UNIVERSITÀ DI PARMA

UNIVERSITÀ DEGLI STUDI DI PARMA

DOTTORATO DI RICERCA IN SCIENZE CHIMICHE

CICLO XXXV

MULTIVALENT PEPTIDO AND GLYCOCALIXARENES AS LIGANDS FOR MICROORGANISMS

Coordinatore:
Chiar.ma Prof.ssa Alessia Bacchi

Tutore:
Chiar.ma Prof.ssa Laura Baldini

Dottorando:
Carlo Alberto Vezzoni

Anni Accademici 2019/2020 – 2021/2022

Contents

ABSTRACT

The present thesis work deals with the design and synthesis of novel calixarene-based multivalent ligands tailored to interact with proteins exposed on the external membrane of different microorganisms. The calixarene macrocycle was chosen as central core of these multivalent ligands because of the efficient methods known for its selective functionalization either at the upper or lower rims and for the possibility to easily modulate, at will, the geometry of the exposed ligating units. This last feature is particularly important when designing multivalent systems for the recognition of biological macromolecules, since it allows to develop ligands of increased efficiency and selectivity.

After a general introduction on calixarenes for protein targeting, the first chapter reports the results of a project aimed at obtaining peptidocalix[4]arenes for the inhibition of the SARS-CoV-2 virus. Our goal was to synthesize ligands able to bind to the virus Spike protein and potentially able to prevent its interaction with its host cell receptor and to block the infection process. This work was triggered by a molecular modelling study to screen *in silico* potential ligands and was followed by the synthesis of some of the selected compounds and by their tests on a model of the virus.

In the second chapter is reported the work performed at the University of Grenoble, where the candidate spent a 6-months research period in the group of prof. Olivier Renaudet. During this period, the attention was focused on the design and synthesis of fucosylated calix[4]arenes for the interaction with three different lectins: *Aspergillus fumigatus* lectin, *Burkholderia ambifaria* lectin and LecB from *Pseudomonas aeruginosa*. In parallel to the synthesis of more classical fucosylated calixarenes, we also synthesized a novel "superstructure" based on a central calix[4]arene core in cone geometry functionalized at the upper rim with four cyclodecapeptides, each of them decorated with four units of fucose, resulting in a peculiar hexadecavalent ligand. All the synthesized compounds were tested in ITC experiments to study their affinity towards the three lectins.

Finally, in the last chapter it is described the preparation of calix[4]arene-based ligands designed for the selective recognition of Gram-positive, Gram-negative and Mycobacteria. To develop ligands capable of discriminating among these three bacterial groups we targeted peculiar epitopes or proteins exposed on the surface of their cell wall. The obtainment of selective ligands for each of these classes of bacteria could be an important aid towards the development of new bacterial sensor devices useful, to medical doctors, for the rapid selection of the appropriate antibiotic, preventing the

administration of broad-spectrum drugs that are among the main causes of the spread of antibiotic resistance. Moreover, these bacteria ligands could even find applications for the preparation of novel targeted antibacterial drugs.

Chapter 1:

Introduction

1. Protein recognition

For all living beings, ranging from microorganisms to humans, proteins are essential. Proteins, for example, serve as structural components for cell support and strength, and they can also be involved in the transportation and storage of molecules.[1,2] Furthermore, they also function as enzymes for the catalysis of many biological processes. Moreover, those located on the outer membranes of viruses and bacteria can be exploited by these pathogens to adhere to host cells and trigger infections.[3,4]

Most of these protein functions are performed thanks to specific recognition events that can occur either in well-defined biding pockets (as the active site of an enzyme) or on the protein surface (as in the case of protein-protein interactions, PPIs).

The comprehension of the mechanisms that control these recognition events, especially those involved in pathological situations, is therefore of great interest for many applications in the medical field. For example, the process of microorganisms' infection of host cells is triggered by a PPI between proteins exposed on the pathogen's surface and proteins present on the host's membrane.[5,6] As a consequence, the development of molecular systems capable of interfering with this PPI can be exploited to prevent cell infection.

2. Calixarenes

Calix[n]arenes (Figure 1) are cyclic oligomers formed by the condensation of phenol and formaldehyde in basic conditions. Initially studied for their ability to selectively complex cations,[7] they have subsequently been used as excellent scaffolds to obtain ligands for biomacromolecules such as proteins, nucleic acids and lipopolysaccharides.[8,9] The reason for their versatility lies in the availability of well-established synthetic procedures that allow to control the size of the macrocycle and to introduce on the reactive positions of the phenol rings (the OH groups, called lower rim, and the aromatic positions para to the OHs, called upper rim) almost any kind of chemical functionalities.[10]

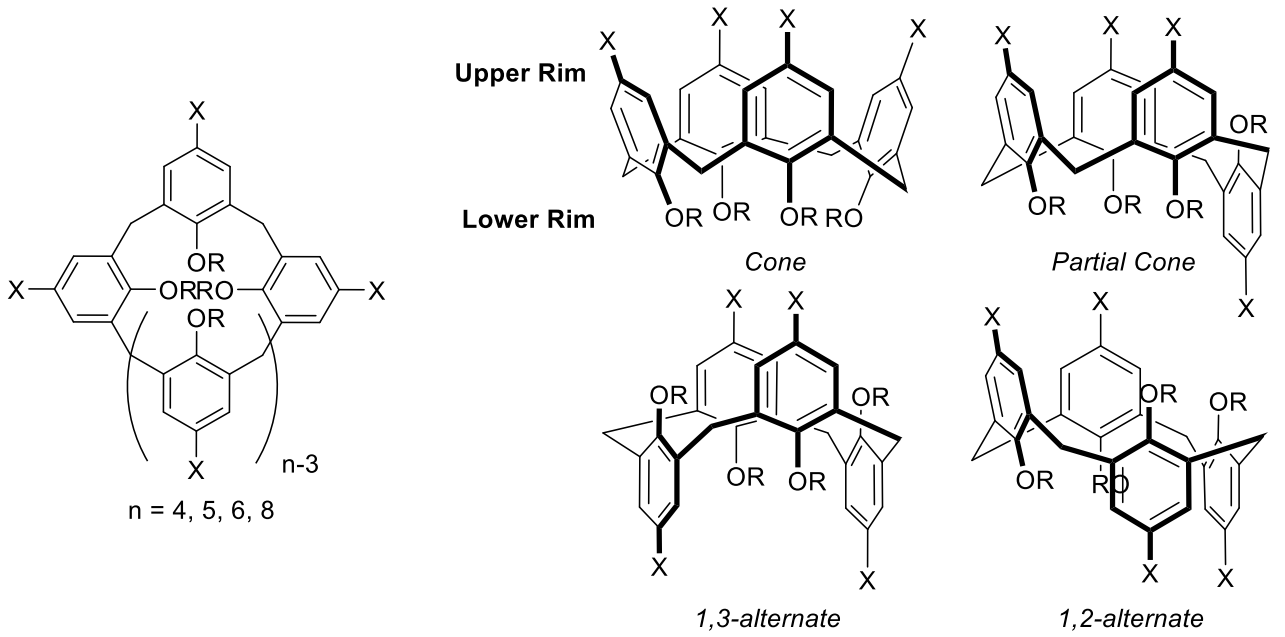

Figure 1: General structure of a calix[n]arene and possible conformations of calix[4]arene.

The conformational mobility of the calixarene scaffold depends on the number of phenol units of the macrocycle. While calix[6]- and calix[8]arenes are quite flexible, due to the larger size of the macrocycle that allows rotation of the aromatic rings around the methylene bridges, the conformation of calix[4]arenes can be blocked in four different structures (named cone, partial cone, 1,3-alternate and 1,2-alternate) by functionalization at the lower rim with alkyl groups larger than ethyl. The possibility to modulate the conformational mobility at will is of great advantage when designing ligands based on the calixarene scaffold, since, depending on the specific aim, it is possible to design mobile ligands that adapt their shape to that of the target (induced fit) or rigid and preorganized ligands that benefit of an entropic advantage.

Additionally, calix[4]arenes in the cone geometry are characterized by an even more subtle conformational flexibility. While calix[4]arenes with no substituents at the lower rim adopt a rigid cone structure thanks to a circular array of quite strong hydrogen bonds between the OH groups (Figure 2, left), calix[4]arenes functionalized with four alkyl groups (larger than ethyl), in solution, experience a rapid conformational interconversion between two structures called flattened or pinched cone, where two distal phenol rings are parallel to each other and the remaining two are tilted outwards (Figure 2, right).[11]

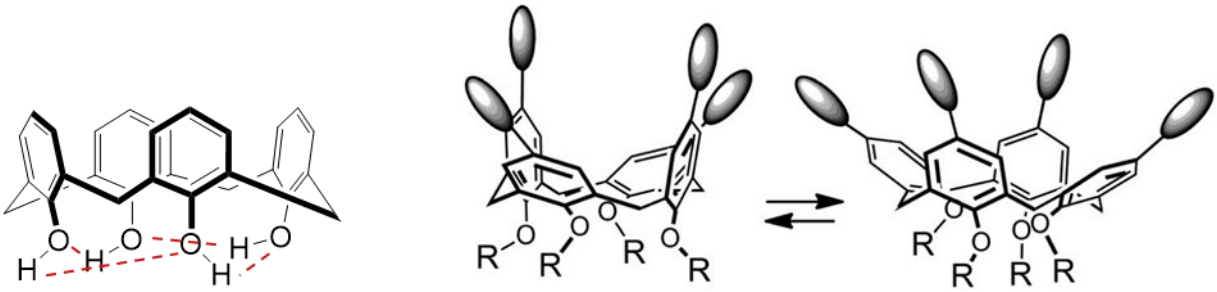

Figure 2: left: rigid cone structure of a calix[4]arene with free OH groups at the lower rim; right: interconversion between the two pinched or flattened cone conformations of calix[4]arenes functionalized at the lower rim with four alkyl groups larger than ethyl.

3. Calixarenes as ligands for proteins

The functionalization of one rim of the calixarene with polar binding sites confers a "hybrid" character to the ligand. This is due to the ability of the calixarene aromatic macrocycle to give apolar interactions, such as π-π, CH-π and hydrophobic effects, in synergy with the electrostatic interactions and/or hydrogen bonds that can be established by the polar substituents. The possibility to combine hydrophilic and hydrophobic binding sites makes the calixarene an ideal scaffold for targeting proteins, which typically exploit both types of residues to achieve efficiency and selectivity in recognition processes. It is not surprising, therefore, that in the last decades numerous examples of calixarene-based ligands for proteins have been reported.[12]

According to the mode of interaction with the protein, calixarene ligands can be divided in three groups:

(i) Ligands targeting quite large areas of the protein surface, with the aim of interfering with PPIs;
(ii) Ligands binding to specific amino acid side chains exposed on the protein surface, thus masking well-defined residues;
(iii) Ligands for the protein binding sites, with the aim of obtaining inhibitors of a protein functionality.

3.1 Calixarenes as inhibitors of PPIs

Protein-protein interactions regulate a plethora of fundamental biological processes, ranging from signal transduction to cell growth and differentiation and apoptosis, which, if misregulated, lead to pathological states.[13] The design of synthetic ligands able to interfere with malfunctioning PPIs can therefore lead to new therapeutic agents.[14,15]

Typically, in a protein-protein complex, the recognition event takes place at the interface of the two proteins, involving large areas (750–1500 $Å^2$) of both of them. These zones are generally characterized by an amphiphilic character due to the presence of hydrophilic, hydrophobic and also charged domains. The instauration of PPIs is commonly based on the presence of many different concurrent intermolecular contacts such as electrostatic interactions, hydrogen bonds but also hydrophobic effects.[16] Moreover, it has been recognized that in protein-protein interfaces are often found a few amino acid residues (called hotspots) that contribute the most, in terms of free energy, to the formation of the protein-protein complexes.[17] These amino acids vary depending on the complex under examination but they can be generally identified by alanine scanning. Knowing if and which are the protein hotspots is a crucial information since it allows to design molecules presenting groups chemically complementary to those in the hotspots which therefore should be able to interfere with the corresponding PPI.[14]

For the complexation of protein surfaces, calixarene derivatives with cone geometry are among the most suitable compounds, thanks to the facial arrangement of the binding groups and the modularity of the scaffold.

Hamilton pioneered this field by showing, in 1997, that calixarenes characterized by a considerable surface area could complementary bind certain protein hotspots.[18] Inspired by the hypervariable peptide loops found in the antibodies antigen recognition site, he developed a collection of calixarene-based ligands decorated at the upper rim by four peptide loops.[19] The general structure consisted of a hydrophobic region, due to the calixarene aromatic rings, enclosed by the peptide loops. The hydrophilic/hydrophobic character of the loops could be easily modulated by the choice of polar or lipophilic amino acids. It was found that the compound decorated with negatively charged loops, composed by two Asp and two Gly (**1a**, Figure 3), was able to strongly bind to a region of the surface of cytochrome c composed of a central lipophilic region surrounded by positively charged Lys residues, forming a complex with a K_D in the nanomolar range.[20]

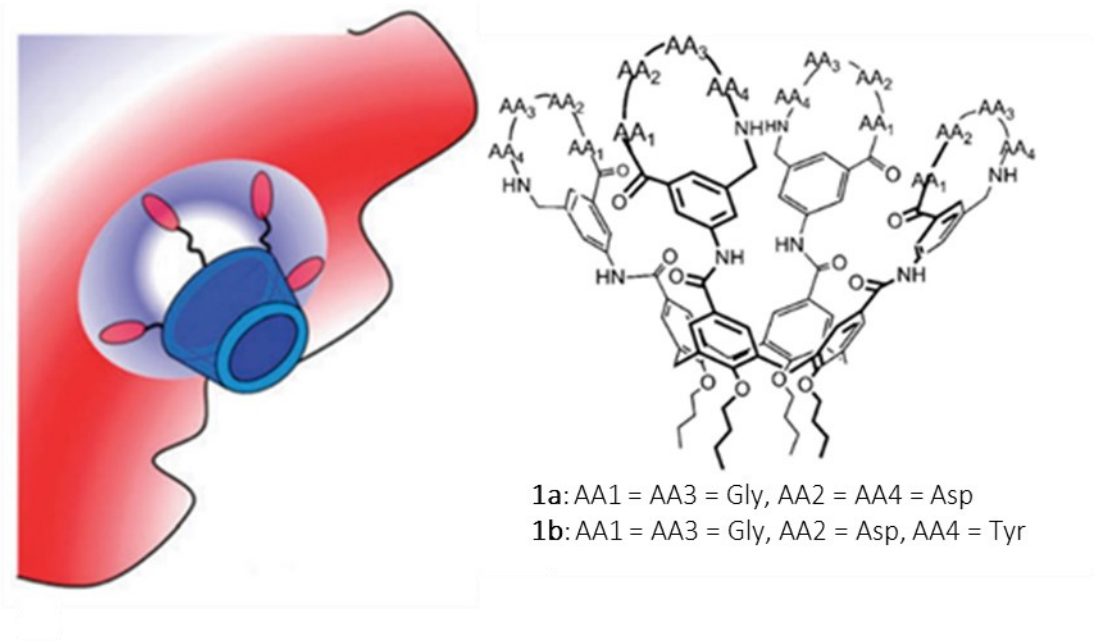

Figure 3: On the left, schematic representation of a calixarene ligand bound to a protein surface, on the right, structure of two peptidocalixarenes developed by Hamilton.[19,21]

Hamilton and coworkers also proved the feasibility of employing calixarene-based ligands for the inhibition of medically relevant PPIs.[21] They focused their attention on a growth factor that is generally involved in angiogenesis and tumor growth, the platelet-derived growth factor (PDGF). They observed that the calixarene decorated at the upper rim with hydrophobic and negatively charged peptide loops (**1b**, Figure 3) was able to selectively and strongly bind PDGF in the same area used by this protein for the interaction with its corresponding receptor, a tyrosine kinase, blocking its biological activity and eventually inhibiting tumor growth. The region involved in such interaction is, in fact, composed of positive and hydrophobic residues.

Another interesting approach in which PPIs are modulated by calixarenes was reported by the De Mendoza research group.[22] The subject of their studies was directed towards the development of ligands able to repair malfunctioning PPIs. They focused their attention on a mutated version of p53 present in a variety of tumors. This protein is involved in processes aimed to protect cells from cancer, in particular regulating cell apoptosis. The biological activity of p53 is, however, strictly linked to its tetrameric structure, where hydrogen bonds, salt bridges and hydrophobic packing hold together the four α-helices. The mutated protein in which Arg337 is replaced by a His loses its biological function because the tetrameric assembly is destabilized since at physiological pH the His is not completely protonated. This results in a weaker hydrogen bond with the corresponding Asp352. De Mendoza showed that the tetraguanidino calixarene **2** (Figure 4) is able to perform as templating ligand holding the tetrameric

structure of the mutated p53 together. The four guanidinium groups, in fact, allow the calixarene to bind four Glu carboxylates. Furthermore, the calixarene lipophilic region is able to interact with a lipophilic pocket formed between the monomers, whose shape is well fitted by the calixarene cone scaffold.[23]

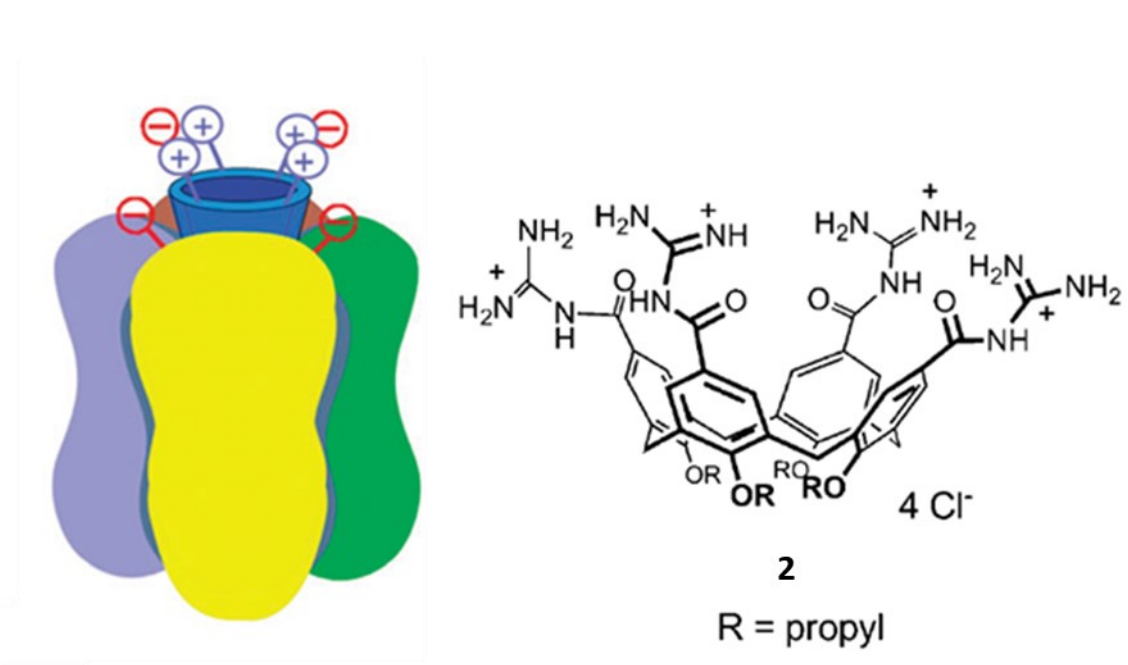

*Figure 4: On the left, schematic representation of the binding of calixarene **2** to mutated p53, on the right, structure of the tetraguanidinocalixarene **2** developed by De Mendoza.*[22]

3.2 Calixarenes for single point recognition

Another strategy employable for the design of ligands capable of PPIs disruption is built on the recognition of single contact points exposed on the target protein surface. In this case, there is no need of developing compounds able to interact with a wide area of the protein, but instead the attention is focused on the design of molecules that selectively target precise amino acidic residues. Usually, these are the charged groups on the amino acids side chains and are targeted by reverse charge ligands.

A clear example of this possibility has been reported by the Crowley group. They have shown that the aromatic cavity of the calixarene can be exploited to complex lipophilic side chains ending with positively charged groups of Arg and Lys, conferring the macrocycle the ability to recognize "single points" on the protein (Figure 5).[24] For their studies, they used tetrasulfonated and tetraphosphonated calix[4]arenes, in which the cone conformation is maintained by the hydrogen bond network between the phenolic OH at the lower rim (Figure 5). The X-ray structure of the tetrasulfonated calixarene-cytochrome c complex shows that the side chain of a Lys exposed on the surface of the

protein is disposed within the hydrophobic cavity of the macrocycle forming a sort of hook, while the ammonium-ε group is directed towards the anionic substituents of the upper rim (Figure 5). In this case, there is the simultaneous presence of hydrophobic interactions and ionic bonds.

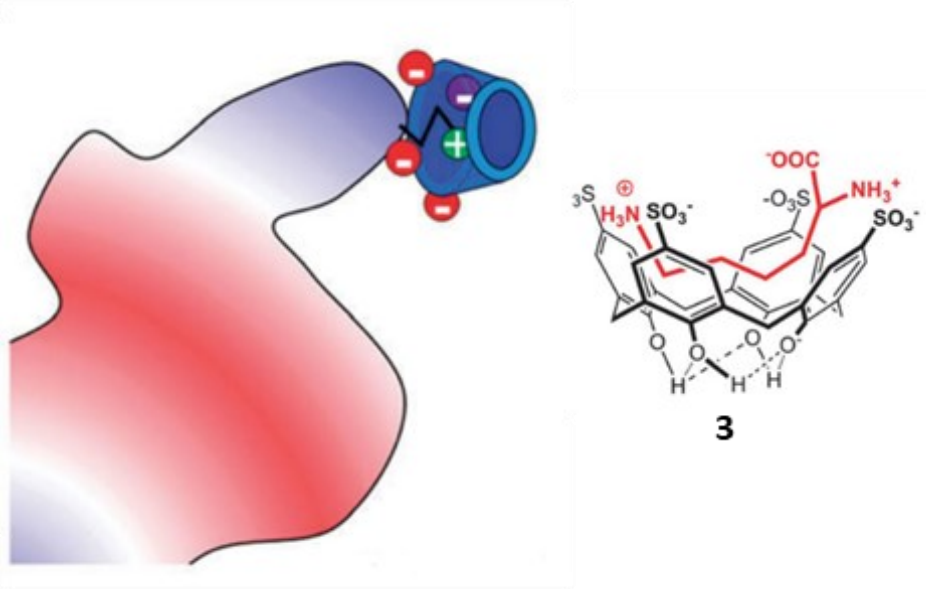

*Figure 5: On the left, schematic representation of single residues binding, on the right, structure of the tetrasulphonated calixarene **3** studied by Crowley complexing a Lys amino acid.*[24]

3.3 Calixarenes targeting proteins binding sites

The most valuable contribution to the field of synthetic agents targeting protein active sites given by calixarenes relies on their multivalent structure. Calixarenes decorated with multiple copies of the same binding unit can, in fact, strongly interact with proteins characterized by multiple binding sites,[8] exploiting the phenomenon of multivalency.

3.3.1 Multivalency

Multivalency[25] can be described as the ability of a particle, molecule or entity to bind another particle, molecule or entity through multiple identical and simultaneous binding site-ligand interactions as shown in Figure 6. These interactions typically have a non-covalent nature and can include hydrogen bonds, cation-π interactions, π-π stacking, electrostatic interactions, hydrophobic effects, and Van der Waals forces. This concept is employed by nature to create specific and strong, yet reversible interactions, particularly when a single substrate-binding site complex would be too weak to ensure selective recognition and stability of the assembled species. A key feature of multivalent

interactions is that they increase the overall binding constant in comparison to the sum of all the binding constants of the individual monovalent events.

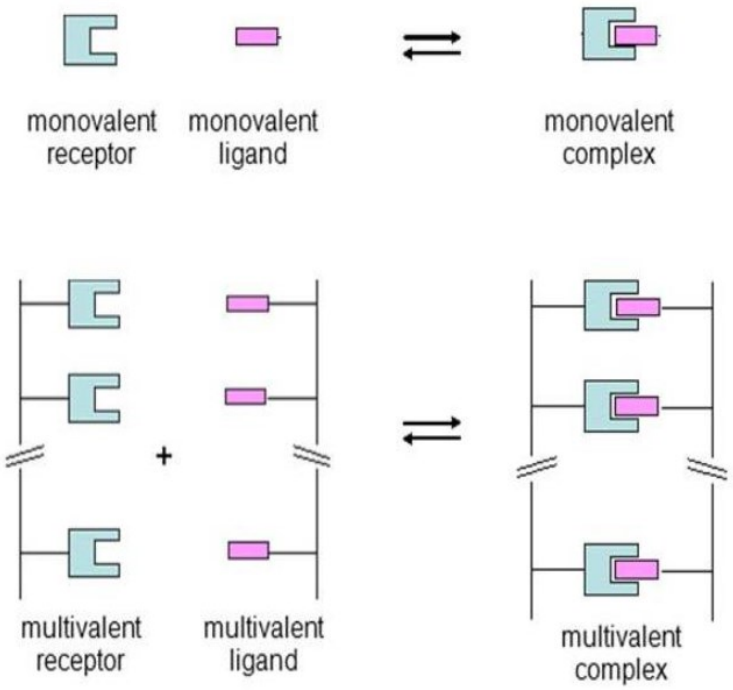

Figure 6: Monovalent and multivalent complex formation (figure from ref. 8).

Multivalency is often characterized by a favorable avidity entropy, which increases with the complex valency, thus promoting binding and counterbalancing the loss of conformational entropy that occurs during multivalent complex formation.

From a thermodynamic perspective, the following formula, proposed by Jencks,[26] can be applied to multivalent binding:

$$\Delta G°_{multi} = n\,\Delta G°_{mono} + \Delta G°_{interaction}$$

Where $\Delta G°_{multi}$ is the standard free energy for multivalent binding and $\Delta G°_{mono}$ is the standard free energy for the corresponding monovalent binding of a ligand to a receptor. The $\Delta G°_{multi}$ also takes into account the $\Delta G°_{interaction}$, which is an additional free energy component that accounts for and balances the favorable and unfavorable effects of tethering.

To evaluate the multivalent effect, a method was proposed by Whitesides,[27] based on the enhancement factor, denoted as β. This is the ratio of the binding constant of a multivalent ligand to a multivalent receptor in a multivalent binding (K_{multi}) and the binding constant of the corresponding monovalent ligand to the same multivalent receptor in a monovalent binding (K_{mono}):

$$\beta = K_{multi}/K_{mono}$$

This factor can be useful when the number of effective binding interactions is not known.

Another useful measure is the relative potency (rp), which is the ratio between the IC50 value of a monovalent ligand ($IC50_{mono}$) and a multivalent ligand ($IC50_{multi}$):

$$rp = IC50_{mono}/IC50_{multi}.$$

IC50 value represents the concentration of a compound needed to inhibit a process by 50%. When the valency of the cluster is known, the enhancement factor and the relative potency can be normalized by dividing their values by the valency, resulting in the parameters β/n and rp/n. These parameters can be used to compare the efficiency of multivalent systems with different valency, topology and linker. Systems with high β/n or rp/n values (>>1) are more efficient than their monovalent counterparts, while systems with low β/n or rp/n values (<<1) have lower affinity and are characterized by a negative multivalent effect.

3.3.2 Multivalent glycocalixarenes for lectin binding

Due to their multivalent structure and the ease of multiple functionalization with identical binding groups, calixarenes are an excellent platform to build multivalent ligands. Among proteins, multivalency is most of all exploited by lectins, i.e. carbohydrate binding proteins that do not possess enzymatic activity but are involved in numerous fundamental processes, among which fertilization, cellular communication and adhesion of viruses, bacteria and toxins to the cell membrane.[28] Lectins are generally endowed of multiple sugar selective binding sites, with which they interact with polyglycosylated substrates such as polysaccharides, glycoproteins, and glycolipids. Even if a single binding site-sugar interaction is weak, the multivalent complex is usually strong due to the simultaneous complexation of multiple identical glycoside residues by multiple equivalent binding sites of the lectin. This specific example of multivalency is also known as the glycoside cluster effect.[29] Chemists in the early 1980s began to focus on the synthesis of polyglycosylated entities, called glycoclusters, with the goal of producing molecules that could exploit multivalency to inhibit fundamental biological processes involving lectins.[30,31,32]

Among the various families of glycoclusters, glycocalixarenes, which are calixarenes with sugars attached at the upper and/or lower rim, have been shown to efficiently recognize lectins due to their ability to easily modulate valency and sugar presentation, as well as their simple preparation and functionalization.[33]

This is the case for cholera toxin (CT), which has 5 identical binding units for the pentasaccharide of the GM1 ganglioside. In this case, a calix[5]arene scaffold was designed (**4**, Figure 7), having five GM1 units at the upper rim connected through a suitable spacer to allow simultaneous complexation of the five saccharide units by the five CT recognition sites, forming a 1:1 complex.[34] The inhibition activity of this macrocyclic ligand was very high, with a gain of 20,000 fold per single GM1 ganglioside.

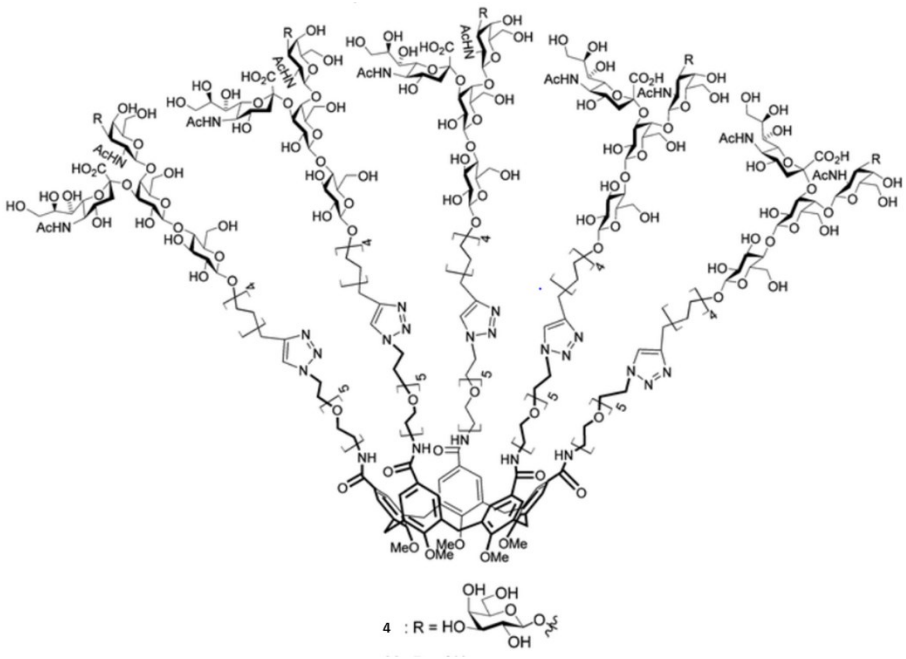

*Figure 7: Structure of the pentavalent calix[5]arene **4**.*

Small libraries can also be prepared with glycocalixarenes of different shapes and valencies to evaluate the best multivalent ligand for a target protein. Once the proper ligand is defined, it can be studied more extensively with the goal of achieving the best multivalent presentation of carbohydrate units towards the target protein.

Andrè and coworkers observed the potential role of different structural characteristics in a family of 14 glycosylthioureidocalix[n]arenes (a small group of which is reported in Figure 8) as inhibitors of human galectins, which are important biological targets in tumor progression.[35]

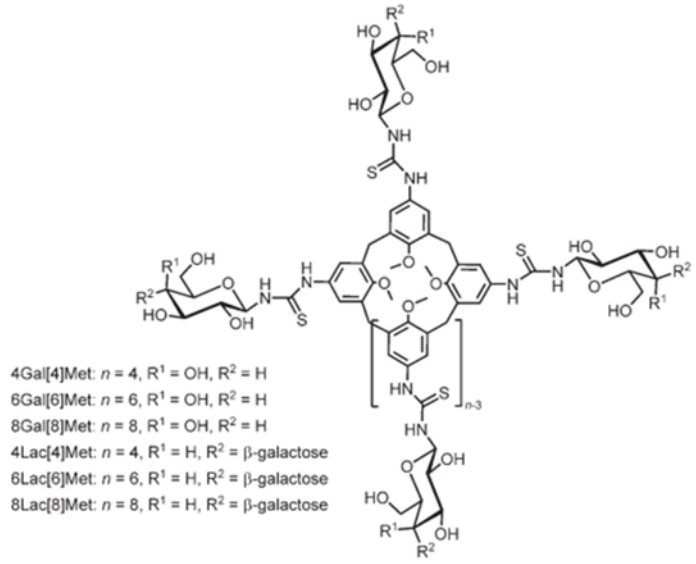

Figure 8: Structures of six of the glycosylthioureidocalixarenes studied by Andrè.

The ligands, some with galactose and some with lactose units, had different properties in terms of valency, binding units, and epitope display. A correlation was found between inhibition potency and structural features, with lactose derivatives generally being more efficient.

Another example is given by Vidal and co-workers who prepared a series of galactosyl glycocalix[4]arenes as potential diagnostic and therapeutic agents against the PA-IL (Lec A) lectin of *Pseudomonas Aeruginosa*. The most efficient derivative was the 1,3-alternate calixarene **6** (Figure 9), which was able to form a complex with two lectins, simultaneously involving all the four galactoses in the recognition process.[36]

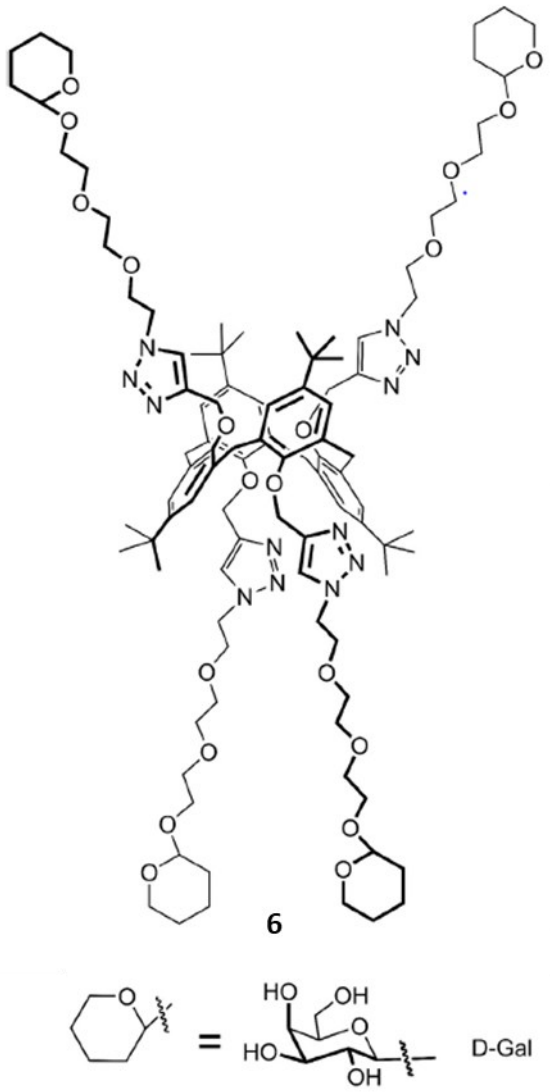

Figure 9: Structure of the best ligand obtained by Vidal.[36]

4. Thesis Outlook

The examples reported above demonstrate that the calixarene macrocycle grants a versatile scaffold for the development of ligands capable of strongly interacting with proteins. A myriad of different functionalities can be introduced on these scaffolds, ranging from amino acids, to charged groups and lipophilic moieties. This allows the researchers to develop adequate ligands for potentially every protein of interest. Moreover, the three-dimensional properties of this macrocycle can be finely tuned to adapt the structure of the ligand to stereochemical demands of the target. Furthermore, it is possible to exploit the intrinsic multivalent nature of calixarenes to develop ligands with higher affinities for multimeric proteins compared to their monovalent analogs.

For these reasons, we decided to exploit this macrocycle for the development of ligands capable of interacting with different proteins and biomacromolecules. In the first chapter of this thesis is described the design and synthesis of peptidocalix[4]arenes for the inhibition of the SARS-CoV-2 virus. We tried to develop molecules capable of interacting with the viral Spike protein, which is involved in the infection process, in order to block its biological activity and prevent cell infection. In the second chapter is described the work carried out at the University of Grenoble during a period of six months. There, we worked on the synthesis of new calixarene-based glycosylated ligands for the interaction with three different fucose-selective lectins: *Aspergillus Fumigatus* Lectin, *Burkholderia ambifaria* Lectin and LecB from *Pseudomonas Aeruginosa*. Finally, in the last chapter is described our work on the development of new calixarene-based ligands for the recognition of specific entities present on the membranes of three different bacterial strains Gram-positive, Gram-negative and Mycobacteria, with the aim of obtaining a quick method for their identification.

5. Bibliography

(1) Ringli, C.; Keller, B.; Ryser, U. Glycine-Rich Proteins as Structural Components of Plant Cell Walls. *Cell. Mol. Life Sci.* **2001**, *58* (10), 1430–1441.

(2) Pickering, A. C.; Fitzgerald, J. R. The Role of Gram-Positive Surface Proteins in Bacterial Niche- and Host-Specialization. *Front. Microbiol.* **2020**, *11*, 2667.

(3) Gómez Borrego, J.; Torrent Burgas, M. Analysis of Host–Bacteria Protein Interactions Reveals Conserved Domains and Motifs That Mediate Fundamental Infection Pathways. *Int. J. Mol. Sci.* **2022**, *23* (19), 11489.

(4) Källström, H.; Liszewski, M. K.; Atkinson, J. P.; Jonsson, A. B. Membrane Cofactor Protein (MCP or CD46) Is a Cellular Pilus Receptor for Pathogenic Neisseria. *Mol. Microbiol.* **1997**, *25* (4), 639–647.

(5) Helena Kallstrom, M. Kathryn Liszewski, J. P.; Jonsson, A. and A.-B. Membrane Cofactor Protein (MCP or CD46) Is a Cellular Pilus Receptor for Pathogenic Neisseria. *Mol. Microbiol.* **1997**, *25* (4), 639–647.

(6) Li, S.; Zhou, W.; Li, D.; Pan, T.; Guo, J.; Zou, H.; Tian, Z.; Li, K.; Xu, J.; Li, X.; et al. Comprehensive Characterization of Human–Virus Protein-Protein Interactions Reveals Disease Comorbidities and Potential Antiviral Drugs. *Comput. Struct. Biotechnol. J.* **2022**, *20*, 1244.

(7) Baldini, L.; Sansone, F.; Casnati, A. Cation Complexation by Calixarenes. *Ref. Modul. Chem. Mol. Sci. Chem. Eng.*, Elsevier, **2013**.

(8) Baldini, L.; Casnati, A.; Sansone, F.; Ungaro, R. Calixarene-Based Multivalent Ligands. *Chem. Soc. Rev.* **2007**, *36* (2), 254–266.

(9) Giuliani, M.; Morbioli, I.; Sansone, F.; Casnati, A. Moulding Calixarenes for Biomacromolecule Targeting. *Chem. Commun.* **2015**, *51* (75), 14140–14159.

(10) Gutsche, C. D. *Calixarenes: An Introduction*, RSC Publishing, Ed. **2008**.

(11) Scheerder, J.; Vreekamp, R. H.; Engbersen, J. F. J.; Verboom, W.; Van Duynhoven, J. P. M.; Reinhoudt, D. N. The Pinched Cone Conformation of Calix[4]Arenes: Noncovalent Rigidification of the Calix[4]Arene Skeleton. *J. Org. Chem.* **1996**, *61* (10), 3476–3481.

(12) Baldini, L.; Casnati, A.; Sansone, F. Biomacromolecule Recognition by Calixarene Macrocycles. In *Comprehensive Supramolecular Chemistry II*; Elsevier, O., Ed.; 2017; pp 371–418.

(13) Toogood, P. L. Inhibition of Protein-Protein Association by Small Molecules: Approaches and Progress. *J. Med. Chem.* **2002**, *45* (8), 1543–1558.

(14) Sheng, C.; Dong, G.; Miao, Z.; Zhang, W.; Wang, W. State-of-the-Art Strategies for Targeting Protein–Protein Interactions by Small-Molecule Inhibitors. *Chem. Soc. Rev.* **2015**, *44* (22), 8238–8259.

(15) Cossar, P. J.; Lewis, P. J.; McCluskey, A. Protein-Protein Interactions as Antibiotic Targets: A Medicinal Chemistry Perspective. *Med. Res. Rev.* **2020**, *40* (2), 469–494.

(16) Yin, H.; Hamilton, A. D. Strategies for Targeting Protein–Protein Interactions With Synthetic Agents. *Angew. Chemie Int. Ed.* **2005**, *44* (27), 4130–4163.

(17) DeLano, W. L. Unraveling Hot Spots in Binding Interfaces: Progress and Challenges. *Curr. Opin. Struct. Biol.* **2002**, *12* (1), 14–20.

(18) Hamuro, Y.; Calama, M. C.; Park, H. S.; Hamilton, A. D. A Calixarene with Four Peptide Loops: An Antibody Mimic for Recognition of Protein Surfaces. *Angew. Chem. Int. Ed. Engl.* **1997**, *36* (23), 2680–2683.

(19) Lin, Q.; Park, H. S.; Hamuro, Y.; Lee, C. S.; Hamilton, A. D. Protein Surface Recognition by Synthetic Agents: Design and Structural Requirements of a Family of Artificial Receptors That Bind to Cytochrome C. *Biopolymers* **1998**, *47* (4), 285–297.

(20) Wei, Y.; Mc Lendon, G. L.; Hamilton, A. D.; Case, M. A.; Purring, C. B.; Lin, Q.; Park, H. S.; Leec, C. S.; Yua, T. Disruption of Protein–Protein Interactions: Design of a Synthetic Receptor That Blocks the Binding of Cytochrome c to Cytochrome c Peroxidase. *Chem. Commun.* **2001**, *1* (17), 1580–1581.

(21) Blaskovich, M. A.; Lin, Q.; Delarue, F. L.; Sun, J.; Park, H. S.; Coppola, D.; Hamilton, A. D.; Sebti, S. M. Design of GFB-111, a Platelet-Derived Growth Factor Binding Molecule with Antiangiogenic and Anticancer Activity against Human Tumors in Mice. *Nat. Biotechnol. 2000 1810* **2000**, *18* (10), 1065–1070.

(22) Gordo, S.; Martos, V.; Santos, E.; Menéndez, M.; Bo, C.; Giralt, E.; De Mendoza, J. Stability and Structural Recovery of the Tetramerization Domain of P53-R337H Mutant Induced by a Designed Templating Ligand. *Proc. Natl. Acad. Sci. U. S. A.* **2008**, *105* (43), 16426.

(23) Martos, V.; Bell, S. C.; Santos, E.; Isacoff, E. Y.; Trauner, D.; De Mendoza, J. Calix[4]Arene-Based Conical-Shaped Ligands for Voltage-Dependent Potassium Channels. *Proc. Natl. Acad. Sci. U. S. A.* **2009**, *106* (26), 10482–10486.

(24) McGovern, R. E.; Fernandes, H.; Khan, A. R.; Power, N. P.; Crowley, P. B. Protein Camouflage in Cytochrome c–Calixarene Complexes. *Nat. Chem. 2012 47* **2012**, *4* (7), 527–533.

(25) Fasting, C.; Schalley, C. A.; Weber, M.; Seitz, O.; Hecht, S.; Koksch, B.; Dernedde, J.;

Graf, C.; Knapp, E. W.; Haag, R. Multivalency as a Chemical Organization and Action Principle. *Angew. Chemie - Int. Ed.* **2012**, *51* (42), 10472–10498.

(26) Jencks, W. P. On the Attribution and Additivity of Binding Energies. *Proc. Natl. Acad. Sci. U. S. A.* **1981**, *78* (7 I), 4046–4050.

(27) Mammen, M.; Choi, S. K.; Witesides, G. M.; Polyvalent Interactions in Biological Systems: Implications for Design and Use of Multivalent Ligands and Inhibitors. *Angew. Chem. Int. Ed. Engl.* **1998**, *37* (20), 2754–2794.

(28) G., H. J., *The Sugar Code*; Weinheim:Wiley-Blackwell, 2009.

(29) Lundquist, J. J.; Toone, E. J. The Cluster Glycoside Effect. *Chem. Rev.* **2002**, *102* (2), 555–578.

(30) Chabre, Y. M.; Giguère, D.; Blanchard, B.; Rodrigue, J.; Rocheleau, S.; Neault, M.; Rauthu, S.; Papadopoulos, A.; Arnold, A. A.; Imberty, A.; et al. Combining Glycomimetic and Multivalent Strategies toward Designing Potent Bacterial Lectin Inhibitors. *Chem. – A Eur. J.* **2011**, *17* (23), 6545–6562.

(31) Chabre, Y. M.; Roy, R. Design and Creativity in Synthesis of Multivalent Neoglycoconjugates. *Adv. Carbohydr. Chem. Biochem.* **2010**, *63*, 165–393.

(32) Pieters, R. J. Maximising Multivalency Effects in Protein-Carbohydrate Interactions. *Org. Biomol. Chem.* **2009**, *7* (10), 2013–2025.

(33) Sansone, F.; Casnati, A. Multivalent Glycocalixarenes for Recognition of Biological Macromolecules: Glycocalyx Mimics Capable of Multitasking. *Chem. Soc. Rev.* **2013**, *42* (11), 4623–4639.

(34) Garcia-Hartjes, J.; Bernardi, S.; Weijers, C. A. G. M.; Wennekes, T.; Gilbert, M.; Sansone, F.; Casnati, A.; Zuilhof, H. Picomolar Inhibition of Cholera Toxin by a Pentavalent Ganglioside GM1os-Calix[5]Arene. *Org. Biomol. Chem.* **2013**, *11* (26), 4340–4349.

(35) André, S.; Sansone, F.; Kaltner, H.; Casnati, A.; Kopitz, J.; Gabius, H. J.; Ungaro, R. Calix[n]Arene-Based Glycoclusters: Bioactivity of Thiourea-Linked Galactose/Lactose Moieties as Inhibitors of Binding of Medically Relevant Lectins to a Glycoprotein and Cell-Surface Glycoconjugates and Selectivity among Human Adhesion/Growth-Regulatory Galectins. *ChemBioChem* **2008**, *9* (10), 1649–1661.

(36) Cecioni, S.; Lalor, R.; Blanchard, B.; Praly, J. P.; Imberty, A.; Matthews, S. E.; Vidal, S. Achieving High Affinity towards a Bacterial Lectin through Multivalent Topological Isomers of Calix[4]Arene Glycoconjugates. *Chem. – A Eur. J.* **2009**, *15* (47), 13232–13240.

Chapter 2:

Design and synthesis of peptidocalix[4]arenes as potential inhibitors of SARS-CoV-2 spike protein

1. INTRODUCTION

COVID19 is a viral disease originally detected in the city of Wuhan, China, in December 2019. Due to its high contagiousness, in the early 2020 the disease quickly spread globally, causing more than 6 million deaths and more than 600 million confirmed cases of infection since the beginning of the pandemic. The need to address this global health emergency has required the effort of the entire scientific community to study this new virus and to develop effective antivirals and vaccines to stop its spreading.

1.1 SARS-CoV-2 structure and mechanism of action

SARS-CoV-2 (Severe Acute Respiratory Syndrome Coronavirus 2), the virus that causes the COVID-19 disease, is a member of the coronavirus family. Coronaviruses are particularly large RNA viruses (26-32 kilobases), in which the genome appears as a single, positive-sense strand of RNA wrapped inside a nucleocapsid.[1] The name of this class of pathogens is linked to the characteristic circular shape of their virion, which is decorated on its surface with the Spike glycoproteins that make it resemble a crown (Figure 1). SARS-CoV-2, in particular, belongs to the Betacoronavirus class, which also includes two other viruses that have caused outbreaks in the last two decades: SARS-CoV (2003) and MERS-CoV (Middle East Respiratory Syndrome, 2012-2013).

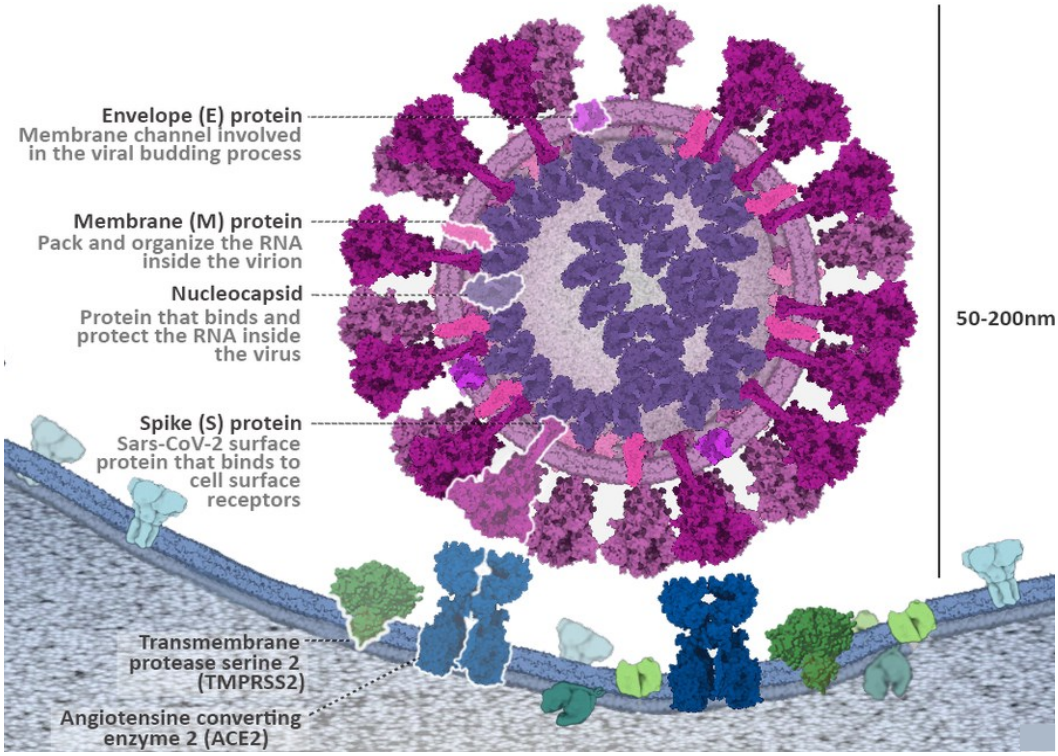

Figure 1: Structure of SARS-CoV-2 (from https://pdb101.rcsb.org/news/2020#5ed7c17cdab5c9354c274f56, Author: Marta Palma Rodríguez).

The SARS-CoV-2 genome was promptly sequenced[2] (Figure 2) and it was seen to code for several proteins with essential roles. Highly conserved sequences were found between this virus and other coronaviruses studied in the past. In particular, SARS-CoV-2 shows more than 70% gene identity with SARS-CoV, with some proteins showing a 95% identical amino acid sequence. In SARS-CoV-2's genetic code, there are two large genes (ORF1a and ORF1b) coding for sixteen non-structural proteins (NSPn). Of these, three have quickly become the target of scientists: the papain-like protease[3] (PLpro), the master protease[4] (3CLpro) and the RNA-dependent RNA polymerase[5] (RdRp). The main function of the two proteases is to break down the polyproteins formed by the translation of viral RNA into functional units. PLpro also has an immunosuppressive effect in infected cells. In contrast, RdRp's role is to synthesize a negative-sense strand of RNA, used as a mould for viral genome replication.

In another section of the genome, there are four genes coding for major structural proteins: N encodes for the nucleocapsid protein, E for the pericapsid protein (a protein involved in the virus budding process) and M is translated into the membrane protein (crucial for the shape and structural organization of the virion). The fourth and final structural protein that has attracted the most attention from the global scientific community is the Spike (S) glycoprotein. This protein plays a central role in the infection process, as it is responsible for the attack on the cellular receptor Angiotensin Converting Enzyme 2 (ACE2) of the host organism.[6] This results in membrane fusion, which allows the virus entry into the cell. Another protein present on the cell membrane, Transmembrane Serine Protease 2 (TMPRSS2),[7] is involved in this process promoting the virus entry into the cell by priming the S protein.

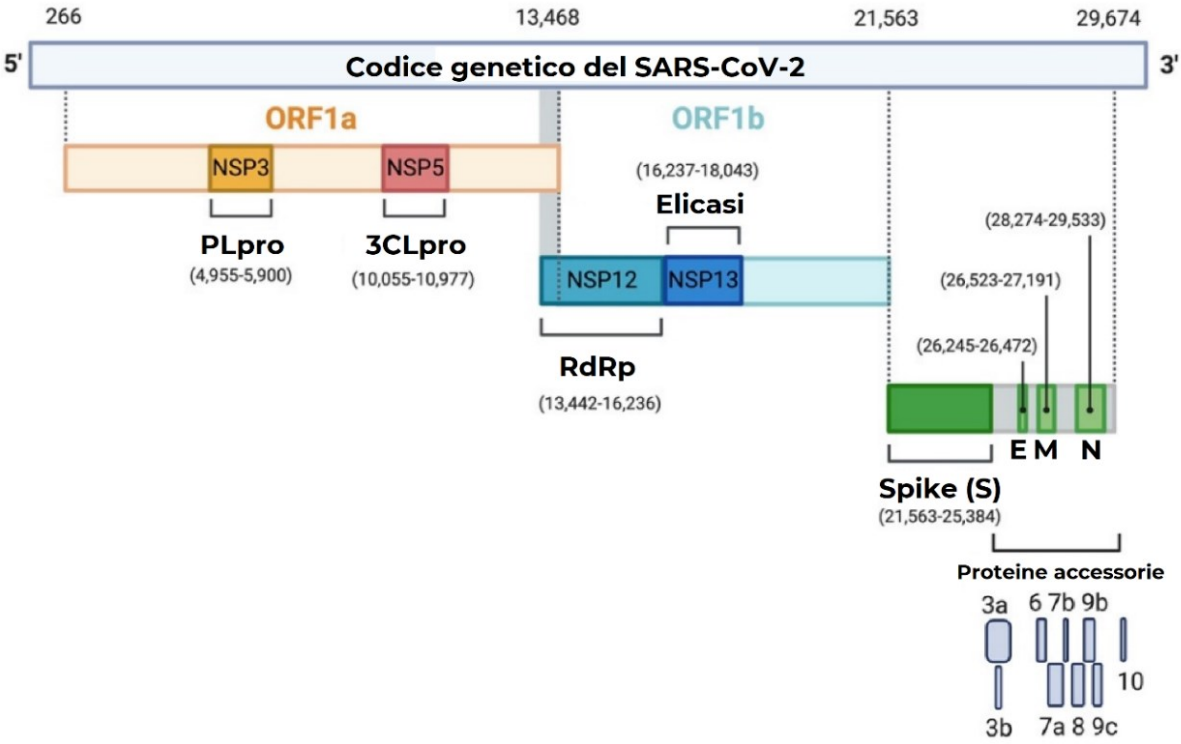

Figure 2: Sequence of the viral genetic code (from Pathogens 2020, 9(5), 331)

All these proteins have become possible targets for the creation of therapeutic agents and vaccines. Once the mechanisms of viral infection and replication had been disclosed,[8] and given the need for the rapid development of a therapy,[2] the possibility of repositioning drugs already on the market for the treatment of other diseases was investigated.[9,10] Some examples, with drug names, possible targets and mechanism of action are given in Table 1. As the months passed and the disease raged on, the efforts of the scientific community never stopped, leading to the development of several well-known vaccines[11] (Pfizer, Moderna, AstraZeneca, Johnson & Johnson), tests capable of reliably and rapidly determining virus positivity, and other compounds capable of interfering on various levels with the infection and replication of SARS-CoV-2.

Table 1: Example of some already existing drugs used also for COVID-19 treatment.

Drug	Standard use	Target	Possible mechanism of action
Remdesivir	Virus Ebola	RdRp	Halting viral replication by blocking nucleotide synthesis
Ribavirina	Hepatitis C, RSV		
Lopinavir+Ritonavir	HIV	3CLpro/PLpro	Proteases' inhibitions
Arbidol (Umifenovir)	Infuenza virus	Spike/ACE2	Preventing virus entry into the cell by hindering the formation of the Spike-ACE2 complex
Clorochina	Malaria	ACE2	Interfere with ACE2 glycosylation by increasing endosomal pH
Camostat mesilato	Viral infections	TMPRSS2	Serine protease inhibition

Among the few proteins of this virus, the most interesting as a potential drug target is the Spike protein (S). This is a trimeric transmembrane protein ranging in size from 180-200 kDa and consisting of a short intracellular C-terminal segment, followed by a transmembrane domain and a large extracellular N-terminal segment that gives it its functionality, and covered with saccharide molecules that render the virus invisible to the immune system.[12] In a simpler representation the protein can be imagined as split into two subunits (Figure 3a), S1, which contains the receptor binding domain (RBD) that is involved in the cell recognition process, and S2, which contains the other domains including the fusion peptide (FP) whose role is to split the cell membrane and promote the formation of a single phospholipidic bilayer during the fusion process.

This protein plays a key role, as it is responsible for the binding to the host's cellular receptor Angiotensin-Converting Enzyme Receptor 2 (ACE2)[13] (Figure 3b). As a result of the interaction, the Spike protein, which is initially in a metastable conformation, undergoes a conformational rearrangement that favors the fusion between the viral and cell membranes, allowing the virus to enter the host cell (Figure 3c). Another protein present on the cell membrane is involved in this process, Serine Protease Transmembrane 210 (TMPRSS2), which promotes the entry of the virus into the cell by priming protein S. Due to its fundamental role in initiating the infection process, the S protein has therefore attracted the attention of the scientific community as a potential target for the development of vaccines and therapeutic agents.

One example is the study conducted by Cheng at al., which proposes toremifene,[14] an anti-estrogen drug already approved by the Food and Drug Administration, as a potential candidate for the treatment of COVID19, as it shows inhibitory activity for SARS-CoV-2. Molecular dynamics and molecular docking studies suggest an interaction

of toremifene with the spike protein such that its secondary structure, in helical region HR1, is disrupted thus preventing the conformational change essential for membrane fusion and entry into the cell by the virus.

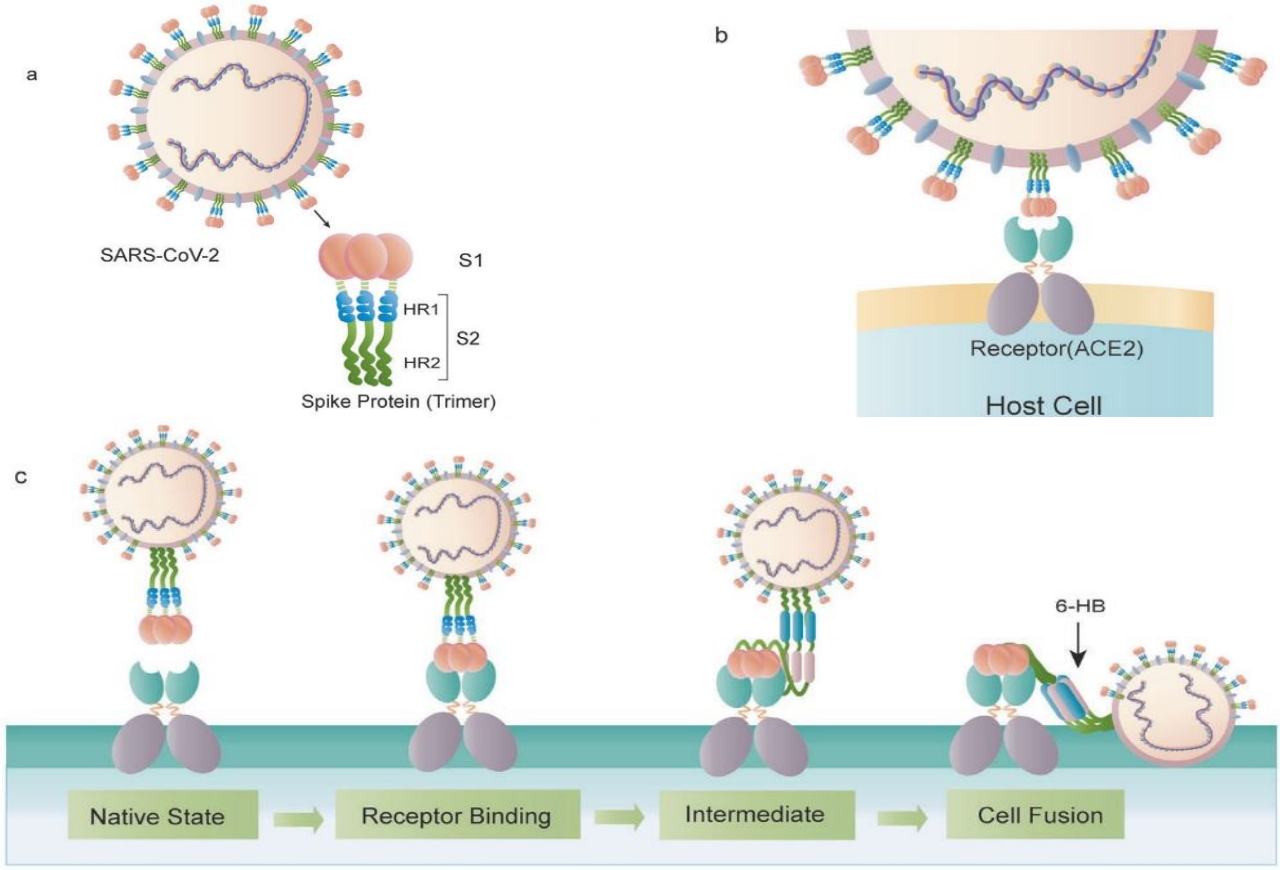

*Figure 3: Structure and activity representation of SARS-CoV-2 Spike protein **a** Schematic structure of proteins S trimers. **b** interaction between protein S and ACE2. **c** Scheme of the S protein-mediated virus-cell interaction and fusion process.*[12]

Another particularly interesting strategy for suppressing the infectious capacity of SARS-CoV-2 could be based on the development of an antiviral capable of inhibiting cell recognition and adhesion by the virus, replacing therefore ACE2 in the interaction with the Spike protein. Of particular interest is, in fact, the possibility of hindering viral infection by preventing the virus from entering the cell, process which is mediated by the cell membrane receptor ACE2 (as in the case of SARS-CoV).[6,15,16] This receptor is involved in several key processes in the body, including the regulation of blood pressure and other cardiovascular functions. Studying the complex formed between ACE2 and the viral S-protein in detail, it can be seen that the region of the latter involved in the interaction, the so-called Receptor Binding Domain[17] (RBD) consists of 193 amino acids (331 to 524). This domain of the S-glycoprotein interacts with the Protease Domain (PD)

of the ACE2 receptor, forming a very stable complex, about 10-20 times more stable than the one formed by the S-protein of SARS-CoV (its greater contagiousness and transmissibility may be attributable to this). The determination by X-ray diffraction, very rapidly and by various research groups, of the ACE2-protein S complex structure made it possible to shed light on the nature of the interactions responsible for the formation of this complex. In figure 4, which shows the structure solved by Qiang Zhou and colleagues,[18] it can be seen that they are separated into three zones. In **A**, there is the presence of the largest number of hydrogen bond type interactions between residues Tyr41, Gln42, Lys353 and Arg357 of ACE2 and Gln498, Thr500 and Asn501 of the RBD. Moving to **B**, two interactions are observed: a hydrogen bond between the virus' Tyr453 and Hys34 of ACE2 and an ion pair between a Lys417 residue and Asp30. Finally, in **C** we find a hydrogen bond between two Gln residues (Gln474 of the RBD and Gln24 of the receptor) and a weak interaction between Phe486 and Met82.

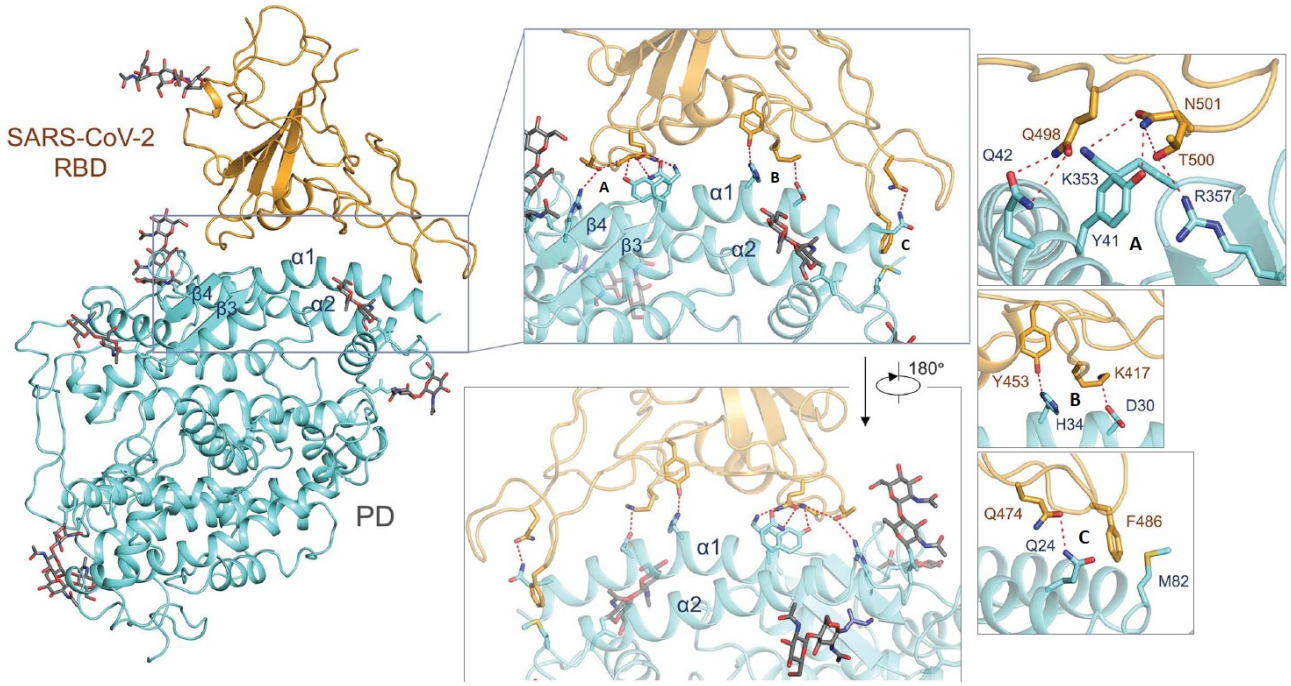

Figure 4: Complex between ACE2 PD and SARS-CoV- 2 RBD (adapted from Rif. 18).

Based on the structure and characteristics of this complex between SARS-CoV-2 RBD and the cellular ACE2 receptor, numerous molecular modelling studies were carried out to see if and how different classes of compounds could be able to prevent the formation of the complex or destabilize it. A study by Chaoyong Yang and colleagues[19] reported the case of a bivalent circular aptamer capable of binding to the RBD of the S protein so as to block viral infection. Molecular docking studies were followed by in vitro tests, which confirmed its high affinity and efficacy in inhibiting SARS-CoV-2. Another research group demonstrated, through interaction studies with atomic force

microscopy, how peptides synthesized to reproduce specific portions of ACE2, in order to mimic the receptor's regions involved in the interaction with the complex, were able to strongly inhibit the formation of the complex between ACE2 and RBD.[20] Finally, in a study by Ujjwal Maulik and colleagues,[21] the results of in silico tests done on several phytochemical compounds (such as emodin and anthraquinone) are reported. Some of these showed an ability to bind to RBD protein S and/or the ACE2-RBD complex comparable to that of chemical compounds whose inhibition properties have already been verified (chloroquine and hydroxychloroquine). All these works show how various types of compounds, ranging from macromolecules such as proteins and nucleic acids to small molecules, both natural and synthetic, have potential applications in this field.

Inspired by these studies, we envisaged that calix[4]arene derivatives appropriately functionalized to interact with the Spike protein could be exploited as inhibitors of the SARS-CoV-2 virus. This idea was based on the observation that the size of the **A** region (Figure 4) is comparable with that of a calix[4]arene, and on the previous studies that successfully reported calixarene ligands able to bind to protein surfaces and disrupt medically relevant protein-protein interactions.[22–24]Thanks to the possibility of functionalizing the calix[4]arene upper rim with amino acids,[25,26] in fact, we could obtain compounds that display some of the residues that ACE2 employs to interact with the Spike protein's RBM. If these new ligands established sufficiently strong interaction with the Spike protein, it might be possible to prevent the formation of the ACE2 - S-RBM complex and thus inhibit the virus' ability to enter the cell, blocking viral infection.

This chapter reports our work aimed at obtaining new calix[4]arenes functionalized with amino acids (peptidocalix[4]arenes) that could be active as SARS-CoV-2 inhibitors. The project was organized in three phases:

(i) A molecular modelling study aimed at identifying the best inhibitors according to a molecular docking analysis;
(ii) The synthesis of the designed compounds;
(iii) The screening of the ligands through viral inhibition tests.

2. RESULTS AND DISCUSSION

2.1 Molecular modelling

2.1.1 Ligands design

The ligand's design was based on the structure of the complex between the ACE2 receptor and the RBD of SARS-CoV-2 obtained by X-ray diffraction by the research

group of prof. Qiang Zhou and colleagues (PDB 6M17).[18] The area of the RBD directly involved in the formation of the complex with the ACE2 receptor is called Receptor Binding Motif (RBM). Observing the relative position of the two protein domains (Figure 5), it is clear how the greatest number of interactions are located in the region indicated as **A**. This region is characterized by the presence of a series of hydrogen bonds between residues of the two proteins, as described above. It was therefore considered interesting to test what effect the presence of a ligand capable of inhibiting the formation of such interactions might have on the virus' ability to bind to ACE2.

The amino acids of ACE2 involved in the complex having a net charge or high polarity (Lys, Arg and Gln) were identified as the most promising binding groups to be attached to the calixarene scaffold. This list of amino acids was expanded with Asn, to test the possible effect of the side-chain length variation, and with Asp and Glu, to see how the presence of negative charges could affect the ligands' binding properties. For synthetic reasons, we decided to study calixarenes functionalized with two pairs of the same amino acids. In fact, a calixarene ligand bearing at the upper rim four different amino acids, even if very interesting, would have been very difficult to produce. As a first step, we reasoned about derivatives in which the amino acid units are all linked to the calixarene platform by amide bonds between their α-COOH group and NH_2 groups at the upper rim of the macrocycle (called **C-linked** derivatives, Figure 6a). The selected pairs of amino acids could be linked either in distal (1,3 and 2,4) or vicinal (1,2 and 3,4) position.

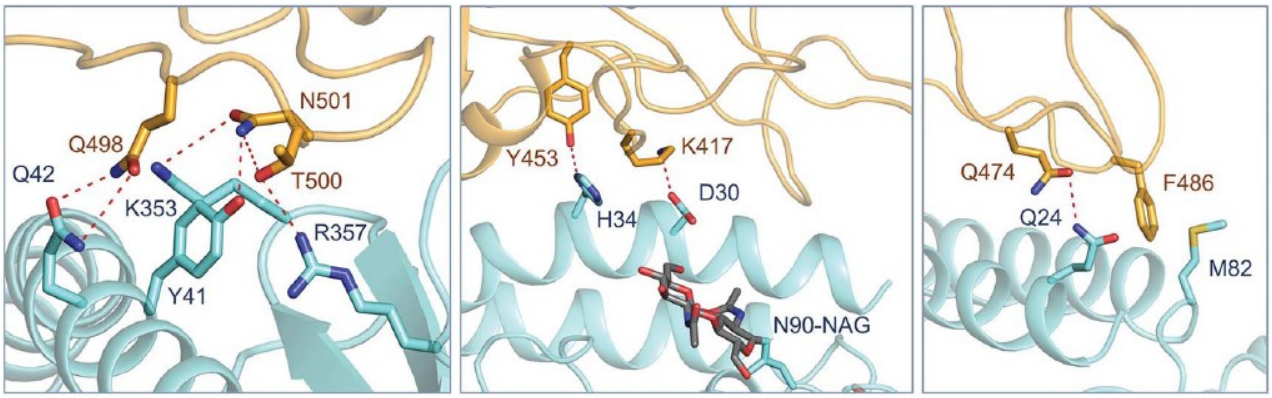

Figure 5: Details of the structure of the ACE2 - Spike-RBM complex relative to the most significant contact points between ACE2 (in blue) and the Sars-CoV-2 RBM (in yellow) (Image adapted from Ref. 18).

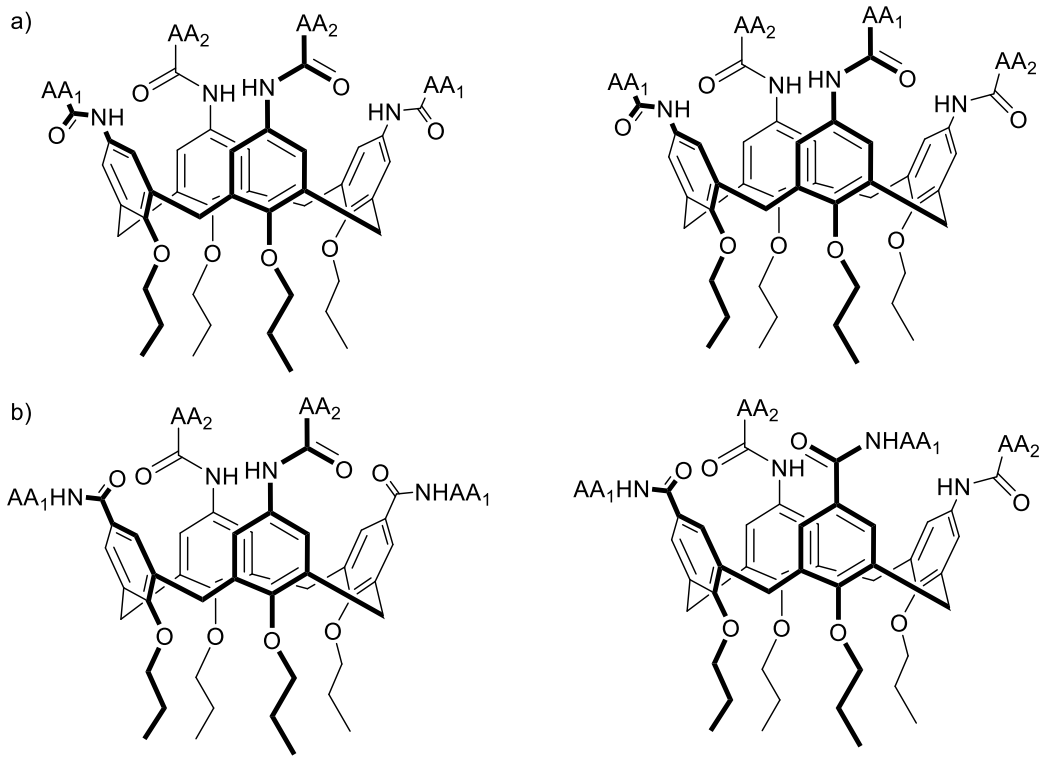

*Figure 6: Generic structure of two peptidocalixarenes (**a**) **C-linked** and (**b**) **C,N-linked**, respectively functionalized with two different amino acids in distal (left) and vicinal (right) position.*

In a second step, we considered derivatives in which two amino acid units are linked to the calixarene via their α-COOH group, like the previous ones, and the other two through their α-NH_2 groups (called **C,N-linked**, Figure6b). Also in this case, both the distal (1,3 and 2,4) and vicinal (1,2 and 3,4) disposition of the amino acid pairs could be explored.

Having established the possible functionalization of the calixarene upper rim, during the computational studies the lower one was considered alkylated with simple methyl groups to avoid wasting computing power in minimizing the conformations of longer chains that, in fact, are not involved in the interaction process examined. For the real compounds, however, it was foreseen that propyl or ethoxyethyl chains would be employed to lock the calixarene scaffold in the cone geometry. We selected this configuration for our ligands, because it projects the amino acid residues towards a common region of space resulting in the best arrangement to interact with the Spike protein's RBD.

Spartan Wavefunction software was used to calculate the energy and fundamental-state equilibrium geometry of the free ligands. The calculation setup used, based on the DFT

Technique, with the B3LYP method and the 6-31G* basis set, is a good compromise between accuracy and time required to complete the task. The calculation was carried out in vacuum not considering the solvent's effects, which certainly is a limitation and a significant approximation, but considering these aspects too would have required too much computing power for our setup. The free amino and carboxylic acid functional groups present on the amino acid side chains were considered in ionic form (NH_2 as NH_3^+ and COOH as COO^-).

2.1.1 Ligands virtual screening

2.1.1.1 C-linked peptidocalixarenes

We therefore started by analyzing derivatives with four amino acid residues linked through their carboxyl group. Due to the reduced computing power at our disposal, to shorten processing time we did not minimize the ligand structures having all the possible amino acid pairs we had selected, but only those in which at least one of the two residues was Lys or Arg (Table 2), since these amino acids are involved in half of the interactions in the **A**-region. The equilibrium geometries of two ligands (**SI1** and **SI9**) are reported in figure 7 as a representative example.

*Table 2: List of the various **C-linked** ligands screened, showing amino acid arrangement and total charge; SI = Spike Inhibitor; K = Lys; Q = Gln; R = Arg; N = Asn; D = Asp; E = Glu. E.g.: KQKQ means that the amino acids in the same pair are in distal position 1,3 and 2,4. KKQQ, suggests instead that they are in vicinal positions 1,2 and 3,4.*

Ligand	Amino Acids	Total Charge
SI1	KQKQ	6
SI2	KKQQ	6
SI3	RQRQ	6
SI4	RRQQ	6
SI5	KEKE	4
SI6	KKEE	4
SI7	RERE	4
SI8	RREE	4
SI9	KDKD	4
SI10	KKDD	4
SI11	RDRD	4
SI12	RRDD	4
SI13	KNKN	6
SI14	KKNN	6
SI15	RNRN	6
SI16	RRNN	6
SI17	KRKR	8
SI18	KKRR	8

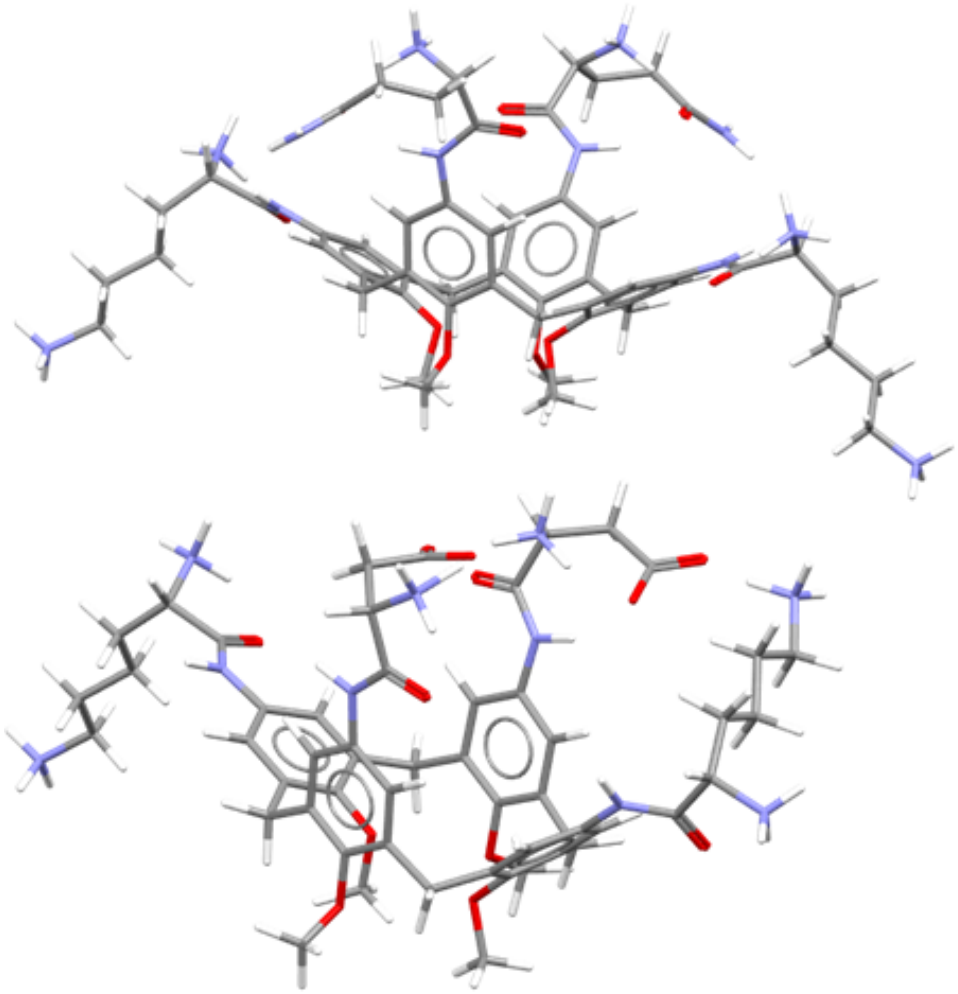

*Figure 7: Equilibrium geometries of **SI1** (above), with two units of Lys and two of Gln at positions 1,3 and 2,4 of the upper rim, respectively, and **SI9** (below), with two units of Lys and two of Asp at the same positions. Images generated with Mercury.*

Once the equilibrium geometries of the potential ligands had been calculated, molecular docking studies were carried out on the RBD of the Spike protein using the AutoDock Vina[27] software, with which all the images below have been generated. The structure of the RBD on which the study was performed was extracted from that of its complex with ACE2 (PDB 6M17).

Before carrying out the calculations, certain parameters and constraints had to be set. The molecular target (RBD) on which the docking would be performed was considered to have a rigid structure, with no bond's rotational freedom. For the ligands, on the other hand, rotational freedom was allowed around the simple bonds of the amino acid parts, while all the other bonds were considered as frozen. As a final step, it was needed to set the region of the protein in which to study the interactions possibly established with the ligand. For this purpose, the region shown in Figure 8a was chosen. This is

larger than region **A** (Figure 5) as it must be able to accommodate the peptidocalixarenic ligand and allow its movement. Subsequently, the area of the RBD explored was extended to the entire region involved in the formation of the complex with the ACE2 receptor (Figure 8b). This was done to see if the ligands studied were more likely to bind in another portion of the RBM itself. The calculations were repeated to check the reproducibility and reliability of the results obtained, which are reported in table 3. The output values represent, for each case, the binding affinity expressed in Kcal/mol. The more negative this value is, the more stable and stronger is the interaction between the ligand and the protein. Unfortunately, the program does not consider the possibility of exchange between the two 'pinched cone' conformations of the calixarene, so it was not possible to determine how much this conformational interconversion could affect the ligands' ability to complex the RBM. At the same time, the program does not allow the phenol rings of the calixarene to rotate around the methylene bridge bonds and thus change the scaffold conformation. This program-imposed limitation was not a problem since we were interested in studying the properties of these ligands locked in the cone conformation, since this is the real ligands' geometry.

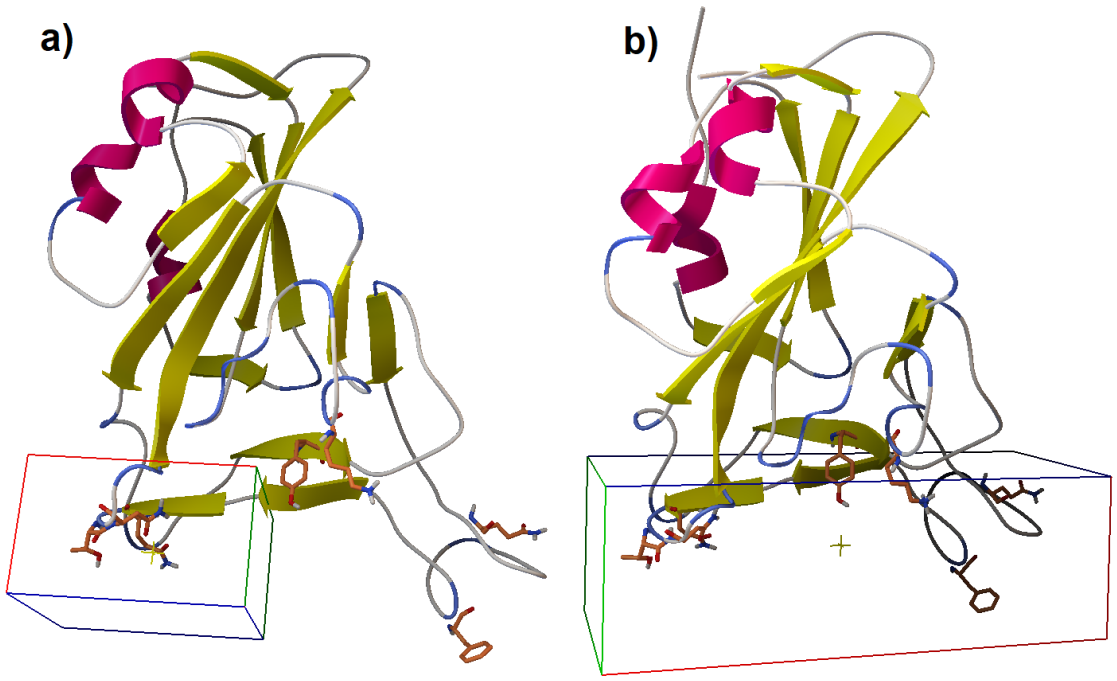

Figure 8: Selected grids for docking: (a) the one set for exploring region A; (b) the one set for exploring the entire Receptor Binding Motif (RBM) and ACE2 interaction zone

Table 3: Molecular docking results on SARS-CoV-2's RBM for C-linked ligands; affinity expressed as arithmetic mean; colors correspond to ligands in Figure 10

Ligands	Amino Acids	Binding Affinity (kcal/mol)	
		BOX1 (Fig. 11a)	BOX2 (Fig. 11b)
SI1	KQKQ	-6.2	-6.3
SI2	KKQQ	-6.0	-6.0
SI3	RQRQ	**-6.9**	-6.5
SI4	RRQQ	**-6.7**	**-7.0**
SI5	KEKE	-6.2	-6.6
SI6	KKEE	-6.0	-6.1
SI7	RERE	**-6.9**	**-6.8**
SI8	RREE	-6.4	-6.6
SI9	KDKD	-6.0	-6.0
SI10	KKDD	-5.5	-5.4
SI11	RDRD	-5.6	**-6.8**
SI12	RRDD	-6.2	-6.2
SI13	KNKN	-5.6	-6.1
SI14	KKNN	-5.9	-6.1
SI15	RNRN	-6.3	**-6.9**
SI16	RRNN	-6.7	-6.7
SI17	KRKR	-6.7	-6.5
SI18	KKRR	-6.1	-6.3

All the complexes resulting from the calculations have been carefully analyzed to identify the most significant interactions. For example, complex **SI1**, between the peptidocalixarene containing two Lys and two Gln units (KQKQ) and the **A** region of the RBM (Figure 9), although less stable than others, is interesting because the peptidocalixarene is able to form a network of hydrogen bonds including, among others (Arg403, Tyr 453, Gly502 and Tyr505), also residues Thr500 and Asn501 (Figure 9b),

which are some of the most significant amino acids directly involved in forming the complex with ACE2.

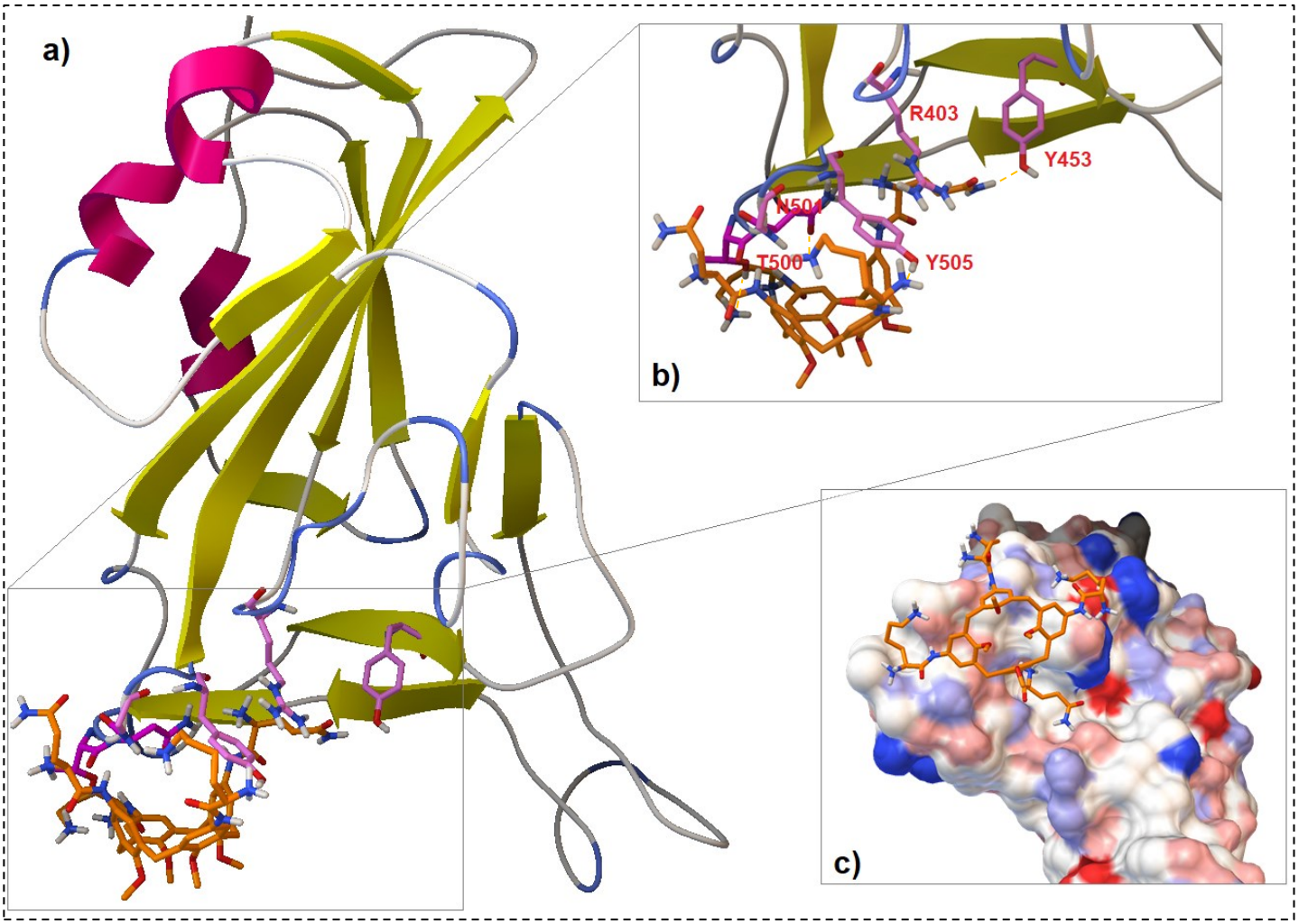

*Figure 9: (a) Complex between the **SI1** ligand and the RBD of the Spike protein obtained by docking; (b) detail of SI1-RBD interactions; (c) overlap with the protein's electronic density surface.*

Furthermore, we can see how the ligand tends to adapt its shape to the protein's surface, arranging the binding groups so that they have complementary charge/polarity to the protein ones (Figure 9c) masking the region of the RBM that interacts the most with ACE2.

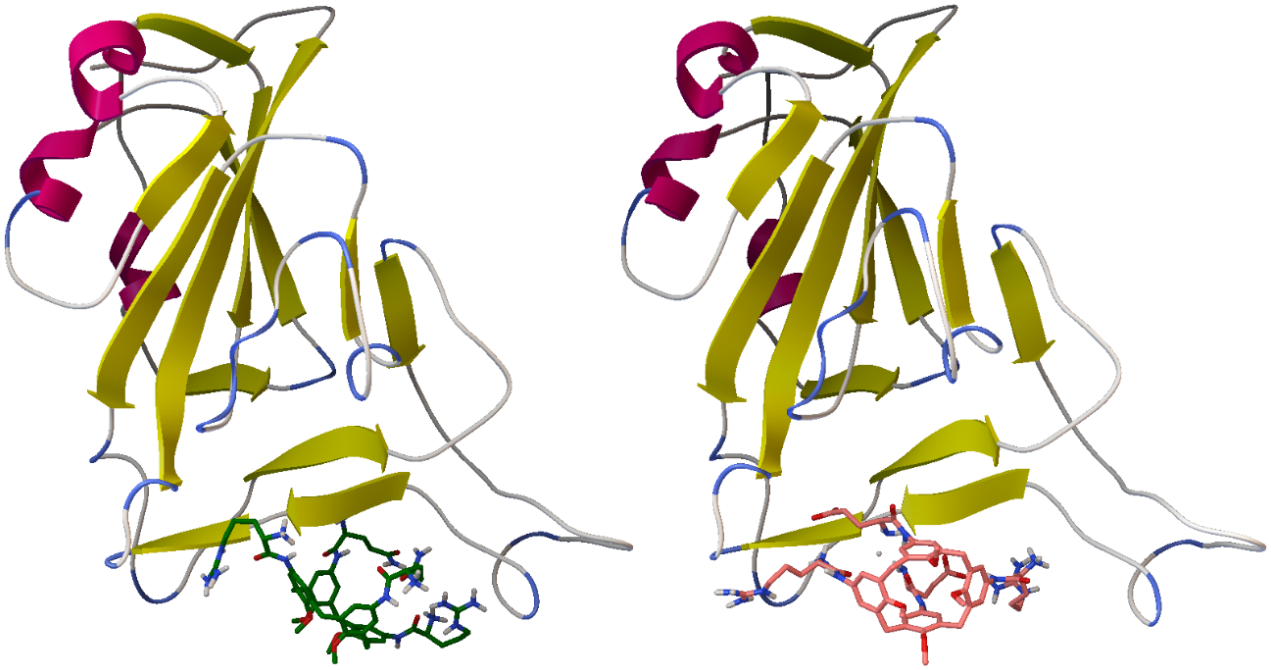

Figure 10: Structure of the complexes obtained by molecular docking between the A zone of the RBM (BOX1) and separately the ligand SI3 (left) and SI7 (right).

The best ligands, however, considering only the BOX1 region, are **SI3** and **SI7**. Both contain Arg and have respectively Gln and Glu as their second amino acid. In both ligands these amino acids occupy the distal positions (**SI3**: RQRQ and **SI7**: RERE). Despite these ligands place the macrocycle between the **A** and **B** region of RBM, they also extend their amino acid substituents to make interactions with some target residues in the **A** zone (Figure 10). Specifically, **SI3** forms interactions with residues Glu484, Gly485, Cys488, Gln493, Gln498 and Asn501, while **SI7** forms a complex with the protein by non-covalently binding residues Glu484, Gln493, Gly496, Thr500, Asn501 and Tyr505. However, once the explored protein region has been extended to the entire RBM (BOX2), the ligand with the highest binding affinity becomes **SI4**, which exposes two Arg units at position 1,2 and two Gln units at position 3,4 (RRQQ). The other ligands found to be slightly less efficient (**SI7**, **SI11**, **SI15**) all have in common with **SI4** the presence of the two Arg units. It can therefore be assumed that this amino acid forms the strongest interactions with the receptor. A detail that stands out is how **SI4** is the only ligand with substituents placed in vicinal position with higher affinity than its analogue with the same amino acids but arranged in the distal positions.

The structure of the complex that **SI4** forms with RBM is shown in Figure 11. The calixarene derivative, surprisingly, is not located in the **A** region of the RBM, where ACE2 establishes the most hydrogen bonds. The ligand forms a hydrogen bond with only one of the residues identified among those involved in the interaction with ACE2, i.e. with Gln498. In contrast, **SI4** establishes a network of hydrogen bonds and ionic interactions

with several RBM residues (Figure 11b), with both the side chains and with the polypeptide skeleton. The RBM residues involved in the interactions are Arg403, Glu484, Cys488, Phe490, Leu492 and Gln498, while the ligand exploits both its ammonium groups and the side chains of each amino acid. Furthermore, observing how the calixarene is arranged with respect to the electron density surface (Figure 11c), it can be seen how its shape adapts to the surface arranging the binding groups in such a way to have complementary charges/polarities with those present on the receptor.

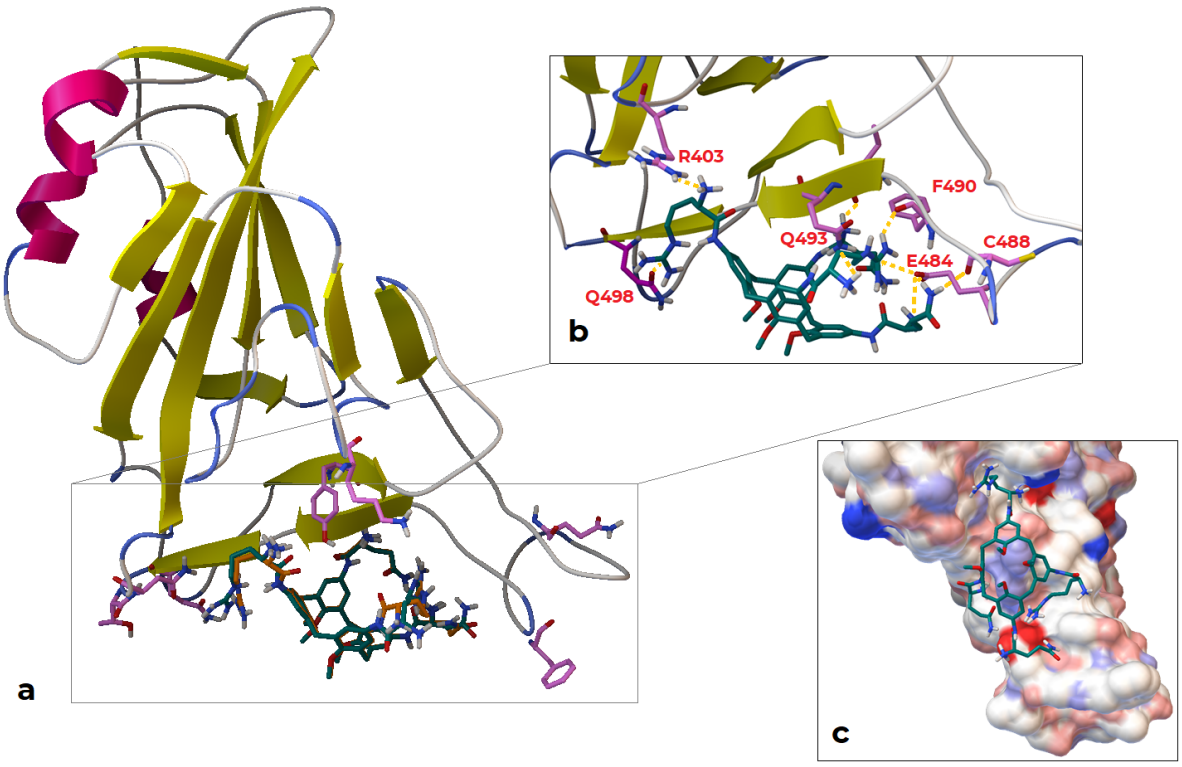

Figure 11: (a) Complex between SI4 ligand and RBM of protein S, obtained by molecular docking; (b) detail of SI4-RBM interactions; (c) overlap with the electronic density surface of the protein receptor.

To check whether there are other regions of the RBD with which the **SI4** ligand could establish more favorable interactions, the entire surface of the RBD was explored. The protein surface was separated into two grids to be able to perform the calculations due to the limitations of the program (Figure 12). Again, the calculations were repeated several times to confirm their reliability.

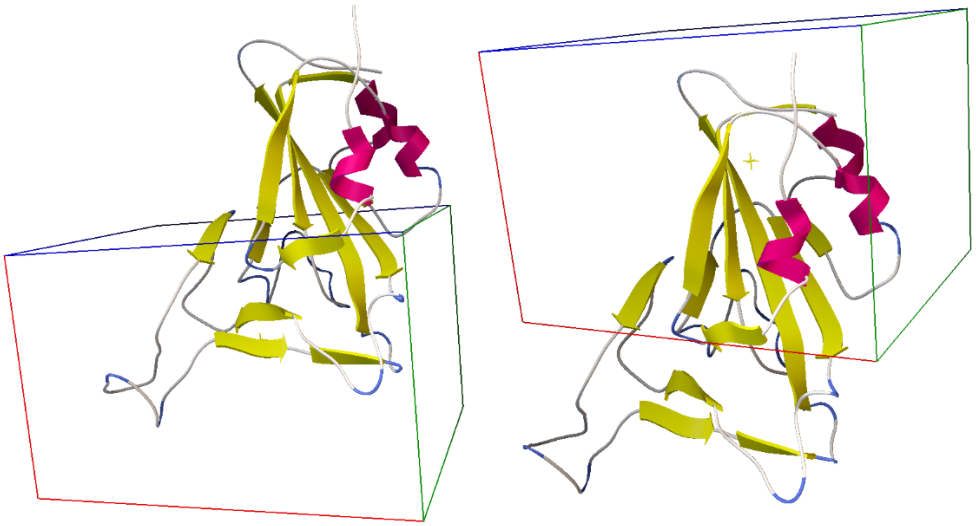

Figure 12: Grids used for the total exploration of the RBD.

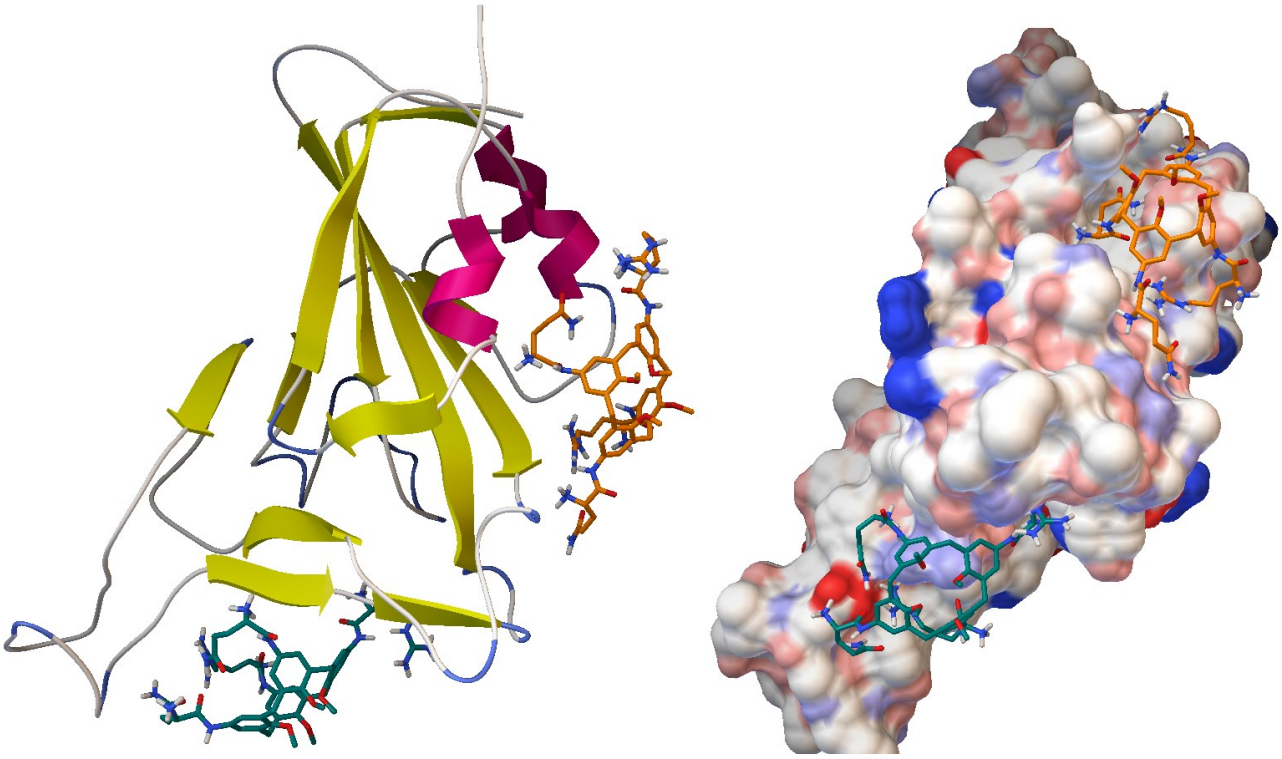

*Figure 13: Structure of the complex between **SI4** and the entire RBD obtained from docking studies for ligand selectivity control; (left) representation of the secondary structure and (right) of the electron density surface.*

From the results (Figure 13), it is possible to observe that the **SI4** ligand tends to interact with the protein in two regions, with equal binding affinities for both. The former is the one seen above, within the RBD, while the latter is not part of the area involved in the interaction with ACE2. This could clearly be a disadvantage, as it would prevent 50% of

the ligand to give the interaction, we considered effective for the inhibition of the formation of the ACE2-protein S complex. Therefore, to obtain the same results, higher concentrations of calixarene would be required. At the same time, however, we cannot exclude the fact that, although not binding to the protein's region of interest, the ligand could have an indirect inhibitory activity through allosteric effects on the RBD.

2.1.1.2 C,N-linked peptidocalixarenes

As a representative of the **C,N-linked** class (Figure 6) we considered ligand **FERSI**. In this compound, two Arg units are C-linked in two distal positions on the upper rim of the calixarene, and two Asn units are N-linked in the other distal positions. The results of the molecular docking on the RBD (Figure 14a) were compared with those of the corresponding C-linked ligand, **SI15**, from the first series (Figure 14b). In addition, given the large number of possible intramolecular interactions in **FERSI**, the corresponding analogue in which the two α-carboxyl groups of the Asn units are in the form of methyl ester (**FERSIM**, Figure 14c) was also studied. Both equilibrium geometries and molecular docking calculations, limited this time to BOX1, were performed using the same virtual screening parameters as before.

a) FERSI	
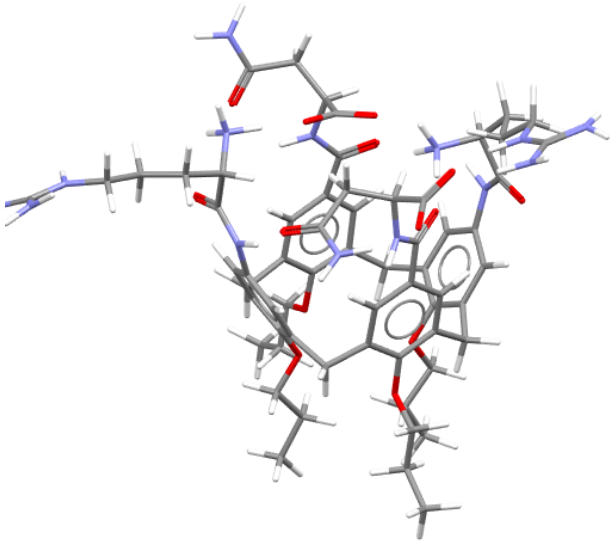	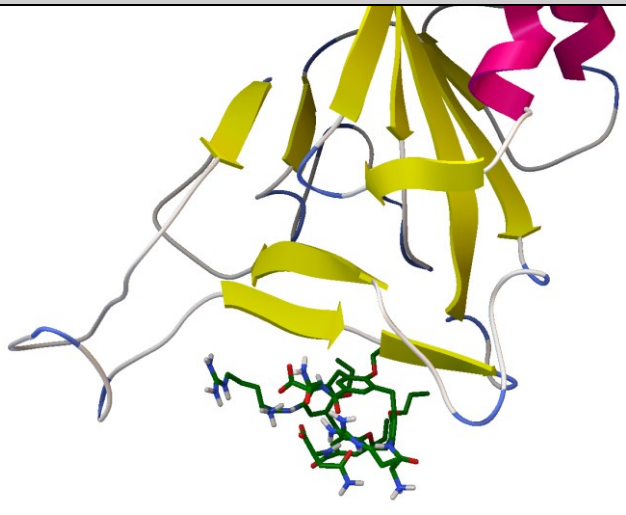
	Binding affinity =-5.4 kcal/mol

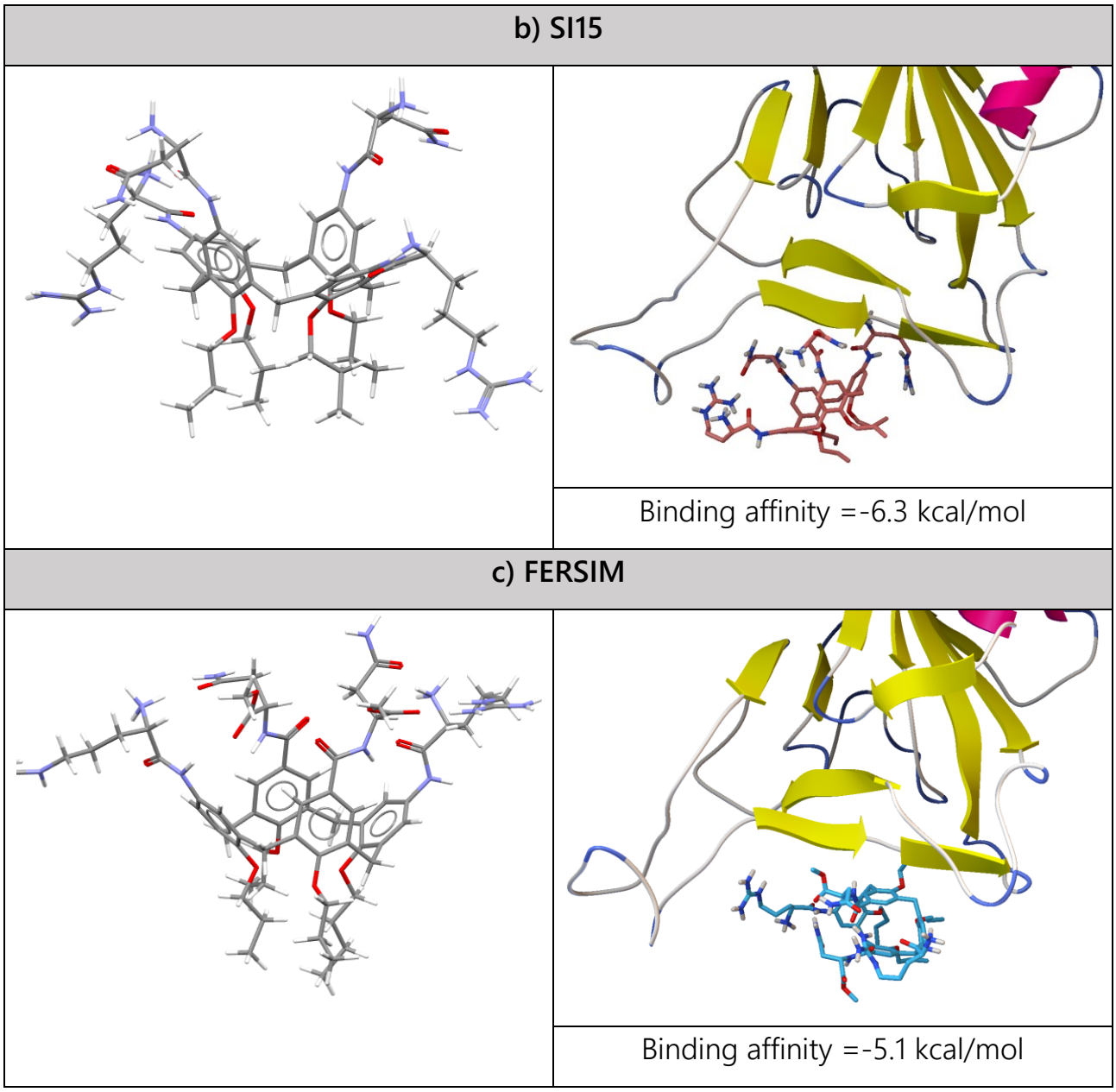

Figure 14: Equilibrium geometries and ligand-RBM complexes obtained from molecular modelling calculations on (a) FERSI, (b) SI15 and (c) FERSIM.

The results show how indeed the presence of intramolecular interactions (ionic pairs and hydrogen bonds) between the amino acids present on the upper rim of **FERSI** reduce its binding ability compared to its C-linked analogue. In fact, the docking output shows that the ligand does not use all the binding groups for the receptor complexation, unlike the C-linked analogue **SI15**. Therefore, while **FERSI** manages to interact with only three residues (Tyr449, Glu484, Gln493), the **SI15** analogue forms a more extensive network of interactions (Tyr449, Glu484, Gly485, Cys488, Gln493, Ser494). Carboxylate methylation (**FERSIM**) does not weaken the intramolecular interactions and consequently no improvement in the binding energy is seen by docking on the RBD with **FERSIM** compared to **FERSI**.

Finally, molecular modelling calculations were performed for two additional C,N-linked potential ligands, in which the amino acids Lys, Gln, Gly and Arg for the former (**CSI1**) and Lys, Glu, Gly and Arg for the latter (**CSI2**) form a small peptide loop, bridged between two distal positions on the upper rim (Figure 15). In this case, we wanted to study how a completely different spatial disposition of the binding units could affect the overall affinity of the ligands.

a) CSI1

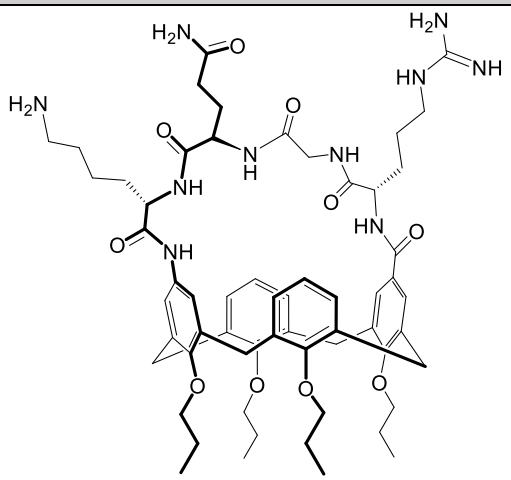

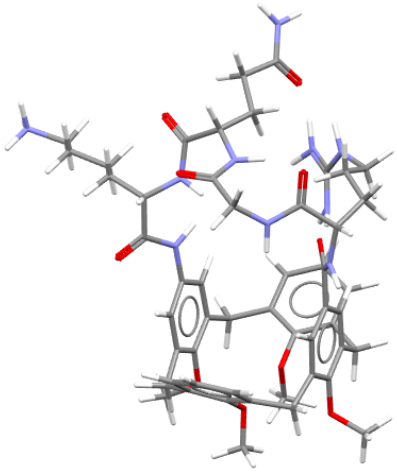

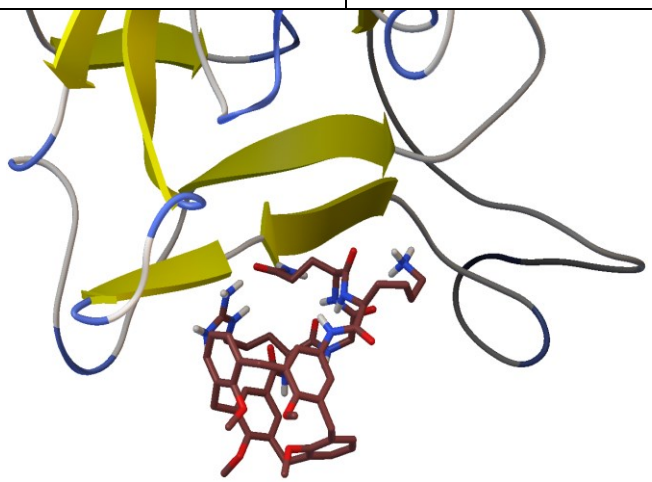

Binding affinity = -5.6 kcal/mol

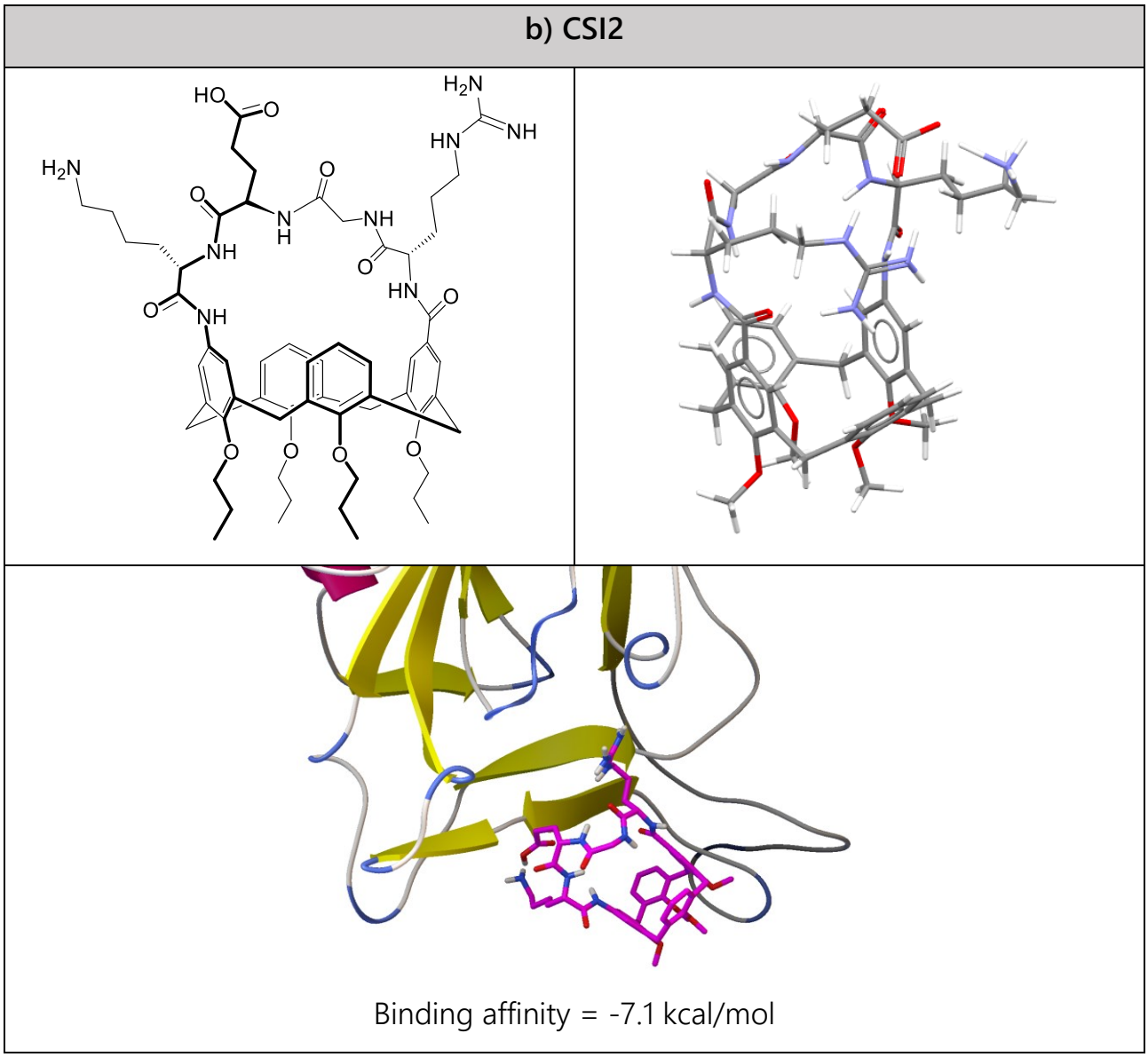

*Figure 15: Structure, equilibrium geometry and ligand-RBM complexes obtained from modelling calculations molecular modelling on macrobicyclic ligands (a) **CSI1**, (b) **CSI2**.*

The result shows that these macrocyclic C,N-linked peptidocalixarenes are arranged with the lipophilic calixarene scaffold oriented towards, but not too close, the protein surface, as in the case of **FERSIM**, while still managing to exploit all the residues to form a complex with the receptor. In particular, the second ligand tested (**CSI2**), has a very good binding affinity and could therefore be used as an RBD inhibitor of the Spike protein. However, due to time restrains we decided not to focus our synthetic efforts on these types of compounds.

2.2 Ligands synthesis

Encouraged by the molecular docking results, we decided to undertake the synthesis of a few C-linked and C,N-linked peptidocalixarenes to test if they could indeed act as ligands for the Spike protein. As a preliminary step, we spent some time on a careful design of the target compounds. We had to take into account both (i) the functionalization of the calixarene scaffold with proper anchoring groups for the amino acids and (ii) the choice of the amino acid pairs. Regarding (i), the introduction of amino and carboxylic acid groups on different positions of the upper rim of a calix[4]arene was well consolidated in the group[28] and did not represent a limitation in the design of the ligands. On the contrary, the choice of amino acids to be used as binding units (ii) had to be dictated not only by the results of the *in silico* studies, but also by both synthetic considerations and by the availability of suitably protected amino acid reagents in the laboratory. This, however, was not considered a significant obstacle, since the docking studies had shown that even peptidocalixarenes that gave lower binding affinity could interact, in the A-zone, with the RBM site involved in the binding with ACE2 and could be viable candidates for studies of inhibition of SARS-CoV-2 infectivity.

2.2.1 C,N-linked ligands

On this type of derivatives, our research group already had experience.[29] Based on the availability of amino acids with the appropriate protecting groups, it was decided to prepare compounds **10** and **11** (Figure 17), where the calixarene scaffold is functionalized with two pairs of Lys and Gln. Lys was chosen instead of Arg, despite the calculations showed how the latter is the amino acid capable of giving the best ligands, because Lys too has a positive charge on the side chain, but, unlike Arg, does not give rise to parasite reactions, such as intramolecular cyclization of the amino acid itself, during the coupling step.

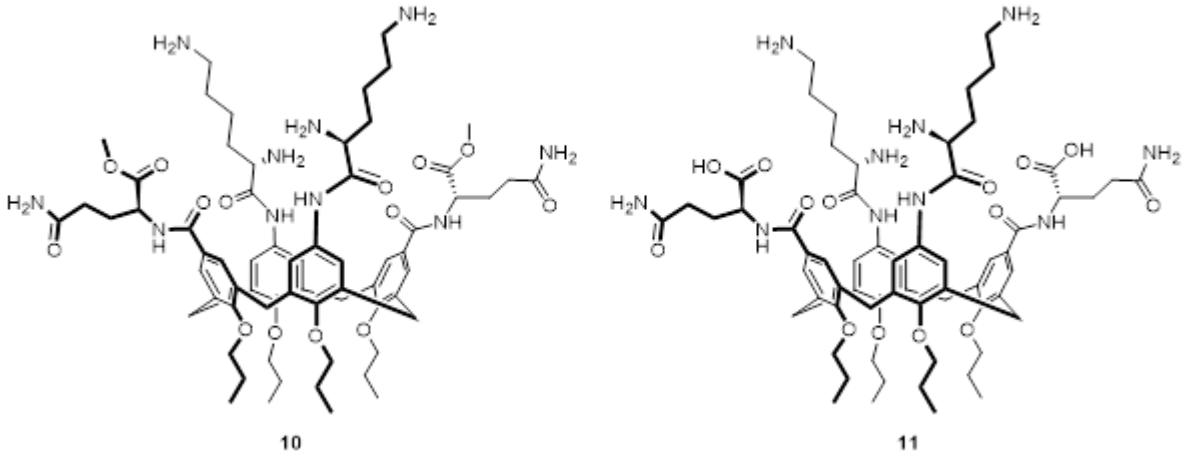

Figure 17: The two distal C,N-linked ligands synthetized

The two compounds, **10** and **11**, differ from each other by the methyl ester group present on the Gln units of **10**. We considered interesting to compare the binding properties of these ligands that, despite having a very similar structure, differ in the overall charge (+4 for compound **10** and +2 for compound **11**, at physiological pH).

2.2.1.1 Calix[4]arene scaffold preparation

The diamino-diacid calixarene **5**, on which the two pairs of amino acids had to be anchored to obtain the desired distal C,N-peptidocalixarenes, was synthesized following a literature procedure as reported in scheme 1.[29]

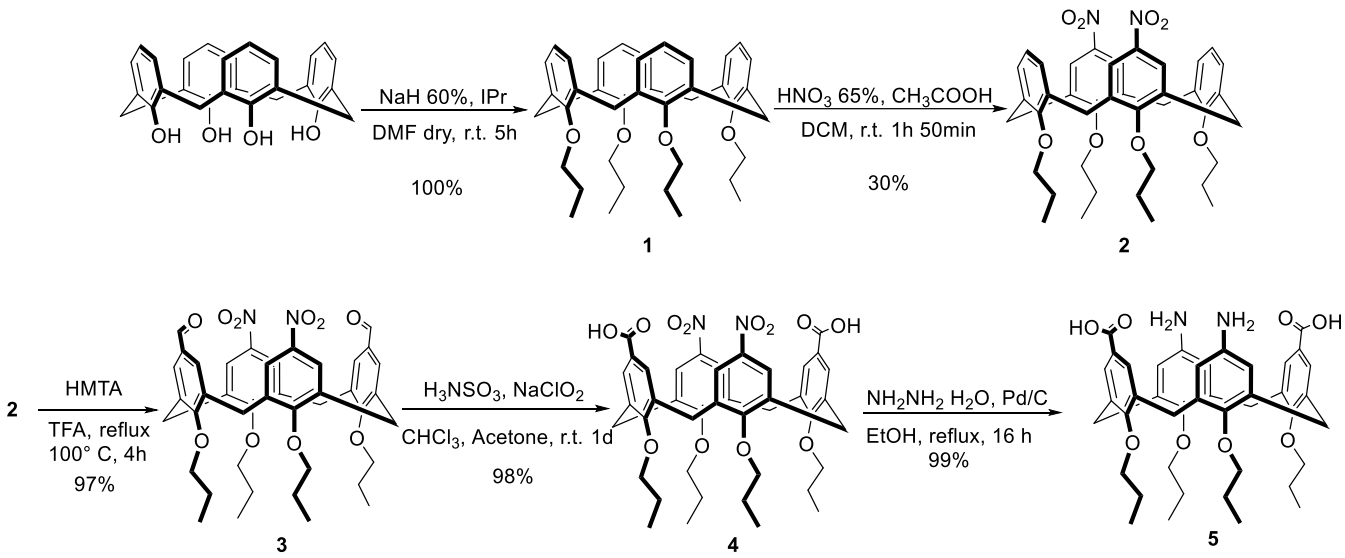

*Scheme 1: Synthesis of compound **5**.*

The synthetic steps to **5** involved alkylation of the calix[4]arene lower rim with propyl chains, followed by nitration of the 1,3-distal positions of the upper rim and formylation of the remaining upper rim positions to obtain intermediate **3**. Oxidation of the aldehyde groups to carboxylic acids and reduction of the nitro groups to amines yielded compound **5**. All the reactions proceeded with very high yields except the nitration step leading to **2**. This reaction was carried out with a mixture of nitric acid and glacial acetic acid. It required continuous monitoring by TLC, as it needed to be quenched quickly when the maximum amount of species carrying two nitro groups (in both 1,3 and 1,2 positions), as opposed to mono-, tri- and tetranitro, was reached. Therefore, the reaction, although long established, was not totally reproducible; moreover, while sometimes a precipitation with DCM and MeOH was enough to isolate **2**, most of the times it was required a chromatographic column to separate the desired product from the rest of the mixture.

Due to the poor reproducibility and difficulties in isolating the desired compound **2**, given by the inherent lack of regioselectivity during the nitration, it was decided to

pursue the synthesis of calixarene **2** following an interesting procedure reported in the literature.[30] In this paper, it is described how to enhance regiochemical control in the calixarene upper rim functionalization by exploiting the ability of the nosyl group to deactivate the position in para to the phenolic O to which it is linked. Subsequently, the nosyl can be removed by simple basic hydrolysis. Through this protection/deprotection procedure (generalized in scheme 2), it is therefore possible to obtain 1,3-disubstituted calixarene in high yields.

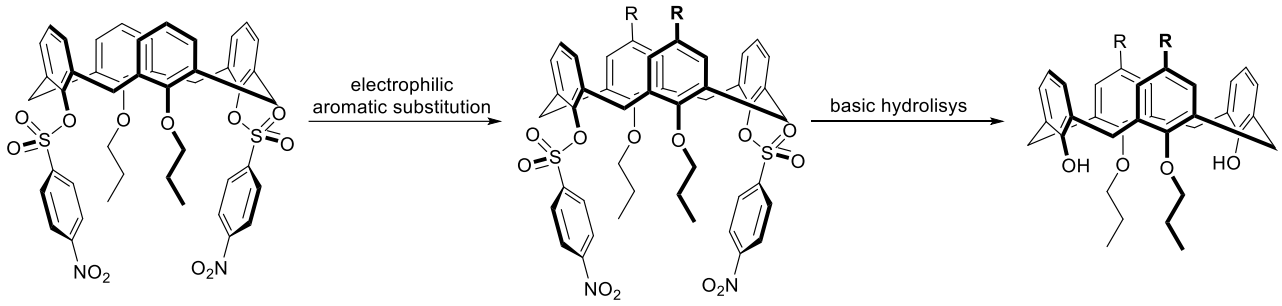

Scheme 2: Schematic synthesis of a 1,3-difunctionalized calix[4]arene.

The synthesis of compound **2** was therefore attempted according to Scheme 3. Compound **1d** was obtained in good yield from p-OH calix[4]arene in 4 steps starting with the alkylation of the distal positions of the lower rim with propyl groups followed by the protection of the two remaining phenolic OHs with the nosyl group and the subsequent nitration of the upper rim. Due to the deactivating ability of the electron-withdrawing nosyl group, indeed, the latter reaction yielded compound **1c** almost quantitatively.

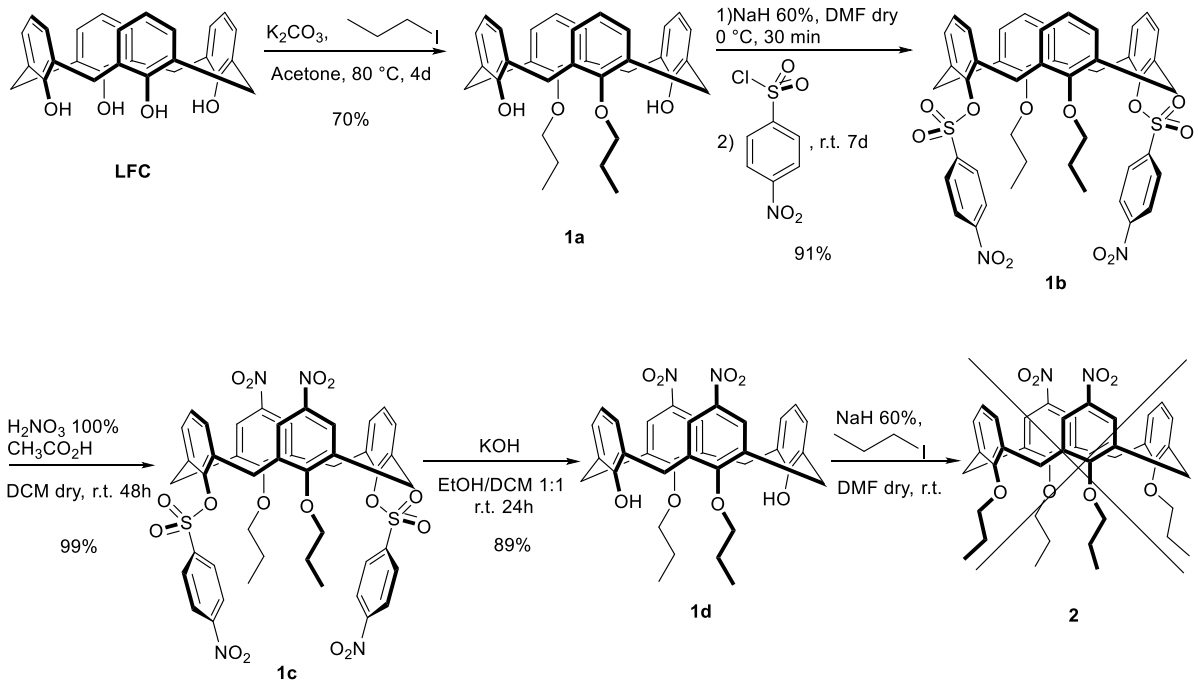

*Scheme 3: Alternative synthesis of **2**.*

Then, calixarene **1c** was deprotected from the nosyl group by hydrolysis with KOH. As reported in the literature,[30] confirmation that nitration occurred only on the positions para to the alkylated OH is deduced from the chemical shift of the phenol OH groups of **1d**. These indeed resonate at higher fields (7.96 ppm) than the ones of the analogous macrocycle with the nitro groups in para to the hydroxyls, which are affected by the electron-attracting effect of NO_2 and are therefore shifted to lower fields (9.44 ppm).

Finally, an attempt was made to alkylate **1d**. The reaction was conducted under standard conditions, using NaH as the base. The template effect of the Na^+ ions was supposed to keep the calixarene locked in the cone configuration. The research group already had experience with the alkylation of dinitro-dialkylcalix[4]arenes with the NO_2 groups para to the hydroxyls, where they had observed the inversion of the aromatic rings and the loss of the cone geometry. The same was not expected to happen during the alkylation of compound **1d**, given the lack of deactivating groups in para to the OHs, but, unexpectedly, a mixture of calixarenes with different conformations was obtained. ^{1}H NMR spectrum showed that in the mixture the cone derivative was only a minor compound (Figure 18). Unfortunately, it was not possible to separate the different calixarene isomers neither by precipitation/crystallization nor by chromatographic separation, as they all have the same elution coefficient.

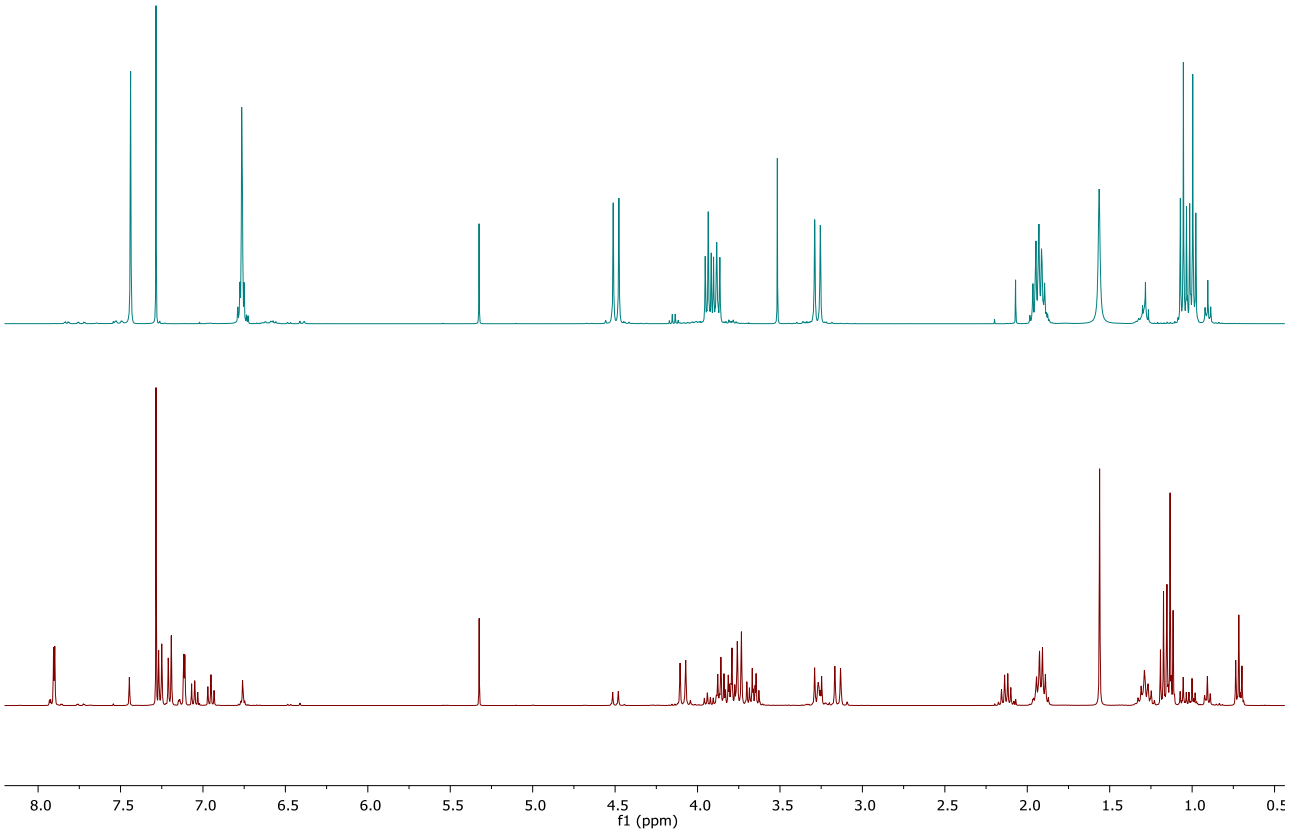

*Figure 18: ^{1}H NMR spectra ($CDCl_3$, 400 MHz) of compound **2** (top) and the mixture of products of the alkylation reaction of compound **1d** (bottom).*

Therefore, even if in theory this synthetic route was the most promising one, it was abandoned due to the difficulties described above.

2.2.1.2 Functionalisation of calixarene 5 with amino acid units

To obtain ligands **10** and **11** we tested several routes to functionalize the upper rim of calixarene **5** with amino acids.

First, an attempt was made to directly functionalize the amino groups of calixarene **5** with the Boc-protected Lys, using a coupling reagent to generate the reactive species in situ (Scheme 4). We tried to proceed without protecting the carboxylic groups of the macrocycle, hoping for a lower reactivity of these compared to those of the amino acid due to the greater steric hindrance that they experience. From evidence collected in the past, it was known about the impossibility of an intramolecular reaction between a carboxylic group and an amino group placed on two neighboring positions on the upper rim.

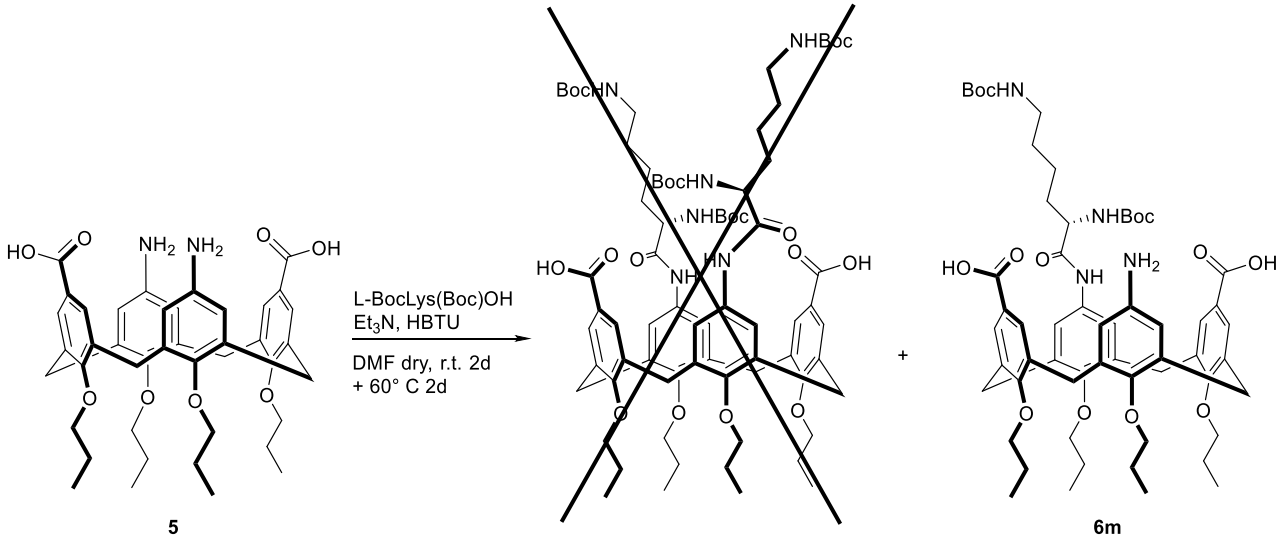

*Scheme 4: Reaction of **5** with L-BocLys(Boc)OH.*

A solution of calixarene **5** and NEt_3, needed to keep the two amines deprotonated, was slowly dripped into a flask containing a solution of Boc-L-Lys(Boc)OH and the coupling agent HBTU, 4 equivalents each. In this way, the amino acid should already be activated upon addition of the calixarene to the reaction flask and the uronium salt should already have been depleted by its reaction with the amino acid, thus excluding the even partial activation of the carboxyl groups of **5** and avoiding side reactions.

An analysis by mass spectrometry of the reaction mixture after 24 hours, however, showed that the crude's main component was the mono-functionalized species accompanied by traces of the desired product but also by secondary products of

calixarene dimerization (dimer, dimer + amino acid). This result revealed a considerable difficulty for the second amino acid to bind to the calixarene and also, albeit marginal, the possibility for a carboxyl group of **5** to be activated by residues of HBTU, evidently present, and react with the amino group of another calixarene molecule. Even trying to promote the formation of the di-functionalized product by heating the reaction to 60° C, did not improve the conversion.

The reaction was therefore quenched and the crude was reacted, considering it as if was mainly formed by the mono-functionalized calixarene **6m**, with the active ester of the same amino acid, previously obtained by condensating Boc-L-Lys(Boc)OH with N-hydroxysuccinimide, in the presence of EDC and DIEA (Scheme 5).

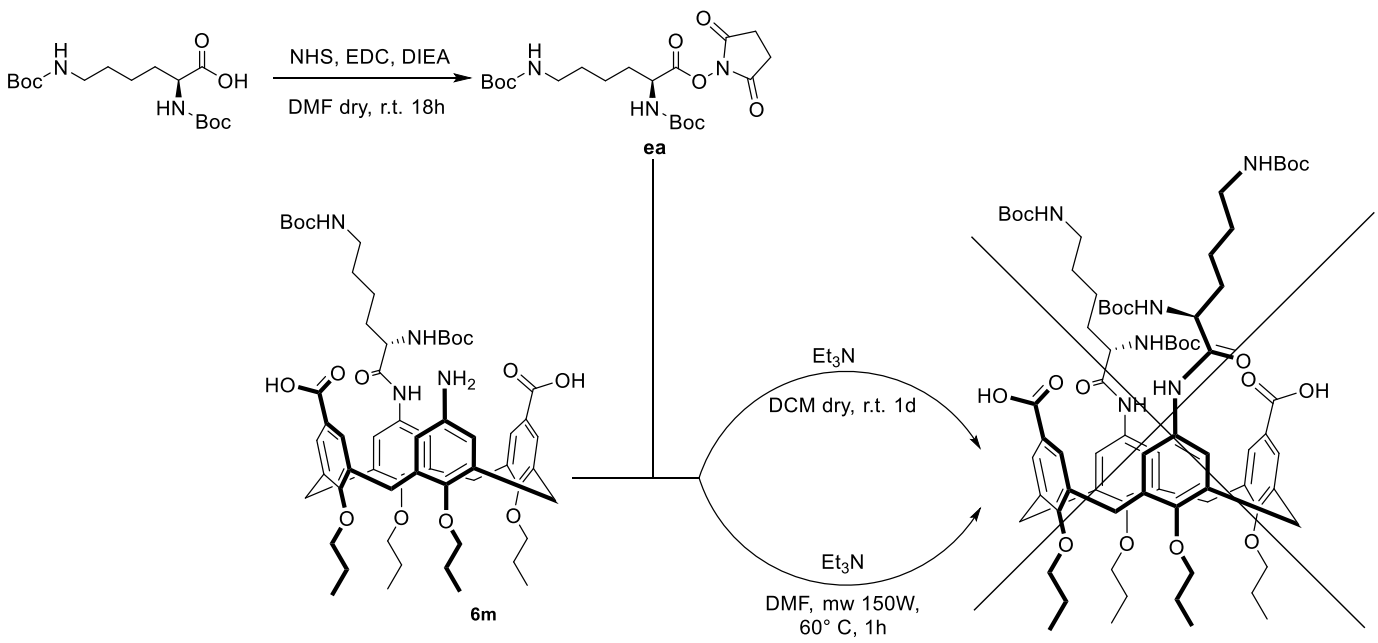

*Scheme 5: Attempt of reacting **6m**.*

With this variation, we wanted to avoid the reaction between calixarene units altogether, even though we knew that the hydroxysuccinimide ester is less reactive than the corresponding HBTU-activated specie. This aspect, considering the verified difficulty of condensing the second Lys unit with **5**, did not bode well for the success of the reaction. Indeed, both under standard conditions and with microwave mediation, the composition of the reaction mixture reaction remained unchanged from that isolated in the previous reaction. It seems, therefore, that it can be assumed that there are intrinsic problems in compound **5** that prevent its direct di-functionalization with the desired amino acid.

A similar process of direct functionalization on the calixarene carboxylic groups was not attempted either, because of the evidence described above. In fact, in this case the reaction between two different calixarene units would be even more favored, since it would be necessary to activate the carboxylic groups of **5**. We therefore decided to follow a synthetic route that had already been reported by our research group for the functionalization of **5** with different amino acids (Scheme 6) and that involves a preliminary step of protection of the calixarene amino groups.[29]

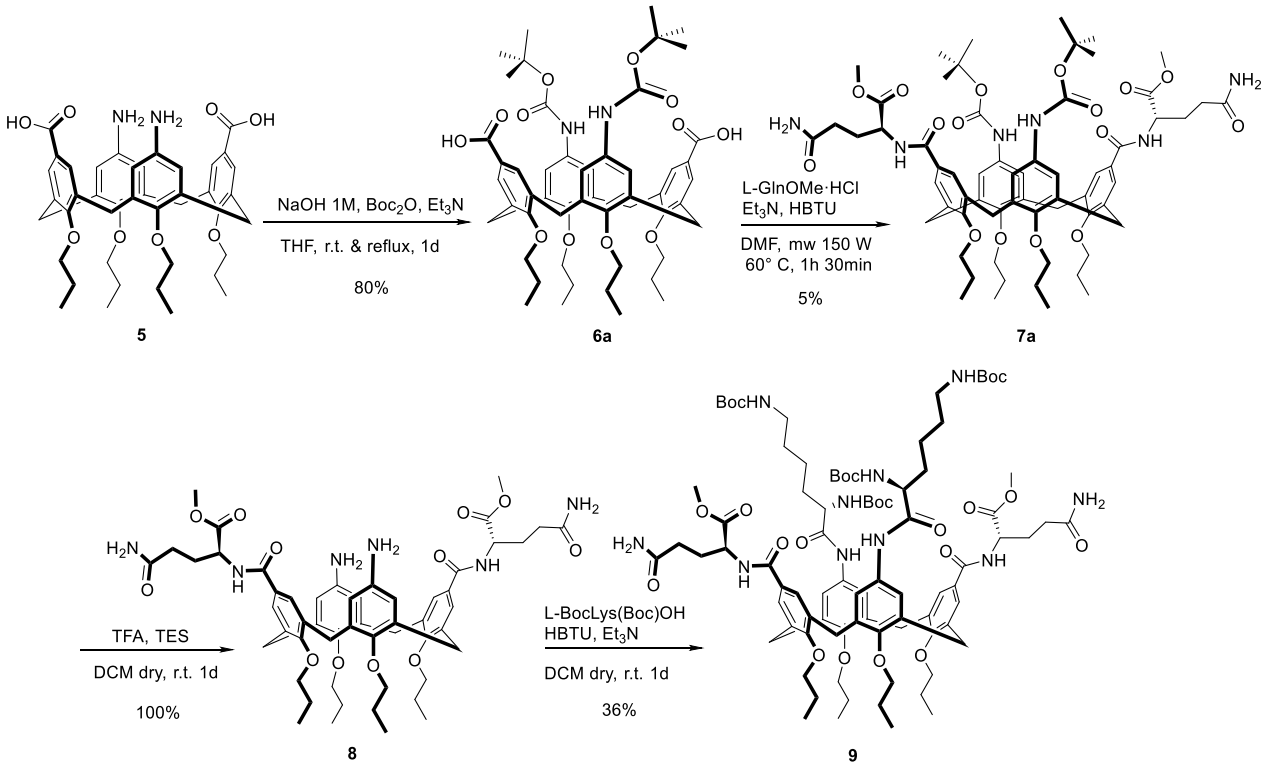

*Scheme 6: Reaction pathway for the synthesis of **9**.*

Compound **5** was thus reacted with di-tert-butyl dicarbonate in presence of aqueous NaOH. This step, however, gave reproducibility problems. The reaction was performed several times, but only once calixarene **6a** formed with a good purity, while the rest of the times it required a chromatographic separation on silica gel, which unfortunately resulted in the degradation of the majority of the product due to the detachment of the Boc groups caused by the acidic character of the stationary phase used. Protection with other groups (Cbz, Alloc and Trt) was then tried, but in these cases, predominant formation of the diprotected product was not observed. In fact, a mixture of mono-, di-, tri- and tetrafunctionalized products formed, leading to the conclusion that the carboxyl groups also reacted with the reagents used to introduce the protecting groups. Thus, the synthesis was carried on with the Boc protected calixarene **6a**.

The first coupling was performed with the aid of microwaves, reacting compound **6a** with L-Gln-OMe, HBTU and NEt_3 in DMF. This resulted in a very complex mixture, which had to be purified with several consecutive chromatographic separations (flash columns and preparative TLC) in order to isolate compound **7a**. The low yield of recovered product was attributed in part to the presence of impurities in reagent **6a**, but also to the fact that on this substrate the coupling reaction was not efficient enough, probably due to steric hindrance.

The Boc groups on calixarene **7a** were then removed by treatment with TFA in presence of TES, giving product **8**. The conjugation of the second amino acid was carried out under standard conditions (DCM anhydrous, room temperature), by adding to a solution of calixarene **8** the amino acid Boc-Lys(Boc)OH, NEt_3 and HBTU. A chromatographic separation with preparative TLC was required to isolate compound **9** in 36% yield.

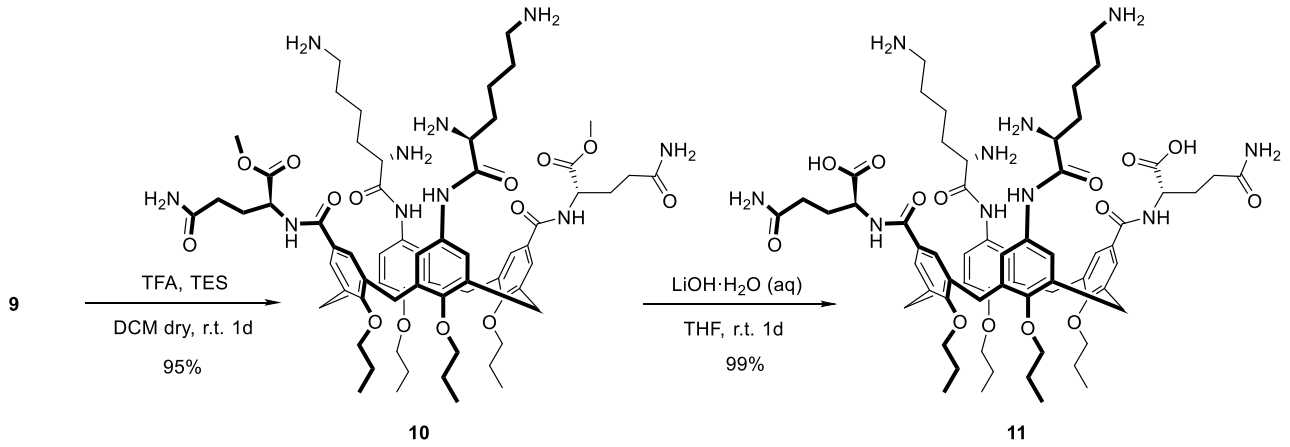

*Scheme 7: Deprotection of compound **9**.*

Ligand **10** was obtained by deprotecting derivative **9** from Boc and ligand **11** by hydrolyzing the methyl ester present at the α-position of Gln of **10** using a stoichiometric amount of aqueous LiOH (Scheme 7). This base was chosen because it is able to react with the ester groups but not with amides and also because it is known to minimize racemization. The final product was obtained as a lithium salt.

With the aim of searching for a higher-yield synthetic pathway to compounds **10** and **11**, we considered that the nitro groups of compound **4** could be exploited as amines protecting groups. Therefore, we tried to directly conjugate the first pair of amino acids onto this compound. We then reduced the NO_2 to NH_2 and resumed with the synthetic route followed previously to reach the final compounds **10** and **11** (Scheme 8).

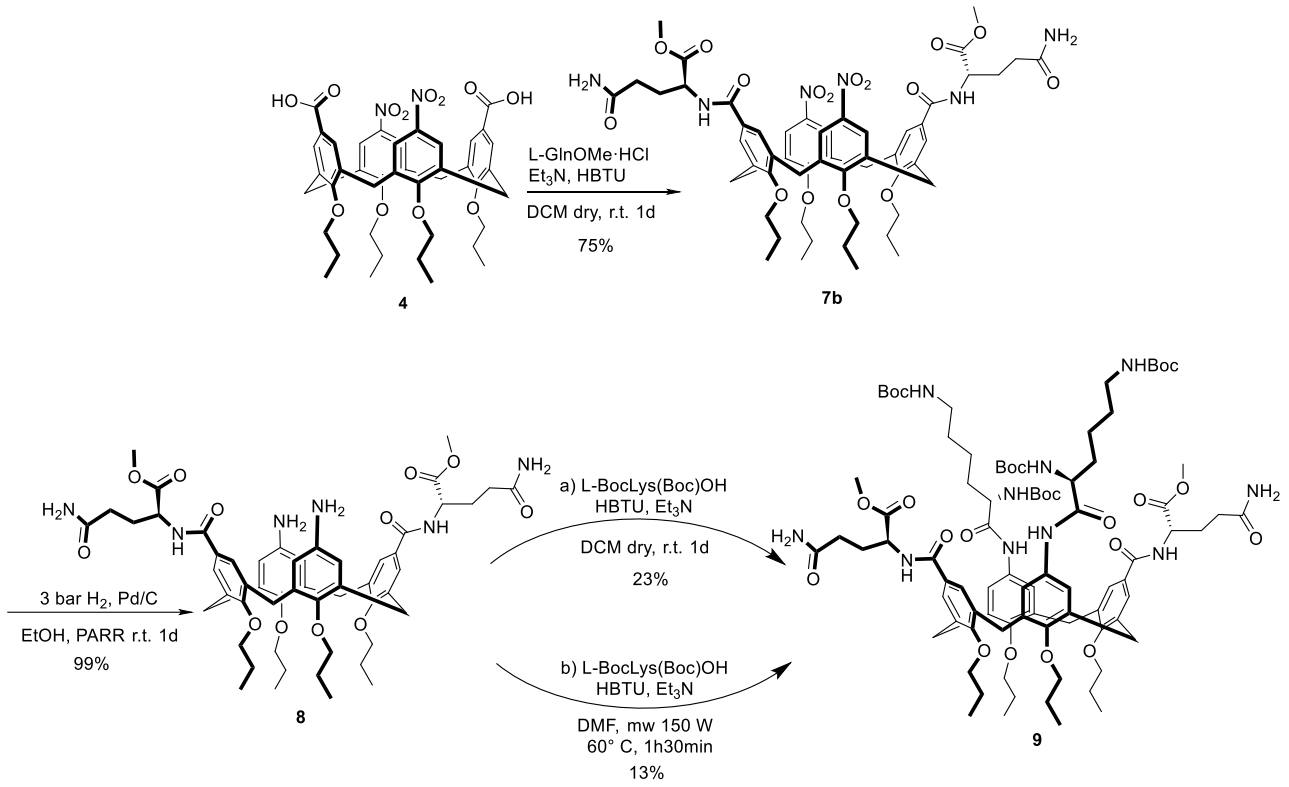

*Scheme 8: Alternative synthetic pathway for the synthesis of **9**.*

The COOH groups of compound **4** were condensed with L-HGlnOMe, in presence of HBTU, in dry DCM at room temperature. Calixarene **7b** was obtained, after purification, in a higher yield (75%) than compound **7a** (5%), suggesting that the steric hindrance of the Boc groups present in the latter molecule could actually hamper the reactivity of the carboxylic acids during the amide coupling reaction.

The second conjugation step was carried out after having reduced the NO_2 to NH_2. The same amide coupling reaction was tested under standard conditions, with DCM at room temperature (Scheme 8, route *a*), and with the aid of microwaves (Scheme 8, route *b*). Unexpectedly, this reaction worked better without microwaves, since in the latter case it was observed the formation of some, not clearly identified, byproducts. In both cases, a chromatographic separation was needed to isolate pure compound **9**.

The use of nitro groups as amine protecting group is clearly the best strategy to obtain compound **9**. In fact, it is possible to see how in this way the overall number of synthetic steps is reduced compared to strategy employing Boc protection of the amines, and furthermore the yield of the first coupling reaction is increased.

Finally, to obtain calixarenes **10** and **11** (Scheme 7) we followed the same deprotection procedures discussed above.

The two potential RBD ligands are both soluble in water, up to 1 mM for **10** and 0.8 mM for **11**. The derivative **11** is less water-soluble than the corresponding α-diester **10**, and this can be explained with the lower positive net charge. From the ^{1}H NMR spectra, recorded in both CD_3OD and D_2O, it can be seen that compound **10** (Figure 19) exhibits narrow, well-defined signals, while calixarene **11** (Figure 20) has broadened peaks. This could be explained by the fact that this compound could form aggregates in solution, or by the presence of some limitation to its conformational freedom due to the intramolecular interactions that could arise from the two carboxylate groups, which are not present in **10**. Dilution tests in D_2O were carried out to see if at lower concentrations signal resolution could be improved but, at least up to the lowest concentration explored, which is 0.2 mM, no significant differences were observed.

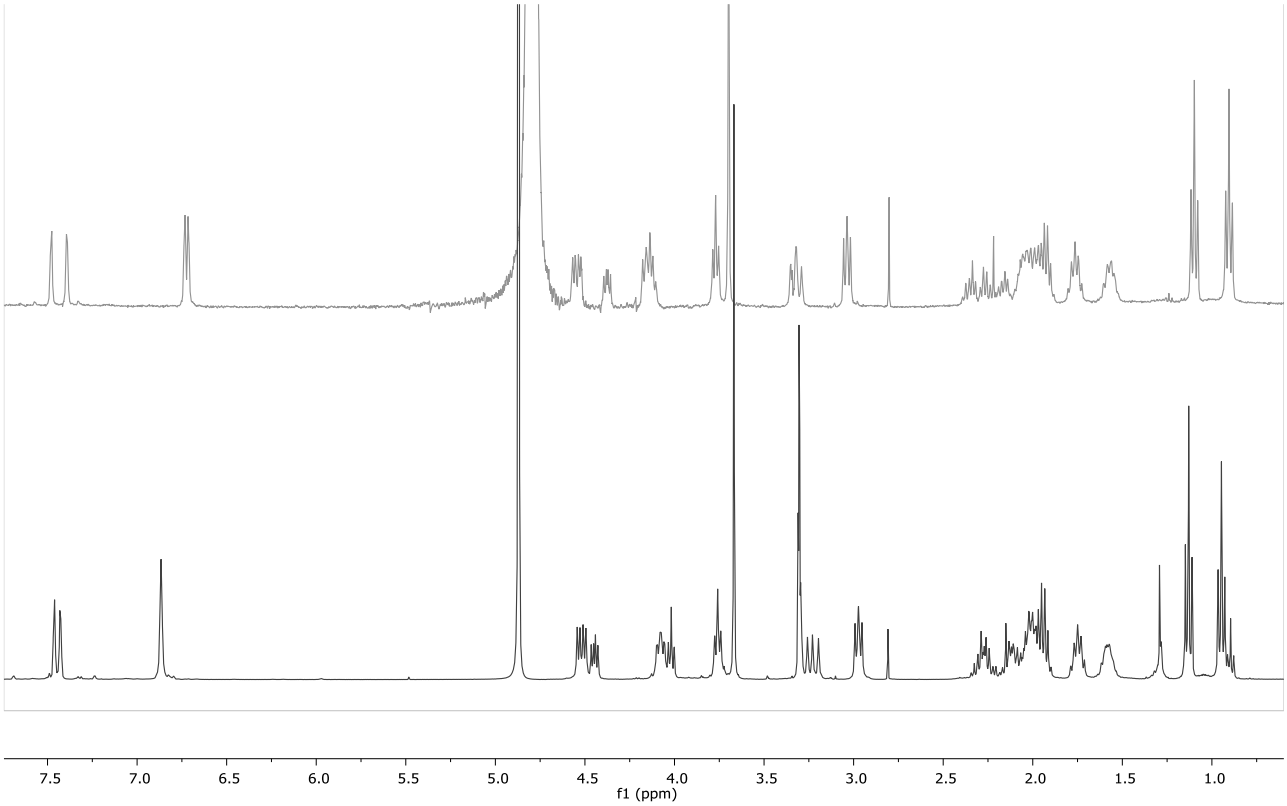

*Figure 19: ^{1}H NMR spectrum (1 mM, 400 MHz) of compound **10** in D_2O (top) and in CD_3OD (bottom).*

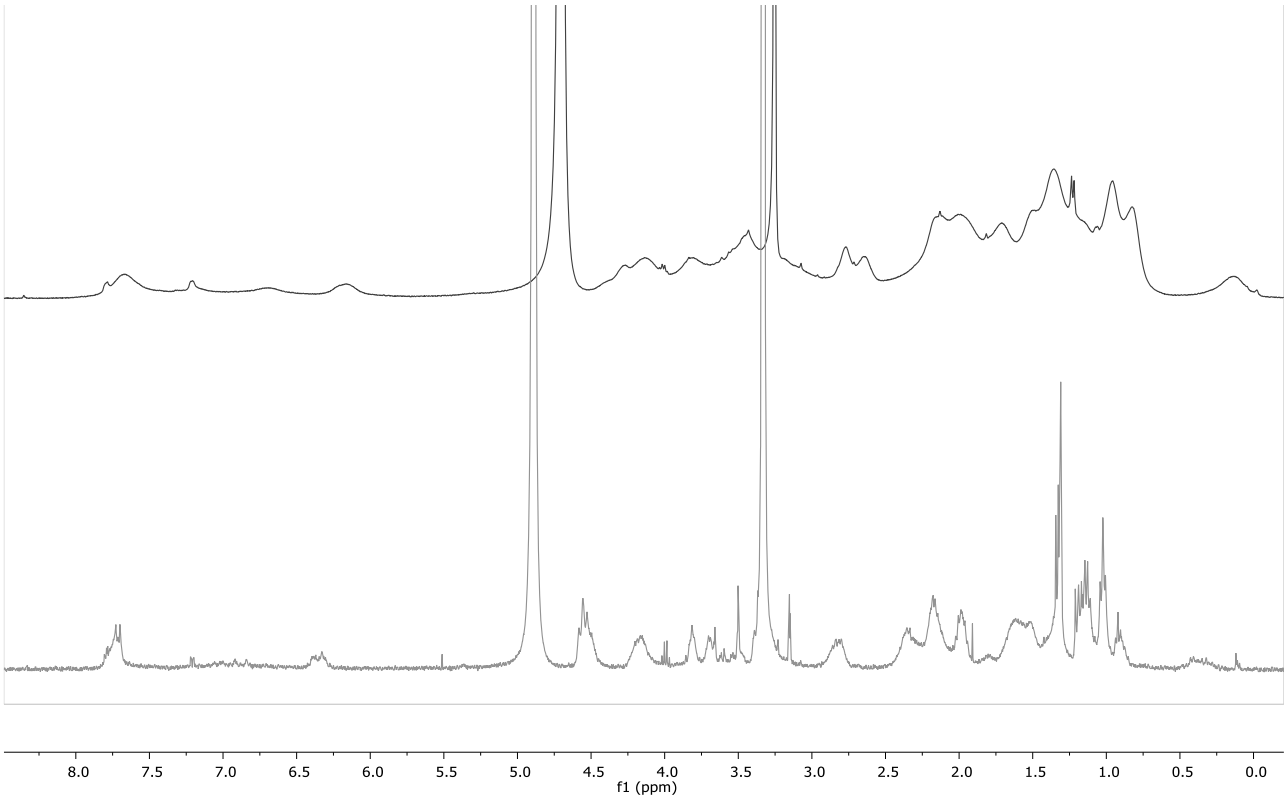

*Figure 20: ^{1}H NMR spectrum (400 MHz) of compound **11** in D_2O (top) and in CD_3OD, 0.8 mM (bottom).*

2.2.2 C-linked ligands

Due to the low yields of some reactions observed in the synthesis of compounds **10** and **11**, attributed to the steric hindrance of the amino acids α-NH_2 or α-COOH groups, when designing the C-linked peptidocalix[4]arene targets, we considered the use of amino acid mimics, i.e. carboxylic acid derivatives having the same side chains of the natural amino acids, but lacking the α-NH_2 group not involved in the linkage to the calixarene. This would avoid an excessive increase in steric bulk at the calixarene's upper rim.

C-linked peptidocalix[4]arenes **21** and **26** (Figure 21) were therefore planned as first synthetic targets of this class of potential ligands.

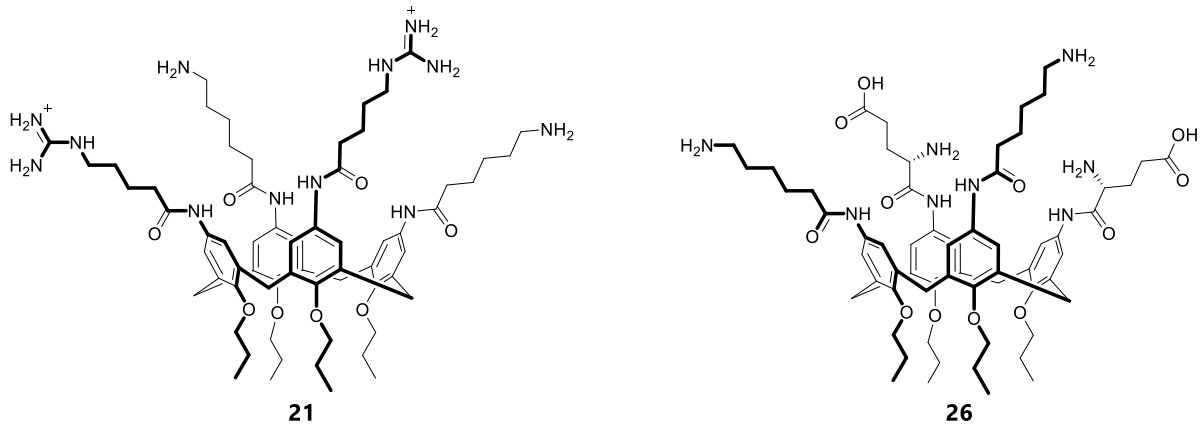

Figure 21: The two C-linked ligands synthetized.

Calixarene **21** is functionalized at the upper rim with two pairs of Lys and Arg mimics, while compound **26** with two Lys mimics and with two Glu units. In particular, ε-aminohexanoic acid was chosen as a mimic of lysine, and δ-guanidinopentanoic acid as a mimic of arginine.

We also tried to synthesize the corresponding distal modified calixarenes. However, as described later in the chapter, we were not able to functionalize our scaffold with the desired distal regiochemistry.

2.2.2.1 Calix[4]arene scaffold preparation

The synthesis of the tetraamine precursor **14**, which serves as a common platform for both target compounds, was carried out following the strategy shown in scheme 9, which was already well established in our research group.[31]

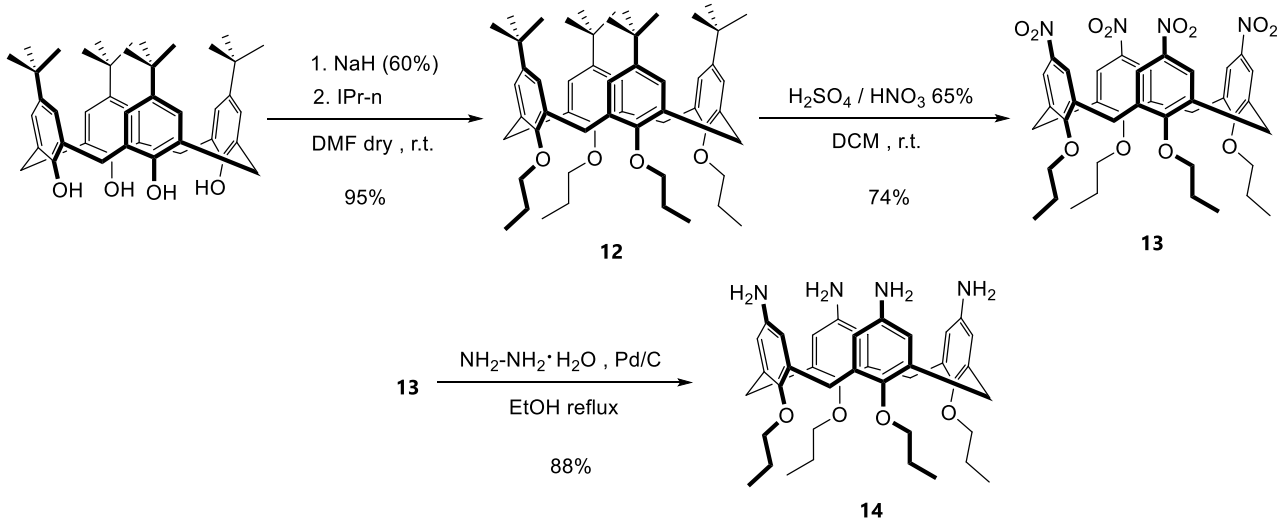

*Scheme 9: Synthesis of compound **14**.*

The synthetic procedure involves the alkylation at the lower rim of the para-tertbutyl calix[4]arene followed by the ipso-nitration at the upper rim, carried out by addition of a sulphonitric mixture in a 1:1 ratio and reduction of the nitro groups to amine by hydrogenation with hydrazine in the presence of Pd/C.

2.2.2.2 Selective protection of two NH_2 groups

In order to functionalize the calixarene with two pairs of different amino acids in vicinal position, we needed to differentiate two amine functions from the others so that they would react at different times. To do this, protection with Boc, for which there is a similar example in the literature,[32] was first explored. The reaction was carried out, as shown in scheme 10, by adding two equivalents of di-tert-butyl dicarbonate in the absence of a base.

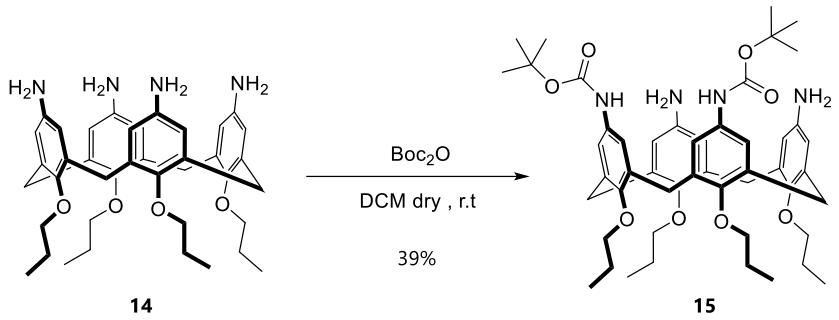

*Scheme 10: Protection of **14**.*

These conditions allowed to install two Boc groups on two vicinal (1,2) amines (compound **15**). Interesting to notice is the fact that the analogous compound where two distal (1,3) amines are protected formed only in traces. The yield was modest, and purification by column chromatography was required to separate the product from tri- and tetra-functionalised compounds. The preference for the formation of the 1,2-isomer over the 1,3 is not attributable to statistical reasons, which would suggest a 2:1 ratio between the two species. This selectivity may depend on conformational and steric factors and the formation of hydrogen bonds.[32] Diagnostic of the obtainment of the desired vicinal isomer is the ^{1}H-NMR spectrum of **15** (Figure 22), in which a peculiar pattern of signals is observed for the equatorial protons of the methylene bridges (3.13-2.88 ppm), which appear as three distinct doublets due to the change in the symmetry of the macrocycle. In addition, four singlets are observed for the aromatic protons (6.65, 6.43, 6.07, 6.06 ppm), as expected for para-substituted calix[4]arenes with substituents at positions 1,2 different from those at positions 3,4.

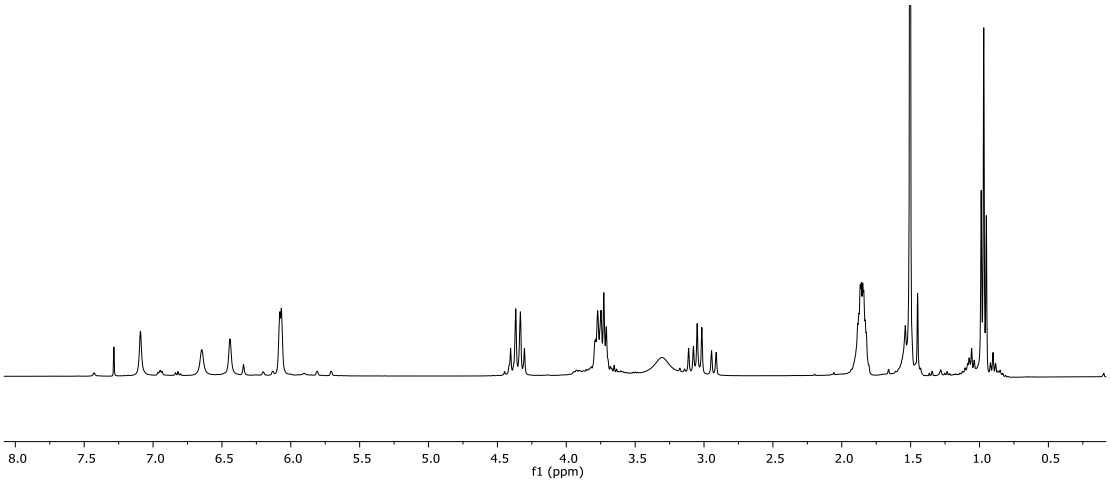

*Figure 22: ^{1}H-NMR (400 MHz, $CDCl_3$) of compound **15***

The same reaction conditions were then used with alternative protecting groups, such as Fmoc, Cbz, and trityl, to see if it was possible to isolate the protected isomer at two distal positions in order to explore also these types of derivatives and not only vicinal-modified calixarenes.

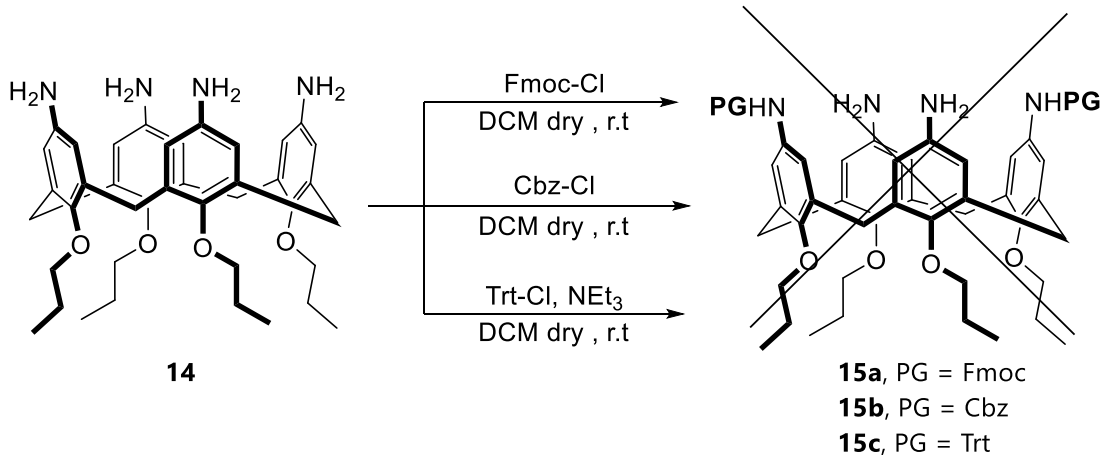

*Scheme 11: Attempts of 1,3 protection of **14**.*

However, in none of these cases (Scheme 11) was observed the formation of the desired product. The reactions of compound **14** with fluorenylmethyloxycarbonyl chloride (Fmoc-Cl) and with benzyl chloroformate (Cbz-Cl), although using two equivalents of these reagents, produced only the corresponding protected compounds on all four positions. On the other hand, the reaction with triphenylmethyl chloride (Trt-Cl) lead to a mixture of compounds from which it was impossible to isolate the product.

2.2.2.3 Functionalisation of calixarene 15 with amino acid units: synthesis of compound 21

The synthetic strategy employed to functionalize intermediate **15** with the two pairs of amino acid mimics is shown in scheme 12.

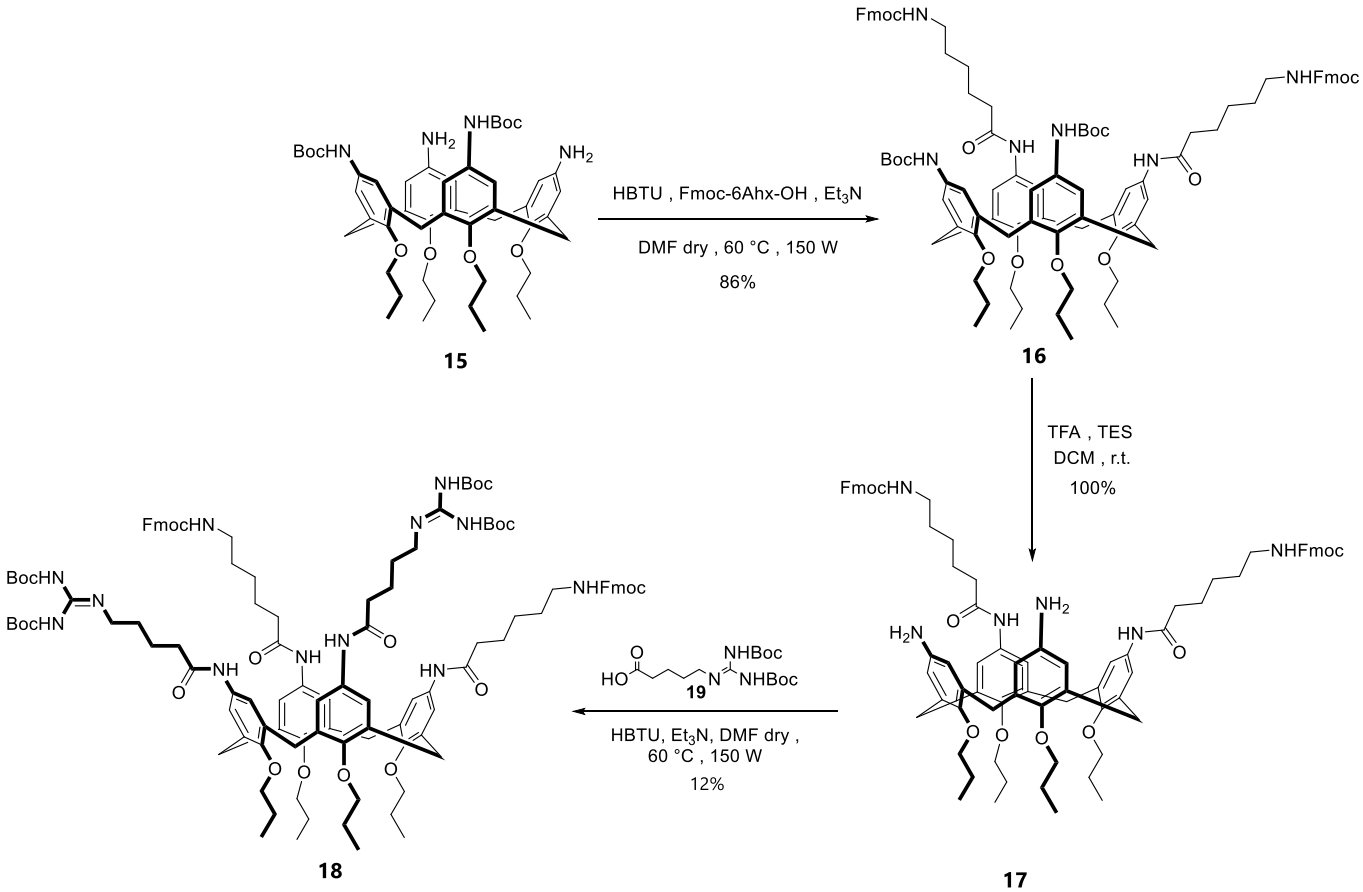

*Scheme 12: Reaction pathway for the synthesis of **18**.*

The first binding unit introduced is the lysine mimic, which must therefore necessarily be protected on the amine function with a protecting group orthogonal to the Boc groups that are already installed on the calixarene scaffold. Compound **15** is therefore reacted with Fmoc-ε-aminohexanoic acid (Fmoc-6Ahx-OH) in presence of triethylamine, using HBTU as coupling agent. Triethylamine was added in a stoichiometric ratio to avoid partial Fmoc deprotection.[33] The reaction was carried out with the aid of microwaves and a chromatographic separation was needed to isolate product **16**, which was obtained in a rather high yield (86%).

The amine-protecting Boc groups were then removed treating **16** with TFA, resulting in the quantitative isolation of the pure product **17.** The reaction was carried out in the presence of triethylsilane (TES) as a sequestering agent for the tert-butyl carbocation.

Before introducing the second pair of binding units, it was necessary to synthesize the mimic of arginine **19** by the reaction of δ-aminopentanoic acid with bisBoc-triflilguanidine to convert the terminal amine of the former to a suitably protected guanidine[34] (Scheme 13).

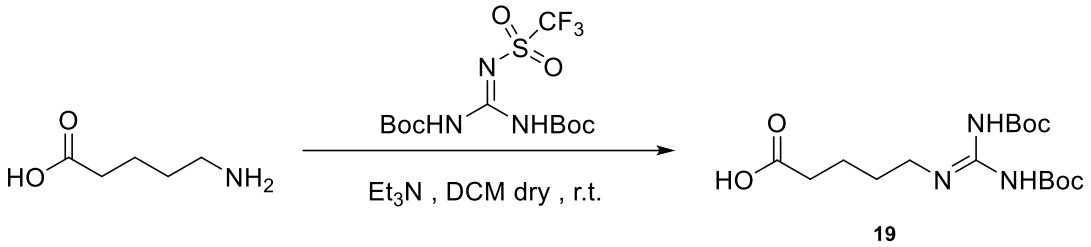

*Scheme 13: Synthesis of **19**.*

Arg mimic **19** was then introduced on calixarene **17** by a coupling reaction, using the same reaction conditions as above. In contrast to the former coupling, however, in this case, a more complex reaction mixture formed and, after chromatographic separation, compound **18** was obtained in poor yield. This could be partly attributed to the lower reactivity of compound **17** due to the steric hindrance caused by the presence of the previously introduced amino acid mimics. Furthermore, a significant amount of another compound, probably the intramolecular cyclization product of **19**, was observed in the reaction crude (Figure 23). This secondary reaction may have contributed to the low yield by removing the amino acid from the conjugation reaction with the calixarene, although steps were taken during synthesis to minimize it, in particular by avoiding the activation of the carboxylic acid of **19** in absence of calixarene **17**.

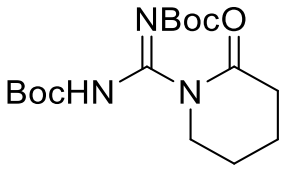

*Figure 23: Cyclization byproduct of **19**.*

We then proceeded with the removal of the protecting groups following the synthetic steps in scheme 14. It was decided to remove first the Fmoc group of the two aminohexanoic acid units, and, in a second step, the guanidine protecting groups of the Arg mimics. The strongly basic character of guanidine and thus its effectively unalterable cationic nature, in fact, suggested that the final compound **21** might be more difficult to purify than the partially deprotected **20**.

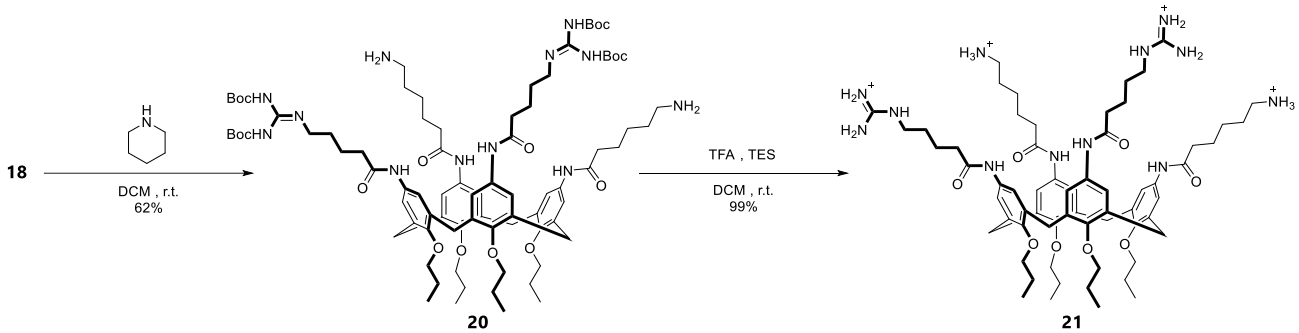

*Scheme 14: Deprotection of compound **18**.*

Fmoc deprotection was carried out in an alkaline medium by treating compound **18** with piperidine. Product **20** was easily purified first with a trituration in diethyl ether to remove the dibenzofulvene that generated as a by-product during the reaction and secondly with a trituration in water to remove the piperidine.

Finally, the removal of the Boc groups from the two guanidine units using TFA in presence of TES made it possible to obtain ligand **21**, after a simple evaporation of the solvents, as confirmed by the ^{1}H-NMR spectrum in which the disappearance of the signals of the protecting groups is observed (Figure 24).

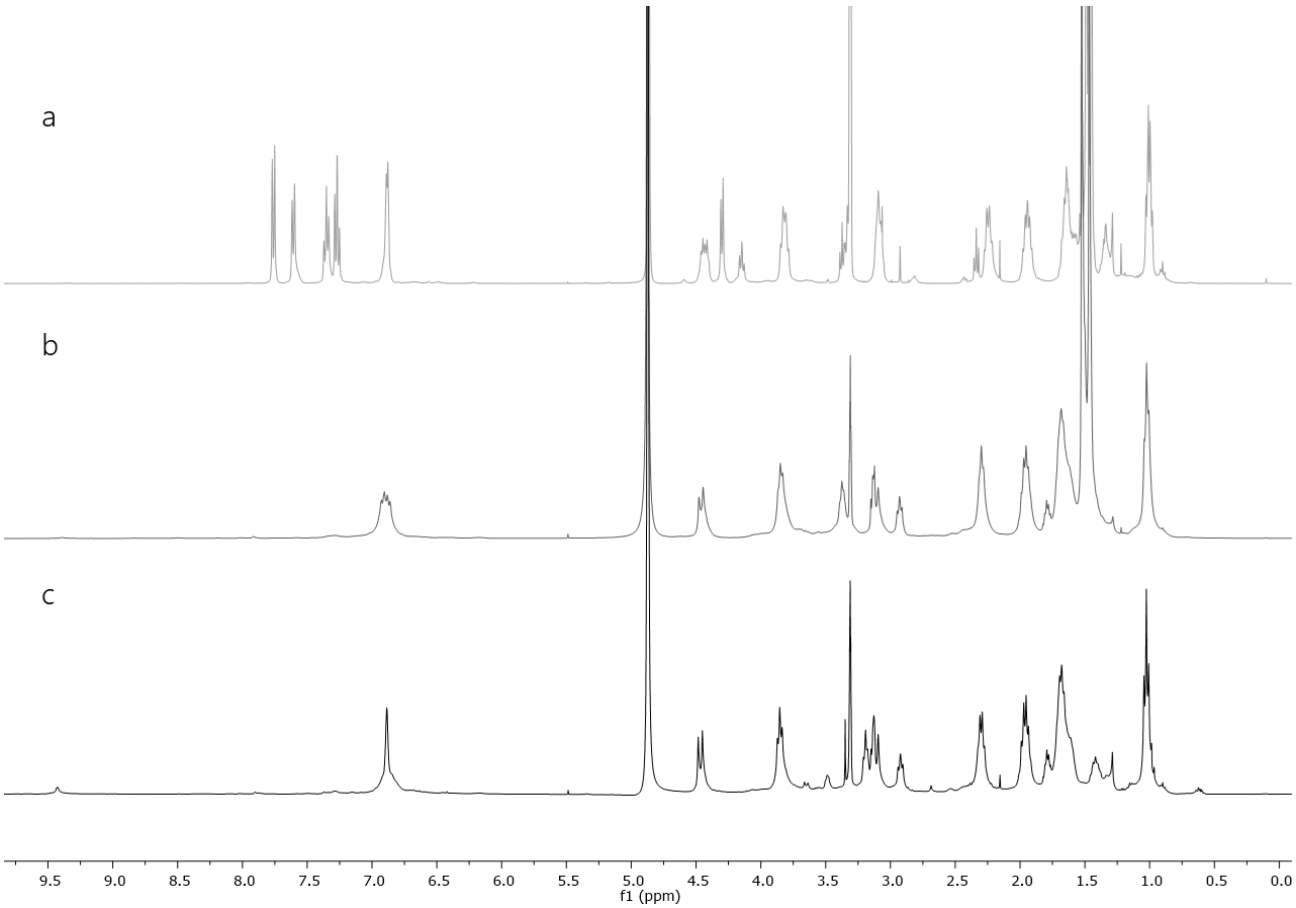

*Figure 24: ^{1}H NMR (400 MHz, CD_3OD) of compounds **18** (a), **20** (b) and **21** (c).*

2.2.2.4 Functionalisation of calixarene 15 with amino acid units: synthesis of compound 26

C-linked peptidocalix[4]arene **26** was synthesized following the same strategy developed for product **21** (Scheme 15).

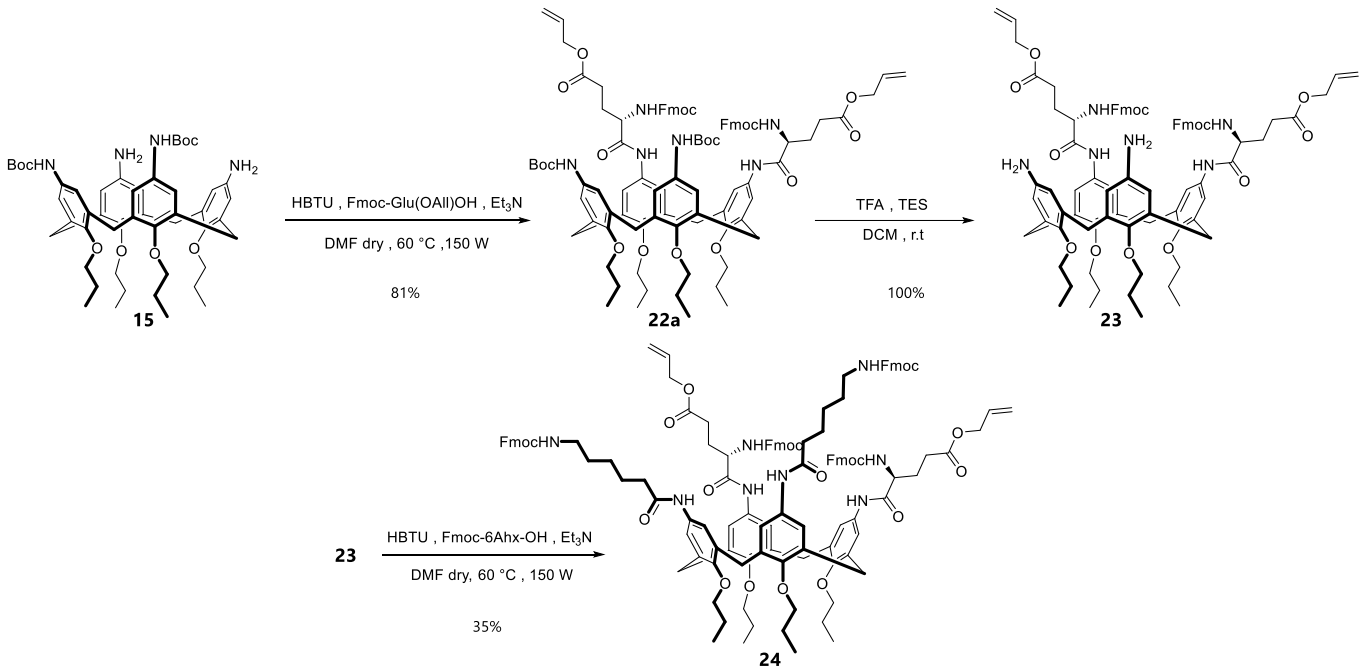

*Scheme 15: Synthesis of compound **24**.*

In the first step, **15** is functionalized with two units of glutamic acid with the amine function protected by a Fmoc group and the carboxyl function of the side chain protected as an allyl ester (Fmoc-Glu(OAll)OH). The coupling reaction was again carried out with the aid of microwaves, using HBTU in presence of triethylmine. Product **22a** was thus obtained in 81 % yield, comparable to that of the first coupling of the previous synthesis (compound **16**). In this step of synthesis, the presence of the sterically hindered Fmoc-protected amino groups, in α to the carboxylic acid involved in the reaction, does not appear to influence the course of the reaction. **22a** was then subjected to the deprotection of the Boc groups in presence of TFA and TES to obtain pure product **23**.

We then proceeded with the second coupling by reacting product **23** with the lysine mimic using the same conditions as before. The reaction mixture obtained was rather complex, so a chromatographic separation was necessary to isolate compound **24**. The latter was obtained in a lower yield than the first coupling step, but better than its analogue (**18**) in the synthesis of the previous target involving arginine mimic. This is probably due to the favorable behavior of the Lys mimic, which does not undergo the undesired cyclization observed for the Arg mimic.

When planning the deprotection of compound **24** (Scheme 16), it was considered advantageous to first remove the allyl group, as compound **25** would still have a sufficiently lipophilic character to allow purification by direct-phase column chromatography.

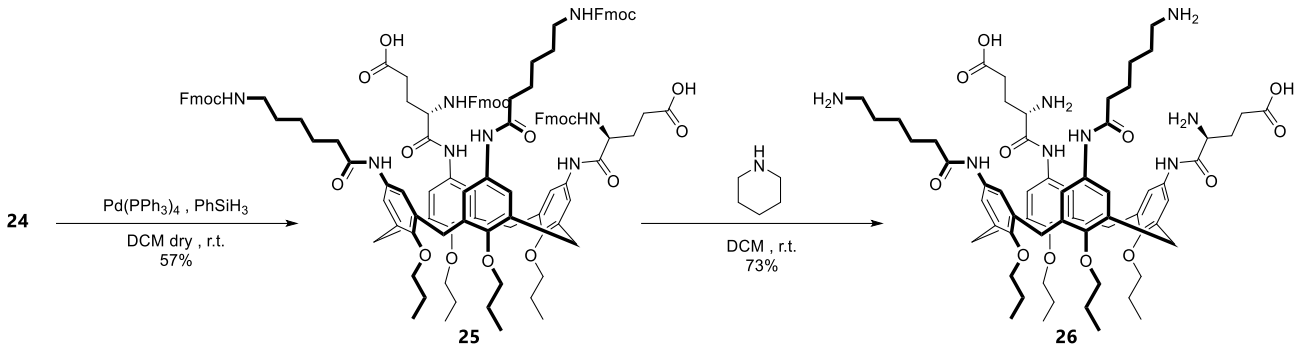

*Scheme 16: Deprotection of compound **24**.*

Allyl ester removal was achieved by a palladium-catalyzed reaction, adapting a procedure reported in the literature.[35] Specifically, $Pd(PPh_3)_4$ was used as catalyst in the presence of phenylsilane as scavenger, which acts as hydride donor without giving rise to side reactions of partial deprotection of the Fmoc, which have been observed in other cases.[36] Chromatographic separation was necessary to isolate compound **25**, and this affected the overall yield of the reaction, which resulted 57%. The successful deprotection was confirmed by the disappearance of the allyl proton signals in the ^{1}H NMR spectrum (Figure 25), although the latter is difficult to interpret. ESI-MS was not diagnostic in identifying the product and for this reason, compound **25** was not characterized, but it was decided to proceed directly with the following synthetic step. In this we removed the Fmoc group under the same reaction conditions used to obtain compound **20**. In this case, however, the purification process was varied from that used in the previous synthesis due to the higher polarity of compound **26**. Trituration was carried out firstly in diethyl ether to remove the dibenzofulvene and then in isopropanol to remove the piperidine. Obtainment of ligand **26** was confirmed by the disappearance of the Fmoc's signals in the ^{1}H NMR spectrum, shown in figure 25.

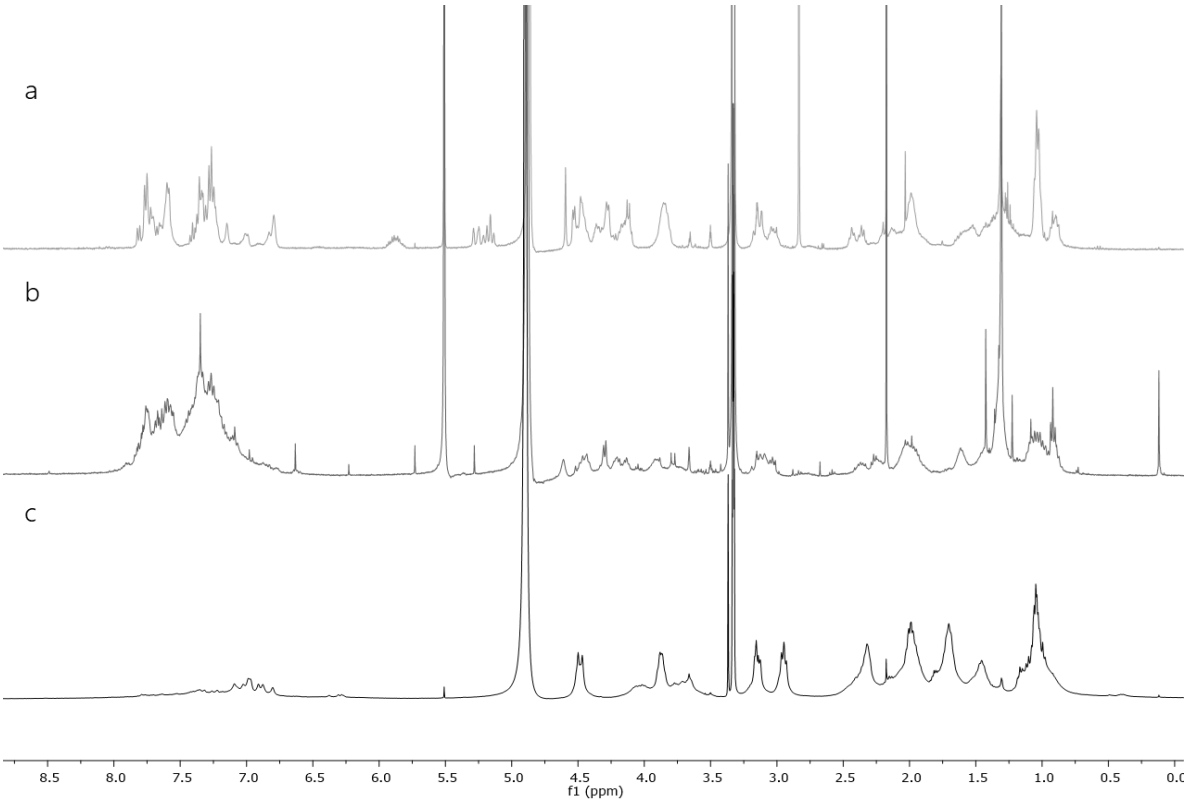

*Figure 24: ^{1}H NMR (400 MHz, CD_3OD) of compounds **24** (a), **25** (b) and **26** (c).*

2.2.3 Alternative approaches for greater differentiation of upper rim units

Having successfully synthesized peptidocalixarenes functionalized with two pairs of different amino acids, we were interested to devise a synthetic strategy that would enable the preparation of a C-linked peptidocalix[4]arene functionalized at the upper rim with three different amino acids or their analogues. This type of compound, due to the simultaneous presence of three different binding units, could have better affinity and selectivity towards the RBM target than the previously discussed calixarenes.

To this aim, the calix[4]arene structure represented in figure 26, which carries a glutamic acid mimic, a lysine mimic and two units of a third amino acid at its upper rim, was identified as the synthetic target. Its synthesis was planned as shown in scheme 17.

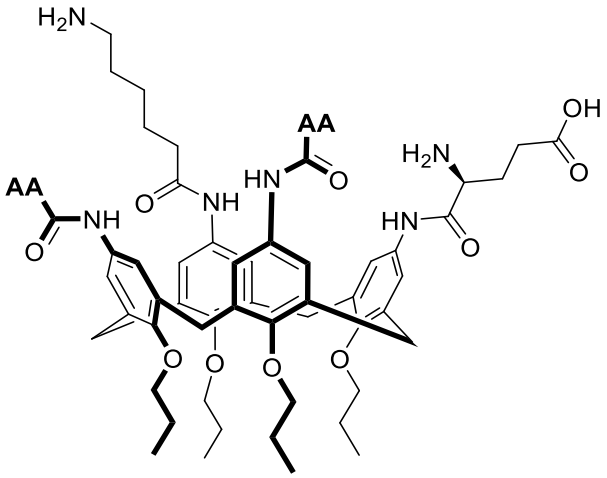

Figure 26: Ligand with a higher degree of complexity

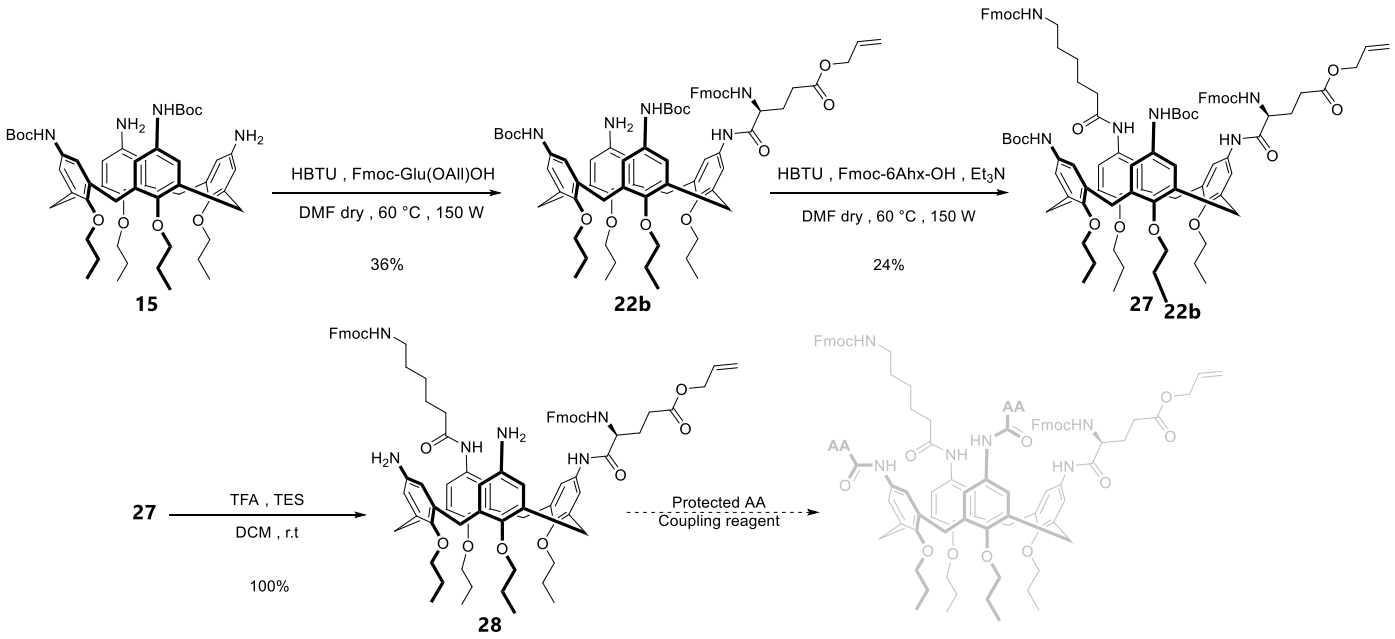

Scheme 17: Strategy for the synthesis of a calixarene with a higher degree of complexity.

In the first step, we attempted to introduce only one glutamic acid unit on the calix[4]arene precursor **15** having two proximal amines protected by the Boc group. In order to succeed in this, the coupling reaction was carried out under the same conditions as before, but without the addition of a base, so that one of the two free amine groups at the upper rim would perform this function. Once the first of the two amines is protonated, only the second, which is also less likely to be protonated due to the presence of the positive charge on the neighboring nitrogen, would react in the formation of the amide bond. The reaction, however, led to the formation of a rather complex mixture. The ESI-MS spectrum (Figure 28) of the mixture shows the presence

of peaks attributable to different species (represented in Figure 27), including the desired monofunctional compound **22b**, which was the main component, and, much less abundant, the difunctionalized compound **22a**. In addition, there are also signals attributable to both the guanidinylation of the reagent and of **22b**, leading respectively to compounds **22c** and **22d**, which can be explained by the undesired reaction between the amino groups and HBTU, when the latter is attacked first by them rather than by the carboxylates of the amino acid.[37]

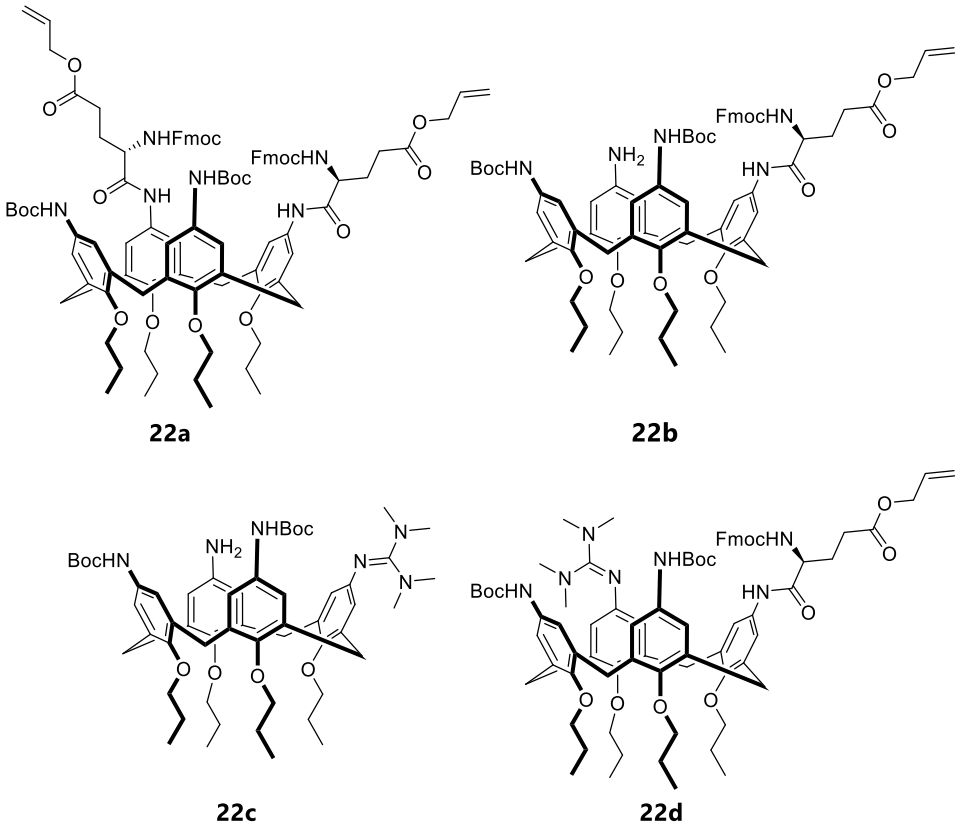

*Figure 27: Compounds found in the reaction's crude for the synthesis of **22b***

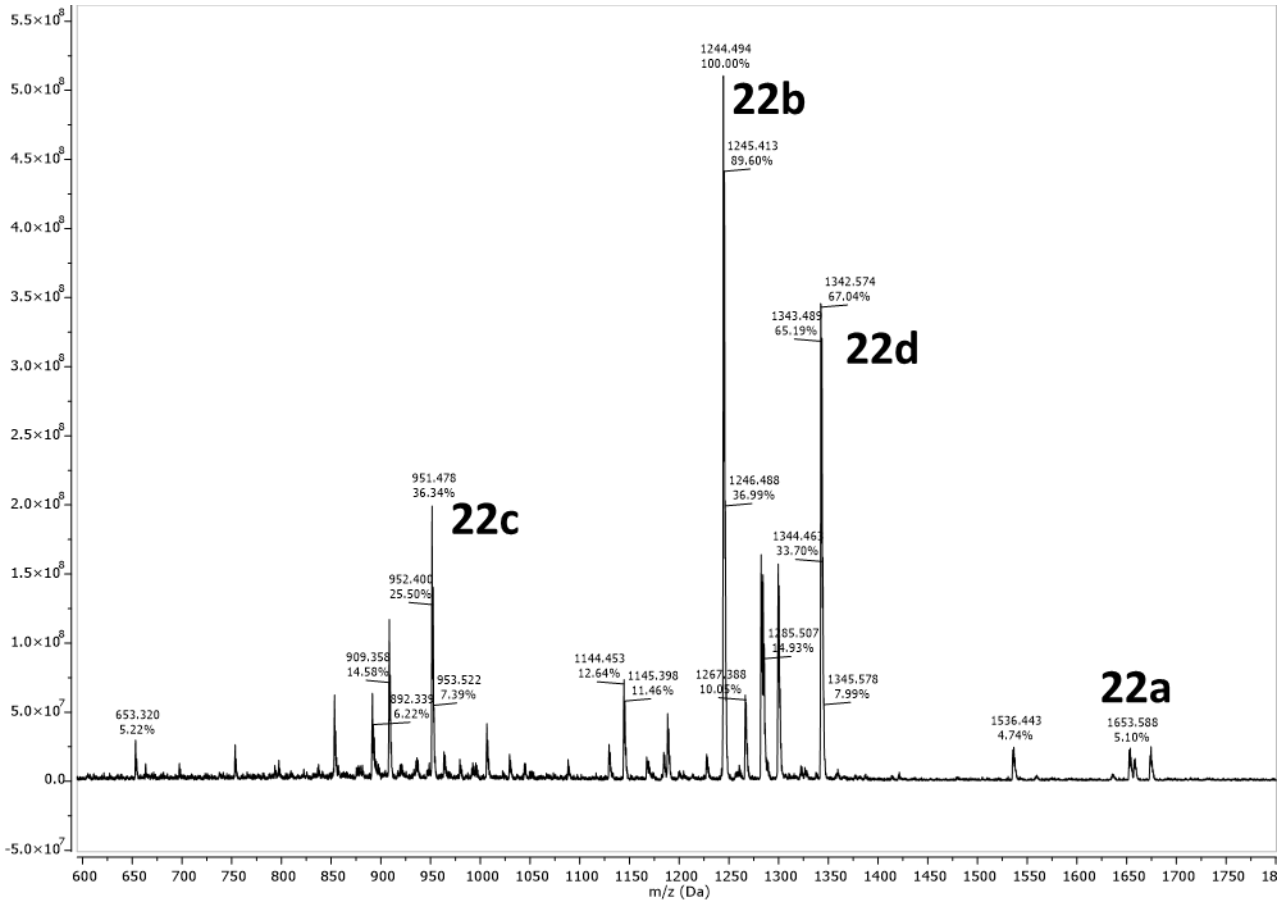

*Figure 28: ESI-MS spectrum of non-purified crude obtained in the synthesis of **22b** where it can be seen signals of compound: **22a** (m/z = 1653.588 [5.10%, M+H]⁺,1536.433 [4.74%, M+H-Boc]⁺), **22b** (m/z = 1244.494 [100.00%, M+H]⁺), **22c** (m/z = 951.478 [36.34%, M+H]⁺) and **22d** (m/z = 1342.574 [67.04%, M+H]⁺).*

Chromatographic separation was therefore required to isolate **22b** in a significant yield (36%), but lower than that obtained in the synthesis of **22a** in presence of a base (81%).

We then proceeded to insert the lysine mimic on the free amine function of **22b** by means of a second coupling reaction. Here, the procedure used in the previous syntheses was employed, using HBTU in the presence of triethylamine, with the aid of microwaves. By chromatographic separation, pure compound **27** was obtained in 24% yield.

The next synthetic step saw the removal of the two Boc protecting groups by standard reaction with TFA and TES, which resulted in product **28**. This product can then be used for further functionalization with two units of a different amino acid or one of its mimics. This route is undoubtedly synthetically demanding, mainly due to the difficulty of purifying the first coupling product, but it allows to obtain a compound with a high degree of complexity. Unfortunately, due to time restrains, we were not able to perform the last step of this pathway and attempt the functionalization of compound **28.**

2.3 Inhibition Test

The synthesized compounds **10**, **11**, **21** and **26** have been tested by professor Gaetano Donofrio of the Dipartimento di Scienze Medico-Veterinarie of the University of Parma.

In order to avoid handling the infectious SARS-CoV-2 he developed a pesudovirus system which allowed him to study the behavior of the coronavirus without the drawbacks of working with it. He was, in fact, able to engineer a lentivirus and force this to expose the SARS-CoV-2 Spike protein on its surface. This pseudovirus was modified also to have its genetic material coding for the expression of the green fluorescent protein.[38]

He then cultured a modified HEK293T based cell line in order to have these cells exposing on their surface the ACE2 receptor. To do so he electroporated the HEK293T cells with a proper plasmid, which coded for the expression of the desired receptor.

With both systems ready, the pseudovirus and the cell line, he was able to study the activity of the peptidocalixarene ligands.

In a preliminary step, a population of these cells was incubated with the pseudovirus. In normal conditions, the pseudovirus is able to infect the cells forcing them to produce the green fluorescence protein. This allows the cell population to be monitored by fluorimetry as a proof of cell transduction. Professor Donofrio also showed that if the pseudovirus is first incubated with human sera coming from SARS-CoV-2 infected patients, and then used to transduce the same cell line discussed above, no fluorescence can be observed, meaning that the antibodies present in the serum are capable of blocking the Spike protein-ACE2 recognition event and therefore prevent cell infection.[38]

Next, he performed the same experiment replacing the human sera with a water based 200 μM solution of one of our ligands. Disappointingly, for the four compounds tested, the cells started to emit green light; therefore, it was assumed that our compounds were not able to prevent the interaction between the Spike protein and the ACE2 receptor, failing to inhibit the pseudovirus, which then infected the cells.

3. CONCLUSIONS

During the time spent working on this project, we were able to synthesize four new peptidocalix[4]arenes, compounds **10**, **11**, **21** and **26**. The many challenges encountered during their preparation improved our expertise on calixarenes synthesis and modification. Furthermore, with the synthesis of intermediate **28**, we set the basis towards the development of an interesting strategy for the preparation of peptidocalixarenes with an increased degree of upper rim differentiation.

Even if, in the end, our compounds did not show inhibitory activity towards a pseudovirus exposing the SARS-CoV-2 Spike protein on its surface, it could still be interesting to perform the inhibition tests with the real SARS-CoV-2 virus to see if the same result would be obtained.

4. EXPERIMENTAL PART

General information

Commercially available reagents and solvents were used without carrying out any prior purification or treatment except as indicated. All moisture- and air-sensitive reactions were conducted under nitrogen atmosphere. Dry solvents were prepared according to standard procedures and stored in the presence of molecular sieves. Monitoring of synthetic processes was performed by direct-phase thin-layer chromatography (TLC) using 60 F254 silica gel plates. For the detection of reagents and products with amine groups, the TLCs were sprayed with a 5% solution of ninhydrin in ethanol; for those with phenolic groups, a solution of $FeCl_3$ in water was used; for those with aldehydic groups, a solution of acidic 2,4-dinitrophenylhydrazine in ethanol was used; and for easily oxidized compounds, a 0.05% solution of $KMnO_4$ in water was used. Flash chromatography columns on silica gel 60 (230-400 mesh), under nitrogen pressure, and commercial preparative TLC 20×20 cm, silica gel F254, 0.5 mm were used for products purification.

Products characterization was performed by ^{1}H and ^{13}C NMR spectroscopy and mass spectrometry using ESI technique. NMR spectra were recorded with Bruker AVANCE 400 spectrometer (^{1}H at 400 MHz, ^{13}C at 100 MHz); chemical shift values are reported in ppm using the resonance frequency of the partially deuterated solvent as a reference. Mass spectra were recorded with a single quadrupole SQ detector spectrometer, Waters. Melting points were determined with Gallenkamp apparatus in closed capillaries.

Molecular Modeling & Docking Studies on the RBD

The computational program Spartan Wavefunction (2014 edition, V1.1.4) was used to perform the molecular modeling studies. The minimization of the equilibrium geometry of the fundamental state in the gas phase was calculated by both ab initio DFT method. The calculation was conducted using the B3LYP hybrid functional approximation and the 6-31G* basis set.

The Autodock Vina program was used for the docking studies. For the calculation, it was necessary to indicate the regions of the RBD with which to determine the binding affinity. In addition, the program requires adjusting a parameter called exhaustiveness (values between 8-100) when exploring regions of the protein greater than 27000 $Å^3$, to reliably find the minimum energy. The indicated cell sizes have the unit corresponding to 0.375 Å. For the calculation in BOX 1, corresponding to the protein's main region of interest, a cell centered in (x, y, z) = (-36.373, 17.564, 1.47), size (50, 50 ,30) and an exhaustiveness of 31 was used. BOX 2 is the one used to explore the entire region of the RBD involved in interaction with the ACE2 cell receptor, and is centered at (x, y, z) = (-38,363, 30,455, 1.56), with dimensions (60, 120 ,40) and an exhaustiveness of 90.

Synthesis of 25,26,27,28-tetrapropoxycalix[4]arene (1)

Tetrahydroxicalx[4]arene (6.0 g, 14.13 mmol) dissolved in dry DMF (150 mL) was placed in a two-necked round-bottom flask under nitrogen flow. Next, NaH 60% (4.52 g, 113.07 mmol) was added. The mixture was stirred for 30 minutes and finally 1-iodopropane (8 mL, 84.8 mmol) is added. The reaction was allowed to react at room temperature under inert atmosphere, periodically checking the progress of the reaction by TLC (eluent: Hexane/AcOEt = 8/2). After 20 hours, the reaction was quenched by the addition of 1M HCl (150 mL). The yellow precipitate that formed was filtered on buchner and dried at the mechanical pump.

Yield = 100% (8.44 g)

^{1}H NMR (400 MHz, $CDCl_3$) δ (ppm): 6.67 – 6.54 (m, 12H, Ar*H*), 4.47 (d, *J* = 13.3 Hz, 4H, H_{ax} di $ArCH_2Ar$), 3.87 (t, *J* = 7.5 Hz, 8H, $OCH_2CH_2CH_3$), 3.17 (d, *J* = 13.3 Hz, 4H, H_{eq} di $ArCH_2Ar$), 1.95 (h, *J* = 7.5 Hz, 8H, $OCH_2CH_2CH_3$), 1.01 (t, *J* = 7.4 Hz, 12H, $OCH_2CH_2CH_3$).

The spectroscopic data found are in agreement with those reported in literature.[39]

25,27-dihydroxy-26,28-dipropoxycalix[4]arene (1a)

In a two-necked round-bottom flask, under nitrogen flow, tetrahydroxicalx[4]arene (1.50 g, 3.54 mmol) was dissolved in 40 mL of dry CH_3CN, then K_2CO_3 (2.06 g, 14.91 mmol) was added and the mixture left stirring. After 30 minutes, 1-iodopropane (1.45 mL, 14.88 mmol) was added to the reaction mixture which was then refluxed for 24 hours. The reaction was monitored with TLC (hexane/AcOEt = 9/1, detected with $FeCl_3$) and after completion it was quenched of 1M HCl (20 mL) and the precipitate was filtered off and recrystallized with cold DCM/hexane. A yellow solid was obtained.

Yield = 70% (1.25 g)

^{1}H NMR (400 MHz, $CDCl_3$) δ (ppm): 8.36 (s, 2H, O*H*), 7.08 (d, J = 7.5 Hz, 4H, Ar*H meta*), 6.95 (d, J = 7.6 Hz, 4H, Ar*H meta*), 6.78 (t, J = 7.5 Hz, 2H, Ar*H para*), 6.67 (t, J = 7.5 Hz, 2H, Ar*H para*), 4.34 (d, J = 12.9 Hz, 4H, H_{ax} di $ArCH_2Ar$), 4.00 (t, J = 6.3 Hz, 4H, $OCH_2CH_2CH_3$), 3.40 (d, J = 13.0 Hz, 4H, H_{eq} di $ArCH_2Ar$), 2.10 (h, J = 7.4 Hz, 4H, $OCH_2CH_2CH_3$), 1.35 (t, J = 7.4 Hz, 6H $OCH_2CH_2CH_3$).

The spectroscopic data found are in agreement with those reported in literature.[40]

25,27-di(*p*-nitrobenzensulfonyloxy)-26,28-dipropoxycalix[4]arene (1b)

In a two-necked round-bottom flask, under nitrogen flow, compound **1a** (1.29 g, 2.53 mmol) was dissolved in 50 mL of dry DMF. NaH 60% (0.40 g, 10.12 mmol) was added and the mixture stirred for 30 min at 0 °C. P-nitrobenzenesulphonyl chloride (2.24 g, 10.12 mmol) was then added and the temperature brought to room temperature. The reaction was monitored by TLC (hexane/AcOEt = 8/2, detected with $FeCl_3$). After 7 days, the reaction was quenched with 50 mL of 1M HCl. A yellow precipitate was recovered, which has been purified by recrystallization in DCM/MeOH to give a yellow solid.

Yield = 91% (2.21 g)

^{1}H NMR (400 MHz, $CDCl_3$) δ (ppm): 8.42 (d, J = 8.8 Hz, 4H, NosAr*H*), 8.06 (d, J = 8.8 Hz, 4H NosAr*H*), 7.07 (d, J = 7.4 Hz, 4H, Ar*H meta*), 6.94 (t, J = 7.5 Hz, 2H, Ar*H para*), 6.43 (t, J = 7.6 Hz, 2H, Ar*H para*), 6.22 (d, J = 7.7 Hz, 4H, Ar*H meta*), 4.01 (d, J = 13.8 Hz, 4H, H_{ax} di $ArCH_2Ar$), 3.89 – 3.79 (m, 4H, $OCH_2CH_2CH_3$), 2.86 (d, J = 13.9 Hz, 4H, H_{eq} di $ArCH_2Ar$), 1.88 (h, J = 7.6 Hz, 4H, $OCH_2CH_2CH_3$), 0.90 (t, J = 7.4 Hz, 6H, $OCH_2CH_2CH_3$).

The spectroscopic data found are in agreement with those reported in literature.[30]

5,17-dinitro-25,27-di(*p*-nitrobenzensulfonyloxy)-26,28-dipropoxycalix[4]arene (1c)

In a two-necked flask, calixarene **1b** (1.08 g, 1.23 mmol) was dissolved in 100 mL of dry DCM, glacial acetic acid (14.7 mL, 257.9 mmol) was added, and 100% HNO_3 (4.4 mL, 104.4 mmol) was then slowly dripped in. The reaction was left stirring for 20 hours at room temperature, and upon completion (determined by TLC: hexane/AcOEt = 8/2) quenched with 300 mL of water. The aqueous phase was extracted with DCM (3x100 mL), the organic phases were combined and washed with water and a saturated solution of $NaHCO_3$. The organic phase was dried over Na_2SO_4 and dried under reduced pressure. An orange solid was obtained.

Yield = 99% (1.19 g)

^{1}H NMR (400 MHz, DMSO-d_6) δ (ppm): 8.53 (d, J = 8.8 Hz, 4H, NosAr*H*), 8.25 (s, 4H, Ar*H*-NO_2), 8.14 (d, J = 8.9 Hz, 4H, NosAr*H*), 6.58 (t, J = 7.6 Hz, 2H, Ar*H para*), 6.36 (d, J = 7.7 Hz, 4H, Ar*H meta*), 3.92 (d, J = 13.8 Hz, 4H, H_{ax} di $ArCH_2Ar$), 3.87 – 3.78 (m, 4H, $OCH_2CH_2CH_3$), 3.30 (d, J = 14.0 Hz, 4H, H_{eq} di $ArCH_2Ar$), 1.73 (h, J = 7.5 Hz, 4H, $OCH_2CH_2CH_3$), 0.77 (t, J = 7.4 Hz, 6H, $OCH_2CH_2CH_3$).

The spectroscopic data found are in agreement with those reported in literature.[30]

5,17-dinitro-25,27-dihydroxy-26,28-dipropoxycalix[4]arene (1d)

Compound **1c** (1.27 g, 1.31 mmol) was dissolved in 400 mL of a 1/1 DCM/EtOH mixture and a solution of powdered KOH (3.69 g, 65.71 mmol) in 1.5 mL of H_2O was added. The

reaction proceeded at room temperature for 24 hours. Upon completion (determined by TLC, hexane/AcOEt eluent = 1/1, detected with $FeCl_3$). The reaction was quenched with 70 mL of 1M HCl. It was then extracted with DCM (3x100 mL), and the organic phase washed with water and brine, anhydrified with the Na_2SO_4 and dried under reduced pressure. A dark orange solid was obtained.

Yield = 89% (0,70 g)

^{1}H NMR (400 MHz, $CDCl_3$) δ (ppm): 7.98 (s, 2H, O*H*), 7.87 (s, 4H, Ar*H*-NO_2), 7.17 (d, J = 7.5 Hz, 4H, Ar*H meta*), 6.77 (t, J = 7.5 Hz, 2H, Ar*H para*), 4.38 (d, J = 13.1 Hz, 4H, H_{ax} di $ArCH_2Ar$), 4.07 (t, J = 6.2 Hz, 4H, $OCH_2CH_2CH_3$), 3.52 (d, J = 13.1 Hz, 4H, H_{eq} di $ArCH_2Ar$), 2.13 (h, J = 6.9 Hz, 4H, $OCH_2CH_2CH_3$), 1.36 (t, J = 7.4 Hz, 6H, $OCH_2CH_2CH_3$).

The spectroscopic data found are in agreement with those reported in literature.[30]

Attempt to synthesize 5,17-dinitro-25,26,27,28-tetrapropossicalix[4]arene (2) from 5,17-dinitro-25,27-dihydroxy-26,28-dipropoxycalix[4]arene (1d)

In a two-necked flask, under nitrogen flow, the compound **1d** (0.70 g, 1.16 mmol) was dissolved in 30 mL of dry DMF, then NaH 60% (0.37 g, 9.37 mmol) was added, and the mixture was stirred for 30 minutes. 1-Iodopropane (0.9 mL, 9.30 mmol) was added, and the reaction was allowed to proceed at room temperature, monitoring the reaction by TLC (hexane/AcOEt = 8/2, revealed with $FeCl_3$). After 24 hours, the reaction was complete and quenched with 30 mL of 1M HCl. A yellow solid was obtained and was then recrystallized in DCM/MeOH. A pale-yellow precipitate was obtained, which by ^{1}H NMR analysis ($CDCl_3$, 400 MHz) was found to be a mixture of calixarenes in multiple conformations, where the one in the cone conformation was not the majority component. It was impossible to separate the different conformations by recrystallization or chromatography because the calixarenes have the same R_f. The reaction did not give us the desired product.

5,17-dinitro-25,26,27,28-tetrapropoxycalix[4]arene (2)

In a round-bottom flask, compound **1** (2.14 g, 3.61 mmol) was dissolved in 200 mL of DCM, and the temperature lowered to 0°C. Glacial CH_3COOH (34 mL) was then added and subsequently 65% v/v HNO_3 (17 mL, 360 mmol) was slowly dripped in. The reaction mixture darkened and developed orange fumes, after which it turned yellow-orange. It was allowed to react at room temperature. The reaction progress was monitored by TLC (eluent: Hexane/AcOEt = 9/1). The reaction is quenched after 2 hours and 40 minutes by adding 250 mL of H_2O. The organic phase was recovered and washed with H_2O until

the pH neutrality, then dried over with Na_2SO_4 and dried under reduced pressure. The product was purified by precipitation in DCM/MeOH. A pale-yellow solid was obtained.

Yield = 34% (0. 83 g)

^{1}H NMR (400 MHz, $CDCl_3$) δ (ppm): 7.45 (s, 4H, Ar*H*-NO_2), 6.82 – 6.71 (m, 6H, Ar*H*), 4.50 (d, J = 13.7 Hz, 4H, H_{ax} di $ArCH_2Ar$), 3.94 (t, J = 7.3 Hz, 4H, $OCH_2CH_2CH_3$-NO_2), 3.89 (t, J = 7.3 Hz, 4H, $OCH_2CH_2CH_3$), 3.27 (d, J = 13.7 Hz, 4H, H_{eq} di $ArCH_2Ar$), 2.00 – 1.86 (m, 8H, $OCH_2CH_2CH_3$), 1.05 (t, J = 7.4 Hz, 6H, $OCH_2CH_2CH_3$-NO_2), 1.00 (t, J = 7.4 Hz, 6H, $OCH_2CH_2CH_3$).

The spectroscopic data found are in agreement with those reported in literature.[41]

5,17-dicarbaldehyde-11,23-dinitro-25,26,27,28-tetrapropoxycalix[4]arene (3)

HMTA (3.35 g, 23.90 mmol), 400 mL of TFA and finally compound **2** (1.01 g, 1.49 mmol) were added sequentially to a two-neck flask, under nitrogen atmosphere. The reaction was refluxed for 4 hours. Upon completion (determined by TLC, eluent: Hexane/AcOEt, 5/2, detected with 2,4-dinitrophenylhydrazine) the reaction was quenched with 400mL of H2O. The aqueous phase is extracted with DCM (3x100 mL), the combined organic phases are washed with H2O until pH neutralization, dried over Na_2SO_4 and dried under reduced pressure. A pale-yellow-colored solid is obtained.

Yield = 97% (1.07 g)

^{1}H NMR (400 MHz, $CDCl_3$) δ (ppm): 9.59 (s, 2H, C*H*O), 7.65 (s, 4H, Ar*H*-NO_2), 7.13 (s, 4H, Ar*H*-CHO), 4.54 (d, J = 13.9 Hz, 4H, H_{ax} di $ArCH_2Ar$), 4.00 (t, J = 7.4 Hz, 4H, $OCH_2CH_2CH_3$), 3.93 (t, J = 7.4 Hz, 4H, $OCH_2CH_2CH_3$), 3.40 (d, J = 14.0 Hz, 4H, H_{eq} di $ArCH_2Ar$), 2.00 – 1.86 (m, 8H, $OCH_2CH_2CH_3$), 1.09 – 0.98 (m, 12H, $OCH_2CH_2CH_3$).

The spectroscopic data found are in agreement with those reported in literature.[42]

5,17-dicarboxylic acid-11,23-dinitro-25,26,27,28-tetrapropoxycalix[4]arene (4)

Compound **3** (2.47 g, 3.35 mmol) was dissolved in 400 mL of a $CHCl_3$/Acetone (1:1) mixture and poured in a round-bottom flask under inert atmosphere. Then, a solution of H_3NSO_3 (2.61 g, 26.92 mmol) and $NaClO_2$ (2.21 g, 24.46 mmol), dissolved in the minimum amount of water, was added to the flask. The mixture was left stirring at room temperature for 24 hours The progress of the reaction was monitored by TLC (eluent: Hexane/AcOEt, 7/3) and upon completion, it was quenched by evaporation under reduced pressure and subsequent trituration in 1M HCl (100 mL) for 15 minutes. The precipitate that formed was filtered on buchner, washed with H_2O, and dried with a mechanical pump obtaining a yellowish solid.

Yield = 98% (2.54 g)

^{1}H NMR (400 MHz, $CDCl_3$) δ (ppm): 12.77 (bs, 2H, COO*H*), 8.16 (s, 4H, Ar*H*-NO_2), 6.79 (s, 4H, Ar*H*-COOH), 4.48 (d, J = 13.8 Hz, 4H, H_{ax} di $ArCH_2Ar$), 4.20 – 4.08 (m, 4H, $OCH_2CH_2CH_3$), 3.72 (t, J = 6.7 Hz, 4H, $OCH_2CH_2CH_3$), 3.34 (d, J = 14.0 Hz, 4H, H_{eq} di $ArCH_2Ar$), 2.00 – 1.83 (m, 8H, $OCH_2CH_2CH_3$), 1.13 (t, J = 7.4 Hz, 6H, $OCH_2CH_2CH_3$), 0.90 (t, J = 7.4 Hz, 6H, $OCH_2CH_2CH_3$).

The spectroscopic data found are in agreement with those reported in literature.[42]

5,17-diamino-11,23-dicarboxylic acid-25,26,27,28-tetrapropoxycalix[4]arene (5)

In a two-neck flask, under nitrogen flow, hydrazine hydrate (2.7 mL, 54.72 mmol) and a catalytic amount of Pd/C (10%) were added to a suspension of compound **4** (0.53 g, 0.68 mmol) in absolute EtOH. The reaction was refluxed for 24 hours and upon completion (determined by TLC, eluent: DCM/MeOH 9/1, detected with ninhydrin) it was quenched and the catalyst removed by filtration. The solvent was evaporated under reduced pressure obtaining a white solid, which was used for the following reactions without further purification

Yield = 99% (0.48 g)

^{1}H NMR (400 MHz, CD_3OD) δ (ppm): 7.74 (s, 4H, Ar*H*-COOH), 5.71 (s, 4H, Ar*H*-NH_2), 4.46 (d, J = 13.3 Hz, 4H, H_{ax} di $ArCH_2Ar$), 4.10 (t, J = 6.5 Hz, 4H, $OCH_2CH_2CH_3$), 3.65 (t, J = 6.5 Hz, 4H, $OCH_2CH_2CH_3$), 3.14 (d, J = 13.3 Hz, 4H, H_{eq} di $ArCH_2Ar$), 2.04 – 1.84 (m, 8H, $OCH_2CH_2CH_3$), 1.16 (t, J = 7.4 Hz, 6H, $OCH_2CH_2CH_3$), 0.92 (t, J = 7.4 Hz, 6H, $OCH_2CH_2CH_3$).

The spectroscopic data found are in agreement with those reported in literature.[29]

5,17-di(Boc-amino)-11,23-dicarboxylic acid-25,26,27,28-tetrapropoxycalix[4]arene (6a)

In a round-bottom flask compound **5** (0.47 g, 0.67 mmol) was suspended in 70 mL of THF. Separately, NaOH (0.056 g, 1.4 mmol) was dissolved in a beaker using the minimum amount of water, then this solution was added to the previous one. Boc_2O (0.38 g, 1.74 mmol) was then added and the mixture was refluxed for 2 hours. The reaction was monitored by TLC (eluent: DCM/MeOH = 9/1, detected with ninhydrin) which suggested its completion. The organic solvent was evaporated, and the remaining aqueous phase was acidified with 1M HCl to pH 6 and extracted with DCM (3x50 mL). The organic phases were combined and washed with H_2O, anhydrified with Na_2SO_4 and dried under reduced pressure. A brown resin was obtained, which was used for the next reaction without any further purification.

Yield = 80% (0.36 g)

^{1}H NMR (400 MHz, $CDCl_3$) δ (ppm): 12.96 (s, 2H, COO*H*), 7.19 (s, 4H, Ar*H*-COOH), 6.82 (s, 4H, Ar*H*-NHBoc), 6.58 (s, 2H, NH-Boc), 4.39 (d, J = 13.6 Hz, 4H, H_{ax} di $ArCH_2Ar$), 4.00 – 3.91 (m, 4H, $OCH_2CH_2CH_3$), 3.65 (t, J = 6.6 Hz, 4H, $OCH_2CH_2CH_3$), 3.12 (d, J = 13.7 Hz, 4H, H_{eq} di $ArCH_2Ar$), 1.90 – 1.82 (m, 8H, $OCH_2CH_2CH_3$), 1.61 (s, 18H, $C(CH_3)_3$), 1.10 (t, J = 7.4 Hz, 6H, $OCH_2CH_2CH_3$), 0.84 (t, J = 7.4 Hz, 6H, $OCH_2CH_2CH_3$).

The spectroscopic data found are in agreement with those reported in literature.[29]

N,N-diBoc-L-Lysine hydroxysuccinimide ester (ea)

In a two-neck round-bottom flask, under nitrogen flow, EDC (0.32 g, 1.69 mmol), N-hydroxysuccinimide (0.20 g, 1.74 mmol) and DIEA (0.3 mL, 1.74 mmol) were added to a solution of Boc-L-Lys(Boc)OH (0.50 g, 1.45 mmol) in 5 mL of dry DMF. The reaction was allowed to react at room temperature, monitoring it with TLC (DCM/AcOEt = 1/1, detected with ninhydrin). After 18 hours, the reaction was completed, and it was quenched with 25 mL of H_2O. The aqueous phase was extracted with AcOEt (3x20 mL). The organic phases were combined and washed with a 5% solution of citric acid, then with a saturated solution of $NaHCO_3$ and finally with brine. It was anhydrified with Na_2SO_4 and dried under reduced pressure, obtaining a white solid.

Yield = 61% (0.39 g)

^{1}H NMR (400 MHz, $CDCl_3$) δ (ppm): 5.30 – 4.97 (m, 1H, Lys-C*H*), 4.82 – 4.56 (m, 1H,), 4.46 – 4.30 (m, 1H), 3.26 – 3.03 (m, 2H, Lys-εCH_2), 2.95 – 2.73 (m, 4H, NHS- (CH_2)$_2$), 2.06 – 1.79 (m, 2H, Lys-βCH_2), 1.60 - 1.47 (m, 22 H Lys-γCH_2δCH_2 + $C(CH_3)_3$).
ESI-MS: m/z calc 443.23 oss: 466.20 [100%, M + Na]$^+$.

The spectroscopic data found are in agreement with those reported in literature.[34]

5,17-di(Boc-amino)-11,23-di[(metoxy-L-Gln)carbonyl]-25,26,27,28-tetrapropoxycalix[4]arene (7a)

In a microwave tube, L-HGlnOMe-HCl (0.31 g, 1.59 mmol) and HBTU (0.60 g, 1.59 mmol) were dissolved in 5 mL of DMF. NEt_3 (0.22 mL, 1.59 mmol) and compound **6a** (0.36 g, 0.40 mmol) were successively added. The mixture was microwaved for 90 minutes, at 150 W of power and 60 °C. Upon completion (TLC, eluent: DCM/MeOH = 96/4) the reaction was quenched with 20 mL of H_2O and the organic phase was extracted with DCM (3x10 mL). The organic phases reunited and washed with H_2O, then dried over Na_2SO_4 and evaporated under reduced pressure. Due to the complexity of the crude two chromatographic columns (eluent: DCM/MeOH = 98/2) and a preparative TLC

(eluent: DCM/AcOEt/hexane = 5/5/1) were necessary to isolate the product. A yellowish solid was obtained.

Yield = 5% (0.0205 g)

^{1}H NMR (400 MHz, CD_3OD) δ (ppm): 7.25 (s, 4H, Ar*H*-COGln), 6.78 (s, 4H, Ar*H*-NHBoc), 4.56 – 4.52 (t, J = 4.8 Hz, 2H, Gln-C*H*), 4.50 (bd, J = 13.0 Hz, 4H, H_{ax} di $ArCH_2Ar$), 3.95 (t, J = 7.4 Hz, 4H, $OCH_2CH_2CH_3$), 3.87 (t, J = 7.5 Hz, 4H, $OCH_2CH_2CH_3$), 3.72 (s, 6H, Gln-OCH_3), 3.23 (t, J = 13.2 Hz, 4H, H_{eq} di $ArCH_2Ar$), 2.37 (t, J = 7.0 Hz, 4H, Gln-$CH_2CH_2CONH_2$), 2.17 (m, 4H, Gln-$CH_2CH_2CONH_2$), 2.03 – 1.92 (m, 8H, $OCH_2CH_2CH_3$), 1.47 (s, 18H, $C(CH_3)_3$), 1.04 (bt, J = 7.4 Hz, 12H, $OCH_2CH_2CH_3$).

^{13}C NMR (101 MHz, CD_3OD) δ (ppm): 176.5 (Gln-$COOCH_3$), 172.6 (Gln-$CONH_2$), 168.7 (Ar-CO-Gln), 159.7 (Ar-CO-Gln *ipso*), 156.9 (Ar-NH-Boc *ipso*), 154.3 (CO-Boc), 152.1, 134.5, 133.0, 127.9, 127.3 - 127.2 (Ar-CO-Gln *orto*), 119.9 - 119.8 (Ar-NH-Boc *orto*), 80.2 - 79.3 ($C(CH_3)_3$), 76.8 - 76.8 ($OCH_2CH_2CH_3$), 53.0 (Gln-CH), 51.4 (Gln-OCH_3), 48.2, 48.0, 47.8, 47.6, 47.4, 47.2, 47.0, 31.6 (Gln-$CH_2CH_2CONH_2$), 30.7 - 30.7 ($ArCH_2Ar$), 27.4 - 27.2 ($C(CH_3)_3$), 26.4 (Gln-$CH_2CH_2CONH_2$), 23.1 – 23.0 ($OCH_2CH_2CH_3$), 9.4 ($OCH_2CH_2CH_3$).

ESI-MS: m/z calc 1194.61 oss: 995.13 [16%, (M -2Boc) + H]$^+$, 1095.23 [45%, (M -Boc) + H]$^+$, 1195.10 [100%, M + H]$^+$, 1217.03 [10%, M + Na]$^+$.

5,17-di[(metoxy-L-Gln)carbonyl]-11,23-dinitro-25,26,27,28-tetrapropoxycalix[4]arene (7b)

In a two-necked round-bottom flask, under nitrogen flow, compound **4** (0.21 g, 0.27 mmol) was dissolved in 25 mL of dry DCM. NEt_3 (0.3 mL, 1.92 mmol), L-HGlnOMe (0.16 g, 0.83 mmol) and HBTU (0.42 g, 1.11 mmol) were then added to the flask. The mixture was allowed to react at room temperature and monitored with TLC (eluent: DCM/AcOEt = 1/1). After 24 hours, the reaction was completed and it was quenched with 20 mL of H_2O. The organic phase was washed with 0.1 M HCl (2x5 mL) and then with water, dried over Na_2SO_4 and evaporated under reduced pressure. The product was purified by chromatographic column (DCM/MeOH = 96/4) obtaining a yellow solid.

Yield = 75% (0.22 g)

^{1}H NMR (400 MHz, CD_3OD) δ (ppm): 7.80 (s, 4H, Ar*H*-COGln), 7.12 – 7.06 (m, 4H, Ar*H*-NO_2), 4.65 (m, 2H, Gln-C*H*), 4.59 (d, *J* = 13.9 Hz, 4H, H_{ax} di $ArCH_2Ar$), 4.20 – 4.11 (m, 4H, $OCH_2CH_2CH_3$), 3.88 (t, *J* = 6.6 Hz, 4H, $OCH_2CH_2CH_3$), 3.82 (s, 6H, Gln-OCH_3), 3.46 (bd, *J* = 14.0 Hz, 4H, H_{eq} di $ArCH_2Ar$), 2.48 (t, *J* = 7.2 Hz, 4H, Gln-$CH_2CH_2CONH_2$), 2.39 – 2.11 (m, 4H, Gln-$CH_2CH_2CONH_2$), 1.98 (es, *J* = 7.5 Hz, 8H, $OCH_2CH_2CH_3$), 1.18 (t, *J* = 7.4 Hz, 6H, $OCH_2CH_2CH_3$), 0.97 (t, *J* = 7.5 Hz, 6H, $OCH_2CH_2CH_3$).

^{13}C NMR (101 MHz, CD_3OD) δ (ppm): 176.5 (Gln-*C*$OOCH_3$), 172.7 (Gln-*C*ONH_2), 168.4 (Ar-*C*O-Gln), 160.8 - 160.4 (Ar *ipso*), 142.6, 136.0, 135.9, 135.2, 128.9, 128.6 (Ar-CO-Gln *orto*), 127.9, 122.7 (Ar-NO_2 *orto*), 77.4 - 76.9 ($OCH_2CH_2CH_3$), 53.1 (Gln-*C*H), 51.4 (Gln-OCH_3), 31.4 (Gln-$CH_2CH_2CONH_2$), 30.6 ($ArCH_2Ar$), 26.4 (Gln-$CH_2CH_2CONH_2$), 23.2 - 22.9 ($OCH_2CH_2CH_3$), 9.7 - 8.8 ($OCH_2CH_2CH_3$).

ESI-MS: m/z calc 1054.45 oss: 1055.42 [100%, M + H]$^+$, 1077.40 [25%, M + Na]$^+$.

m.p. = 137-147 °C

5,17-diamino-11,23-di[(metoxy-L-Gln)carbonyl]-25,26,27,28-tetrapropoxycalix[4]arene (8)

(a) Compound **7a** (0.021 g, 0.017 mmol) was dissolved in 2 mL of DCM, then TFA (2 mL) and TES (5 μL, 0.034 mmol) were added to the solution, which was allowed to react at room temperature for 24 hours. Upon completion (TLC, DCM/MeOH eluent = 95/5, detected with ninhydrin) the reaction was quenched by drying the solvent under reduced pressure obtaining a white solid.

Yield = 100% (21.7 mg, calculated with the PM of the compound as trifluoroacetate salt)

^{1}H NMR (400 MHz, CD_3OD) δ (ppm): 7.54 (m, 4H, Ar*H*-COGln), 6.46 (m, 4H, Ar*H*-NH_2), 4.57 (d, *J* = 13.6 Hz, 4H, H_{ax} di $ArCH_2Ar$), 4.57 (m, 2H, Gln-C*H*), 4.09 (t, *J* = 7.8 Hz, 4H, $OCH_2CH_2CH_3$), 3.86 (t, *J* = 7.0 Hz, 4H, $OCH_2CH_2CH_3$), 3.78 (s, 6H, Gln-OCH_3), 3.37 (bd, *J* = 13.8 Hz, 4H, H_{eq} di $ArCH_2Ar$), 2.43 (t, J = 6.9 Hz, 4H, Gln-$CH_2CH_2CONH_2$), 2.32 – 2.12 (m, 4H, Gln-$CH_2CH_2CONH_2$), 2.04 – 1.94 (m, 8H, $OCH_2CH_2CH_3$), 1.13 (t, *J* = 7.4 Hz, 6H, $OCH_2CH_2CH_3$), 1.01 (t, *J* = 7.5 Hz, 6H, $OCH_2CH_2CH_3$).

^{13}C NMR (101 MHz, CD_3OD) δ (ppm): 176.7 (Gln-*C*$OOCH_3$), 172.5 (Gln-*C*ONH_2), 168.2 (Ar-*C*O-Gln), 160.34 - 159.8 (Ar *ipso*), 155.1, 135.9, 135.6, 128.1 (Ar-CO-Gln *orto*), 127.5, 121.4 - 121.2 (Ar-NH_2 *orto*), 77.2 – 77.0 ($OCH_2CH_2CH_3$), 53.0 (Gln-*C*H), 51.4 (Gln-OCH_3), 31.4 (Gln-$CH_2CH_2CONH_2$), 30.5 ($ArCH_2Ar$), 26.3 (Gln-$CH_2CH_2CONH_2$), 23.1 - 23.0 ($OCH_2CH_2CH_3$), 9.6 - 9.0 ($OCH_2CH_2CH_3$).

ESI-MS: m/z calc 994.51 oss: 995.45 [100%, M + H]$^+$, 1017.57 [50%, M + Na]$^+$.

m.p. > 150 °C (decomposition).

b) In a PARR reactor, compound **7b** (0.22 g, 0.21 mmol) was dissolved in 5 mL of EtOH and a catalytic amount of Pd/C (10%) was then added. It was allowed to react with an H2 pressure of 3 bar. The reaction was checked with TLC (eluent DCM/MeOH = 95/5, detected with ninhydrin). The reaction was completed after 24 hours and the catalyst was removed by filtration. After drying, a yellowish solid was obtained. Even if the purity of the product was not satisfactory, a chromatographic separation was not conducted

because of the presence of the free amine species which would hamper elution on silica gel.

5,17-di[(Boc-L-Lys(Boc))amino]-11,23-di[(metoxy-L-Gln)carbonyl]-25,26,27,28-tetrapropoxycalix[4]arene (9)

In a two-necked round-bottom flask, under nitrogen flow, compound **8** (0.022 g, 0.022 mmol) was dissolved in 5 mL of dry DCM. NEt_3 (0.02 mL, 0.15 mmol), Boc-L-Lys(Boc)OH (0.023 g, 0.065 mmol) and HBTU (0.033 g, 0.087 mmol) were then added to the flask and the mixture was stirred for 16 hours. Upon completion (TLC, eluent: DCM/AcOEt = 1/1) the reaction was quenched with 20 mL H_2O. The aqueous phase was extracted with DCM (3x5 mL), the organic phases were combined, washed with water, dried over Na_2SO_4 and evaporated under reduced pressure. The product was isolated by chromatographic separation (DCM/MeOH = 96/4) obtaining a colorless resin.

Yield = 36% (0.011 g)

^{1}H NMR (400 MHz, CD_3OD) δ (ppm): 7.43 (m, 2H, Ar*H*-COGln), 7.25 (m, 2H, Ar*H*-COGln), 7.11 – 6.90 (m, 2H, Ar*H*-NHLys), 6.56 (s, 2H, Ar*H*-NHLys), 4.55 (m, 2H, Gln-C*H*), 4.54 (d, *J* = 12.7 Hz, 4H, H_{ax} di $ArCH_2Ar$), 4.03 (t, J = 7.6 Hz, 4H, $OCH_2CH_2CH_3$), 4.00 (m, 2H, Lys-C*H*), 3.84 (t, J = 7.2 Hz, 4H, $OCH_2CH_2CH_3$), 3.75 (m, 6H, Gln-OCH_3), 3.29 (d, *J* = 13.3 Hz, 4H, H_{eq} di $ArCH_2Ar$), 3.02 (t, *J* = 6.4 Hz, 4H, Lys-εCH_2NHBoc), 2.39 (t, *J* = 7.3 Hz, 4H, Gln-$CH_2CH_2CONH_2$), 2.31 – 2.07 (m, 4H, Gln-$CH_2CH_2CONH_2$), 1.99 (es, J = 7.6 Hz, 8H, $OCH_2CH_2CH_3$), 1.85 – 1.55 (m, 4H, Lys-βCH_2), 1.51 (hm, 4H, Lys-δCH_2), 1.46 (m, 36H, $C(CH_3)_3$), 1.40 – 1.26 (m, 4H, Lys-γCH_2), 1.17 – 0.92 (m, 12H, $OCH_2CH_2CH_3$).

^{13}C NMR (101 MHz, CD_3OD) δ (ppm): 176.4 (Gln-*C*$OOCH_3$), 172.5 (Gln-*C*ONH_2), 172.0 (Ar-NH*C*O-Lys), 168.3 (Ar-*C*O-Gln), 160.2 (Ar-CO-Gln *ipso*), 157.1 – 156.8 (*C*O-Boc), 153.0 (Ar-NHCO-Lys *ipso*), 135.6 - 135.34, 134.1 - 134.0, 131.9, 127.1, 127.9 – 127.8 (Ar-CO-Gln *orto*), 121.8 – 120.6 (Ar-NH-Lys *orto*), 76.9 ($OCH_2CH_2CH_3$), 55.2 (Lys-*C*H), 53.0 (Gln-*C*H), 51.4 (Gln-OCH_3), 39.7 (Lys-εCH_2NHBoc), 31.7 (Lys-βCH_2), 31.6 (Gln-$CH_2CH_2CONH_2$), 30.8 – 30.7 ($ArCH_2Ar$), 29.3 (Lys-δCH_2), 27.5 ($C(CH_3)_3$), 26.4 (Gln-$CH_2CH_2CONH_2$), 23.1 – 23.0 ($OCH_2CH_2CH_3$), 22.9 (Lys-γCH_2), 9.6 - 9.2 ($OCH_2CH_2CH_3$).

ESI-MS: m/z calc 1650.90 oss: 1352.85 [18%, (M-3Boc) + 2H]$^+$, 1451.93 [38%, (M-2Boc) + H]$^+$, 1551.95 [100%, (M-Boc) + H]$^+$, 1652.03 [46%, M + H]$^+$, 1674.07 [56%, M + Na]$^+$, 1690.00 [13%, M + K]$^+$.

5,17-di[(L-Lys)amino]-11,23-di[(metoxy-L-Gln)carbonyl]-25,26,27,28-tetrapropoxycalix[4]arene (10)

In a round-bottom flask, compound **9** (0.039 g, 0.023 mmol) was dissolved in 3 mL of DCM, then TFA (2 mL) and TES (19 µL, 0.16 mmol) were added. The mixture was allowed to react at room temperature and monitored with TLC (DCM/MeOH eluent = 9/1, detected with ninhydrin). The reaction was quenched after 24 hours by drying under reduced pressure. A pale orange-coloured solid was obtained.

Yield = 100% (39.25 mg)

^{1}H NMR (400 MHz, CD_3OD) δ (ppm): 7.44 (m, 2H, Ar*H*-NHLys), 6.87 (m, 4H, Ar*H*-COGln), 4.52 (dd, *J* = 13.1 Hz, 4H, H_{ax} di $ArCH_2Ar$), 4.45 (m, 2H, Gln-C*H*), 4.07 (t, J = 7.6 Hz, 4H, $OCH_2CH_2CH_3$), 4.02 (t, J = 6.5 Hz, 2H, Lys-C*H*), 3.76 (t, J = 6.8 Hz, 4H, $OCH_2CH_2CH_3$), 3.67 (s, 6H, Gln-OCH_3), 3.24 (dd, *J* = 13.5 Hz, 4H, H_{eq} di $ArCH_2Ar$), 2.97 (m, 4H, Lys-εCH_2NH_2), 2.30 (m, 4H, Gln-$CH_2CH_2CONH_2$), 2.30 – 2.05 (m, 4H, Gln-$CH_2CH_2CONH_2$), 2.02 (hm, 4H, Lys-βCH_2), 2.06 - 1.89 (m, J = 7.2 Hz, 8H, $OCH_2CH_2CH_3$), 1.75 (m, 4H, Lys-δCH_2), 1.58 (bm, 4H, Lys-γCH_2), 1.13 (t, J = 7.4 Hz, 6H, $OCH_2CH_2CH_3$), 0.95 (t, J = 7.5 Hz, 6H, $OCH_2CH_2CH_3$).

^{13}C NMR (101 MHz, CD_3OD) δ (ppm): 176.9 (Gln-$COOCH_3$), 172.5 (Gln-$CONH_2$), 168.1 (Ar-*C*O-Gln), 166.7 (Ar-NH*C*O-Lys), 158.7 (Ar-CO-Gln *ipso*), 154.3 (Ar-NHCO-Lys *ipso*), 136.5, 133.6 – 133.3, 131.8, 127.4 – 126.7, 127.1 (Ar-CO-Gln *orto*), 121.4 – 121.0 (Ar-NH-Lys *orto*), 77.3 – 76.6 ($OCH_2CH_2CH_3$), 53.5 (Lys-*C*H), 52.9 (Gln-*C*H), 51.3 (Gln-OCH_3), 38.9 (Lys-εCH_2NH_2), 31.7 (Gln-$CH_2CH_2CONH_2$), 30.8 (Lys-βCH_2), 30.6 ($ArCH_2Ar$), 26.8 (Lys-δCH_2), 26.3 (Gln-$CH_2CH_2CONH_2$), 23.2 – 22.3 ($OCH_2CH_2CH_3$), 21.6 (Lys-γCH_2), 9.8 – 8.9 ($OCH_2CH_2CH_3$).

ESI-MS: m/z calc 1250.70 oss: 626.47 [50%, M + H]$^{2+}$, 648.54 [100%, M + Na]$^{2+}$, 1251.60 [39%, M + H]$^{+}$, 1253.54 [61%, M + Na]$^{+}$.

m.p. > 200 °C (decomposition).

5,17-di[(L-Lys)amino]-11,23-di[(L-Gln)carbonyl]-25,26,27,28-tetrapropoxycalix[4]arene (11)

In a round-bottom flask, compound **10** (0.010 g, 0.0056 mmol) was dissolved in 2 mL of freshly distilled THF. LiOH monohydrate (1.43 mg, 0.034 mmol) was dissolved separately in the minimal amount of water and poured into the flask. is the mixture was left to react at room temperature. After 24 hours, the reaction was completed (TLC, DCM/MeOH = 1/1) and it was quenched by drying under reduced pressure. A yellowish solid was obtained.

Yield = 100% (10.5 mg)

^{1}H NMR (400 MHz, CD_3OD) δ (ppm): 7.71 – 7.65 (m, 2H, Ar*H*-NHLys), 6.45 – 6.35 (m, 4H, Ar*H*-COGln), 4.55-4.35 (m, 6H, H_{ax} di $ArCH_2Ar$, Gln-C*H*), 4.14 – 4.06 (m, 4H,

OC*H*$_2$CH$_2$CH$_3$), 4.02 (t, J = 6.5 Hz, 2H, Lys-C*H*), 3.76 (t, J = 6.8 Hz, 4H, OC*H*$_2$CH$_2$CH$_3$), 3.24 (m, 4H, H_{eq} di ArCH$_2$Ar), 2.90 – 2.72 (m, 4H, Lys-εC*H*$_2$NH$_2$), 2.50 – 0.6 (m, 40H, Gln-CH$_2$C*H*$_2$CONH$_2$, Gln-C*H*$_2$CH$_2$CONH$_2$, Lys-βC*H*$_2$, OCH$_2$C*H*$_2$CH$_3$, Lys-δC*H*$_2$, Lys-γC*H*$_2$, OCH$_2$CH$_2$C*H*$_3$). ESI-MS: m/z calc 1222.66 oss: 612.47 [29%, M + H]$^{2+}$, 632.68 [100%, (M-2H) + Na]$^{2+}$, 1223.37 [13%, M + H]$^+$, 1245.51 [30%, M + Na]$^+$, 1263.67 [100%, (M + 2H) + K]$^+$.

m.p. > 200 °C (decomposition).

5,11,17,23-tetraterz-butyl-25,26,27,28-tetrapropoxycalix[4]arene (12)

In a two-necked round-bottom flask, under nitrogen flow, tetraterz-butyl-tetrahydroxycalix[4]arene (10.0 g, 15.41 mmol) was dissolved in 175 mL of dry DMF. NaH 60% (4.93 g, 123.28 mmol) was then added and allowed to react under magnetic stirring at room temperature for 30 minutes. n-IPr (4.93 mL, 123.28 mmol) was then added and allowed to react under mechanical stirring at room temperature. The reaction was monitored by TLC (hexane/ethyl acetate 7:3, with $FeCl_3$ detector) and upon completion the reaction mixture was treated with 1N HCl solution and the product was cold filtered. A pale-yellow solid was obtained. The product was purified by recrystallization with methanol which yielded a white powdery solid in 95% yield (11.99 g).

^{1}H NMR (400 MHz, $CDCl_3$) δ 6.77 (s, 8H, ArH), 4.41 (d, *J* = 12.4 Hz, 4H, ArCH_{ax}H$_{eq}$Ar), 3.81 (t, *J* =7.6 Hz, 8H, OC*H*$_2$CH$_2$CH$_3$), 3.11 (d, *J* = 12.5 Hz, 4H, ArCH$_{ax}$$H_{eq}$Ar), 2.02 (q, *J* = 7.6 Hz, 8H, OCH$_2$C*H*$_2$CH$_3$), 1.07 (s, 36H, C(C*H*$_3$)$_3$), 0.99 (t, *J* = 7.5 Hz, 12H, OCH$_2$CH$_2$C*H*$_3$).

The spectroscopic data found are in agreement with those reported in literature.[43]

5,11,17,23-tetranitro-25,26,27,28-tetrapropoxycalix[4]arene (13)

In a round-bottom flask, compound **12** (11.99 g, 14.68 mmol) was dissolved in 110 mL of DCM. The sulphonitric mixture, previously prepared by adding 3.91 mL of H_2SO_4 (74.3 mmol) to 5.12 mL of HNO_3 65% (74.3 mmol) in an Erlenmeyer flask, was then slowly added into the flask. Upon addition, the solution first turned yellow and then switched to an increasingly intense violet. It was allowed to react under magnetic stirring at room temperature. The reaction was monitored by TLC (DCM eluent) and after 4 days, the reaction was completed. The reaction mixture was then quenched with H_2O. The organic phase was extracted, washed with H_2O to neutrality and then anhydrified with Na_2SO_4. The solvent was evaporated under reduced pressure obtaining a red solid. The product was then recrystallized with methanol to obtain product **13** (yellow/orange solid) in 75% yield.

^{1}H NMR (400 MHz, $CDCl_3$) δ 7.57 (s, 8H, ArH), 4.53 (d, *J* = 14.0 Hz, 4H, ArCH_{ax}H$_{eq}$Ar), 3.96 (t, *J* = 7.5 Hz, 8H, OCH_2CH$_2$CH$_3$), 3.40 (d, *J* = 14.0 Hz, 4H, ArCH$_{ax}H_{eq}$Ar), 1.91 (h, *J* = 7.5 Hz, 8H, OCH$_2CH_2$CH$_3$), 1.02 (t, *J* = 7.5, 12H, OCH$_2$CH$_2CH_3$).

The spectroscopic data found are in agreement with those reported in literature.[43]

5,11,17,23-tetramino-25,26,27,28-tetrapropoxycalix[4]arene (**14**)

Compound **13** (8.45 g, 10.936 mmol), hydrazine monohydrate (21.25 mL, 437.44 mmol) and a catalytic amount of Pd/C are introduced in a two-necked round-bottom flask filled with 50 mL of EtOH. The mixture was allowed to react under magnetic stirring at reflux. The reaction was monitored by TLC (DCM eluent, with ninhydrin detector), and after 19 hours, the reaction was completed. The catalyst was then removed by filtration and the solvent evaporated under reduced pressure. Then the reaction mixture was dissolved in DCM, which was then treated with H_2O. The organic phase was extracted, dried over Na_2SO_4 and the solvent evaporated under reduced pressure. Product **14** (yellowish-white solid) was obtained with a yield of 88% (6.29 g).

^{1}H NMR (400 MHz, CD_3OD) δ 6.12 (s, 8H, ArH), 4.33 (d, *J* = 13.1 Hz, 4H, ArCH_{ax}H$_{eq}$Ar), 3.73 (t, *J* = 7.4 Hz, 8H, OCH_2CH$_2$CH$_3$), 2.91 (d, *J* = 13.2 Hz, 4H, ArCH$_{ax}H_{eq}$Ar), 1.88 (h, *J* = 7.4 Hz, 8H, OCH$_2CH_2$CH$_3$), 0.99 (t, *J* = 7.5 Hz, 12H, OCH$_2$CH$_2CH_3$).

The spectroscopic data found are in agreement with those reported in literature.[43]

5,11-di(Boc-ammino)-17,23-diammino-25,26,27,28-tetrapropoxycalix[4]arene (**15**)

In a two-necked round-bottom flask, under nitrogen flow, compound **14** (0.600 g, 0.925 mmol) was dissolved in 60 mL of dry DCM. Boc_2O (0.404 g, 1.85 mmol) previously dissolved in 10 mL of dry DCM was then added to the mixture. After 19 hours of stirring at room temperature, the reaction is completed (TLC, hexane/ethyl acetate 1:1). The solvent was evaporated under reduced pressure. The product was purified by column chromatography, using hexane/ethyl acetate 1:1 as eluent, obtaining a yellowish solid in 39% yield (0.306 g).

^{1}H NMR (400 MHz, $CDCl_3$) δ 7.06 (s, 2H, CONH), 6.62 (s, 2H, ArH), 6.44 (s, 2H, ArH), 6.10 (s, 2H, ArH), 4.41 – 4.26 (m, 4H, ArCH_{ax}H$_{eq}$Ar), 3.79-3.65 (m, 8H, OCH_2CH$_2$CH$_3$), 3.07 (d, *J* = 13.7 Hz, 1H, ArCH$_{ax}H_{eq}$Ar), 3.01 (d, *J* = 13.7 Hz, 2H, ArH), 2.92 (d, *J* = 13.0 Hz, 1H, ArH), 1.90 – 1.76 (m, 8H, OCH$_2CH_2$CH$_3$), 1.47 (s, 18H, C(CH$_3$)$_3$), 0.94 (t, *J* = 7.4 Hz, 12H, OCH$_2$CH$_2CH_3$).

^{13}C NMR (101 MHz, $CDCl_3$) δ 154.2, 153.8, 150.3, 139.6, 135.9, 135.8, 135.7, 135.5, 131.7, 122.3 (Ar*H*), 115.8 (Ar*H*), 115.7 (Ar*H*), 79.6 (*C*(CH$_3$)$_3$), 76.5 (OCH_2CH$_2$CH$_3$), 31.1 (ArCH$_2$Ar), 28.5 (C(CH$_3$)$_3$), 23.1 (OCH$_2CH_2$CH$_3$), 10.3 (OCH$_2$CH$_2CH_3$).

ESI-MS: m/z calc 853.11, oss: 653.26 [100%,M+H-2Boc]$^+$, 753,35 [61%, M+H-Boc]$^+$, 853,42 [41%, M+H]$^+$

Attempt to synthesize 5,17-di(Fmoc-ammino)-11,23-diammino-25,26,27,28-tetrapropoxycalix[4]arene (15a)

In a two-necked round bottom flask, under nitrogen flow, **14** (0.100 g, 0.153 mmol) was dissolved in 10 mL of dry DCM, then Fmoc-Cl (0.079 g, 0.306 mmol), dissolved in 1 mL of dry DCM, was added to the solution. The reaction was allowed to proceed under mechanical agitation at room temperature. The reaction was monitored by TLC (eluent hexane/ethyl acetate 1:1). After 21 hours, the reaction was complete. The solvent was evaporated under reduced pressure. A mixture of products that impossible to purify was obtained.

Attempt to synthesize 5,17-di(Cbz-ammino)-11,23-diammino-25,26,27,28-tetrapropoxycalix[4]arene (15b)

In a two-necked round bottom flask, under nitrogen flow, **14** (0.100 g, 0.153 mmol) was dissolved in 10 mL of dry DCM, then Cbz-Cl 50% in toluene (0.104 g, 0.306 mmol), was added to the solution. The reaction was allowed to proceed under mechanical agitation at room temperature. The reaction was monitored by TLC (eluent hexane/ethyl acetate 1:1). After 21 hours, the reaction was complete. The solvent was evaporated under reduced pressure. A mixture of products that impossible to purify was obtained.

Attempt to synthesize 5,17-di(Trt-ammino)-11,23-diammino-25,26,27,28-tetrapropoxycalix[4]arene (15c)

In a two-necked round bottom flask, under nitrogen flow, **14** (0.100 g, 0.153 mmol) was dissolved in 6 mL of dry DCM, then Trt-Cl (0.094 g, 0.337 mmol), was dissolved in 3 mL of dry DCM and added to the solution. The reaction was allowed to proceed under mechanical agitation at room temperature for 6 hours. Net_3 (0.17 mL) was then added and after 2 hours another portion of Trt-Cl (0.043 g, 0.153 mmol) was added too. The reaction was monitored by TLC (eluent hexane/ethyl acetate 1:1). After 6 hours from the last addition, the reaction was complete. The solvent was evaporated under reduced pressure. A mixture of products that impossible to purify was obtained.

5,11-di(Boc-amino)-17,23-di[(acid-Fmoc-ε-aminohexanoyl)amino]-25,26,27,28-tetrapropoxycalix[4]arene (16)

In a microwave vial, compound **15** (0.389 g, 0.456 mmol), HBTU (0.692 g, 1.824 mmol), Fmoc-6Ahx-OH (0.483 g, 1.368 mmol) and NEt_3 (0.127 mL, 0.912 mmol) were solubilized in 3 mL of dry DMF. The mixture was microwaved at 60°C, 150W in dynamic power mode for 1h. The reaction was monitored by TLC (ethyl acetate eluent, with ninhydrin detector), and by ESI-MS. DCM and H_2O were added to the mixture. The organic phase was then extracted, washed with H_2O to neutrality and then dried over with Na_2SO_4. The solvent was evaporated under reduced pressure. Product **16** (yellowish glassy solid) was isolated by column chromatography, using DCM/ethyl acetate 2:8 as eluent, with a yield of 86% (0.603g).

^{1}H NMR (400 MHz, CD_3OD) δ 7.75 (d, J = 7.6 Hz, 4H, FmocArH), 7.60 (d, J = 7.5 Hz, 4H, FmocArH), 7.41 – 7.21 (m, 8H, FmocArH), 6.86 (s, 4H, ArH), 6.67 (s, 4H, ArH), 4.40 (d, J = 13.1 Hz, 4H, ArC$H_{ax}$$H_{eq}$Ar), 4.29 (d, J = 7.0 Hz, 4H, OCH_2CH), 4.14 (t, J = 7.0 Hz, 2H, OCH_2CH), 3.85 – 3.70 (m, 8H, OC$H_2$$CH_2CH_3$), 3.16 – 2.97 (m, 8H, NHCH_2, Ar$CH_{ax}H_{eq}$Ar), 2.27 (t, J = 7.4 Hz, 4H, COCH_2), 1.99-1.81 (m, 8H, $OCH_2CH_2CH_3$), 1.70-1.56 (m, 4H, $COCH_2CH_2$), 1.56-1.18 (m, 26H, $NHCH_2CH_2$, $NHCH_2CH_2CH_2$, $C(CH_3)_3$), 0.99 (td, J = 7.5, 4.9 Hz, 12H, $OCH_2CH_2CH_3$).

^{13}C NMR (101 MHz, CD_3OD) δ 172.7 ($NHCOCH_2$), 157.5, 154.4, 153.1, 152.3, 143.9, 141.2, 134.8, 132.6, 132.2, 127.4 (FmocArH), 126.7 (FmocArH), 124.8 (FmocArH), 120.6 (ArH), 119.8 (ArH), 119.5 (FmocArH), 79.2 ($C(CH_3)_3$), 76.6 ($OCH_2CH_2CH_3$), 66.2 (OCH_2CH), 48.5 (OCH_2CH), 40.2 (NHCH_2), 36.3 (COCH_2), 30.7 (ArCH_2Ar), 29.2 ($NHCH_2CH_2$), 27.4 ($C(CH_3)_3$), 25.9 ($NHCH_2CH_2CH_2$), 25.1 ($COCH_2CH_2$), 22.9 ($OCH_2CH_2CH_3$), 9.4 ($OCH_2CH_2CH_3$).

ESI-MS: m/z calc 1522.81 oss: 1523.94 $[100\%, M+H]^+$

5,11-diamino-17,23-di[(acid-Fmoc-ε-aminohexanoyl)amino]-25,26,27,28-tetrapropoxycalix[4]arene (17)

In a round-bottom flask, compound **16** (0.647 g, 0.425 mmol) and TES (0.2 mL) were dissolved in DCM (1 mL), then TFA (2 mL) was added. The reaction was allowed to proceed under mechanical stirring at room temperature for 24 hours, then upon completion (TLC, eluent DCM/ethyl acetate 1:1) the solvent was evaporated under reduced pressure. The solid obtained was dissolved in DCM and washed with H_2O until neutral pH. Product **17** (orange glassy solid) was obtained in a quantitative yield (0.55 g).

^{1}H NMR (400 MHz, CD_3OD) δ 7.78 (d, *J* = 7.5 Hz, 4H, FmocArH), 7.63 (d, *J* = 7.5 Hz, 4H, FmocArH), 7.33 (dt, *J* = 34.2, 7.5 Hz, 8H, FmocArH), 6.79 (s,2H, ArH), 6.67 (s, 2H, ArH), 6.16 (s, 4H, ArH), 4.58 – 4.26 (m, 8H, Ar$CH_{ax}H_{eq}$Ar, OCH_2CH), 4.17 (t, *J* = 7.0 Hz, 2H,

OCH_2CH), 3.92 – 3.64 (m, 8H, $OCH_2CH_2CH_3$), 3.19 – 2.85 (m, 8H, $ArCH_{ax}H_{eq}Ar$, $NHCH_2$), 2.26 (t, *J* = 7.6 Hz, 4H, $COCH_2$), 2.02 – 1.78 (m, 8H, $OCH_2CH_2CH_3$), 1.73 – 1.25 (m, 12H, $COCH_2CH_2$, $NHCH_2CH_2CH_2$, $NHCH_2CH_2$), 1.16 – 0.86 (m, 12H, $OCH_2CH_2CH_3$).

^{13}C NMR (101 MHz, CD_3OD) δ 173.1 ($NHCOCH_2$), 157.5, 153.8, 150.3, 143.9, 141.2, 135.5, 135.1, 131.8, 127.4 (FmocArH), 126.7 (FmocArH), 124.8 (FmocArH), 122.2 (ArH), 121.9 (ArH), 119.5 (FmocArH), 116.5 (ArH), 116.3 (ArH), 76.5 ($OCH_2CH_2CH_3$), 66.2 (OCH_2CH), 40.2 ($NHCH_2$), 36.0 ($COCH_2$), 30.7 ($ArCH_2Ar$), 29.1 ($NHCH_2CH_2$), 25.9 ($NHCH_2CH_2CH_2$), 25.1 ($COCH_2CH_2$), 23.0 ($OCH_2CH_2CH_3$), 22.9 ($OCH_2CH_2CH_3$), 9.4 ($OCH_2CH_2CH_3$), 9.4 ($OCH_2CH_2CH_3$).

ESI-MS: m/z calc 1323.69 oss: 1101.65 [22%,M+H-Fmoc]$^+$, 1324.67 [100%, M+H]$^+$

δ-(2,3-diBoc)guanidinopentanoic acid (19)

In a round-bottom flask, δ-aminopentanoic acid (0.300 g, 2.561 mmol) was suspended in NEt_3(0.5 mL). Then a solution of bisBoc-triflilguanidine (1.00 g, 2.561 mmol) and NEt_3 (0.1 mL) in DCM (1 mL) was slowly added to the mixture. The reaction proceeded at room temperature and was monitored by TLC (eluent hexane/ethyl acetate 1:1 + 0.4% acetic acid). After 26 hours, the reaction was completed. The mixture was then treated with a saturated $NaHCO_3$ solution. The organic phase was extracted, washed with H_2O to neutrality and then dried over Na_2SO_4. The solvent was evaporated under reduced pressure. Product **19** was purified by column chromatography, using 1:1 hexane/ethyl acetate + 0.4 % acetic acid as eluent, with a yield of 37 % (0.339 g).

^1H NMR (400 MHz, CD_3OD) δ 3.38 (t, *J* = 6.5 Hz, 2H, CH_2COOH), 2.35 (t, *J* = 6.9 Hz, 2H, NCH_2), 1.73-1.57 (m, 4H, CH_2CH_2COOH, NCH_2CH_2), 1.53 (9H, $C(CH_3)_3$) 1.47 (9H, $C(CH_3)_3$).

The spectroscopic data found are in agreement with those reported in literature.[44]

5,11-di[(acid-diBoc-δ-guanidinopentanoyl)ammino]-17,23-di[(acid-Fmoc-ε-aminohexanoyl)amino]-25,26,27,28-tetrapropoxycalix[4]arene (18)

In a microwave vial, compound **17** (0.202 g, 0.105 mmol), HBTU (0.230 g, 0.608 mmol), 6a (0.238 g, 0.661 mmol) and NEt_3 (0.07 mL) were solubilized in dry DMF. The mixture was microwaved at 60°C, 150W in dynamic power mode for 1h. The reaction was monitored by TLC (DCM/ethyl acetate 1:1, with ninhydrin detector), then quenched by the addition of DCM and H_2O. The organic phase was then extracted, washed with H_2O to neutrality and then dried over Na_2SO_4. The solvent was evaporated under reduced pressure and the product purified by column chromatography, using DCM/ethyl acetate 1:1 as eluent, with a yield of 12% (0.037 g).

^{1}H NMR (400 MHz, CD_3OD) δ 7.76 (d, *J* = 7.5 Hz, 4H, FmocArH), 7.61 (d, *J* = 7.4 Hz, 4H, FmocArH), 7.40-7.21 (m, 8H, FmocArH), 6.96-6.82 (m, 8H, ArH), 4.52-4.35 (m, 4H, ArC$H_{ax}$$H_{eq}$Ar), 4.30 (d, *J* = 6.9 Hz, 4H, OCH_2CH), 4.15 (t, *J* = 7.0 Hz, 2H, OCH_2CH), 3.89-3.75 (m, 8H, O$CH_2CH_2CH_3$), 3.41 – 3.33 (m, 4H, CNCH_2), 3.15 – 3.02 (m, 8H, NHCH_2,Ar$CH_{ax}$$H_{eq}$Ar), 2.35-2.13 (m,8H, $NHCH_2CH_2CH_2CH_2CH_2$, $CNCH_2CH_2CH_2CH_2$), 2.03 – 1.86 (m, 8H, $OCH_2CH_2CH_3$), 1.74 – 1.24 (m, 60H, $CNCH_2CH_2$, $CNCH_2CH_2CH_2$, $NHCH_2CH_2$, $NHCH_2CH_2CH_2CH_2$, $NHCH_2CH_2CH_2$, $C(CH_3)_3$), 1.00 (m, 12H, $OCH_2CH_2CH_3$).

^{13}C NMR (101 MHz, CD_3OD) δ 172.5, 172.2, 163.2, 157.5, 156.2, 153.0, 152.8, 143.9, 141.2, 134.8, 132.3, 127.4 (FmocArH), 126.8 (FmocArH), 124.8 (FmocArH), 120.6 (ArH), 119.6 (FmocArH), 83.1, 78.9 ($C(CH_3)_3$), 76.7 (O$CH_2CH_2CH_3$), 66.2 (OCH_2CH), 40.2 (NHCH_2), 40.1 (CNCH_2), 36.3-35.8 ($NHCH_2CH_2CH_2CH_2$, $CNCH_2CH_2CH_2CH_2$), 30.7 (ArCH_2Ar), 29.3 ($NHCH_2CH_2$), 28.3 ($CNCH_2CH_2$), 27.2 ($C(CH_3)_3$), 26.8 ($C(CH_3)_3$), 26.0 ($NHCH_2CH_2CH_2$), 25.1 ($NHCH_2CH_2CH_2CH_2$), 23.0 ($OCH_2CH_2CH_3$), 22.6 ($CNCH_2CH_2CH_2$), 9.4 ($OCH_2CH_2CH_3$).

ESI-MS: m/z calc 2006.50 oss: 803.97 [100%, M+H-4Boc]$^{2+}$, 854.03 [16%, M+H-3Boc] $^{2+}$, 904.07 [14%, M+H-2Boc] $^{2+}$, 1004.18 [9%, M+H] $^{2+}$, 1907.02 [0.61%, M+H-Boc]$^{+}$

5,11-di[(acid-diBoc-δ-guanidinopentanoyl)amino]-17,23-di[(acid-ε-aminohexanoyl)amino]-25,26,27,28-tetrapropoxycalix[4]arene (**20**)

Compound **18** (0.051 g, 0.025 mmol) was dissolved in a 20% solution of piperidine in dry DCM and left under magnetic stirring at room temperature. The reaction was monitored by TLC (DCM/ethyl acetate 3:7, with Ninhydrin detector) and after 2 hours, it was completed. The solvent was evaporated under reduced pressure. The solid obtained was triturated in diethylether and then in water. Product **20** (yellow glassy solid) was obtained with a 62% (0.0247 g) yield.

^{1}H NMR (400 MHz, CD_3OD) δ 7.04 – 6.76 (m, 8H, ArH), 4.46 (d, *J* = 13.7 Hz, 4H, ArC$H_{ax}$$H_{eq}$Ar), 3.93 – 3.71 (m, 8H, O$CH_2CH_2CH_3$), 3.44-3.33 (m, 4H, $CNCH_2$), 3.21 – 3.03 (m, 4H, Ar$CH_{ax}$$H_{eq}$Ar), 2.93 (t, *J* = 7.6 Hz, 4H, NHCH_2), 2.35-2.20 (m, 8H, $NHCH_2CH_2CH_2CH_2CH_2$, $CNCH_2CH_2CH_2CH_2$), 2.05-1.90 (m, 8H, $OCH_2CH_2CH_3$), 1.85-1.74 (m, 4H, $NHCH_2CH_2CH_2CH_2$) 1.74– 1.55 (m, 16H, $CNCH_2CH_2$, $CNCH_2CH_2CH_2$, $NHCH_2CH_2$, $NHCH_2CH_2CH_2$), 1.55 – 1.33 (m, 36H, $C(CH_3)_3$), 1.02 (t, *J* = 7.4 Hz, 12H, $OCH_2CH_2CH_3$).

^{13}C NMR (101 MHz, CD_3OD) δ 172.2, 163.2, 156.2, 153.0, 152.8, 134.8, 132.3, 120.6 (ArH), 83.1, 79.0 ($C(CH_3)_3$), 76.8 (O$CH_2CH_2CH_3$), 44.4, 40.1 ($CNCH_2$), 39.2 (NHCH_2), 35.9 ($NHCH_2CH_2CH_2CH_2CH_2$, $CNCH_2CH_2CH_2CH_2$), 30.8 (ArCH_2Ar), 28.4 ($CNCH_2CH_2$), 27.3 ($C(CH_3)_3$), 27.0 ($C(CH_3)_3$), 26.9 ($C(CH_3)_3$), 26.9 ($C(CH_3)_3$), 25.6 ($NHCH_2CH_2CH_2$), 24.8 ($NHCH_2CH_2CH_2CH_2$), 23.0 ($OCH_2CH_2CH_3$), 22.7 ($CNCH_2CH_2$), 22.4 ($CNCH_2CH_2CH_2$), 9.4 ($OCH_2CH_2CH_3$).

ESI-MS: m/z calc 1562.02 oss: 581.52 [100%, M+H-4Boc]$^{2+}$, 1564.14 [5%, M+H]$^{+}$, 1585.09 [9%, M+Na]$^{+}$

5,11-di[(acid-δ-guanidinopentanoyl)amino]-17,23-di[(acid-ε-aminohexanoyl)amino]-25,26,27,28-tetrapropoxycalix[4]arene (21)

TFA (0.5 mL) was added to a solution of compound **20** (0.0247 g, 0.0158 mmol) and TES (0.1 mL) in DCM (1 mL). The reaction was stirred at room temperature for 24 hours and upon completion (TLC, DCM/methanol eluent 9:1, with ninhydrin detector) the solvent was evaporated under reduced pressure. Product **21** (a yellowish glassy solid) was obtained in a quantitative yield (17 mg).

^{1}H NMR (400 MHz, CD_3OD) δ 6.99 – 6.76 (m, 8H, ArH), 4.47 (d, J = 13.1 Hz, 4H, Ar$CH_{ax}H_{eq}$Ar), 3.92-3.76 (m, 8H, O$CH_2$$CH_2CH_3$), 3.24 – 3.02 (m, 8H, CNCH_2, Ar$CH_{ax}H_{eq}$Ar), 2.92 (t, J = 7.7 Hz, 4H, NHCH_2), 2.36-2.28 (m, 8H $NHCH_2CH_2CH_2CH_2CH_2$, $CNCH_2CH_2CH_2CH_2$), 2.05-1.86 (m, 8H, O$CH_2CH_2CH_3$), 1.83-1.53 (m, 16H, $NHCH_2CH_2CH_2CH_2$, $CNCH_2CH_2$, $CNCH_2CH_2CH_2$, $NHCH_2CH_2$), 1.50 – 1.36 (m, 4H, $NHCH_2CH_2CH_2$), 1.03 (t, J = 7.5 Hz, 12H, $OCH_2CH_2CH_3$).

ESI-MS: m/z calc 1161.55 oss: 581.40 [100%, M+H]$^{2+}$, 1161.77 [19%, M+H]$^{+}$

5,11-di(Boc-amino)-17,23-di[(Fmoc-L-Glu(OAll))amino]-25,26,27,28-tetrapropoxycalix[4]arene (22a)

In a microwave vial compound **15** (0.101 g, 0.118 mmol), HBTU (0.179 g, 0.472 mmol), Fmoc-Glu(OAll)OH (0.148 g, 0.353 mmol) and NEt_3 (0.024 g, 0.234 mmol) were dissolved in dry DMF. The solution was microwaved at 60°C, 150W in dynamic power mode for 90 minutes. Then the reaction is monitored by TLC (eluent DCM/ethyl acetate 1:1, with ninhydrin detector), and by ESI-MS. The reaction mixture was treated with DCM and H_2O. The organic phase was extracted, washed with H_2O to neutrality and then dried over Na_2SO_4. The solvent was then evaporated under reduced pressure. Product **22a** was obtained by column chromatography, using DCM/ethyl acetate/hexane 5:5:1 as eluent, in 81% yield (0.157 g).

^{1}H NMR (400 MHz, CD_3OD) δ 7.83 –7.56 (m, 8H, FmocArH), 7.43 – 7.17 (m, 8H, FmocArH), 7.07 (s, 2H, ArH), 6.89-6.60 (m, 6H, ArH), 6.00 – 5.78 (m, 2H, CH_2CHCH_2), 5.35 – 5.12 (m, 4H, CH_2CHCH_2), 4.65 – 4.24 (m, 12H, CH_2CHCH_2, Ar$CH_{ax}H_{eq}$Ar, OCH_2CHFmoc), 4.22-4.09 (m, 4H, NHCH, OCH_2CHFmoc), 3.95 – 3.78 (m, 8H, O$CH_2CH_2CH_3$), 3.21 – 3.08 (m, 4H, Ar$CH_{ax}H_{eq}$Ar), 2.52 – 2.30 (m, 4H, $NHCHCH_2CH_2$-), 2.10-1.86 (m, 12H, NHCHCH_2, O$CH_2CH_2CH_3$), 1.48-1.27 (m, 18H, $C(CH_3)_3$), 1.04 (t, *J* = 7.4 Hz, 12H, $OCH_2CH_2CH_3$).

^{13}C NMR (101 MHz, CD_3OD) δ 172.7, 170.5, 156.9, 154.4, 153.3, 152.2, 143.8, 141.2, 134.8, 132.7, 132.2, 131.8 (CH_2*CH*CH_2), 127.4 (FmocArH), 126.8 (FmocArH), 124.9 (FmocArH), 121.0 (ArH), 120.7 (ArH), 119.9 (ArH), 119.5 (FmocArH), 117.0 (CH_2CH*CH_2*), 79.2 (*C*(CH_3)$_3$), 76.7 (O*CH_2*CH_2CH_3), 66.6 (O*CH_2*CHFmoc), 64.9 (*CH_2*$CHCH_2$), 53.4 (NH*CH*-), 30.7 (Ar*CH_2*Ar), 29.9 (NHCHCH_2*CH_2*), 27.4 (C(*CH_3*)$_3$), 27.1 (OCH_2*CH_2*CH_3), 23.0 (NHCH*CH_2*), 9.4 (OCH_2CH_2*CH_3*).

ESI-MS: m/z calc 1635.96 oss: 1535.54 [9%, M+H-Boc]$^+$, 1657.66 [100%, M+Na]$^+$

5,11-diamino-17,23-di[(Fmoc-L-Glu(OAll))amino]-25,26,27,28-tetrapropoxycalix[4]arene (23)

In a round-bottom flask, compound **22a** (0.157 g, 0.096 mmol), TES (0.03 mL) and then TFA (2 mL) were dissolved in 1mL of DCM. Upon completion (TLC, DCM/ethyl acetate 1:1) the solvent was evaporated under reduced pressure obtaining a brown solid which was then dissolved in DCM and washed with H_2O until neutral pH. Product **23** (orange glassy solid) was obtained in quantitative yield after solvent removal.

^{1}H NMR (400 MHz, CD_3OD) δ 7.80-7.48 (m, 8H, FmocArH), 7.41-7.18 (m, 8H, FmocArH), 7.18 – 6.71 (m, 8H, ArH), 5.99-5.79 (m, 2H, CH_2*CH*CH_2), 5.33 – 5.09 (m, 4H, CH_2CH*CH_2*), 4.63 – 4.25 (m, 12H, *CH_2*$CHCH_2$, Ar*C*$H_{ax}$$H_{eq}$Ar, O*$CH_2$*CHFmoc), 4.24 – 4.03 (m, 4H, NH*CH*,OCH_2*CH*Fmoc), 3.94 – 3.65 (m, 8H, OCH_2*CH_2*CH_3), 3.30 – 3.00 (m, 4H, ArCH_{ax}*H_{eq}*Ar), 2.57 – 2.29 (m, 4H, NHCHCH_2*CH_2*), 2.21-2.03 (m, 4H, NHCH*CH_2*), 2.03 – 1.77 (m, 8H, OCH_2*CH_2*CH_3), 1.17 – 0.92 (m, 12H, OCH_2CH_2*CH_3*).

^{13}C NMR (101 MHz, CD_3OD) δ 172.7, 172.7, 171.1, 157.2, 156.6, 153.3, 143.9, 143.7, 141.2, 141.1, 132.2 (CH_2*CH*CH_2), 127.4 (FmocArH), 126.8 (FmocArH), 124.9 (FmocArH), 122.6 (*Ar*H), 120.9 (ArH), 119.6 (Fmoc*Ar*H), 117.1 (CH_2CH*CH_2*), 77.0-76.9 (O*CH_2*CH_2CH_3), 66.7 (O*CH_2*CHFmoc), 65.0 (*CH_2*$CHCH_2$), 55.0 (NH*CH*), 47.0 (OCH_2*CH*Fmoc), 46.9 (OCH_2*CH*Fmoc), 30.1 (Ar*CH_2*Ar), 30.0 (NHCHCH_2*CH_2*), 27.0 (OCH_2*CH_2*CH_3), 23.0 (NHCH*CH_2*), 9.5-9.4 (OCH_2CH_2*CH_3*).

ESI-MS: m/z calc 1435.73 oss: 143.23 [100%, M+H]$^+$, 1457.26 [60%, M+Na]$^+$, 1473.30 [24%, M+K]$^+$

5,11-di[(acid-Fmoc-ε-aminohexanoyl)amino]-17,23-di[(Fmoc-L-Glu(OAll))amino]-25,26,27,28-tetrapropoxycalix[4]arene (24)

Compound **23** (0.09 g, 0.063 mmol), HBTU (0.095 g, 0.25 mmol), Fmoc-6Ahx-OH (0.0663 g, 0.188 mmol) and NEt_3 (0.017 mL, 0.125 mmol) were added to a microwave vial containing dry DMF. The solution was microwaved at 60°C, 150W in dynamic power mode for 1h. The reaction was monitored by TLC (DCM/ethyl acetate eluent 3:7, with

ninhydrin detector), and then treated with DCM and H_2O. The organic phase was extracted, washed with H_2O to neutrality and then dried over Na_2SO_4. The solvent was evaporated under reduced pressure. Product **24** (yellow/brown glassy solid) was isolated by column chromatography, using DCM/ethyl acetate 1:1 as eluent, in a 35% (0.045 g) yield.

^{1}H NMR (400 MHz, CD_3OD) δ 7.83 – 7.48 (m, 8H, FmocArH), 7.50 – 7.18 (m, 8H, FmocArH), 7.17 – 6.71 (m, 8H, ArH), 5.94 – 5.77 (m, 2H, CH_2*CH*CH_2), 5.35 – 5.05 (m, 4H, CH_2CH*CH*$_2$), 4.55-4.37 (m, 8H, *CH*$_2$$CHCH_2$, Ar*CH*$_{ax}$$H_{eq}$Ar), 4.39 – 4.02 (m, 8H, OCH_2*CH*Fmoc, NH*CH*-, O*CH*$_2$$CHFmoc$), 3.96-3.73 (m, 8H, O*CH*$_2$$CH_2CH_3$), 3.21 – 2.90 (m, 8H, $ArCH_{ax}$*H*$_{eq}$Ar, NH*CH*$_2$), 2.49 – 2.25 (m, 4H, $NHCHCH_2$*CH*$_2$), 2.23 – 1.78 (m, 16H, $NHCH_2CH_2CH_2CH_2$*CH*$_2$, NHCH*CH*$_2$, OCH_2*CH*$_2$$CH_3$), 1.66-147 (m, 4H, $NHCH_2CH_2CH_2C$*H*$_2$), 1.46 – 1.10 (m, 8H, $NHCH_2C$*H*$_2$,$NHCH_2CH_2C$*H*$_2$), 1.09-0.97 (m,12H, OCH_2CH_2*CH*$_3$).

^{13}C NMR (101 MHz, CD_3OD) δ 172.7, 157.4, 156.9, 153.3, 143.9, 143.7, 141.2, 134.7, 132.2 (CH_2*CH*CH_2), 127.4 (FmocArH), 126.7 (FmocArH), 124.8 (FmocArH), 121.1-120.7 (ArH), 119.5 (FmocArH), 117.0 (CH_2CH*CH*$_2$), 76.8 (O*CH*$_2$$CH_2CH_3$), 66.2 (O*CH*$_2$CHFmoc), 65.0 (*CH*$_2$$CHCH_2$), 54.8 (NH*CH*), 46.5 ($OCH_2$*CH*Fmoc), 40.2 (NH*CH*$_2$), 36.2 ($NHCH_2CH_2CH_2CH_2$*CH*$_2$), 30.6 (Ar*CH*$_2$Ar), 29.9($NHCHCH_2$*CH*$_2$), 29.1 (NHCH*CH*$_2$), 27.1 ($NHCH_2$*CH*$_2$), 25.9 ($NHCH_2CH_2C$*H*$_2$), 25.0 ($NHCH_2CH_2CH_2C$*H*$_2$), 23.0 (O$CH_2$*CH*$_2$$CH_3$), 22.3, 9.4 ($OCH_2CH_2$*CH*$_3$).

ESI-MS: m/z calc 2106.53 oss: 1052.92 [100%, M+H]$^{2+}$

5,11-di[(acid-Fmoc-ε-aminohexanoyl)amino]-17,23-di[(Fmoc-L-Glu)amino]-25,26,27,28-tetrapropoxycalix[4]arene (25)

In a two-necked round-bottom flask, under argon flow, compound **24** (0.042 g, 0.021 mmol), $PhSiH_3$ (0.01 mL 0.083 mmol) and $Pd(PPh_3)_4$ in catalytic amount were dissolved in 2 mL of degassed dry DCM. The reaction was monitored by TLC (DCM/MeOH 95:5 eluent, with green bromocresol detector). After 24 hours the mixture was treated with DCM and H_2O. The organic phase was extracted, washed with H_2O and the solvent evaporated under reduced pressure. The crude was purified by column chromatography, using 95:5 ethyl acetate as eluent, obtaining the desired product as a white solid in a 57% (0.026 g) yield.

The product was immediately used without characterization.

5,11-di[(acido-ε-aminohexanoyl)amino]-17,23-di[(L-Glu)amino]-25,26,27,28-tetrapropoxycalix[4]arene (26)

Compound **25** (0.026 g, 0.0128 mmol) was dissolved in a 20% solution of piperidine in DCM. After 2 hours TLC (DCM/methanol 9:1, with Ninhydrin detector) indicated reaction completion. The solvent was then evaporated under reduced pressure. The solid obtained was triturated in diethyl ether and then in isopropanol obtaining the desired product with a of 73% (0.0102g) yield.

^{1}H NMR (400 MHz, CD_3OD) δ 7.47 – 6.74 (m, 8H, ArH), 4.56-4.41 (m, 4H, ArCH_{ax}H$_{eq}$Ar), 3.94-3.80 (m, 4H, OCH_2CH$_2$CH$_3$), 3.74 – 3.61 (m, 2H, NHC*H*), 3.21-3.07 (m, 4H, ArCH$_{ax}$$H_{eq}$Ar), 3.01-2.85 (m, 4H, NHCH_2), 2.45 – 2.23 (m, 8H, NHCH$_2$CH$_2$CH$_2$CH$_2$CH_2, NHCHCH$_2$CH_2), 2.09 – 1.85 (m, 12H, NHCHCH_2, OCH$_2$CH_2CH$_3$), 1.79-1.57 (m, 8H, NHCH$_2$CH_2, NHCH$_2$CH$_2$CH$_2$CH_2), 1.52 – 1.35 (m, 4H, NHCH$_2$CH$_2$CH_2), 1.13 – 0.90 (m, 12H, OCH$_2$CH$_2$CH_3).

^{13}C NMR (101 MHz, CD_3OD) δ 172.4, 153.3, 134.8, 132.3, 131.7, 120.7 (ArH), 54.1 (NHC*H*), 39.1 (NHCH_2), 35.9 (NHCH$_2$CH$_2$CH$_2$CH$_2$CH_2), 33.2 (NHCHCH_2), 30.7 (ArCH_2Ar), 29.9 (NHCHCH_2), 26.9 (NHCH$_2$CH_2), 25.6 (NHCH$_2$CH$_2$CH_2), 24.7 (NHCH$_2$CH$_2$CH$_2$CH_2), 23.3-23.0 (OCH$_2$CH_2CH$_3$), 9.8-8.9 (OCH$_2$CH$_2$CH_3).

ESI-MS: m/z calc 1137.43 oss: 1137.68 [100%, M+H]$^+$

5,11-di(Boc-amino)-17-amino-23-[(Fmoc-L-Glu(OAll))amino]-25,26,27,28-tetrapropoxycalix[4]arene (22b)

In a microwave vial, compound **15** (0.297 g, 0.349 mmol), HBTU (1.236 g, 3.258 mmol) and Fmoc-Glu(OAll)OH (1.0 g, 1.711 mmol) were dissolved in dry DMF. The solution was microwaved at 60°C, 150W in dynamic power mode for 1.30h. The reaction was monitored by TLC (eluent DCM/ethyl acetate/hexane 5:5:1, with ninhydrin detector), and upon completion it was treated with DCM and H_2O. The organic phase was extracted, washed with H_2O to neutrality and dried over Na_2SO_4. The solvent was evaporated under reduced pressure. Product **22b** (yellow/brown glassy solid) was isolated by column chromatography, using DCM/ethyl acetate/hexane 5:5:1 as eluent, with a 36% (0.405 g, 0.125 mmol) yield. From the same separation process, product **22a** (yellow/brown glassy solid) was also isolated with a 10% yield (0.133 g).

^{1}H NMR (400 MHz, CD_3OD) δ 7.86 – 7.51 (m, 4H, FmocArH), 7.44 – 7.23 (m, 4H, FmocArH), 7.14-6.18 (m, 8H, ArH), 6.03 – 5.78 (m, 1H, CH$_2$C*H*CH$_2$), 5.38 – 5.10 (m, 2H, CH$_2$CHCH_2), 4.62-4.31 (m, 8H, CH_2CHCH$_2$, ArCH_{ax}H$_{eq}$Ar, OCH_2CHFmoc), 4.31-4.19 (m, 2H, NHC*H*,OCH$_2$C*H*Fmoc), 4.02 – 3.62 (m, 8H, OCH_2CH$_2$CH$_3$), 3.20 – 3.01 (m, 4H, ArCH$_{ax}$$H_{eq}$Ar), 2.58-2.36 (m, 2H, NHCHCH$_2$CH_2), 2.10-1.79 (m,12H, NHCHCH_2, OCH$_2$CH_2CH$_3$), 1.62 – 1.20 (m, 18H, C(CH_3)$_3$), 1.16 – 0.81 (m, 12H, OCH$_2$CH$_2$CH_3).

^{13}C NMR (101 MHz, CD_3OD) δ 172.7, 166.1, 157.2, 154.5, 153.3, 152.2, 143.8, 141.2, 132.3 (CH$_2$C*H*CH$_2$), 127.4 (FmocArH), 126.8 (FmocArH), 124.9 (FmocArH), 120.8 (ArH), 120.4

(ArH), 119.8 (ArH), 119.6 (FmocArH), 117.1 ($CH_2CH\mathit{CH_2}$), 79.3 ($\mathit{C}(CH_3)_3$), 76.7 ($OCH_2\mathit{CH_2}CH_3$), 66.6 ($O\mathit{CH_2}$CHFmoc), 65.0 ($\mathit{CH_2}CHCH_2$), 56.1 (NH*CH*), 30.6-29.9 (Ar$\mathit{CH_2}$Ar), 27.4 (C($\mathit{CH_3}$)$_3$), 27.1 ($OCH_2\mathit{CH_2}CH_3$), 22.8 ($NHCH\mathit{CH_2}$), 9.7-9.1 ($OCH_2CH_2\mathit{CH_3}$).

ESI-MS: m/z calc 1244.54 oss: 1144.70 [15%, M+H-Boc]$^+$, 1244.76 [100%, M+H]$^+$, 1266.74 [16%, M+Na]$^+$

5,11-di(Boc-amino)-17-[(acid-Fmoc-ε-aminohexanoyl)amino]-23-[(Fmoc-L-Glu(OAll))amino]-25,26,27,28-tetrapropoxycalix[4]arene (27)

In a microwave vial, compound **22b** (0.150 g, 0.12 mmol), HBTU (0.091 g, 0.240 mmol), Fmoc-6Ahx-OH (0.051 g, 0.145 mmol) and NEt_3 (0.017 mL, 0.125 mmol) were dissolved in dry DMF. The solution was microwaved at 65°C, 150W in dynamic power mode for 1 hour and then monitored by TLC (eluent DCM/ethyl acetate 1:1, with ninhydrin detector). The reaction mixture was treated with DCM and H_2O, the organic phase was extracted, washed with H_2O to neutrality and dried over Na_2SO_4. The solvent was evaporated under reduced pressure. Product **27** (yellow/brown glassy solid) was isolated by column chromatography, using DCM/ethyl acetate 1:1 as eluent, with a 24% (0.045 g) yield.

^{1}H NMR (400 MHz, CD_3OD) δ 7.86 – 7.21 (m, 16H, FmocArH), 7.14 – 6.42 (m, 8H, ArH), 5.99 – 5.83 (m, 1H, $CH_2C\mathit{H}CH_2$), 5.35 – 5.13 (m, 2H, $CH_2CHC\mathit{H_2}$), 4.61 – 4.51 (m, 2H, $C\mathit{H_2}CHCH_2$), 4.47 – 4.37 (m, 4H, Ar$C\mathit{Hax}H_{eq}$Ar), 4.39 – 4.26 (m, 4H, $OC\mathit{H_2}$CH), 4.23 – 4.17 (m, 1H, $OCH_2C\mathit{H}$), 4.22 – 4.16 (m, 1H, NHC*H*), 4.17 – 4.11 (m, 1H, $OCH_2C\mathit{H}$), 3.90 – 3.70 (m, 8H, $OC\mathit{H_2}CH_2CH_3$), 3.13 – 3.07 (m, 2H, $NHC\mathit{H_2}$), 3.10 – 3.01 (m, 4H, $ArCH_{ax}\mathit{H_{eq}}$Ar), 2.50 – 2.37 (m, 2H, $NHCHCH_2C\mathit{H_2}$), 2.26 – 2.13 (m, 2H, $NHCH_2CH_2CH_2CH_2C\mathit{H_2}$), 2.13 – 1.99 (m, 2H, $NHCHC\mathit{H_2}CH_2$), 1.98 – 1.85 (m, 8H, $OCH_2C\mathit{H_2}CH_3$), 1.65 – 1.52 (m, 2H, $NHCH_2CH_2CH_2C\mathit{H_2}$), 1.52 – 1.46 (m, 2H, $NHCH_2C\mathit{H_2}$), 1.47 – 1.35 (m, 18H, C($C\mathit{H_3}$)$_3$), 1.36 – 1.26 (m, 2H, $NHCH_2CH_2C\mathit{H_2}$), 1.08 – 0.93 (m, 12H, $OCH_2CH_2C\mathit{H_3}$).
^{13}C NMR (101 MHz, CD_3OD) δ 172.7, 171.6, 170.7, 157.5, 157.0, 154.5, 154.3, 153.6, 152.8, 152.5, 152.0, 144.0, 143.8, 141.2, 135.3, 134.3, 132.7, 132.3 ($CH_2\mathit{C}HCH_2$), 131.7, 127.4-126.7 (FmocArH), 124.8 (FmocArH), 121.1-119.6 (*A*rH), 119.5 (Fmoc*Ar*H), 117.0 ($CH_2CH\mathit{C}H_2$), 79.2 ($\mathit{C}(CH_3)_3$), 76.7 ($OCH_2CH_2CH_3$), 66.6- 66.2 (OCH_2CH), 65.0 ($\mathit{C}H_2CHCH_2$), 54.8 (NH*C*H), 47.1 ($OCH_2\mathit{C}H$), 40.2 ($NH\mathit{C}H_2$), 36.3 ($NHCH_2CH_2CH_2CH_2\mathit{C}H_2$), 30.7 (Ar$\mathit{C}H_2$Ar), 30.0 ($NHCHCH_2\mathit{C}H_2$), 29.2 ($NHCH_2\mathit{C}H_2$), 27.4 (C($\mathit{C}H_3$)$_3$), 27.1 ($NHCH\mathit{C}H_2$), 25.9 ($NHCH_2CH_2\mathit{C}H_2$), 25.0 ($NHCH_2CH_2CH_2\mathit{C}H_2$), 23.1-22.9 ($OCH_2\mathit{C}H_2CH_3$), 9.6-9.3 ($OCH_2CH_2\mathit{C}H_3$).
ESI-MS: m/z calc 1578.80 oss: 1579.89 [100%, M+H]$^+$, 1601.74 [23%, M+Na]$^+$

5,11-diamino-17-[(acid-Fmoc-ε-aminohexanoyl)amino]-23-[(Fmoc-L-Glu(OAll))amino]-25,26,27,28-tetrapropoxycalix[4]arene (28)

In a round-bottom flask, compound **27** (0.045 g, 0.033 mmol), TES (0.02 mL) and then TFA (1.0 mL) were added to 1.0 mL of DCM. The reaction was allowed to proceed under mechanical stirring at room temperature while it was monitored by TLC (DCM/ethyl acetate 1:1, with ninhydrin detector). After 24 hours, the reaction was completed, and the solvent was removed under reduced pressure obtaining a yellowish solid in quantitative yield (44 mg).

^{1}H NMR (400 MHz, CD_3OD) δ 7.80 – 7.22 (m, 16H, FmocArH), 7.06 – 6.37 (m, 8H, ArH), 5.96 – 5.82 (m, 1H, CH_2CHCH_2), 5.33 – 5.13 (m, 2H, CH_2CHCH_2), 4.59 – 4.50 (m, 2H, CH_2CHCH_2), 4.48 – 4.37 (m, 4H, $ArCH_{ax}H_{eq}Ar$), 4.40 – 4.24 (m, 4H, OCH_2CH), 4.24 – 4.11 (m, 1H, NHCH) , 4.24 – 4.07 (m, 2H, OCH_2CH), 3.89 – 3.72 (m, 8H, $OCH_2CH_2CH_3$), 3.17 – 3.10 (m, 2H, $NHCH_2$), 3.14 – 3.03 (m, 4H, $ArCH_{ax}H_{eq}Ar$), 2.54 – 2.40 (m, 2H, $NHCHCH_2CH_2$), 2.34 – 2.17 (m, 2H, $NHCH_2CH_2CH_2CH_2CH_2$), 2.16 – 1.94 (m, 2H, $NHCHCH_2CH_2$), 1.97 – 1.84 (m, 8H, $OCH_2CH_2CH_3$), 1.68 – 1.54 (m, 2H, $NHCH_2CH_2CH_2CH_2$), 1.55 – 1.41 (m, 2H, $NHCH_2CH_2$), 1.42 – 1.25 (m, 2H, $NHCH_2CH_2CH_2$), 1.07 – 0.90 (m, 12H, $OCH_2CH_2CH_3$).
^{13}C NMR (101 MHz, CD_3OD) δ 176.1, 172.7, 171.1, 157.5, 157.1, 154.4, 154.2, 153.4, 143.9, 143.7, 141.2, 136.6, 136.3, 136.2, 136.1, 135.9, 135.2, 135.1, 134.9, 134.7, 134.6, 134.5, 132.3 (CH_2CHCH_2), 127.5-124.8 (FmocArH), 121.4-120.1 (ArH), 119.6 (FmocArH), 117.1 (CH_2CHCH_2), 76.9-76.8 ($OCH_2CH_2CH_3$), 66.7-66.1 (OCH_2CH), 65.0 (CH_2CHCH_2), 54.9 (NHCH), 47.1 (OCH_2CH), 40.2 ($NHCH_2$), 36.2 ($NHCH_2CH_2CH_2CH_2CH_2$), 30.6-30.4 ($ArCH_2Ar$), 30.0 ($NHCHCH_2CH_2$), 29.2 ($NHCH_2CH_2$), 27.0 ($NHCHCH_2$), 26.0 ($NHCH_2CH_2CH_2$), 25.1 ($NHCH_2CH_2CH_2CH_2$), 23.0 ($OCH_2CH_2CH_3$), 9.5-9.3 ($OCH_2CH_2CH_3$).
ESI-MS: m/z calc 1379.71 oss: 1157.63 [22%, M+H-Fmoc]$^+$, 1380.64 [100%, M+H]$^+$

4. BIBLIOGRAPHY

(1) Lu, R.; Zhao, X.; Li, J.; Niu, P.; Yang, B.; Wu, H.; Wang, W.; Song, H.; Huang, B.; Zhu, N.; et al. Genomic Characterisation and Epidemiology of 2019 Novel Coronavirus: Implications for Virus Origins and Receptor Binding. *Lancet,* **2020**, *395* (10224), 565–574.

(2) Morse, J. S.; Lalonde, T.; Xu, S.; Liu, W. R. Learning from the Past: Possible Urgent Prevention and Treatment Options for Severe Acute Respiratory Infections Caused by 2019-NCoV. *ChemBioChem* **2020**, *21* (5), 730–738.

(3) Báez-Santos, Y. M.; St. John, S. E.; Mesecar, A. D. The SARS-Coronavirus Papain-like Protease: Structure, Function and Inhibition by Designed Antiviral Compounds. *Antiviral Res.* **2015**, *115*, 21–38.

(4) Zhang, L.; Lin, D.; Sun, X.; Curth, U.; Drosten, C.; Sauerhering, L.; Becker, S.; Rox, K.; Hilgenfeld, R. Crystal Structure of SARS-CoV-2 Main Protease Provides a Basis for Design of Improved a-Ketoamide Inhibitors. *Science,* **2020**, *368* (6489), 409–412.

(5) Zhang, L.; Zhou, R. Binding Mechanism of Remdesivir to SARS-CoV-2 RNA Dependent RNA Polymerase, *J. Phys. Chem. B.*, **2020**, 124, 32, 6955–6962

(6) Zhang, H.; Penninger, J. M.; Li, Y.; Zhong, N.; Slutsky, A. S. Angiotensin-Converting Enzyme 2 (ACE2) as a SARS-CoV-2 Receptor: Molecular Mechanisms and Potential Therapeutic Target. *Intensive Care Med.* **2020**, *46* (4), 586–590.

(7) Hoffmann, M.; Kleine-Weber, H.; Schroeder, S.; Krüger, N.; Herrler, T.; Erichsen, S.; Schiergens, T. S.; Herrler, G.; Wu, N. H.; Nitsche, A.; et al. SARS-CoV-2 Cell Entry Depends on ACE2 and TMPRSS2 and Is Blocked by a Clinically Proven Protease Inhibitor. *Cell* **2020**, *181* (2), 271-280.

(8) Guzzi, P. H.; Mercatelli, D.; Ceraolo, C.; Giorgi, F. M. Master Regulator Analysis of the SARS-CoV-2/Human Interactome. *J. Clin. Med. 2020, Vol. 9, Page 982* **2020**, *9* (4), 982.

(9) Liu, C.; Zhou, Q.; Li, Y.; Garner, L. V.; Watkins, S. P.; Carter, L. J.; Smoot, J.; Gregg, A. C.; Daniels, A. D.; Jervey, S.; et al. Research and Development on Therapeutic Agents and Vaccines for COVID-19 and Related Human Coronavirus Diseases. *ACS Cent. Sci.* **2020**, *6* (3), 315–331.

(10) Pant, S.; Singh, M.; Ravichandiran, V.; Murty, U. S. N.; Srivastava, H. K. Peptide-like and Small-Molecule Inhibitors against Covid-19. *J. Biomol. Struct. Dyn.* **2020**, 1–10.

(11) Forni, G.; Mantovani, A.; Forni, G.; Mantovani, A.; Moretta, L.; Rappuoli, R.; Rezza, G.; Bagnasco, A.; Barsacchi, G.; Bussolati, G.; et al. COVID-19 Vaccines: Where We Stand and Challenges Ahead. *Cell Death Differ. 2021 282* **2021**, *28* (2), 626–639.

(12) Huang, Y.; Yang, C.; Xu, X. feng; Xu, W.; Liu, S. wen. Structural and Functional Properties of SARS-CoV-2 Spike Protein: Potential Antivirus Drug Development for COVID-19. *Acta Pharmacol. Sin. 2020 419* **2020**, *41* (9), 1141–1149.

(13) Alanagreh, L.; Alzoughool, F.; Atoum, M. The Human Coronavirus Disease COVID-19: Its Origin, Characteristics, and Insights into Potential Drugs and Its Mechanisms. *Pathog.*, **2020**, *9* (5).

(14) Martin, W. R.; Cheng, F. Repurposing of FDA-Approved Toremifene to Treat COVID-19 by Blocking the Spike Glycoprotein and NSP14 of SARS-CoV-2. *J. Proteome Res.* **2020**, *19* (11), 4670–4677.

(15) Li, W.; Moore, M. J.; Vasllieva, N.; Sui, J.; Wong, S. K.; Berne, M. A.; Somasundaran, M.; Sullivan, J. L.; Luzuriaga, K.; Greeneugh, T. C.; et al. Angiotensin-Converting Enzyme 2 Is a Functional Receptor for the SARS Coronavirus. *Nat. 2003 4266965* **2003**, *426* (6965), 450–454.

(16) Li, W.; Zhang, C.; Sui, J.; Kuhn, J. H.; Moore, M. J.; Luo, S.; Wong, S. K.; Huang, I. C.; Xu, K.; Vasilieva, N.; et al. Receptor and Viral Determinants of SARS-Coronavirus Adaptation to Human ACE2. *EMBO J.* **2005**, *24* (8), 1634–1643.

(17) Tai, W.; He, L.; Zhang, X.; Pu, J.; Voronin, D.; Jiang, S.; Zhou, Y.; Du, L. Characterization of the Receptor-Binding Domain (RBD) of 2019 Novel Coronavirus: Implication for Development of RBD Protein as a Viral Attachment Inhibitor and Vaccine. *Cell. Mol. Immunol. 2020 176* **2020**, *17* (6), 613–620.

(18) Yan, R.; Zhang, Y.; Li, Y.; Xia, L.; Guo, Y.; Zhou, Q. Structural Basis for the Recognition of SARS-CoV-2 by Full-Length Human ACE2. *Science,* **2020**, *367* (6485), 1444–1448.

(19) Sun, M.; Liu, S.; Wei, X.; Wan, S.; Huang, M.; Song, T.; Lu, Y.; Weng, X.; Lin, Z.; Chen, H.; et al. Aptamer Blocking Strategy Inhibits SARS-CoV-2 Virus Infection. *Angew. Chemie Int. Ed.* **2021**, *60* (18), 10266–10272.

(20) Yang, J.; Petitjean, S. J. L.; Koehler, M.; Zhang, Q.; Dumitru, A. C.; Chen, W.; Derclaye, S.; Vincent, S. P.; Soumillion, P.; Alsteens, D. Molecular Interaction and Inhibition of SARS-CoV-2 Binding to the ACE2 Receptor. *Nat. Commun. 2020 111* **2020**, *11* (1), 1–10.

(21) Basu, A.; Sarkar, A.; Maulik, U. Molecular Docking Study of Potential Phytochemicals and Their Effects on the Complex of SARS-CoV2 Spike Protein and Human ACE2. *Sci. Reports 2020 101* **2020**, *10* (1), 1–15.

(22) Wei, Y.; Mc Lendon, G. L.; Hamilton, A. D.; Case, M. A.; Purring, C. B.; Lin, Q.; Park, H. S.; Leec, C. S.; Yua, T. Disruption of Protein–Protein Interactions: Design of a Synthetic Receptor That Blocks the Binding of Cytochrome c to Cytochrome c

Peroxidase. *Chem. Commun.* **2001**, *1* (17), 1580–1581.

(23) Lin, Q.; Hamilton, A. D. Design and Synthesis of Multiple-Loop Receptors Based on a Calix[4]arene Scaffold for Protein Surface Recognition. *Comptes Rendus Chim.* **2002**, *5* (5), 441–450.

(24) Sebti, S. M.; Hamilton, A. D. Design of Growth Factor Antagonists with Antiangiogenic and Antitumor Properties. *Oncogene* **2000**, *19* (56), 6566–6573.

(25) Sansone, F.; Baldini, L.; Casnati, A.; Lazzarotto, M.; Ugozzoli, F.; Ungaro, R. Supramolecular Chemistry And Self-Assembly Special Feature: Biomimetic Macrocyclic Receptors for Carboxylate Anion Based on C-Linked[4]Arenes. *Proc. Natl. Acad. Sci. U. S. A.* **2002**, *99* (8), 4842.

(26) Lazzarotto, M., Sansone, F., Baldini, L., Casnati, A., Cozzini, P., Synthesis and Properties of Upper Rim C-Linked Peptidocalix[4]arenes. *Eur. J. Org. Chem.* **2001**, No. 3, 596–602.

(27) Trott, O.; Olson, A. J. AutoDock Vina: Improving the Speed and Accuracy of Docking with a New Scoring Function, Efficient Optimization, and Multithreading. *J. Comput. Chem.* **2010**, *31* (2), 455–461.

(28) Arosio, D.; Fontanella, M.; Baldini, L.; Mauri, L.; Bernardi, A.; Casnati, A.; Sansone, F.; Ungaro, R. A Synthetic Divalent Cholera Toxin Glycocalix[4]Arene Ligand Having Higher Affinity than Natural GM1 Oligosaccharide. *J. Am. Chem. Soc.* **2005**, *127* (11), 3660–3661.

(29) Baldini, L.; Sansone, F.; Scaravelli, F.; Casnati, A.; Ungaro, R. Proximal and Distal N,C-Linked Tetra-Peptidocalix[4]Arenes as Bifunctional Receptors: Synthesis, Conformation and Preliminary Binding Studies. **2010**, *22* (11–12), 776–788.

(30) Hudecek, O.; Curinova, P.; Budka, J.; Lhoták, P. Regioselective Upper Rim Substitution of Calix[4]Arenes. *Tetrahedron* **2011**, *67* (29), 5213–5218.

(31) Dudic, M.; Colombo, A.; Sansone, F.; Casnati, A.; Donofrio, G.; Ungaro, R. A General Synthesis of Water Soluble Upper Rim Calix[n]Arene Guanidinium Derivatives Which Bind to Plasmid DNA. *Tetrahedron* **2004**, *60* (50), 11613–11618.

(32) Saadioui, M.; Shivanyuk, A.; Bohmer, V.; Vogt, W. Selective N-Protection of a Tetraamino Calix[4]Arene Tetraether. *J. Org. Chem.* **1999**, *64* (10), 3774–3777.

(33) Chang, C. -D; Waki, M.; Ahmad, M.; Meienhofer, J.; Lundell, E. O.; Haug, J. D. Preparation and Properties of Nalpha-9-Fluorenylmethyloxycarbonylamino Acids Bearing Tert.-Butyl Side Chain Protection. *Int. J. Pept. Protein Res.* **1980**, *15* (1), 59–66.

(34) Thomas, J. B.; Atkinson, R. N.; Namdev, N.; Rothman, R. B.; Gigstad, K. M.; Fix, S. E.;

Mascarella, S. W.; Burgess, J. P.; Vinson, N. A.; Xu, H.; et al. Discovery of an Opioid κ Receptor Selective Pure Antagonist from a Library of N-Substituted 4β-Methyl-5-(3-Hydroxyphenyl)Morphans. *J. Med. Chem.* **2002**, *45* (16), 3524–3530.

(35) Guibé, F. Allylic Protecting Groups and Their Use in a Complex Environment Part II: Allylic Protecting Groups and Their Removal through Catalytic Palladium π-Allyl Methodology. *Tetrahedron* **1998**, *54* (13), 2967–3042.

(36) Dessolin, M.; Guillerez, M. G.; Thieriet, N.; Guibé, F.; Loffet, A. New Allyl Group Acceptors for Palladium Catalyzed Removal of Allylic Protections and Transacylation of Allyl Carbamates. *Tetrahedron Lett.* **1995**, *36* (32), 5741–5744.

(37) Dubey L. V., Dubey I. Y., Side reactions of onium coupling reagents BOP and HBTU in the synthesis of silica polymer supports, *Ukr. Bioorg. Acta*, 2005, *1*, 13-19.

(38) Donofrio, G.; Franceschi, V.; Macchi, F.; Russo, L.; Rocci, A.; Marchica, V.; Costa, F.; Giuliani, N.; Ferrari, C.; Missale, G. A Simplified Sars-Cov-2 Pseudovirus Neutralization Assay. *Vaccines* **2021**, *9* (4), 389.

(39) Balogh-Nair, V. Macrocyclic Synthesis: A Practical Approach Edited by David Parker., *J. Am. Chem. Soc.* **1997**, *119* (48), 11721–11721.

(40) Ugozzoli, F.; Casnati, A.; Pochini, A.; Ungaro, R.; Arnaud, F.; Fanni, S.; Schwing, M. J.; Egberink, R. J. M.; Jong, F. de; Reinhoudt, D. N. Synthesis, Complexation, and Membrane Transport Studies of 1,3-Alternate Calix[4]Arene-Crown-6 Conformers: A New Class of Cesium Selective Ionophores. *J. Am. Chem. Soc.* **1995**, *117* (10), 2767–2777.

(41) Kelderman, E.; Verboom, W.; Engbersen, J. F. J.; Reinhoudt, D. N.; Heesink, G. J. T.; van Hulst, N. F.; Derhaeg, L.; Persoons, A. Nitrocalix [4]Arenes as Molecules for Second-Order Nonlinear Optics. *Angew. Chem. Int. Ed. English* **1992**, *31* (8), 1075–1077.

(42) Struck, O.; Verboom, W.; Smeets, W. J. J.; Spek, A. L.; Reinhoudt, D. N. Calix[4]Arene Dimers; Self-Assembly via Hydrogen Bonding at Theupper Rim. *J. Chem. Soc. Perkin Trans. 2* **1997**, *2* (2), 223–228.

(43) Sansone, F.; Chierici, E.; Casnati, A.; Ungaro, R. Thiourea-Linked Upper Rim Calix[4]Arene Neoglycoconjugates: Synthesis, Conformations and Binding Properties. *Org. Biomol. Chem.* **2003**, *1* (10), 1802–1809.

(44) Casnati, A.; Fabbi, M.; Pelizzi, N.; Pochini, A.; Sansone, F.; Ungaro, R.; Di Modugno, E.; Tarzia, G. Synthesis, Antimicrobial Activity and Binding Properties of Calix[4]Arene Based Vancomycin Mimics. *Bioorg. Med. Chem. Lett.* **1996**, *6* (22), 2699–2704.

Chapter 3:

Multivalent glycocalix[4]arenes as ligands for lectins

1. INTRODUCTION

1.1 Lectins

Lectins are proteins that, recognizing and binding to specific carbohydrates, play a key role in many physiological and pathological processes such as cell communication, pathogen invasion, and tumor metastasis.[1,2] For example, when bacteria or viruses infect a host, they use the lectins present on their surface to bind to specific carbohydrates displayed on the host cells.[3,4,5] Although lectins have rather high specificity for their carbohydrate ligands, the interactions between a single recognition site and a single substrate present in the two partners involved in the process are usually weak, with affinities in the low millimolar to high micromolar range. To overcome this issue, lectins often form multimers presenting multiple sites that bind clusters of carbohydrate ligands, giving rise to the so-called glycoside cluster effect. The achieved whole interaction is significantly stronger due to the multiple simultaneous binding events.[6,7,8]

In nature, in fact, multivalent interactions are exploited in biological processes to enhance the affinity and specificity of ligands for their targets, as well as to create cluster receptors for certain cellular signaling pathways. These interactions are an important part of the way in which cells communicate and function.

The multivalent effect, or, for glycoconjugates, the glycoside cluster effect, was first postulated by Lee and Lee in 1995.[8] This concept refers to the enhanced binding affinity and specificity that can be achieved through the use of multivalent glycoconjugates, which have multiple glycans attached to a single carrier molecule, compared to those of a monovalent ligand. These structures can in fact better mimic the multivalent interactions that occur naturally in biological systems and can, therefore, be used to study or modulate various biological processes.

The multivalent effect can be observed when the ligand has the right valency, geometry, and size to maximize its interaction with the receptor. The mechanisms by which this occurs depend on the geometry and number of the receptor's binding sites. It is important to consider these factors when designing multivalent glycoconjugates in order to achieve the desired effect. Important mechanisms, described below, are involved during the establishment of multivalent interactions. Furthermore, it is worth noting that the multivalent effect observed for a multivalent ligand/multimeric receptor pair is often dependent on a combination of different interaction mechanisms.[9]

The chelate mechanism consists in the simultaneous binding to the same multimeric protein of more than one unit belonging to a multivalent ligand. In this case, the ligand is able to bind several sites on the protein at the same time, forming a chelate structure.

This can increase the affinity and specificity of the interaction and may also modulate the activity of the protein (Figure 1A). This indeed is the multivalent effect in agreement with the definition of glycoside cluster effect coined by Lee and Lee studying the interactions between oligomeric mannose binding lectins and ligands displaying multiple copies of mannose-based epitopes.[8]

Similarly, it is also possible to observe the multivalent effect when two monomeric receptors come into contact. This can occur, for example, when membrane receptors cluster together on the surface of a cell. In these cases, the multivalent effect can be used to modulate the activity of the receptors and the signaling pathways that they are involved in (Figure 1B).

A chelate effect can also be achieved when a multivalent ligand affects a secondary site, during the binding process, in addition to the main interaction site. This can increase the selectivity of the interaction, as the ligand will be able to bind more specifically to the desired target. This can be especially useful in situations where several potential targets are present, as it can help to prevent unwanted binding to off-target molecules (Figure 1C).

Finally, another mechanism of multivalent interaction is the statistical re-association or binding-rebinding mechanism which can occur when a single binding site is presented to a high local concentration of the binding unit. This can lead to an increased likelihood of interaction due to the increased availability of the ligand species (Figure 1D).

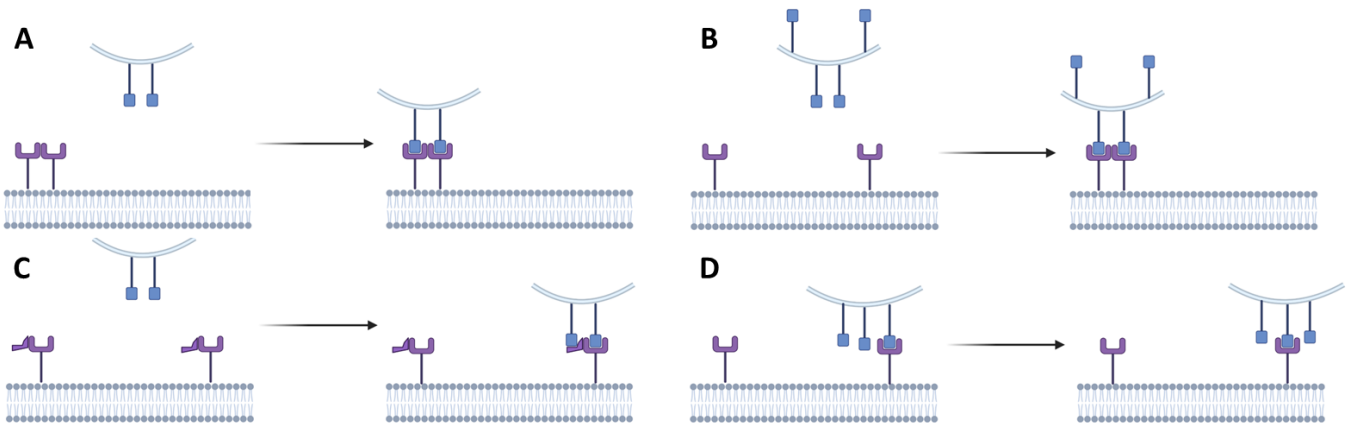

Figure 1: Different multivalent interaction mechanisms A) chelate mechanism; B) clustering mechanism; C) chelate mechanism involving secondary site D) statistical re-association (adapted from Kiessling et al. Curr. Opin. Chem. Biol., 2000, 4 (6), 696–703).

These mechanisms of multivalent interactions can be explained in terms of thermodynamic processes. The affinity of a ligand for a target is controlled by the binding energy. When a multivalent ligand is presented to a multimeric receptor, the

energy cost of binding of the first unit also allows the binding of the others without requiring additional energy since they are already in place.

Synthetic molecules that can compete with lectins natural ligands have been shown to potentially prevent cell adhesion and biofilm formation by taking advantage of the glycoside cluster effect.[10,11,12,13,14,15] Interesting inhibition properties have, for instance, been observed with both fucose- and galactose-based compounds against *Pseudomonas aeruginosa*, highlighting the potential of this lectin-directed anti-adhesion strategy against pathogenic bacteria.[16,17]

Actually, fucose is a saccharide particularly significant in the context of infections caused by microorganisms exploiting lectins-glycoconjugates interactions to trigger the first phases of the disease. It is found in both human tissue and plant cell walls, making it a common target for pathogens seeking to infect either of them.[18,19] It is known, in fact, that many opportunistic pathogens are capable of spreading from soil to plants and humans. Fucose is also known to be a marker of inflammation in mammal tissues.[20] For example, fucosylated glycoconjugates are often over-expressed in the airways of individuals affected by cystic fibrosis.[21] This disease, and more generally lung infections are often caused by pathogens able to produce and secrete soluble lectins as means for adhesion to fucosylated glycoconjugates found on the surface of human cells. These glycoconjugates, such as histoblood group epitopes, are indeed exploited as anchoring sites by the pathogens and are, therefore, involved in the overall infection process.[22] Soluble fucose-binding lectins have been identified in several types of pathogenic microorganisms, including *Pseudomonas aeruginosa*,[23] *Burkholderia ambifaria*,[24] and *Aspergillus fumigatus* (Figure 2).[25]

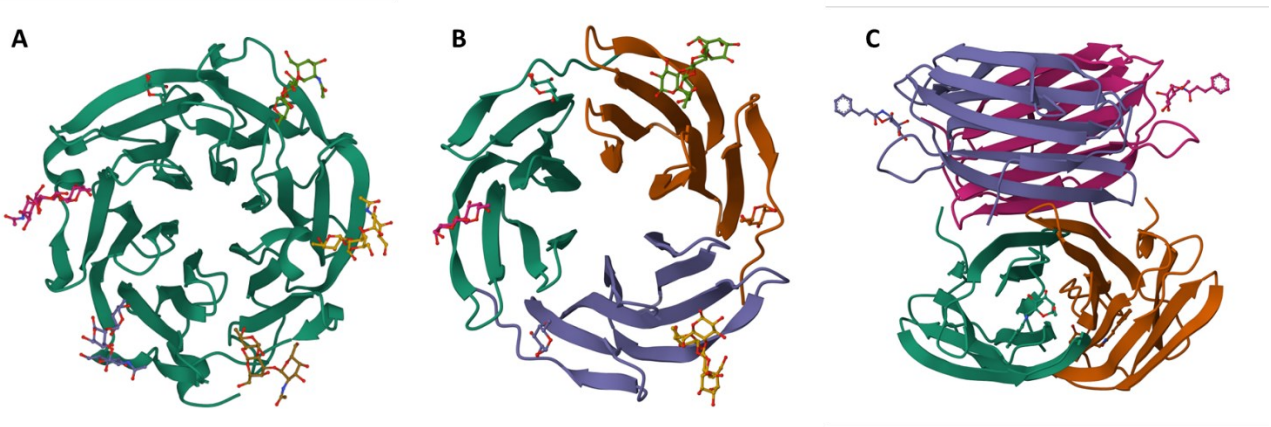

Figure 2: Lectin studied, a) Aspergillus Fumigatus Lectin, b) Burkholderia ambifaria lectin, c) Pseudomonas aeruginosa LecB

Of particular interest is a structural family of lectins that includes BambL and AFL produced respectively by *B. ambifaria* and *A. fumigatus*. Both lectins are composed of

repeated small beta sheets of approximately 40 amino acids and can with unusual high affinity bind to up to six fucose residues, exploiting six binding sites all positioned in the same space region.[24,25] The affinity for fucose in this family of lectins is indeed rather strong, with binding occurring in the micromolar range, which is not common for protein-carbohydrate interactions. To prevent pathogen adhesion to host cells and the subsequent infection process, fucose based compounds can therefore be used as synthetic ligands to intercept bacteria that bind to this crucial carbohydrate. Monomeric fucoside derivatives, such as for example (2E)-hexenyl α-L-fucopyranoside, have been tested by professor Fahy against AFL and proved to be effective inhibitors.[26]

LecB from *Pseudomona aeruginosa* is a smaller protein compared to AFL wighting only 48 kDa, but as the previous two lectins, it is composed prevalently by beta sheet. Differently by the other two lectins in exam, this protein has less fucose binding sites, only four, and they are divided in two pairs each of them pointing to opposite spatial regions.

Since also these fucose binding lectins are multimeric proteins, in order to increase the possibility of interfering with their activity multivalent glycocompounds can be exploited.[10,27] Examples of ligands built with this strategy are the calixarene-based fucosylated clusters reported by professor Vidal, which have been shown to have strong affinity for LecB, in the nanomolar range, and provide, in a mice used as infection model, almost complete protection against *P. aeruginosa*[5] infection. However, even if this approach gave interesting results with LecB, it has not been widely tested for β-propeller lectins like BambL and AFL. Not many examples of multivalent ligands for this class of lectins have been reported in literature. Some of them describe fucosylated glycoclusters with 4, 6, or 8 residues synthesized using mannose-centered and branched-phosphodiester scaffolds, which display affinities of approximately 43 nM for BambL[28]. Other multivalent compounds, such as hexavalent cyclotriveratrylene[29] and penta- and decavalent pillarenes,[30,31] have also demonstrated very strong affinity, in the low twenties nanomolar range, for the same lectin. Professor Renaudet has also shown how it is possible to exploit multivalent RAFT-based glycoconjugates to selectively target the fucose binding AFL, BambL and LecB.[32]

On the basis of these considerations, we decided to prepare new multivalent fucosylated ligands for the inhibition of these fucose selective lectins.

1.2 Ligands

A wide range of molecular scaffolds, including calixarenes, cyclodextrins, dendrimers, and nanoparticles, have been developed for a variety of uses in the field of glycoscience.[33,34,35]

These compounds have been extensively used as carriers for glycans, creating multivalent glycosylated compounds with enhanced binding affinity and specificity towards carbohydrate-binding proteins thanks to the glycoside cluster effect.[6]

1.2.1 Calixarenes as lectins ligands

During the years, many multivalent calixarene based ligands have been published, and our research group also contributed with many interesting ones. A noteworthy ligand developed in 2013, for example, is a calix[5]arene bearing at the upper rim five units of an analog of the glycosphingolipid ganglioside GM1 for the inhibition of cholera toxin. This pentavalent ligand showed remarkable properties, in fact, it was demonstrated that it was able to inhibit the target protein even at picomolar concentrations.[36] Another interesting example, published in 2008, was related to the use of a lactosylated calixarenes as ligands for galectins.[37] Even in this case the calixarene was able to perform the task it was developed for, providing multivalent effect and selectivity to the ligands. This and other examples prove how versatile the calixarene macrocycle is as scaffold to prepare many different multivalent ligands.

1.2.2 RAFT-based ligands

Over the past two decades, cyclopeptides have also become very important in this field. Initially used to present peptide fragments that mimic natural proteins,[38,39] they have been found to be well-suited for in vivo applications thanks to their conformational stability, combined with a high resistance to enzymatic degradation, and lack of immunogenicity.

Due to these interesting properties, cyclopeptides have recently been modified with a range of glycans in order to understand, stimulate, or inhibit multivalency based biological processes.[40]

The synthesis of this class of compounds is well established and modular. This allowed many researchers to easily functionalize these scaffolds exploring a wide range of different possibilities. A noteworthy approach relies on the introduction of multiple copies of a binding unit on the same cyclopeptide core in order to exploit the principles of multivalency to aid the development of new ligands for different biomolecules.

During my Ph.D. I had the opportunity to work for a few months in the laboratories of professor Renaudet at the University of Grenoble. His research group have been using

the RAFT platform for more than a decade for various biologically oriented applications.[40,41] During this time, he mastered the techniques needed for the proper functionalization of this scaffold. RAFT is the acronym for cyclopeptides identified as Regioselectively Addressable Functionalized Templates. (Figure 3A). RAFT is a highly versatile platform which allows for the selective functionalization of its specific sites resulting in the possible introduction of many different molecules of interest, each oriented in a precise spatial arrangement. The RAFT platform acts indeed as a template molecule and can be used to create a wide range of multivalent glycoconjugates with different valences, geometries, and functionalities.

This versatile scaffold was first discovered in the late 1990s by the Mutter group, and was later developed further by Renaudet, Dumy, and others. Its core is based on a cyclodecapeptide that contains two Gly-Pro antiparallel beta turns that help to stabilize its conformation in solution. The presence of four lysine moieties on the upper face permits the multiple conjugation of peptides, sugars, or other species, while the functionalization of one or two lysine residues on the lower side can be exploited for the anchoring to a surface or for the introduction of fluorescent tags, biosensors, or other compounds, depending on the desired biological application (as shown in Figure 3B). In addition, RAFT is easily chemically accessible, and its cyclic structure makes it stable in vivo and non-immunogenic, making it suitable for in vivo applications.[39,42,43]

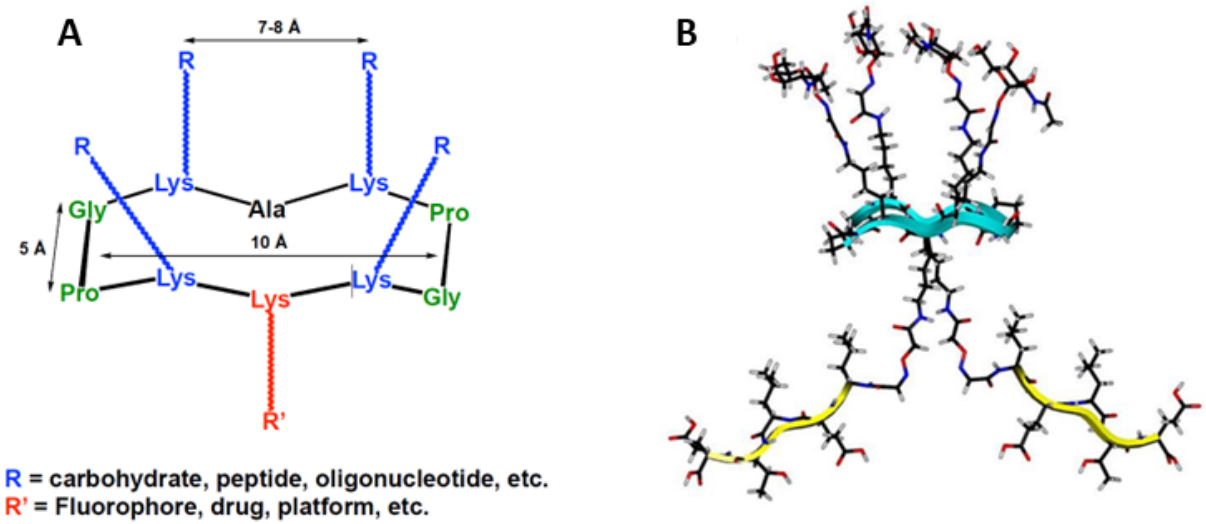

Figure 3: A) General structure of the RAFT platform B) Stick representation of a RAFT functionalized with carbohydrate residues at the upper domain and peptides at the lower domain as an example of the possible modifications of this scaffold.

Due to the very interesting nature of this scaffold, we decided to combine it with calix[4]arenes in a "superstructure" as the main platform to build polyglycosylated ligands on for the lectins mentioned above. In our case, one of the Lys residues cited above was replaced by an Ala, since the presence of a second Lys was not required. The

calixarene part could give to these compound interesting properties. Since the polyphenolic macrocycle can be easily prepared in different geometries, we could orient the cyclopeptides linked to the same core in different region of the space, generating ligands with modulated properties. We also decided to study the binding properties of simpler calix[4]arenes directly functionalized with fucose units without the presence of RAFTs. In particular, we focused our attention on three different calix[4]arene scaffolds: the cone, the 1,3-alternate and the mobile one. This because we wanted to investigate, also in this case, how the different spatial orientation of the binding groups affect the ligand affinity.

2. RESULTS AND DISCUSSION

In the following pages are described the synthesis and the properties of the three calix[4]arenes based- and the "superstructure" based- ligands.

2.1 Synthesis of fucosylated calix[4]arenes

As stated above, we decided to prepare three calix[4]arene based multivalent ligands. These compounds, in order to be able to benefit from multivalent interactions during the binding of the fucose-selective lectins, had to be functionalized with multiple copies of α-fucose (Figure 4).

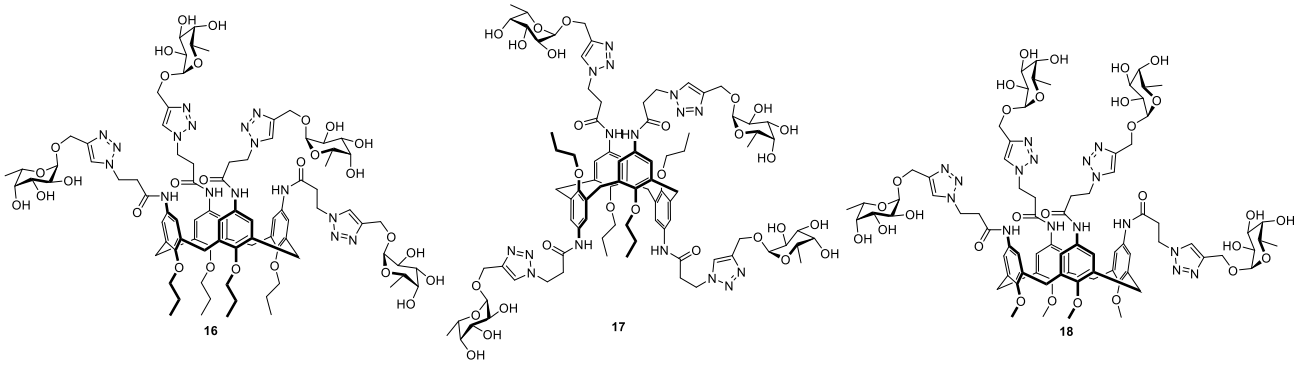

Figure 4: The three synthesized ligands.

Calixarene **16** is locked in a cone configuration, which results in the exposition of the four fucose units in a narrow, confined region of space. This high level of preorganization may facilitate the target binding for the glycosylated ligand, as the binding groups are presented in a more predictable and uniform manner. This particular geometry could promote a binding-rebinding mechanism of interaction. In fact, it is difficult to imagine, due to the relative dimensions, a single calixarene able to interact simultaneously with more than a single lectin binding site and therefore exploiting

different mechanisms. On the other hand, the lower rim propyl chains could promote aggregation phenomena leading to species in solution with augmented valency. This arrangement could also ensure the same multivalent mechanism of interaction due to the high density of equally oriented fucoses present on the surface of the aggregate, but it could even allow the simultaneous interaction between a calixarene-based aggregate species with more lectins giving rise to intermolecular crosslinked networks.

Calixarene **17**, on the other hand, has a 1,3-alternate configuration and exposes the four saccharides in different directions. As shown in figure 4, two of the groups are projected in one direction while the others in the opposite one. This different spatial orientation may statistically make more difficult for the glycosylated ligand to bind to the target protein but could allow for a situation in which a single ligand is bridging two different lectins.

Calixarene **18** is not locked into a defined configuration like the previous two. Its conformational freedom is preserved due to the lower rim functionalization with the small methyl groups, that allow the molecule to adopt different conformations, switching from one to the other depending on the boundary conditions. This derivative may be more versatile than the previous two because it can potentially adapt itself to the target binding site more easily. On the other hand, the lack of preorganization and the consequent need of higher costs in terms of entropy during the recognition process with the target could penalize this glycosylated ligand for the binding.

2.1.1 Synthesis of the tetra-azido-calix[4]arenes precursors

The first part of the ligand synthesis concerned the preparation of the tetraazido calixarene scaffolds showed in figure 5. It was indeed planned to introduce four azido moieties on the three geometrically different calixarenes and react these compounds with four units of an alkyne-bearing L-fucose to obtain the desired ligands **16**, **17**, **18**, exploiting the copper catalyzed alkyne-azide cycloaddition reaction (CuAAC).

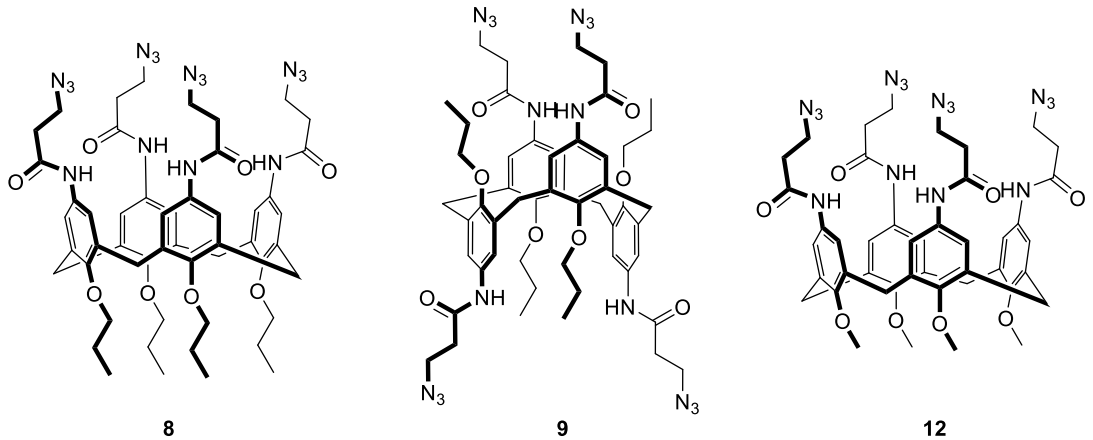

*Figure 5: Tetraazido calix[4]arenes used as precursor for the preparation of compound **8**, **9**, **12**.*

The envisioned synthesis is linear and started with the lower rim alkylation of the tetrahydroxy calixarene, which was actually the only different step in the preparation of the three azido calixarenes. In scheme 1are reported the experimental conditions used.

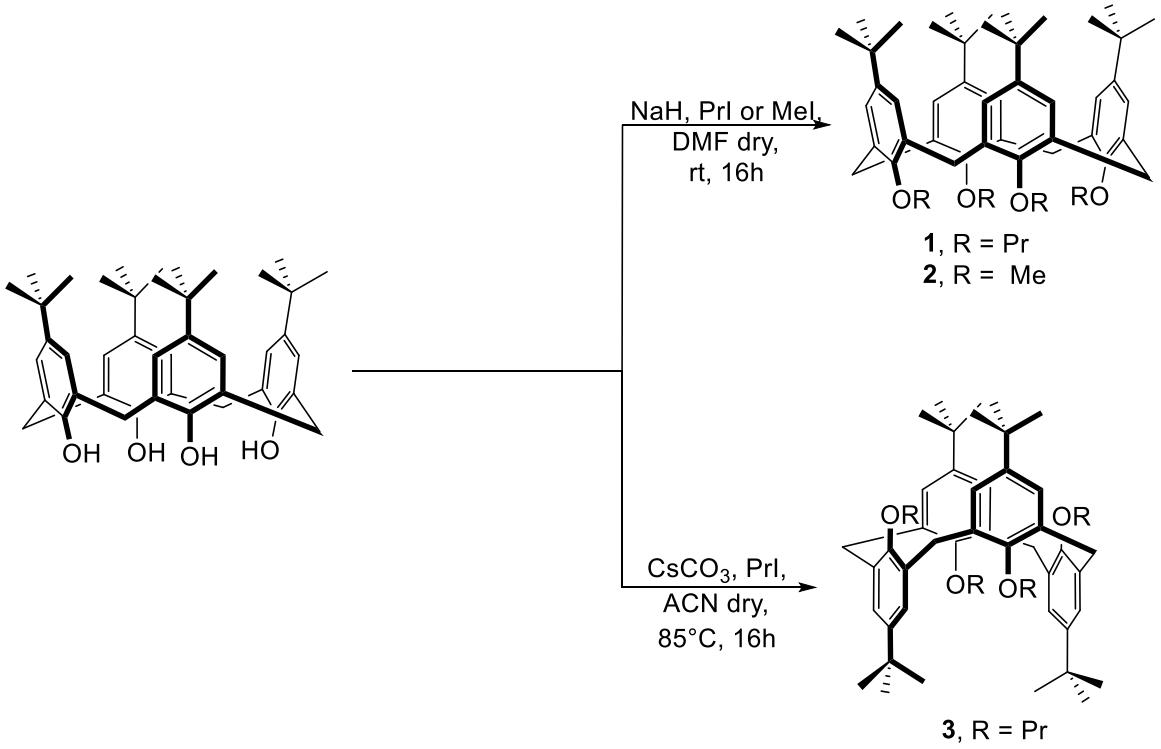

*Scheme 1: Synthesis of compounds **1**, **2** and **3**.*

As well-known, the base used in this process was the key factor which allowed us to obtain the compounds blocked in the desired geometry. NaH, in fact, permits the formation of the cone configuration calixarene in conjunction with 1-iodopropane,[44] or the mobile one while employing 1-iodomethane as the alkylating agent.[45] To obtain the 1,3-alternate geometry, instead, the base needed is $CsCO_3$.[46] After the alkylation step, the synthesis proceeded identically for each compound. We introduced the four desired azido groups by reacting the tetraamino calixarene with 3-azido propionic acid.

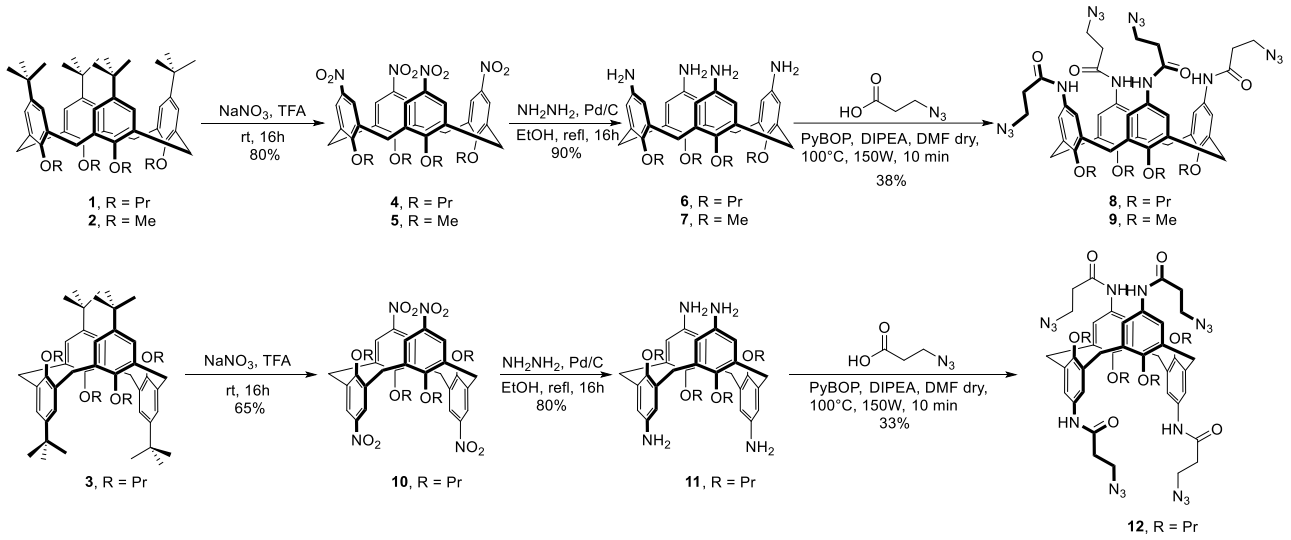

*Scheme 2: Reaction pathway for the preparation of **8**, **9** and **12**.*

The synthetic steps performed to obtain the tetraamino derivatives are reported in scheme 2. The sequence consists of an ipso-nitration performed with $NaNO_3$ in presence of TFA to have **4**, **5** and **10**, followed by a reduction with hydrazine in presence of a catalytic amount of Pd/C. This two-step sequence led us to the desired tetraamino calixarenes **6**, **7** and **11** in very good yields.

After obtaining compounds **6**, **7** and **11** we reacted them with 3-azidopropionic acid. The reaction was carried out in DMF with the aid of microwaves employing PyBOP as the coupling agent. This standard protocol allowed us to obtain the desired tetra azido derivatives **8**, **9**, **12**. The yield of this coupling reaction was surprisingly low for each calixarene. The most difficult aspect of this reaction was the product purification. Lengthy and multiple column chromatography was needed to purify the products, which in the end were never obtain completely free from contaminants. The purification process surely compromised the overall yield of the isolated product.

2.1.2 Synthesis of α-propargyl-L-fucose

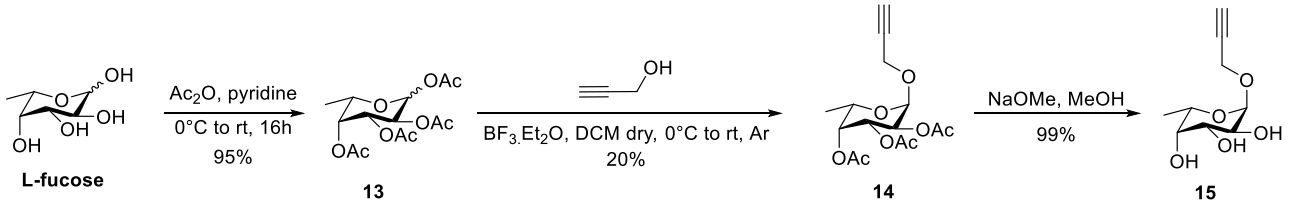

*Scheme 3: Synthesis of **15**.*

Following the already known sequence of transformations reported in scheme 3, we were able to prepare the α-propargyl fucose we needed.[47] The synthesis started with an exhaustive acetylation of L-fucose carried out in acetic anhydride using pyridine as both the solvent and the base. Compound **13** was then glycosylated by reaction with

propargyl alcohol in presence of boron trifluoride diethyl etherate in dry DCM. The resulting crude purification was very demanding since it was composed by a 70:30 mixture of the two anomers, with the undesired β one being the main component. This ratio was however expected. In fact, a key role in the stereochemical outcome of this reaction is played by the neighboring acetyl group that acts as a participant group during the glycosylation partially blocking the α-face and therefore promoting the formation of the unwanted anomer. Due to the little chemical dissimilarity between the two anomers a lengthy chromatographic separation was necessary to isolate compound **14**. This mandatory process negatively affected the overall yield of the reaction.

Once we had compound **14** in our hands, we removed the acetyl groups with sodium methoxide, in Zemplén conditions, obtaining the desired compound **15** in almost quantitative yield. We in fact planned to link to the calixarenes the fucose units in their deprotected form, taking into account a purification procedure by RP-HPLC.

2.1.3 α-Propargylfucose-calixarene conjugation

Once both the azido-calixarene scaffolds and the propargylfucose were obtained, we proceeded with their conjugation.

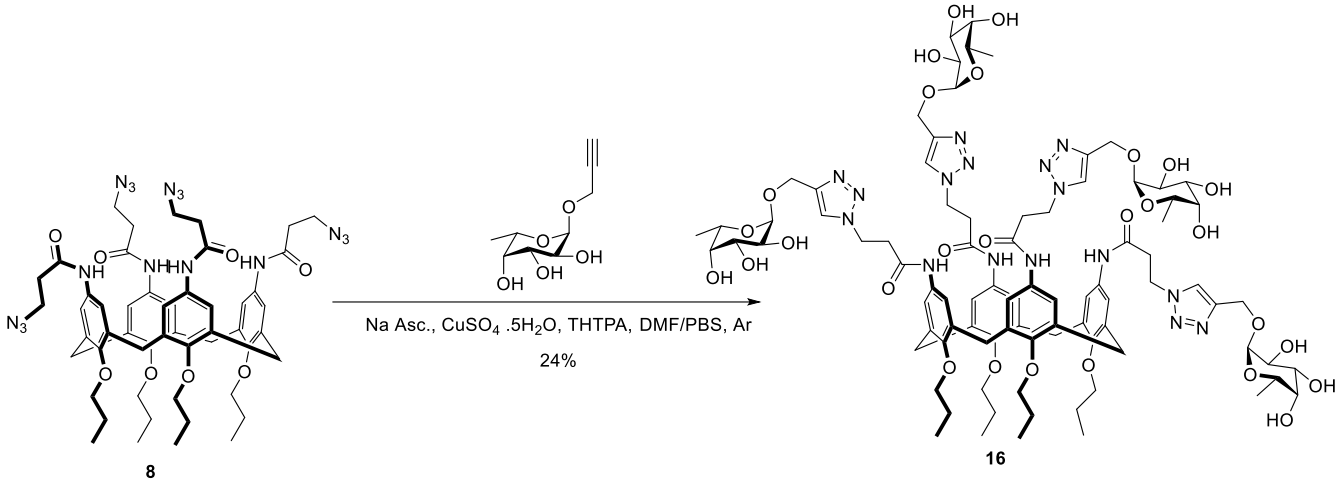

*Scheme 4: Synthesis of compound **16**.*

We started with the cone compound **8** (Scheme 4). This was reacted in a DMF-PBS mixture with propargylfucose **15** in presence of $CuSO_4$, sodium ascorbate and tris(3-hydroxypropyltriazolylmethyl)amine known as THTPA. This latter water-soluble compound acts as a ligand for Cu(I), which forms in situ, preventing its oxidation to Cu(II) and therefore enhancing its catalytic activity during the cycloaddition. The reaction proceeded smoothly at room temperature. The crude was then treated with the ion-exchange resin Chelex, which allowed us to remove the copper ions from the solution. This was necessary because the following purification of the crude by

semipreparative HPLC, without the preliminary removal of the copper ions, would have resulted in longer times and poorer peaks resolution.

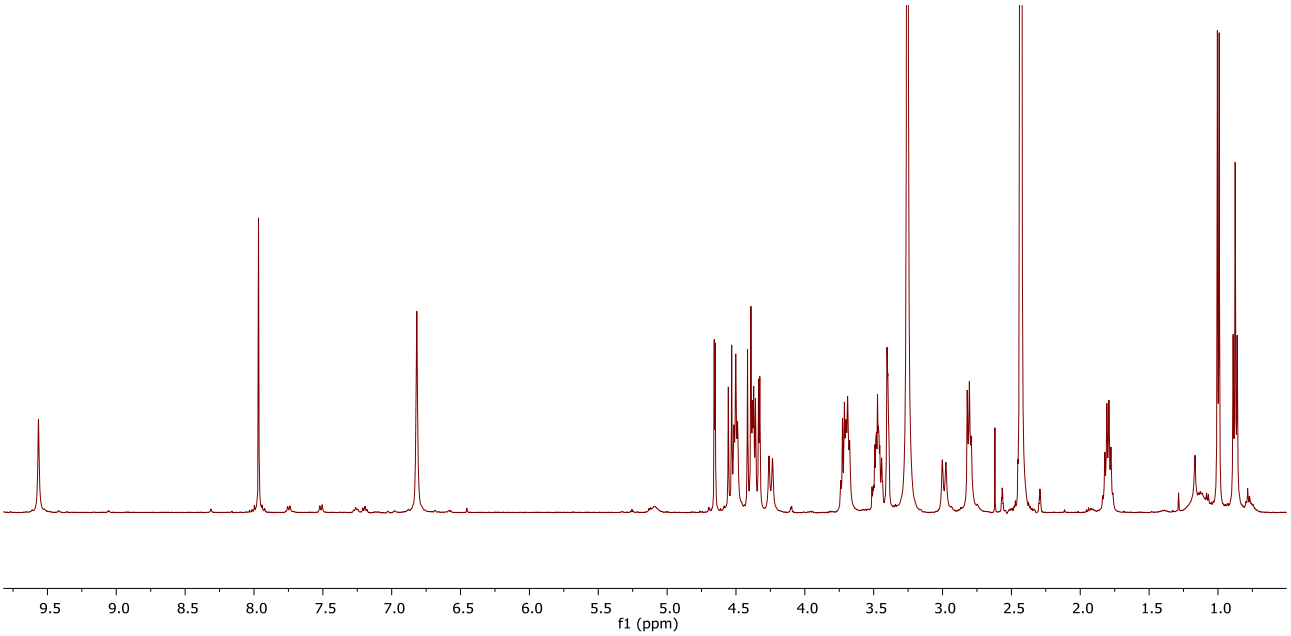

*Figure 6: ^{1}H-NMR of compound **16**, acquired in DMSO-d_6 at 500 MHz and 25 °C.*

The ^{1}H-NMR spectrum of the isolated compound (Figure 6) confirmed, in accordance with the results of MS and 2D-NMR, that compound **16** was successfully formed during the reaction and was correctly purified afterwards. In particular, it is possible to observe some diagnostic signals and their relative integration values. The singlet at 7.97 ppm, corresponding to the triazole protons, the singlet at 6.82 ppm for the calixarene aromatic protons and the doublet due to the fucose methyl groups at 0.91 ppm show a 1:2:3 integral values ratio, confirming the tetra functionalization of the macrocyclic scaffold.

Interestingly, using D_2O as the NMR solvent we obtained the spectrum reported in which the signals were very different from the ones observed in DMSO. The overall broadness of the calixarene signals and the multiple signals relative to the methyl group of the fucose overlapped at high field suggested that there was a complex situation in

solution. Compound **16** can, in fact, as mentioned before, form aggregates in solution thanks to its amphiphilic nature and this NMR spectrum seems to prove this hypothesis.

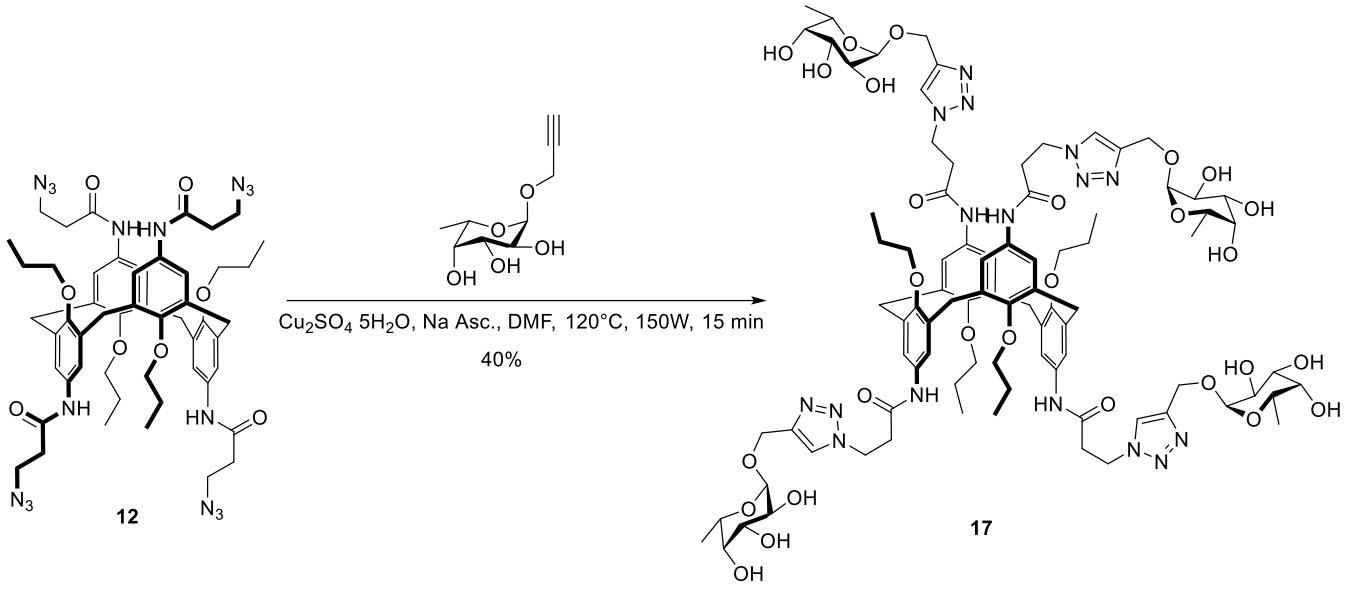

*Scheme 5: Preparation of compound **17**.*

The same procedure described above was also tested with the 1,3-alternate scaffold **12**. In this case, however, due to not completely clear limitation, this protocol did not give us the desired tetravalent ligand (Scheme 5). We were able to only recover the difunctionalized compound, observing an unexhaustive conversion of the sugar. Initially we tried to perform the same reaction at higher temperatures, but this decreased only the time required to see the formation of the divalent compound, without however enhancing the conversion of the starting material and without pushing on the reaction towards the three and/or the tetrafucosylated macrocycles. We then tried to avoid the PBS and only use the minimum amount of water necessary to solubilize the salty reagents. We, in fact, thought that a solubility issue could be at the basis of the poor reactivity of our scaffold. Even these conditions, however, did not promote the formation of the desired product.

We then tried to run the reaction in a microwave reactor. There, using only DMF as a solvent, we were able to reach high temperatures which then promoted the solubilization of all the reagents. At room temperature, in fact, the mixture was heterogeneous but once the temperature increased to 120 °C, it became a homogeneous solution. Using this protocol, we observed the formation of the desired product in only 15 minutes of irradiation. After cooling to room temperature, the crude was treated with Chelex resin as described previously. Semipreparative HPLC purification gave us in 40% yield the tetravalent ligand **17**, that was then characterized by both MS and NMR.

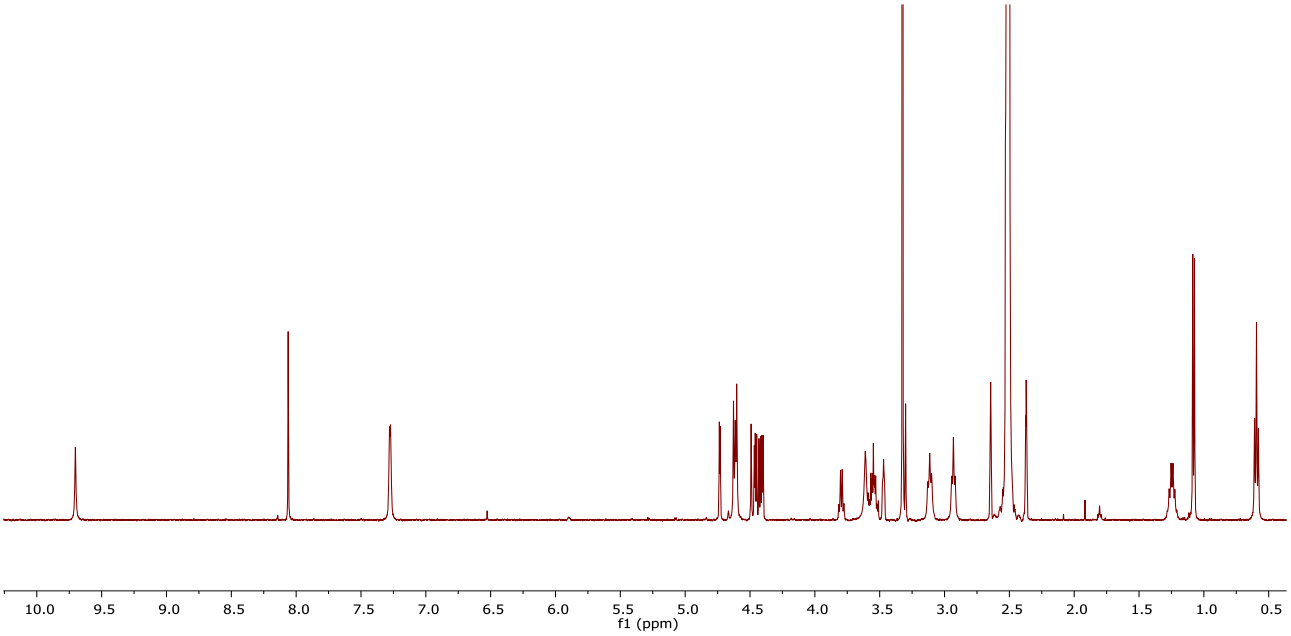

*Figure 7: ^{1}H-NMR of compound **17** recorded in DMSO-d_6 at 500 MHz and 25 °C.*

Looking in the ^{1}H NMR spectrum (Figure 7) at the three diagnostic signals used for the characterization of compound **16**, it was possible also in this case to confirm the successful outcome of the click reaction. Their integral ratio was indeed again 1:2:3, as it must be in a tetra functionalized calixarene.

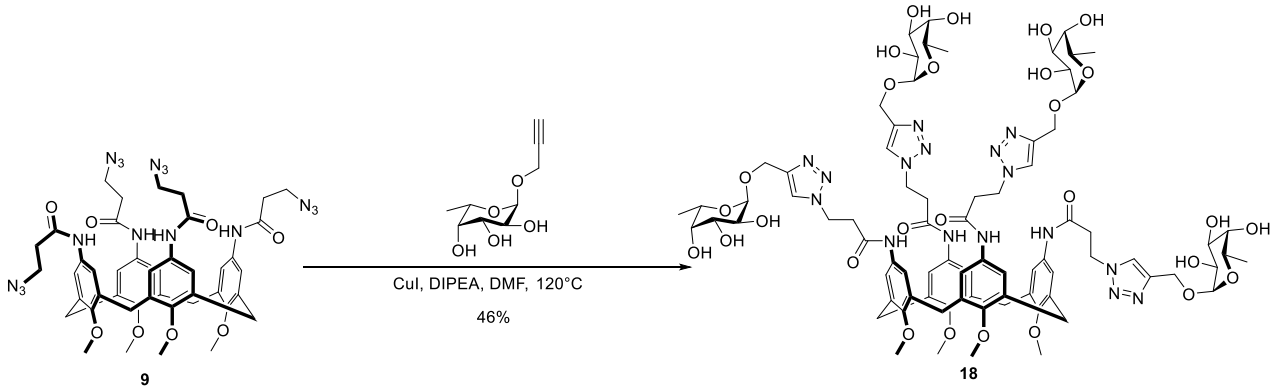

*Scheme 6: Synthesis of compound **18**.*

Moving to the conformationally mobile calixarene **9**, we initially went back to the protocol described for the synthesis of **16**, but we found the same issues met in the first unsuccessful attempts for the synthesis of the 1,3-alternate ligand **17**. Unfortunately, in this case, even performing the reaction assisted by the microwave radiation did not allow to obtain the desired tetravalent compound **18**.

We had therefore to change the reaction conditions again. We decided to change the catalytic system in order to improve the reaction yield. We replaced the standard

$CuSO_4$/Na ascorbate pair with the less common, but still widely used, CuI/DIPEA. The copper atom in this catalytic system is already in the correct oxidation state to perform its catalytic activity. By using these new conditions and conducting the reaction in a microwave reactor, we were able to recover the desired product **18** after HPLC purification (Scheme 6). The use of CuI/DIPEA as the catalytic system and the microwave reactor as the heat source thus proved to be effective in promoting the reaction.

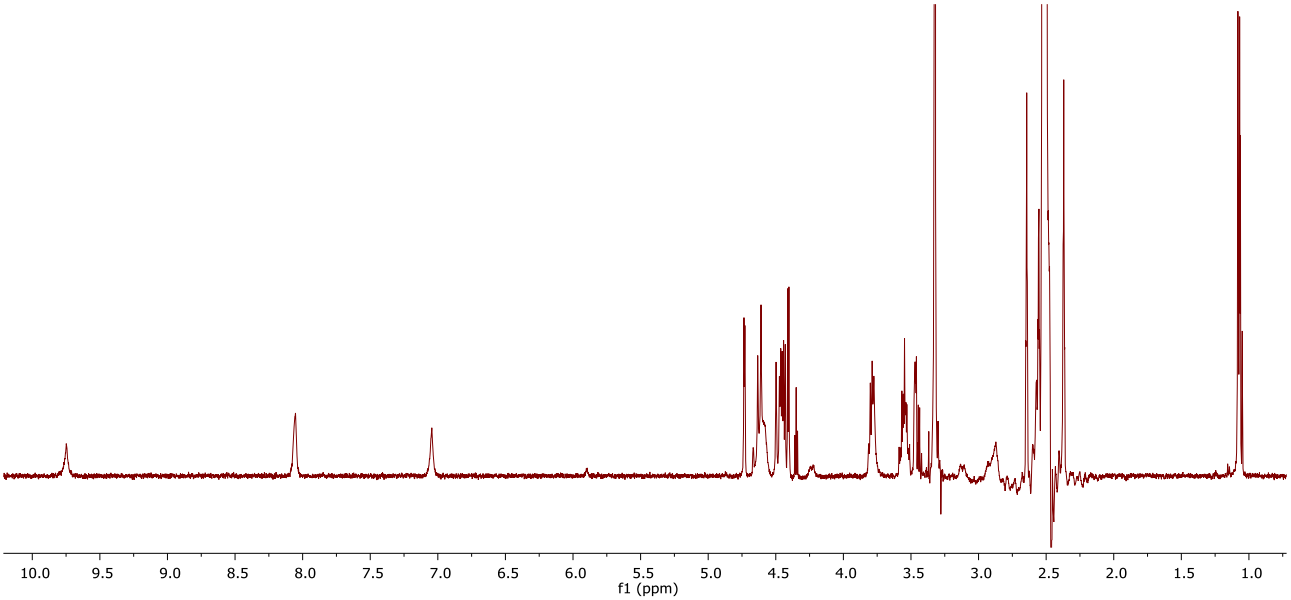

*Figure 8: ^{1}H-NMR of compound **18** recorded in DMSO-d_6 at 500 MHz and 25 °C.*

In the ^{1}H NMR spectrum reported in figure 8 the integrals of the three diagnostic signals taken into consideration before have a slightly unbalance. The signal of the triazole protons at 8.06 ppm and that for the fucose methylene groups at 1.08 integrate for the correct amount, respectively 4 and 12, but the calixarene signal relative to its aromatic protons at 7.05 ppm is less than the half of the value it should be. This could be explained by the observed broadening of the signals relative to the calixarene scaffold reasonably due to its high degree of conformational freedom. However, the presence of only one singlet for the aromatic protons supported the equivalence of the functionalization for the four aromatic rings and then the successful cycloaddition for all the azide units of **9**.

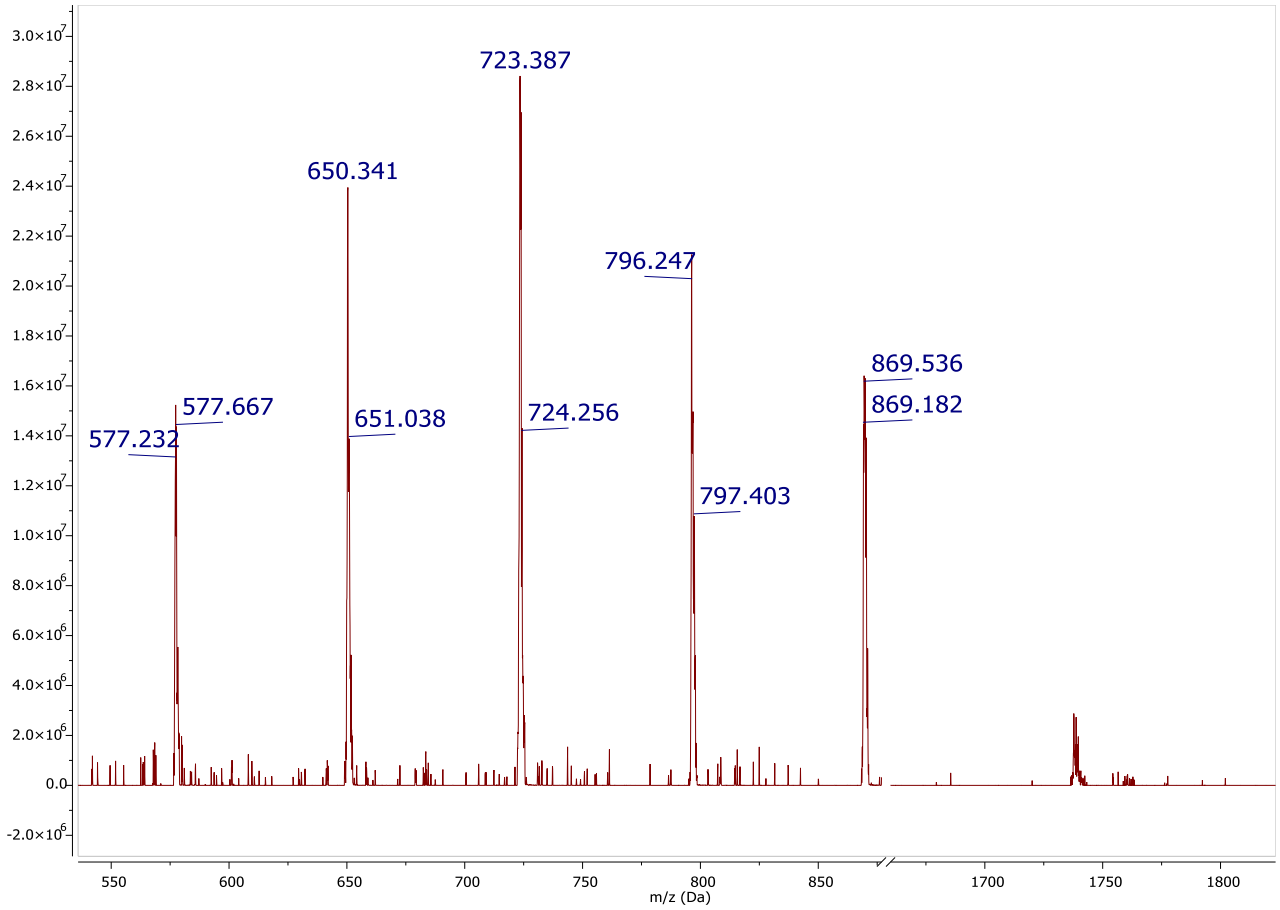

*Figure 9: ESI-MS spectrum of **18***

In any case, the ESI-MS analysis (Figure 9) allowed to dispel any doubt about the reaction outcome. In the MS spectrum it is in fact possible to observe the signals related to the molecular ion of **18** at m/z = 1737, and its dicationic form at m/z = 869, while no peaks relative to partially fucosylated calixarenes are present. The four signals with m/z from 577 to 796, in fact, are in sequence all separated by 73 Dalton from each other, relating to dicationic species wherein, by fragmentation due to the analysis conditions, one or more fucose units are released upon glycosidic bond breaking. As an example, in figure 10 is reported the compound structure generating the signal at 797 m/z. Analogously, those at m/z = 724, 650 and 577 lack two, three and four units of fucose, respectively.

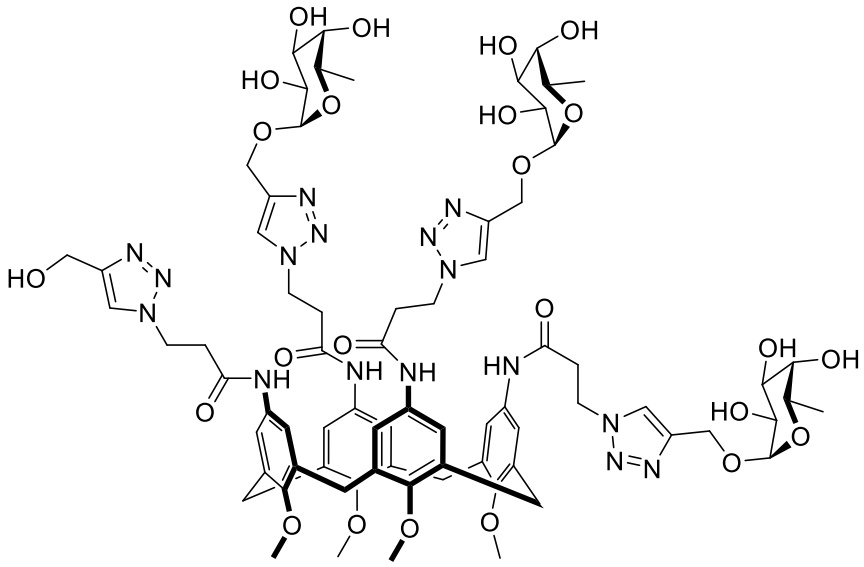

*Figure 10: One of the detected structure upon MS fragmentation of **18**.*

2.2 Calixarene-RAFT-based superstructure synthesis

Since prof. Renaudet's group acquired, during the years, considerable experience in the field of RAFT synthesis and functionalization, we decided to combine his expertise in this field with ours on calixarene synthesis to prepare a new class of polyglycosylated multivalent ligands (Figure 11).

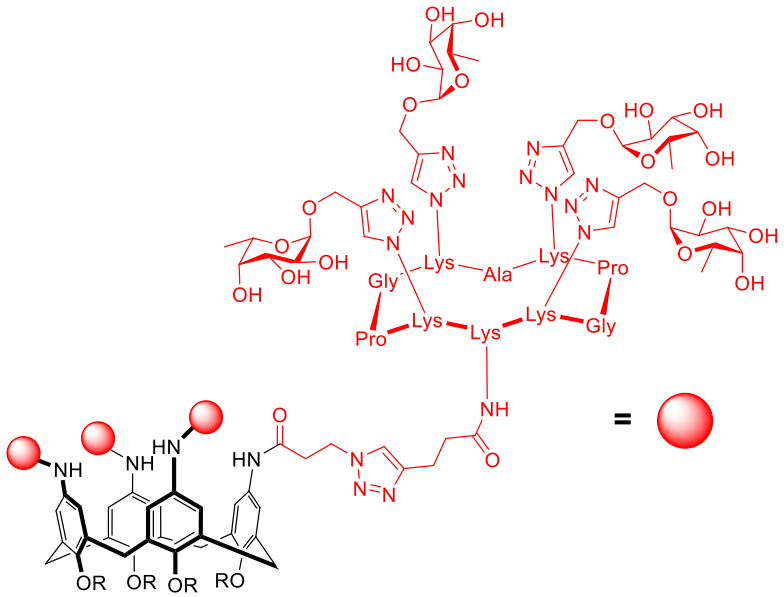

Figure 11: General structure of the new multivalent ligands synthesized.

These new compounds have a central calix[4]arene core that is decorated with four units of a glycosylated RAFT, resulting in hexadecavalent ligands. These molecules,

depending on the geometry of the calixarene core, can orient in different directions the four RAFT units. In fact, employing a cone configuration calix[4]arene will result in the obtainment of a ligand exposing the RAFT units all in the same direction, while utilizing a 1,3-alternate calix[4]arene allow to synthesize a ligand having to cyclopeptide units pointing in a direction and the other two in the opposite one. The situation with a mobile calixarene is difficult to predict in advance, but its conformational freedom could enhance the versatility of this system that could better adapt to different binding sites disposition. The RAFT part of these molecules ensures a high solubility in aqueous media, and all the properties of these scaffolds discussed above. It also gives to these compounds an augmented numbers of binding units compared to the single calixarene. Due to the high structural complexity of these new multivalent structures, we thought to also prepare a control molecule where all the sugar units are replaced by α-galactose. We did this to check if the possible binding that we would have observed during the next interaction experiments was specifically related to the sugar epitopes of these ligands and not to their inner structure.

The synthetic strategy adopted for the preparation of these compounds was, once again, based on click chemistry as the main tool used to fuse the different building blocks together (Figure 12). Since, at this point, we already had in our hands the tetrafunctionalized azido-calix[4]arenes **8**, **9**, **12**, we proceeded with the preparation of the tetravalent glycosylated-RAFTs bearing an alkyne moiety on the lower face. This was needed to link the RAFT platforms onto the central calixarene core.

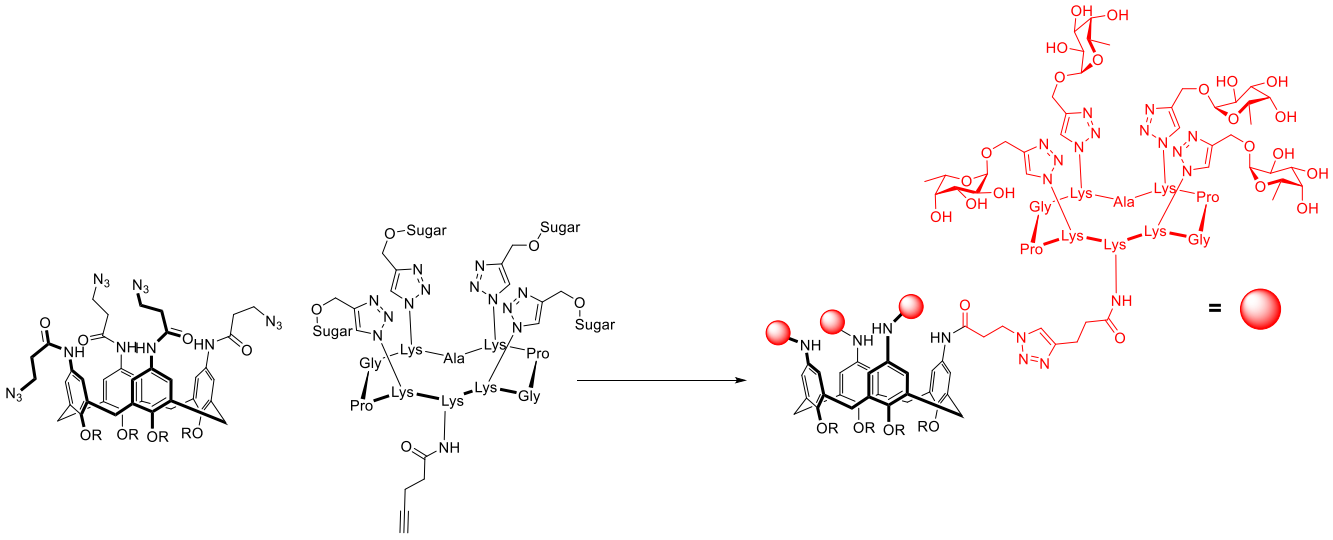

Figure 12: General approach used in the synthesis of the calixarene-RAFT combine ligands

2.2.1 RAFT synthesis

The first step in the cyclodecapeptide synthesis consisted in the preparation of the linear decapeptide that would be subsequently cyclized into the desired RAFT. To do so, we performed the initial part of our synthesis on solid phase, exploiting the Fmoc/tBu strategy. We chose a sasrin resin as the solid support. The main property of this resin is that it allows for a very mild acid cleavage of the elongated peptide chain once the synthesis has been completed. The amino acidic sequence needed to obtain the desired RAFT is:

$$Lys(N_3)\text{-}Lys(Boc)\text{-}Lys(N_3)\text{-}Pro\text{-}Gly\text{-}Lys(N_3)\text{-}Ala\text{-}Lys(N_3)\text{-}Pro\text{-}Gly$$

All the amino acids, opportunely protected with a Fmoc group on their α-amine, are commercially available except for the lysine bearing on the side chain an azido group. This compound had, therefore, to be prepared.

An azido group can be easily incorporated on an amino acid by an azide substitution of a halogenated derivative,[48] or by transfer of a diazo group. This last strategy is particularly interesting because it allows to convert, in a single step, primary amines to azides in high yields, without affecting the stereochemistry of the molecule. Generally, the diazo transfer reaction is carried out using triflate azide under bivalent transition metal catalysis.[49,50] However, this protocol has many disadvantages due to the main reagent instability and low solubility in aqueous media. In 2007, the Goddart-Borger group developed an alternative reagent, imidazole-1-sulfonyl-azide, that is more stable and easier to prepare than triflate azide.[51] The use of this improved reagent allowed us to synthesize compound **19** starting from Fmoc-Lys-OH in a single step (Scheme 7).

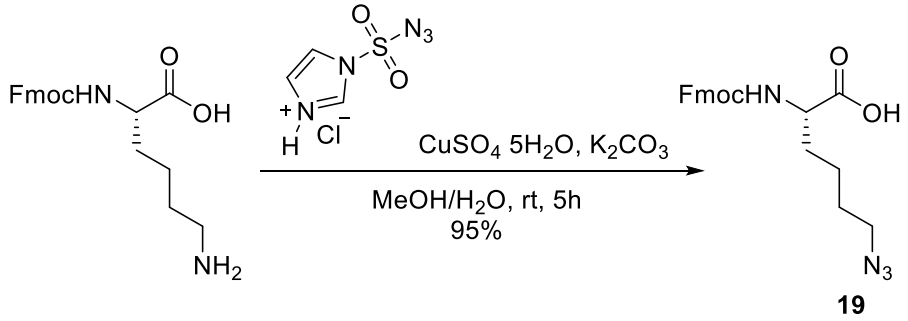

*Scheme 7: Preparation of compound **19**.*

We performed the diazotransfer reaction by treating the Fmoc-protected lysine with the above-mentioned imidazole-1-sulfonyl azide in its hydrochloride form, in presence of copper sulfate and potassium carbonate. These conditions allowed us to obtain compound **19** in a very high yield. During this transformation the two terminal nitrogens of the azidating agent are transferred to the amine to form the desired azide.[52]

Once we had all the needed amino acids, we began the solid phase synthesis. The elongation of the linear peptide was performed manually on the acid-labile Gly-Sasrin resin. The additional advantage with this resin, other than the mild cleavage conditions, is that it is commercially available in the form of already functionalized with Fmoc-protected Gly. The synthesis of the linear peptide started with an achiral residue, the preloaded glycine, in order to avoid any possible epimerization process that can occur during the final cyclisation step since, during this, the first amino acid used to build the linear chain would be the activated one. The deprotection cycles of the N-terminal amines were carried out with a 20% piperidine solution. The peptide couplings were performed with PyBOP as coupling agent in the presence of DIPEA. Once the desired linear peptide was formed, it was cleaved from the resin obtaining compound **20**. by treating our beads with a 1% solution of TFA in DCM. These mildly acid conditions were well tolerated by the Boc protecting group present on the elongated chain. The decapeptide was then cyclized in highly diluted conditions, less than 0.5 mM, to promote the intramolecular reaction while minimizing the risk of the intermolecular one which would result in polymerization. After this step, the only Boc group present in compound **21** was removed by treatment with TFA obtaining, after HPLC purification, compound **22** (Scheme 8).[53] The overall yield, starting from the SPPS to the obtainment of compound **22**, was 37%.

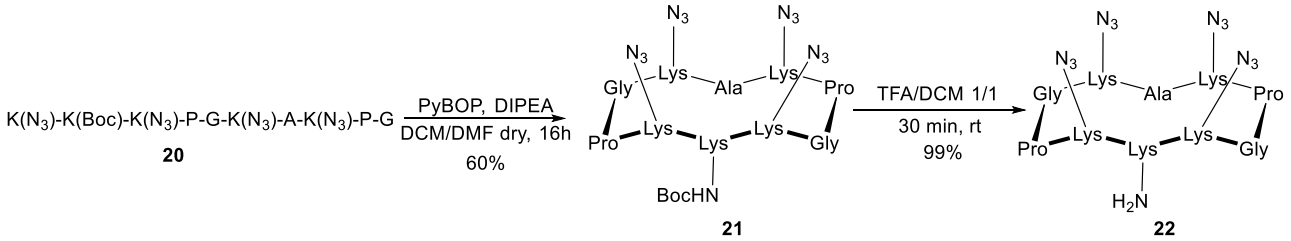

*Scheme 8: Synthesis of **22**.*

The Boc protecting group needed to be removed at this stage since the following synthetic step involved the conjugation of the decapeptide with four units of propargylfucose. This prevented us to remove the carbamate later because the glycosidic bond of the four carbohydrates would have not tolerated the highly acidic conditions required for the deprotection.

2.2.2 RAFT fucosylation

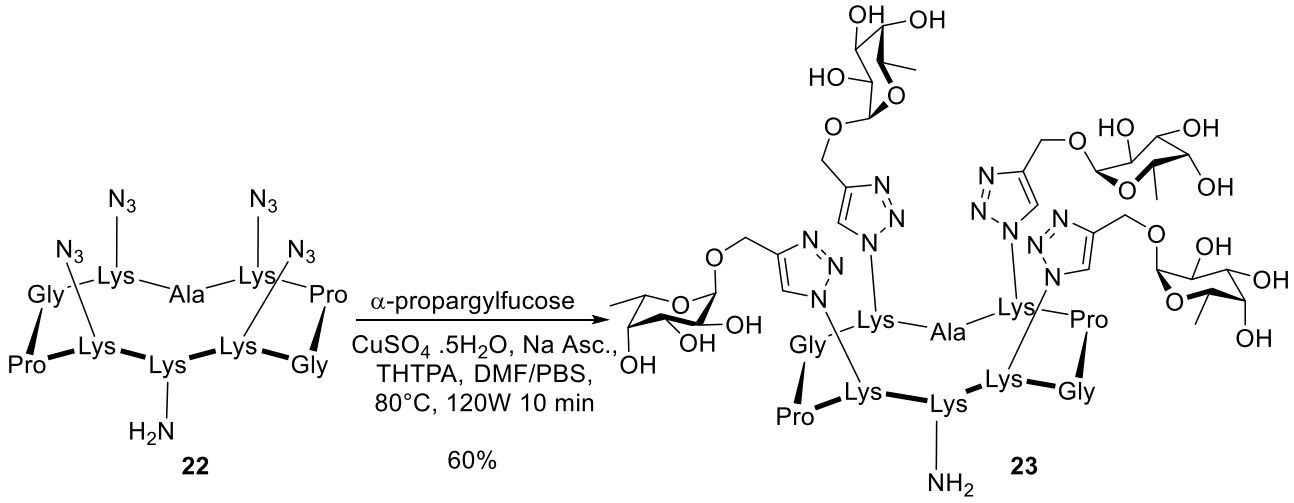

*Scheme 9: Synthesis of compound **23**.*

As introduced above, the purified compound **22** was linked to the α-propargylfucose (Scheme 9). The CuAAC allowed us to join the five molecules together. The catalytic system we employed was the standard $CuSO_4$/Na ascorbate pair, enhanced by the addition of THTPA. The solvent used was a mixture of DMF and PBS, the latter needed to keep the pH at 7.4 and promote reagents solubilization. The reaction was carried out in a microwave reactor at 80 °C. This protocol permitted us to obtain the desired fucosylated-cyclopeptide **23** after only ten minutes of irradiation. At this point, Chelex resin was added to the solution, then, after filtration, the product was purified by semipreparative HPLC, obtaining the pure compound **23** in 60% yield.

At this point, as described previously, we needed to introduce the alkyne functionality on **23** (Scheme 10).

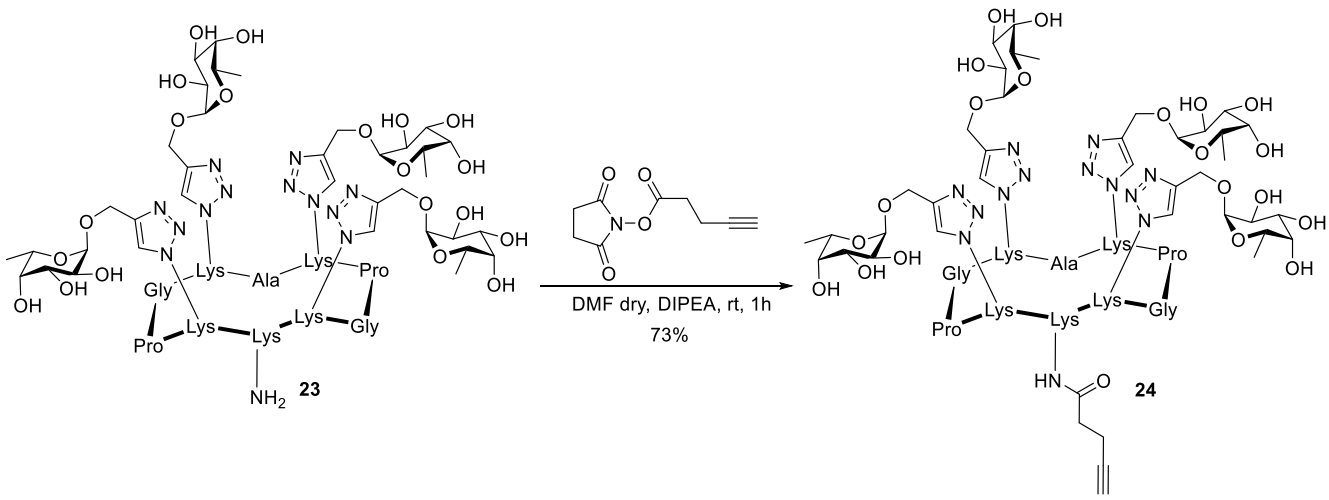

*Scheme 10: Synthesis of compound **24**.*

This, in fact, was necessary to be able to link four fucosylated RAFTs to the calixarene platforms (**8**, **9**, **12**), once again via CuAAC. The alkyne must not be too close to the cyclopeptide since steric hindrance could negatively affect the outcome of the click reaction. Furthermore, the spacer length is crucial for the conformational freedom of the ligand. However, it is useful to avoid too long spacers to prevent that the linked RAFT substantially acts as an impaired version of its free, unbound, form. We wanted to avoid this scenario and instead exploit the ligand preorganization introduced by the calixarene presence, which could result in a better ligand. We therefore chose the 4-pentynoic acid as the spacer. Its chain length represented for us a good balance between enhancing the cycloaddition reaction outcome and preventing the ligand to have too much conformational freedom. Furthermore, the limited number of saturated carbons should not affect the water solubility of the ligand.

To introduce this alkyne moiety, we performed a peptide coupling reaction between the activated ester of 4-pentynoic acid and the free amine of **23**. The reaction proceeded smoothly and after one hour, and HPLC purification, we were able to obtain the desired compound **24** in a satisfactory 73% yield. Its ESI-MS spectrum is reported in figure 13. Here it is possible to observe the signal at m/z = 2013 which corresponds to the molecular ion of the product and the signal at m/z = 1867 related to the molecular ion having lost, due to a fragmentation, a unit of fucose. The signals with m/z around and below 1000 are all related to dicationic species. The signal at m/z = 1007 is relative to the molecular ion of **24**, while the one at 934 to a corresponding fragment. All the other signals are spaced by 73 Dalton and are generated by detachment of fucose units, arriving at m/z = 715 which corresponds to the completely de-glycosylated RAFT.

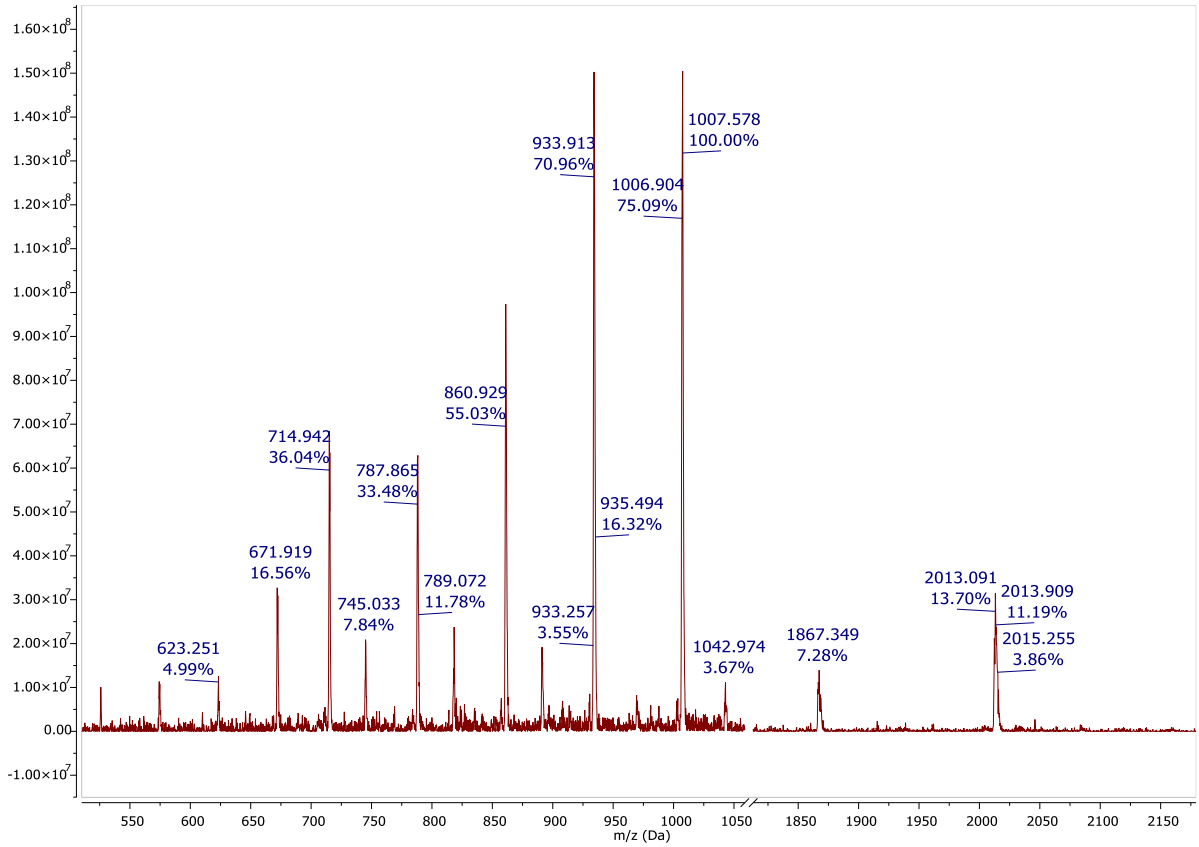

*Figure 13: ESI-MS spectrum of compound **24**.*

2.2.3 Calixarenes-RAFT conjugation

At this point we had all the compounds necessary to perform the RAFT-calixarene conjugation. We aimed to prepare the hexadecavalent ligands in three different configurations, using the calixarene cores described above.

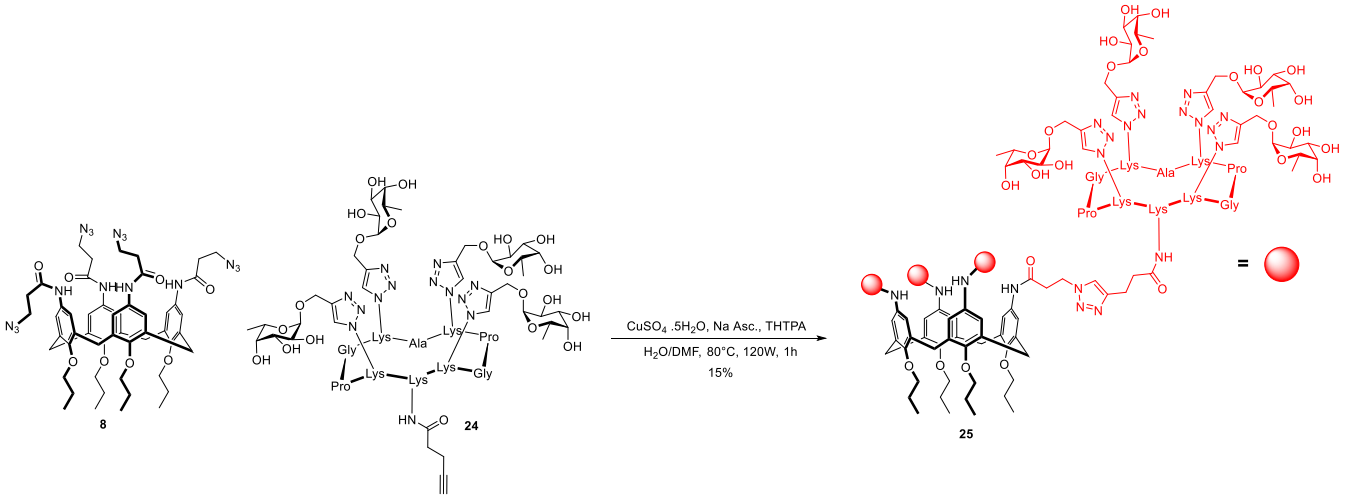

*Scheme 11: Synthesis of compound **25**.*

Once again, we employed click chemistry to link compounds **8** and **24** together (Scheme 11). We used similar conditions as described above, being the only difference, in this case, that we avoided the use of PBS and only employed distilled water as solvent.

The choice was also based on the evidence, collected before, that calixarenes do not need this buffer to be solubilized and for the non-cone configurations it was even detrimental. The lengthy synthesis of both the reactants allowed us to only have few milligrams of each at this point, therefore we used only a slightly excess of RAFT compared to the calixarene, 4.4 equivalents to 1. Three cycles of microwave irradiation, each twenty minutes long, were performed. After the first iteration it was still possible to see unreacted calixarene by ESI-MS analysis. The second cycle was crucial for converting all the limiting reagent, while the third one was carried out to limit the amount of possible intermediates. These, however, together with the desired product, were very difficult to identify because, once the molecular weight increased over the region explorable with ESI-MS, we could not analyze our reaction mixture in a rapid and simple way. MALDI-MS was not an option because, due to the low quantities involved, we couldn't exploit it as monitoring technique.

Since the only clue we had was the exhaustive consumption of the starting calixarene scaffold, we proceeded by quenching the reaction and then purifying the crude by HPLC. This process gave us two compounds that, after MALDI-MS analysis, revealed to be the desired one, compound **25**, and the tri-functionalized calixarene **26** (Figure 14).

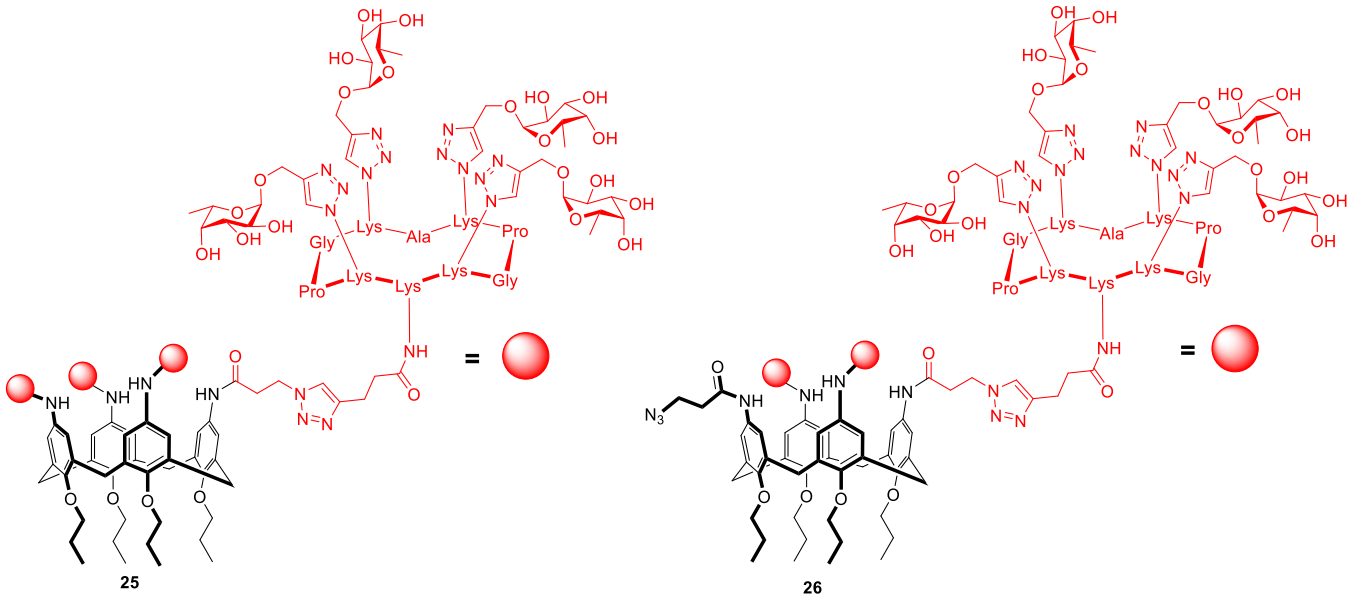

*Figure 14: Structure of the two multivalent compounds **25** and **26**.*

Below are reported the MALDI-MS spectra for both compound **25** (Figure 15) and **26** (Figure 16).

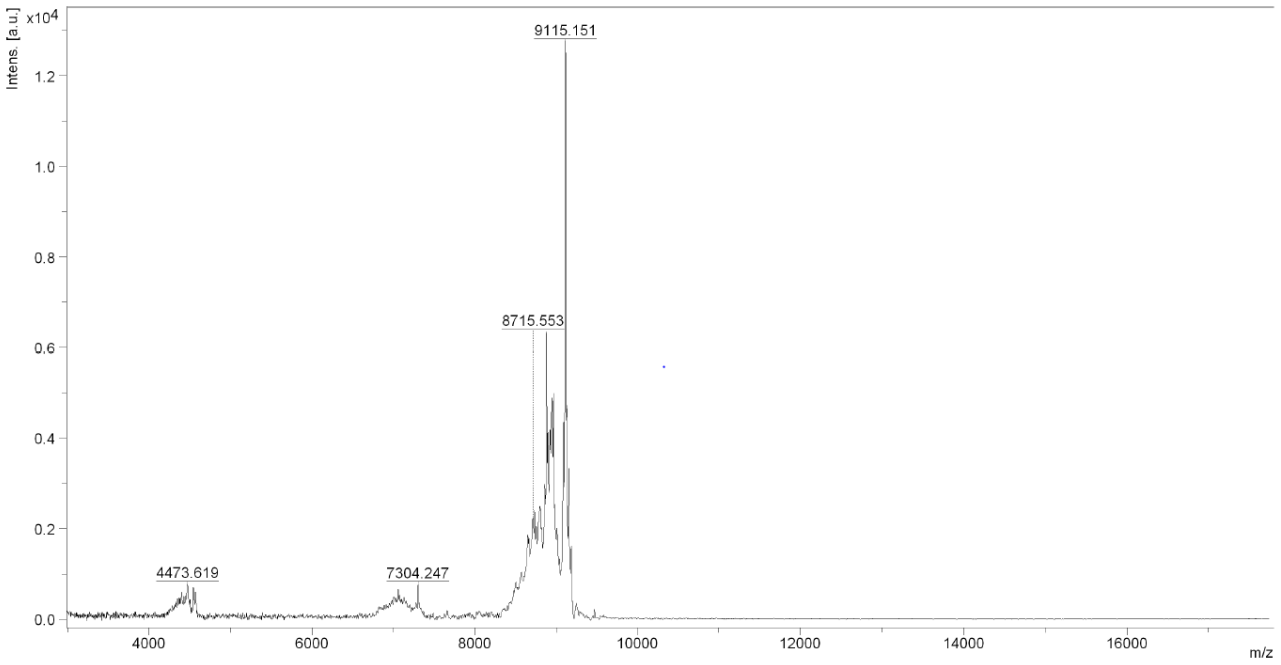

*Figure 15: MALDI-MS spectrum of compound **25**.*

In the spectrum of the former the main signal is the one at m/z = 9115 m/z which corresponds to the adduct with sodium of compound **25**. However, it is also possible to notice how, even after HLPC purification, it was impossible to obtain a pure product. In fact, the signal around m/z = 7000 m/z is related to the trifunctionalized compound **26**.

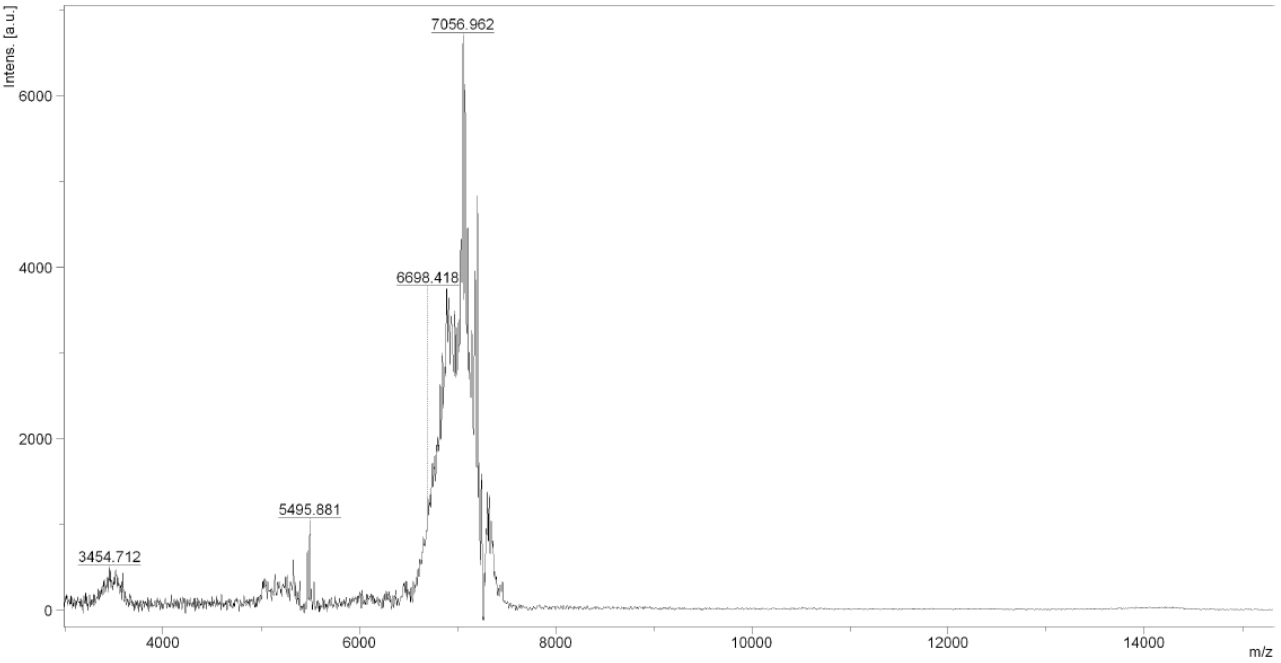

*Figure 16: MALDI-MS spectrum of compound **26**.*

The MALDI-MS analysis of compound **26** gave us similar results, with the main signal relatable to the trifunctionalized derivative. Also in this case the compound is not completely pure as evidenced by the presence of signals around 5000 m/z which are possibly related to a difunctionalized species.

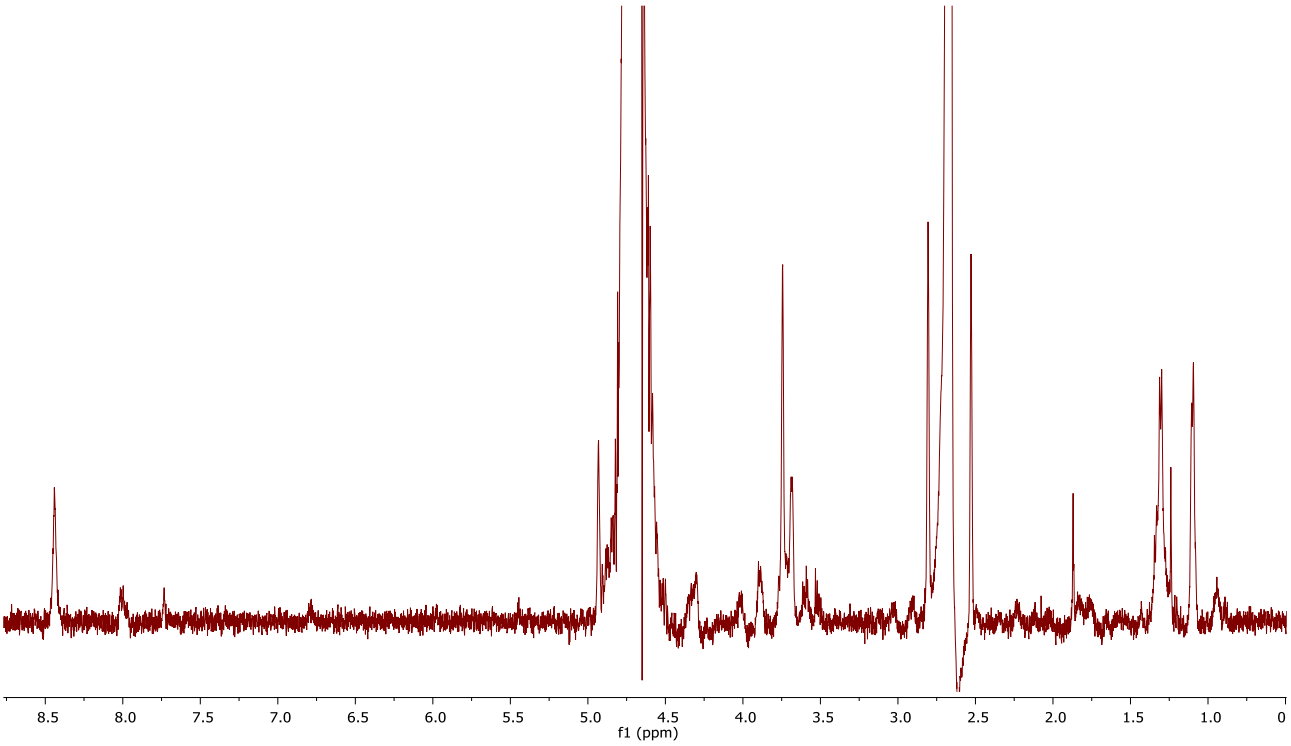

*Figure 17: 1H-NMR of compound **25** recorded in a mixture of deuterated water and DMSO (9:1) at 500 MHz and 25 °C.*

^{1}H-NMR of product **25** was also collected, and it is shown in figure 17. The spectrum results difficult to comment because of the very low concentration, but few key signals can be observed. In particular it is possible to see: the signal at 8.52 ppm, related to the triazolic protons; the signal at 8.08 ppm, which is linked to the aromatic protons of the calixarene core; the on at 5.02 ppm, generated by the anomeric protons of the sugars which is partially overlapped to the residual water signal and lastly the signal at 1.18 ppm, which is related to the fucose methyl groups. The integral values for these signals are a bit off due to them disappearing into the noise or being overlaid to others. Setting the doublet at 1.18 ppm to 48, the integrals for the signals at 8.52, 8.08 and 5.02 ppm are respectively 21, 5 and 20, when ideally, they should be 20, 4, 16.

The overall yield of the isolated compound **25** was very low, around 15%. This could be explained by the fact that the reaction was probably quenched too early and the intermediate **26**, and the others not isolated, were not able to react further. However, due to quantity limitations and time restrain we could not try to optimize the protocol.

We then moved on with the other tetraazido calixarenes.

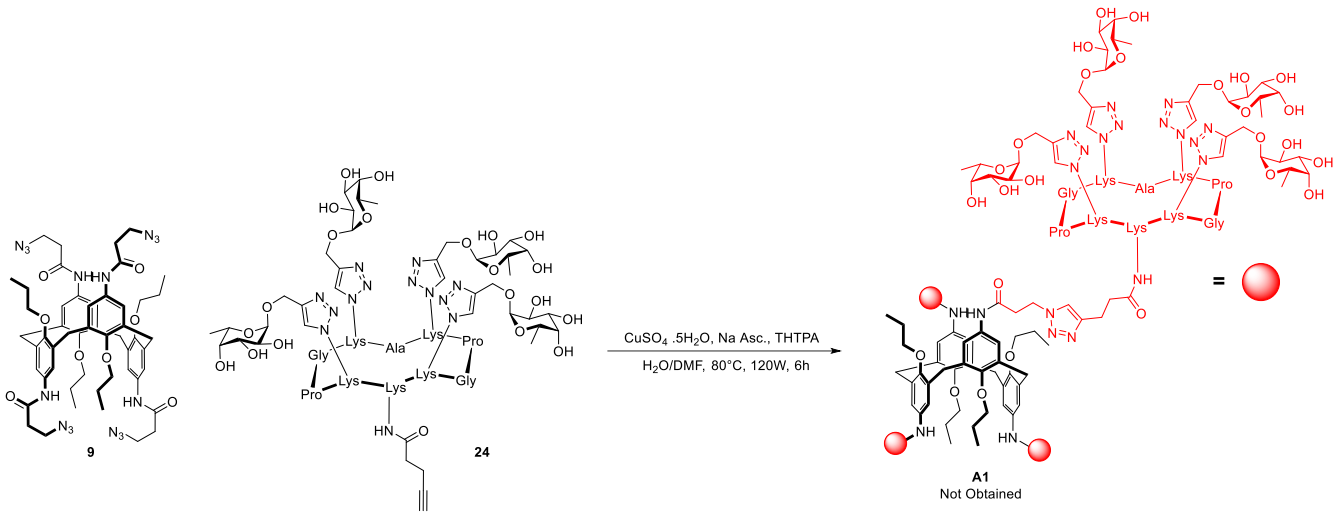

*Scheme 12: Attempt of preparation of compound **A1**.*

The protocol described above was also followed for the conjugation on the 1,3-alternate calixarene **9** (Scheme 12). However, in this case, even after six hours of total microwave irradiation, we did not observe the formation of the desired product and the conversion of the starting material stopped at the difunctionalized intermediate. This can be seen in figure 18 where the MALDI-MS spectrum shows at around m/z = 5000 the signals relatable to this intermediate product. No addition of both the RAFT and the catalytic system influenced the mixture composition.

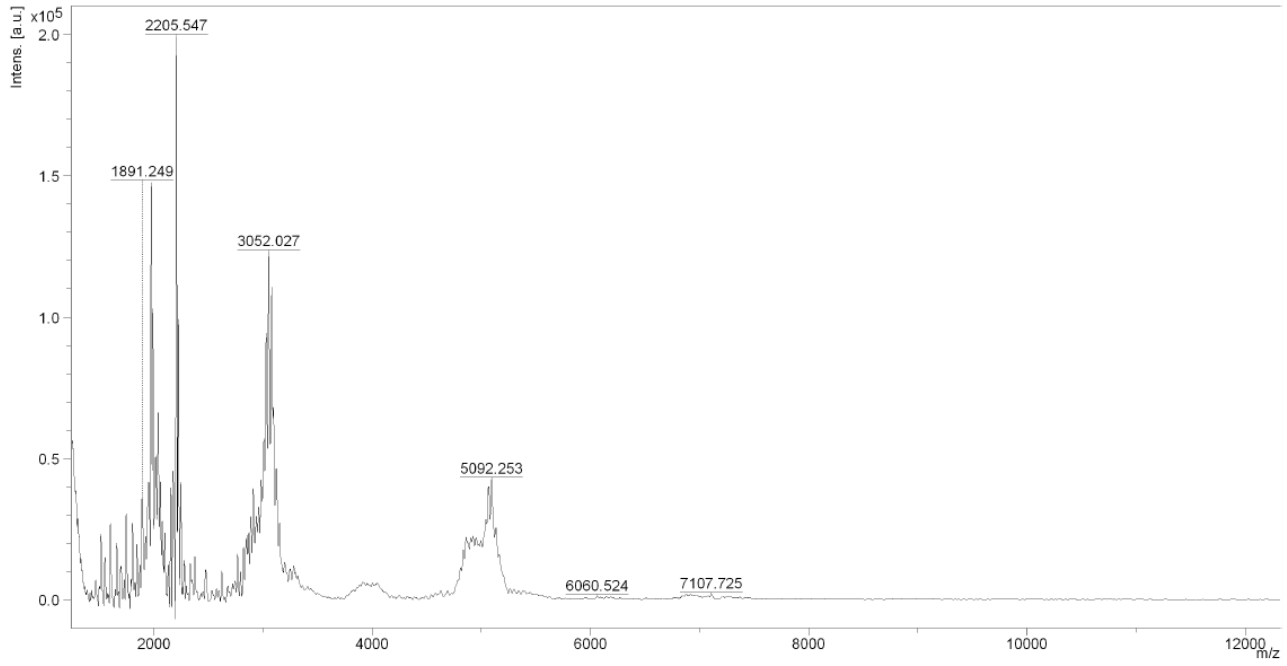

Figure 18: MALDI-MS spectrum of the crude.

After this, we tried to conjugate the mobile tetraazido calixarene **12** to the RAFT scaffold too (Scheme 13).

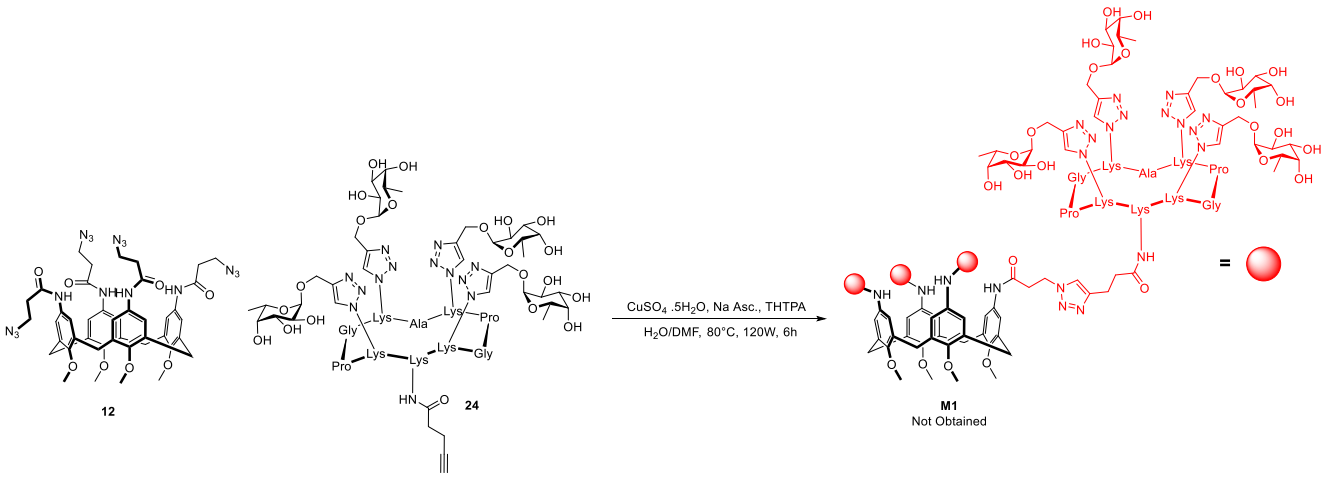

*Scheme 13: Attempt of preparation of compound **M1**.*

Unexpectedly, with the conformationally mobile calixarene **12** we did not observe any conversion of the starting material. Even after multiple iterations of microwave irradiation the composition of the crude did not change.

2.2.4 Synthesis of galactosylated control molecules

Since we were able to synthesize only the multivalent ligand having as core the cone calix[4]arene **8**, we proceeded in the preparation of only the control compound having the same architecture. This ligand was obtained following the same synthetic steps described above. The only difference was that, in this case, the saccharide unit employed consisted in the α-propargyl galactoside (Scheme 14).

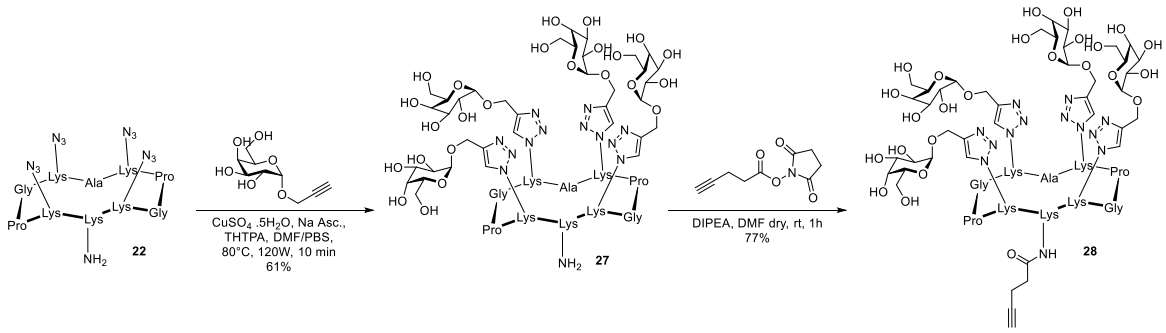

*Scheme 14: Reaction pathway for the synthesis of compound **28**.*

After the preparation of the galactosylated RAFT **28** we proceeded with its linking on the cone tetraazido calixarene **8** by CuAAC. We followed the same protocol that allowed us to obtain compound **25**. These conditions proved valid also in this case and we were able to obtain the desired product **29** after HPLC purification (Scheme 15).

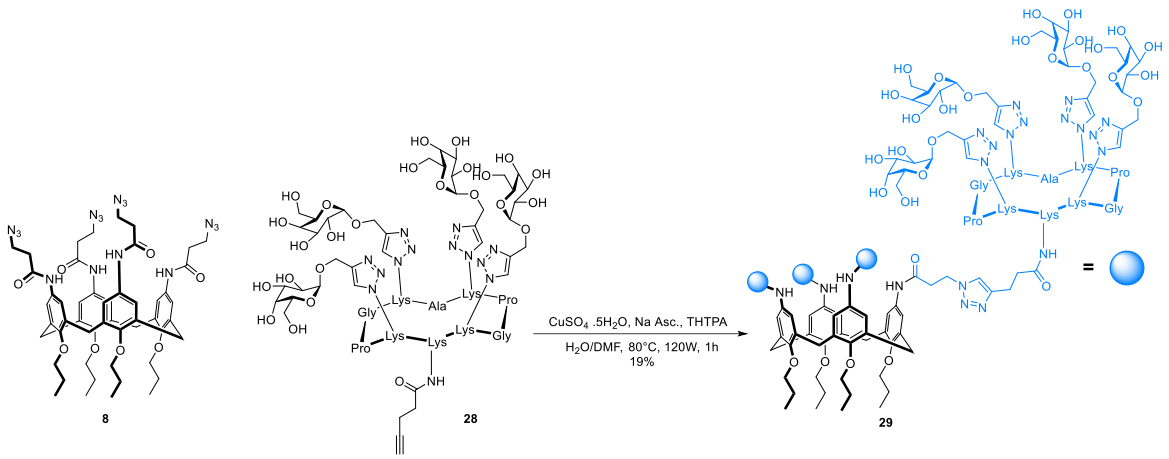

*Scheme 15: Synthesis of compound **29**.*

In figure 19 is reported the relative MALDI analysis. The base peak is related to the sodium adduct of the molecular ion of **29**, ensuring the positive outcome of the reaction. As in the previous cases, however, it is possible to see signals related to partially functionalized scaffolds. Since we had little time left before the end of my period in the Renaudet's lab, and since this compound had only to act as a control, we proceeded with the following studies.

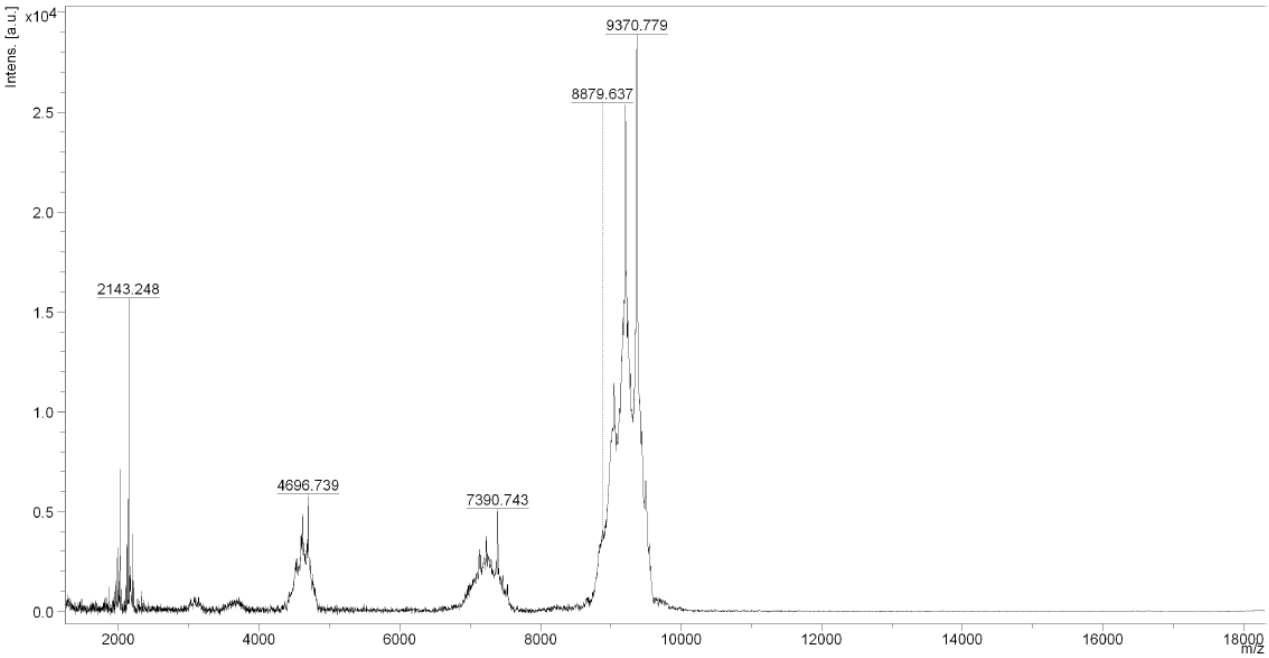

*Figure 19: MALSI-MS spectrum of compound **29**.*

2.3 ITC experiments

Once all the ligands were synthesized, we proceeded to study them using isothermal titration calorimetry (ITC). This technique allowed us to gather precious information about their binding affinities towards the three lectins examined: BambL from *Burkholderia ambifaria*, AFL from *Aspergillus Fumigatus*, and LecB from *Pseudomonas Aeruginosa*.

Professor Renaudet and coworkers had already described the process and conditions for the expression of these lectins. This was carried out in *Escherichia coli* while protein purification was done on an affinity column.[54] ITC experiments were conducted using a PEAQ-ITC microcalorimeter at 25 °C. The lyophilized neoglycoconjugates and lectins were dissolved in a buffer solution composed of Tris-HCl (20 mM), NaCl (100 mM), and $CaCl_2$ (100 µm), in order to maintain constant both the pH at 7.5 and the ionic strength of the medium. The lectins (15-50 µM) were placed in the 200 µL sample cell, which was also kept at 25 °C. The titrations were performed using 19 injections of neoglycoconjugates (30-800 µM, 2 µL per injection), with a 150 s interval between injections to allow the system to equilibrate after each addition. The data were analyzed using the MicroCal PEAQ-ITC software, which fits the experimental data to a theoretical titration curve and determines the enthalpy change (ΔH), dissociation constant (K_D), and the stoichiometry (n). Entropy contributions (TΔS) and free energy variations (ΔG) are derived from the equation $\Delta G = \Delta H - T\Delta S = - RT\ln K_a$ (where T is the absolute temperature and R = 8.314 $J \cdot mol^{-1} \cdot K^{-1}$ and $K_a = 1/K_D$). Two independent titrations were performed for each ligand tested.

2.3.1 BambL titration

The first step consisted in the titration of the lectin with the monovalent α-propargyl fucoside **15** (Figure 21), and it was carried out to determine the affinity of a single fucose unit for BambL. We determined a K_D of 1060 nM with a stoichiometry of 1.66 units of ligand per protein pointing for an average occupation of roughly four over six binding sites of the protein.[55]

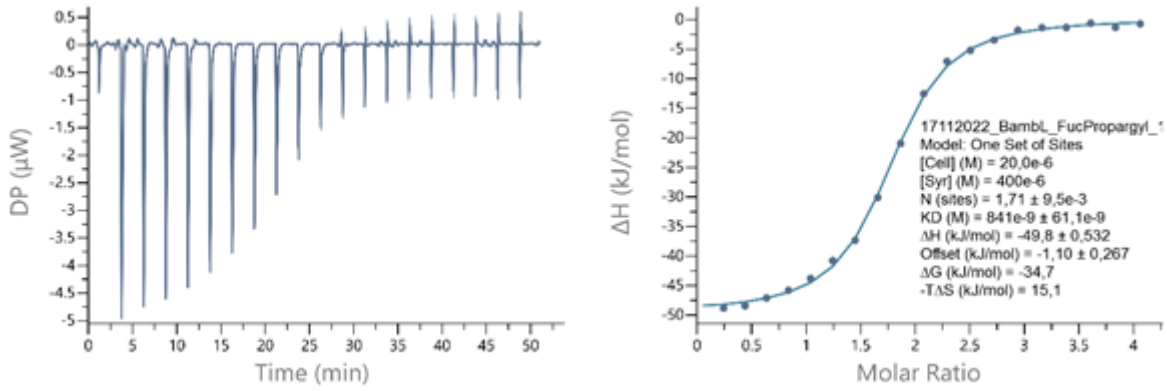

*Figure 21: Left: thermograms obtained by injections of **15** in a solution of BambL. Right: corresponding integrated titration curves.*

We used the result of this determination as a guideline to compare the values obtained by testing our ligands. All the results are reported in table 1.

Table 1: BambL: Thermodynamic data refer to moles of glycoconjugate and stoichiometry is expressed as the number of glycoconjugate molecules per lectin. Standard deviations are indicated on experimentally derived values (at least two experiments). Coefficient α is the relative potency compared to the monovalent compound. Coefficient β is the relative potency per fucose residue.

Compound	Valency	K_D (nM)	*n*	-ΔH (kJ/mol)	-ΔG (kJ/mol)	-TΔS (kJ/mol)	α	β
15	1	1060±220	1.66	48.8±1.0	34.2	14.6	-	-
16	4	4.86±3.2	0.85	52.4±4.0	48.2	4.2	218	55
17	2+2	47.4±16.3	0.63	119±1.0	42.0	77.0	22	5.5
18	4	51.5±2.5	0.62	122±0.5	41.7	80.3	21	5
25	16	21.3±0.9	0.16	502±3.0	43.8	458	50	3
26	12	18.4±0.7	0.25	340±1.0	44.2	296	58	5

In the case of BambL, all compounds could be evaluated and no aggregation causing precipitation was observed during all the calorimetric titrations. Concerning the tetravalent compounds **16**, **17** and **18**, the first one showed the highest affinity ($K_D \cong 5$ nM) and a significant relative potency ($\alpha = K_D mono/K_D multi$) with respect to the monovalent reference compound **15** of 218 corresponding to a normalized value ($\beta = \alpha/n$) of 55 per fucose unit. Despite the same valency, ligands **17** and **18**, substantially equivalent to each other, resulted at least 10-fold less efficient than **16**.

Interestingly, the enthalpy/entropy balance is much more favorable in the case of **16** where the entropic cost, resulting from the loss of flexibility upon lectin binding, is around 20 times lower than for **17** and **18** (4.24 versus 78.8 and 79.9 kJ/mol). This suggests that the spatial arrangement of the epitope units all pointing in the same direction as for **16** is, in this recognition process, more effective than a divalent presentation in two opposite directions as it is the case of **17**. Substitution of the propyloxy groups at the lower rim of the calixarene (**16**) with methoxy ones (**18**) has a negative effect on the affinity probably due to the increased flexibility of the overall structure and, as the data evidence, a significantly higher cost in term of entropy only partially counterbalanced by a more favorable enthalpy.

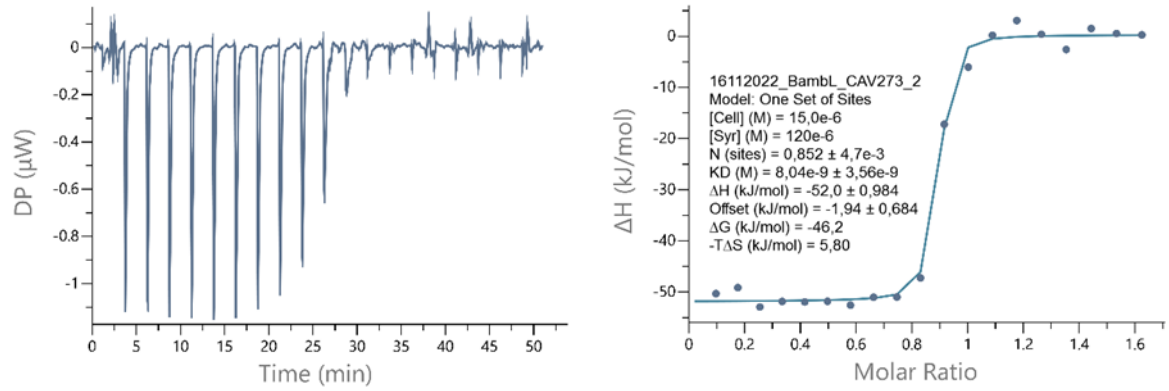

*Figure 22: Left: thermograms obtained by injections of **16** in a solution of BambL. Right: corresponding integrated titration curves.*

For ligands **17** and **18**, the stoichiometry ligand/protein close to 0.5 indicates their ability of binding to two protein trimers that is compatible with the 1,3-alternate geometry of **17**. Probably the same or a very similar geometry is assumed also by the conformationally mobile derivative **18**. This is actually reasonable, considering that it was already demonstrated that mobile methoxycalix[4]arenes with polar groups at the upper rim tend to rearrange in that conformation when in water solution to minimize the contact between the polar environment and the lipophilic portions of their structure.[56] Compound **16**, having a n value of 0.85, binds on average 1.15 lectin trimers then it is substantially all engaged in a 1:1 complex (experimental data in Figure 22). Considering the length of the spacers linking the fucose units to the calixarene scaffold (surely smaller than 13 Å) and the distance between the lectin trimer binding sites (17.3 Å), it is difficult to imagine the possibility that even two epitope units are each one simultaneously interacting with one the binding sites. Therefore, the results for this ligand suggest that the gain in affinity comes from local binding-rebinding of the multiple fucose units to a single binding site of the lectin. This can also be inferred by

observing that ΔH values for **15** and **16** are very similar but the latter has greater entopic stabilization than the former.

Stoichiometries observed with dodeca- and hexadecavalent glycodendrimers **25** (Figure 24) and **26** (Figure 23) suggest that a single molecule is able to simultaneously bind six and four lectin trimers, respectively. Furthermore, ΔH values for **25** and **26** suggest that, unless very favorable chelate effects are present, the former employs around ten fucose units during the binding while the latter seven. This would imply that for both ligands at least one of the four or three RAFT units is involved in interactions with two copies of trimers. However, the gain in binding enthalpy allowed by this multivalent interaction is strongly counterbalanced by its huge entropic cost. The resulting K_D values are therefore only slightly lower than for tetravalent compounds **17** and **18** and their relative potency per sugar the same as that of them. Interestingly, dodecavalent compound **26** has an affinity very similar to that of compound **25**, and the normalized relative potency slightly smaller, suggesting that adding a fourth tetravalent arm to the structure does not lead to an improved binding due to the resulting entropic cost.

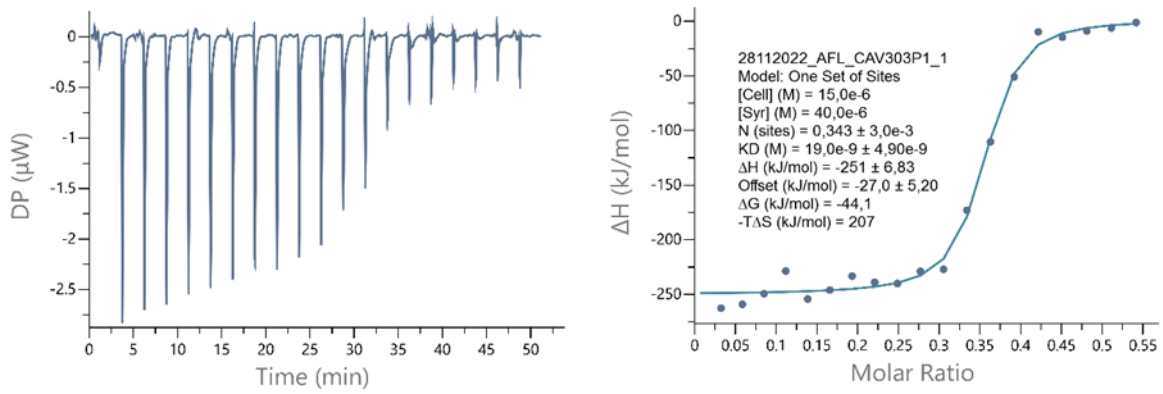

*Figure 23: Left: thermograms obtained by injections of **26** in a solution of BambL. Right: corresponding integrated titration curves.*

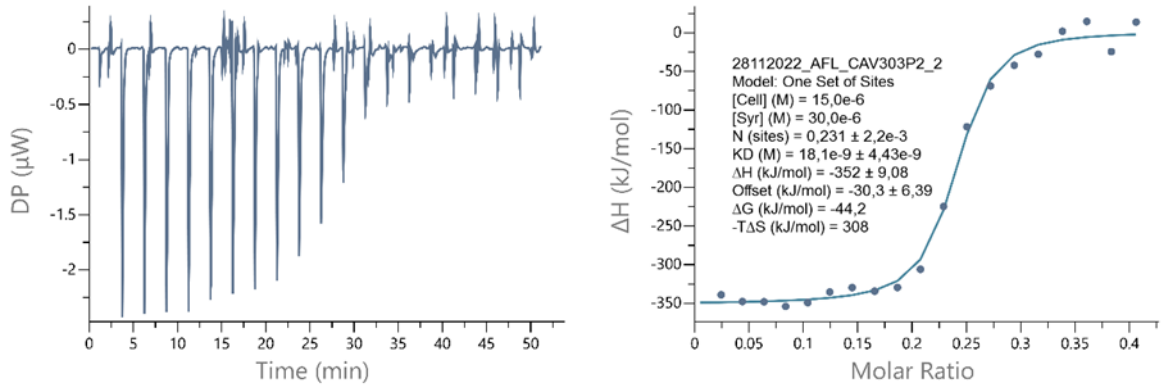

*Figure 24: Left: thermograms obtained by injections of **25** in a solution of BambL. Right: corresponding integrated titration curves.*

Among all the tested compounds, **16** clearly stands out. It is the most potent ligand of BambL with a K_D below 5 nM and each sugar epitope installed on the cone calix[4]arene scaffold is 55 folds more potent when compared to the monovalent reference. The interesting behaviour of **16** could be explained with the possibility for this ligand of forming aggregates in solution, due to its amphiphilic nature, and therefore have an enhanced valency compared to its monomeric form. In this situation, in fact, on the aggregate surface are shown multple copies of fucose, each very close to the others. This strongly enhanche the binding-rebinding process because every time a fucose unit leaves the lectin binding site there is immediately a new one able to interact with it due to the aboundance of binding units on the aggregate surface.

The control molecule **29**, the galactosylated hexadecavalent superstructure, behaved as expected and had no affinity for the lectin. This proved that the binding observed using the dodeca- and hexadecavalent ligands was not aspecific, but due to the fucose binding units installed on these ligands.

2.3.2 AFL titration

The same experiment setup described above was repeated also for the studies with AFL. The results obtained are reported in table 2.

Table 2: AFL: Thermodynamic data refer to moles of glycoconjugate and stoichiometry is expressed as the number of glycoconjugate molecules per lectin. Standard deviations are indicated on experimentally derived values (at least two experiments). Coefficient α is the relative potency compared to the monovalent compound. Coefficient β is the relative potency per fucose residue.

Compound	Valency	K_D (nM)	*n*	-ΔH (kJ/mol)	-ΔG (kJ/mol)	-TΔS (kJ/mol)	α	β
15	1	36900±13000	1.01	56.8±23.2	25.3	31.5	-	-
16	4			Agglutination				
17	2+2			Agglutination				
18	4			Agglutination				
25	16	14.8±3.4	0.24	359±7	44.8	314	2501	156
26	12	17.1±1.9	0.33	264±12.5	44.4	219	2158	180

In the case of AFL, the tetravalent compounds **16**-**18** were assayed but data were not useful due to the agglutination phenomenon that occurred in the last part titration

experiments, before it the ΔH release could reache the final plateau. Agglutination phenomena in the studies of interactions between multivalent ligands and multimeric proteins are usually due to the formation of rather extended intermolecular complexes where a high number of ligands crosslink a high number of multimeric proteins giving rise to rather large complexes that precipitate. However, with dodeca- and hexadecavalent compounds (Figure 25 and Figure 26), this agglutination phenomenon did not take place and K_D in the same range as those observed with BambL were measured (15-20 nM).

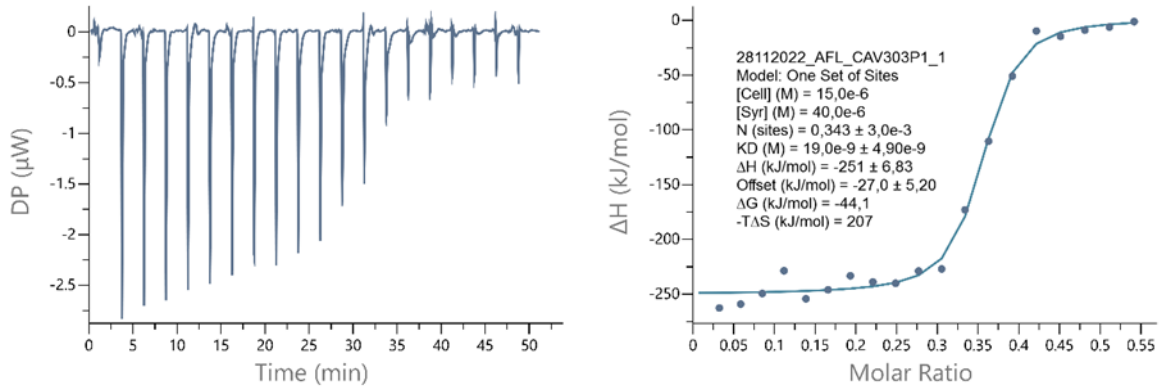

*Figure 25: Left: thermograms obtained by injections of **26** in a solution of AFL. Right: corresponding integrated titration curves.*

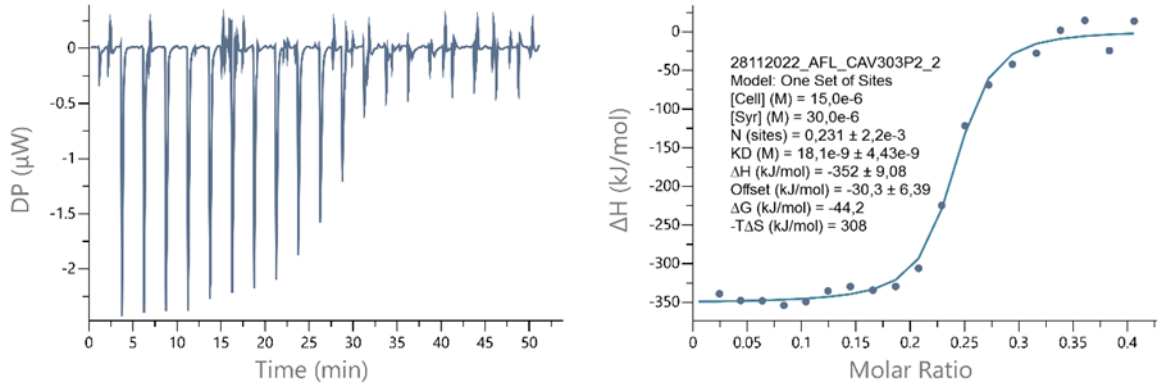

*Figure 26: Left: thermograms obtained by injections of **25** in a solution of AFL. Right: corresponding integrated titration curves.*

Given the thermodynamic data, binding of these compounds to AFL is likely based on local binding-rebinding in which several proteins are involved. Looking at n values is in fact possible to note how **25** binds to 4 lectins and **26** to 3; this means that each of them interacts with one protein for every RAFT unit present on the multivalent ligand. As it is the case with BambL, the binding is enthalpy driven, and disfavored by a strong entropic penalty. However, due to the lower affinity of monovalent fucoside **15** for AFL

if compared to BambL, compounds **26** and **25** showed remarkable relative potency factors of 2158 and 2501, respectively, corresponding to normalized values of 180 and 156. Once again, going from dodeca- (**26**) to hexadecavalent (**25**) presentation of the epitopes does not have a significant effect on the affinity, which even decreases for each fucoside unit, most likely due to a steric hindrance preventing interaction with additional lectin molecules.

Looking at the aggregation phenomena observed with the simpler tetravalent ligands **16**, **17** and **18**, as previously described, it is reasonable to state that they are due to agglutination processes induced by their interaction with AFL. Nothing of similar was observed with the RAFT based ligands **25** and **26** despite their higher valency that, in principle should favor the formation of intermolecular lectin-ligand aggregated species. No quantitative data are available so that no conclusion can actually be drawn, but on the basis of the results obtained with BambL, we could speculate that the aggregation is determined by a higher affinity of the tetravalent ligands with respect to the dodeca- and hexadecavalent one and/or that this determines the rapid formation of large intercrosslinked aggregates.

2.3.3 LecB titration

Unfortunately, we could not get any data with lecB except for the monovalent reference, which gave values similar to already published data with alpha methyl fucoside.[57] The agglutination occurs at the very beginning of the titration (second or third injection) for each multivalent ligand, preventing from having any reproducible and reliable data. This behavior, however, could be a symptom of a very high affinity of our multivalent ligands for LecB which results in agglutination of these protein.

3. CONCLUSIONS

During the six months spent in the laboratories of professor Renaudet, we were able to synthesize three novel fucosylated calixarenes **16**, **17** and **18**. Moreover, we designed and developed a new class of multivalent ligands by combining two well known scaffold, calixarenes and RAFT, obtaining compound **25** and **26**. However, additional studies are needed to further investigate why the use of calixarenes not in cone geomery prevented the formation of the tetra functionalized scaffold.

Finally, we tested these multivalent ligands in ITC experiments with three different fucose-selective lectins, BambL, AFL and LecB. Interesting data were obtained during the investigation of BambL, in which we observed how **16** behaved completely different from the other two calixarenes resulting in a very potent ligand for this protein, with a

nanomolar K_D. Furthermore, we observed, thanks to β, that the ligands based on the calixarene-RAFT conjugation did not improve the binding of ligands based only on the calixarene scaffold.

Agglutinaniton phenomena prevented us to extensively study all our ligands with AFL and LecB, however we were able to investigate the binding of **25** and **26** with the former protein. Here we observed extremely high α values, above 2000 for both ligands, suggesting that the disposition of the sugar units on these compounds greatly enhance the binding properties of each fucose.

4. EXPERIMENTAL PART

General information

Commercially available reagents and solvents were used without carrying out any prior purification or treatment except as indicated. All moisture- and air-sensitive reactions were conducted under nitrogen atmosphere. Dry solvents were prepared according to standard procedures and stored in the presence of molecular sieves. Monitoring of synthetic processes was performed by direct-phase thin-layer chromatography (TLC) using 60 F254 silica gel plates. For the detection of reagents and products with amine groups, the TLCs were sprayed with a 5% solution of ninhydrin in ethanol; for those with phenolic groups, a solution of $FeCl_3$ in water was used; for those with aldehydic groups, a solution of acidic 2,4-dinitrophenylhydrazine in ethanol was used; and for easily oxidized compounds, a 0.05% solution of $KMnO_4$ in water was used. Flash chromatography columns on silica gel 60 (230-400 mesh), under nitrogen pressure, and commercial preparative TLC 20×20 cm, silica gel F254, 0.5 mm were used for products purification.

Products characterization was performed by ^{1}H and ^{13}C NMR spectroscopy and mass spectrometry using ESI technique. NMR spectra were recorded with Bruker AVANCE 500 spectrometer (^{1}H at 500 MHz, ^{13}C at 125 MHz); chemical shift values are reported in ppm using the resonance frequency of the partially deuterated solvent as a reference. Mass spectra were recorded with a single quadrupole SQ detector spectrometer, Waters.

Cone 5,11,17,23-tetra-*tert*-butyl-25,26,27,28-tetrapropoxycalix[4]arene (1)

In a two-necked round-bottom flask, under nitrogen flow, tetra-tert-butyl-tetrahydroxycalix[4]arene (8.0 g, 12.35 mmol) was dissolved in 125 mL of dry DMF. NaH 60% (2.38 g, 98.8 mmol) was then added and allowed to react under magnetic stirring at room temperature for 30 minutes. n-PrI (9.0 mL, 74.1 mmol) was then added and allowed to react under mechanical stirring at room temperature. The reaction was monitored by TLC (hexane/ethyl acetate 7:3) and upon completion the reaction mixture was treated with 1N HCl solution and the product was filtered. A pale-yellow solid was obtained. The product was purified by recrystallization with methanol which yielded a white powdery solid in quantitative yield (10.0 g).

^{1}H NMR (400 MHz, $CDCl_3$) δ 6.77 (s, 8H, ArH), 4.41 (d, *J* = 12.4 Hz, 4H, ArC$H_{ax}$$H_{eq}$Ar), 3.81 (t, *J* = 7.6 Hz, 8H, OC$H_2$$CH_2CH_3$), 3.11 (d, *J* = 12.5 Hz, 4H, $ArCH_{ax}H_{eq}Ar$), 2.02 (q, *J* = 7.6 Hz, 8H, $OCH_2CH_2CH_3$), 1.07 (s, 36H, $C(CH_3)_3$), 0.99 (t, *J* = 7.6 Hz, 12H, $OCH_2CH_2CH_3$).

The spectroscopic data found are in agreement with those reported in literature.[58]

Cone 5,11,17,23-tetranitro-25,26,27,28-tetrapropoxycalix[4]arene (4)

In a round-bottom flask, compound **1** (10.0 g, 12.25 mmol) was dissolved in 75 mL of TFA, then sodium nitrate (41.7g, 490 mmol) was added. The solution first turned yellow and then switched to an increasingly intense violet. It was allowed to react under magnetic stirring at room temperature. The reaction was monitored by TLC (DCM eluent) and after 2 days, the reaction was completed. The reaction mixture was then quenched with H_2O. The organic phase was extracted, washed with H2O to neutrality and then anhydrified with Na_2SO_4. The solvent was evaporated under reduced pressure obtaining a red solid. The product was then recrystallized with methanol to obtain product **4** (yellow/orange solid) in 75% yield.

^{1}H NMR (400 MHz, $CDCl_3$) δ 7.57 (s, 8H, ArH), 4.53 (d, *J* = 14.0 Hz, 4H, ArCH_{ax}H$_{eq}$Ar), 3.96 (t, *J* = 7.5 Hz, 8H, OCH_2CH$_2$CH$_3$), 3.40 (d, *J* = 14.0 Hz, 4H, ArCH$_{ax}$$H_{eq}$Ar-), 1.91 (h, *J* = 7.5 Hz, 8H, OCH$_2$$CH_2CH_3$), 1.02 (t, *J* = 7.5, 12H, OCH$_2$CH$_2$$CH_3$).

The spectroscopic data found are in agreement with those reported in literature.[59]

Cone 5,11,17,23-tetraamino-25,26,27,28-tetrapropoxycalix[4]arene (6)

Compound **4** (8.45 g, 10.936 mmol), hydrazine monohydrate (21.25 mL, 437.44 mmol) and a catalytic amount of Pd/C are introduced in a two-necked round-bottom flask filled 50 mL of EtOH. The mixture was allowed to react under magnetic stirring at reflux. The reaction was monitored by TLC (DCM eluent), and after 19 hours, the reaction was completed. The catalyst was then removed by filtration and the solvent evaporated under reduced pressure. Then the reaction mixture was dissolved in DCM, which was then treated with H_2O. The organic phase was extracted, dried over Na_2SO_4 and the solvent evaporated under reduced pressure. Product **6** (yellowish-white solid) was obtained with a yield of 88% (6.29 g).

^{1}H NMR (400 MHz, CD_3OD) δ 6.12 (s, 8H, ArH), 4.33 (d, *J* = 13.1 Hz, 4H, ArCH_{ax}H$_{eq}$Ar), 3.73 (t, *J* = 7.4 Hz, 8H, OCH_2CH$_2$CH$_3$), 2.91 (d, *J* = 13.2 Hz, 4H, ArCH$_{ax}$$H_{eq}$Ar), 1.88 (h, *J* = 7.4 Hz, 8H, OCH$_2$$CH_2CH_3$), 0.99 (t, *J* = 7.5 Hz, 12H, OCH$_2$CH$_2$$CH_3$).

The spectroscopic data found are in agreement with those reported in literature.[60]

***1,3-Alternate* 5,11,17,23-tetra-tert-butyl-25,26,27,28-tetrapropoxycalix[4]arene (3)**

In a two necked round bottom flask, under inert atmosphere, tetra tert-butyl-hydroxycalix[4]arene (10 g, 15.42 mmol) was dissolved in dry CH_3CN (70 ml) at room temperature. $CsCO_3$ (50 g, 154.25 mmol) was added, and the reaction was stirred for 15 minutes. After the addition of 1-iodopropane (15 ml, 154.25 mmol) the temperature was raised to 85°C for 48 h. The reaction was monitored by TLC (eluent: hexane/EtOAc 9:1), quenched with HCl 1M (50 ml) and extracted with DCM. The organic phase was washed with H_2O (50 ml) until neutral pH. The organic extract was dried over anhydrous Na_2SO_4, filtered, and concentrated under reduced pressure, giving a white solid. The residue was crystallized using petroleum ether. After filtration on Buchner **3** was obtained as white solid (5.5g, 6.74 mmol) in 44% yield.

^{1}H-NMR: (400 MHz, $CDCl_3$) δ (ppm): 6.98 (s, 8H, ArH), 3.83 (s, 8H, $ArCH_2Ar$), 3.33 (t, *J* = 7.6 Hz, 8H, OCH_2), 1.29 (s, 36H, $C(CH_3)_3$), 1.26-1.00 (m, 8H, OCH_2CH_2), 0.64 (t, J = 7.6 Hz, 12H, $OCH_2CH_2CH_3$).

The spectroscopic data found are in agreement with those reported in literature.[46]

1,3-Alternate 5,11,17,23-tetra-nitro-25,26,27,28-tetrapropoxycalix[4]arene (10)

Calixarene **3** (5.5 g, 7.74 mmol) and NaNO3 (22.9 g, 270 mmol) were put into a round-bottom flask, then CF_3COOH (41.4 mL, 540 mmol) was added dropwise. The mixture was stirred at room temperature for 16 hours. The reaction was quenched by addition of water (400 ml) and extracted with DCM (2x200 ml). The combined organic layers were washed with water (150 ml) and dried over Na_2SO_4. The solvent was removed under reduced pressure. The residue was purified by recrystallization in DCM/MeOH obtaining a yellowish solid (3.17 g, 4.11 mmol) in 61% yield.

^{1}H-NMR (400 MHz, $CDCl_3$): δ(ppm) 7.98 (s, 8H, ArH), 3.82 (t, 8H, *J* = 7.2 Hz, OCH_2), 3.76 (s, 8H, $ArCH_2Ar$), 1.95-1.85 (m, 8H, OCH_2CH_2), 1.07 (t, 12H, *J* = 7.4 Hz, $OCH_2CH_2CH_3$).

The spectroscopic data found are in agreement with those reported in literature.[46]

1,3-Alternate 5,11,17,23-tetra-amino-25,26,27,28-tetrapropoxycalix[4]arene (11)

$NH_2NH_2{\cdot}H_2O$ (7.99 mL, 164.5 mmol) and Pd/C (10%) (catalytic amount) were added to a suspension of compound **10** (3.17 g, 4.11 mmol) in ethanol (50 mL). The reaction mixture was refluxed at 85°C and stirred for 18 hours. The catalyst was then filtered off and the solvent was removed under reduced pressure. The pure product was obtained as light-yellow solid (2.41 g, 3.70 mmol) in 90% yield.

^{1}H-NMR (400 MHz, MeOD): δ(ppm) 6.54 (s, 8H, ArH), 3.58 (s, 8H, $ArCH_2Ar$), 3.36 (t, 8H, *J* = 7.2 Hz, OCH_2), 3.16 (s, 8H, NH_2), 1.64-1.55 (m, 8H, OCH_2CH_2), 0.93 (t, *J* = 7.4 Hz, 12H, $OCH_2CH_2CH_3$).

The spectroscopic data found are in agreement with those reported in literature.[46]

Cone-5,11,17,23-tetrakis-(3-azidopropanamide)-25,26,27,28-tetrapropoxycalix[4]arene (8)

Calixarene **6** (400 mg, 0.61 mmol) was dissolved in dry DMF (5 mL) then 3-azidopropionic acid (0.3 mL, 3.06 mmol), PyBOP (1.9 g, 3.66 mmol) and DIPEA (0.31 mL, 1.83 mmol) were added to the solution, which was stirred at room temperature for 16 hours. The reaction was quenched with water (5 mL) and extracted with DCM (2x 10 mL). The organic phase was dried over Na_2SO_4 and the solvent was evaporated under reduced pressure. The crude was purified by column chromatography (eluent, cyclohexane/ethyl acetate 4/6) obtaining a white solid (80 mg, 0.077 mmol) in 13% yield.

^{1}H NMR (500 MHz, CD_3OD) δ(ppm): 6.80 (s, 8H, ArH), 4.37 (d, *J*=13.0, 4H, $ArCH_{ax}H_{eq}Ar$), 3.77 (t, *J*=7.5, 8H, $ArOCH_2$), 3.50 (t, *J*=6.4, 8H, $COCH_2CH_2N$), 3.03 (d, *J*=13.1, 4H, $ArCH_{ax}H_{eq}Ar$), 2.41 (t, *J*=6.4, 8H, $COCH_2CH_2N$), 1.88 (q, *J*=7.5, 8H, $ArOCH_2CH_2$), 0.93 (t, *J*=7.5, 12H, $ArOCH_2CH_2CH_3$).

ESI-MS: m/z calculated for $C_{52}H_{64}N_{16}O_8$ $[M+H]^+$: 1041.510, found: 1041.183.

***1,3-Alternate*-5,11,17,23-tetrakis-(3-azidopropanamide)-25,26,27,28-tetrapropoxycalix[4]arene (12)**

Compound **11** (100 mg, 0.15 mmol) was dissolved in dry DMF (1 mL) and poured in a microwave vial, then 3-azidopropionic acid (0.1 mL, 0.9 mmol), PyBOP (500 mg, 0.95 mmol) and DIPEA (0.3 mL, 0.6 mmol) were added to the solution. The mixture was heated at 100°C (150 W) for 10 minutes, then it was quenched by addition of water (5 mL) and exctracted with DCM (2x 5 mL). The organic phase was anhydrified over Na2SO4 then the solvent was removed under reduced pressure. The crude was purified by column chromatography (eluent, cyclohexane/ethyl acetate 6/4) obtaining a white solid (50 mg, 0.048 mmol) in a 32% yield.

^{1}H NMR (400 MHz, CD_3OD) δ(ppm): 7.36 (s, 8H, ArH), 3.77 (s, 8H, $ArCH_2Ar$), 3.65 (t, *J*= 6.4 Hz, 8H, $COCH_2CH_2N$), 3.28 (t, *J*= 7.4 Hz, 8H, $ArOCH_2$), 2.62 (t, *J*=6.4 Hz, 8H,

$COCH_2CH_2N$), 1.33 (q, *J*= 7.3 Hz, 8H, $ArOCH_2CH_2$), 0.72 (t, *J*= 7.5 Hz, 12H, $ArOCH_2CH_2CH_3$).

ESI-MS: m/z calculated for $C_{52}H_{64}N_{16}O_8$ $[M+H]^+$: 1041.510, found: 1041.393

5,11,17,23-tetrakis-(3-azidopropanamide)-25,26,27,28-tetramethoxycalix[4]arene (9)

Compound **7** (200 mg, 0.37 mmol) was dissolved in dry DMF (2 mL) and poured in a microwave vial, then 3-azidopropionic acid (0.18 mL, 1.85 mmol), PyBOP (1154 mg, 2.22 mmol) and DIPEA (0.2 mL, 1.11 mmol) were added to the solution. The mixture was heated at 100°C (150 W) for 10 minutes, then it was quenched by addition of water (5 mL) and exctracted with DCM (2x 5 mL). The organic phase was anhydrified over Na2SO4 then the solvent was removed under reduced pressure. The crude was purified by column chromatography (eluent, cyclohexane/ethyl acetate 5/5) obtaining a white solid (75 mg, 0.081 mmol) in a 22% yield.

It was not possible to isolate the pure product, we used the crude for the following reaction.

ESI-MS: m/z calculated for $C_{44}H_{48}N_{16}O_8$ $[M+H]^+$: 929.973, found: 931.450; 466.418 ($[M+2H]^{2+}$)

Propargyl 2,3,4-tri-O-acetyl-α-L-fucopyranoside (14)

L-Fucose (1.0 g, 6.09 mmol) was dissolved in dry pyridine (10 mL), the temperature was lowered to 0°C then acetic anhydride (4.6 mL, 48.73 mmol) was slowly added to the solution. The mixture was stirred at room temperature for 16 hours, then it was quenched by the addition of 1M HCl (40 mL) and exctracted with ethyl acetate. The organic phase was dried ove Na_2SO_4 and evaporated under reduced pressure. The product **13** obtained was immediately used for the glycosylation reaction. It was dissolved in dry DCM (15 mL) and propargyl alcohol (1.51 mL, 26.24 mmol). After cooling the mixture to 0°C, $BF_3{\cdot}Et_2O$ (3.24 mL, 26.24 mmol) was added dropwise. The reaction was stirred for 16 hours at room temperature then in was quenched by a slow addition of water (20 mL). The organic phase was separated, dried over Na_2SO_4 and evaporated under reduced pressure. The oily crude was purified by column chromatography (eluent, cyclohexane/ethyl acetate 6/4) obtaining the desired product (400 mg, 1.22 mmol) in 20% yield as a clear oil.

^{1}H NMR (500 MHz, $CDCl_3$) δ(ppm): 5.29 (dd, *J* = 10.9, 3.3 Hz, 1H, H_3), 5.24 (dd, *J* = 3.4, 1.3 Hz, 1H, H_4), 5.19 (d, *J* = 3.8 Hz, 1H, H_1), 5.09 (dd, *J* = 10.9, 3.8 Hz, 1H, H_2), 4.19 (d, *J* = 2.4 Hz, 2H, OC*H*$_2$CCH), 4.14 (qd, *J* = 6.6, 1.1 Hz, 1H, H_5), 2.38 (t, *J* = 2.4 Hz, 1H, OCH_2CCH), 1.08 (d, *J* = 6.6 Hz, 3H, CH_3).

The spectroscopic data found are in agreement with those reported in literature.[47]

Propargyl α-L-fucopyranoside (15)

Compound **14** (400 mg, 1.22 mmol) was dissolved in MeOH, then a solution of NaOMe (25% in MeOH) was slowly added until pH 9. The mixture was stirred at room temperature for 30 minutes, then it was quenched by the addition of Amberlyst IR-120 (200 mg). After 10 minutes of stirring the suspension was filtered and the solvent evaporated under reduced pressure. A white solid (295 mg ,1.22 mmol) was obtained with quantitative yield.

^{1}H NMR (400 MHz, D_2O) δ(ppm): 4.99 (d, *J* = 3.6 Hz, 1H, H_1), 4.25 (d, *J* = 2.5 Hz, 2H, OC*H*$_2$CCH), 4.05 (q, *J* = 6.6 Hz, 1H, H_5), 3.85 – 3.69 (m, 3H, H_2, H_3, H_4), 2.83 (t, *J* = 2.4 Hz, 1H, OCH_2CCH), 1.15 (d, *J* = 6.6 Hz, 3H, CH_3).

The spectroscopic data found are in agreement with those reported in literature. [47]

Cone 5,11,17,23-tetrakis-[4-(α-methyl-L-fucosyl)-1,2,3-triazolyl]propanoylamido-25,26,27,28-tetrapropoxycalix[4]arene (16)

Calixarene **8** (20 mg, 0.019 mmol) and α-propargylfucose (17.2 mg, 0.085 mmol) were dissolved in DMF (500 uL) and PBS (pH 7.4, 0.9 mL), then a solution of $CuSO_4{\cdot}5H_2O$ (2.4 mg, 0.019 mmol) and THTPA (8.3 mg, 0.019 mmol) in PBS (0.2 mL) was added. Then a solution of sodium ascorbate (11.3 mg, 0.057 mmol) in PBS (0.2 mL) was added to the previous one. The mixture was stirred for 16 hours, then quenched addition of Chelex resin and stirred for 30 minutes at room temperature. The crude was filtrated and purified by RP-HPLC (Rt = 9.03 min, C18, λ = 214 nm, 5-100% CH_3CN in 25 minutes) obtaining after lyophilization a white solid (8.6 mg, 0.0046 mmol) in 24% yield.

^{1}H NMR (500 MHz, DMSO-*d*$_6$) δ(ppm): 9.57 (s, 4H, ArNHCO), 7.97 (s, 4H, NCHCN), 6.82 (s, 8H, ArH), 4.65 (d, J = 3.4 Hz, 4H, H_1), 4.60 – 4.30 (m, 28H, OC*H*$_2$CCH, $COCH_2CH_2N$, OHs), 4.25 (d, J = 12.8 Hz, 4H, $ArCH_{ax}H_{eq}Ar$), 3.71 (m, 12H, $ArOCH_2$, H_5), 3.54 – 3.35 (m, 12H, H_2, H_4, H_3), 2.99 (d, J = 13.0 Hz, 4H, $ArCH_{ax}H_{eq}Ar$), 2.81 (t, J = 10.5 Hz, 8H,

COC*H*$_2$CH$_2$N), 1.80 (q, J = 7.2 Hz, 8H, ArOCH$_2$C*H*$_2$), 1.00 (d, J = 6.1 Hz, 12H, CH$_3$), 0.87 (t, J = 7.4 Hz, 12H, ArOCH$_2$CH$_2$C*H*$_3$).

^{13}C NMR (126 MHz, DMSO-d_6) δ(ppm): 167.7 (NHCO), 152.5 (CH$_2$*C*NCHN), 144.3 (Ar), 134.6 (Ar), 133.2 (Ar), 124.6 (NCHCN), 119.9 (Ar$_{ortho}$), 99.1 (C1), 76.9, 72.0, 70.0, 68.5, 66.6, 60.6, 59.8, 45.9, 36.4, 31.3 (Ar*C*H$_2$Ar), 23.1 (ArOCH$_2$*C*H$_2$), 16.9 (CH$_3$), 10.6 (ArOCH$_2$CH$_2$*C*H$_3$).

ESI-MS: m/z calculated for C$_{88}$H$_{121}$N$_{16}$O$_{28}$ [M+H]$^+$: 1851.010, found: 1852.290

RP-HPLC (C18, λ = 250 nm, 0-100% CH$_3$CN in 15 minutes): R$_t$ = 9.080 minutes

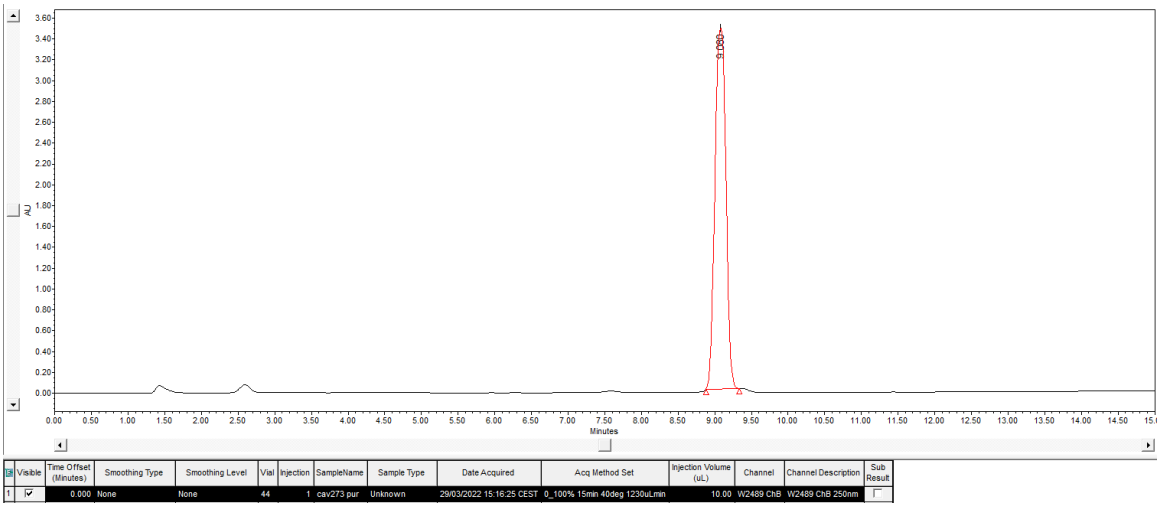

1,3-Alternate-5,11,17,23-tetrakis-[4-(α-methyl-L-fucosyl)-1,2,3-triazolyl]propanoylamido-25,26,27,28-tetrapropoxycalix[4]arene (17)

Calixarene **12** (22 mg, 0.02 mmol) and α-propargylfucose (19.2 mg, 0.095 mmol) were introduced in a microwave vial and dissolved in DMF (0.7 mL), then CuSO$_4$·5H$_2$O (2.5 mg, 0.02 mmol) and THTPA (8.5 mg, 0.02 mmol) were added. The mixture was heated at 110°C (150 W) for 15 minutes, then the reaction was quenched by addition of Chelex resin followed by stirring for 30 minutes at room temperature. The resin was filtered off and the crude purified by RP-HPLC (Rt = 7.12 min, C18, λ = 214 nm, 5-100% CH3CN in 25 minutes), obtaining after lyophilization a white solid (14.7 mg, 0.008 mmol) in 40% yield.

^{1}H NMR (500 MHz, DMSO-d_6) δ (ppm): 9.70 (s, 4H, ArNH), 8.06 (s, 4H, NCHCN), 7.28 (s, 8H, ArH), 4.73 (d, *J* = 3.4 Hz, 4H, H$_1$), 4.66 – 4.35 (m, 27H, OC*H*$_2$CCH, COCH$_2$*CH*$_2$N, OHs), 3.80 (q, *J* = 6.5 Hz, 4H, H$_5$), 3.61 (s, 8H, ArCH$_2$Ar), 3.55 (m, 8H, H$_2$, H$_3$), 3.47 (m, 4H, H$_4$), 3.11 (t, *J* = 7.5 Hz, 8H, ArOCH$_2$), 2.93 (t, *J* = 6.7 Hz, 8H, COC*H*$_2$CH$_2$N), 1.25 (q, *J* = 7.5 Hz, 8H, ArOCH$_2$C*H*$_2$), 1.08 (d, *J* = 6.6 Hz, 12H, CH$_3$), 0.59 (t, *J* = 7.4 Hz, 12H, ArOCH$_2$CH$_2$C*H*$_3$).

^{13}C NMR (126 MHz, DMSO-d_6) δ (ppm): 167.5 (NHCO), 152.9 (CH_2CNCHN), 144.2 (Ar), 134.2 (Ar), 124.6 (NCHCN), 120.8 (Ar_{ortho}), 99.1 (C1), 72.5 ($ArOCH_2$), 72.1 (C_4), 70.0, 68.4 (C_5), 66.6, 60.6, 46.1, 38.4 ($ArCH_2Ar$), 36.7 ($COCH_2CH_2N$), 22.8 ($ArOCH_2CH_2$), 16.9 (CH_3), 10.2 ($ArOCH_2CH_2CH_3$).

ESI-MS: m/z calculated for $C_{88}H_{121}N_{16}O_{28}$ $[M+H]^+$: 1851.010, found: 1850.991

RP-HPLC (C18, λ = 250 nm, 0-100% CH3CN in 15 minutes): R_t = 5.006 minutes

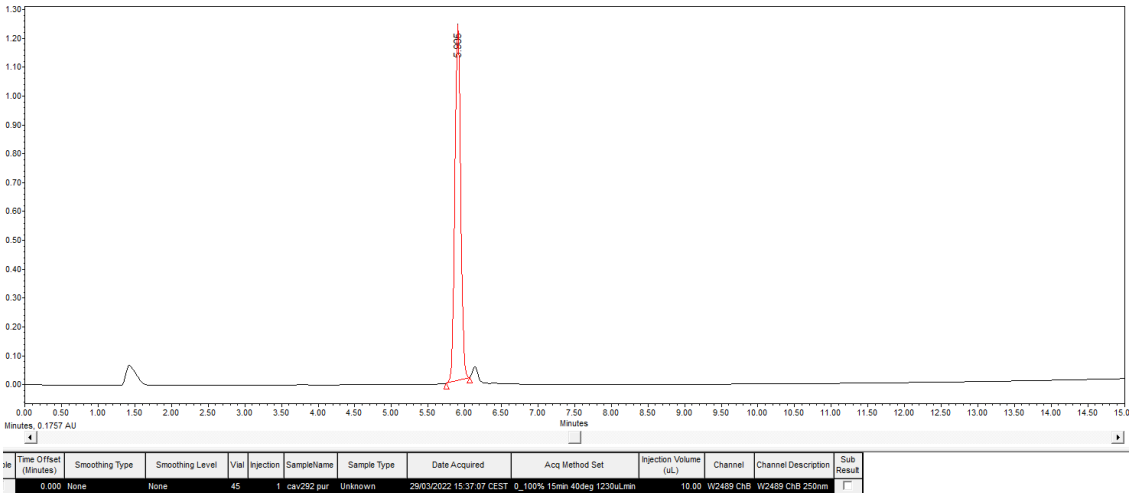

5,11,17,23-tetrakis-[4-(α-methyl-L-fucosyl)-1,2,3-triazolyl]propanoylamido--tetramethoxycalix[4]arene (18)

Calixarene **9** (10 mg, 0.0107 mmol) and α-propargylfucose (9.6 mg, 0.047 mmol) were introduced in a microwave vial and dissolved in DMF (1 mL), then CuI (2.6 mg, 0.027 mmol) and DIPEA (0.026 mL, 0.14 mmol). The mixture was heated at 110°C (150 W) for 15 minutes, then was quenched by addition of Chelex resin and stirred for 30 minutes at room temperature. The resin was filtered off and the crude purified by RP-HPLC (Rt = 7.53 min, C18, λ = 214 nm, 5-100% CH3CN in 25 minutes), obtaining after lyophilization a white solid (8.5 mg, 0.0049 mmol) in 46% yield.

^{1}H NMR (500 MHz, DMSO-d_6) δ(ppm): 9.75 (bs, 4H, ArNHCO), 8.06 (s, 4H, NCHCN), 7.05 (s, 8H, ArH), 4.73 (d, J = 3.4 Hz, 4H, H_1), 4.68 – 4.37 (m, 28H, OCH_2CCH, $COCH_2CH_2N$, OHs), 4.23 (d, J = 12.2 Hz, 4H, $ArCH_{ax}H_{eq}Ar$), 3.89 - 3.42 (m, 28H, H_2, H_3, H_4, H_5, OCH_3), 3.13 (d, J = 12.4 Hz, 4H, $ArCH_{ax}H_{eq}Ar$), 3.00 – 2.82 (m, 8H, $COCH_2CH_2N$), 1.08 (d, J = 6.6 Hz, 12H, CH_3).

^{13}C NMR (126 MHz, DMSO-d_6) δ(ppm): 124.5, 99.1 (C1), 72.0 (OCH_3), 70.0, 68.5 (C_5), 16.9 (CH_3).

The ^{13}C NMR signals reported are those recorded with HSQC, the ^{13}C spectrum, even after 6000 scans, did not show any signals.

ESI-MS: m/z calculated for $C_{80}H_{105}N_{16}O_{28}$ $[M+H]^+$: 1738.800, found: 1738.725

RP-HPLC (C18, λ = 250 nm, 0-100% CH3CN in 15 minutes): R_t = 5.970 minutes

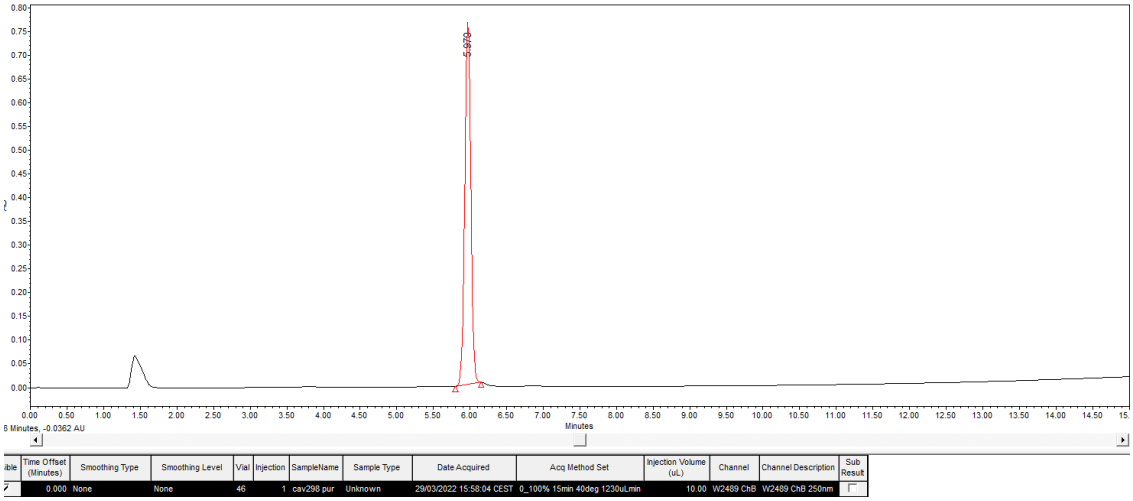

6-azido-2S-{[(9H-fluorenyl-9-ylmethoxy)carbonyl]amino}hexanoic acid (19)

To a stirred solution of Fmoc-protected Lysine (5.00 g, 13.55 mmol) of MeOH/H_2O (2:1, 150 mL), $CuSO_4 \cdot 5H_2O$ (34 mg, 0.135 mmol), K_2CO_3 (18.73 g, 135.5 mmol) and 1H-imidazole-1-sulfonyl azide hydrochloride (4.41 g, 16.26 mmol) were added. The reaction was stirred at room temperature for 5 hours, then the solvent was concentrated under reduced pressure. The resulting crude was acidified with aq. HCl (3M) until pH 1, then washed with water (2 x 100 mL), brine (2 x 100 mL) and concentrated under vacuum to give the desired product (5.07 g, 12.87 mmol) as yellow resin in 95% yield.

^1H-NMR (400 MHz, DMSO-*d6*) δ(ppm): 8.95 (s, 1H), 7.89 (d, J = 7.4 Hz, 2H, ArH), 7.73 (d, J = 7.4 Hz, 2H, ArH), 7.47 – 7.27 (m, 4H, ArH), 6.70 (br d, J = 6.8 Hz, NHCOO) 4.34 – 4.18 (m, 3H, CH, $COOCH_2$), 3.65 (q, J = 6.48 Hz, 1H, CHN), 3.32 (t, J = 6.8 Hz, 2H, CH_2N_3), 1.80 – 1.54 (m, 2H, CH_2), 1.50 – 1.45 (m, 2H, CH_2), 1.37 (m, 2H, CH_2)

The spectroscopic data found are in agreement with those reported in literature.[61]

Solid Phase Peptide Synthesis

Adapted from an already published protocol from professor Renaudet.[53] Assembly of all linear protected peptides was performed manually by solid phase peptide synthesis (SPPS) using the standard 9-fluorenylmethoxycarbonyl/tert-butyl (Fmoc/tBu) protection

strategy. Fmoc-Gly-Sasrin resin was chosen as solid phase. The reactor consisted in a 150 mL volume polypropylene syringe-shaped cylinder, loadable up to 4 g of resin and equipped with a filter and a valve in the lower end, to removal solvent through filtration assisted by compressed air. Fmoc-protected resin (1.0 g, 0.79 mmol/g) was weighed and then gently stirred thanks to an orbital laboratory agitator (IKA Vibrax VXR basic, USA), firstly with 10 mL of DCM then with 10 mL DMF, each for 10 min separately. After the swelling phase, to remove the -Fmoc protecting group, the resin was treated with a fresh 20% piperidine solution in DMF, two times for 10 minutes and one times for 5 minutes. Before proceeding with the coupling phase, the resin was washed 10 times for one minute with DMF and one time for one minute with DCM, to remove piperidine traces. The first coupling phase was performed in 10 mL DMF with N-Fmoc-protected amino acids (2.0 eq.), in situ activators PyBOP (2.0 eq.) and DIPEA (3.0 eq.). The solution's pH was checked to be equal to 9-10 and the reaction mixture was gently stirred for 60 min at room temperature. Then, the resin was washed three times for one min with DCM and five times for one min with DMF, until the neutrality of solution's pH. The procedure for the peptide elongation was repeated from the Fmoc-deprotection step and after repeating this protocol for the required coupling steps, the final linear peptide sequence was obtained.

Cleavage

The linear peptide synthesized on Gly-SASRIN resin was treated 10 times (10 mL) for 10 minutes with a mixture of TFA/DCM (1/99). The collected solutions were combined, neutralized with DIPEA and concentrated under reduced pressure. The resulting oil was dissolved in a minimum quantity of DCM, and it was added dropwise to a calibrated falcon filled with ice-cold diethyl ether to induce precipitation. After one centrifugation (4000 g, 3 min), the supernatant is discarded, and the precipitation process is repeated twice more. After desiccation a white solid (0.92 g, 0.74 mmol) was obtained.

Tetraazide-Lys(Boc)-RAFT (21)

Linear peptide **20** was dissolved in DMF (1.5L) and the pH values was adjusted to 8-9 by addition of DIPEA. PyBOP (500 mg, 0.96 mmol) was added, and the solution stirred at room temperature for 16 hours. Solvent was removed under reduced pressure and the residue dissolved in a minimum of DCM. It was added dropwise to a calibrated falcon filled with ice-cold diethyl ether to induce precipitation. After one centrifugation (4000 rpm, 3 min), the supernatant was discarded, and the precipitation process is repeated

twice more. After desiccation, the resulting white solid was subjected to the following reaction.

Tetraazide-RAFT (22)

The Boc-containing compound **21** was dissolved in a mixture of TFA/DCM (3:2, 10 mL of total volume) and the reaction mixture was stirred for 30 minutes at room temperature. The solvent was removed under reduced pressure, and the residue dissolved into DCM. This solution was added dropwise to ice-cold diethyl ether causing the precipitation of the Boc deprotected product, which was filtrated and dried under vacuum. The crude was purified by semipreparative RP-HPLC (R_t = 12.28 minutes, C18, λ = 214 nm, 5-60% CH_3CN in 15 minutes) obtaining the desire compound (291 mg, 0.26 mmol), after two steps, in a 35% overall yield.

ESI-MS: m/z calculated for $C_{47}H_{78}N_{23}O_{10}$ $[M+H]^+$: 1125.6302, found: 1125.6216.

Tetrafucosylated-RAFT (23)

α-propargyl fucose (45 mg, 0.22 mmol) and compound **22** (50 mg, 0.045 mmol) were dissolved in a 1:2 mixture of DMF and PBS buffer (pH 7.5, 3 mL). A solution of $CuSO_4{\cdot}5H_2O$ (5.5 mg, 0.022 mmol) and THPTA (19 mg, 0.044 mmol) in PBS was added to a solution of sodium ascorbate (26 mg, 0.133 mmol) in PBS. This mixture was added to the solution containing the azide and alkyne which was degassed with argon and microwaved for 10 minutes at 80°C (120 W). Chelex resin was then added to the reaction mixture which was stirred for 45 minutes. The resin was filtered off, rinsed with water and the filtrate purified by semipreparative RP-HPLC (R_t = 4.43 minutes, C18, λ = 214 nm, 5-100% CH_3CN in 15 minutes). Fractions containing the product were combined and lyophilized obtaining a white foam (52 mg, 0.027 mmol) in 60% yield.

ESI-MS: m/z calculated for $C_{83}H_{133}N_{23}O_{10}$ $[M+H]^+$: 1934.110, found: 1934.211.

Tetrafucosylated-5-pentynamide-RAFT (24)

Free amine compound **23** (50 mg, 0.025 mmol) was dissolved in dry DMF (2 mL), DIPEA was added to reach pH between 9-10, then succinimide ester of pentynoic acid (7.3 mg, 0.038 mmol) was added. The reaction mixture was stirred at room temperature. for one hour. The mixture was then diluted with water (2 mL) and purified by semi-preparative RP-HPLC (R_t = 8.85 minutes, C18, λ = 214 nm, 5-50% CH3CN in 15 minutes). Fractions containing the product were combined and lyophilized obtaining a white solid (13 mg, 0.0063 mmol) in 25% yield.

ESI-MS: m/z calculated for $C_{88}H_{138}N_{23}O_{31}$ $[M+H]^+$: 2014.192, found: 2014.011.

Cone 5,11,17,23-Tetrakis {tetra-[4-(a-methyl-L-fucosyl)-1,2,3-triazolyl]-RAFT}-25,26,27,28-tetrapropoxycalix[4]arene (25)

Calixarene **8** (1 mg, 0.0014 mmol) and RAFT **24** (13 mg, 0.0063 mmol) were dissolved in a 1:1 solution of water:DMF (1 mL). A solution containing $CuSO_4 \cdot 5H_2O$ (0.18 mg, 0.0007 mmol), sodium ascorbate (0.84 mg, 0.0043 mmol) and THTPA (0.62 mg, 0.0014 mmol) in 0.4 mL of water/DMF (1/1) was then added to the previous one. The mixture was microwaved for 15 minutes at 80°C (150 W) then quenched by addition of Chelex resin and stirred for 30 minutes. The resin was then filtered off and the crude purified by RP-HPLC (R_t = 8.78 minutes, C18, λ = 214 nm, 5-100% CH_3CN in 25 minutes) obtaining after lyophilization a white foam (1.8 mg, 0.00021 mmol) in 15% yield.

^1H NMR (500 MHz, D_2O/DMSO-d_6 9/1, selected signals reported) δ(ppm): 8.44 (s, 20H, NCHN), 8.00 (s, 8H, ArH), 4.93 (bs, 16H, H_1), 1.10 (s, 48H, CH_3).

MALDI-MS: m/z calculated for $C_{404}H_{612}N_{108}O_{132}$: 9092.96, found: 9115.151 $[M+Na]^+$.

RP-HPLC (C18, λ = 250 nm, 0-90% CH_3CN in 15 minutes) R_t = 8.460 minutes

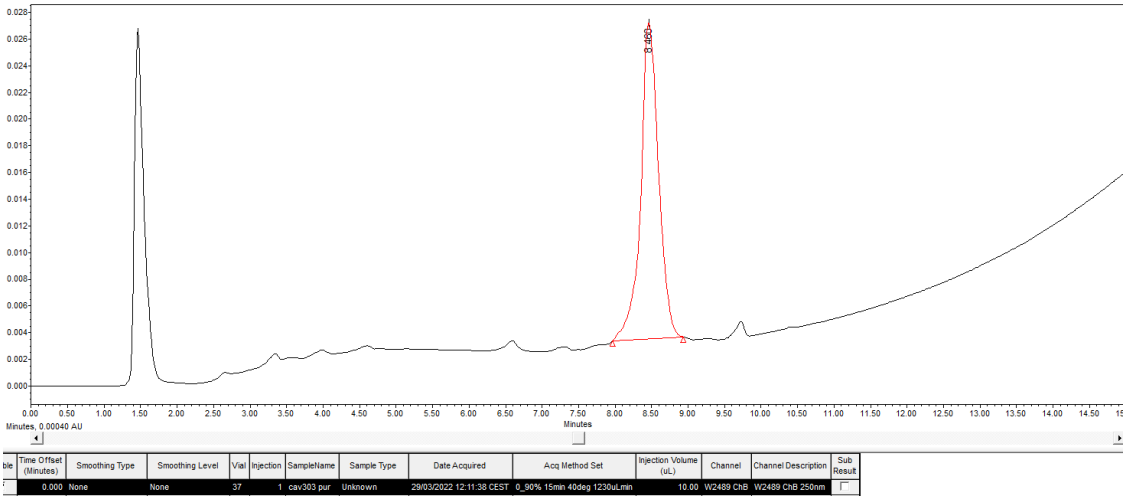

During the purification was also isolated the trifunctionalized compound **26**.

MALDI-MS: m/z calculated for $C_{316}H_{475}N_{85}O_{101}$ $[M+H]^+$: 7080.77, found: 7104.125 $[M+Na]^+$.

RP-HPLC (C18, λ = 250 nm, 0-100% CH_3CN in 15 minutes) R_t = 8.217 minutes

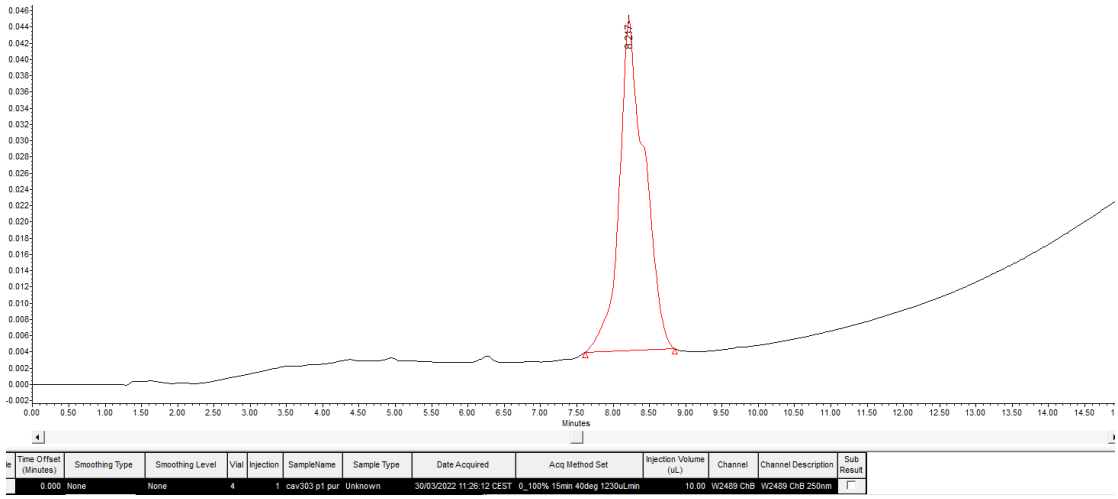

Tetragalactosylated-RAFT (27)

α-propargyl galactose (292 mg, 1.33 mmol) and azide-functionalized raft **22** (300 mg, 0.27 mmol) were dissolved in a 1:2 mixture of DMF and PBS buffer (pH 7.5, 5 mL). A solution of $CuSO_4 \cdot 5H_2O$ (34 mg, 0.135 mmol) and THPTA (120 mg, 0.27 mmol) in PBS was added to a solution of sodium ascorbate (162 mg, 0.81 mmol) in PBS. This mixture was added to the solution containing the azide and alkyne which was degassed with argon and microwaved for 10 minutes at 80°C (150 W). Chelex resin was then added to the reaction mixture which was stirred for 45 minutes. The resin was filtered off, rinsed with water and the filtrate purified by semipreparative RP-HPLC (R_t = 5.03 minutes, C18, λ = 214 nm, 5-100% CH_3CN in 15 minutes). Fractions containing the product were combined and lyophilized obtaining a white foam (330 mg, 0.165 mmol) in 61% yield.

ESI-MS: m/z calculated for $C_{83}H_{134}N_{23}O_{34}$ $[M+H]^+$: 1995.948, found: 1997.132.

Tetragalactosylated-5-pentynamide-RAFT 28

Free amine compound **27** (330 mg, 0.165 mmol) was dissolved in dry DMF (5 mL), DIPEA was added to reach pH around 9-10, then succinimide ester of pentynoic acid (48 mg, 0.248 mmol) was added. The reaction mixture was stirred at room temperature for 1 hour. The mixture was diluted with water and purified by semi-preparative RP-HPLC (R_t = 4.80 minutes, C18, λ = 214 nm, 5-100% CH_3CN in 15 minutes). Fractions containing the product were combined and lyophilized obtaining a white solid (264 mg, 0.127 mmol) in 77% yield.

ESI-MS: m/z calculated for $C_{83}H_{134}N_{23}O_{34}$ $[M+H]^+$: 2075.960, found: 2077.155.

5,11,17,23- Tetrakis {tetra-[4-(α-methyl-L-fucosyl)-1,2,3-triazolyl]-RAFT}-25,26,27,28-tetrapropoxycalix[4]arene 29

Calixarene **8** (2 mg, 0.0019 mmol) and RAFT **28** (19 mg, 0.0096 mmol) were dissolved in a 1:1 solution of water:DMF (1 mL). A solution containing $CuSO_4$ $5H_2O$ (0.25 mg, 0.001 mmol), sodium ascorbate (1.2 mg, 0.006 mmol) and THTPA (0.87 mg, 0.0019 mmol) in 0.4 mL of water/DMF (1/1) was then added to the previous one. The mixture was microwaved for 15 minutes at 80°C (150 W) then quenched by addition of Chelex resin and stirred for 30 minutes. The resin was then filtered off and the crude purified by RP-HPLC (R_t = 7.31 minutes, C18, λ = 214 nm, 5-100% CH_3CN in 15 minutes) obtaining after lyophilization a white foam (3.3 mg, 0.000361 mmol) in 19% yield.

MALDI-MS: m/z calculated for $C_{404}H_{612}N_{108}O_{148}$ $[M+H]^+$: 9348.950, found: 9370.779 $[M+Na]^+$.

RP-HPLC (C18, λ = 250 nm, 0-100% CH_3CN in 15 minutes) R_t = 7.310 minutes

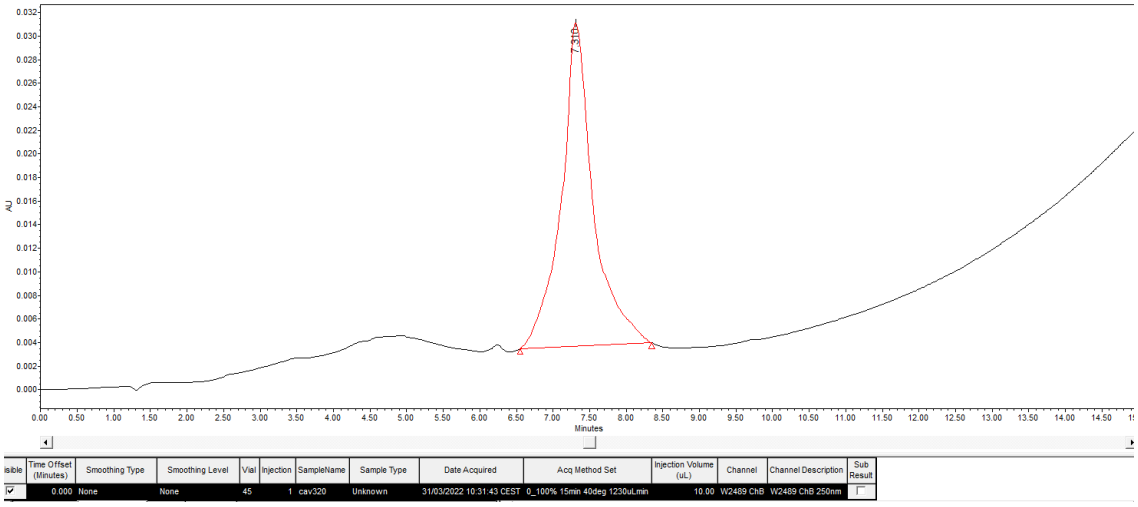

5. BIBLIOGRAPHY

(1) Lis, H.; Sharon, N. Lectins: Carbohydrate-Specific Proteins That Mediate Cellular Recognition†. *Chem. Rev.* **1998**, *98* (2), 637–674.

(2) Varki, A.; Cummings, R. D.; Esko, J. D.; Freeze, H. H.; Stanley, P.; Bertozzi, C. R.; Hart, G. W.; Etzer, M. E. ; Essentials of Glycobiology. *Cold Spring Harb.*, **2009**, *039*, 2015–2017.

(3) Sharon, N. Carbohydrate-Lectin Interactions in Infectious Disease. *Adv. Exp. Med. Biol.* **1996**, *408*, 1–8.

(4) Imberty, A.; Varrot, A. Microbial Recognition of Human Cell Surface Glycoconjugates. *Curr. Opin. Struct. Biol.* **2008**, *18* (5), 567–576.

(5) Boukerb, A. M.; Rousset, A.; Galanos, N.; Méar, J. B.; Thépaut, M.; Grandjean, T.; Gillon, E.; Cecioni, S.; Abderrahmen, C.; Faure, K.; et al. Antiadhesive Properties of Glycoclusters against Pseudomonas Aeruginosa Lung Infection. *J. Med. Chem.* **2014**, *57* (24), 10275–10289.

(6) Lundquist, J. J.; Toone, E. J. The Cluster Glycoside Effect. *Chem. Rev.* **2002**, *102* (2), 555–578.

(7) Mammen M., Choi S. K.., Whitesides G. M., Polyvalent Interactions in Biological Systems: Implications for Design and Use of Multivalent Ligands and Inhibitors, *Angew. Chem. Int. Ed.*, 1998, 37(20), 2754- 2794.

(8) Lee, Y. C.; Lee, R. T. Carbohydrate-Protein Interactions: Basis of Glycobiology. *Acc. Chem. Res.* **1995**, *28* (8), 321–327.

(9) Kiessling, L. L.; Gestwicki, J. E.; Strong, L. E. Synthetic Multivalent Ligands in the Exploration of Cell-Surface Interactions. *Curr. Opin. Chem. Biol.* **2000**, *4* (6), 696–703.

(10) Bernardi, A.; Jiménez-Barbero, J.; Casnati, A.; De Castro, C.; Darbre, T.; Fieschi, F.; Finne, J.; Funken, H.; Jaeger, K. E.; Lahmann, M.; et al. Multivalent Glycoconjugates as Anti-Pathogenic Agents. *Chem. Soc. Rev.* **2013**, *42* (11), 4709–4727.

(11) Johansson, E. M. V.; Crusz, S. A.; Kolomiets, E.; Buts, L.; Kadam, R. U.; Cacciarini, M.; Bartels, K. M.; Diggle, S. P.; Cámara, M.; Williams, P.; et al. Inhibition and Dispersion of Pseudomonas Aeruginosa Biofilms by Glycopeptide Dendrimers Targeting the Fucose-Specific Lectin LecB. *Chem. Biol.* **2008**, *15* (12), 1249–1257.

(12) Cecioni, S.; Imberty, A.; Vidal, S. Glycomimetics versus Multivalent Glycoconjugates for the Design of High Affinity Lectin Ligands. *Chem. Rev.* **2015**, *115* (1), 525–561.

(13) Reichardt, N. C.; Martín-Lomas, M.; Penadés, S. Opportunities for Glyconanomaterials in Personalized Medicine. *Chem. Commun.* **2016**, *52* (92), 13430–13439.

(14) Cid, J. J.; Assali, M.; Fernández-García, E.; Valdivia, V.; Sánchez-Fernández, E. M.; Garcia Fernández, J. M.; Wellinger, R. E.; Fernández, I.; Khiar, N. Tuning of Glyconanomaterial Shape and Size for Selective Bacterial Cell Agglutination. *J. Mater. Chem. B* **2016**, *4* (11), 2028–2037.

(15) Khanal, M.; Raks, V.; Issa, R.; Chernyshenko, V.; Barras, A.; Garcia Fernandez, J. M.; Mikhalovska, L. I.; Turcheniuk, V.; Zaitsev, V.; Boukherroub, R.; et al. Selective Antimicrobial and Antibiofilm Disrupting Properties of Functionalized Diamond Nanoparticles Against Escherichia Coli and Staphylococcus Aureus. *Part. Part. Syst. Charact.* **2015**, *32* (8), 822–830.

(16) Chemani, C.; Imberty, A.; De Bentzmann, S.; Pierre, M.; Wimmerová, M.; Guery, B. P.; Faure, K. Role of LecA and LecB Lectins in Pseudomonas Aeruginosa-Induced Lung Injury and Effect of Carbohydrate Ligands. *Infect. Immun.* **2009**, *77* (5), 2065–2075.

(17) Hauber, H. P.; Schulz, M.; Pforte, A.; Mack, D.; Zabel, P.; Schumacher, U. Inhalation with Fucose and Galactose for Treatment of Pseudomonas Aeruginosa in Cystic Fibrosis Patients. *Int. J. Med. Sci.* **2008**, *5* (6), 371–376.

(18) Becker, D. J.; Lowe, J. B. Fucose: Biosynthesis and Biological Function in Mammals. *Glycobiology* **2003**, *13* (7), 41R-51R.

(19) Anderson, C. T.; Wallace, I. S.; Somerville, C. R. Metabolic Click-Labeling with a Fucose Analog Reveals Pectin Delivery, Architecture, and Dynamics in Arabidopsis Cell Walls. *Proc. Natl. Acad. Sci. U. S. A.* **2012**, *109* (4), 1329–1334.

(20) Gringhuis, S. I.; Kaptein, T. M.; Wevers, B. A.; Mesman, A. W.; Geijtenbeek, T. B. H. Fucose-Specific DC-SIGN Signalling Directs T Helper Cell Type-2 Responses via IKKε- and CYLD-Dependent Bcl3 Activation. *Nat. Commun. 2014 51* **2014**, *5* (1), 1–13.

(21) Glick, M. C.; Kothari, V. A.; Liu, A.; Stoykova, L. I.; Scanlin, T. F. Activity of Fucosyltransferases and Altered Glycosylation in Cystic Fibrosis Airway Epithelial Cells. *Biochimie* **2001**, *83* (8), 743–747.

(22) Heggelund, J. E.; Varrot, A.; Imberty, A.; Krengel, U. Histo-Blood Group Antigens as Mediators of Infections. *Curr. Opin. Struct. Biol.* **2017**, *44*, 190–200.

(23) Garber, N.; Guempel, U.; Gilboa-Garber, N.; Royle, R. J. Specificity of the Fucose-Binding Lectin of Pseudomonas Aeruginosa. *FEMS Microbiol. Lett.* **1987**, *48* (3), 331–334.

(24) Audfray, A.; Claudinon, J.; Abounit, S.; Ruvoën-Clouet, N.; Larson, G.; Smith, D. F.; Wimmerová, M.; Le Pendu, J.; Römer, W.; Varrot, A.; et al. Fucose-Binding Lectin from Opportunistic Pathogen Burkholderia Ambifaria Binds to Both Plant and Human Oligosaccharidic Epitopes. *J. Biol. Chem.* **2012**, *287* (6), 4335–4347.

(25) Houser, J.; Komarek, J.; Kostlanova, N.; Cioci, G.; Varrot, A.; Kerr, S. C.; Lahmann, M.; Balloy, V.; Fahy, J. V.; Chignard, M.; et al. A Soluble Fucose-Specific Lectin from Aspergillus Fumigatus Conidia--Structure, Specificity and Possible Role in Fungal Pathogenicity. *PLoS One* **2013**, *8* (12).

(26) Kerr, S. C.; Fischer, G. J.; Sinha, M.; McCabe, O.; Palmer, J. M.; Choera, T.; Yun Lim, F.; Wimmerova, M.; Carrington, S. D.; Yuan, S.; et al. FleA Expression in Aspergillus Fumigatus Is Recognized by Fucosylated Structures on Mucins and Macrophages to Prevent Lung Infection. *PLoS Pathog.* **2016**, *12* (4).

(27) Chabre, Y. M.; Giguère, D.; Blanchard, B.; Rodrigue, J.; Rocheleau, S.; Neault, M.; Rauthu, S.; Papadopoulos, A.; Arnold, A. A.; Imberty, A.; et al. Combining Glycomimetic and Multivalent Strategies toward Designing Potent Bacterial Lectin Inhibitors. *Chem. – A Eur. J.* **2011**, *17* (23), 6545–6562.

(28) Ligeour, C.; Audfray, A.; Gillon, E.; Meyer, A.; Galanos, N.; Vidal, S.; Vasseur, J. J.; Imberty, A.; Morvan, F. Synthesis of Branched-Phosphodiester and Mannose-Centered Fucosylated Glycoclusters and Their Binding Studies with Burkholderia Ambifaria Lectin (BambL). *RSC Adv.* **2013**, *3* (42), 19515–19524.

(29) Galanos, N.; Chen, Y.; Michael, Z. P.; Gillon, E.; Dutasta, J. P.; Star, A.; Imberty, A.; Martinez, A.; Vidal, S. Cyclotriveratrylene-Based Glycoclusters as High Affinity Ligands of Bacterial Lectins from Pseudomonas Aeruginosa and Burkholderia Ambifaria. *ChemistrySelect* **2016**, *1* (18), 5863–5868.

(30) Buffet, K.; Nierengarten, I.; Galanos, N.; Gillon, E.; Holler, M.; Imberty, A.; Matthews, S. E.; Vidal, S.; Vincent, S. P.; Nierengarten, J. F. Pillar[5]Arene-Based Glycoclusters: Synthesis and Multivalent Binding to Pathogenic Bacterial Lectins. *Chem. – A Eur. J.* **2016**, *22* (9), 2955–2963.

(31) Galanos, N.; Gillon, E.; Imberty, A.; Matthews, S. E.; Vidal, S. Pentavalent Pillar[5]Arene-Based Glycoclusters and Their Multivalent Binding to Pathogenic Bacterial Lectins. *Org. Biomol. Chem.* **2016**, *14* (13), 3476–3481.

(32) Goyard, D.; Baldoneschi, V.; Varrot, A.; Fiore, M.; Imberty, A.; Richichi, B.; Renaudet, O.; Nativi, C. Multivalent Glycomimetics with A Ffi Nity and Selectivity toward Fucose-Binding Receptors from Emerging Pathogens. **2018**.

(33) Renaudet, O.; Roy, R. Multivalent Scaffolds in Glycoscience: An Overview. *Chem. Soc. Rev.* **2013**, *42* (11), 4515–4517.

(34) Cecioni, S.; Imberty, A.; Vidal, S. Glycomimetics versus Multivalent Glycoconjugates for the Design of High Affinity Lectin Ligands. *Chem. Rev.* **2015**, *115* (1), 525–561.

(35) Kim, Y.; Hyun, J. Y.; Shin, I. Multivalent Glycans for Biological and Biomedical Applications. *Chem. Soc. Rev.* **2021**, *50* (18), 10567–10593.

(36) Garcia-Hartjes, J.; Bernardi, S.; Weijers, C. A. G. M.; Wennekes, T.; Gilbert, M.; Sansone, F.; Casnati, A.; Zuilhof, H. Picomolar Inhibition of Cholera Toxin by a Pentavalent Ganglioside GM1os-Calix[5]Arene. *Org. Biomol. Chem.* **2013**, *11* (26), 4340–4349.

(37) André, S.; Sansone, F.; Kaltner, H.; Casnati, A.; Kopitz, J.; Gabius, H. J.; Ungaro, R. Calix[n]Arene-Based Glycoclusters: Bioactivity of Thiourea-Linked Galactose/Lactose Moieties as Inhibitors of Binding of Medically Relevant Lectins to a Glycoprotein and Cell-Surface Glycoconjugates and Selectivity among Human Adhesion/Growth-Regulatory Galectins. *ChemBioChem* **2008**, *9* (10), 1649–1661.

(38) Dawson, P. E.; Kent, S. B. H. Convenient Total Synthesis of a 4-Helix TASP Molecule by Chemoselective Ligation. *J. Am. Chem. Soc.* **1993**, *115* (16), 7263–7266.

(39) Mutter, M.; Dumy, P.; Garrouste, P.; Lehmann, C.; Mathieu, M.; Peggion, C.; Peluso, S.; Razaname, A.; Tuchscherer, G. Template Assembled Synthetic Proteins (TASP) as Functional Mimetics of Proteins. *Angew. Chem. Int. Ed. English* **1996**, *35* (13–14), 1482–1485.

(40) Galan, M. C.; Dumy, P.; Renaudet, O. Multivalent Glyco(Cyclo)Peptides. *Chem. Soc. Rev.* **2013**, *42* (11), 4599–4612.

(41) Dumy, P.; Eggleston, I. M.; Cervigni, S.; Sila, U.; Sun, X.; Mutter, M. A Convenient Synthesis of Cyclic Peptides as Regioselectively Addressable Functionalized Templates (RAFT). *Tetrahedron Lett.* **1995**, *36* (8), 1255–1258.

(42) Tuchscherer, G.; Dömer, B.; Sila, U.; Kamber, B.; Mutter, M. The TASP Concept : Mimetics of Peptide Ligands, Protein Surfaces and Folding Units. *Tetrahedron* **1993**, *49* (17), 3559–3575.

(43) Renaudet, O.; Dumy, P. Chemoselectively Template-Assembled Glycoconjugates as Mimics for Multivalent Presentation of Carbohydrates. *Org. Lett.* **2003**, *5* (3), 243–246.

(44) Verboom, W.; Durie, A.; Egberink, R. J. M.; Asfari, Z.; Reinhoudt, D. N. Ipso Nitration of P-Tert-Butylcalix[4]Arenes. *J. Org. Chem.* **1992**, *57* (4), 1313–1316.

(45) Gutsche, C. D.; Dhawan, B.; Levine, J. A.; Hyun No, K.; Bauer, L. J. Calixarenes 9 : Conformational Isomers of the Ethers and Esters of Calix[4]arenes. *Tetrahedron* **1983**, *39* (3), 409–426.

(46) Sansone, F.; Dudič, M.; Donofrio, G.; Rivetti, C.; Baldini, L.; Casnati, A.; Cellai, S.; Ungaro, R. DNA Condensation and Cell Transfection Properties of Guanidinium Calixarenes: Dependence on Macrocycle Lipophilicity, Size, and Conformation. *J. Am. Chem. Soc.* **2006**, *128* (45), 14528–14536.

(47) Buffet, K.; Gillon, E.; Holler, M.; Nierengarten, J. F.; Imberty, A.; Vincent, S. P. Fucofullerenes as Tight Ligands of RSL and LecB, Two Bacterial Lectins. *Org. Biomol. Chem.* **2015**, *13* (23), 6482–6492.

(48) Isaad, A. L. C.; Barbetti, F.; Rovero, P.; D'Ursi, A. M.; Chelli, M.; Chorev, M.; Papini, A. M. Nα-Fmoc-Protected ω-Azido- and ω-Alkynyl-L-Amino Acids as Building Blocks for the Synthesis of "Clickable" Peptides. *Eur. J. Org. Chem.* **2008**, *2008* (31), 5308–5314.

(49) Alper, P. B.; Hung, S. C.; Wong, C. H. Metal Catalyzed Diazo Transfer for the Synthesis of Azides from Amines. *Tetrahedron Lett.* **1996**, *37* (34), 6029–6032.

(50) Nyffeler, P. T.; Liang, C. H.; Koeller, K. M.; Wong, C. H. The Chemistry of Amine-Azide Interconversion: Catalytic Diazotransfer and Regioselective Azide Reduction. *J. Am. Chem. Soc.* **2002**, *124* (36), 10773–10778.

(51) Goddard-Borger, E. D.; Stick, R. V. An Efficient, Inexpensive, and Shelf-Stable Diazotransfer Reagent: Imidazole-1-Sulfonyl Azide Hydrochloride. *Org. Lett.* **2007**, *9* (19), 3797–3800.

(52) Pandiakumar, A. K.; Sarma, S. P.; Samuelson, A. G. Mechanistic Studies on the Diazo Transfer Reaction. *Tetrahedron Lett.* **2014**, *55* (18), 2917–2920.

(53) Bossu, I.; Berthet, N.; Dumy, P.; Renaudet, O. Synthesis of Glycocyclopeptides by Click Chemistry and Inhibition Assays with Lectins. **2011**, *30* (7–9), 458–468.

(54) Lameignere, E.; Malinovská, L.; Sláviková, M.; Duchaud, E.; Mitchell, E. P.; Varrot, A.; Šedo, O.; Imberty, A.; Wimmerová, M. Structural Basis for Mannose Recognition by a Lectin from Opportunistic Bacteria Burkholderia Cenocepacia. *Biochem. J.* **2008**, *411* (2), 307–318.

(55) Audfray, A.; Claudinon, J.; Abounit, S.; Ruvoën-Clouet, N.; Larson, G.; Smith, D. F.; Wimmerová, M.; Le Pendu, J.; Römer, W.; Varrot, A.; et al. Fucose-Binding Lectin from Opportunistic Pathogen Burkholderia Ambifaria Binds to Both Plant and Human Oligosaccharidic Epitopes. *J. Biol. Chem.* **2012**, *287* (6), 4335–4347.

(56) Giuliani, M.; Faroldi, F.; Morelli, L.; Torre, E.; Lombardi, G.; Fallarini, S.; Sansone, F.;

Compostella, F. Exploring Calixarene-Based Clusters for Efficient Functional Presentation of Streptococcus Pneumoniae Saccharides. *Bioorg. Chem.* **2019**, *93*.

(57) Gillon, E.; Varrot, A.; Imberty, A. LecB, a High Affinity Soluble Fucose-Binding Lectin from Pseudomonas Aeruginosa. *Methods Mol. Biol.* **2020**, *2132*, 475–482.

(58) Iwamoto, K.; Araki, K.; Shinkai, S. Conformations and Structures of Tetra- O -Alkyl-p-Tert -Butylcalix[4]Arenes. How Is the Conformation of Calix[4]Arenes Immobilized? *J. Org. Chem.* **1991**, *56* (16), 4955–4962.

(59) Rincón, A. M.; Prados, P.; De Mendoza, J. A Calix[4]Arene Ureidopeptide Dimer Self-Assembled through Two Superposed Hydrogen Bond Arrays. *J. Am. Chem. Soc.* **2001**, *123* (15), 3493–3498.

(60) Klimentová, J.; Vojtíšek, P. New Receptors for Anions in Water: Synthesis, Characterization, X-Ray Structures of New Derivatives of 5,11,17,23-Tetraamino-25,26,27,28-Tetrapropyloxycalix[4]Arene. *J. Mol. Struct.* **2007**, *826* (1), 48–63.

(61) Pícha, J.; Buděšínský, M.; Macháčková, K.; Collinsová, M.; Jiráček, J. Optimized Syntheses of Fmoc Azido Amino Acids for the Preparation of Azidopeptides. *J. Pept. Sci.* **2017**, *23* (3), 202–214.

Chapter 4:

Calix[4]arene-based derivatives for bacteria recognition

1. INTRODUCTION

The human body and bacteria are deeply connected through a bond that can be symbiotic and beneficial or lead to infections, sometimes deadly. The bacterial composition present in the human body, called microbiota, determines the state of health/disease based on diet (fatty acids, indigestible carbohydrates, prebiotics and polyphenols) and other external and non-external factors (environment, sex, age, genetic background).[1] Bacteria provide us with some biological functions that our metabolism is not able to perform independently, such as the fermentation of undigested substrates, which include starch, polysaccharides, and some proteins, or the transformation and/or elimination of toxic substances.[2] The microbiota also plays a major role in the proper functioning of the human immune system, as it is involved in the induction of protective responses against pathogens and in maintaining regulatory processes to allow tolerance towards harmless antigens. It has been shown that exposure to non-pathogenic bacteria causes an increase in the number of lymphocytes in the mucous membranes and increases the size of germinal centers in the lymph nodes; in addition, immunoglobulins in the serum also undergo a significant increase. The microbiota also induces the development of regulatory B and T cells, which are necessary for tolerance towards various antigens that pass through the intestine, avoiding unnecessary inflammatory processes.[2] The dialogue between the host and the bacterial population is based on molecular signals.

Infections caused by pathogenic bacteria, as well as other environmental factors such as smoking, can alter the composition of the specific microbiota of the organ, leading to the development of certain microbial populations (E. Coli, Yersinia and Clostridium difficile, for example) and the subsequent onset of chronic inflammation in the intestine. The homeostasis of the bacterial population in the host is therefore related to human health and its perturbation, also called dysbiosis, can lead to diseases even in other organs, such as the liver, bones, and nervous system. It is therefore essential to understand the interconnection between the population of the microbiota and the general state of health of humans. Easy identification of bacterial strains can certainly facilitate this difficult task. One of the main obstacles in the study of these processes is indeed the specific identification of the bacterial strain and the quantitative detection of its metabolites.

The timely identification of pathogenic bacterial agents is furthermore very important considering that there is a rapid insurgence of antibiotic resistant bacteria.

This is a serious issue which is claiming the lives of many people every year, and as shown in figure 1, and every region of the globe is more or less affected by it.[3]

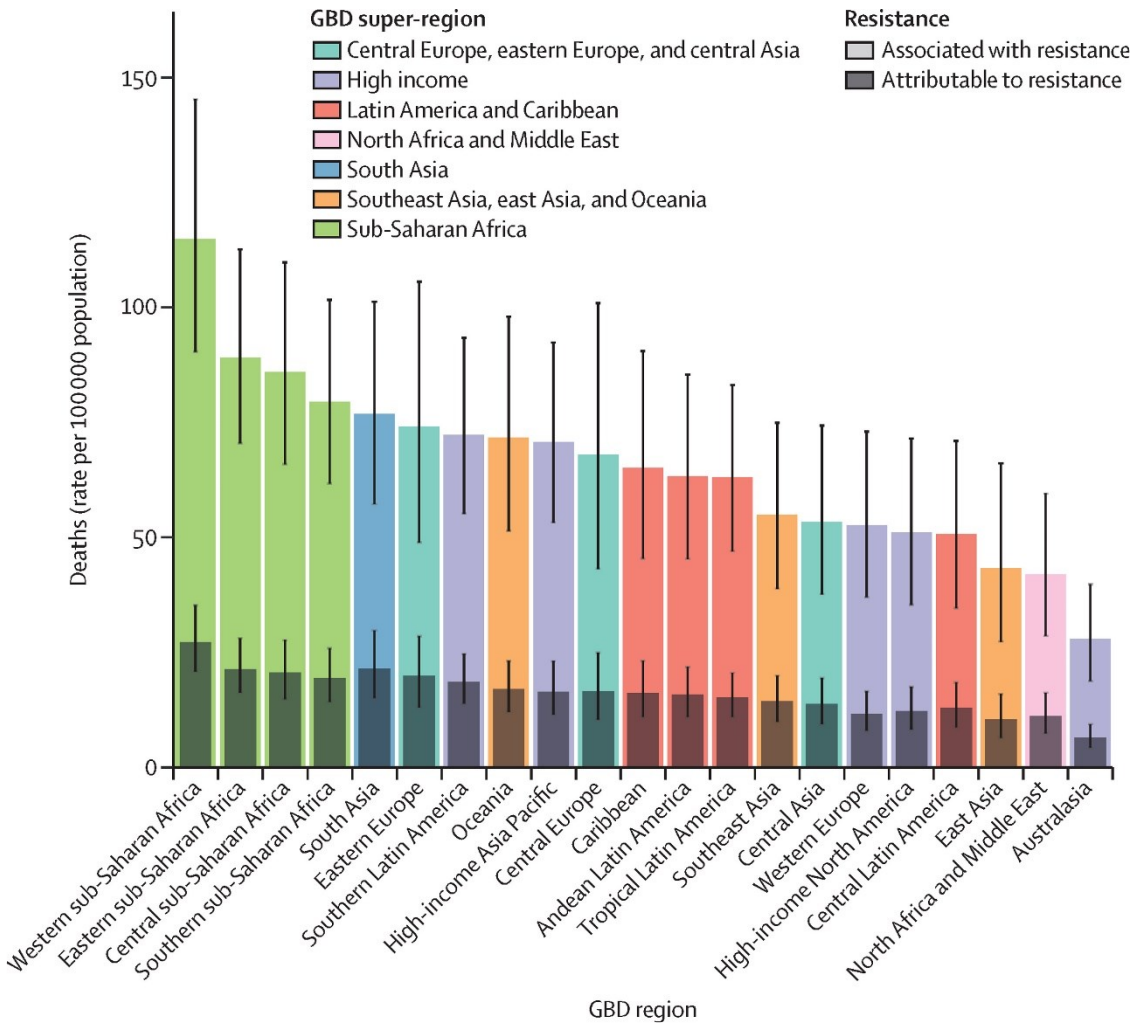

Figure 1: Death rate due to bacterial antimicrobial resistance by GBD region for all ages, in 2019.[3]

The main solution to this problem would be the release of new antibiotics to the market, possibly having bacteria targets different from those exploited up to now. However, since the 1990 no new class of these crucial drugs entered the market.

In this scenario a fast identification of the nature of a bacterial infection is key. In fact, the timely identification of pathogenic bacterial agents in acute infections can lead to an improvement in therapeutic treatments, reducing the use of broad-spectrum antibiotics for antibiotics specific for the strain to be treated. In fact, in 20-50% of cases, patients receive inadequate antibiotic therapy, as the severity of the situation and the urgency of treatment lead to an empirical choice of therapy.[4] In addition to an increase in the effectiveness of treatment, specific therapy could lead to a decrease in the continuous development of antibiotic-resistant bacteria, due to inadequate prescription of these drugs.

Commonly used methods for bacterial identification include outdated and lengthy biological assays or modern sequencing techniques, which are however still complex, expensive, and lengthy. The biological approach is based on the isolation of the

bacterium using specific culture media and subsequent enzymatic reactions and/or morphological analyses. These biochemical protocols, in addition to requiring several steps and therefore taking up to several days, are also easily subject to errors. There are alternatives like faster molecular methods that can however simultaneously verify the presence of only a limited number of pathogens on the same sample. In the 1980s, for example, a revolutionary method was introduced that uses the polymerase chain reaction (PCR) to amplify specific bacterial gene sequences. After the development of electrospray ionization (ESI) and matrix-assisted laser desorption/ionization (MALDI) techniques, mass spectrometry has also been used for bacterial identification. One approach is PCR-ESI-QTOF-MS, which is advantageous because it requires minimal or no sample preparation and can provide information about the bacterial strain. Another valid alternative is MALDI-MS analysis, which returns the protein profile of whole microorganisms by efficiently identifying biomarkers related to ribosomal proteins. Adequate databases, equipped with algorithms capable of comparing mass fragmentation profiles, are obviously necessary. One of the main limitations of bacterial identification by mass spectrometry is the initial cost of the equipment and its configuration; in addition, since only one instrument is needed for a large number of daily samples, the occurrence of technical problems can lead to an interruption of the routine analysis and consequent decision-making problems for doctors, especially in emergency situations, such as in the case of sepsis.[5]

Modern sequencing techniques are very promising; they are based on sequencing the entire bacterial genome or on amplifying and subsequently sequencing an amplicon of the 16S rRNA gene, which represents a hypervariable region of the genome and can therefore provide a specific signature for each bacterial species. The first step is to extract DNA from the bacterial cells, and for this purpose, there are various kits available on the market, then it needs to be purified, amplified, and finally sequenced. There are different techniques for the latter step, which are based on different principles, such as fluorescence, pH variation, or the use of nanopores.[6] As mentioned previously, this approach has the disadvantage of being expensive and not fast enough. A faster and functional method for identifying one or more pathogenic bacteria has not yet been found.

In this context, the BacHound project (Supramolecular nanostructures for bacteria detection) was funded by MUR (Ministry of University and Research). Its aim is to develop nanosensors for the detection of different bacterial strains, through the recognition of molecular patterns present on the bacterial cell wall or given by the presence of specific metabolites. These new diagnostic tools must be reliable, selective and should give a fast response, in order to provide rapid and complete information

about the composition of the bacterial population and its variation in physiological and pathological conditions.

The BacHound project proposes to take advantage of some principles of Supramolecular Chemistry, such as self-assembly and multivalency using, as the main platforms, systems already proven to be effective in the biomedical field like calixarenes. These compounds will be functionalized with appropriate units, which target specific molecular patterns associated with pathogens (PAMPs). Molecular recognition is based on a combination of electrostatic interactions, hydrophobic effects and other complementary noncovalent interactions. Once it will be established that a given system can interact with the desired bacteria strain, these systems will have to be further modified and associated with an appropriate reporter, which must cause modulation of the signal depending on the interaction with the target, thus allowing their application as biomolecular sensors.

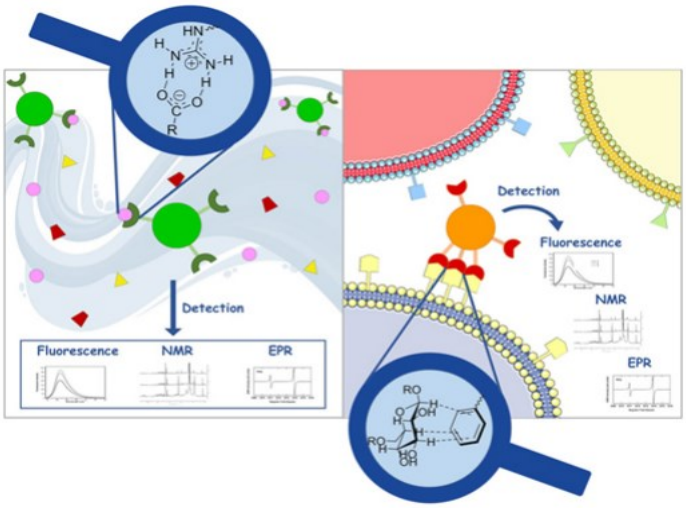

Figure 2: On the left is represented the recognition of metabolites in biological fluids, while on the right is highlighted the recognition of PAMPs on the bacterial surface.

Advanced techniques can, at least in this preliminary scouting process, be used to monitor the signal variation, such as:

-NMR chemosensing, which exploits the transfer of magnetization between organic molecules and interacting analytes,

-EPR (electron paramagnetic resonance), which identifies and analyzes paramagnetic species, exciting electronic spins,

-the Indicator Displacement Assay (IDA), an optical detection method where the indicator is not covalently bound to the receptor but constitutes a reporter initially complexed to receptor and displaced by the incoming analyte. Upon release into the

solution, the indicator undergoes a change in its optical properties which can be monitored by absorbance or fluorescence.

Finally, the principal component analysis (PCA) using nanosensor assay will allow the detection of specific groups of metabolites and bacterial strains associated with health/disease states.

The aforementioned nanosystems must be able to discriminate at least between the three types of bacteria first: Gram-positive, Gram-negative and mycobacteria, and respond differently based on the bacterial species. For this discrimination, it is thought to take advantage of the different molecular/structural composition of the bacterial wall (Figure 3).

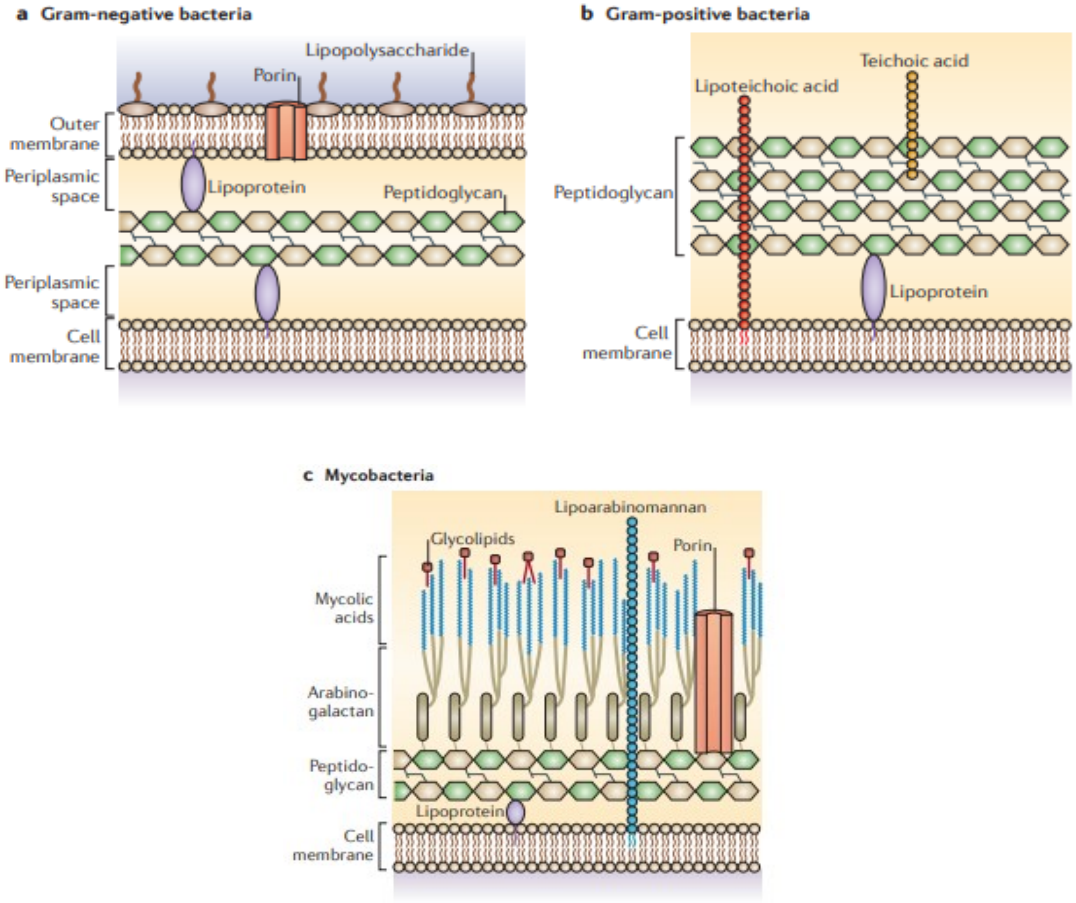

Figure 3: Bacterial cell wall of a) Gram-negative b) Gram-positive c) Mycobacteria.

The wall of Gram-negative bacteria is composed of a thin layer of peptidoglycan, located in the periplasmic space between the two lipid membranes. On the outer membrane are exposed lipopolysaccharides, which can be exploited as molecular targets for this class of bacteria. Gram-positive bacteria, on the other hand, have teichoic and lipoteichoic acids on their surface and have a thicker and much more

exposed layer of peptidoglycan, which makes up the predominant part of the wall. Finally, mycobacteria are associated with a wall composed of a thin layer of peptidoglycan, to which arabinogalactans are, in turn, connected with mycolic acids. This last layer gives the wall a marked hydrophobic character.

Therefore, BacHound aims to synthesize and study new multivalent systems, which exploit some of the key interactions identified as crucial to recognize bacteria such as those represented in figure 4. In particular, the ones based on the electrostatic interaction between the negatively charged membrane of Gram-negative (but to some extent also of Gram-positive) bacteria could be used to differentiate them from the more hydrophobic mycobacteria.

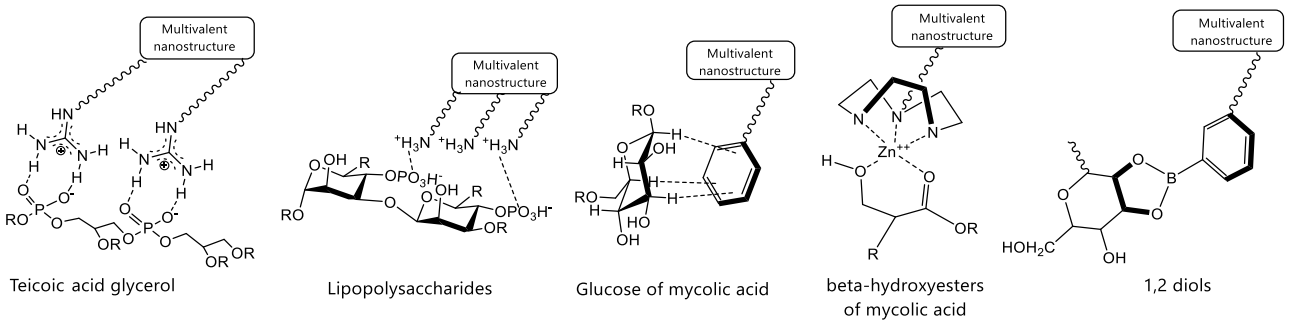

Figure 4: Potential interactions for bacterial wall recognition. For example, nanosystems containing guanidine or ammonium groups, positively charged metal complexes or phenylboronic acid could be exploited.

Synthetic compounds capable of interacting with bacteria have already been reported in the literature. Recent studies, for example, have shown that poly(amidoamine) dendrimers functionalized with modified boronic acid (B-PAMAM(G4)) (Figure 5) can be used as cross-linking molecules for the formation of aggregates with bacteria.[7] The structure of the dendrimer allows for the presence of numerous interaction sites. After only five minutes of adding these dendrimers to a bacterial suspension, the formation of aggregates is observed, which are visible to the naked eye. The change in optical density at 600 nm was monitored. The formation of aggregates has been shown to depend on pH, in fact, in basic conditions, aggregates are formed by both Gram-positive and Gram-negative bacteria, while at neutral pH only Gram-positive bacteria form aggregates. The recognition of the bacterial surface takes place through the end of the arms that present the phenylboronic acid; it is known, in fact, that boronic acid binds to diols and therefore also to sugars. The discrimination between the two classes, as already stated previously, is based on the different composition of the bacterial cell wall.

Other studies regarding the use of dendrimers modified with phenylboronic acid and labeled with a fluorescent dansyl group (Figure 5) have shown their potential use as sensors for the detection of bacteria within twenty minutes, with potential antibacterial activity towards Gram-negative bacteria.[8]

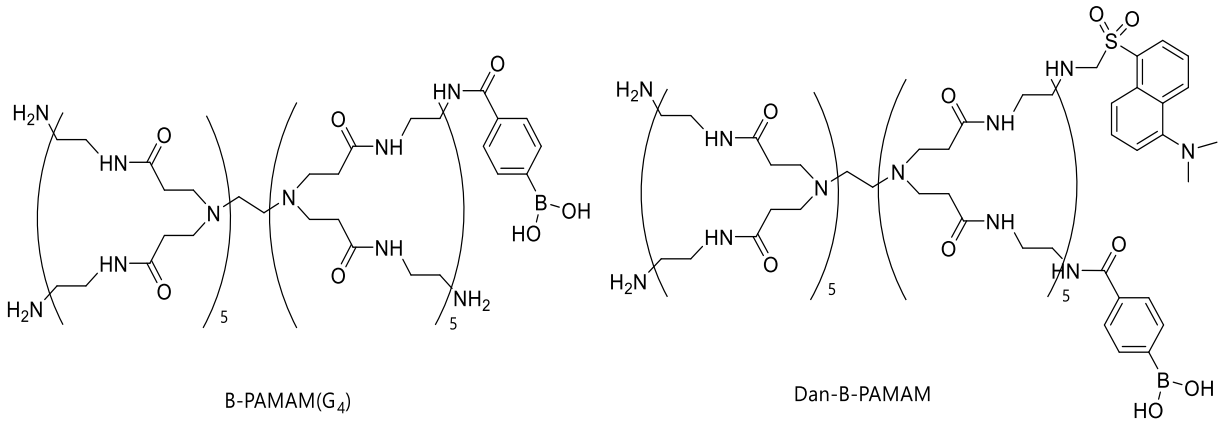

Figure 5: Poly(amidoamine) dendrimers functionalized with phenylboronic acid.

Using calixarenes and AuNPs, the detection of small metabolites in biological fluids can also be designed but will not be treated into details in this introduction because not pursued in the present thesis. By monitoring the signal change associated with reporters covalently linked to positively or negatively charged nanostructures it could be possible to recognize target metabolites such as short-chain fatty acids or polyamines and polycations, respectively.

1.1 Gram-positive bacteria

We chose to focus on the synthesis of receptors for the detection of Gram-positive bacteria, using the amino acid chain of peptidoglycan as a target and, in particular, the unique D-ala-D-ala amino acid sequence present in the peptidoglycan. This should ensure to the designed nanostructure a specific recognition towards this class of bacteria. This sequence is indeed very rare in nature and present only in Gram-positive bacteria. The antibiotic Vancomycin (Figure 7) owes its action and specificity to its peculiar characteristic of binding to the D-ala-D-ala sequence of peptidoglycan, inhibiting its growth and causing the lysis of the cell wall of these bacteria.[9]

Peptidoglycan is the predominant component in the cell wall of Gram-positive bacteria, where it forms a thick polymer layer from 20 to 80 nm that represents about 90% of the dry weight of the cell. The main components are two acetylated amino sugars: N-acetylglucosamine (NAG) and N-acetylmuramic acid (NAM), linked by β-1,4-glycosidic bonds (Figure 6). Short amino acid chains with the sequence L-ala-γ-D-glu-L-lys-D-ala-

D-ala are connected to NAM units through an amide bond. Peptidoglycan chains of different saccharides are joined together, forming interpeptide bonds, known as cross-linking units, which hold together the structure and increase its chemical and mechanical resistance. This cross-linking is formed by the binding between the ε-amino group of lys in position 3 of one chain and the terminal carboxy group of Ala in position 4 of the next chain. This binding, in Gram-positive bacteria, is often mediated by a pentaglycine moiety that is arranged as a bridge unit, as can be seen in figure 6.

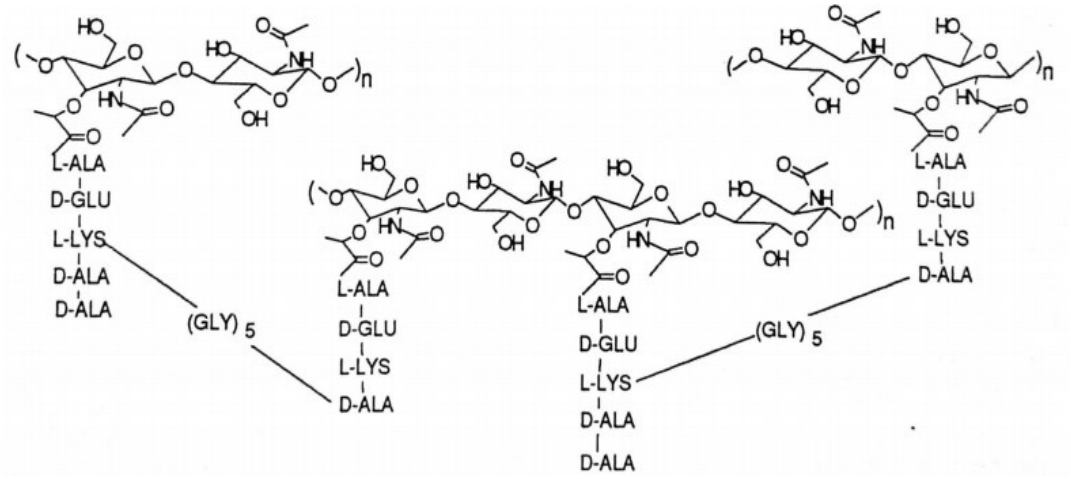

Figure 6: Peptidoglycan structure of Gram-positive bacteria.

In order to recognize the peptidoglycan, we thought to prepare a macrocyclic calixarene-based system, previously synthesized and studied by our research group, which showed vancomycin-like properties.[10] The macrobicyclic peptidocalix[4]arene shown in Figure 7, had been previously studied as an antimicrobic system able to inhibit the growth of Gram-positive bacteria. Its action was supposed to take place by the inhibition of the biosynthesis of the cell wall of Gram-positive bacteria. Its complexation to the terminal D-ala-D-ala sequence of peptidoglycan could in fact hinders, so as vancomycin does, the cross-linking processes catalyzed by transpeptidases.[10]

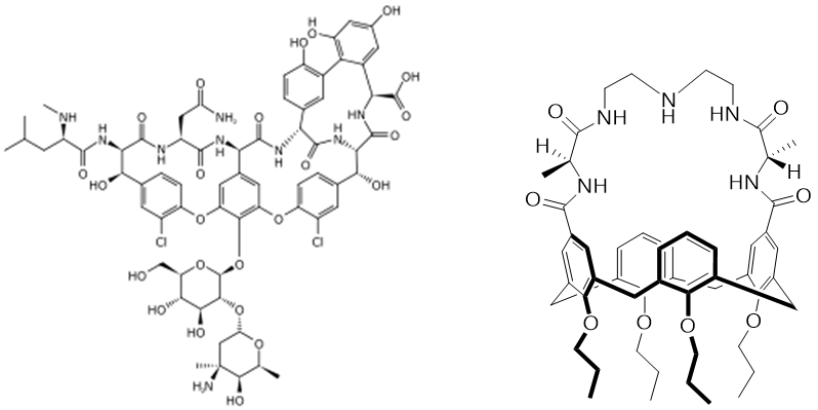

Figure 7: Vancomycin (left) and its mimic peptidocalix[4]arene (right).

The macrobicyclic peptidocalixarene of Figure 7 is highly preorganized; it has, in fact, a rigid structure with the binding groups already oriented in the proper direction to establish valuable interactions during the complexation process. Therefore, it is not subject to significant and enthalpy costly conformational changes upon binding to the guest (D-ala-D-ala terminal part of peptidoglycan) and, moreover, the presence of the bridge reduces the entropic disadvantage of complexation. Keeping the other energetic factors constant, that is the number of possible attractive interactions taking place between the host and the guest, a high degree of preorganization generally highly increases the binding constants. In the design of the receptor, we also try to follow the concept of complementarity, that is, the functionalization of the macromolecule with groups that give the most efficient interactions possible, without however generating non-binding repulsions or intra-annular tensions.

Moreover, this macrocyclic receptor for peptidoglycan, contains a basic amine function in the middle of the bridge and introduced to interact directly with the carboxylate of the terminal D-alanine, thus providing a strong electrostatic contribution, especially important in water, to the energy required for complexation. A single basic function has been inserted to obtain well-defined host/guest (amino acid chain) complexes with a 1:1 stoichiometry and to avoid complexes with variable stoichiometries.

From previous studies on the antimicrobial properties of this receptor, it is clear that the amino function plays a crucial role in complexation, as the activity of the macrocycle decreases significantly if the central amino nitrogen is transformed into a carbamoyl nitrogen, which cancels its basicity.[10] Moreover, in addition to the electrostatic interactions between the protonated amine of the bridge and the carboxylate of alanine, evidence has been collected of hydrogen bond formation between the C=O or amide NH on the host and those on the guest. It has also been hypothesized that CH-π interactions may occur between the methyl group of central alanine and the lipophilic cavity of the calixarene, interactions that would be enhanced in water due to the hydrophobic effect. The proposed schematic structure for the complex between the peptidocalix[4]arene and the simplified model of the N-Ac-D-ala-D-ala terminal peptidoglycan is illustrated in figure 8.[11]

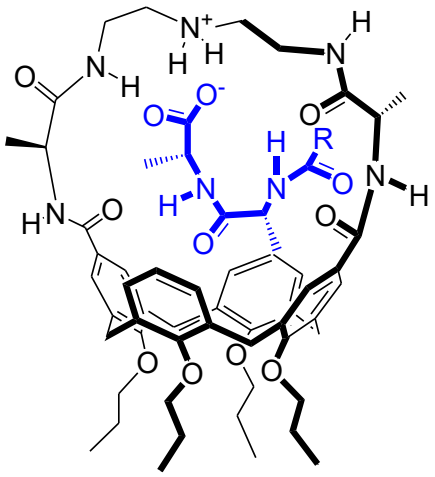

Figure 8: Proposed structure of the complex with N-acyl-D-ala-D-ala.

Previous studies have shown that the size of the peptide bridge in the receptor in the figure is the optimal compromise between conformational rigidity and the volume necessary to accommodate the ligand-ala-D-ala ligand. Analogs with larger dimensions, i.e. with four alanines in the peptide bridge or with different amino acids in terms of structure (phenylalanine, glycine) or stereochemistry (D instead of L) have been synthesized, but these structural variations of the host have always led to a decrease in activity.[9] Therefore, the above-mentioned system was re-synthesized in order to study its interaction with Gram-positive bacteria, but not with the aim of developing antimicrobial systems, but rather for explore the possibility to use it in bacteria detection. Moreover, since we had to deal with biological samples containing bacteria, an analog of the abovementioned compound with ethoxyethyl chains, much more hydrophilic than propyl, on the lower rim (compound **19** in Figure 9) was also synthesized to favor solubility in an aqueous biological sample. Also, in this latter case (**19**), we proposed to investigate the complexation properties first with a simplified model of the bacterial wall, then with the bacteria itself. Preliminary studies were therefore carried out on the interaction between the receptor **19** and two mimics of the amino acid chain of peptidoglycan, such as N-Ac-D-ala-D-ala and N-Ac-L-lys-D-ala-D-ala, using mass spectrometry and ^{1}H NMR analysis.

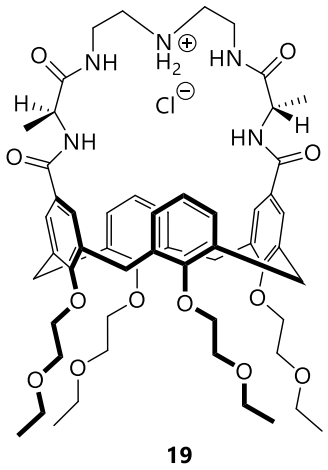

19

*Figure 9: The second peptidocalix[4]arene **19** synthesized.*

1.2 Gram-negative bacteria

The cell membrane of this class of bacteria is characterized by a high content of lipopolysaccharides (LPS), which bear negatively charged saccharide units. (Figure 10)

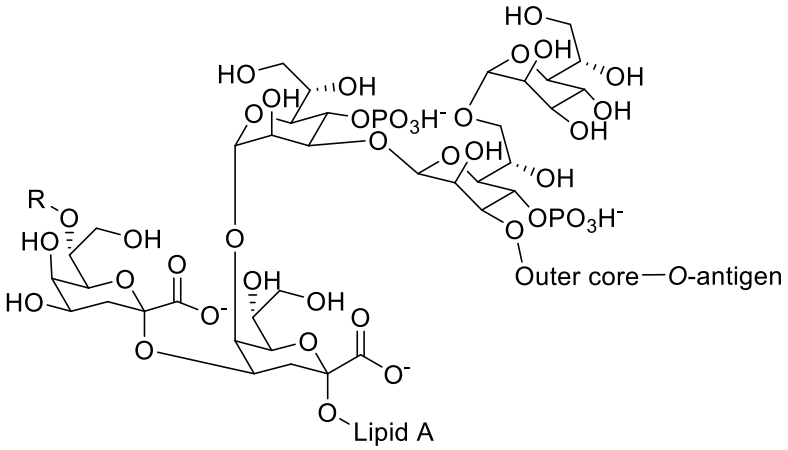

Figure 10: General representation of Gram-negative lipopolysaccharide

The localization, on the Gram-negative bacteria surface, of multiple negative charges was a characteristic that we wanted to exploit to prepare ligands for this type of bacteria. For this reason we envisioned that positively charged calix[4]arenes could have the correct characteristics for this task. In fact, positively charged compounds could form strong electrostatic interactions with the negatively charged moieties like the phosphate groups in LPS. Guanidinium is a perfect candidate to obtain charged, water soluble, calixarenes as our research group showed during the years with various examples.[12] Moreover, Regouf-de-Vains and coll. showed that calix[4]arene bearing ammonium and guanidinium groups have antimicrobial activity versus Gram-negative and Gram-

positive bacteria although without demonstrating a high selectivity for one of the two families.[13,14]

We therefore decide to prepare the following three guanidinylated calix[4]arenes (Figure 11).

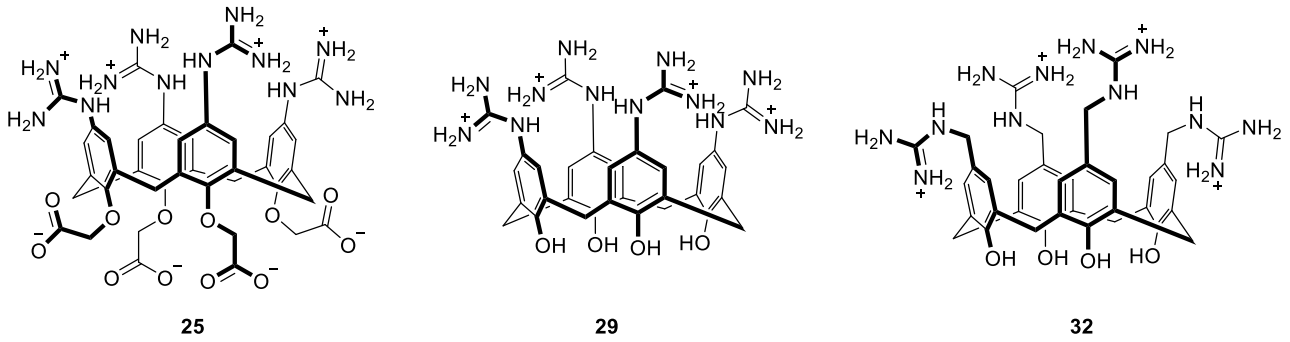

Figure 11: The three p-guanidinylated calix[4]arene synthesized.

The water solubility of these compounds is ensured by the presence of a highly charged upper rim decorated with four guanidinium groups, and a polar lower rim which is composed by OH groups or carboxylic acids. The solubility in water was an essential property that we wanted to pursue for our compounds as they had to be tested in aqueous solution.

The guanidinium group present on each compound, should favor the selectivity towards Gram-negative bacteria and prevent any sort of interaction with the lipophilic mycobacteria. In fact, at physiological pH (and even up to pH ≅ 9) this group is protonated, and therefore positively charged.[15]

Compounds **29** and **32** only differ by a methylene group, used in **32** as a spacer between the aromatic rings and the guanidinium groups. We thought that this structural variation could have been interesting to study how the affinity of these compounds for their target would change based on the conformational freedom of the guanidinium groups. In fact, compound **32** should be able to better position its charged groups thanks to the increased mobility given by the CH_2. Compound **32**, indeed, could partially adapt its binding group to the binding site without altering the calixarene cone conformation. On the other hand, compound **29** cannot do so since the guanidinium groups are directly linked to the aromatic rings, hence every modification of the position of these group would require some sort of cone distortion. It is worth keeping in mind that in these two compound the cone configuration is strongly enhanced by the network of hydrogen bonds that is established by the phenolic OH at the lower rim.

Compound **25**, has four acetate acid at the lower rim that, should be completely deprotonated from pH =6.[16] Furthermore, its cone geometry is further rigidified in a

more regular cone structure upon complexation, by the four -OCH_2COO^- units at the lower rim, of alkali or alkaline earth metal ions which are present at high concentration in biological samples.

1.3 Mycobacteria

In this context, mycobacteria are a class of bacteria that includes over 50 species. Although most of them are non-pathogenic, among these species should be also accounted *Mycobacterium tuberculosis* and *Mycobacterium leprae*, two powerful and difficult to eradicate pathogens that can cause long-term and sometimes latent and difficult to identify infections. It is estimated that *M. tuberculosis* causes about 9.4 million new cases and 1.7 million deaths worldwide each year. It was one of the first pathogens for which was described the phenomenon of multidrug resistance (MDR), that is the property of a pathogen to resist multiple unrelated antimicrobial drugs with different mechanisms of action.

Mycobacteria, like Gram-positive bacteria, are characterized by the presence of a peptidoglycan-based cell wall, but unlike them, they expose on their surface a thick layer of glycolipids such as PIM (phosphatidylinositol mannoside), mycolic acids and trehalose esters (Figure 12), which are also known to be involved in pathogenesis mechanisms and in the modulation of the immune response.

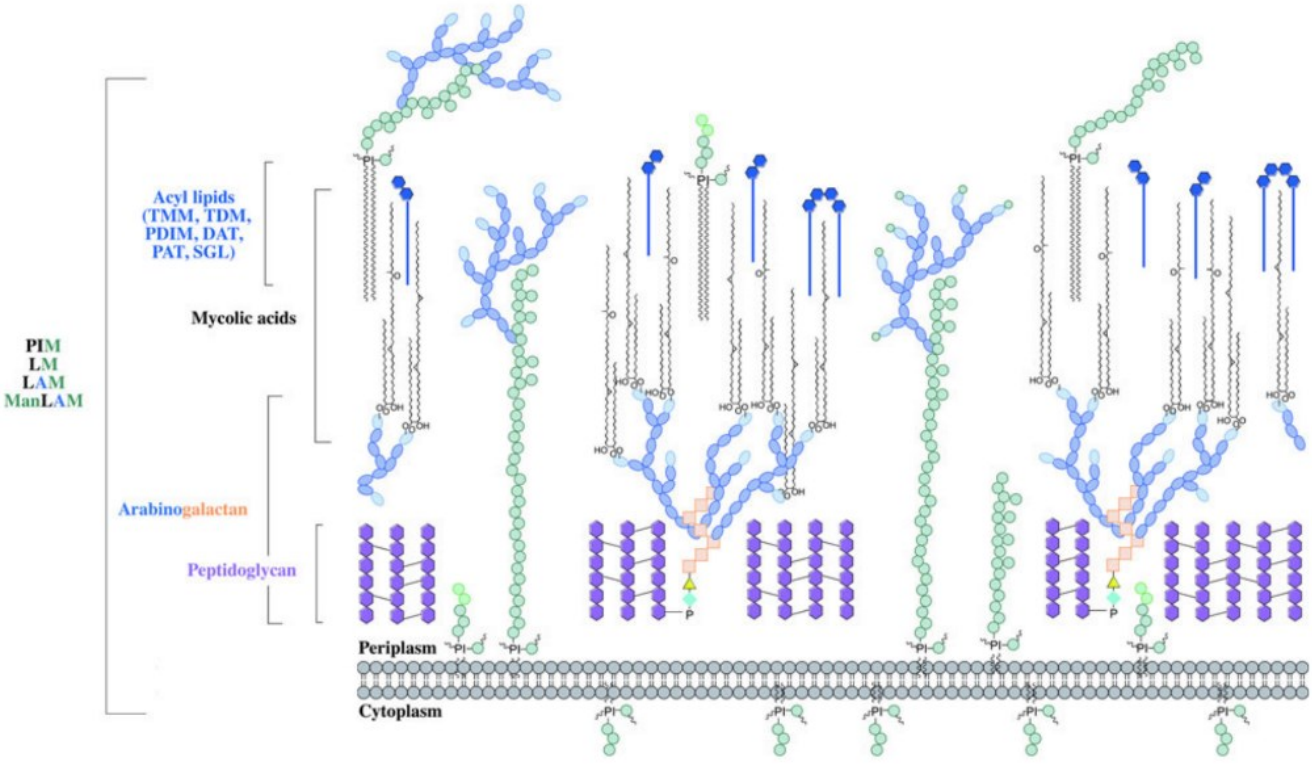

Figure 12: Schematic representation of the mycobacterial cell wall.[17]

The biosynthesis of trehalose in mycobacteria occurs in the cytoplasm from glucose through the enzymes TPS/TPP (trehalose-6-phosphate synthase / trehalose-6-phosphate phosphatase), then it is converted into mycolic acid-mono trehalose (TMM); once it passes through the plasma membrane via the protein MmpL3, TMM is converted into TDM thanks to the Ag85 enzyme complex.[18] TDM forms the end of the mycobacterial membrane (or mycomembrane); meanwhile, a second TMM molecule gives its mycolic group to an arabinogalactan terminal residue, which also becomes part of the outer structure (Figure 13).[18]

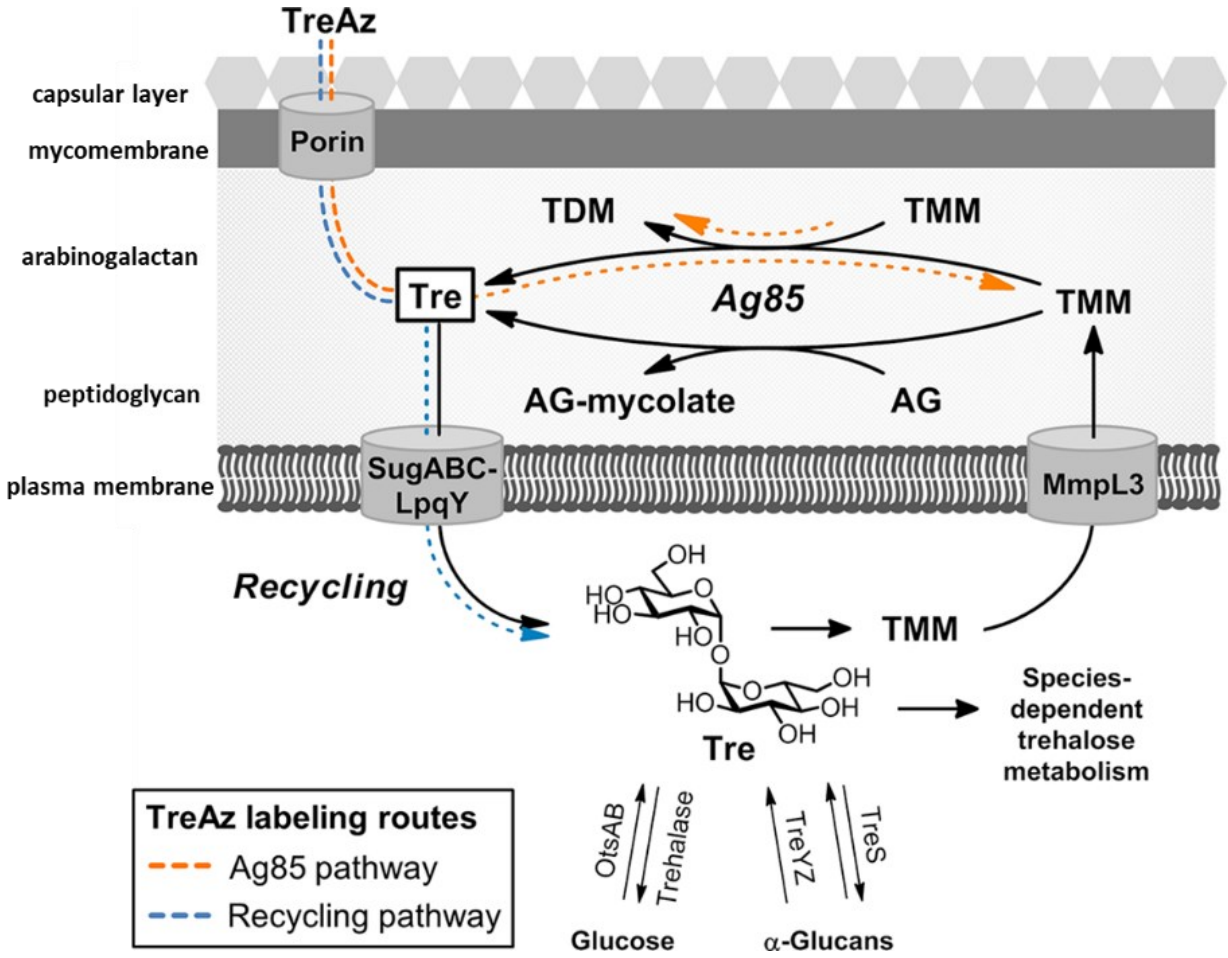

Figure 13: Schematic representation of some of the main pathways in which trehalose is involved in mycobacteria.[19]

New synthetic analogs of trehalose have recently been studied for the purpose of creating mimics that act as antibiotics, as well as for the specific detection of mycobacteria. Ishikawa et al. report trehalose dibehenate, which is the diester of behenic acid or docosanoic acid, as an analog of TDM and capable of acting as a ligand for the Mincle receptor, with positive results.[20] Other authors have reported chemically modified analogs with various functional groups. For example, Kamariza et al. have designed a trehalose analog conjugated with a fluorescent probe, which can be recognized by the mycobacterium and can be incorporated into the mycomembrane,

passing through various metabolic pathways.[21] Additionally, the dimethylaminonaphthalimide probe is quenched in aqueous solution, but fluorescent when in contact with the hydrophobic mycomembrane representing a huge advantage for the mycobacteria detection.[22] Another reported approach was based on the design of a trehalose analog (called O-alkTMM) with a single acyl chain attached at position 6, in order to mimic monomycolate trehalose (TMM); this compound was found to be extremely selective for mycobacteria, being incorporated into the metabolism of Ag85, without showing activity against Gram-positive or Gram-negative bacteria such as *B.Subtilis* or *E.Coli*.[23]

Exploiting a similar strategy professor Kiessling showed how it was possible to prepare a trehalose-based fluorogenic probe for the real-time imaging of mycobacteria.[24] This probe is made of a central trehalose core functionalized in position 6 and 6' with two different ester groups. In fact, on the former position, it bears an alkyl chain terminating with a BODIPY unit, while on the latter it has been modified whit an azo-arene. This azo compound, when is close enough, is able to quench the BODIPY fluorescence. The probe has been designed to report on to the enzymes known as mycolyltransferases, which play a role in constructing the mycolic acid membrane. This membrane, anchored by peptidoglycan, functions as a barrier to protect cells from antibiotics and the host's immune system. The probe in question, called quencher-trehalose-fluorophore (QTF), is a synthetic version of the substrate that mycolyltransferases typically work with. The enzymes process, therefore, QTF by diverting their normal activity of transesterification to hydrolysis, which in turn triggers fluorescence since the two groups, the fluorophore and the quencher, are no more close each to the other.

Another example of a trehalose-based probe has been published few years ago by the recent Nobel laureate professor Bertozzi. She, in fact, showed how it was possible to exploit, thanks to an azido modified trehalose, not only the Ag85 pathway of this sugar, but also its recycling pathway to selectively target mycobacteria.[19]

Trehalose glycolipids, which are located in the mycobacterial cell wall, are made in the cytoplasm through metabolic processes involving either glucose or α-glucans (Figure 13).[25] These lipids then combine with mycolic acid to form TMM, which is transported across the plasma membrane by the Mmpl3 complex.[26,27] The Ag85 complex then transfers the mycolate from TMM to either arabinogalactan or another molecule of TMM, forming the foundation of the mycobacterial cell wall. Both processes release a free molecule of trehalose.

Due to the extreme importance of this disaccharide, mycobacteria have developed a recycling system able to recognize and bring back into the cytoplasm the wasted

trehalose molecules. This system is based on the trehalose-specific transporter SugABC-LpqY also called trehalose transporter system.[28] The selectivity of this system is ensured by the LpqY protein (Figure 14).

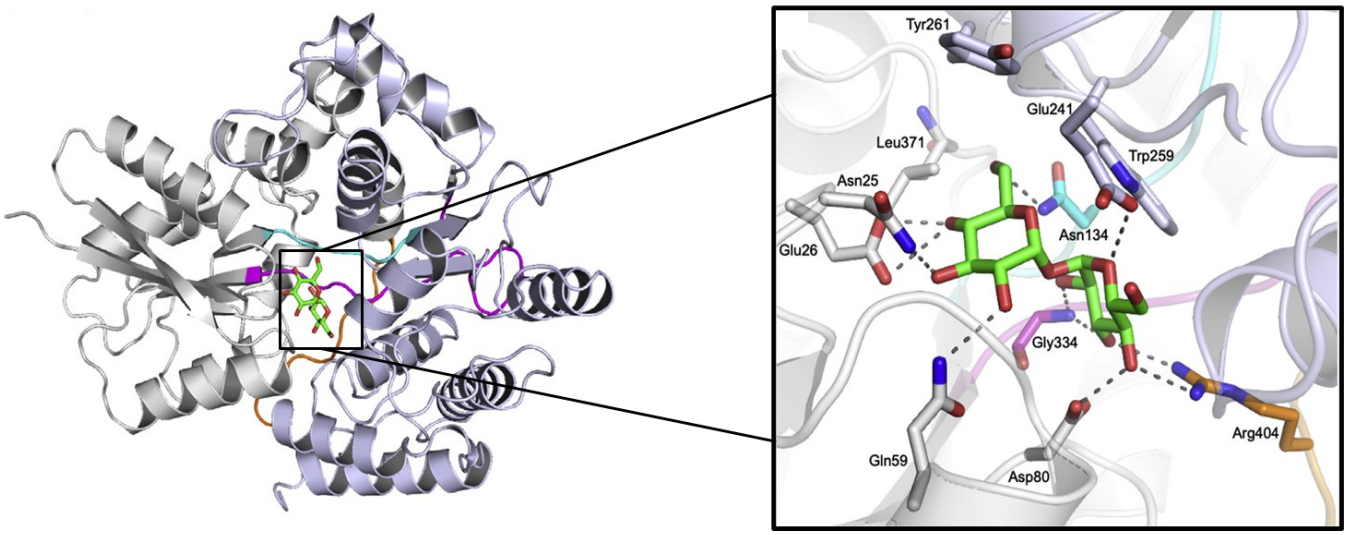

Figure 14: Overall view of the complex of LpqY and trehalose (left), and amplification of the trehalose binding site on Mycobacterium tubercolosys (Mtr) LpqY (right) showing the trehalose and the interacting residues in stick representation.[29]

Here it is possible to see how the disaccharide docks perfectly inside the protein binding pocket. The complex is held together by a strong network of hydrogen bonds. Furthermore, it is worth noting how the sugar is hosted during the binding. While one glucose unit is completely buried inside the cavity, the other sugar unit is placed close to the entrance of the carbohydrate binding pocket. A closer look reveals that the 4 and 6 positions of this latter sugar are the less hindered ones, and therefore are the best ones to use to introduce modifications onto the trehalose backbone.

Professor Fullham, in fact, showed how, despite the high selectivity of this protein towards natural trehalose, some modifications of this disaccharide are well tolerated and lead to carbohydrate-protein complexes of similar stability.[29]

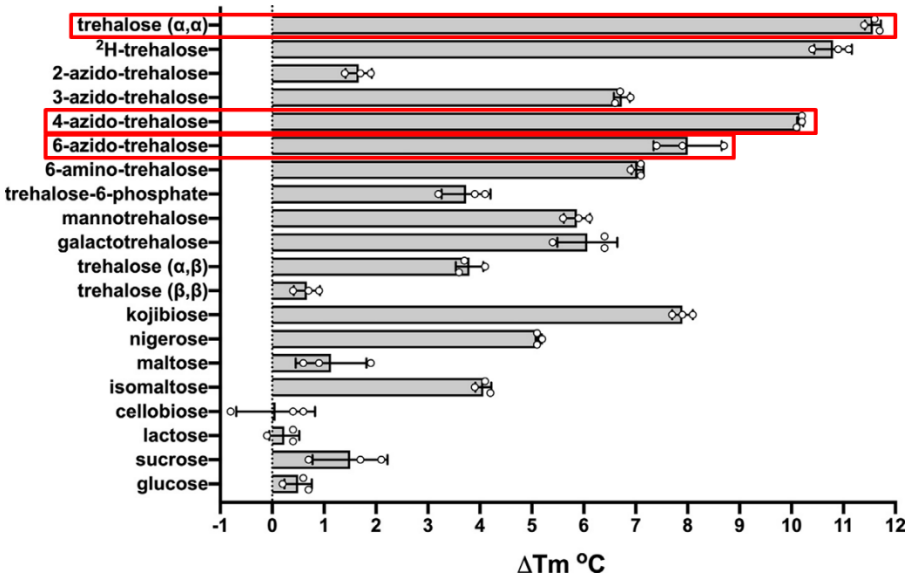

Figure 15: Thermal shift assay investigating a selection of potential ligands for Mtr LpqY. Bar graph showing the ΔTm shift of Mtr LpqY for a series of carbohydrates. Highlighted in red are trehalose and its two best azido analogs.[29]

In particular, it is possible to see in figure 15 how trehalose analogs bearing an azido group either in position 6 or 4 are still able to generate a variation of the complex melting temperature similar to the one produced by trehalose. Furthermore, the 4-azido analog resulted in higher thermal shifts compared to their 6-azido counterpart and this is in accordance with the structure of the LpqY-trehalose complex.

With this background in mind, we decided to develop new trehalose-based ligands capable of interacting with mycobaceteria both for detection and if possible, also as drugs.

To do so we envisaged that calixarenes could have been a valuable molecular scaffold on which synthetize our ligands. In fact, during the years our research group has reported the synthesis and applications of multiple calixarene-base glycoconjugates which revealed to have very interesting properties.[30,31] Therefore, we already had the expertise required for the preparation of new trehalose based calixarenes.

Moreover, we also planned to prepare multivalent trehalose calixarene derivatives. Although it was not yet demonstrated that multivalent might help the recognition of *Mycobacteria,* it could be something new to test and in any case a rebinding mechanism (see Chapter 3) can certainly strengthen the binding. Therefore, we decided to initially synthesized a divalent cone-calix[4]arene functionalized at the upper rim with two units of 6-triazolyl trehalose and bearing at the lower rim either four propyl or four ethoxyethyl chains (Figure 16). The synthesis of the tetrapropoxy scaffold is easier but could incur in solubility problems in highly polar and protic solvents like water, while

the tetra-ethoxyethyl derivative benefits from an increased water solubility but requires more synthetic steps to be obtained.

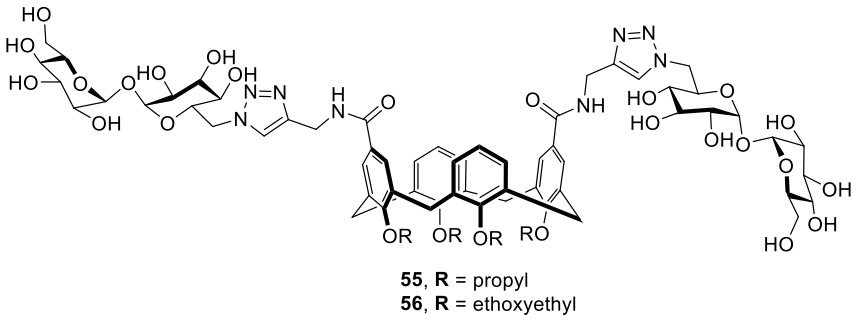

Figure 16: The first two divalent glycocalix[4]arenes synthesized.

We also decided to evaluate how different trehalose modifications could affect the binding process, and since, in theory, the 4-analogs should be even better ligands than 6-derivatized ones, we also prepared compound **57** (Figure 17). Furthermore, in the perspective to verify if multivalence could play a role in the recognition process we also prepared two tetravalent ligands **59** and **60** which are respectively functionalized with multiple copies of 6-azido and 4-azido trehalose (Figure 17), respectively.

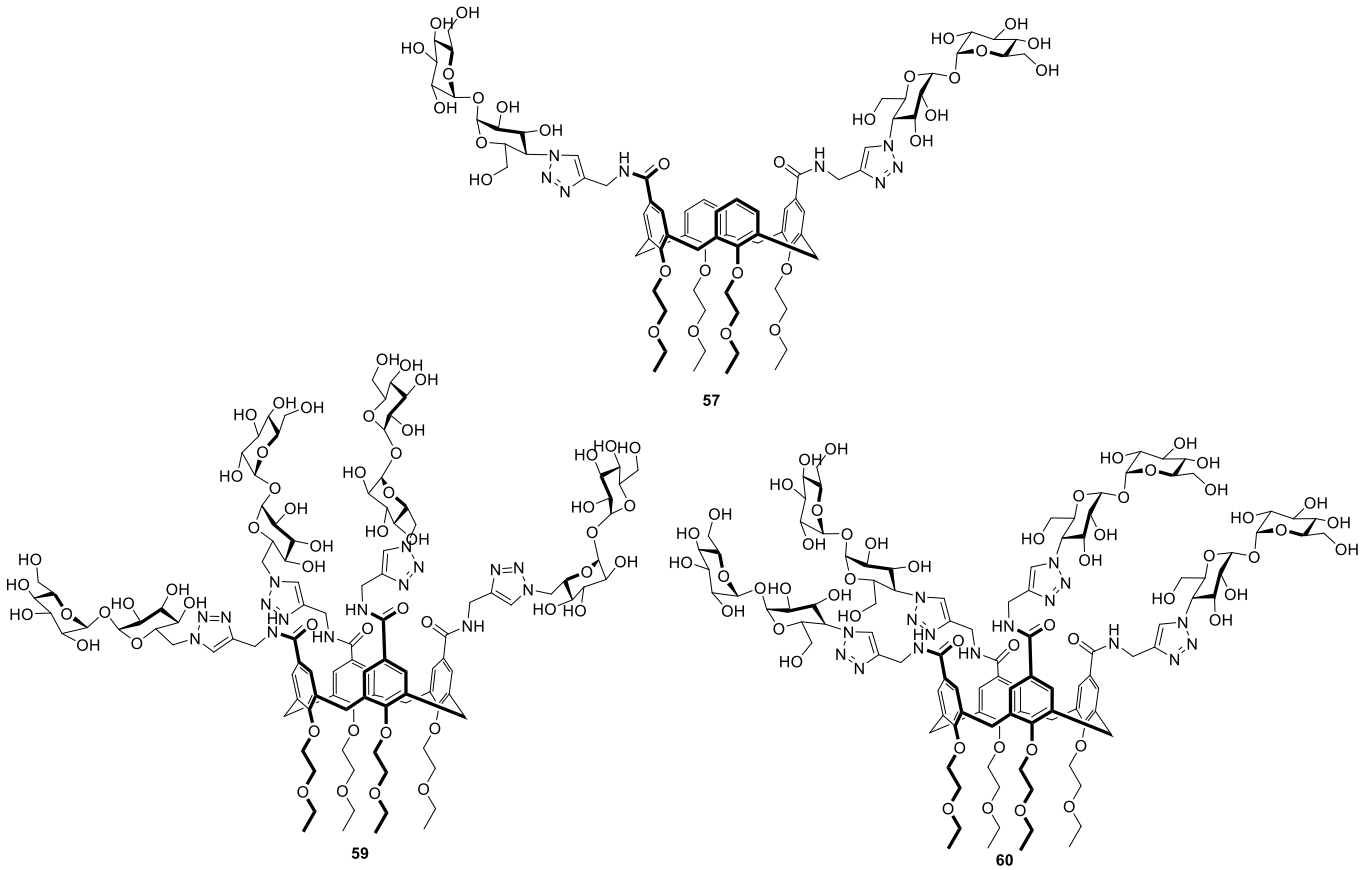

Figure 17: Structure of the other three trehalose-functionalized calixarenes.

2. RESULTS AND DISCUSSION

2.1 Gram-positive Bacteria recognition

In order to obtain the two macrocyclic peptidocalix[4]arenes shown in figure 18, a convergent synthetic strategy was chosen. The pseudopeptide bridge was independently synthesized and then condensed onto the appropriately functionalized calixarene having two dichlorocarbonyl groups in distal positions.

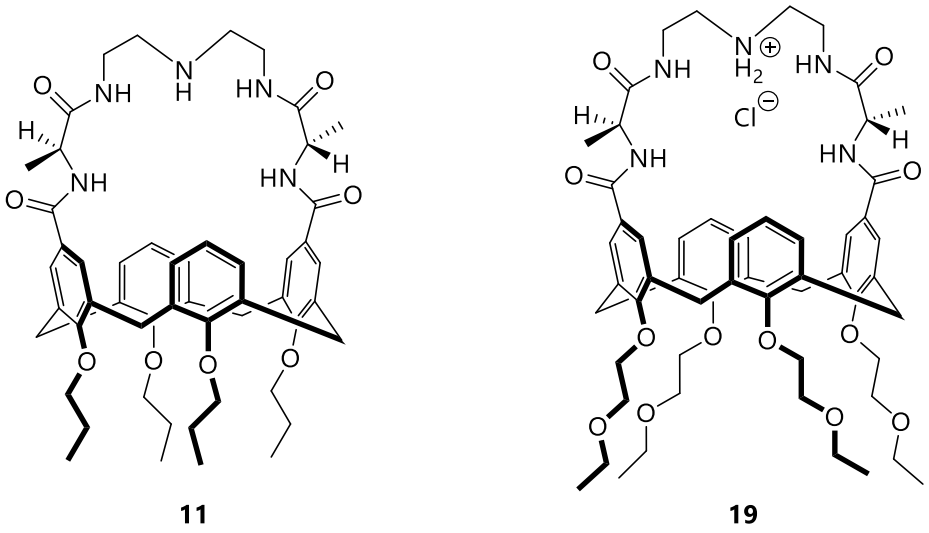

11 **19**

Figure 18: Structure of the two peptidocalix[4]arenes, mimics of vancomycin, synthesized.

2.1.1 Pseudopeptide bridge synthesis

To synthesize the pseudopeptide bridge, diamine **4** had to be condensed with the 1,3-dichlorocarbonyl functionalized calixarenes **9**. The synthetic strategy illustrated in scheme 1 was followed to prepare compound **4**.

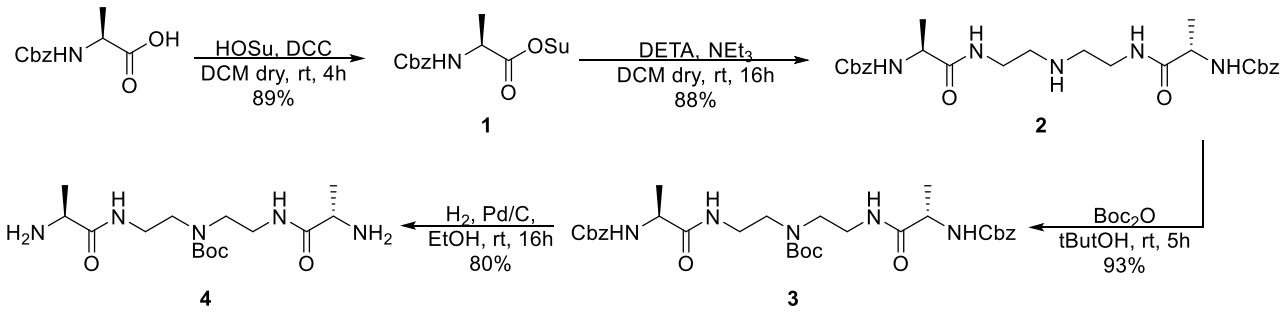

*Scheme 1: Synthesis of compound **4**.*

The synthesis began with L-alanine, whose amino function is protected as a carbamate by the carbobenzyloxy group (Cbz); the first step involved the *in situ* activation of the amino acid carboxy group as an active ester using N,N'-dicyclohexylcarbodiimide (DCC) and N-hydroxysuccinimide (HOSu), obtaining compound **1**.

Subsequently, two equivalents of this derivative were reacted with one equivalent of diethylenetriamine (DETA) in presence of triethylamine, obtaining the difunctionalized product **2**. Here, only the terminal N atoms of DETA were functionalized, thanks to the greater nucleophilicity of these two primary amines. The excellent final yield and purity of the isolated compound **2** (89%) prove that the secondary amine does not react significantly.

The following reaction involved the protection of the secondary amine of compound **2** with a different protecting group, orthogonal to the Cbz. For this task we chose the Boc group. This, in fact, ensured us for the possibility to perform selective deprotection later in the synthesis. The tert-butyloxycarbonyl group (Boc) was introduced using tert-butyl dicarbonate (Boc_2O) in tert-butanol, obtaining the desired compound **3**.

At this point, the two Cbz protecting groups were removed by catalytic hydrogenation; the reaction was carried out in a Parr hydrogenator, at a pressure of 2 atm H_2, using 10% Pd/C as a catalyst. At the end of the reaction, the catalyst was simply removed by filtration. Following these three simple and efficient reactions, the pseudopeptide bridge **4,** which has the central amine protected and the two terminal amine groups free, was easily obtained in 73% overall yield.

The ^1H NMR spectrum in CD_3OD of compound **4** is shown in figure 19: the methyl groups of the two alanines give a doublet at high fields, while the signal of the methine groups of the Cα of the amino acid is shifted to lower fields, around 3.46 ppm. The tert-butyl of the Boc protecting group instead gives a singlet at 1.50 ppm, and the methylenes of diethylenetriamine give a wide multiplet around 3.30 ppm.

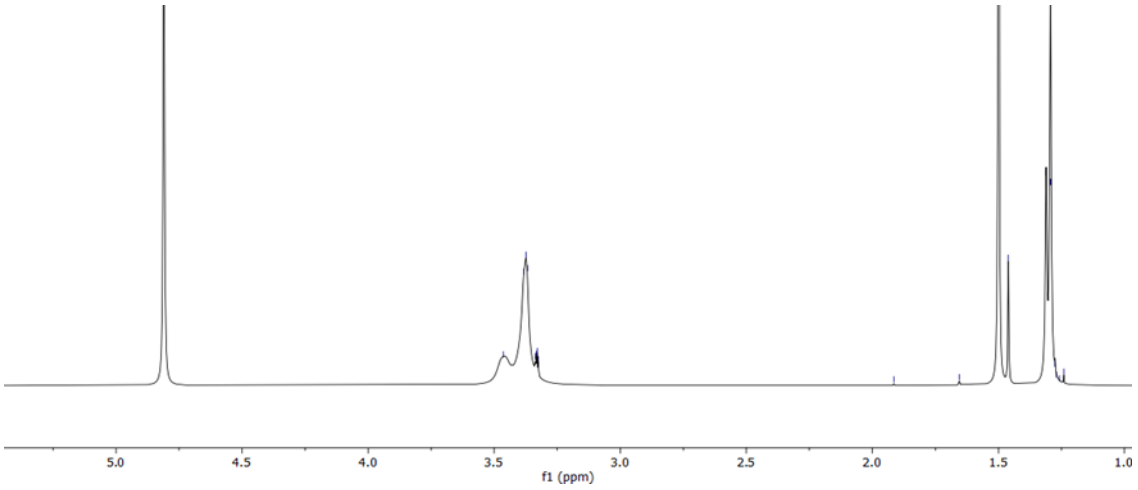

*Figure 19: ^1H NMR spectrum of compound **4** recorded in CD_3OD (400 MHz, 298K).*

2.1.2 Calixarenes synthesis

To obtain the tetrapropoxycalix[4]arene derivative **9**, the synthetic strategy shown in scheme 2 was followed. This led us to the desired compound in six steps starting from tetrahydroxycalix[4]arene.

In this part, a simplified numeration is adopted to identify the aromatic rings of the calix[4]arene according to their relative position. Aromatic rings having a distal relationship are identified as 1,3, while rings in a proximal disposition identified as aromatic nuclei in 1,2.

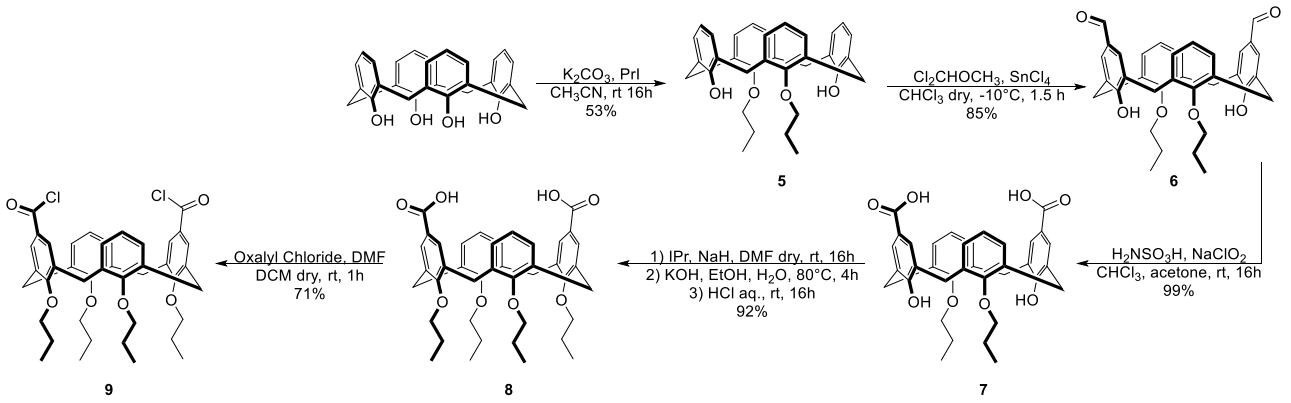

*Scheme 2: Reaction pathway for the synthesis of compound **9**.*

The first reaction involved a lower rim selective alkylation of the tetrahydroxycalix[4]arene. In order to obtain 1,3-dipropoxycalix[4]arene **5**, a weak base, K_2CO_3, and Pr-I, both in slight excess (4.2 equivalents), were used. The dialkylation occurs in successive steps, first by mono-deprotonation of the phenol OH due to the weak base, and then its alkylation. The monoalkyl derivative formed in the reaction environment, is then monodeprotonated again. The more acidic phenolic hydroxyl group, which is the one deprotonated under these weakly basic conditions, is the one in the distal position to the already formed ether group. The higher acidity of the OH group distal to the ether is due to the fact that its conjugated base is stabilized by two intramolecular hydrogen bonds, unlike the anion formed by deprotonation of the hydroxyl in proximal position to the ether group which can be stabilized by only one intramolecular hydrogen bond. The greater stabilization of the first mentioned species ensured the selective functionalization of the calixarene, allowing us to obtain the 1,3-dialkylated product **5** in reasonably high yields.

The following step involved the selective formylation of the para positions on the phenolic, unfunctionalized, rings 2,4. Compound **6** was obtained as the only product, thanks to the greater reactivity of the para positions of the two free OH phenolic rings

compared to those of the corresponding aryl ethers. For this transformation was decided to follow the Gross formylation protocol which employs, as formylating agent, the α,α-dichloro-methylmethyl ether activated by $SnCl_4$.

Subsequently, the oxidation of the two aldehydes to carboxylic acids was carried out using sodium chlorite and sulfamic acid. This last reagent acts as a scavenger of the hypochlorite ion formed in the reaction environment. This ion, in fact, is a stronger oxidizing agent than the chlorite one, and its presence often lead to unwanted overoxidation products.[32]

The diacid **7**, obtained in quantitative yield, was then reacted with 1-iodopropane and NaH to alkylate the two remaining free phenolic groups and lock the calixarene in the cone conformation. The use of NaH in DMF allows the two remaining hydroxy functions to be alkylated while keeping the phenolic rings all pointing in the same direction of the space and the calix[4]arene in the cone conformation. Since the reaction involves an excess (8 equiv.) of base and alkylating agent, the carbonyl functions present at the upper rim, despite being less nucleophilic than the phenolic hydroxyls groups, react, leading to an esterification of one or both carboxy functions.

The crude product of the alkylation reaction, consisting of compound **8** in a mixture with its mono- and diester, was then immediately subjected to a saponification reaction using a 10% solution of KOH in water/ethanol. In this way, after acidification, the two desired carboxy functions were restored. Compound **8** was thus obtained in a 92% overall yield.

The following step involved the activation of the two carboxy functions as acyl chlorides. Compound **8** was reacted with oxalyl chloride in dry DCM using N,N-dimethylformamide as a catalyst. Compound **9** was successfully obtained, and its ^{1}H-NMR spectrum is shown in figure 20.

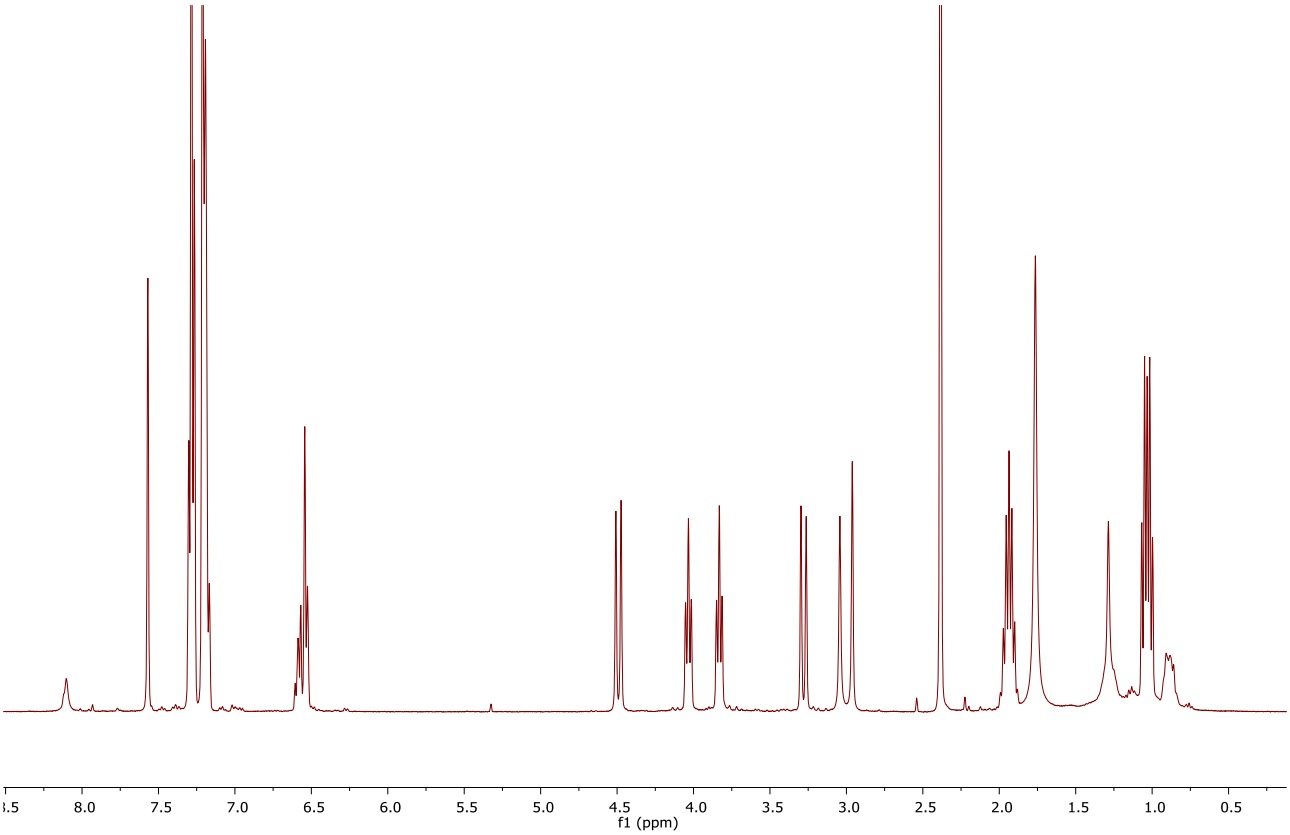

*Figure 20: ^{1}H NMR spectrum of compound **9** in $CDCl_3$ (400 MHz, 298K). The spectrum contains toluene (~2.35 and 7.10-7.30 ppm) and DMF (2.9, 3.1 and 8.1 ppm) as residuals from the reaction and its treatment.*

In the spectrum it is possible to observe the signals related to the protons of the propyl chains at 0.97-1.09, 1.94, 3.83 and 4.03 ppm, which correspond respectively to the methyl and methylene protons. The methylene bridge protons of the calixarene instead give two doublets at 3.28 and 4.52 ppm, while as for the aromatic protons there is a multiplet around 6.5 ppm, which corresponds to the signal of the six protons of the aromatic rings not functionalized at the upper rim, while those in ortho to the chloro-carbonyls give a singlet at 7.57 ppm. In the spectrum there are still present the signals related to the catalyst (s at 2.95, s at 3.04, s at 8.1 ppm) and toluene used for the washing of the reaction crude (s at 2.38 and m at 7.20 and 7.28 ppm), as the product was used immediately in the cyclization reaction.

The following reaction was crucial since it combined the two converging branches of the overall synthesis, and especially because it involved the formation of a macrocycle, which is generally a difficult task. Compound **9** was reacted with pseudopeptide bridge **4** in a condensation reaction, as shown in scheme 3.

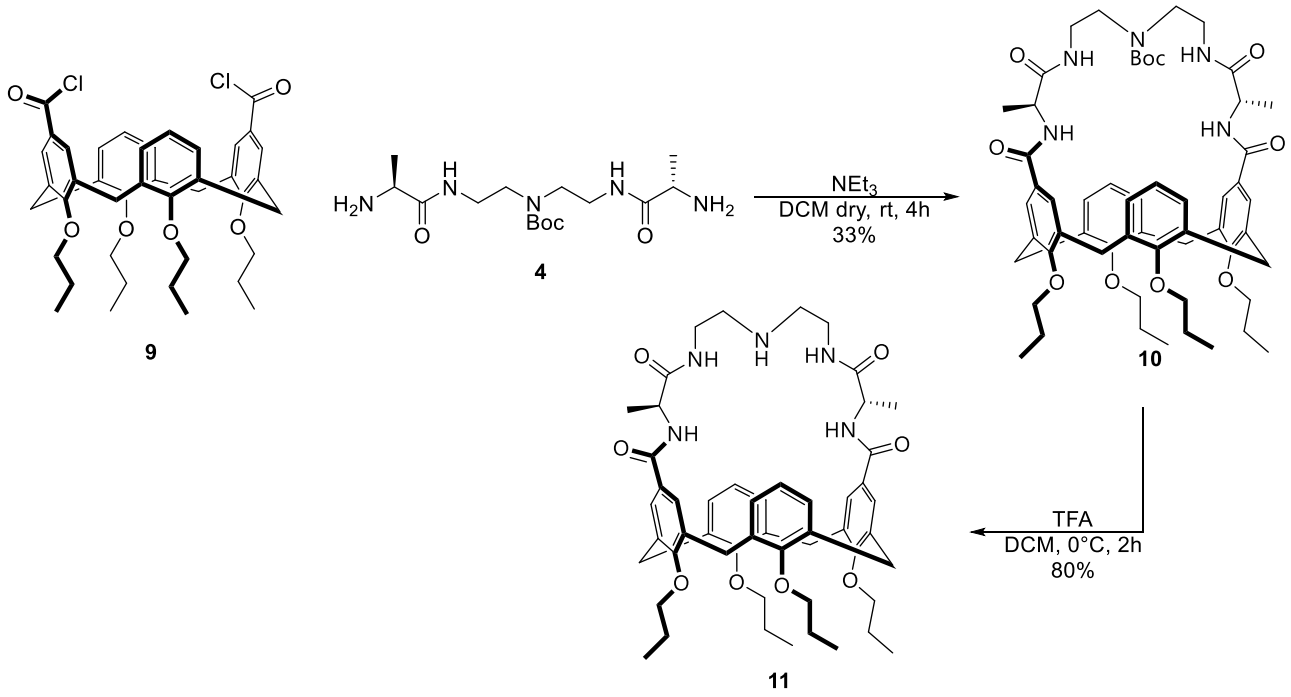

*Scheme 3: Synthesis of **11**.*

The cyclization reaction took place in dry DCM in the presence of triethylamine. To avoid secondary reactions that could have led to polymer formation, it was carried out under high dilution conditions. Two syringes containing the reagents were therefore prepared and their content slowly dripped into a round bottom flask containing the solvent. The concentration of the two reagents in the syringes were 9.3 mM for compound **9** and 10.2 mM for compound **4**, however in the reaction flask, the concentrations were significantly lower and at the end of the dripping, they reached values around 1 mM. Compound **10** was purified by flash chromatography on silica gel, and, despite the difficulties of the reaction and purification, the yield of the isolated product was satisfactory (33%) for a cyclization reaction. The ^{1}H-NMR spectrum of **10** in $CDCl_3$ is shown in figure 21. Comparing the spectrum with that of compound **9**, here it is possible to observe the signal corresponding to the methyl group of the two alanine moieties at high fields, a doublet at 1.36 ppm, while the methine group gives a signal at 4.57 ppm. The methylene groups of diethylentriamine give several broad signals, which partially overlap with the doublet of the equatorial protons of the calixarene methylene bridges. In the low-field region, in addition to the signals corresponding to the aromatic protons of the calixarene, there are broad signals at 6.55, 6.75 and 8.08 ppm, assignable to amide protons. In general, the signals, especially those of the pseudopeptide part of the bridge, are somewhat broad, partly due to the formation of hydrogen bonds, as the spectrum is recorded in $CDCl_3$, and partly due to the existence of structural isomerism around the amide bonds and the carbamate.

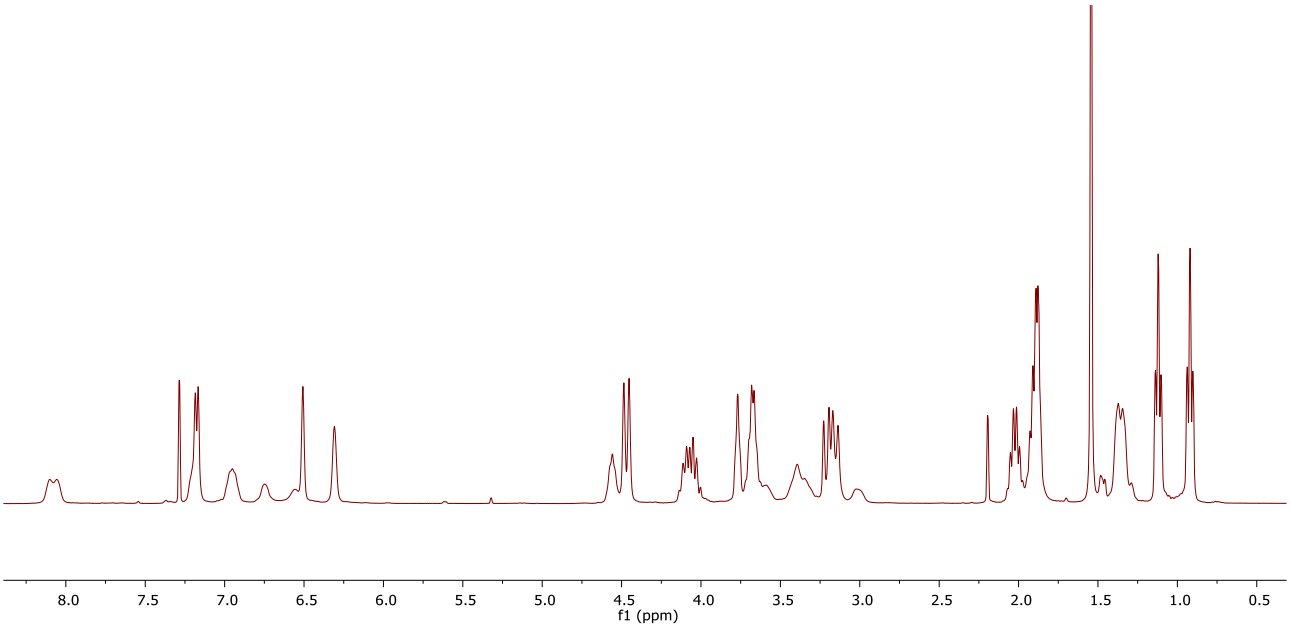

*Figure 21: ^{1}H NMR spectrum of compound **10** in $CDCl_3$ (400 MHz, 298K).*

The final step involved the removal of the Boc protecting group using trifluoroacetic acid. In an acidic environment, the amine function was protonated, and the tert-butyl cation and CO_2 released. The solution was then washed with 1M LiOH until neutrality was reached. In the ^{1}H-NMR spectrum (Figure 22), in addition to the disappearance of the signal corresponding to the tert-butyl protons of Boc, there is a shift to high fields of the methine proton of alanine.

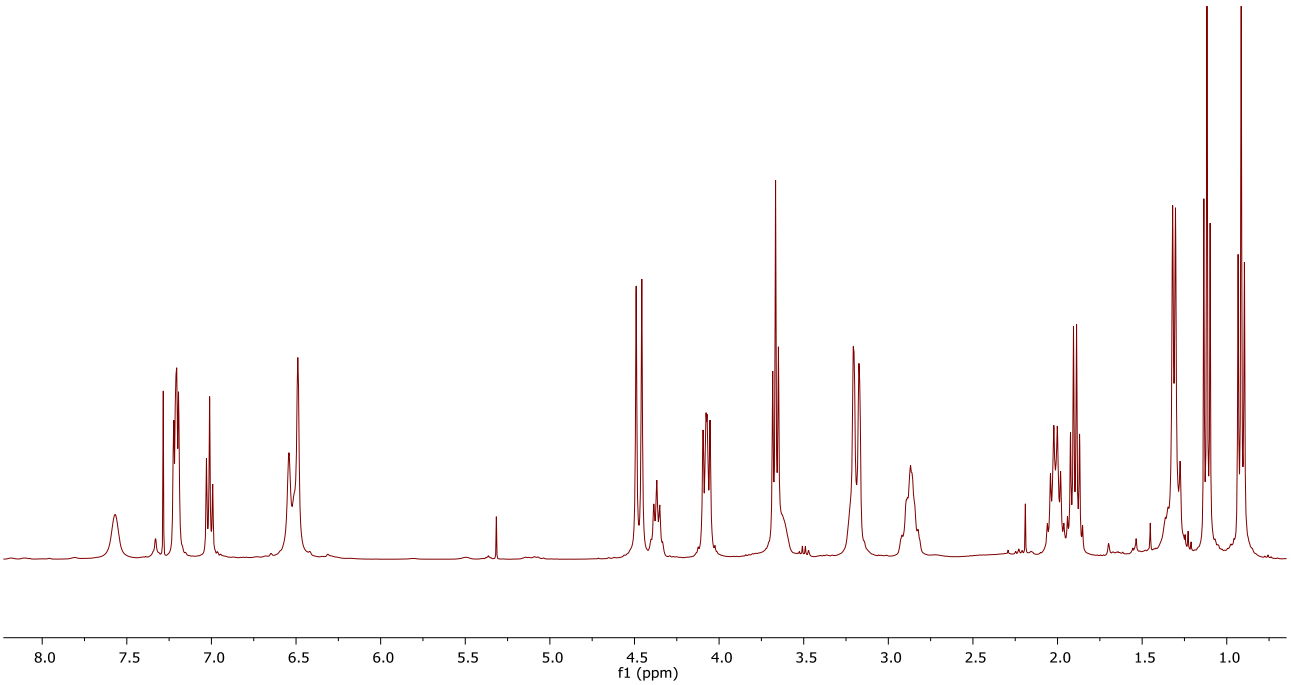

*Figure 22: ^{1}H NMR spectrum of compound **11** in $CDCl_3$ (400 MHz, 298K).*

It is interesting to note that, even if the spectrum has always been recorded in $CDCl_3$ and at room temperature, the signals of **11** are significantly narrower than those of **10**, supporting the hypothesis that the presence of the carbamate in **10** may originate the presence of structural isomerism at the pseudopeptide bridge level.

This compound is soluble in apolar solvents; the propyl chains at the lower rim make the calixarene skeleton very lipophilic while prevent a high solubility in water.

We also implemented the synthesis of the novel and more water-soluble version (**19**) of the peptidocalix[4]arene **11**, in order to carry out binding studies and biological assays in aqueous environment, which although more challenging and competitive, resembles best the conditions that will have to be used for bacteria interaction. To have a proper solubility in water, we decided to introduce more hydrophilic, like ethoxyethyl chains, chains at the lower rim. However, even if the new compound **19** is very similar to the previously prepared compound **11**, we had to plan a new synthetic route for this derivative. The new strategy showed some significant differences and difficulties, that will be highlighted in the following of this chapter.

To obtain compound **17**, the synthetic strategy illustrated in scheme 4 was followed.

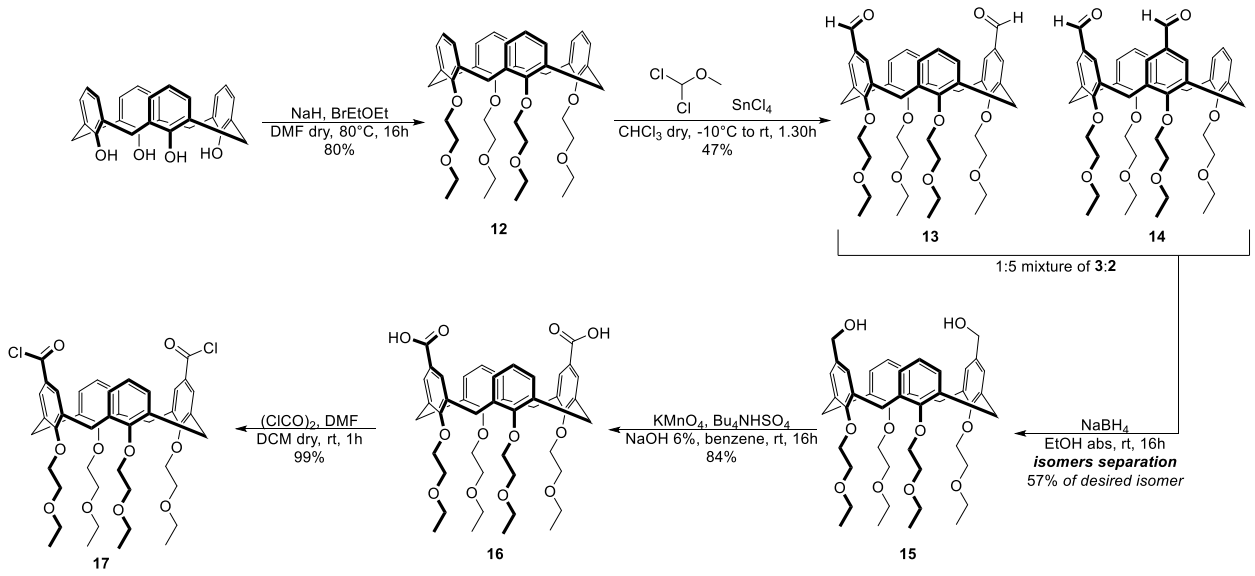

*Scheme 4: Reaction pathway for the synthesis of compound **17**.*

The starting reagent is tetrahydroxycalix[4]arene. The synthetic pathway adopted in this case is significantly different from that of scheme 2. While for propyl derivatives, selective functionalization at the lower rim and transfer of this 1,3 selectivity to the upper rim with formylation reaction was possible, in the case of ethoxyethyl derivatives, this strategy had not previously led to satisfactory results. In this case, it was known that it

was possible to obtain, although with some problems, the 1,3-diacid (**16**) starting from tetra-ethoxyethylcalix[4]arene **12** via upper rim formylation. The first reaction of this synthesis consisted in a tetraalkylation at the lower rim, using NaH and 1-bromo-2-ethoxyethane.

The following step involved the upper rim diformylation in order to obtain the distal 1,3-diformylated derivative. Gross formylation was used also in this case, but unlike compound **6**, where the functionalization at the lower rim of the reagent induced total selectivity at the upper rim, here, the parameters that had to be optimized to ensure the correct regioselectivity were temperature, catalyst, and equivalent of formylating agent. As reported in literature, in order to obtain the diformylated derivative, $SnCl_4$ was used as a catalyst and the reaction was carried out in chloroform at -10°C.[33] Despite the conditions reported in the literature, however, purification of the crude by flash chromatography led to the isolation of a mixture of 1,3- and 1,2-diformylcalix[4]arenes (**13** and **14**, respectively), the ^{1}H-NMR spectrum of which is shown in figure 23.

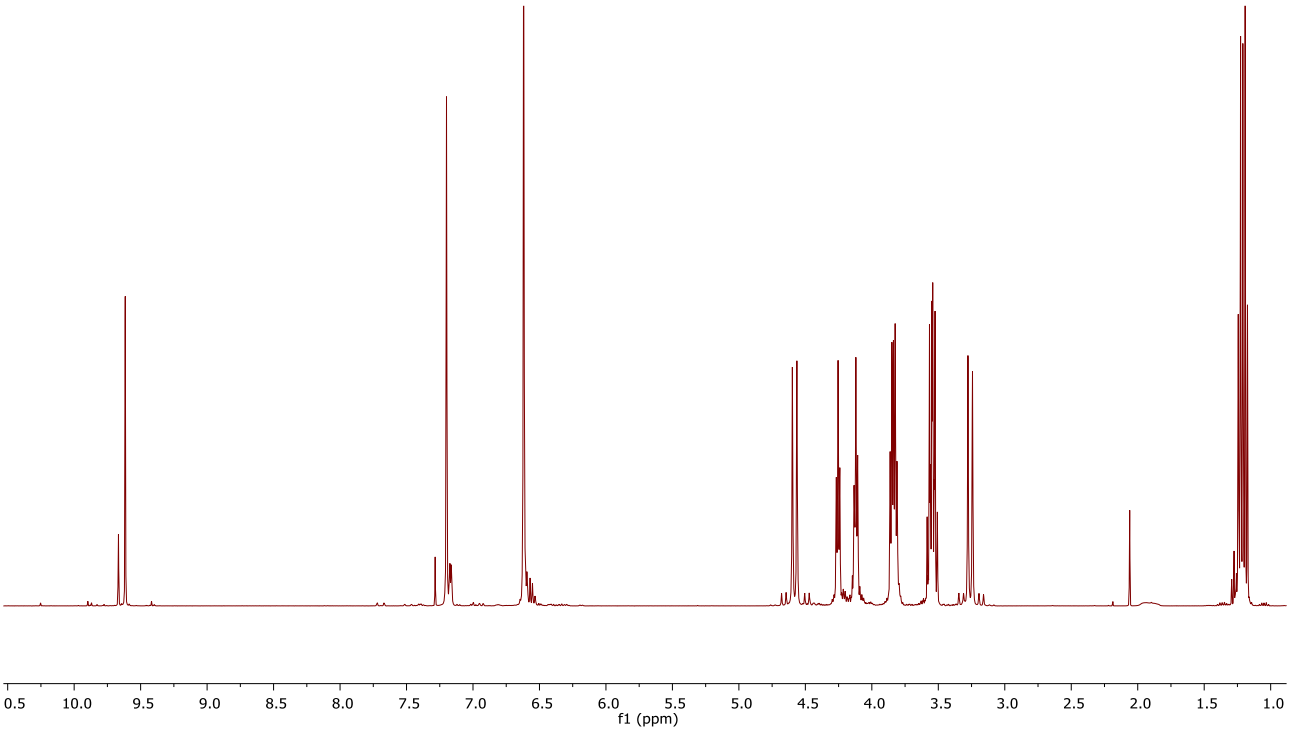

*Figure 23: ^{1}H NMR spectrum of the mixture of 1,2-diformylcalix[4]arene (**14**), minor isomer, and 1,3-diformylcalix[4]arenes (**13**), major isomer.*

The ^{1}H-NMR spectrum indeed shows two signals at 9.67 and 9.62 ppm, which are the formyl protons of the two different species. From this, we could estimate a 1:5 ratio between the two isomers, but this signal alone does not allow us to understand which is the predominant product between 1,2- and 1,3-diformyl derivatives. However, this information can be inferred from the signals of the $ArCH_2Ar$ protons, H_{ax}, and H_{eq},

respectively around 4.6 and 3.2 ppm. In fact, it is possible to observe a clear prevalence of the 1,3-difunctionalized isomer, which gives two intense doublets, while it can be noted, with a much lower intensity, the typical pattern of signals, three doublets with intensity 1:2:1, of the protons of the methylene bridges of the 1,2-diformylcalix[4]arene, partly superimposed with those of compound **13**. From this data, it is therefore possible to establish that the 1:5 ratio between the two 1,2-/1,3-diformyl isomers in the sample is in favor of the 1,3-diformylcalix[4]arene.

The two compounds, however, are no longer separable through flash chromatography, as they have the same retention factor in various eluents, so, as suggested in literature, the mixture of regioisomers was separated only after reduction to the corresponding dialcohols.[34] The mixture of compounds **13** and **14** was reduced using $NaBH_4$ in ethanol. The two alcohol compounds were easily separated and compound **15**, functionalized on the 1,3-distal rings, was obtained pure after flash chromatography on silica gel. The ^{1}H-NMR spectra of the two dialcoholcalix[4]arenes are shown in figure 24 and figure 25. Contrary to what is observed for the diformyls, in the case of the two isomeric dialcohols, the NMR spectra are very similar to each other. The assignment of the structure of the two samples was done analogously to what is reported in the literature.[34] It is interesting to note, in fact, that even in the case of 1,2-dialcoholcalix[4]arene (Figure 25), the signals do not show the expected multiplicity: for example, for the $ArCH_2Ar$ group protons, a single doublet is observed for the axial and another single doublet for the equatorial protons, when one could expect three doublets for the one and three doublets for the other in a 1:2:1 ratio, as previously observed for the 1,2-diformyl derivative.

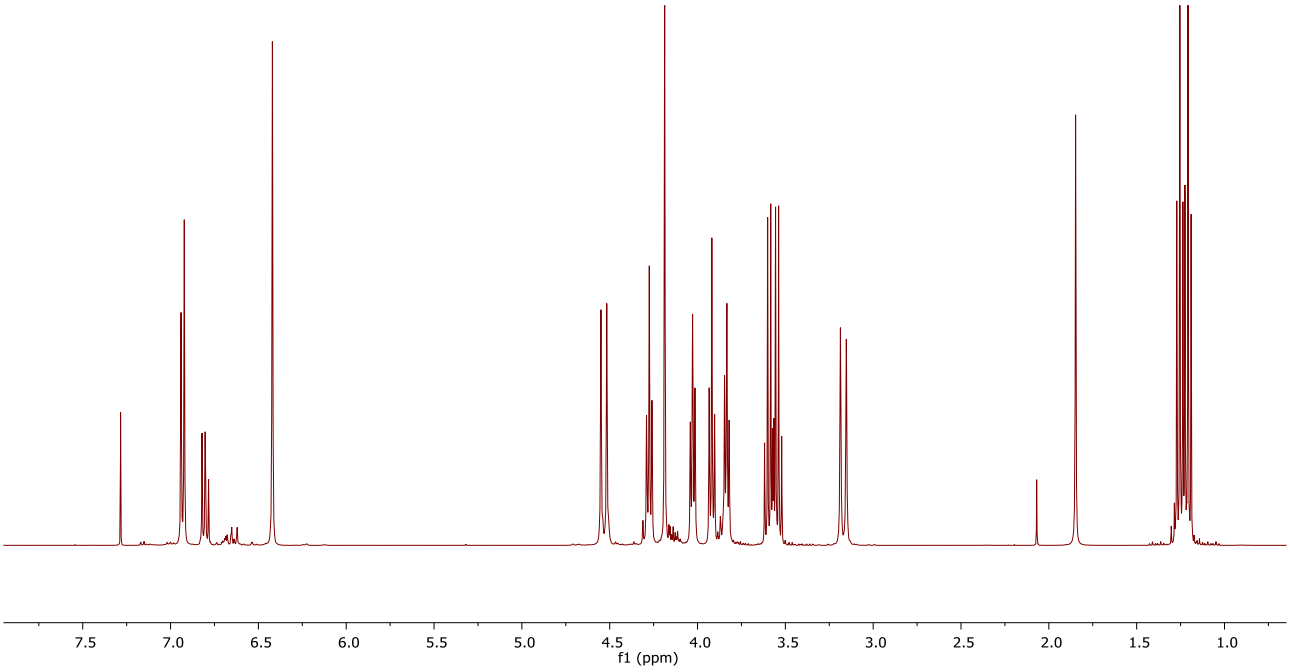

*Figure 24: ^{1}H NMR spectrum of 1,3-dialcoholcalix[4]arene **15** in $CDCl_3$ (400 MHz, 298K).*

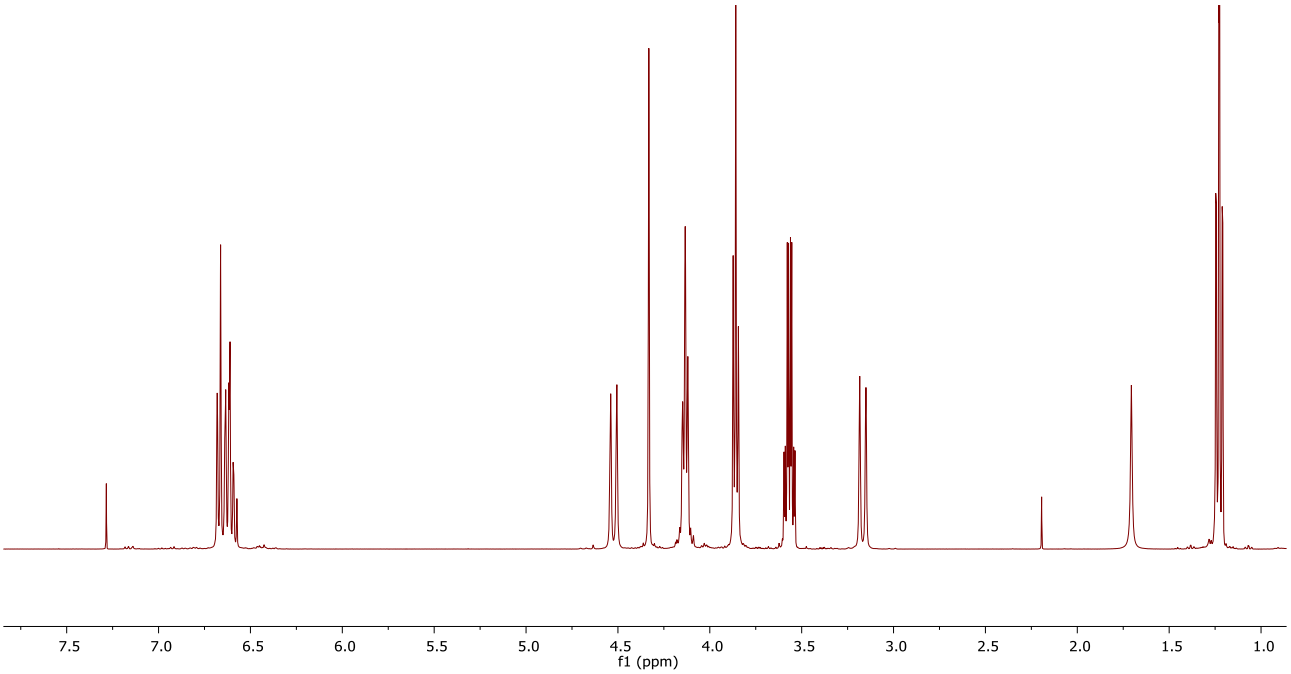

Figure 25: ^{1}H NMR spectrum of 1,2 dialcoholcalix[4]arene in $CDCl_3$ (400 MHz, 298K)

The careful analysis and comparison of the spectra, however, makes it clear that 1,3-dialcohol is the compound of the spectrum in figure 24. This derivative, in fact, has a flattened cone structure, with a C_{2v} symmetry with the aromatics bearing the CH_2OH group almost parallel to each other, probably also due to the establishment of an intramolecular H bond between the alcoholic hydroxyls in $CDCl_3$. This causes a high field resonance of the signals of the ArH nuclei bearing the CH_2OH groups falling these protons in the shielding cone of the other two (unsubstituted) ArH nuclei. The flattened cone also causes a greater differentiation of the signals of the ethoxyethyl chains at the lower rim. In the 1,2-dialcohol derivative of figure 25, on the other hand, the calixarene assumes a more regular cone structure due to its inability to form intramolecular H bonds, as evidenced by the presence of all signals clustered at 6.7-6.5 ppm for the aromatics and the presence of unique signals (two triplets, a quartet and another triplet) for the ethoxyethyl groups.

The following reaction consisted in the oxidation of the alcoholic functions to carboxylic acids; for this reason, potassium permanganate was used as the oxidizing agent. The reaction was carried out in a biphasic environment, consisting of benzene and an aqueous solution of NaOH 6% and $KMnO_4$. $Bu_4N^+HSO_4^-$ was used as the phase transfer agent.

Compound **16** was then reacted with oxalyl chloride in dry DCM in the presence of DMF as a catalyst, analogously to what was done on the propylated calixarene **8**. The ^{1}H-NMR spectrum of the acyl chloride **17** is shown in figure 26.

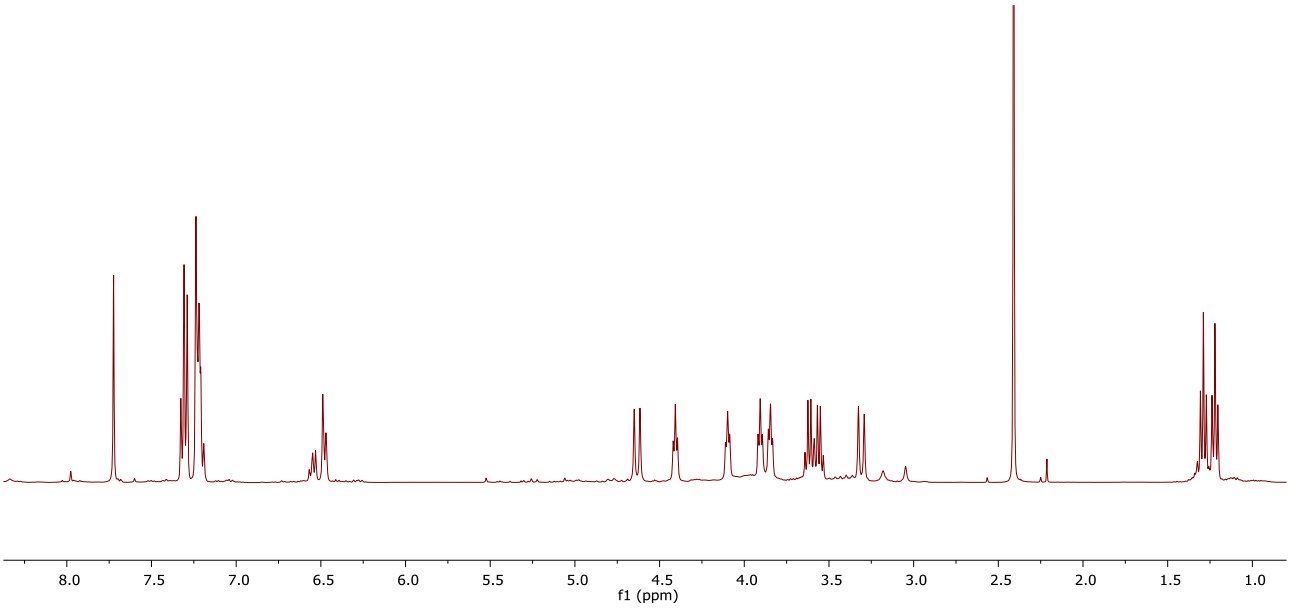

*Figure 26: ^{1}H NMR spectrum of compound **17** in $CDCl_3$ (400 MHz, 298K).*

In the ^{1}H NMR spectrum, the presence of two triplets at high fields, corresponding to the protons of the methyl groups, can be observed. The signals of the methylene chain of the ethoxyethyl chain are instead located between the two doublets at 3.31 and 4.63 ppm, that are the signals of the bridging methylenes. In the aromatic region can be observed the signals of the aromatic protons of the unfunctionalized rings around 6.50 ppm while at 7.72, the signal of the aromatic protons in ortho to the chlorocarbonyl, as already observed for compound **9**. In this case too, the signals of toluene (s at 2.40 and m at 7.23 and 7.30 ppm), added during purification procedures, are visible in the spectrum.

Calixarene derivative **17** was then condensed with the peptide segment previously used, as reported in scheme 5.

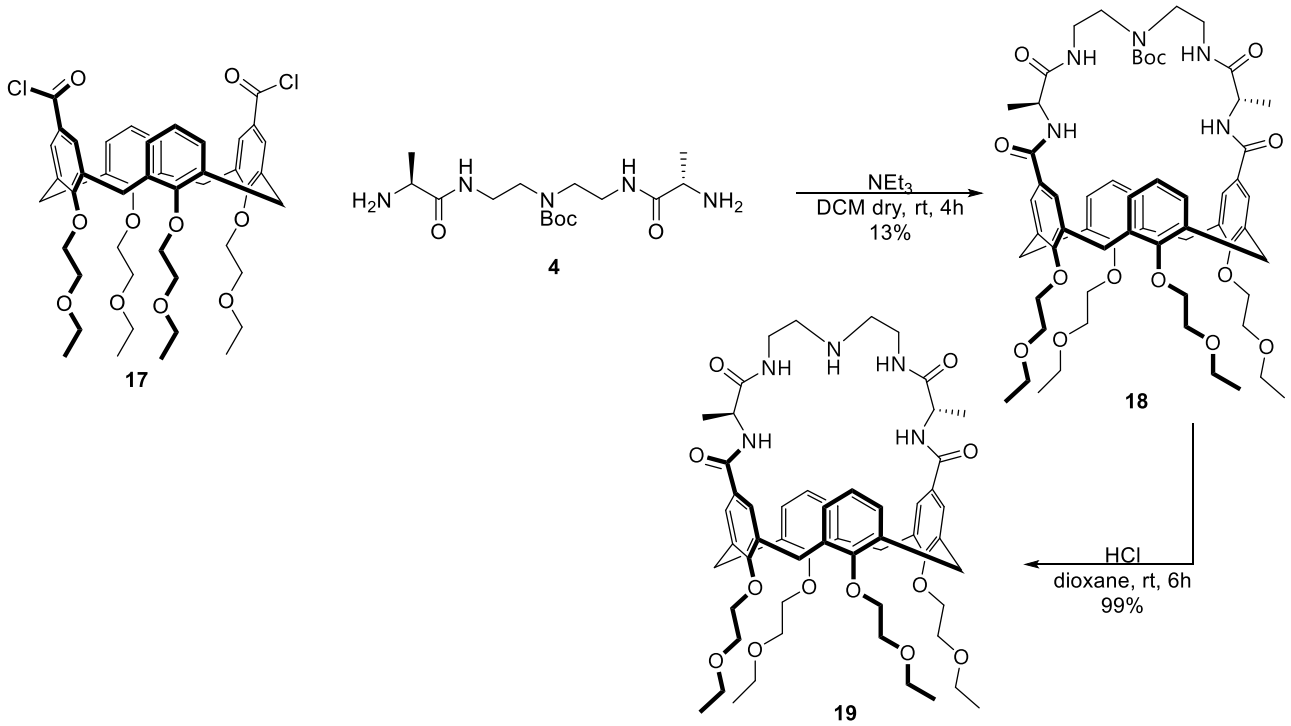

*Scheme 5: Preparation of compound **19**.*

The cyclization reaction was carried out following the procedure used to obtain compound **18**. The conditions of high dilution obtained by preparing the two syringes at a concentration of 17 mM for compound **17** and 21 mM for compound **4**, in 20 mL of total volume, and dripping them into a flask containing 160 mL of solvent (dry DCM); in this way, the concentration in the round-bottom flask at the end of dripping phase is around 2 mM. Compound **19** was also purified by flash chromatography on silica and its ^{1}H-NMR spectrum is shown in figure 27. In this case, however, the yield (13%) was significantly lower compared to the 33% obtained for compound **10**. 2+2 cyclization or polymerization products can obviously be byproducts, but they have not been isolated and characterized so far, so it is not clear why there was a drop in yield compared to **10**. The reaction was carried out only once and it will be necessary to optimize its conditions to enhance the yield in the future if more than a few milligrams of compound **19** will be needed.

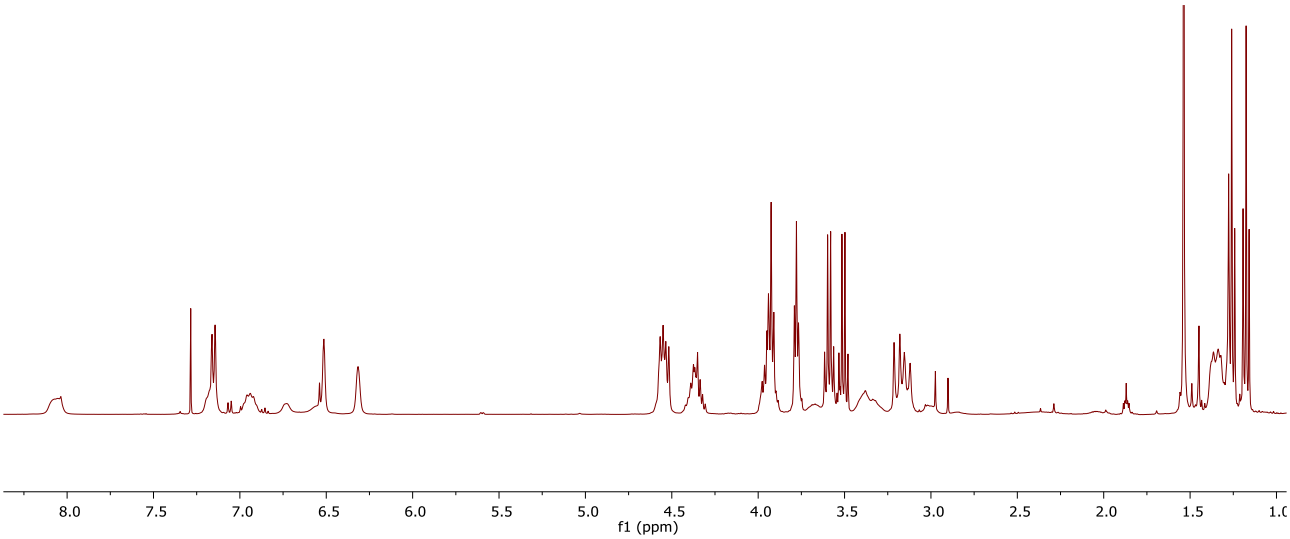

*Figure 27: ^{1}H NMR spectrum of compound **18** in $CDCl_3$ (400 MHz, 298K).*

The spectrum of compound **18**, excluding the signals of protons belonging to the ethoxyethyl chains, is very similar to that recorded for compound **10**. In this case too, the signals of the methyl and methine protons, this time partially superimposed to the axial protons of the bridging methylenes, of the two alanines and those corresponding to the methylenes of diethylenetriamine and amide protons appear in the spectrum after the reaction. Also, in this case the spectrum in $CDCl_3$ is rather broad especially for the signals of the pseudo-peptide bridge.

For the deprotection step from the Boc group, 37% hydrochloric acid was chosen this time, because, given the supposed water solubility, basic washes to restore neutrality and the tedious procedure of exchanging the triflate anion with the chloride had to be avoided. The presence of the triflate anion would be discouraged in the final product because it could interact more strongly with the ammonium salt on the pseudo-peptide bridge, perhaps also occupying the cavity of the macrocycle and thus presumably hindering the interaction with the peptidoglycan mimic in binding studies. Compound **19** was purified by trituration in diethyl ether and the corresponding ^{1}H-NMR spectrum is shown in figure 28.

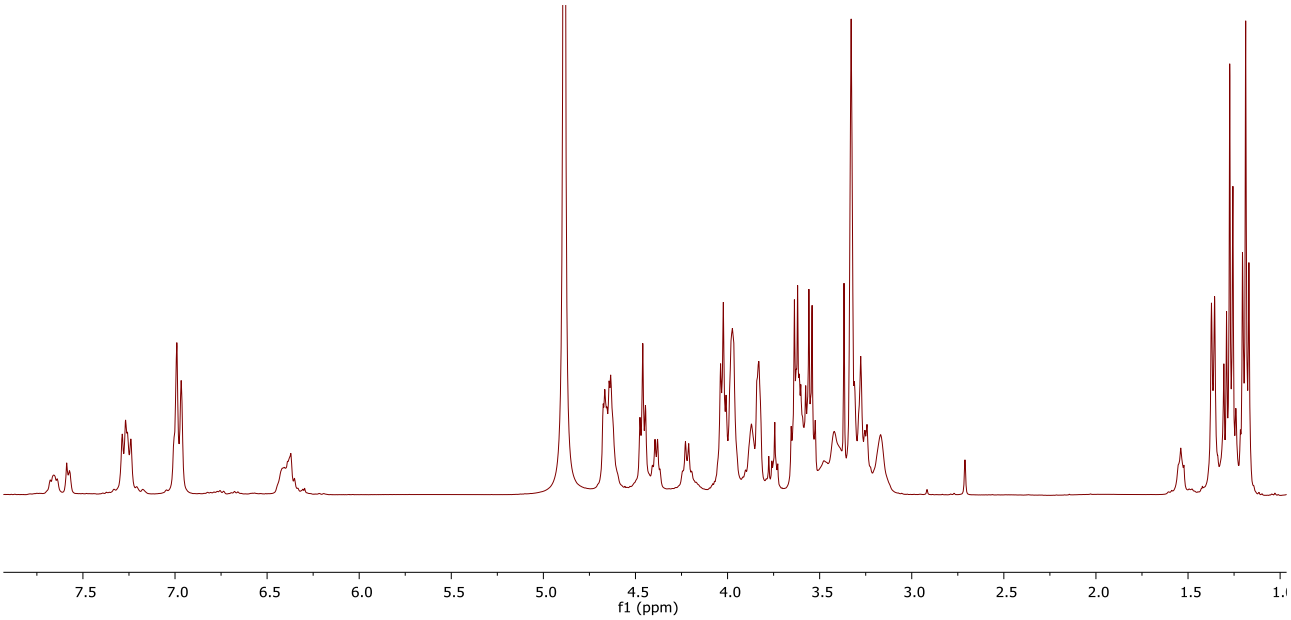

*Figure 28: ^{1}H NMR spectrum of compound **19** in CD_3OD (400 MHz, 298K)*

As in compound **11**, the spectrum of the deprotected macrocyclic compound shows narrower peaks, the disappearance of the signal corresponding to the Boc protons and the shift to high fields of the methine proton of alanine. In this case, the spectrum was recorded in deuterated methanol due to the increased polarity of the compound, acquired thanks to functionalization with the ethoxyethyl chains.

Solubility studies were carried out to verify whether the presence of ethoxyethyl chains instead of propyl chains at the lower rim is really sufficient to make receptor **19** soluble in water. Solubility in water at concentrations up to 2 mM was actually observed and at this concentration the ^{1}H-NMR spectrum (Figure 29) was recorded in deuterated water.

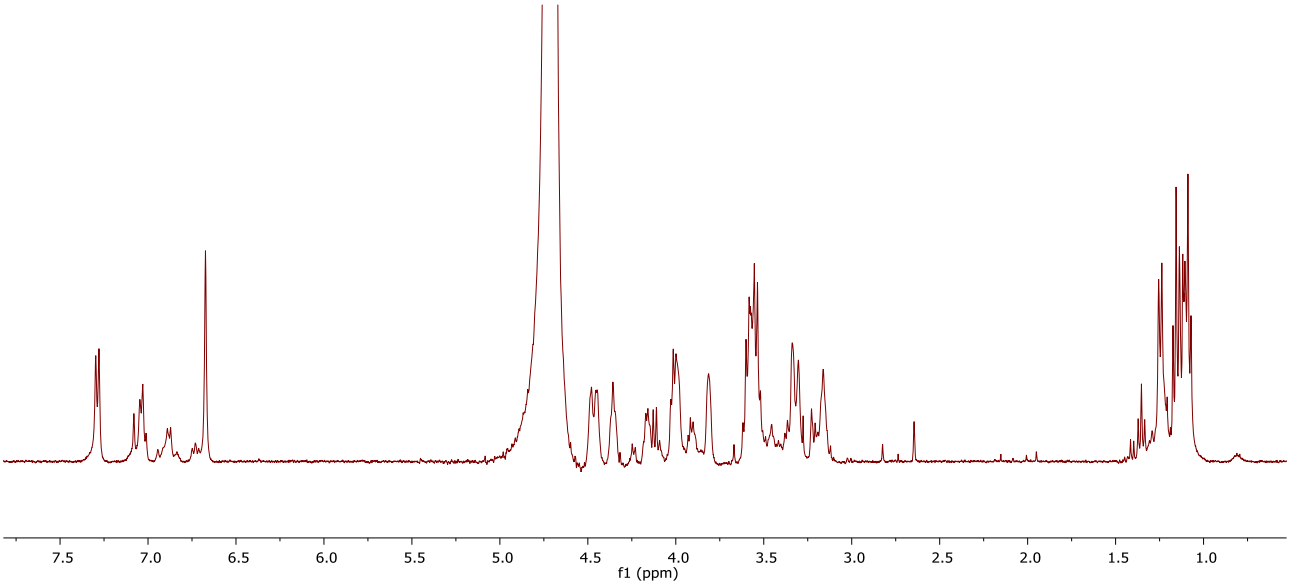

*Figure 29: ^{1}H NMR spectrum of compound **19** in D_2O (2 mM, 400 MHz, 298K).*

2.1.3 Preliminary studies of complexing properties

As mentioned in the introduction, receptors **11** and **19** were synthesized for their potential complexing properties towards the cell wall of Gram-positive bacteria, in particular towards the amino acid chain of peptidoglycan. To verify the formation of the complex, preliminary studies were conducted using two simplified models of peptidoglycan, i.e, N-Ac-D-ala-D-ala and N-Ac-L-lys-D-ala-D-ala (Figure 30).

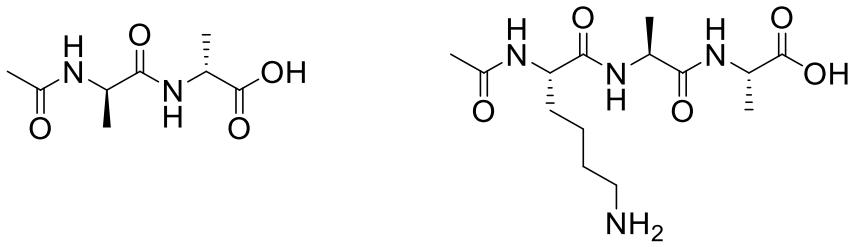

Figure 30: Guests used is the complexation experiments.

NMR is an extremely sensitive technique to chemical environment variations and therefore it allows to follow the shift of the proton signals of the receptor and/or ligand upon complexation. In the case of fast exchange on the NMR time-scale, it is also possible to evaluate the complexation constant through non-linear regressions of one or more of the proton signals in function of the receptor/substrate ratio and concentration changes. Usually, more sensitive are those protons of the receptor/ligand which are involved in the interaction or close to the region of interaction between the two partners.[35]

For receptor **11**, complexation studies had already been conducted in $CDCl_3$, using N-Ac-D-ala-D-ala as the guest.[10] The dipeptide, however, was not soluble in the chosen apolar solvent, so solid-liquid extraction experiments were also carried out. The guest was suspended in $CDCl_3$ and the calixarene receptor was added in equimolar quantities, leading to the formation of the complex and the consequent transfer of the dipeptide into solution. NMR analysis confirmed the formation of a 1:1 stoichiometry complex; the interaction between the guest and the receptor led to a change in the chemical shift of several proton signals of the macrocycle, including the amine and methylene protons of the diethylenetriamine and the amide protons of alanine. These signals underwent a shift to lower fields, indicating the formation of electrostatic interactions and/or hydrogen bonding between the two molecules. To quantitatively evaluate the receptor affinity for D-ala-D-ala, NMR experiments were carried out in homogeneous phase using N-lauroyl-D-ala-D-ala, which is soluble in chloroform due to the long fatty acid chain. These complexation studies were also extended to more polar solvents (CD_3OD) or combination of solvents ($CDCl_3$+2/10%DMSO-d_6), showing a general drop of binding

affinity compared to dry $CDCl_3$.[36] Receptor **11**, however, due to its insolubility in water could not never be tested under physiological conditions.

The receptor **19**, after being characterized in terms of structure, was studied to evaluate its complexing properties in solution towards two models of peptidoglycan, N-Ac-D-ala-D-ala and N-Ac-L-lys-D-ala-D-ala. Given its solubility in water, initially the ^{1}H-NMR analyses were carried out in D_2O, at an initial concentration of host (compound **19**) equal to 2mM, with successive additions of increasing volumes of a D_2O solution of guest prepared at 25 mM. The NMR experiments were recorded with both guests, but no significant changes in the signals were observed for either the host or the guest that could confirm the formation of the complex between the two molecules.

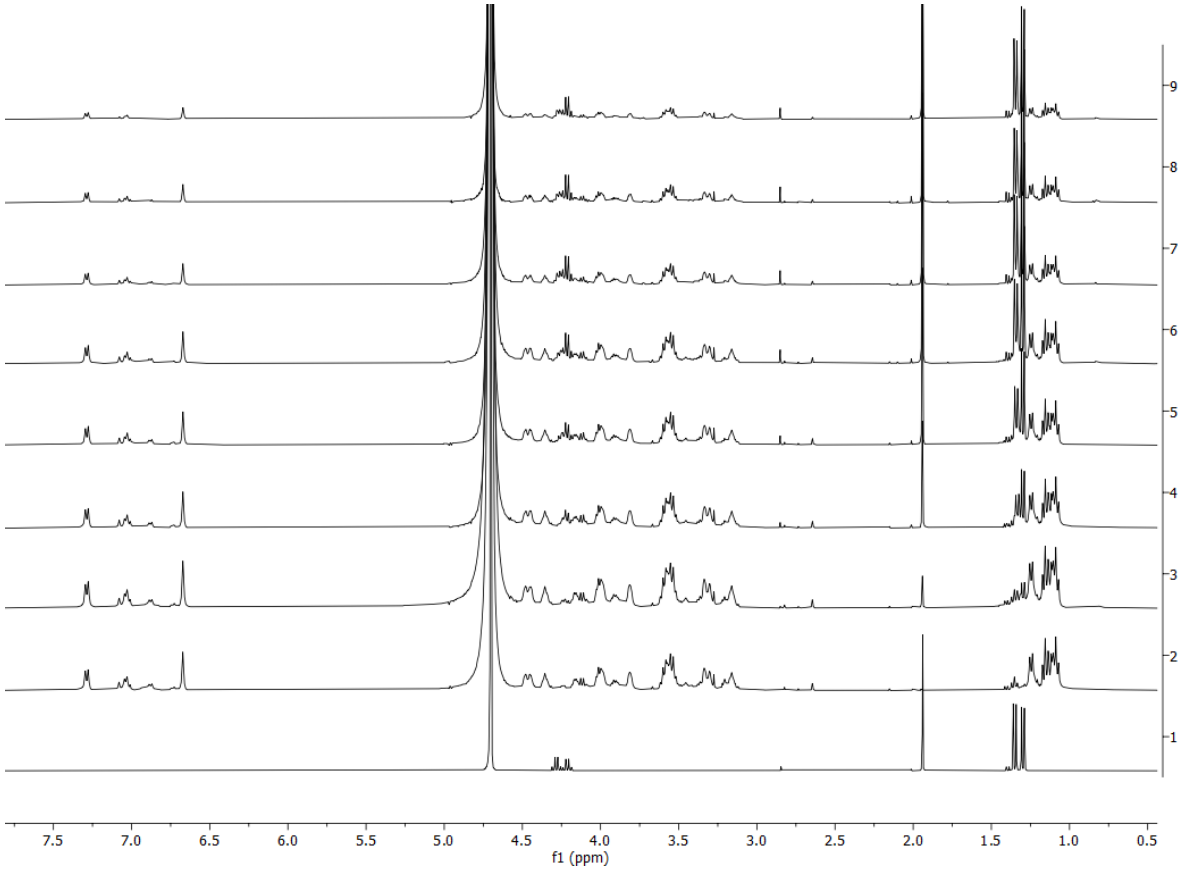

*Figure 31: From the bottom: Spectrum of N-Ac-D-ala-D-ala (trace 1), spectrum of compound **19** (trace 2), and spectra of **19** with increasing concentrations of guest (traces 3-9). All the spectra were recorded in D_2O (400 MHz, 298K)*

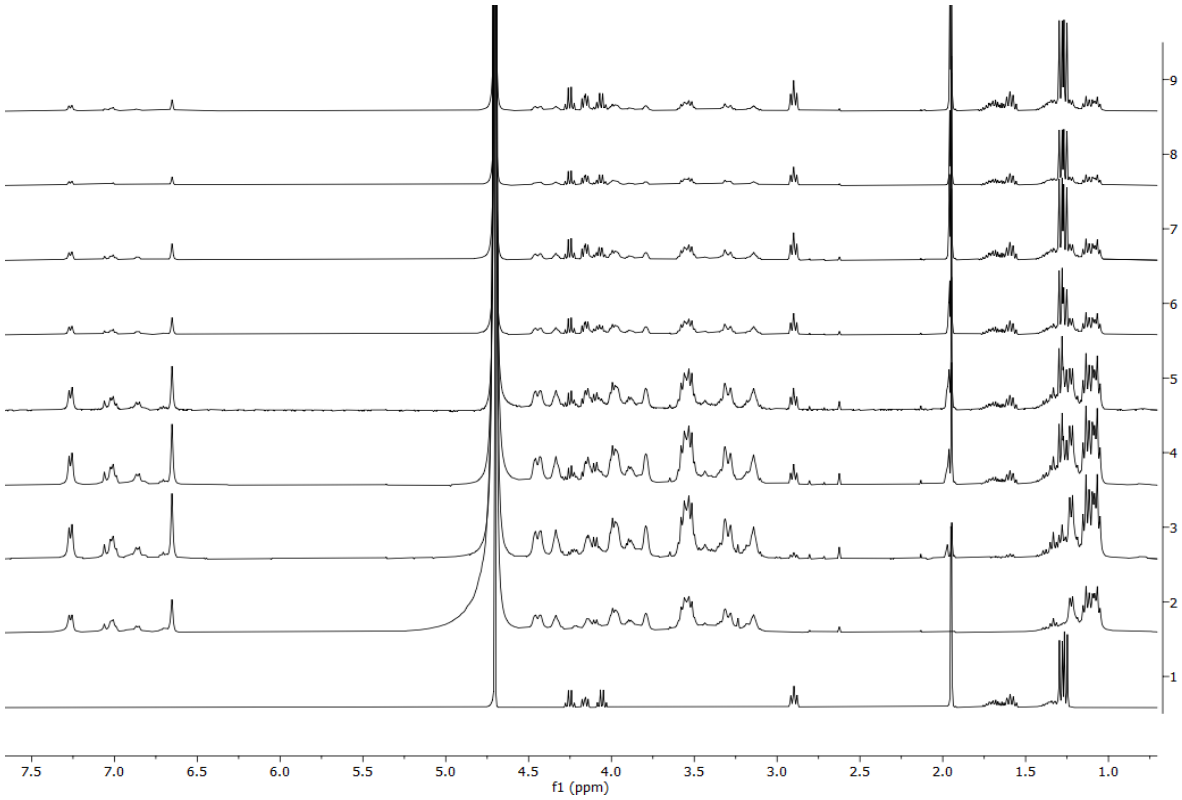

*Figure 32: From the bottom: Spectrum of N-Ac-L-Lys-D-ala-D-ala (trace 1), spectrum of compound **19** (trace 2) and spectra of **19** with increasing concentrations of guest (traces 3-9). All the spectra were recorded in D_2O (400 MHz, 298K)*

The obtained spectra (Figure 31 and Figure 32) are the simple overlap of the NMR spectra of the two species taken individually.

The absence of interaction can be explained by the fact that the solvent used is polar and protic and can strongly compete with the substrate in forming hydrogen bonds with the binding sites of the peptidocalixarene, and therefore can make the complexation of the dipeptide energetically unfavorable. Another attempt at complexation in deuterated methanol, slightly less polar than D_2O, was made using N-Ac-D-ala-D-ala as the guest, given its solubility in the organic solvent, but no appreciable changes in the proton signals were observed in this case either (Figure 33).

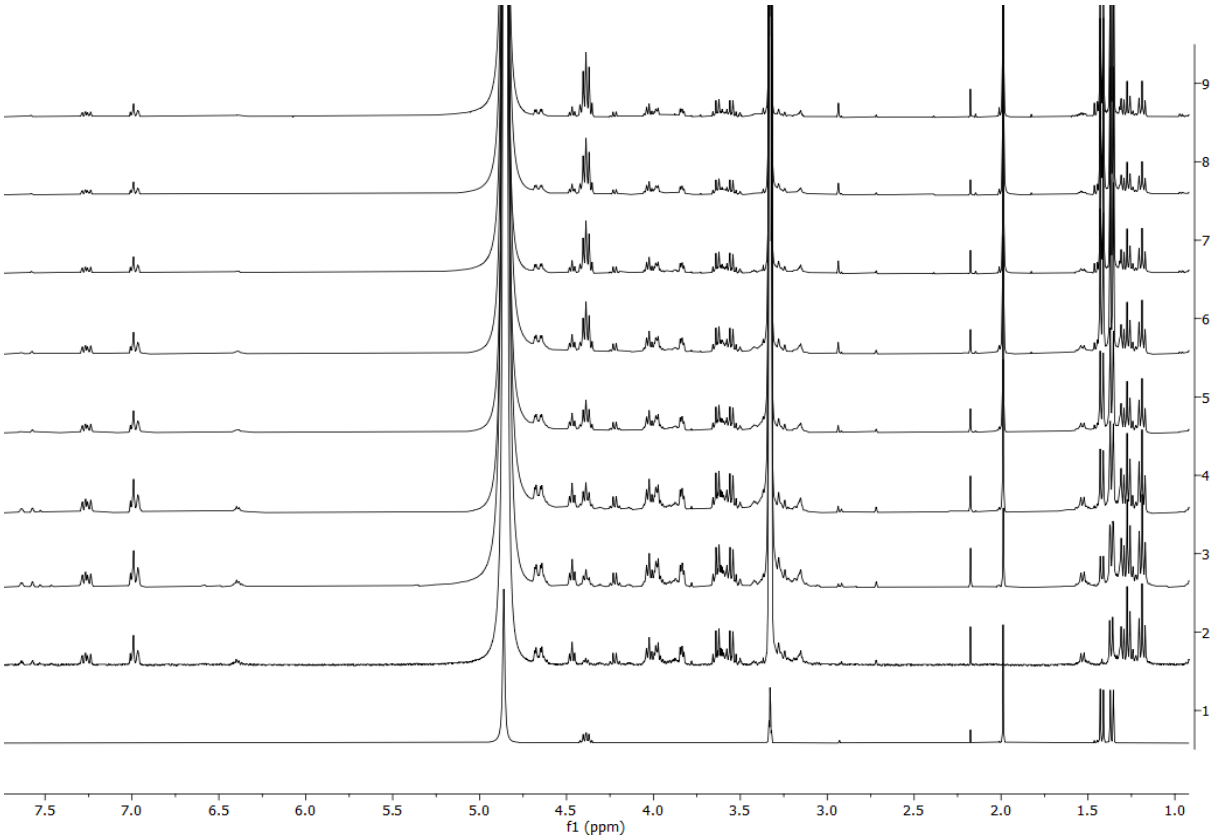

*Figure 33: From the bottom: Spectrum of N-Ac-D-ala-D-ala (trace 1), spectrum of compound **19** (trace 2), and spectra of **19** with increasing concentrations of guest (trace 2-9). All the spectra were recorded in CD_3OD (400 MHz, 298K)*

Complexation properties of receptor **19** were also investigated by ESI mass spectrometry. After optimizing the operating conditions, i.e. setting the parameters of the capillary potential and cone to 3.3 KV and 30 V respectively, several solutions in methanol containing host and guest at different ratios, specifically 1:1, 1:2 and 1:5, were analyzed and gave rise to peaks ascribable to the complexes. However, the increase of the concentrations of the guest did not result in a significant increase in the intensity of the signals of the complex. It was observed, instead, that the value of the cone potentials influences the ratio between the molecular ion of the receptor and the ligand-receptor complex; in fact, by recording the spectra first with a cone potential of 40 V and then at 30 V, a slight increase in intensity of the peak corresponding to the complex (from 1 to 3%) was observed, taking the molecular ion of the receptor as a reference.

The analyses were carried out both with positive and negative ionization mode. In particular, the signal related to the complex between the receptor and N-Ac-L-lys-D-ala-D-ala was observed through ESI-MS analysis both in positive and negative mode, while that related to the receptor and N-Ac-D-ala-D-ala is only visible through negative ionization mode. Their respective mass spectra are shown in figures 34-36 in methanol and in figure 37 in water.

The molecular mass of the receptor is m/z 1009.54, while that of the N-Ac-D-ala-D-ala and N-Ac-L-lys-D-ala-D-ala are m/z 202.09 and 330.19, respectively.

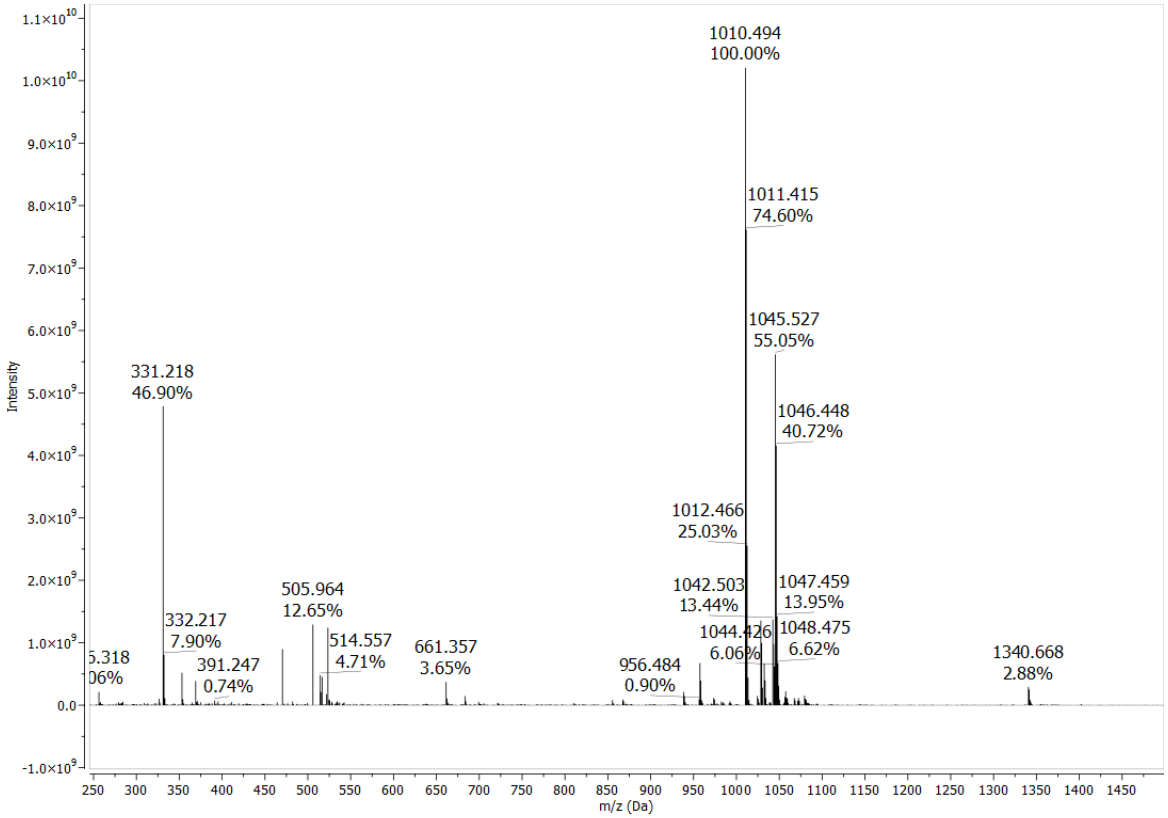

*Figure 34: ESI-MS(+) spectrum of a 1 mM methanol solution of receptor **19** and N-Ac-L-lys-D-ala-D-ala in a 1:1 ratio.*

In the mass spectrum, it is possible to observe the signal at m/z 331.22, which corresponds to the protonated molecular ion of the guest, the one at m/z 1010.50, which corresponds to the protonated molecular ion of receptor **19**, and finally the last one at m/z 1340.67, which corresponds to the monoprotonated 1:1 stoichiometry complex between receptor **19** and N-Ac-L-lys-D-ala-D-ala. It was therefore possible to confirm the formation of the complex, although the intensity of the complex signal is quite low.

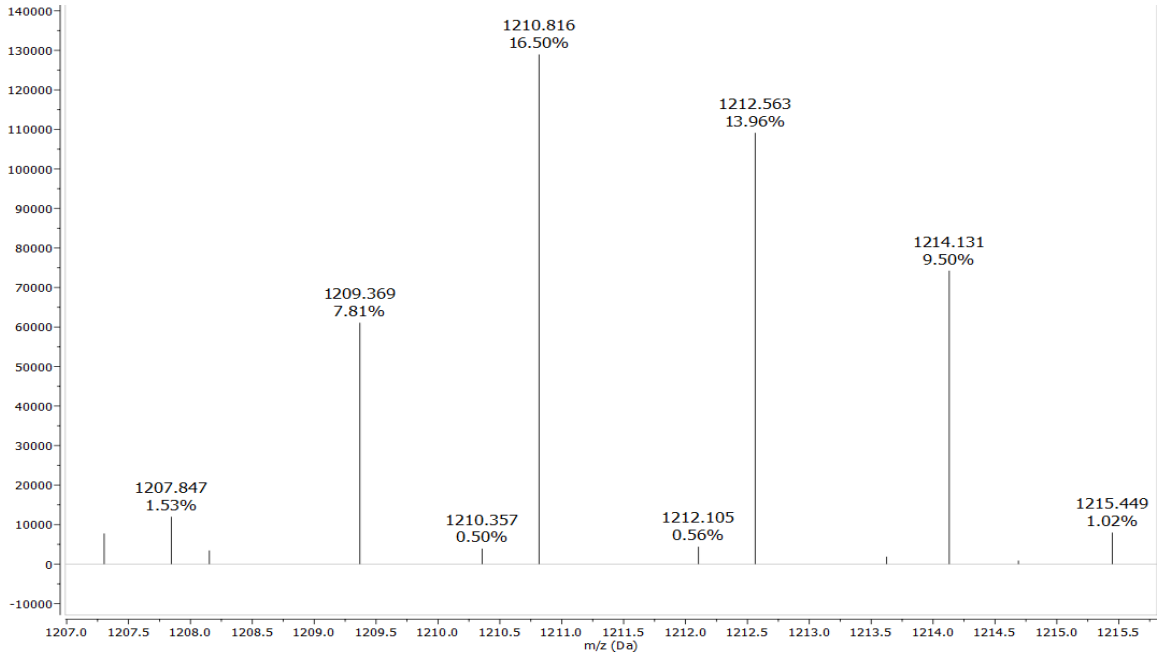

*Figure 35: ESI-MS(-) spectrum of a 1 mM methanol solution of receptor **19** and N-Ac-D-ala-D-ala in a 1:1 ratio.*

In the case of the dipeptide N-Ac-D-ala-D-ala, Figure 35 shows the amplification of the spectrum in the window between 1207 and 1215 m/z, highlighting the peak at m/z 1210.82 corresponding to the 1:1 host/guest complex between receptor **19** and N-Ac-D-ala-D-ala.

A competition experiment was also carried out, starting from a 1 mM solution containing receptor **19** and the two guests having **19**:N-Ac-D-ala-D-ala:N-Ac-L-lys-D-ala-D-ala = 1:1:1. The experiment was recorded with negative ionization mode, as the complex with N-Ac-D-ala-D-ala is not visible in positive mode.

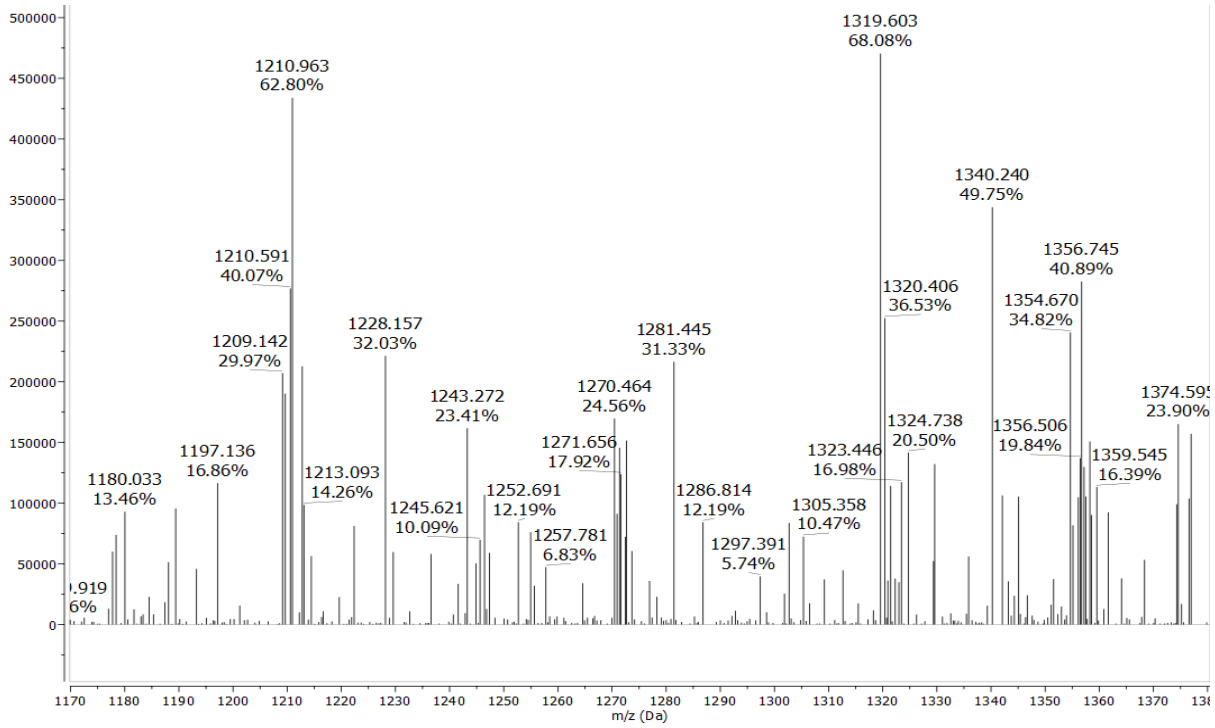

*Figure 36: ESI-MS(-) spectrum of a 1 mM methanol solution of receptor **19** and of the two guests in a 1:1:1 ratio.*

Although this competitive experiment is characterized by a significant noise and signals not identified, it is interesting to observe that the peaks (m/z: 1210.96 and 1340.24) of both complexes are present in the spectrum. The higher intensity of the signal corresponding to the complex with N-Ac-D-ala-D-ala (63%) compared to the analogous complex with N-Ac-L-lys-D-ala-D-ala (49%) suggests that lysine does not significantly contribute to the interactions that are established for the formation of the complex.

Since signals related to host/guest complexes were observed in methanol, the analyses were also repeated in water, where similar results were found (example reported in Figure 37).

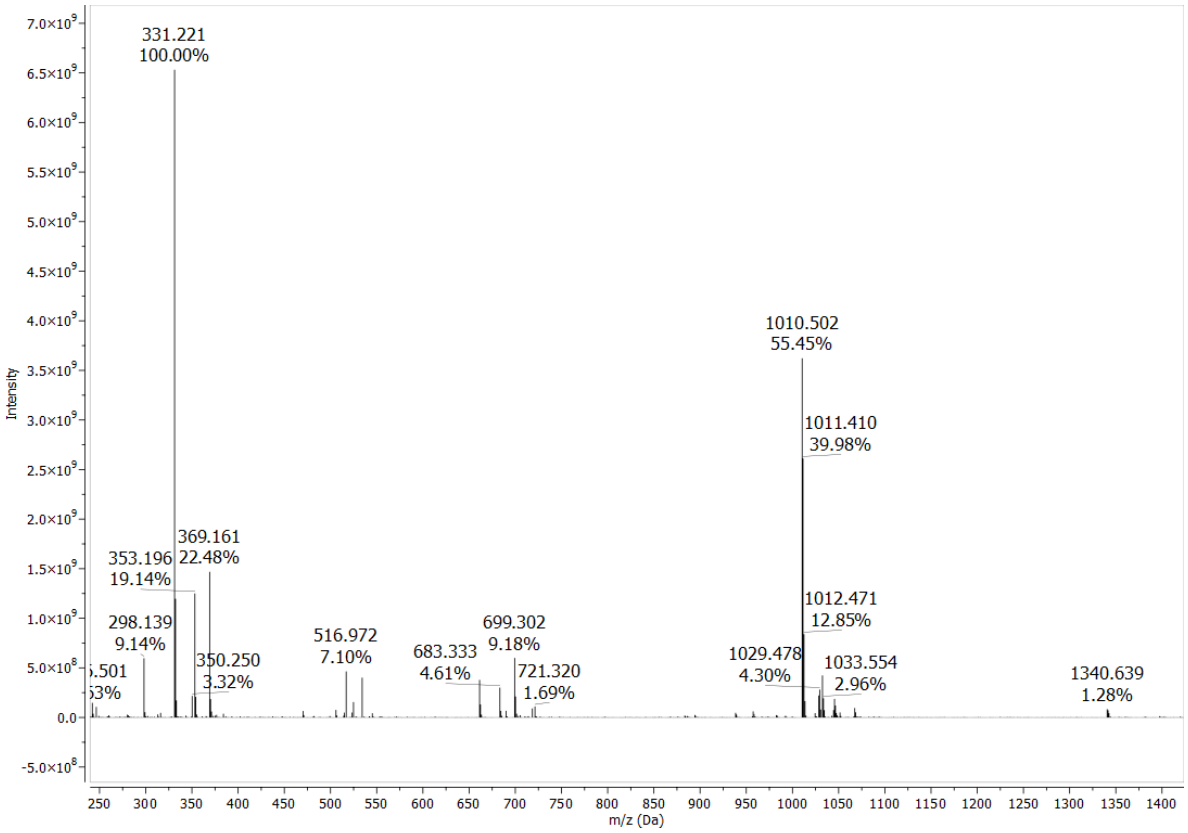

*Figure 37: ESI-MS(+) spectrum of a 1 mM aqueous solution of receptor **19** and N-Ac-L-lys-D-ala-D-ala in a 1:1 ratio.*

As for the previously reported mass spectrum in methanol, it is possible to observe the signals at m/z 331.22 corresponding to the protonated molecular ion of the guest, at m/z 1010.50 corresponding to the protonated molecular ion of receptor **19**, and finally at m/z 1340.64 corresponding to the 1:1 monoprotonated complex **19**xN-Ac-L-lys-D-ala-D-ala.

Studying N-Ac-D-ala-D-ala, we observed a signal at m/z 1210.41 corresponding to the deprotonated complex between receptor **19** and dipeptide. Moreover, even in aqueous solvent during the competitive experiment, we observed signals at m/z 1209.52 and 1338.65 corresponding to the complexes between receptor **19** and the two guests.

2.2 Gram-negative bacteria

The synthesis of the three calix[4]arenes, designed as ligands for Gram-negative bacteria (Figure 38) is disclosed below.

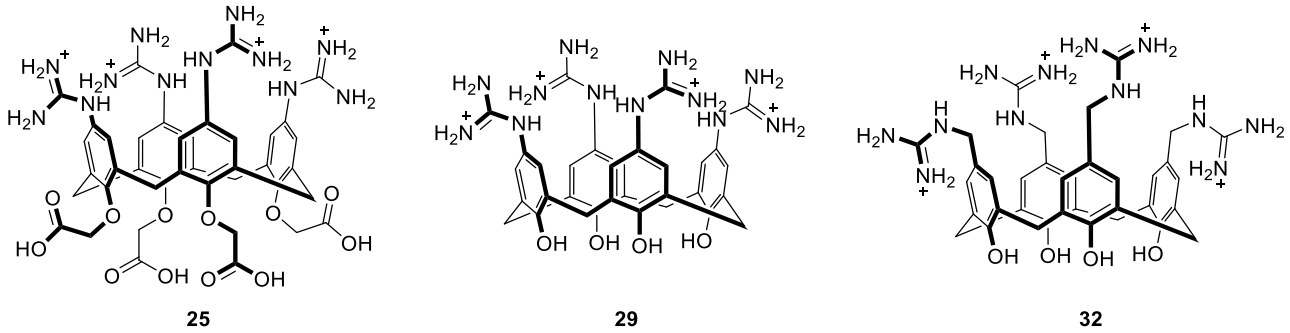

Figure 38: The three guanidinocalix[4]arenes synthesized.

2.2.1 Synthesis of compound 25

Compound **25** was synthesized as described in scheme 6.

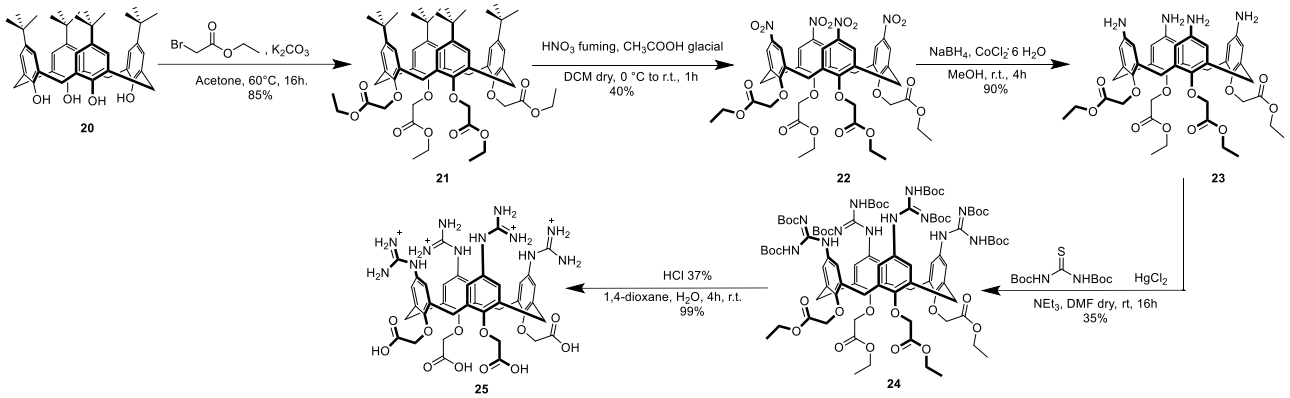

*Scheme 6: Reaction pathway followed for the synthesis of **25**.*

The synthesis started with the alkylation of p-tertbutyl-tetrahydroxy calix[4]arene **20** with ethyl bromoacetate, carried out in acetone at 60°C in presence of potassium carbonate. Compound **21** was obtained, after filtration, in 85% yield. The following reaction consisted in an ipso nitration.[37] This is a typical reaction carried out on alkylated calixarenes, in this case however we had ester groups at the lower rim and therefore extra precautions had to be took in place to promote the formation of the desired product. In this case we used dry conditions, employing only water free reagents like fuming nitric acid and glacial acetic acid. This had to be done because it was observed poor reactivity and by-product formation when the reaction was carried out in non-dry conditions. The desired tetranitro calixarene **22** was obtained, after chromatographic purification, in 40% yield. Compound **22** was then reduced to the corresponding tetraamino calixarene **23** exploiting $NaBH_4$ and $CoCl_2$. The reaction proceeded smoothly, and we were able to obtain compound **23** in 90% yield. This compound was then readily reacted with bis(Boc)thiourea to install the protected guanidine functions. The presence, during this reaction, of mercury(II) chloride in essential. In fact, we tried

to substitute the highly toxic $HgCl_2$ with other metal ions which usually have a good affinity towards sulfur, like copper and silver, but we observed no conversion of the starting material. We also tried other guanidinylating agents such as 1,3-di-Boc-2-(trifluoromethylsulfonyl)guanidine, but with no success. We, therefore, continued to use mercury(II) chloride. Compound **24** was obtained after column chromatography in 35% yield. It was subsequently Boc deprotected and hydrolyzed with concentrated HCl in dioxane. In this way we were able to collect the desired product **25**, whose ^{1}H NMR is reported below (Figure 39).

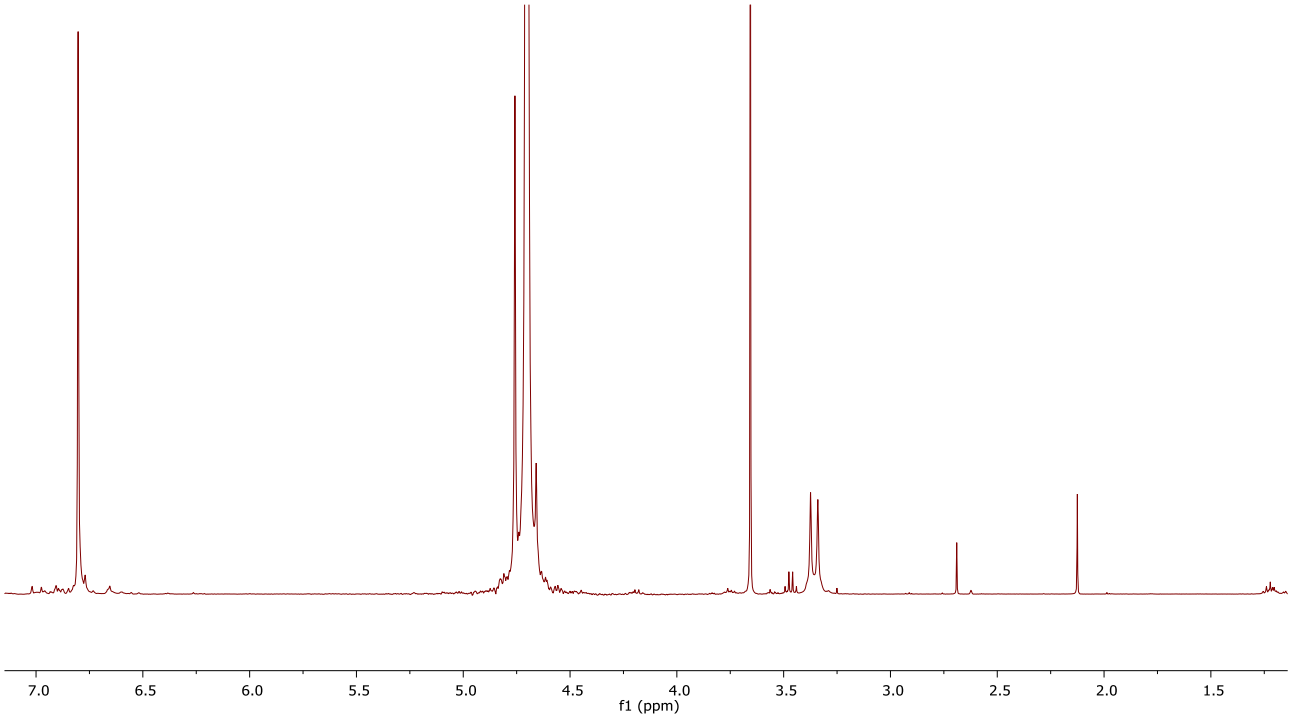

*Figure 39: ^{1}H NMR of compound **25** recorded in D_2O at 298K at 400 MHz (the singlet at 3.70 is due to residual dioxane).*

Here it is possible to observe the singlet at 6.80 ppm corresponding to aromatic protons and the doublet at 3.36 ppm generated by the equatorial proton of the calixarene methylene bridge. The other two key signals are overlaid with the solvent peak, however looking closer it is possible to see the singlet at 4.76 ppm which corresponds to the lower rims methylene groups, and it is also possible to note half of what should be the doublet generated by the axial proton of the calixarene bridge at 4.66 ppm. This has been verified also by an HSQC where it is possible to see how these two doublets correlate to a ^{13}C signal at 30.4 ppm which corresponds to the typical chemical shift of the calixarene bridge carbon.

The integral ratio between the only two clearly identifiable signals in the proton NMR spectrum is as expected 2:1.

2.2.2 Synthesis of compound 29

To synthesized compound **29** we followed the reaction pathway reported in scheme 7.

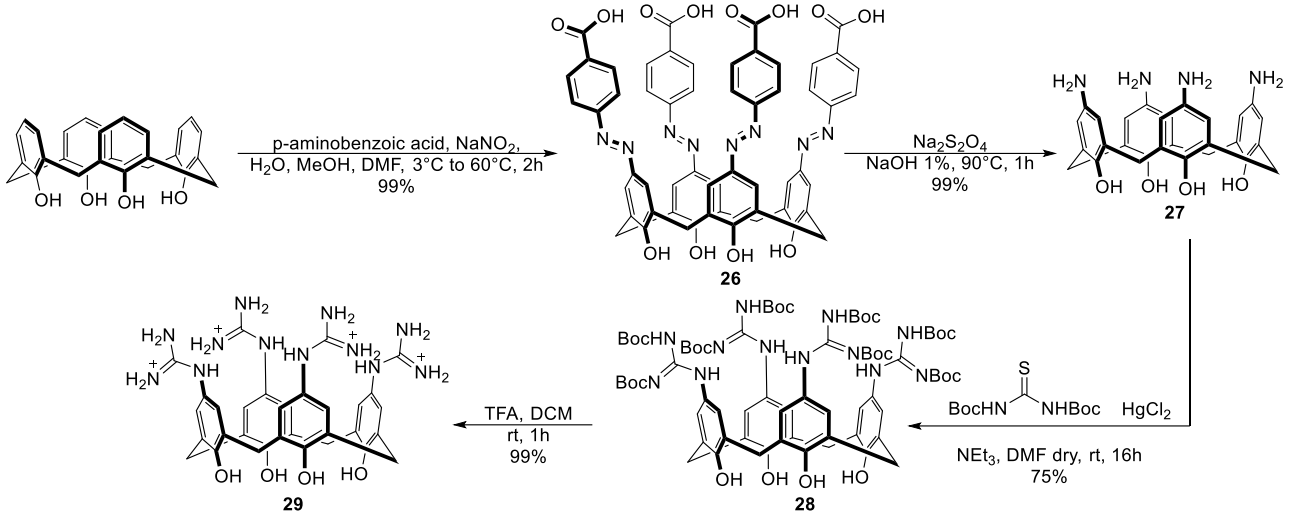

*Scheme 7: Synthetic steps employed for the preparation of compound **29**.*

We started by preparing the diazonium salt of p-aminobenzoic acid, following the classic protocol with $NaNO_2$ and HCl. Once we obtained this intermediate we reacted it with the tetrahydroxycali[4]arene obtaining the azocalixarene **26** after a simple precipitation.[38] This compound was then reduced to its amine counterpart using sodium dithionite in basic water. Both these reactions had quantitative yields. Compound **27** is very unstable and tends to form quinonimines very easily. In fact, if the flask is left open to the air, the product changes almost immediately color going from white to dark blue. For this reason, we immediately subjected this compound, once obtained, to the guanidinylation reaction. We carried out this step in the same conditions described above, and we were able to isolate, after column chromatography on silica gel, compound **28** in high yield (75%). This was then Boc deprotected using TFA in DCM and after evaporation of the solvents, we obtained a white powder whose ^1H NMR is reported in figure 40.

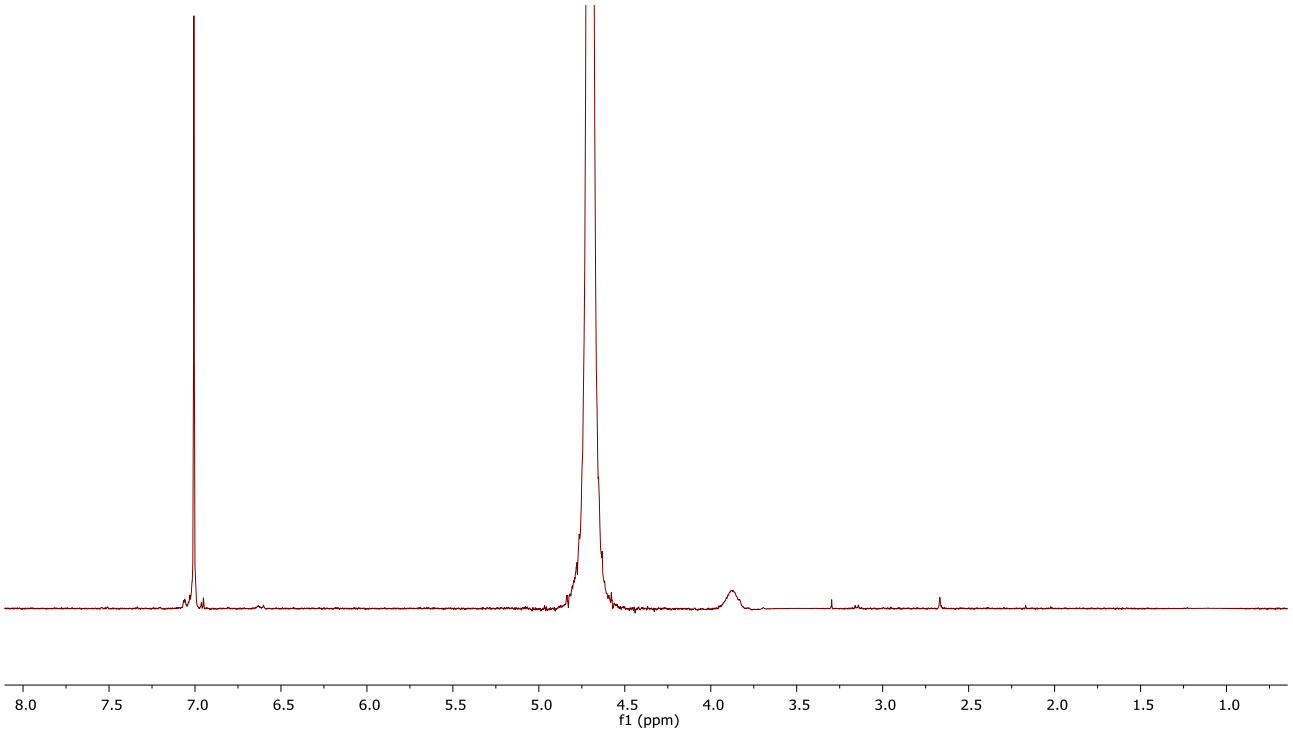

*Figure 40: ^{1}H NMR of compound **29** recorded in D_2O (298K, 400 MHz).*

In this spectrum, excluding the residual D_2O peak, only two signals are visible, the singlet at 7.01 ppm corresponding to the calixarene aromatic protons and the broad singlet at 3.88 ppm generated by the protons of the calixarene methylene bridge. Their integral ratio is 2:0.5 which is a bit off. We decided to record the same spectrum at 80°C to have sharper signals (Figure 41).

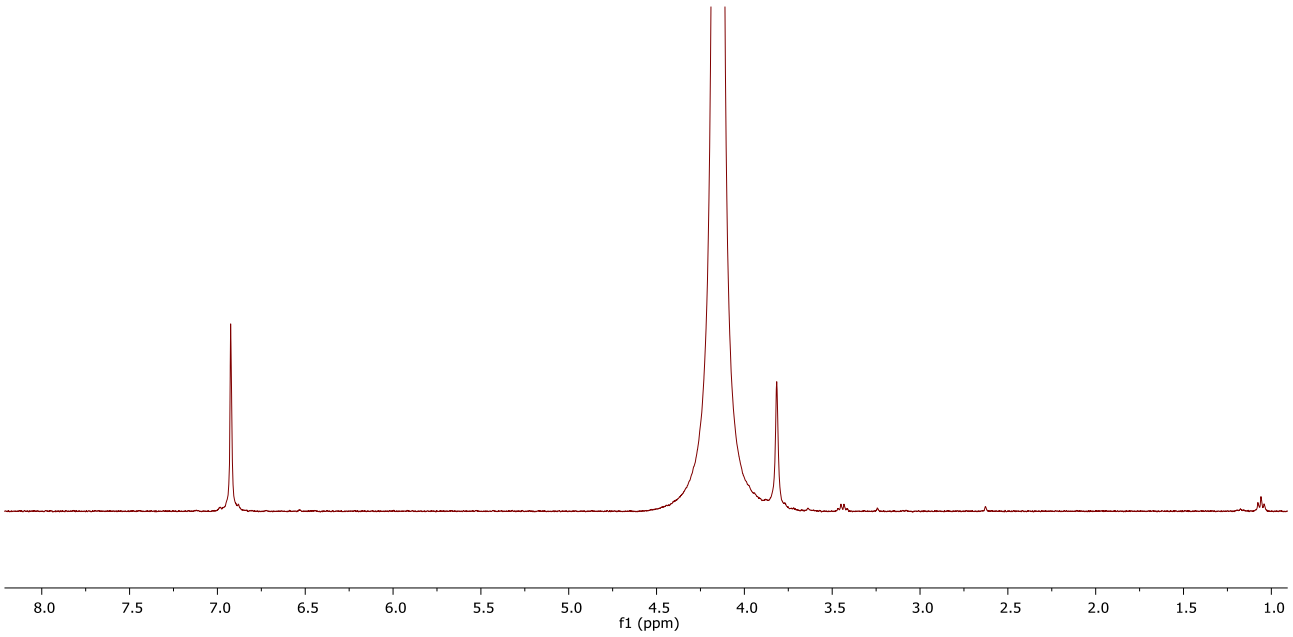

*Figure 41: ^{1}H NMR of compound **29** recorded in D_2O at 353K at 400 MHz.*

Here it is possible to see two singlets at 6.92 and 3.82 ppm and their integral ratio is 1:1. Therefore, the NMRs confirmed that the desired product was obtained, which was also proved by ESI-MS analysis.

2.2.3 Synthesis of 32

The last guanidinylated calixarene, compound **32** was prepared as reported in scheme 8.

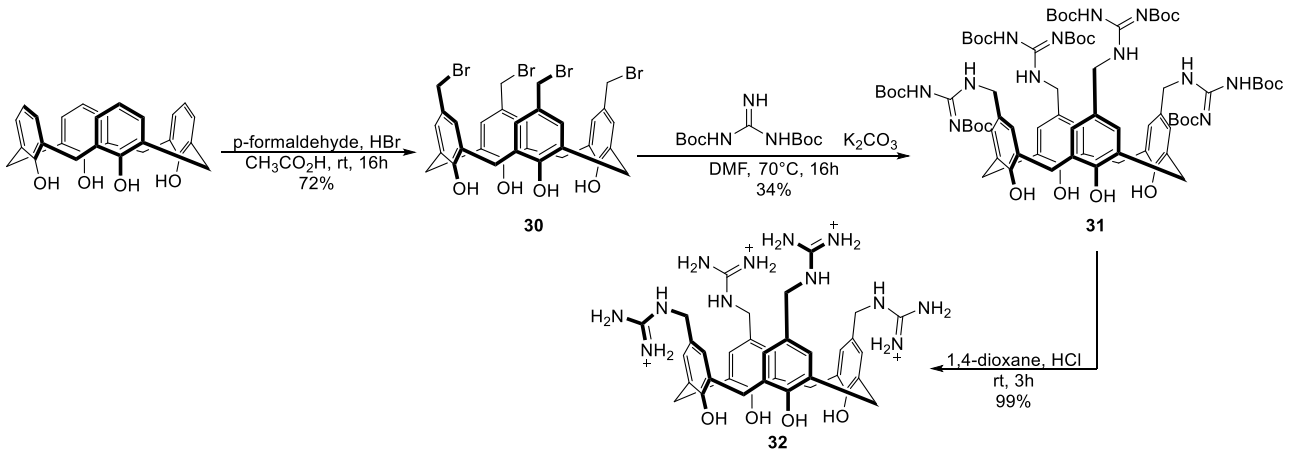

*Scheme 8: Synthesis of compound **32**.*

The first step involved the insertion onto the calixarene aromatic para position of a bromo methylene group. We performed this transformation employing paraformaldehyde and HBr in acetic acid.[39] Compound **30** was obtained in 72% yield after precipitation in chloroform. The tetra functionalized bromo calixarene **30** was then reacted with bis(Boc)guanidine using potassium carbonate as a base and DMF. Chromatographic purification was needed to isolate the desired compound **31**, obtained in 34% yield. The last step involved the Boc deprotection of the guanidine groups carried out using, once again, concentrated HCl in dioxane. Following these steps, we were able to obtain the desired product **31**, whose ^{1}H NMR spectra are reported in figure 42.

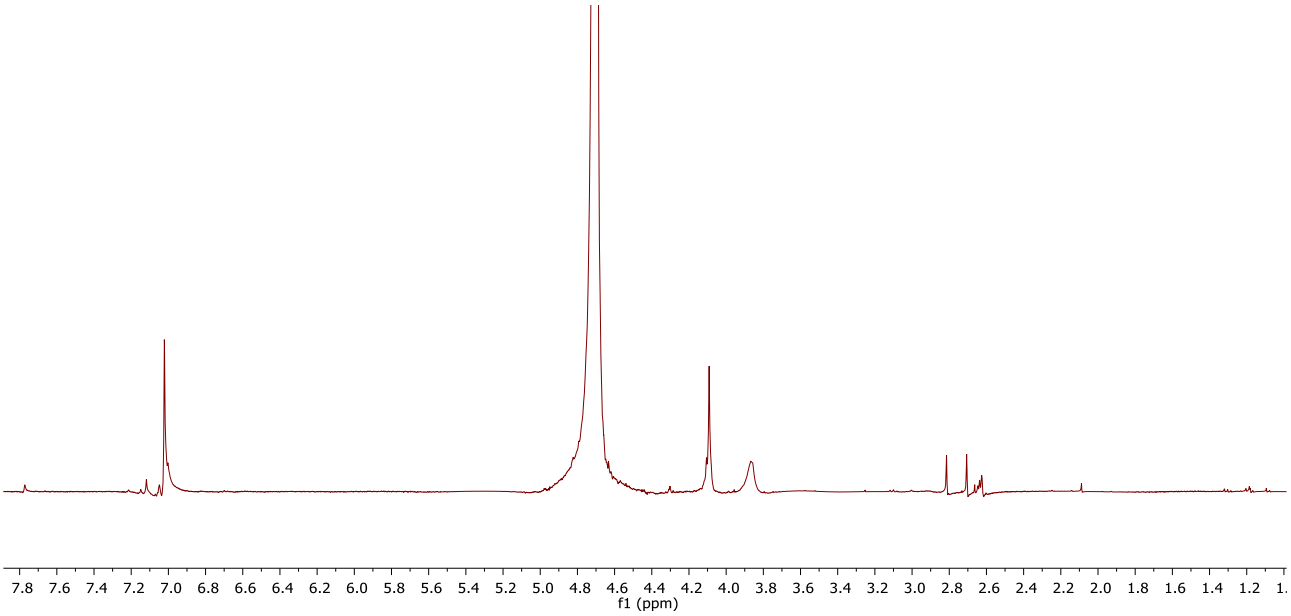

*Figure 42: ^{1}H NMR of compound **32** recorded in D_2O at 298K at 400 MHz.*

Here it is possible to observe the singlets at 7.02, 4.09 and 3.87 ppm. They correspond respectively to the aromatic protons, the methylene protons located between the aromatic rings and the guanidinium groups and finally the calixarene methylene bridge protons (HSQC correlation with ^{13}C signal at 30.5 ppm).

2.3 Mycobacteria

This part of the project requires the preparation of trehalose units functionalized with azide groups and their reactions with calixarene structures functionalized at the upper rim with terminal alkyne groups. In this way, the copper(I)-catalyzed azide-alkyne cycloaddition reaction, also known as the "click" reaction, could be exploited to link the calixarene to the saccharide structure.

The first calix[4]arene scaffold we decided to prepare was the difunctionalized compound **33**. The two alkyne moieties at the upper rim ensured the possibility of trehalose conjugation by CuAAC. (Scheme 9) We started with the diacyl chloride of tetrapropoxy calix[4]arene **7**. The amide formation reaction was carried out using TEA and propargylamine in dry DCM, obtaining compound **33** in 40% yield after purification by flash column chromatography.

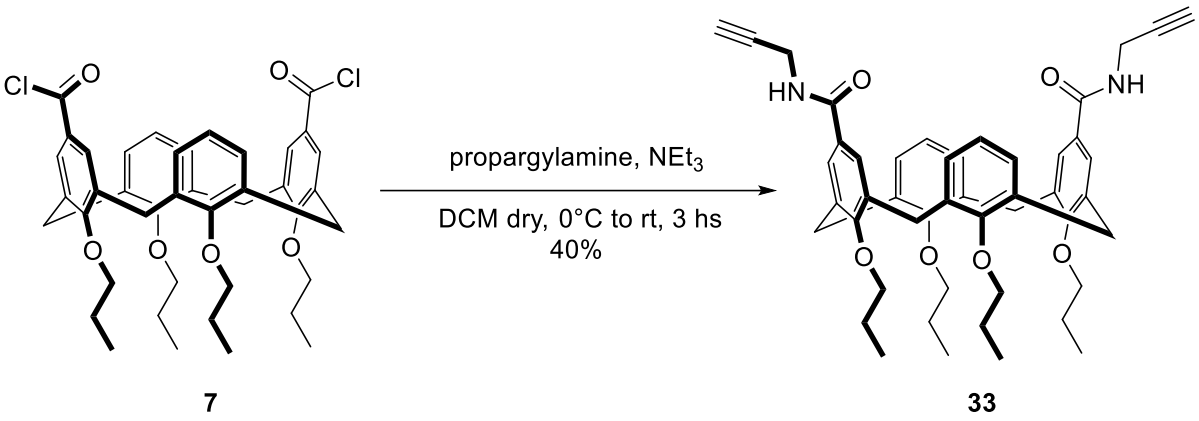

*Scheme 9: Preparation of compound **33**.*

The ^{1}H NMR spectrum of compound **33** is reported in figure 43.

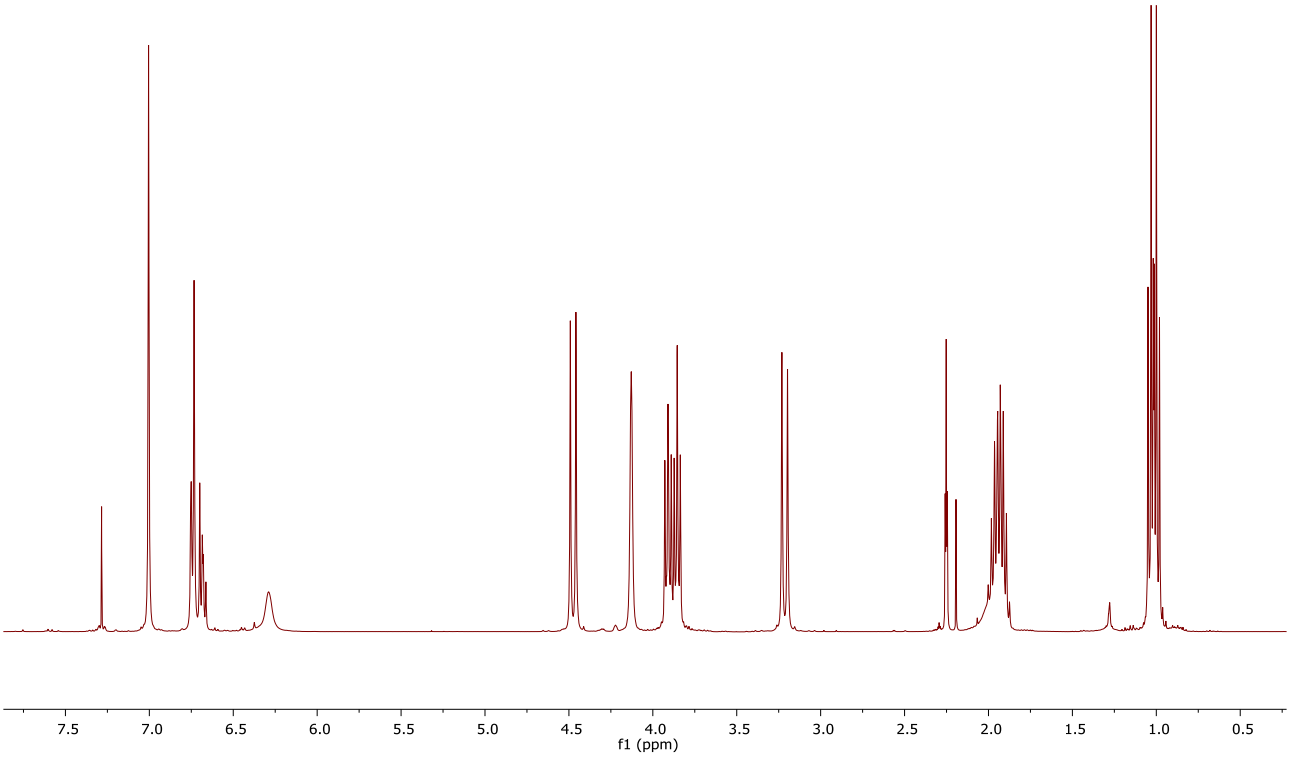

*Figure 43: ^{1}H NMR of compound **33** recorded in $CDCl_3$ at 298K and 400 MHz.*

The calixarene cone configuration is proved by the two doublets relative to the axial and equatorial protons of the methylene bridge that resonate respectively at 4.47 and 3.21 ppm. This multiplicity of the protons of the aromatic nuclei and of those of propyl groups confirms the high symmetry of the functionalized scaffold confirming the 1,3-difunctionalization of the upper rim. It is also possible to observe the three signals relative to the installed propargylamide functionality: the broad singlet at 6.29 ppm, (NHCO), the doublet at 4.13 ppm (the CH_2NH group) and finally the triplet at 2.25 ppm, ascribed to the alkyne proton.

Since we reasoned that the four propoxy groups at the lower rim, together with the calixarene aromatic backbone, could have resulted in a high hydrophobicity of this scaffold preventing the water solubility of the final glycoconjugate, we decided to also synthetize a calixarene derivative having ethoxyethyl groups at the lower rim. This expedient was often successfully used in calixarene chemistry to make these macrocycles more water soluble (*see* also compound **19** in this chapter).

2.3.1 Hydrophilic scaffold synthesis

Starting from diacyl chloride **17**, the amide bond formation was carried out using the same conditions described above and obtaining compound **34** after purification by flash column chromatography (Scheme 10) in 49% yield. This derivative, interestingly, crystallized in chloroform and allowing us to solve its X-ray structure (Figure 44).

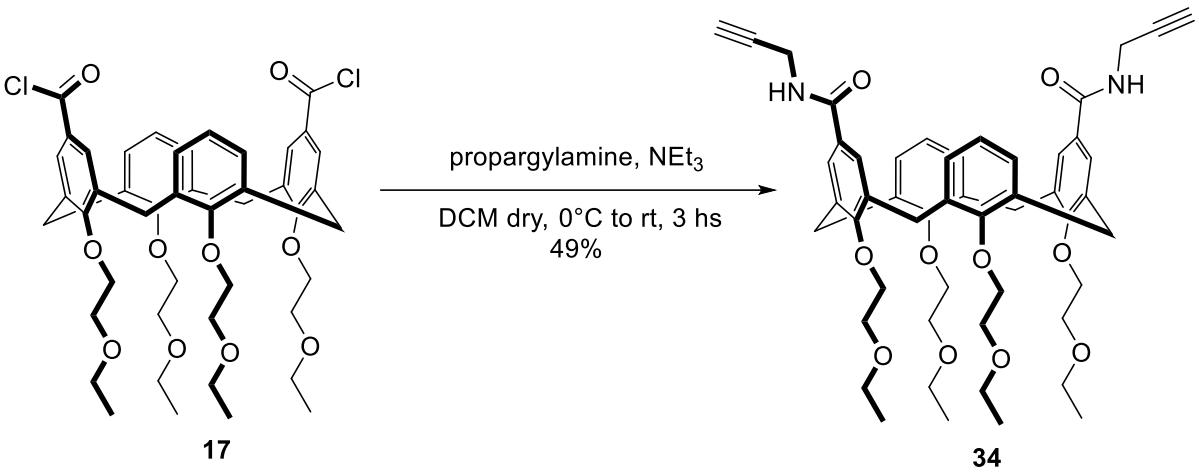

*Scheme 10: Synthesis of **34**.*

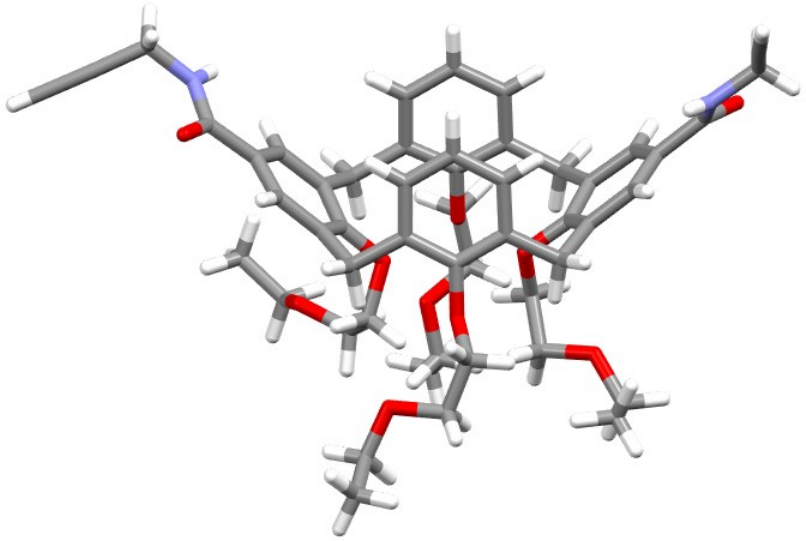

*Figure 44: Cristal structure of compound **34**.*

The calix[4]arene **34** adopts a flattened "open" cone conformation, with the two aromatic groups bearing the propargylamide units at the upper rim diverging and almost perpendicular to each other. The reason for this conformation, observed in the solid state, is that the two amide groups establish intermolecular interactions with other adjacent molecules in the crystal structure. From a first analysis carried out using the Mercury software, the main intermolecular interactions established by molecule **34** within the crystal were obtained. Propargylamide groups form hydrogen bonds with adjacent molecules: the NH of one propargylamide is a hydrogen bond donor towards a carbonyl oxygen acceptor of an adjacent molecule. With a distance within the sum of Van der Waals radii + 0.1 Å, a terminal alkyne group establishes a CH-π interaction with a close aromatic ring.

We then proceeded with the synthesis of the calixarene scaffold with four amide functions (compound **38**) (Scheme 11). Firstly, compound tetraethoxyethylcalix[4]arene was formylated at all four positions on the upper rim exploiting the Duff formylation with hexamethylenetetramine (HMTA) and TFA as solvent The reaction, however, even in large excess of HMTA, did not reach its completion so that, after a flash chromatographic purification, compound **35** could be isolated in only 55% yield. Subsequently, this derivative was oxidized to carboxylic acid using the Pinnick reaction. Compound **36** was obtained by precipitation in acidic water. It was then reacted with oxalyl chloride and catalytic amounts of DMF, and then with propargylamine and NEt_3, according to the same acyl chloride and amide formation reaction protocols followed to obtain compound **38**.

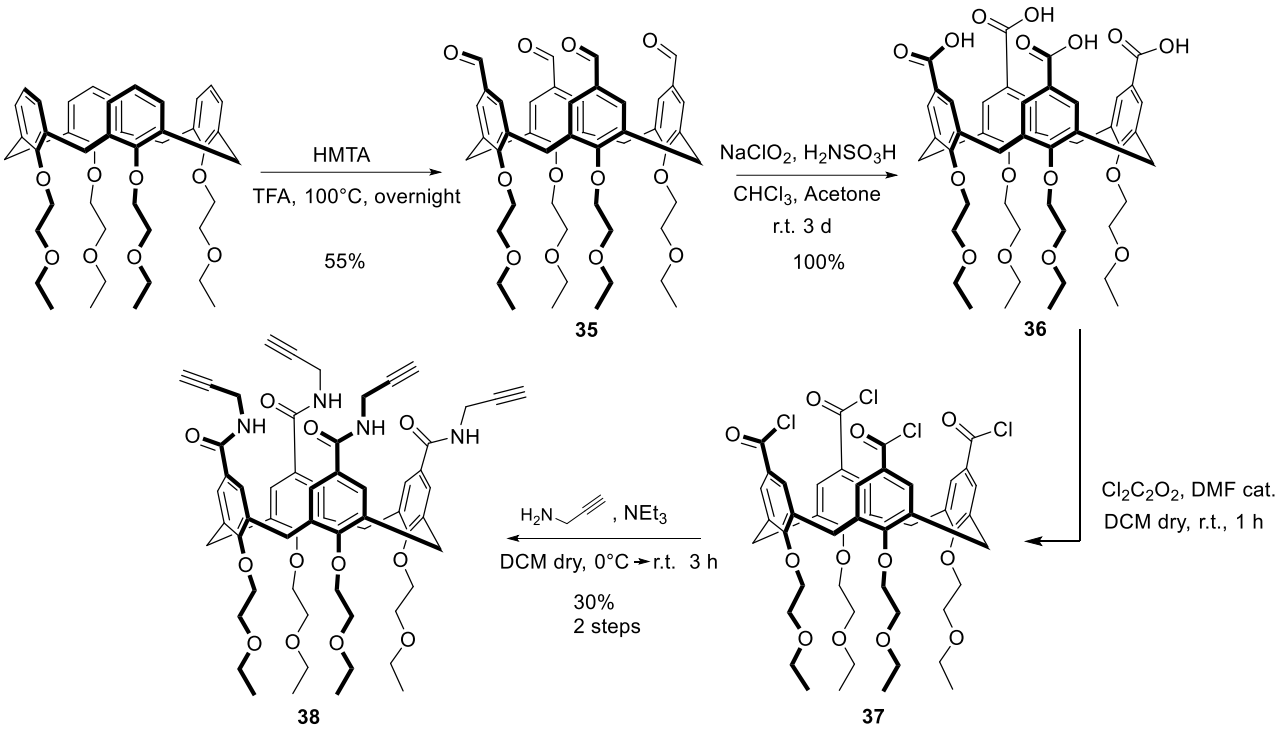

*Scheme 11: Synthesis of compound **38**.*

The NMR spectra confirm the presence of the propargylamide group on compounds **34** and **38**: the ^{1}H-NMR spectrum of compound **34** (Figure 45) shows a multiplet at 4.16 ppm due to the superimposition of the signals of the methylene protons of the Ar-CONHC**H$_2$**CCH chain and of one of the triplets of the ethoxyethyl chain. A second signal at 2.27 ppm is assigned to the alkyne proton, which is a triplet due to the coupling with the Ar-CONHC**H$_2$**CCH protons (J = 2.5 Hz). The HSQC spectrum (Figure 46) confirms the assignment of the multiplet at 4.16 ppm due to its correlation with both the ^{13}C signals of the -ArO**C**H$_2$CH$_2$OCH$_2$CH$_3$ at 73.4 ppm, and of the Ar-CONH**C**H$_2$CCH at 29.6 ppm.

The ^{1}H-NMR spectrum of compound **38** (Figure 47) shows a doublet at 4.06 ppm corresponding to the -CH$_2$ protons of the Ar-CONHCH$_2$CCH chain, and a triplet at 2.56 ppm corresponding to the terminal alkyne -CCH proton. This assignment is confirmed by the fact that both the doublet and triplet have the same ^{4}J = 2.5 Hz, and by the fact that in the 2D-COSY spectrum the two signals correlate with each other. The ^{4}J coupling of the -CH$_2$ protons of the Ar-CONHCH$_2$CCH chain is also present in the spectrum of compound **34** but is not observable from the monodimensional spectrum due to overlap with other peaks as previously discussed. Here the tetrafunctionalization of the calixarene is confirmed by the presence of only one singlet at 7.30 ppm for the aromatic protons.

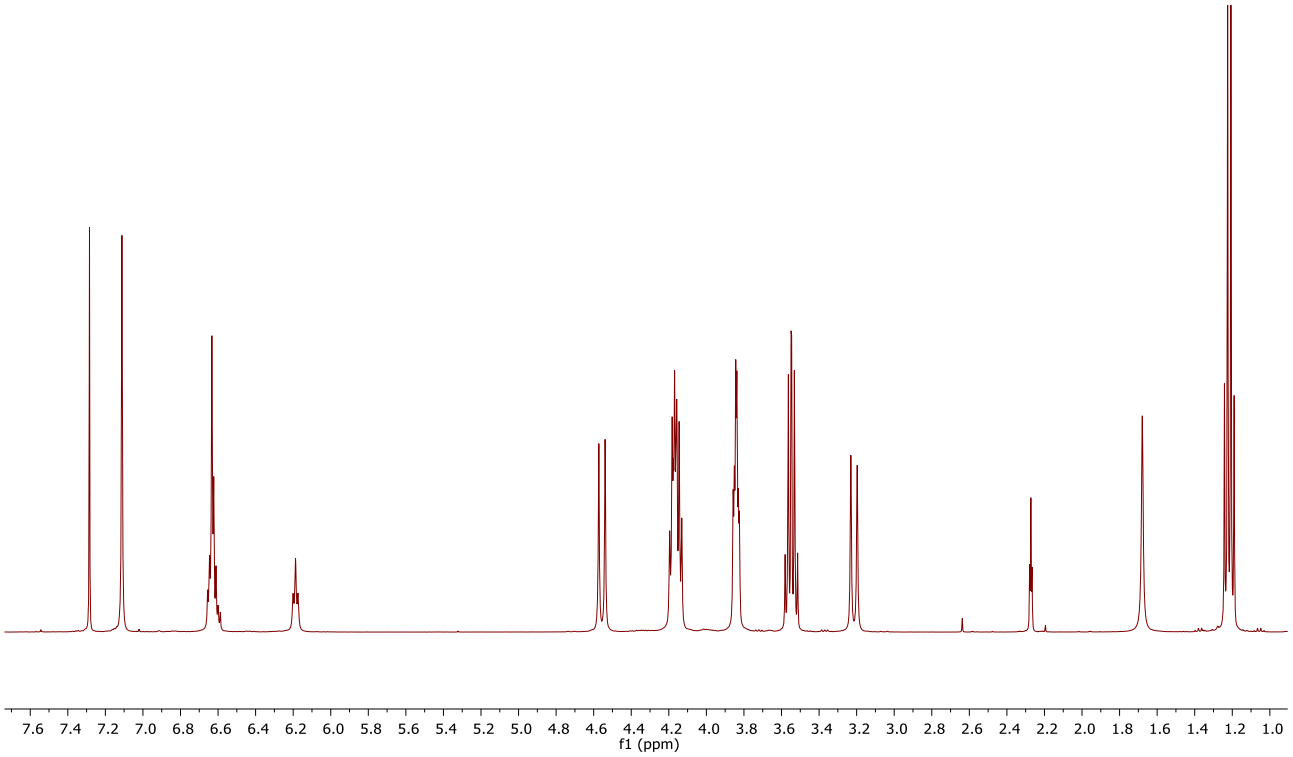

*Figure 45: ^{1}H NMR of compound **34** recorded in $CDCl_3$ at 298K and 400 MHz.*

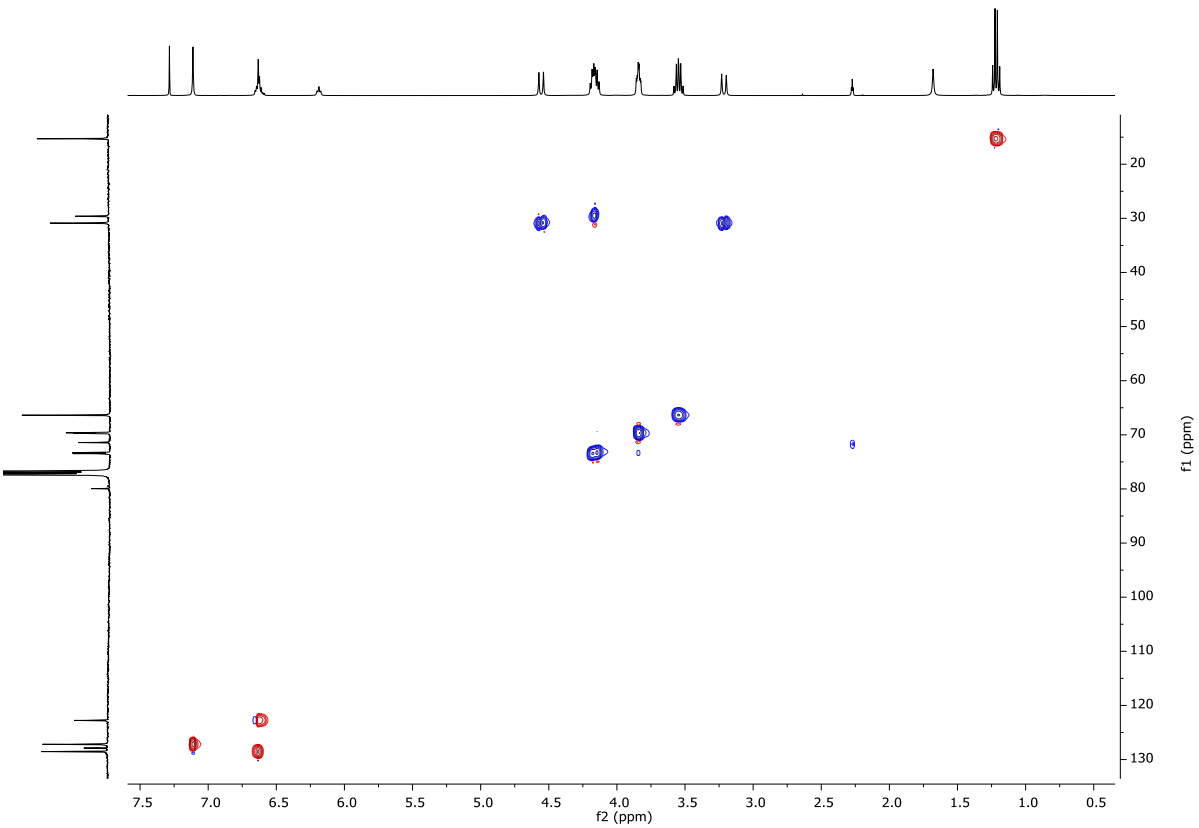

*Figure 46: HSQC spectrum of compound **34** recorded in $CDCl_3$ at 298K and 400 MHz.*

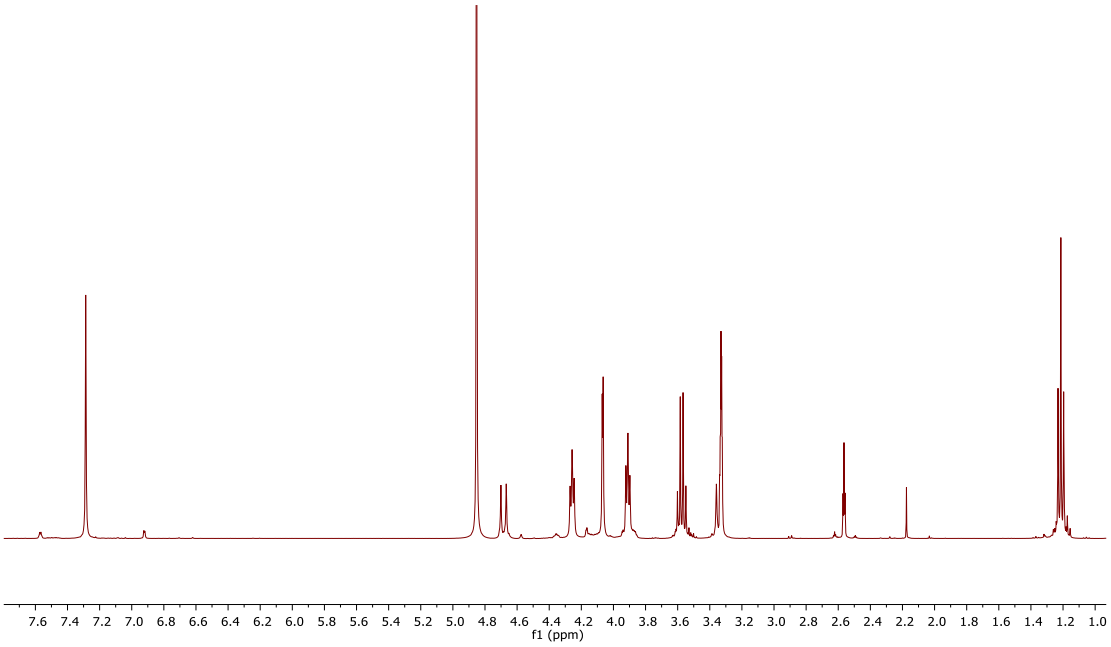

*Figure 47: ^{1}H NMR of compound **38** recorded in CD_3OD at 298K and 400 MHz.*

2.3.2 Trehalose functionalization

In order to link the desired trehalose units to our alkyne-bearing calixarene scaffolds we had to introduce an azido group into the disaccharide structure. As stated in the introduction, modifications of groups in C_6 and/or C_4 positions are well tolerated and do not significantly modify the affinity for the trehalose binding proteins. We therefore started with the easiest molecule to obtain, that is the 6-azido trehalose. The synthetic steps used to obtain the protected 6-azidotrehalose **41** are reported in scheme 12.

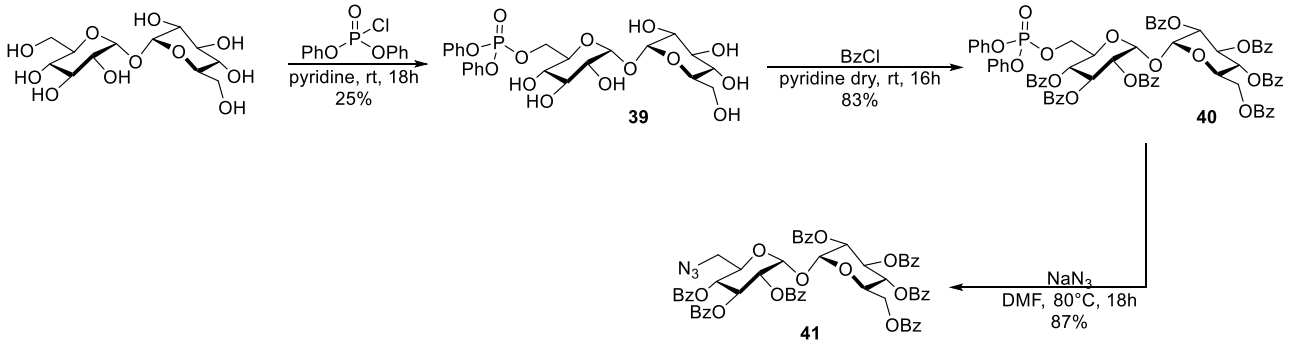

*Scheme 12: Preparation of compound **41**.*

The synthesis starts with the phosphorylation of one of the two primary alcohols, performed in pyridine at room temperature. This reaction, being statistically driven, was not allowed to reach completion and, in fact, was stopped once the maximum amount of the desired compound was formed. Due to the multiple intermediates present in the crude a chromatographic purification was needed. The nature of this reaction did not

allow us to prepare the desired product in more than 25% yield. Once compound **39** was obtained, it was fully protected by reacting it with benzoyl chloride in dry pyridine. Compound **40** was then solubilized in DMF and treated with sodium azide in 87% yield. This very short synthetic sequence permitted us to obtain the first trehalose azido analog in a 18% overall yield.

The relative ^{1}H NMR is reported in figure 48.

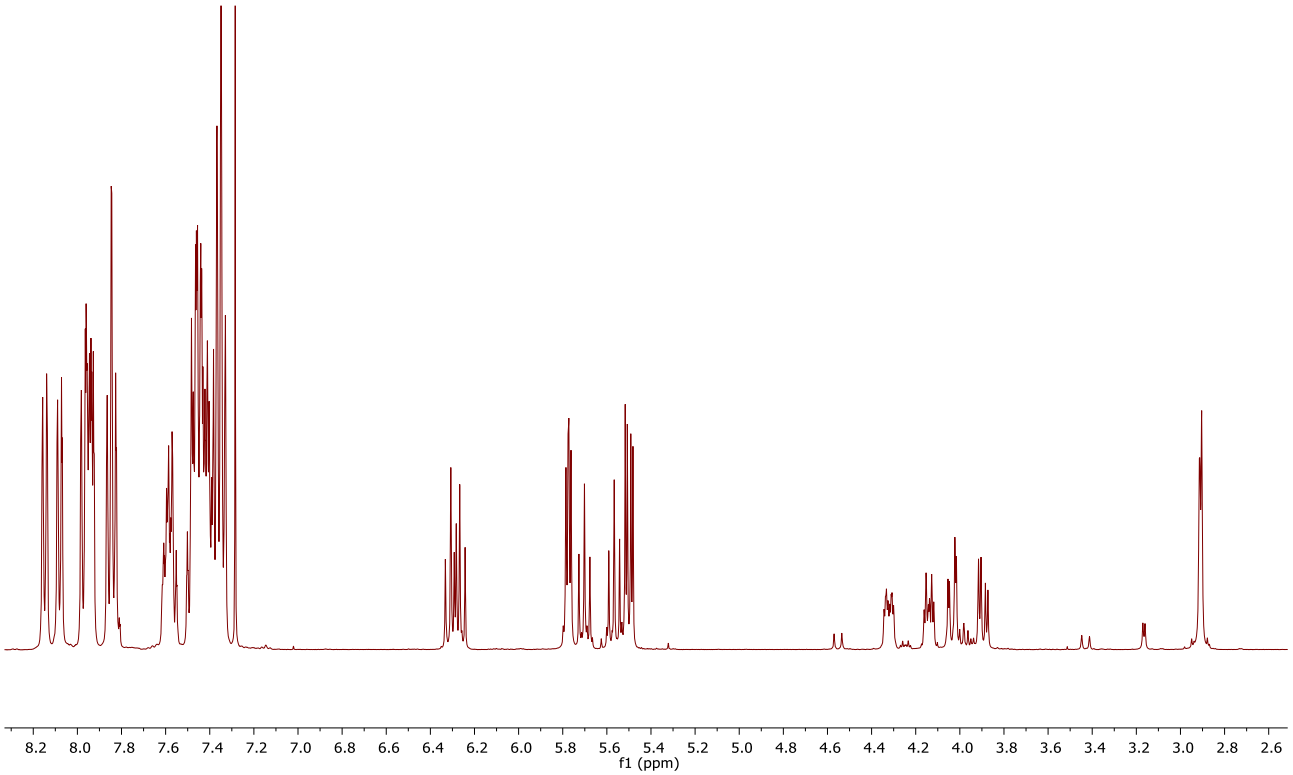

*Figure 48: ^{1}H NMR of compound **41** recorded in $CDCl_3$ at 298K and 400 MHz.*

The spectrum confirms the obtainment of the desired product. In fact, it is possible to observe two different sets of signals for each of the glucose ring. In particular, it is possible to notice two different signals for H_5 and H_5', respectively two doublets of doublets of doublets at 4.32 and at 4.14 ppm. Furthermore, the most significant signals are those generated by H_{6a} and H_{6b} of the two rings. The two doublets of doublets at 4.03 and 3.89 ppm can be attributed to the H_6 of the unmodified ring while those of the azido-ring generates a multiplet at 2.90 ppm. This is in accordance with the different functionalization of the 6 and 6' position, where the former carries a strongly electron withdrawing benzoyl group while the latter an azido group. The heptabenzoylation of the saccharide is also confirmed by the ratio of the integrals of the aromatic signals and the H_5 signal which is, as expected, 35:1.

We then moved on with the synthesis of the 4-azido trehalose. Initially we followed a synthetic sequence reported in scheme 13.[40]

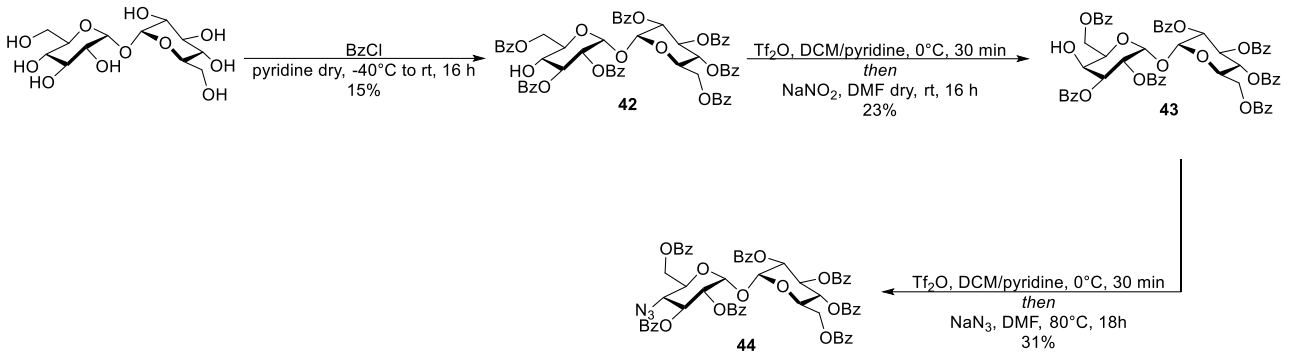

*Scheme 13: Synthesis of compound **44**.*

The first reaction involved the selective hepta-protection of the disaccharide. This was possible due to the lower reactivity of the OH groups in position 4 and 4' towards benzoyl chloride. The difference between these alcohols and the other secondary ones is, however, very small and for this reason the reaction had to be, initially, carried out at -40°C. During this transformation we observed a very complex crude. In fact, multiple compounds were present at the same time as the perbenzoylated sugar, the hexa protected one, and the desired product. Lengthy chromatographic purification on silica gel allowed us to obtain the desired hepta-protected sugar, but in a very low overall yield. We then proceeded with the epimerization of compound 7, following the Lattrell-Dax protocol,[41] that consists in treating the disaccharide with triflic anhydride followed by reaction of the resulting triflate with sodium nitrite in dry DMF. However, we were unable to reproduce the selectivity reported in the literature,[40] and we obtained a mixture of the two epimers with the starting one being the most abundant and the desired compound **43** in only 23% yield. We then treated compound **43** with triflic anhydride to generate a good leaving group and, again without isolation of the triflate we performed the reaction with sodium azide. Since we had epimerized one trehalose ring from gluco- to galacto- (*see* compound **43**) this nucleophilic substitution gave us the desired compound having the azido group in equatorial position, as the natural C_4 OH of trehalose. The reaction was successful in giving us the desired product despite the disappointing low yield. The proton NMR is reported in figure 49.

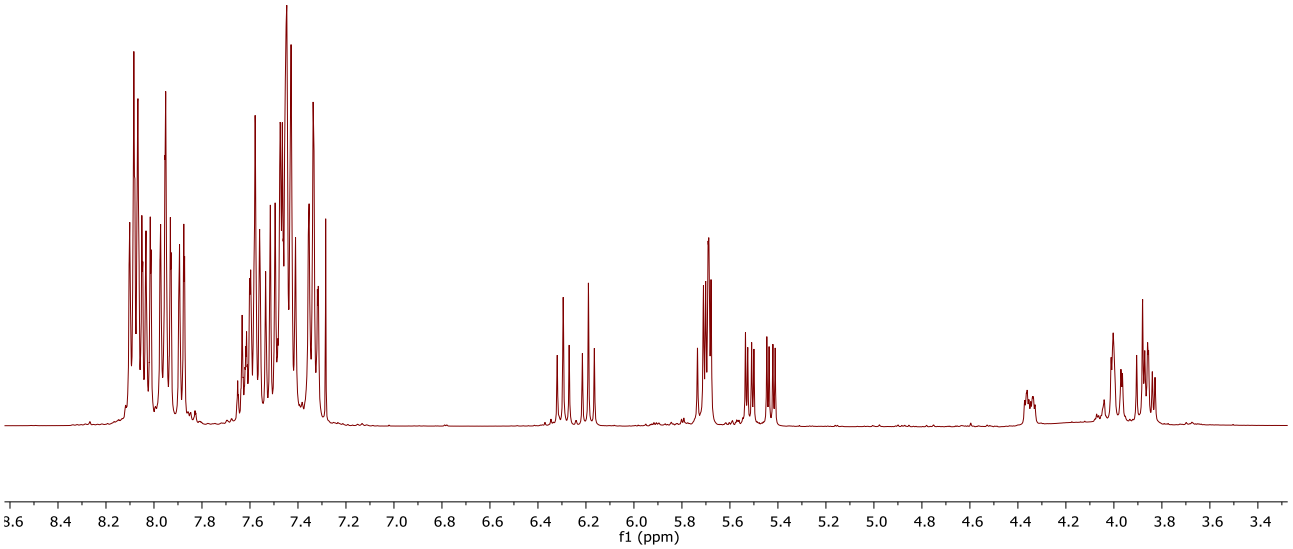

*Figure 49: ^{1}H NMR of compound **44** recorded in $CDCl_3$ at 298K and 400 MHz.*

Here, thanks also to the COSY spectrum reported in figure 50 it is possible to observe two triplets at 6.29 and 6.19 ppm respectively generated by H_3' and H_3. This are important to be assign because, through their correlations we could assign all the other signals and, in particular, the multiplets generated by $H_{4/4'}$. As expected, the two protons in position 4 and 4' resonate at very different ppm due to their different functionalization.

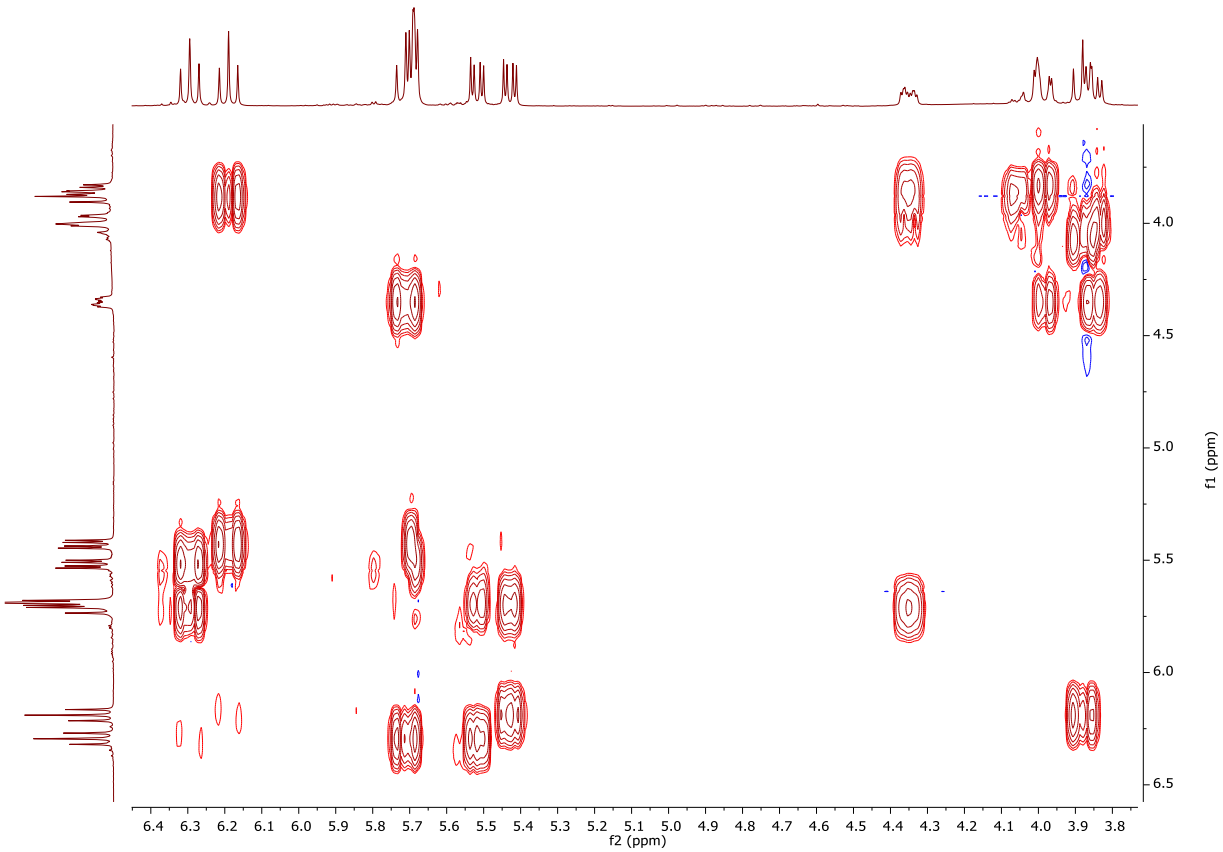

*Figure 50: COSY spectrum of compound **44** recorded in $CDCl_3$ at 298K and 400 MHz.*

Following this strategy, we were able to obtain compound **44** but only in a global 1% yield. The lengthy purification of the first intermediate, combined with the very low yield, pushed us to develop an alternative synthesis of this trehalose analog in order to be able to prepare the larger quantities necessary for calixarene functionalization.

2.3.2.1 Improved strategy of C4 functionalization

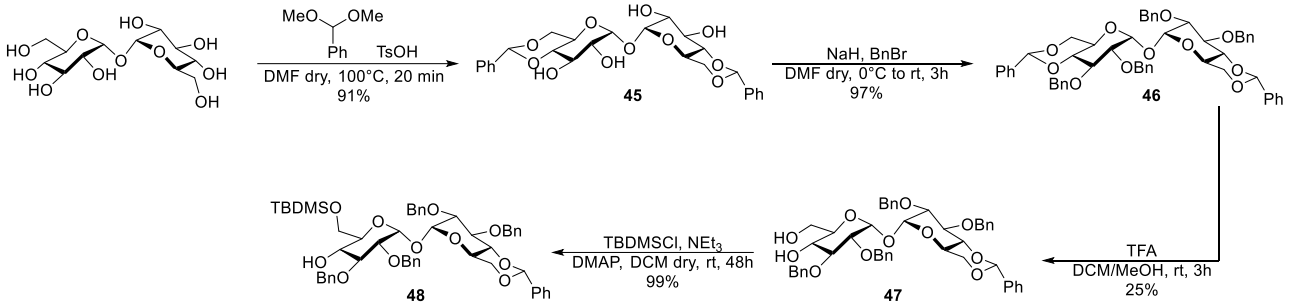

*Scheme 14: Synthetic pathway for the preparation of compound **48**.*

This alternative strategy, partially depicted in scheme 14, avoided the use of benzoyl protecting groups and is based on benzyls and acetals. The first key intermediate, compound **48**, was obtained following an already reported sequence of transformation.[42]

We started with the acetal protection of the OH groups in position 4 and 6 of both glucose rings. This reaction was been carried out in dry DMF at 100 °C by reacting anhydrous trehalose with α,α-dimethoxytoluene in presence of catalytic amounts of p-toluenesulfonic acid. Compound **45**, obtained by simple solvent removal, was readily reacted with benzyl bromide and sodium hydride. Even in this case no crude purification was performed and compound **46** was subjected to an acidic deprotection of one of the two acetal protecting groups. This desymmetrization reaction was carried out in a 1/1/0.5 mixture of DCM, methanol and TFA. These reagents ratios and the total reaction time, not exceeding 180 minutes, ensured the formation of the minimum amount of the bis-deprotected sugar. In these conditions the reaction yield was only of 25% but it was easily recovered the unreacted starting material, that can be subjected again to the deprotection. We also tried running the reaction for longer times and using higher amounts of TFA, and this let us obtain higher yield of compound **47** in a single step, but we also recovered high amounts of the bis-deprotected sugar. Since the purification of **47** is easier and the starting material (**46**) can be easily recycled, we think that the conditions reported in scheme 14 are the best ones for this deprotection reaction. The last step of this sequence consisted in the selective protection of the only primary alcohol with the TBDMS group. This was easily achieved by reacting **47** with *tert*-

butyldimethylsilylchloride in presence of TEA and DMAP. The reaction allowed us to obtain intermediate **48** in almost quantitative yield. Its proton NMR is reported in figure 51.

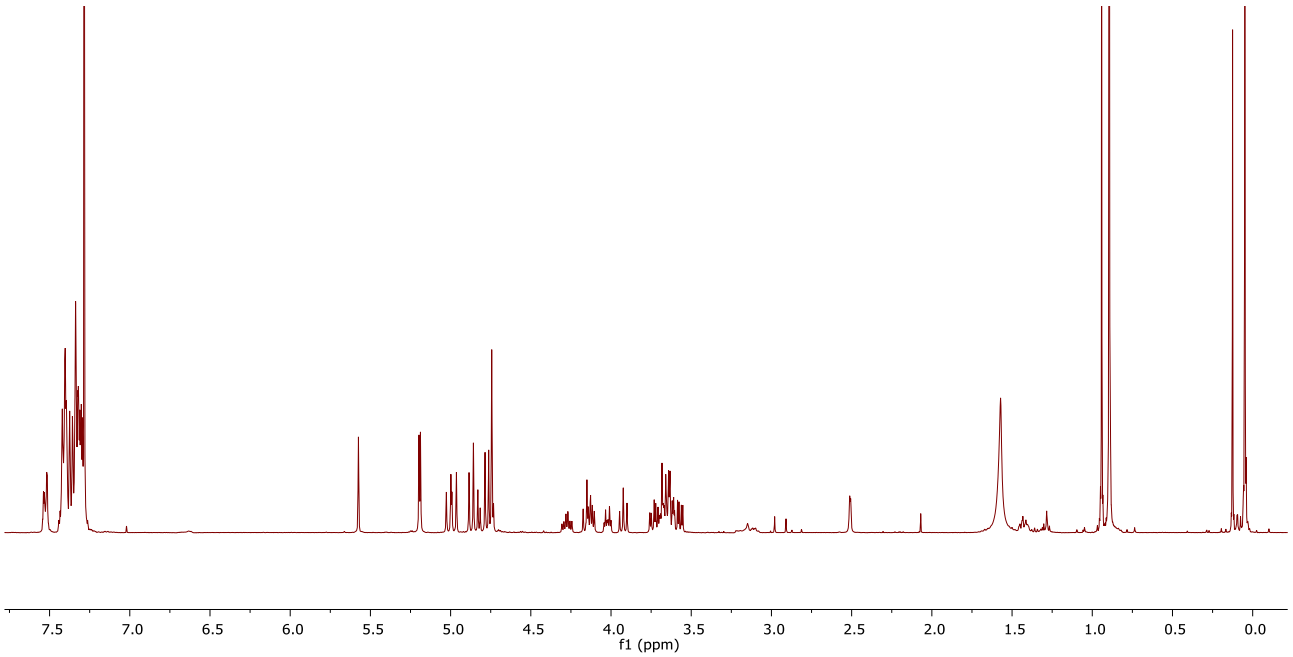

*Figure 51: ^{1}H NMR of compound **48** recorded in $CDCl_3$ at 298K and 400 MHz.*

The key signals here are: the singlet at 5.57 ppm which is generated by the acetal protecting group proton, and the two singlets at 0.89 and 0.05 ppm which are ascribable to the tertbutyl groups and the two methyl groups of TBDMS. It is also possible to observe two other singlets near them, which are probably generated by TBDMSOH which was not removed during the workup. Unexpectedly here the two protons of H_1 and H_1' resonate at the same chemical shift of 5.19 ppm.

Once again, to introduce an azido group in equatorial position we had to first epimerize the free OH group to obtain a galacto-sugar. For this transformation we exploited an oxydative/reductive protocol (Scheme 15).

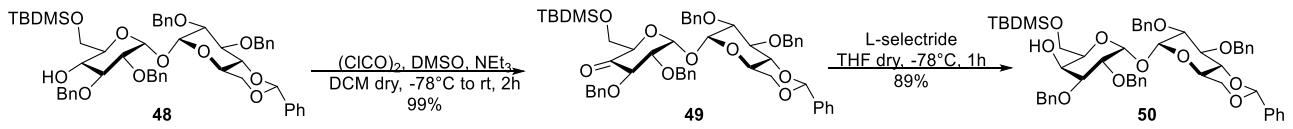

*Scheme 15: Synthesis of compound **50**.*

Firstly, in fact, we oxidized the only free alcohol to the corresponding ketone using Swern conditions. Compound **49** was obtained in very high yields and with no purification needed.

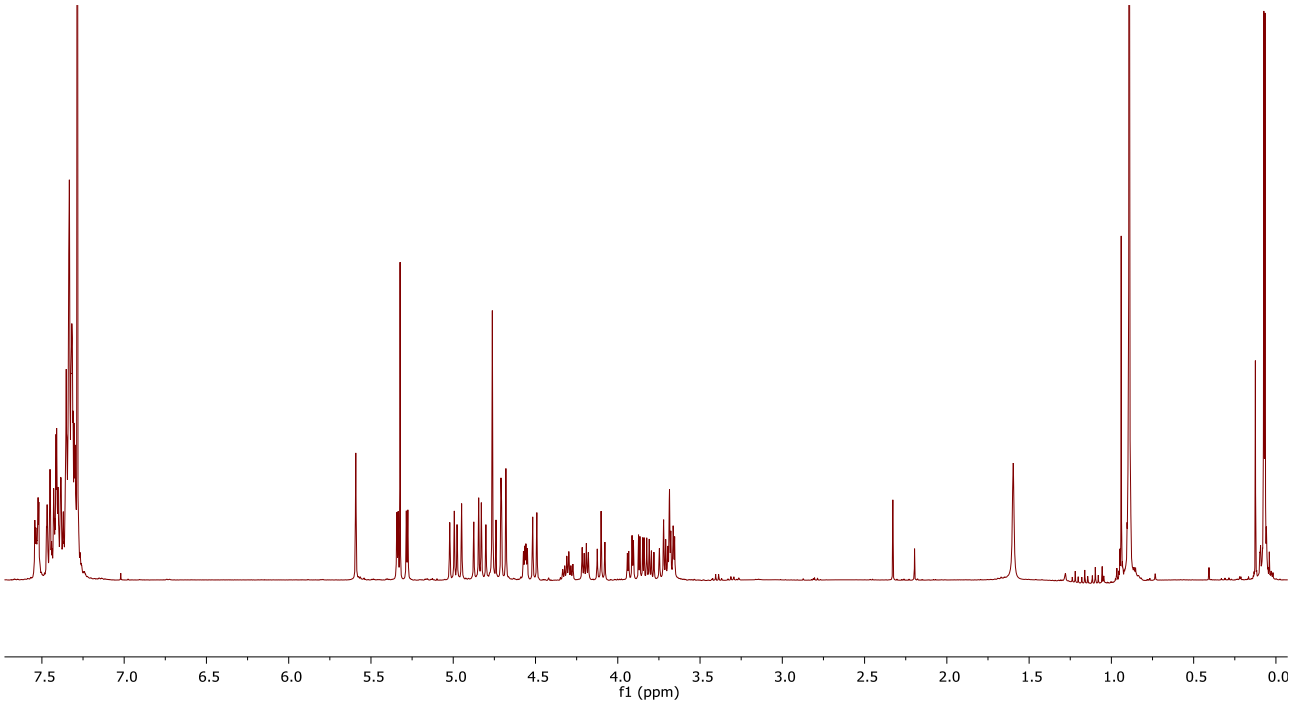

*Figure 52: ^{1}H NMR of compound **49** recorded in CDCl3 at 298K and 400 MHz.*

Here we can notice that the ^{1}H spectrum (Figure 52) has changed compared to that of the reagent. The H_5' signal is now clearly recognizable at 4.56 ppm, a chemical shift which suggest the neighboring presence of an electron withdrawing group, like a ketone. Interestingly integration of the signals highlights the presence of only thirteen protons for the pyranose rings, as requested for the product.

The oxidation is further supported by the ^{13}C APT spectrum (Figure 53) where it is possible to observe a signal at 202.7 ppm, clearly ascribable to a ketone carbon.

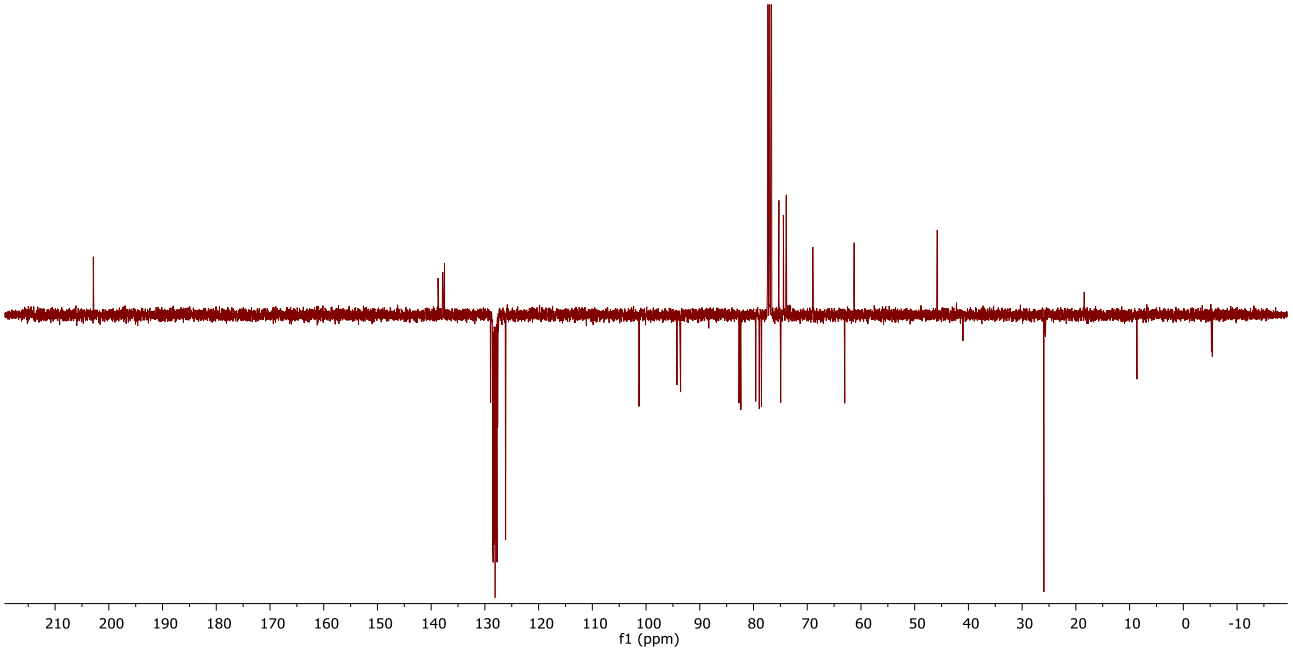

*Figure 53: ^{13}C APT spectrum of compound **49** recorded in $CDCl_3$ at 298K and 400 MHz.*

We envisaged that ketone **49** could have been easily reduced to the desired epimer **50** by simply using $NaBH_4$ as the reducing agent. The selectivity of this reaction can be explained by Cram's chelate model. In theory, the metal should in fact coordinate both the carbonyl group and the benzyl ether in position 3, leading to a staggered conformation in which only one enantioface, the desired one, is capable of reacting with the incoming H^- nucleophile. The selectivity observed was, unfortunately, not so remarkable, since we recovered, after chromatographic separation, about 65% of the desired product while the rest was the other epimer. Reiteration of these two fast reactions, Swern oxidation and reduction, could have been a strategy to enhance the overall yield, however we decided to tune the reduction condition to enhance its enantioselectivity. To do so, we tried to switch the reducing agent to a bulkier one, as L-selectride, that possibly would have permitted the reduction on the correct ketone face.

As reported in scheme 15, we reduced **49** using L-selectride in dry THF at -78°C. The low temperature was also needed to enhance the enhance the stereochemical outcome of the reaction. With this protocol we were able to obtain the desired galacto-trehalose **50** in 89% yield. Its proton NMR is reported in figure 54.

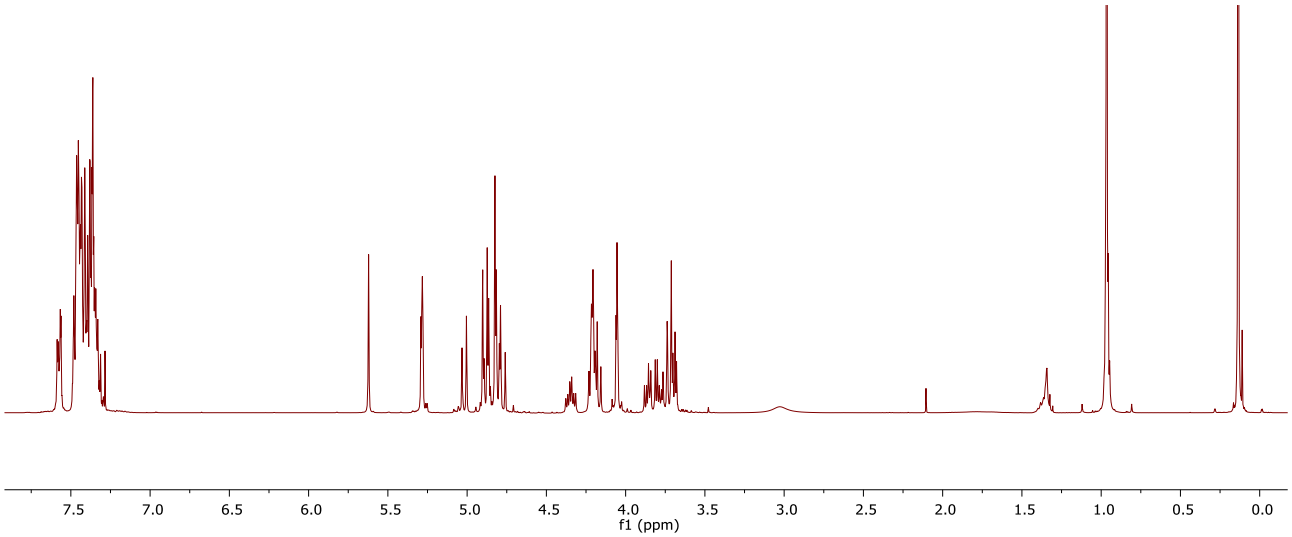

*Figure 54: ^1H NMR of compound **50** recorded in $CDCl_3$ at 298K and 400 MHz.*

Here it is possible to observe that all the protecting groups are still installed onto the disaccharide. The observation that the signal of H5', previously resonating at 4.56 ppm, moved under the multiplet at 4.05 ppm support the success of the reaction and of the correct setereochemistry. In figure 55 is reported the stacking of the NMR spectra of compound **48**, **49** and **50**, that allows to better compare and notice the changes occurring in the spectra during the reaction pathway.

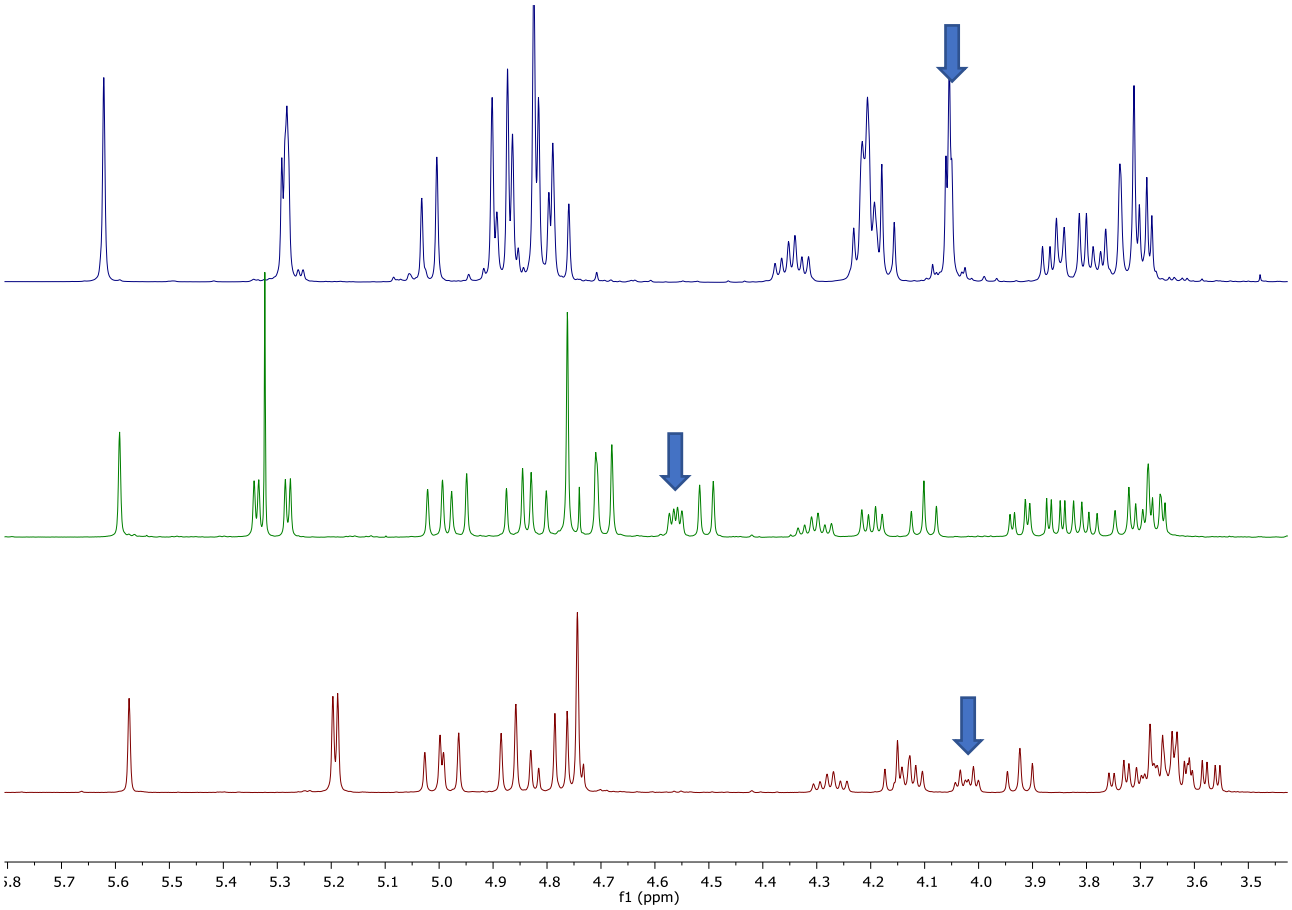

*Figure 55: Stacking of the proton NMR spectra of compound **48**, **49** and **50** (from bottom to top).*

The most easily trackable signal is, as described above, the one of H_5' which, due to its position, is clearly affected by the induced transformations.

The last step of the synthesis involved the introduction of the azido group in the desired equatorial position.

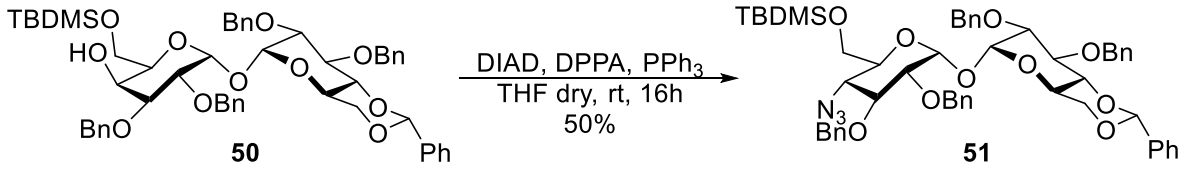

*Scheme 16: Mitsunobu reaction on compound **50**.*

To do so we employed Mitsunobu conditions (Scheme 16), by reacting **50** with diisopropyl azodicarboxylate, diphenyl phosphoryl azide, and triphenyl phosphine. Surprisingly we could not achieve conversions of the starting material higher than 50%, even after multiple reagents additions. However, after chromatographic purification, we were able to obtain the desired 4-azido trehalose **51** at least in high stereoselectivity. The relative NMR spectrum is reported in figure 56.

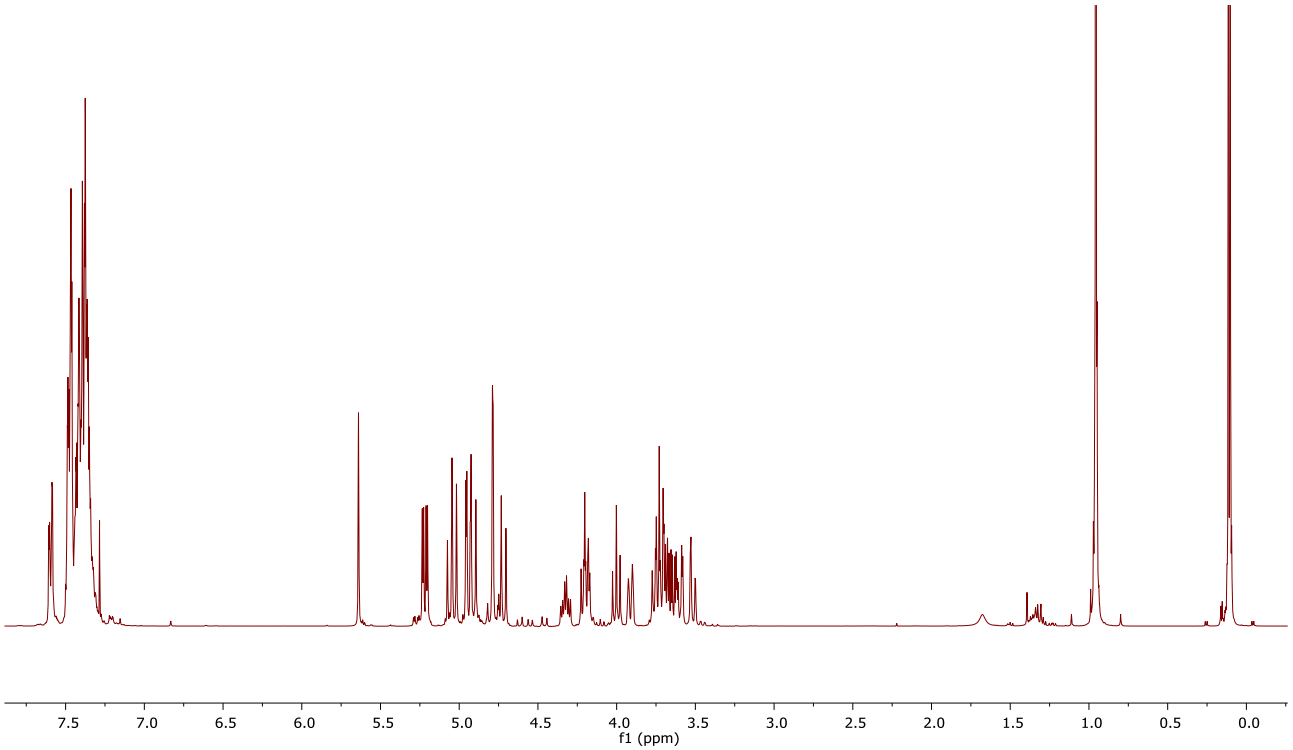

*Figure 56: ^{1}H NMR of compound **51** recorded in $CDCl_3$ at 298K and 400 MHz.*

The spectrum of compound **51** shows that the H5' neighboring groups changed their position once again and, in fact, its signal is clearly recognizable at 3.90 ppm (better view in the stacking reported in figure 57). It resonates at lower ppm as expected by the α substitution of an OH group by an azido one.

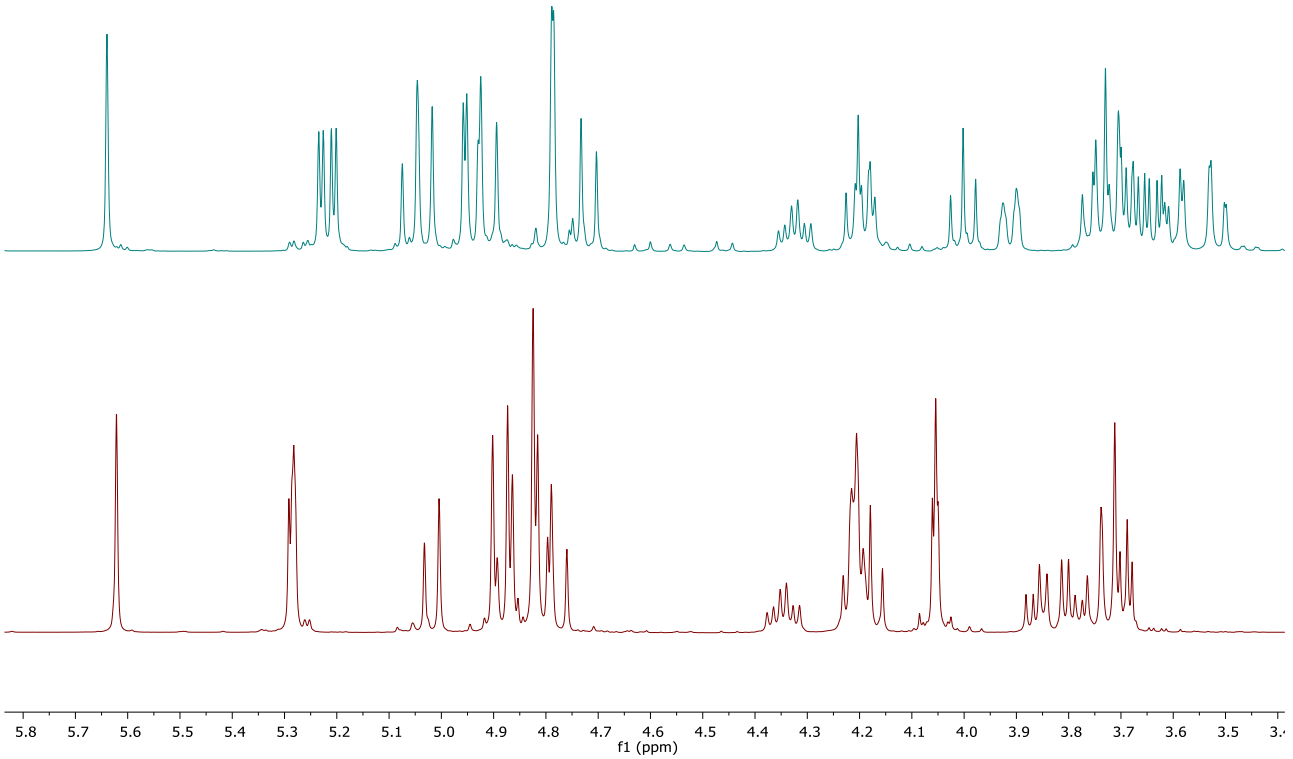

*Figure 57: Stacking of the ^{1}H NMR spectra of compounds **50** (bottom) and **51** (top).*

We also recorded the IR spectrum of compound **51** (Figure 58) where it is clearly observable the stretching of an azido group at 2107 cm^{-1}.

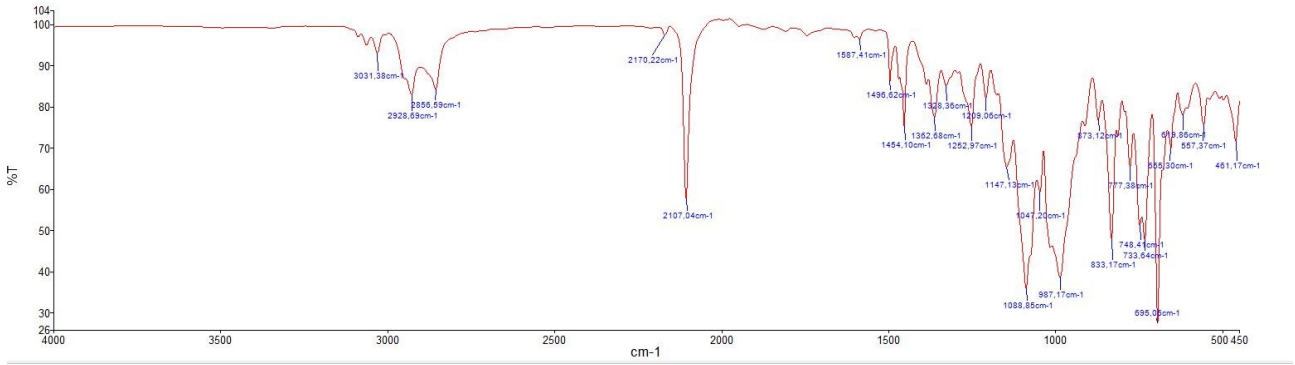

*Figure 58: IR spectrum of compound **51**.*

This new synthetic strategy, therefore, allowed us to prepare the desired disaccharide in a global yield of 9.7%. On top of that, it is important to notice that this sequence (Scheme 14 + 15 + 16) is preferable compared to the previous one (Scheme 13) also because into two steps (the deprotection of **46**, and the Mitsunobu on **50**) unreacted reagents are recovered quantitatively and can be re-used.

2.3.3 Mannose functionalization

In parallel with the synthesis of trehalose derivatives, it was also decided to synthesize another azido-sugar to be clicked onto the calixarene scaffold to have a glycocalixarene to be used in biological test as negative control. The conjugation of this saccharide to propargyl derivatives **34** and **38** should result in calixarene glycoconjugates very similar to the target compounds containing trehalose, but with a different sugar and this new glycoconjugate could be very useful to verify that the biological activity of the trehalose calixarenes is due to the presence of trehalose units and is not simply related to any carbohydrates or even to the calixarene structure per se. It was therefore decided to synthesize the 6-azido-α-methyl mannoside, a monosaccharide quite similar to the terminal glucose unit of trehalose but with a different stereochemistry on the C2 atom.

It was, therefore, decided to proceed using methyl-α-D-mannopyranoside as the starting substrate (Scheme 17). The -OH group on C6, given the greater nucleophilicity, is the only -OH groups that is sulfonated to give compound **52**, using stoichiometric ratios 1:1 of tosyl chloride. Subsequently, positions 2,3,4 were protected with benzoyl chloride obtaining compound **53**. This was then reacted with sodium azide in DMF to obtain compound **54**.

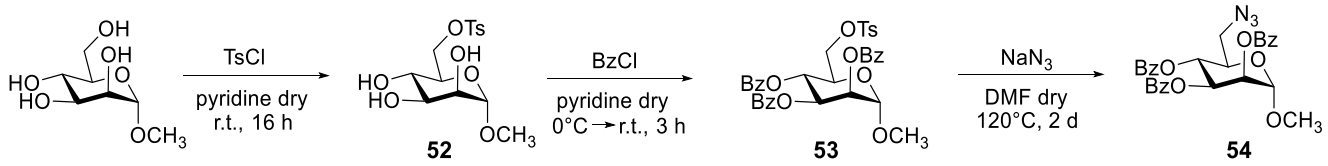

*Scheme 17: Preparation of compound **54**.*

The desired product has been obtained in 29% overall yield and its proton NMR is reported in figure 59.

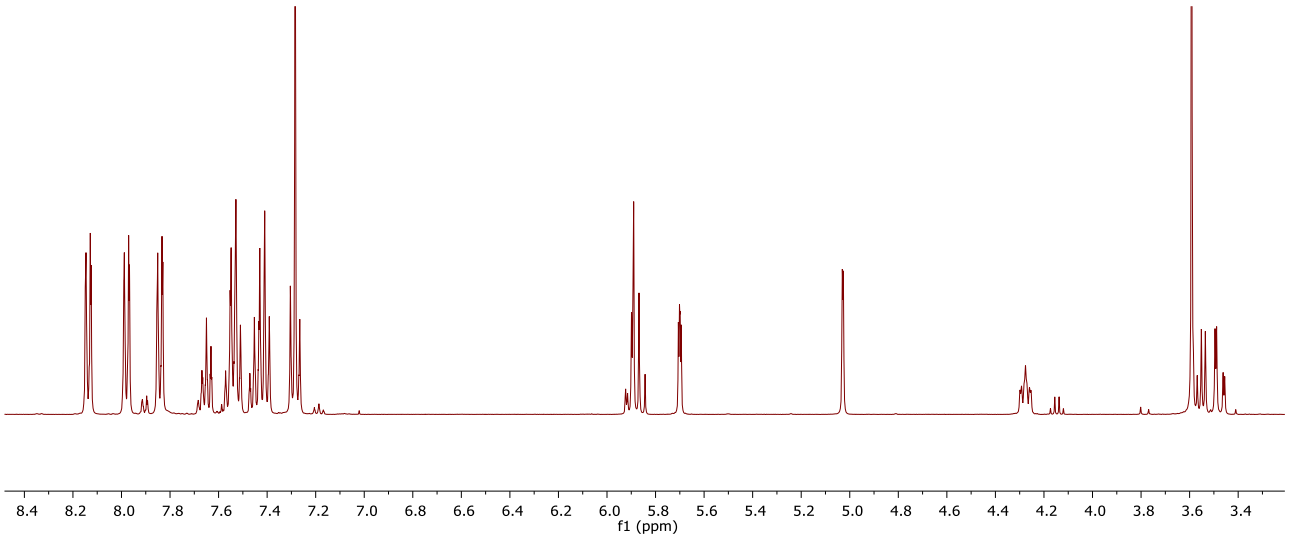

*Figure 59: ^{1}H NMR of compound **54** recorded in $CDCl_3$ at 298K and 400 MHz.*

Typical of this product are: i) a multiplet at 5.90 ppm generated by H_3 and H_4, ii) the doublet of doublets at 5.70 ppm with two small J of 2.9 and 1.8 Hz and therefore assigned to H_2; iii) a doublet resonating at 5.03 ppm due H_1; the multiplet at 4.28 ppm of H_5. The last two protons, H_{6a} and H_{6b} give two doublets of doublets in the 3.57-3.42 ppm region in accordance with the presence of a neighboring azido group.

2.3.4 Glycoconjugates synthesis

Once both the calixarene scaffolds and the saccharide structures were obtained, they were combined to prepare the glycoconjugates reported in figure 60.

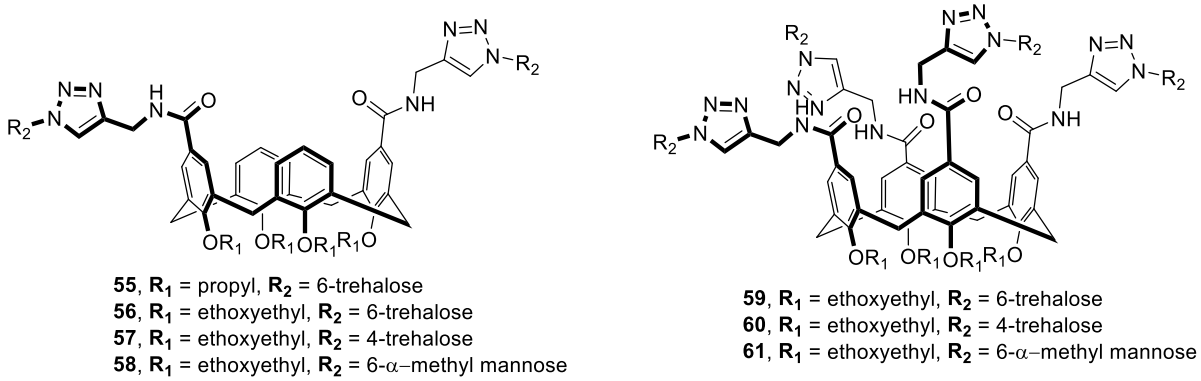

Figure 60: The desired glycoconjugates.

The two reagents (azido sugar and alkynylcalixarene) were linked together thanks to a CuAAC. The general conditions employed are reported in scheme 18.

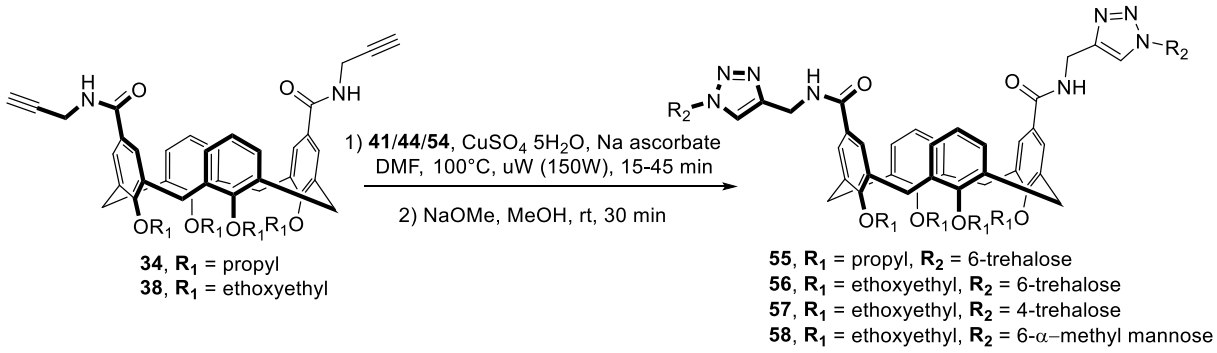

*Scheme 18: Schematic representation of the conditions employed for the synthesis of **55**, **56**, **57** and **58**.*

All cycloadditions were carried out in DMF at 100°C with the aid of microwaves using an in situ generated Cu(I) catalyst. We observed that a maximum of 45 minutes of reaction were enough to form the desired products. Generally, the crude was purified by column chromatography. After this the compounds were all deprotected following the Zemplèn protocol, obtaining the target glycoconjugates in decent yields (detailed in the experimental section).

Below are reported (Figure 61-62), as an exemplification, the ^{1}H NMR spectra of two of these divalent conjugates.

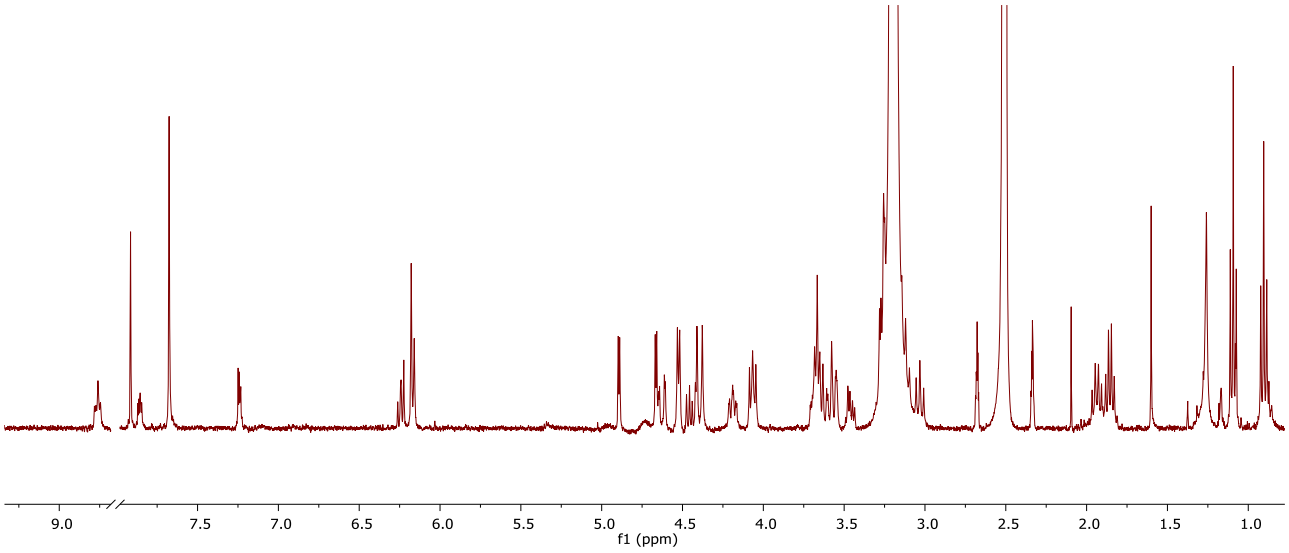

*Figure 61: ^{1}H NMR of compound **55** recorded in deuterated DMSO at 298K and 400 MHz.*

Here it is possible to observe few diagnostic signals that suggest the obtainment of the desired compound **55**. Noteworthy are the two singlets at low fields at 7.91 and 7.68 ppm, which are generated by the triazole protons and the aromatic protons of the functionalized calixarene ring, respectively. The ratio of their integrals, as expected, is 1:2. This proved that the alkyne-modified scaffold reacted twice in a CuAAC and that the sugars is really linked to the calixarene scaffold. The calixarene has been modified as intended and this can be deduced by the presence of the doublet at 4.98 ppm generated by the trehalose H_1 proton, which in addition has the same integral as the signal of the triazole protons. Interestingly, the wide difference in chemical shift between unsubstituted (~6.25 ppm) and para-substituted (7.68 ppm) ArH protons indicates that, in polar solvents (so as in water should be), the macrocycle adopts a flattened cone conformation with the bulky trehalose functionalized arm diverging one from the other.

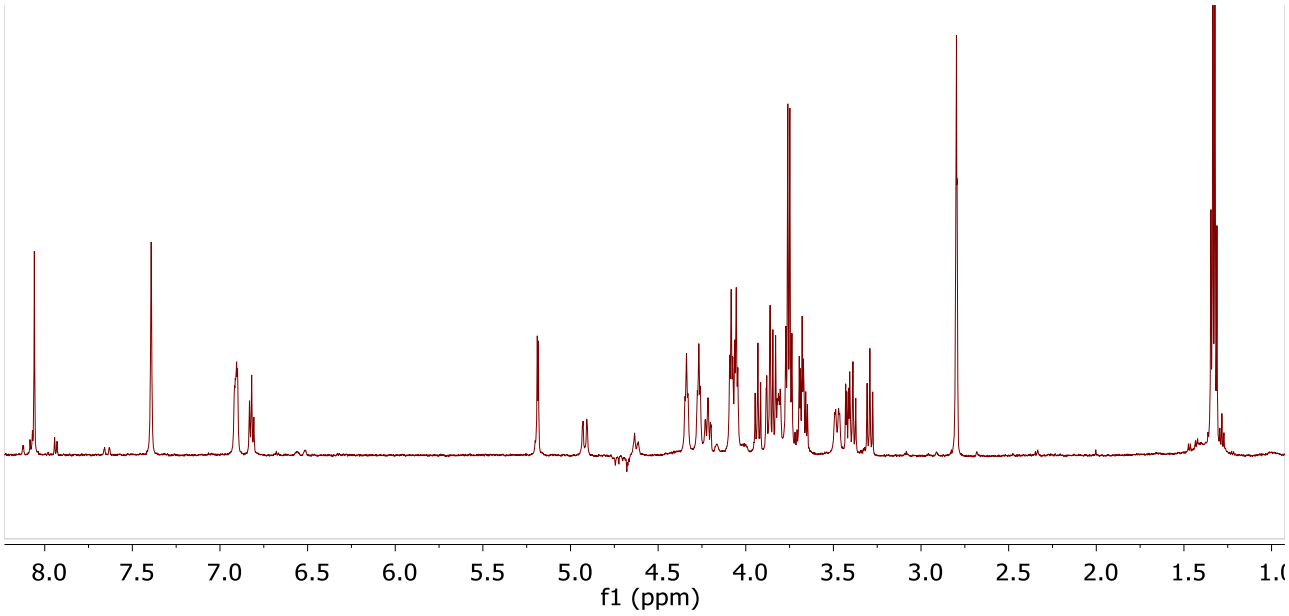

*Figure 62: ^{1}H NMR of compound **56** recorded in deuterated PBS and 20% of deuterated DMSO at 298K and 400 MHz.*

The same diagnostic signals described above can be found also in the ^{1}H NMR spectrum of compound **56**. This compound, bearing ethoxyethyl chains at the lower rim, is soluble in phosphate buffer D_2O solution with 20% DMSO-d_6 proving it can be used in biological tests. Also, in this case the calixarene macrocycle is in a flattened cone conformation, even though the difference in chemical shifts between the unfuctionalized (6.85 ppm) and functionalized (7.40 pmm) ArH protons is less marked than in case of compound **55**.

For the synthesis of the tetravalent glycoconjugates (Scheme 19) we followed the same protocol described above for the divalent ones, just changing the equivalents of azido-sugars used.

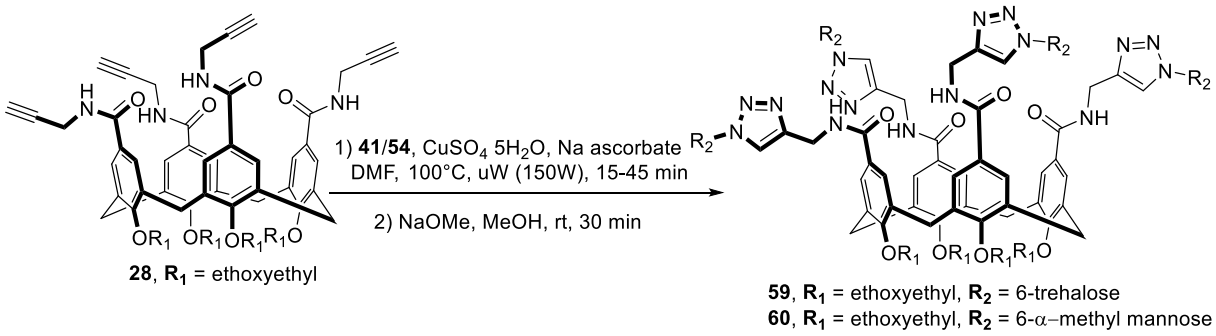

*Scheme 19: Schematic representation of the conditions employed for the synthesis of **59** and **60**.*

The ^{1}H NMR spectra of compound **59** is reported in figure 63.

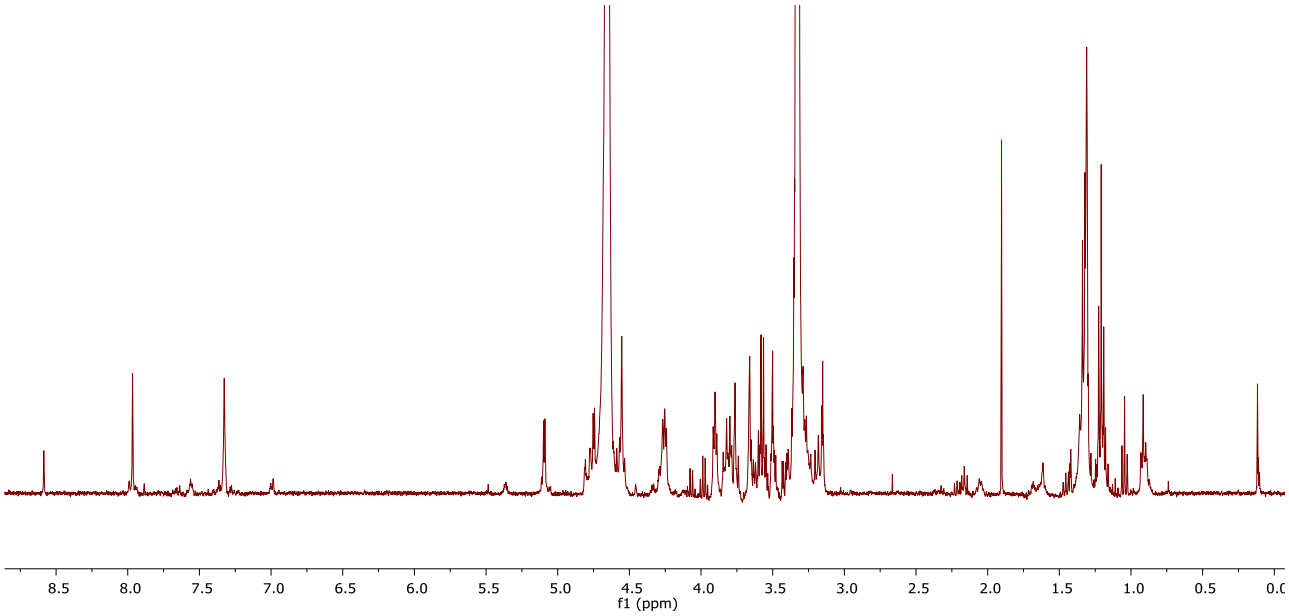

*Figure 63: ^{1}H NMR of compound **59** recorded in CD_3OD at 298K and 400 MHz.*

The NMR spectrum of the tretra functionalized calixarene **59** shows three main signals which prove the compound identity. These are: the singlet a 7.97 and 7.33 pmm and the doublet at 5.09 ppm. These signals correspond respectively to the triazole protons, the calixarene aromatic ones and finally to the H_1 of the terminal glucose ring of trehalose. Their integral ratio is, as expected, 1:2:1.

Unfortunately, due to time restrains we were not able to complete the synthesis of the tetraglycosylated calix[4]arene. However, we were able, at least, to run the click reaction which gave us compound **61** in 30% yield (Scheme 20).

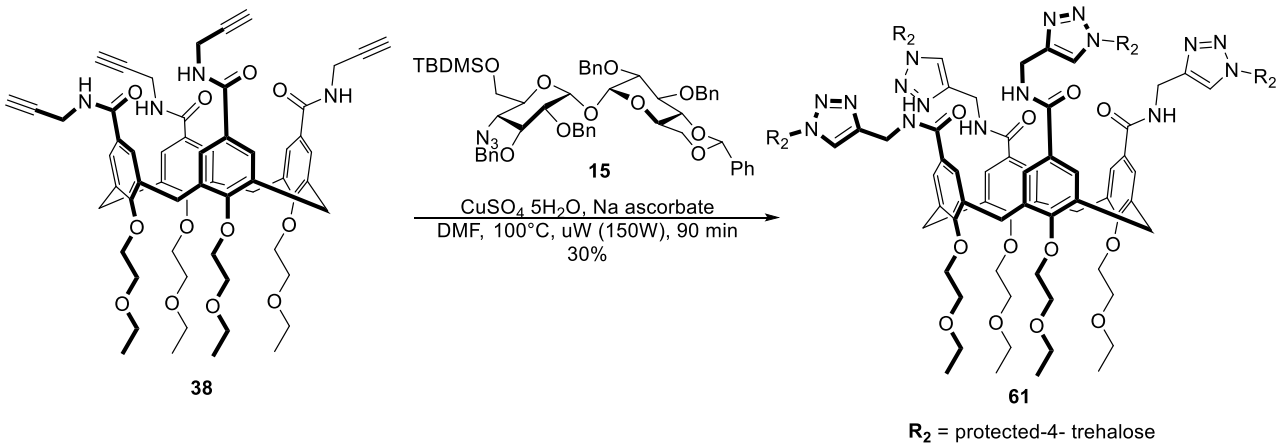

*Scheme 20: Synthesis of compound **61**.*

2.4 NMR studies

The synthesis of the calixarene ligands described above took many months. During this time, we started studying if the compounds obtained in the meantime showed any recognition properties towards bacteria. We were helped in this task by our collaborators, of the research group of Professor Cristina Airoldi at the University of Milano Bicocca. We, in fact, decided to test the affinity of our compounds by performing NMR experiments, in particular STD, with live bacteria, employing *Pseudomonas putida*, *Staphylococcus epidermidis* and *Mycobacterium smegmatis* as models respectively for Gram-positive, Gram-negative and Mycobacteria.

The tested compounds are collected, altogether, in figure 64. It is possible to see that also a negatively charged calixarene (**CM1**), which was already present in our laboratory, was tested. In particular, **CM1** was used as a control molecule. In fact, this compound, due to the four negative charges present on its upper rim at physiological pH, should not be able to interact with any of the studied bacteria cell walls. This control is very useful to assess that the interactions observed with these ligands are due to their upper rim functionalization and not simply to the presence of the calixarene macrocycle.

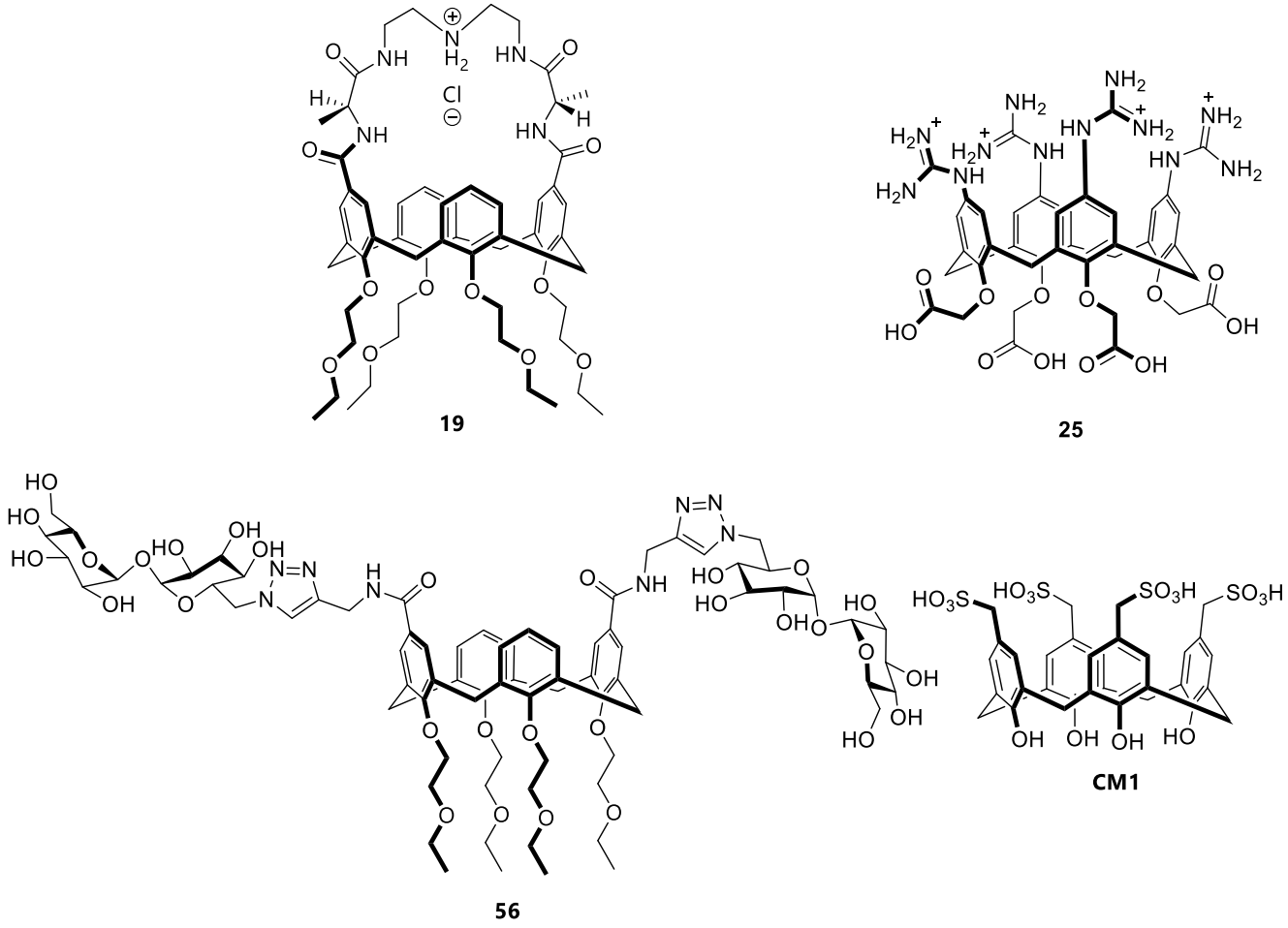

Figure 64: Calixarenes tested during the STD-NMR experiments.

Initially we tested, by STD experiments (Figure 65), the ability of compound **19** to interact with the Gram-positive *S. epidermidis*.

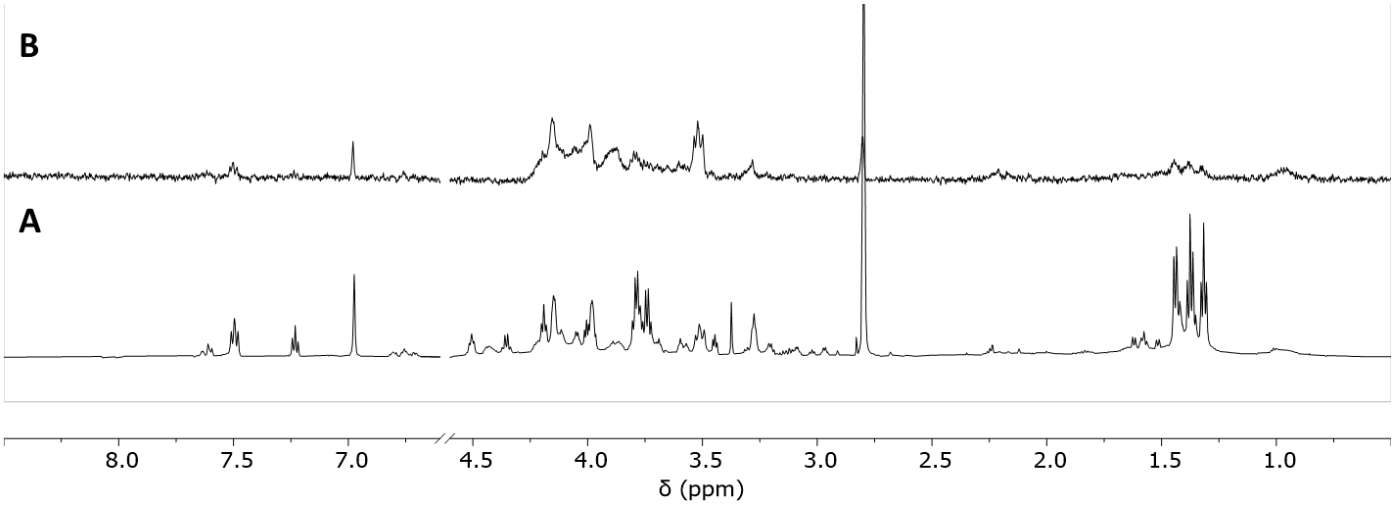

*Figure 65: **A)** ^{1}H NMR spectrum of **19** 2mM + S. epidermidis (OD 1.5 in 750 µL ×2 pelleted and resuspended in 250 µL), d-PBS + d6-DMSO (20%). **B) 19** 2mM + S. epidermidis (OD 1.5 in 750 µL ×2 pelleted and resuspended in 250 µL), d-PBS + d6-DMSO (20%), STD, 3s, 5.15 ppm.*

Quite interestingly, due to the presence of some of the peaks of the calixarene ligand **19** in the STD spectrum (Figure 65B), we can assume that compound **19** is binding to the bacteria.

To prove its possible selectivity for Gram-positive bacteria, we tested compound **19** also with the Gram-negative *P. putida* and the mycobacteria *M. Smegmatis*. The recorded STD spectra are respectively reported in figure 66 and figure 67.

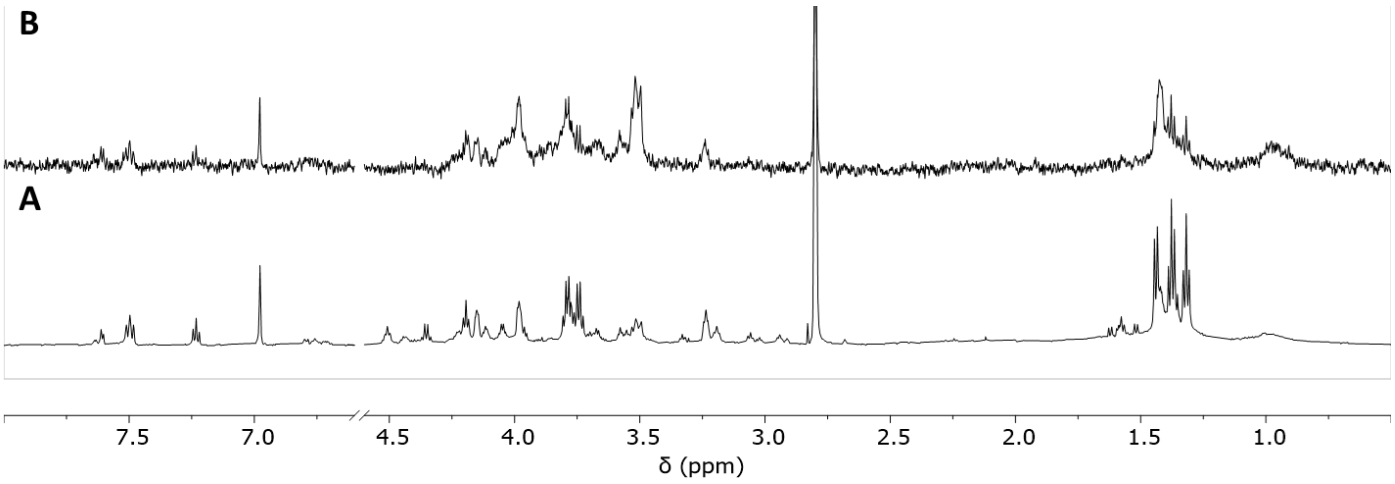

*Figure 66: **A**) **19** 2mM + P. putida (OD 1.5 in 750 µL ×2 pelleted and resuspended in 250 µL), d-PBS + d6-DMSO (20%). ^{1}H NMR spectrum **B**) **19** 2mM + P. putida (OD 1.5 in 750 µL ×2 pelleted and resuspended in 250 µL), d-PBS + d6-DMSO (20%). STD, 3s, 5.15 ppm.*

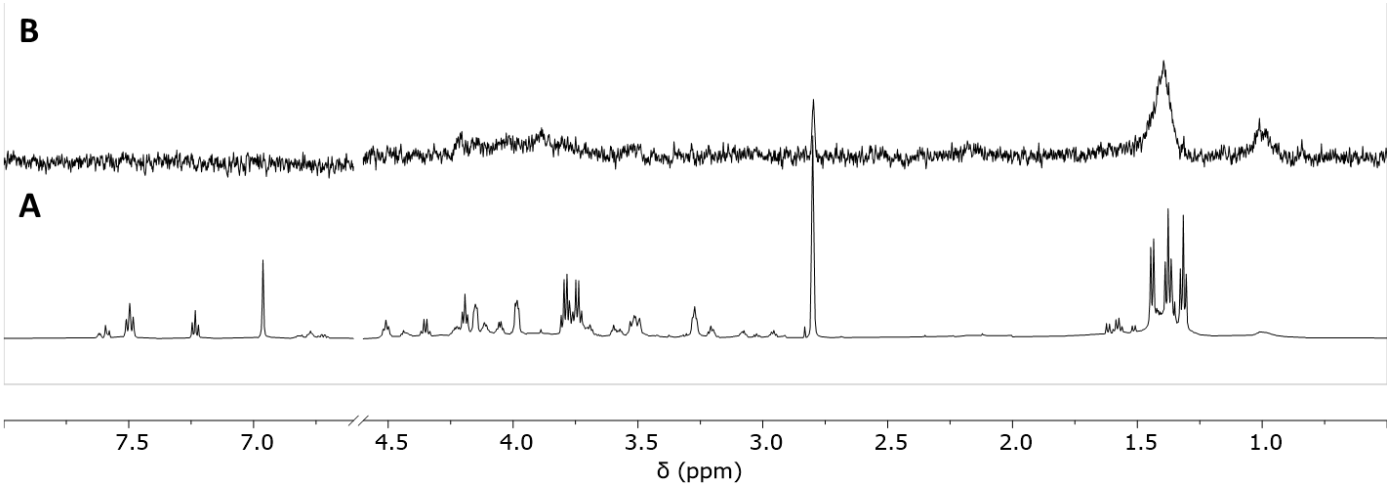

*Figure 67: **A**) **19** 2mM + M. smegmatis (OD 1.5 in 750 µL ×2 pelleted and resuspended in 250 µL), d-PBS + d6-DMSO (20%), ^{1}H NMR spectrum. **B**) **19** 2mM + M. smegmatis (OD 1.5 in 750 µL ×2 pelleted and resuspended in 250 µL), d-PBS + d6-DMSO (20%), STD, 3s, 5.15 ppm.*

From this data emerges that our ligand is not Gram-positive selective, in fact its STD spectrum in presence of *P. Putida* has also some clearly recognizable ligand signals. This behavior points out how the interaction with the D-Ala-D-Ala fragment of peptidoglycan, observed in apolar solvents by ESI-MS studies, is not necessarily the most important one when complex environments, like a polar solvent or, especially, live bacteria, are into play. Indeed, up to the present state of our research, it was not yet possible to clearly identify which are the molecular targets on bacteria of ligand **19**. Although peptidoglycan is present also in the cell wall of Gram-negative bacteria, it is rather deep in its structure and well protected by the outer phospholipid bilayer, so that its access from the exterior of the cell wall by **19** looks quite difficult. Another hypothesis is that the targets of **19** are different onto the two different classes of bacteria. However, some sort of selectivity can be inferred, at least toward mycobacteria, since the STD spectrum of our peptidocalixarene **19** in presence of *M. Smegmatis* (Figure 67B) is rather flat, apart from the bacteria residual signals at high fields, suggesting that no interactions between the two partners was established in these conditions.

To follow, we also studied the interaction of tetraguanidinium-tetracarboxylate compound **25** with our set of bacterial strain, again by using NMR. In this case, however, no STD studies was needed, since the information about the selectivity of this ligand towards the different bacteria strains could be easily deducible form simple ^{1}H NMR spectra recorded on the different solutions, where both the ligand and the bacteria are present (Figure 68).

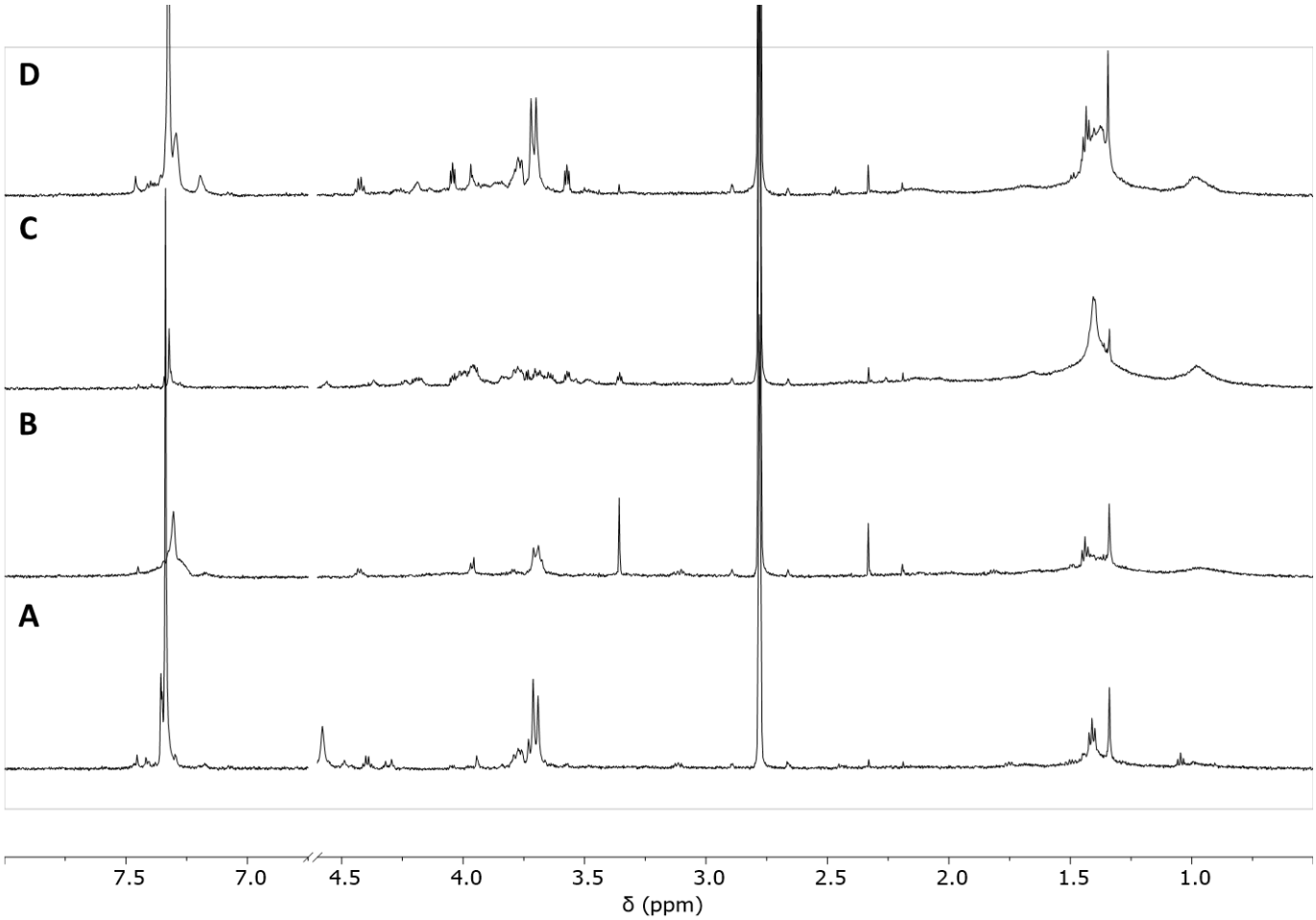

*Figure 68: [1]H NMR spectra of: **A**) **25** 2mM, d-PBS + d6-DMSO (20%). **B**) **25** 2mM + P. putida (OD 1.5 in 750 µL ×2 pelleted and resuspended in 250 µL), d-PBS + d6-DMSO (20%). **C**) **25** 2mM + S. epidermidis (OD 1.5 in 750 µL ×2 pelleted and resuspended in 250 µL), d-PBS + d6-DMSO (20%). **D**) **25** 2mM + M. smegmatis (OD 1.5 in 750 µL ×2 pelleted and resuspended in 250 µL), d-PBS + d6-DMSO (20%).*

In the case of ligand **25**, it was already possible to directly evaluate the interaction with the bacteria by comparing the signals of the ligand alone (Figure 68A) in absence of any bacteria, with those in the presence of either *P. Putida* or *S. Epidermidis*. With both these bacteria, in fact, the signal of the ligand broadened extensively (Figure 68B and Figure 68C) proving the binding. On the other hand, it is also worth noting how the spectrum of the free ligand and of that of the solution containing both compound **25** and *M. Smegmatis* (Figure 68D) are very similar, and simply due to a superposition of the signals of some of the protein residues to those of **25**, with no broadening of the latter signals observable. This indicates no binding of **25** to the Mycobacteria. All these are clear indications which suggest how compound **25** is able to strongly bind to both Gram-positive and Gram-negative bacteria (*S. Epidermidis*, *P. Putida*) but cannot interact with Mycobacteria. In fact, the line broadening is due to the formation, in solution, of a complex between the ligand and the bacteria. This new object, due to its dimensions, has shorter relaxation times compared to those of a relatively small molecule like the

unbound ligand, resulting in it having broader NMR signals. This situation is clearly not observable while having the mycobacterium in solution since the NMR spectrum has very sharp signals for the ligand, proving that no interactions have been established between the two partners.

The lack of selectivity observed between these two classes of bacteria can be rationalized by the fact that, overall, both the surfaces of Gram-positive and Gram-negative are negatively charged, even if the latter is much more negative than the former. The positively charged guanidinium groups at the upper rim of the calixarene **25** interact therefore with both type of bacteria being apparently unable to distinguish between them. A competitive experiment could be interesting to study if the different charge density could be really a discriminant factor to trigger a selectivity between Gram-positive and Gram-negative bacteria by **25**.

In this case too, mycobacteria showed no affinity towards the ligand, proving how difficult is to develop systems capable of interacting with them.

Finally, we tried to test the two trehalose bisfunctionalized calixarenes **55** and **56** bearing, respectively, propyl or ethoxyethyl chains at the lower rim. However, the solubility of **55** in the solvents used (d-PBS and even 20% DMSO) was not enough to allow us to perform the required NMR experiments. The increase of the amount of d-DMSO was not an option because this could result in the death of the bacteria, thus impairing the experiment.

We were able, however, to test compound **56**, that bearing ethoxyethyl chains results to be much more soluble in the mixture of solvents used. The STD experiments, collected in presence of *M. smegmatis*, are reported in figure 69.

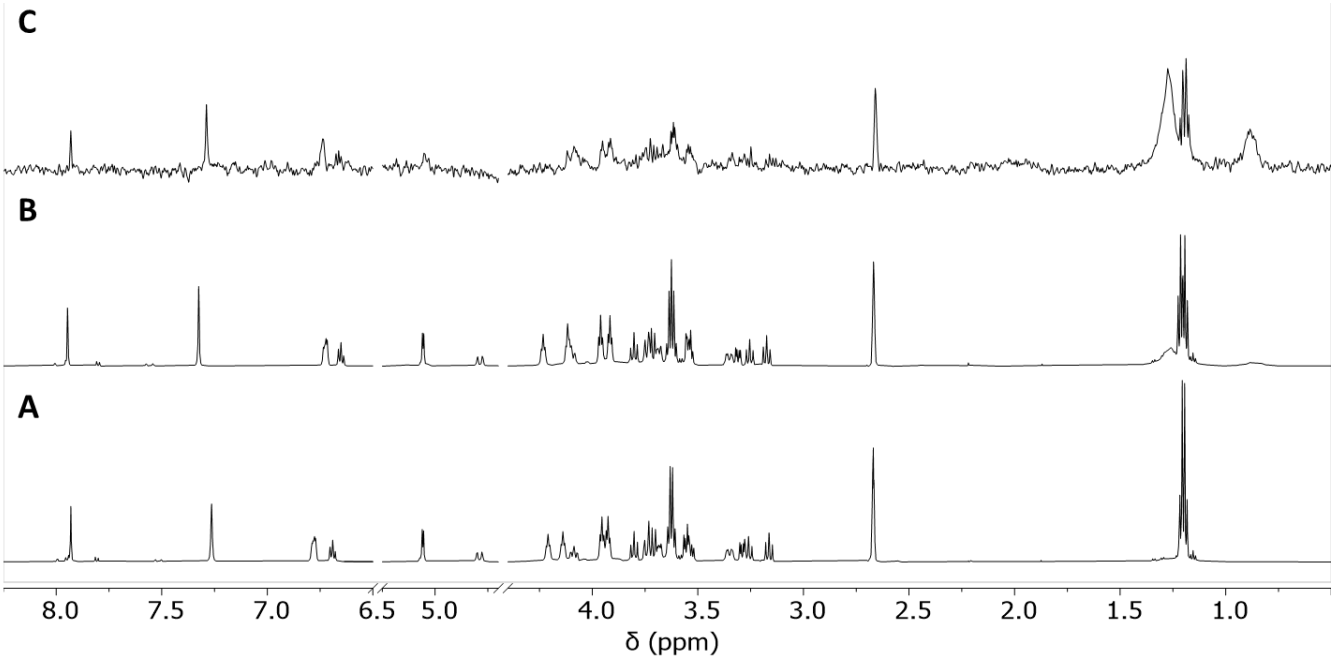

*Figure 69: **A**) **56** 2mM, d-PBS + d6-DMSO (20%). 1H NMR, **B**) **56** 2mM + M. smegmatis (OD 1.5 in 750 µL ×2 pelleted and resuspended in 250 µL), d-PBS + d6-DMSO (20%). 1H NMR, **C**) **56** 2mM + M. smegmatis (OD 1.5 in 750 µL ×2 pelleted and resuspended in 250 µL), d-PBS + d6-DMSO (20%). STD, 3s, 0.0 ppm*

Interestingly, it is still possible to observe the signals of ligand **56** in the STD spectrum (Figure 69C), suggesting that this compound is able to interact with this type of mycobacteria. However, as shown in figure 70 and figure 71, this ligand can also bind to both Gram-positive and Gram-negative bacteria.

Compound **56**, therefore, is a good ligand for bacteria cell wall, but it is not a selective ligand for mycobacteria, as was hypothesized. Yet, these results are still very interesting because none of the calixarenes studied before were able to bind to this type of bacteria and, in general, it is well known that Mycobacteria are difficult to be targeted. We are, however, still interested to study the behavior of the remaining trehalose-base ligands **59** and **60** that, for reason of time, could not be achieved up to now. These studies will allow to verify if the different functionalization of the trehalose, but also the increase of valency of the ligands, could enhance both the selectivity and affinity of these ligands towards *M. smegmatis*.

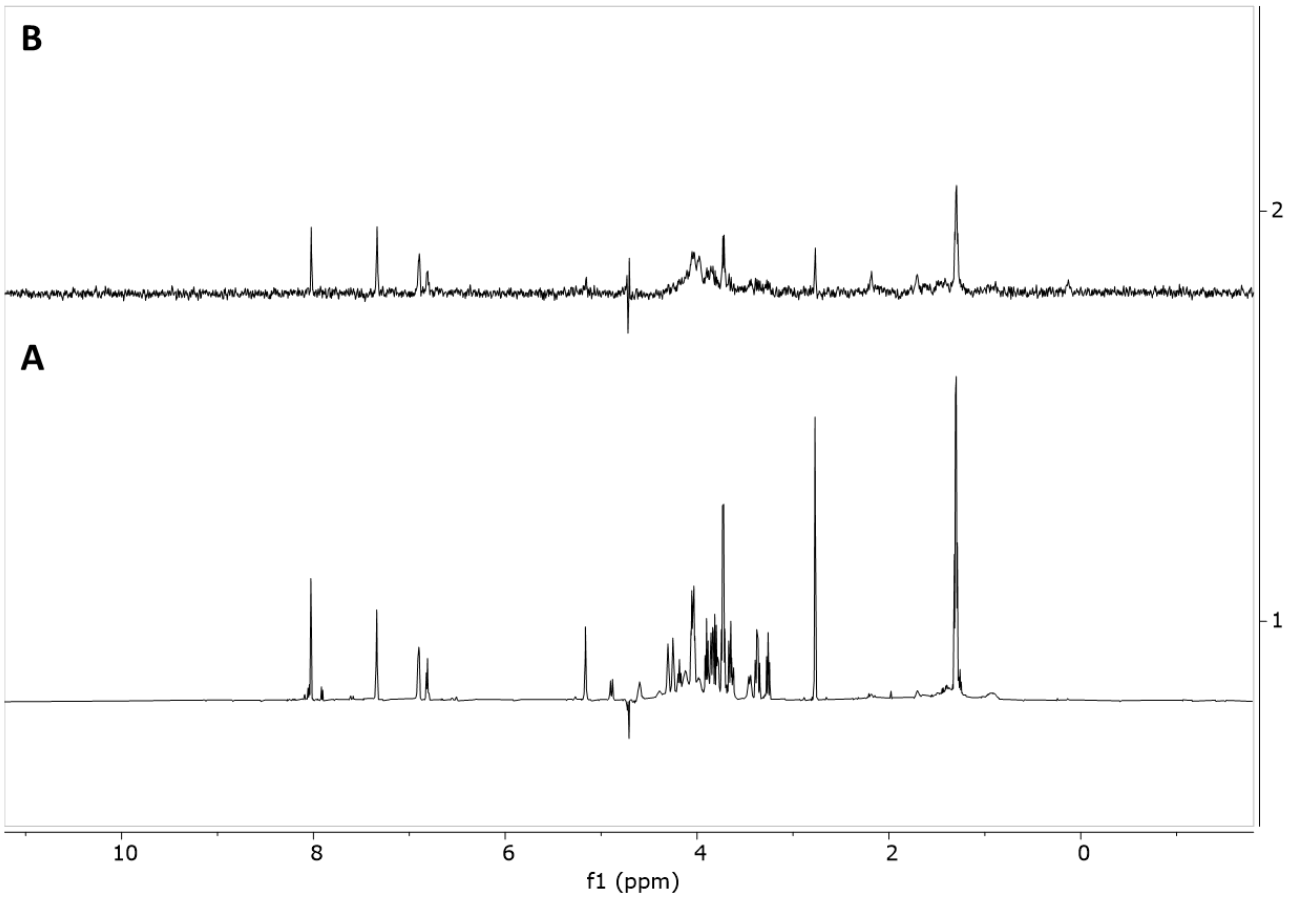

*Figure 70: **A**) **56** 2mM + S. epidermidis (OD 1.5 in 750 µL ×2 pelleted and resuspended in 250 µL), d-PBS + d6-DMSO (20%). ^{1}H NMR, **B**) **56** 2mM + S. epidermidis (OD 1.5 in 750 µL ×2 pelleted and resuspended in 250 µL), d-PBS + d6-DMSO (20%). STD, 3s, 0.0 ppm*

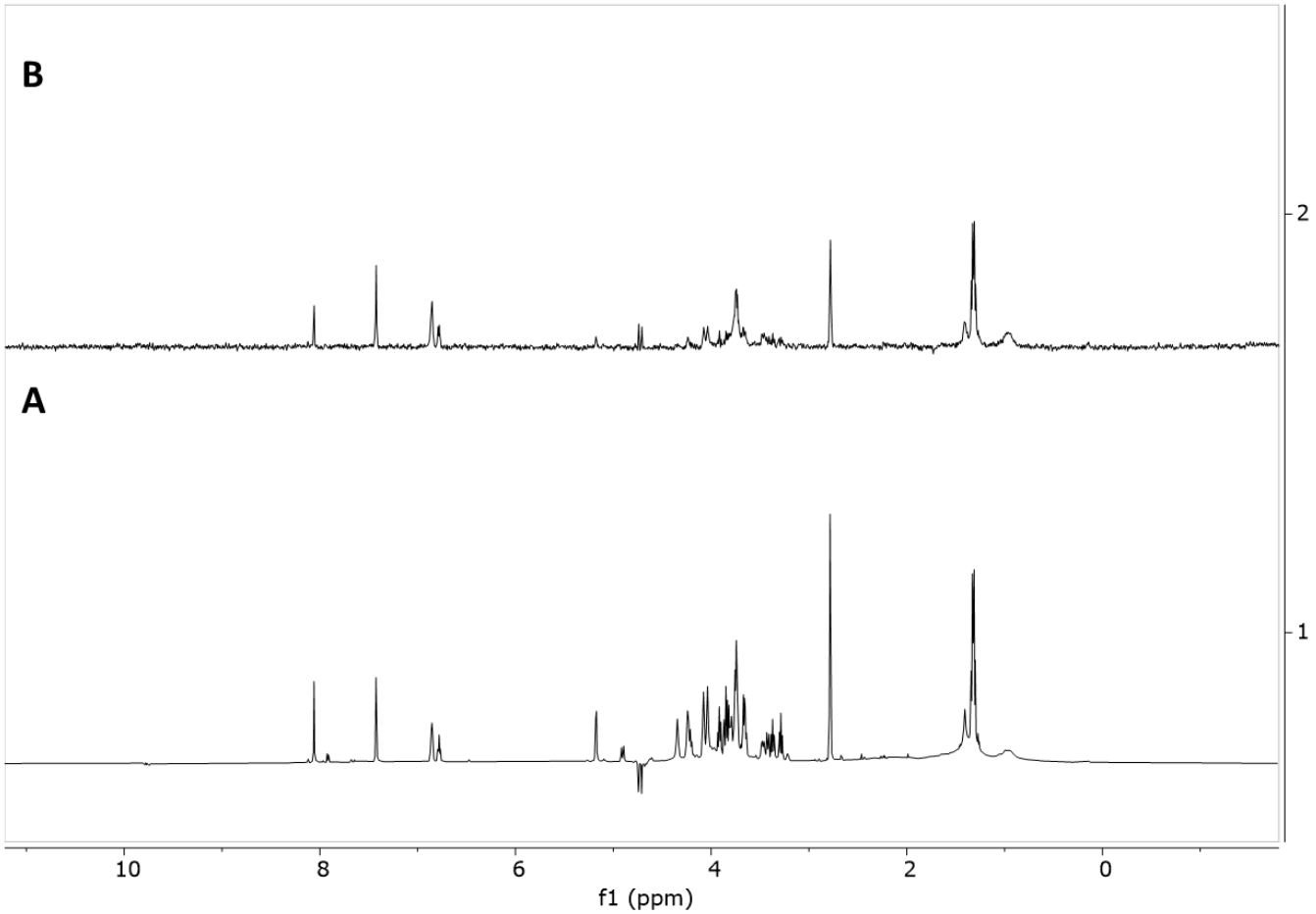

*Figure 71: **A**) **56** 2mM + P. Putida (OD 1.5 in 750 µL ×2 pelleted and resuspended in 250 µL), d-PBS + d6-DMSO (20%) ^{1}H NMR, **B**) **56** 2mM + P. Putida (OD 1.5 in 750 µL ×2 pelleted and resuspended in 250 µL), d-PBS + d6-DMSO (20%). STD, 3s, 0.0 ppm*

Finally, as introduced before, we also studied the behavior of a tetramethylsulfonated calix[4]arene (**CM1**), used as a control, with the three different bacteria strains. In this case it is reported in figure 72 the STD spectrum when *S. epidermidis* was used (the other two spectra can be found in the experimental section of this chapter).

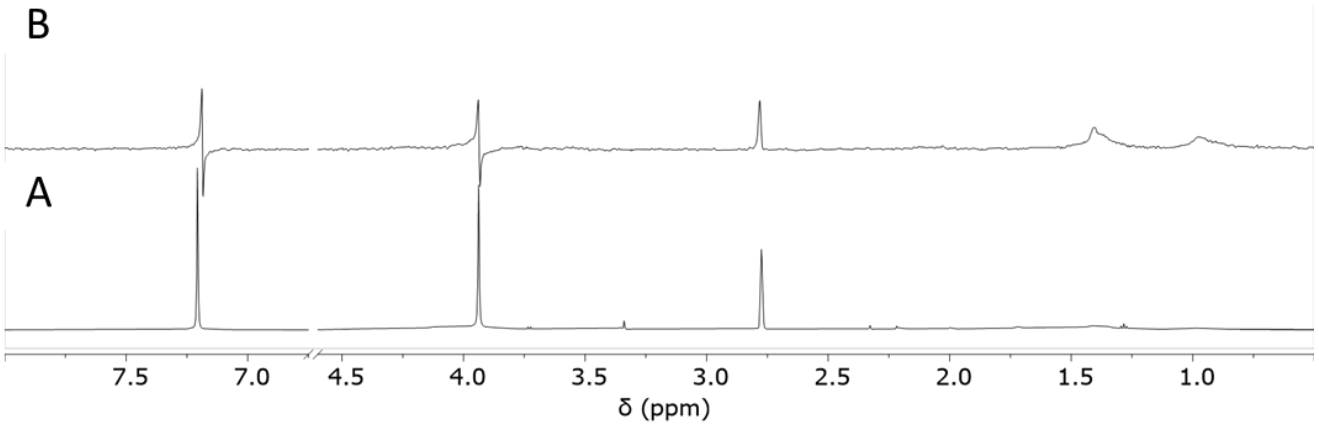

*Figure 72: **A**) **CM1** 2mM, d-PBS + d6-DMSO (20%) ^{1}H NMR **B**) **CM1** 2mM + S. epidermidis (OD 1.5 in 750 µL ×2 pelleted and resuspended in 250 µL), d-PBS + d6-DMSO (20%) STD, 3s, 0.5 ppm*

In this case, although the only two signals of **CM1** around 7.2 and 3.9 ppm are still visible in the STD spectrum, they are antiphase signals. Their positive part is equal to the negative one resulting in no STD signal. Therefore, the only true signals observable in the STD are those of the bacteria resonating at high fields. This proved that **CM1** is not able to interact with bacteria and that the interactions observed before with the other calixarene ligands are not due to the calixarene backbone with the bacteria cell wall but to the particular functionalization at the upper rim, that is the presence of the cyclopeptide bridge for ligand **19**, of the guanidinium units for **25** and of the trehalose carbohydrates for **56.**

3. CONCLUSIONS

This chapter highlighted the different strategies employed by us to synthesize many new calix[4]arene-based ligands for different bacteria classes. NMR experiments confirmed that our derivatives are able to interact with these microorganisms. However, unfortunately, the compounds tested until now, did not have the selectivity we hope they would have. We demonstrated that the interactions observed between our calixarenes and the bacteria are due to the proper scaffold functionalization an not to its backbone. Useful information has still been gathered from the STD studies and these could help us, in the future, to optimize the design of our ligands to improve their selectivity.

4. EXPERIMETAL PART

General information

Commercially available reagents and solvents were used without carrying out any prior purification or treatment except as indicated. All moisture- and air-sensitive reactions were conducted under nitrogen atmosphere. Dry solvents were prepared according to standard procedures and stored in the presence of molecular sieves. Monitoring of synthetic processes was performed by direct-phase thin-layer chromatography (TLC) using 60 F254 silica gel plates. For the detection of reagents and products with amine groups, the TLCs were sprayed with a 5% solution of ninhydrin in ethanol; for those with phenolic groups, a solution of $FeCl_3$ in water was used; for those with aldehydic groups, a solution of acidic 2,4-dinitrophenylhydrazine in ethanol was used; and for easily oxidized compounds, a 0.05% solution of $KMnO_4$ in water was used. Flash chromatography columns on silica gel 60 (230-400 mesh), under nitrogen pressure, and commercial preparative TLC 20×20 cm, silica gel F254, 0.5 mm were used for products purification.

Products characterization was performed by ^{1}H and ^{13}C NMR spectroscopy and mass spectrometry using ESI technique. NMR spectra were recorded with Bruker AVANCE 400 spectrometer (^{1}H at 400 MHz, ^{13}C at 100 MHz); chemical shift values are reported in ppm using the resonance frequency of the partially deuterated solvent as a reference. Mass spectra were recorded with a single quadrupole SQ detector spectrometer, Waters. Melting points were determined with Gallenkamp apparatus in closed capillaries.

2,5-dioxopyrrolidin-1-yl ((benzyloxy)carbonyl)-L-alaninate (1)

In a round-bottom flask ((benzyloxy)carbonyl)-L-alanine was dissolved in dry DCM (90 mL), the temperature was then lowered to 0°C and HOSu (1.70 g, 14.8 mmol) and DCC (3.05 g, 14.8 mmol) were added to the solution. The mixture was left reacting at room temperature for 4 hours. Once assessed the completion of the reaction by TLC (AcOEt/Hex 7:3) the mixture was filtered with cold DCM to remove DCU. The solvent was evaporated under reduced pressure. The white solid obtained was then triturated with 2-propanol and filtered.

Yield: 89% (3.90 g)

^{1}H NMR (400 MHz, $CDCl_3$) δ(ppm): 7.43 – 7.31 (m, 5H, ArH), 5.28 (d, *J* = 7.6 Hz, 1H, NH), 5.21 – 5.11 (m, 2H, CH_2 Cbz), 4.84-4.77 (m, 1H, CH), 2.87 (s, 4H, CH_2 OSu), 1.63 (d, *J* = 7.3 Hz, 3H, CH_3).

The spectroscopic data found are in agreement with those reported in literature.[43]

2,5,8,11,14-Pentaazapentadecanedioic acid, 3(S),13(S)-dimethyl-4,12-dioxo-bis(phenylmethyl) ester (2)

In a two-neck round-bottom flask under inert atmosphere, compound **1** (1.67 g, 5.23 mmol) was solubilized in dry DCM (65 mL). DETA (0.26 mL, 2.38 mmol) and Et_3N (0.33 mL, 2.38 mmol) were then added. The reaction was allowed to proceed under magnetic stirring for 5 hours at room temperature. Upon completion (as determined by TLC, Hex/AcOEt 1:1) the reaction mixture was treated with a saturated aqueous solution of Na_2CO_3 (30 mL). After two washings with distilled H_2O (30 mL) the organic phase was separated and dried under reduced pressure to give a with solid.

Yield: 90% (1.09 g)

^{1}H NMR (400 MHz, CD_3OD) δ (ppm): 7.40 – 7.27 (m, 10H, ArH), 5.15 – 5.03 (m, 4H, CH_2 Cbz), 4.11 (q, *J* = 7.2 Hz, 2H, CH), 3.43-3.37 + 3.28-3.22 (m, 4H, CH_2N), 2.72 (bs, 4H, CH_2N), 1.33 (d, *J* = 7.2 Hz, 6H, CH_3).

The spectroscopic data found are in agreement with those reported in literature.[10]

((5S)-5-methyl-3,6,14-trioxo-1-phenyl-2-oxa-4,7,10,13-tetraazahexadecan-10-tertbutoxycarbonyl-(15S)-15-yl)benzylcarbamate (3)

In a two-necked round-bottom flask equipped with a condenser and dropping funnel, compound **2** (1.09 g, 2.13 mmol) was solubilized in tBuOH (95 mL). Boc_2O (0.56 g, 2.55 mmol) was dissolved in tBuOH (30 mL) and slowly added to the mixture. The reaction is allowed to proceed under magnetic stirring at reflux for 3 hours. The reaction was monitored by TLC (hexane/AcOEt 1:1 eluent) multiple times. Upon completion the solvent was evaporated under reduced pressure. The crude was dissolved in DCM (30 mL) and washed with distilled H_2O (2x30 mL). The organic layer was separated, dried over anhydrous Na_2SO_4 and evaporated over reduced pressure to give a white solid.

Yield: 93% (1.22 g)

^{1}H NMR (400 MHz, CD_3OD) δ (ppm): 7.44 – 7.25 (m, 10H, ArH), 5.16 – 5.04 (m, 4H, CH_2 Cbz), 4.12 (q, *J* = 7.2 Hz, 2H, CH), 3.35-3.30 (m, 8H, CH_2N), 1.48 (s, 9H, $(CH_3)_3C$), 1.33 (d, *J* = 7.2 Hz, 6H, CH_3).

The spectroscopic data found are in agreement with those reported in literature.[10]

tert-butyl bis(2-(2-aminopropanamido)ethyl)carbamate (4)

Compound **3** (0.56 g, 0.91 mmol) was solubilized in absolute EtOH and poured into a Parr's hydrogenator reactor. 10% Pd/C (catalytic amount) was then added, and the reaction was allowed to proceed for 24 hours in Parr's apparatus, maintaining the hydrogen pressure at 2 atm. The reaction was monitored by TLC (AcOEt eluent). The Pd/C was removed by filtration, and the solvent was evaporated from the filtrate under reduced pressure, resulting in an oil used as such in the following reactions.

Yield: 80% (0,25 g)
^{1}H NMR (400 MHz, CD_3OD) δ (ppm): 3.48-3.46 (m, 2H, CH), 3.30 (m, 8H, CH_2N), 1.50 (s, 9H, $(CH_3)_3C$), 1.34 – 1.23 (m, 6H, CH_3).

The spectroscopic data found are in agreement with those reported in literature.[10]

25,27-dipropoxy-26,28-dihydroxycalix[4]arene (5)

Tetrahydroxycalix[4]arene (2.0 g, 4.7 mmol) and K_2CO_3 (2.73 g, 19.76 mmol) are suspended in dry ACN (70 mL) in a two-neck round-bottom flask under inert atmosphere. The mixture was left stirring for 30 minutes, then Iodopropane (1.92 mL, 19.76 mmol) was added. The reaction was allowed to proceed under magnetic stirring at reflux for 20 hours. Upon completion (determined by TLC, Hex/AcOEt 9:1) a 1M HCl solution (50 mL) was added to the mixture. The white solid that precipitated was then filtered and purified by recrystallization in DCM/Hex.

Yield: 53% (1.27 g)

^{1}H NMR (400 MHz, $CDCl_3$) δ (ppm): 8.36 (s, 2H, OH), 7.08 (d, *J* = 7.5 Hz, 4H, ArH), 6.95 (d, *J* = 7.5 Hz, 4H, ArH), 6.77 (t, *J* = 7.5 Hz, 2H, ArH), 6.67 (t, *J* = 7.5 Hz, 2H, ArH), 4.35 (d, *J* = 12.9 Hz, 4H, Ar$CH_{ax}H_{eq}$Ar), 4.01 (t, *J* = 6.2 Hz, 4H, $OCH_2CH_2CH_3$), 3.41 (d, *J* = 12.9 Hz, 4H, Ar$CH_{ax}H_{eq}$Ar), 2.10 (sext, *J* = 7.1 Hz, 4H, $OCH_2CH_2CH_3$), 1.35 (t, *J* = 7.4 Hz, 6H, $OCH_2CH_2CH_3$).

The spectroscopic data found are in agreement with those reported in literature.[44]

5,17-diformyl-25,27-dipropoxy-26,28-dihydroxycalix[4]arene (6)

In a three-necked round-bottom flask under inert atmosphere compound **5** (1.21 g, 2.38 mmol) and dry $CHCl_3$ (100 mL) were added, then the temperature was lowered to -10°C thanks to an ice-salt bath. Cl_2CHOCH_3 (0.581 mL, 6.42 mmol) and $SnCl_4$ (2.21 mL, 18.85 mmol) were then added, and the reaction was allowed to proceed at -10°C under magnetic stirring for 3 hours. The reaction was monitored by TLC (Hex/AcOEt, eluent 7:3) and once completed the mixture was treated with 1M HCl (30 mL). The organic

phase was then washed with distilled H_2O three times to neutrality. The organic layer was separated, dried over anhydrous Na_2SO_4 and evaporated under reduced pressure. The product was recrystallized with MeOH and filtered, obtaining a white solid.

Yield: 85% (1.15 g)
^{1}H NMR (400 MHz, $CDCl_3$) δ (ppm): 9.81 (s, 2H, CHO), 9.29 (s, 2H, OH), 7.66 (s, 4H, ArH), 7.00 (d, *J* = 7.6 Hz, 4H, ArH), 6.82 (t, *J* = 7.6 Hz, 2H, ArH), 4.33 (d, *J* = 13.1 Hz, 4H, $ArCH_{ax}H_{eq}Ar$), 4.04 (t, *J* = 6.2 Hz, 4H, $OCH_2CH_2CH_3$), 3.53 (d, *J* = 13.2 Hz, 4H, $ArCH_{ax}H_{eq}Ar$), 2.11 (sext *J* = 7.4 Hz, 4H, $OCH_2CH_2CH_3$), 1.36 (t, *J* = 7.4 Hz, 6H, $OCH_2CH_2CH_3$).

The spectroscopic data found are in agreement with those reported in literature.[45]

5,17-bis(hydroxycarbonyl)-25,27-dipropoxy-26,28-dihydroxycalix[4]arene (7)

In a two-necked round-bottom flask under inert atmosphere, compound **6** (1.00 g, 1.77 mmol) was solubilized in a $CHCl_3$/Acetone mixture (1:1, 90+90 mL), then cooled at 0°C with an ice bath. H_2NSO_3H (0.69 g, 7.09 mmol) and $NaClO_2$ (0.56 g, 6.20 mmol) were previously dissolved in the minimum amount of H_2O and then added to the mixture. The reaction was allowed to proceed under magnetic stirring for 4 hours at room temperature. Upon reaction completion (determined by TLC, Hex/AcOEt 1:1 eluent) the solvent was evaporated under reduced pressure, then the crude was treated with a 1M HCl solution (30 mL), which induced the precipitation of a white solid. The product is obtained sufficiently pure once it has been cold filtered through a buchner filter.

Quantitative yield (1,06 g)

^{1}H NMR (400 MHz, DMSO-d_6) δ (ppm): 12.44 (s, 2H, COOH), δ 9.20 (s, 2H, OH), 7.81 (s, 4H, ArH), 7.07 (d, *J* = 7.6 Hz, 4H, ArH), 6.83 (t, *J* = 7.6 Hz, 2H, ArH), 4.17 (d, *J* = 12.8 Hz, 4H, $ArCH_{ax}H_{eq}Ar$), 3.98 (t, *J* = 5.9 Hz, 4H, $OCH_2CH_2CH_3$), 3.60 (d, *J* = 13.1 Hz, 4H, $ArCH_{ax}H_{eq}Ar$), 2.01 (sext, *J* = 7.3 Hz, 4H, $OCH_2CH_2CH_3$), 1.31 (t, *J* = 7.4 Hz, 6H, $OCH_2CH_2CH_3$).

The spectroscopic data found are in agreement with those reported in literature.[34]

5,17-bis(hydroxycarbonyl)-25,26,27,28-tetrapropoxycalix[4]arene (8)

Compound **7** (1.13 g, 1.89 mmol) was dissolved in dry DMF (25 mL) in a two-necked round-bottom flask under inert atmosphere. Pr-I (1.47 mL, 15.09 mmol) and NaH 60% (0.36 g, 9.05 mmol) were then added. After 24 h, the reaction was monitored by TLC (Hex/AcOEt eluent 1:1) which indicated its completion. The reaction mixture was quenched with distilled H_2O (5 mL) and then with 1M HCl (5 mL). The organic phase was extracted with AcOEt (40 mL) and washed with distilled H_2O (3x30 mL). The organic

layer was separated, dried over anhydrous Na_2SO_4 and evaporated under reduced pressure.

The crude, without any characterisation, was hydrolyzed to obtain **8**.

In a round-bottom flask the crude was dissolved in a 10% solution of KOH in H_2O and EtOH (30 mL). The reaction was allowed to proceed under magnetic stirring for 24 hours at reflux. Upon reaction completion (TLC Hex/AcOEt, 1:1 eluent) the alcoholic fraction was evaporated under reduced pressure, then the crude was acidified with 1M HCl, causing the precipitation of the product as a white solid, which was then recovered by filtration.

Yield: 92% (1,19 g)

^{1}H NMR (400 MHz, $CDCl_3$) δ(ppm): 12.94 (s, 2H, COOH), δ 7.20 (d, *J* = 7.5 Hz, 4H, ArH), 7.07 (t, *J* = 7.1 Hz, 2H, ArH), 6.79 (s, 4H, ArH), 4.44 (d, *J* = 13.6 Hz, 4H, ArCH_{ax}H$_{eq}$Ar), 4.03 (t, *J* = 8.3 Hz, 4H, OCH_2CH$_2$CH$_3$), 3.69 (t, *J* = 6.7 Hz, 4H, OCH_2CH$_2$CH$_3$), 3.17 (d, *J* = 13.7 Hz, 4H, ArCH$_{ax}$$H_{eq}$Ar), 1.91 (m, 8H, OCH$_2CH_2CH_3$), 1.12 (t, *J* = 7.4 Hz, 6H, OCH$_2$CH$_2$CH_3), 0.89 (t, *J* = 7.5 Hz, 6H, OCH$_2$CH$_2$CH_3).

The spectroscopic data found are in agreement with those reported in literature.[34]

5,17-bis(chlorocarbonyl)-25,26,27,28-tetrapropoxycalix[4]arene (9)

In a dry-flamed two-necked round-bottom flask, under inert atmosphere, compound **8** (0.6 g, 0.88 mmol) was dissolved in dry DCM (4 mL), then oxalyl chloride (2 mL, 22.93 mmol) and DMF (catalytic amount) were added. The reaction was allowed to proceed under magnetic stirring for 30 minutes. The reaction was monitored by TLC (hexane/AcOEt eluent 7:3) and after completion the solvent was evaporated under reduced pressure and used without further purification.

Yield: 71% (0,45 g)

^{1}H NMR (400 MHz, $CDCl_3$) δ (ppm): 7.57 (s, 4H, ArH), 6.67 – 6.43 (m, 6H, ArH), 4.57 – 4.42 (m, 4H, ArCH_{ax}H$_{eq}$Ar), 4.03 (t, *J* = 7.2 Hz, 4H, OCH_2CH$_2$CH$_3$), 3.83 (t, *J* = 6.9 Hz, 4H, OCH_2CH$_2$CH$_3$), 3.28 (d, *J* = 13.6 Hz, 4H, ArCH$_{ax}$$H_{eq}$Ar), 1.94 (m, 8H, OCH$_2CH_2CH_3$), 1.09 – 0.97 (m, 12H, OCH$_2$CH$_2$CH_3).

The spectroscopic data found are in agreement with those reported in literature.[46]

5,17-((N^1,N^7-bis((L)-alaninamide)-N^4-tert-butoxycarbonyl-1,4,7-triazaheptane)-dicarboxyamide)-25,26,27,28-tetrapropoxycalix[4]arene (10)

A solution of compound **4** (0.07 g, 0.12 mmol) in dry DCM (20 mL) and Et_3N (50 µL) was loaded into a 20 mL syringe. Compound **9** (0.13 g, 0.20 mmol) was solubilized in dry DCM (20 mL) and loaded in another syringe. The two solutions are dripped simultaneously and at the same rate through automated drippers into a three-necked round-bottom flask under inert atmosphere containing dry DCM (130 mL) and Et_3N (0.08 mL, 0.56 mmol). The reaction was allowed to proceed under magnetic stirring for 1 hour from the end of the additions (33 minutes drip time). The reaction completion was determined by TLC (Hex/THF, eluent 4:6). The solvent was evaporated under reduced pressure and the crude was subjected to flash column chromatography (Hex/THF, 4:6) to obtain a white solid.

Yield: 33% (0,06 g)

^{1}H NMR (400 MHz, $CDCl_3$) δ (ppm): 8.08 (bs, 2H, N*H*CH_2), 7.18 (d, *J* = 8.8 Hz, 4H, ArH), 6.95 (bs, 2H, ArH), 6.75 + 6.55 (bs, 2H, NHCOAr), 6.51 + 6.31 (s, 4H, ArH), 4.61-4.52 (m, 2H, CH), 4.47 (d, *J* = 13.3 Hz, 4H, ArC*H*$_{ax}$H$_{eq}$Ar), 4.17 – 3.95 + 3.71-3.60 (m, 8H, OC*H*$_2$CH$_2$CH$_3$), 3.79 – 3.74, 3.59, 3.45-3.30 and 3.06-2.96 (m, 8H, CH_2N), 3.21 + 3.15 (d, *J* = 13.0 Hz, 4H, ArCH$_{ax}$*H*$_{eq}$Ar), 2.08-1.84 (m, 8H, OCH$_2$C*H*$_2$CH$_3$), 1.55 (s, 9H, $(CH_3)_3C$), 1.36 (d, *J* = 10.5 Hz, 6H, CH_3), 1.12 (t, *J* = 7.5 Hz, 6H, OCH$_2$CH$_2$C*H*$_3$), 0.92 (t, *J* = 7.5 Hz, 6H, OCH$_2$CH$_2$C*H*$_3$).
The spectroscopic data found are in agreement with those reported in literature.[10]

5,17-((N^1,N^7-bis((L)-alaninamide)-1,4,7-triazaheptane)-dicarboxyamide)-25,26,27,28-tetrapropoxycalix[4]arene (11)

Compound **10** (0.056 g, 0.06 mmol) was dissolved with DCM (5 mL) in a round-bottom flask, the temperature was lowered to 0°C with an ice bath then TFA (0.45 mL) was added. The reaction was monitored by TLC (Hex/THF eluent 4:6) and after 1 hour, upon completion, the solvent was evaporated under reduced pressure. A 1M aqueous LiOH solution was then added (until pH neutrality) then the organic phase was separated and the aqueous one was extracted with DCM (4x5 mL). The solvent was evaporated under reduced pressure and a white solid was collected.

Yield: 80% (0,04 g)
^{1}H NMR (400 MHz, $CDCl_3$) δ (ppm): 7.57 (s, 2H, NH), 7.23-7.19 (m, 4H, ArH), 7.01 (t, *J* = 7.4 Hz, 2H, ArH), 6.54 and 6.49 (s, 4H, ArH), 4.47 (d, *J* = 13.2 Hz, 4H, ArC*H*$_{ax}$H$_{eq}$Ar), 4.40-4.34 (m, 2H, CH), 4.10-4.05 (m, 4H, OC*H*$_2$CH$_2$CH$_3$), 3.67 (t, *J* = 6.8 Hz, 4H, OC*H*$_2$CH$_2$CH$_3$), 3.27 – 3.14 (m, 4H, ArCH$_{ax}$*H*$_{eq}$Ar), 3.62, 3.25-3.26 and 2.93-2.91 (m, 8H, CH_2N), 2.09 – 1.95 (m, 4H, OCH$_2$C*H*$_2$CH$_3$), 1.90 (q, *J* = 7.1 Hz, 4H, OCH$_2$C*H*$_2$CH$_3$), 1.31 (d, *J* = 6.8 Hz, 6H, CH_3), 1.12 (t, *J* = 7.4 Hz, 6H, OCH$_2$CH$_2$C*H*$_3$), 0.91 (t, *J* = 7.5 Hz, 6H, OCH$_2$CH$_2$C*H*$_3$).

The spectroscopic data found are in agreement with those reported in literature.[10]

25,26,27,28-tetrakis(2-ethoxyethoxy)calix[4]arene (12)

In a round-bottom flask were added 25,26,27,28-tetrahydroxycalix[4]arene (5.0 g, 11.78 mmol), DMF (150 mL) and NaH (60% dispersion in oil, 3.0 g, 75.03 mmol). The mixture was heated to 40°C and left under magnetic stirring for 40 minutes then BrEtOEt (6.64 mL, 58.90 mmol) was added. The reaction was allowed to proceed under magnetic stirring at 40°C for 16 hourss. During this time, it was monitored by TLC (Hex/AcOEt, eluent 8:2). Upon completion the reaction was quenched with 1M HCl (40 mL), causing precipitation of the product, which was immediately filtered. The solid was purified by recrystallization in hot MeOH. The needle-like white crystals formed were then recovered by filtration.

Yield: 80% (6.6 g, 9.42 mmol)

^{1}H NMR (400 MHz, $CDCl_3$) δ (ppm) 6.76 – 6.48 (m, 12H, ArH), 4.52 (d, *J* = 13.3 Hz, 4H, Ar$CH_{ax}H_{eq}$Ar), 4.14 (t, *J* = 5.8 Hz, 8H, ArOCH_2CH_2), 3.87 (t, *J* = 5.8 Hz, 8H, ArOCH_2CH_2), 3.57 (q, *J* = 7.0 Hz, 8H, OCH_2CH_3), 3.17 (d, *J* = 13.4 Hz, 4H, Ar$CH_{ax}H_{eq}$Ar), 1.23 (t, *J* = 7.0 Hz, 12H, OCH_2CH_3).

The spectroscopic data found are in agreement with those reported in literature.[47]

5,17-diformyl-25,26,27,28-tetrakis(2-ethoxyethoxy)calix[4]arene (13)

In a two-necked round-bottom flask under inert atmosphere, compound **12** (2.6 g, 3.65 mmol) was dissolved in dry $CHCl_3$ (85 mL), then the temperature was lowered to -10° then Cl_2CHOCH_3 (9.81 mL, 108.43 mmol) and $SnCl_4$ (13.04 mL, 111.38 mmol) were added. The reaction was allowed to proceed at -10°C for 30 minutes. Upon completion (TLC Hex/AcOEt, 6:4) the reaction was quenched by carefully adding 200 mL of distilled H_2O. The organic phase was separated and washed with a saturated solution of Na_2CO_3 (100 mL), distilled H_2O (2x100 mL) and finally dried with anhydrous Na_2SO_4. The solvent was removed under reduced pressure. The product was subjected to flash column chromatographic (stationary phase: silica, eluent: hexane/AcOEt 6:4). The isolated fraction was a mixture of 5,11-diformyl- and 5,17-diformyl-25,26,27,28-tetra(2-ethoxyethoxy)calix[4]arene in a 1:5 ratio which was not possible to separate each from the other.

Yield: 47% (1.31 g)

^{1}H NMR of the major isomer (400 MHz, $CDCl_3$) δ(ppm): 9.67 and 9.62 (s, 2H, CHO), 7.20-7.16 (m, 4H, ArH), 6.62-6.52 (m, 6H, ArH), 4.66, 4.58 and 4.49 (d, *J* = 13.6 Hz, 4H, Ar$CH_{ax}H_{eq}$Ar), 4.25 (t, *J* = 5.3 Hz, 4H, ArOCH_2CH_2), 4.12 (t, *J* = 5.5 Hz, 4H, ArOCH_2CH_2),

3.86-3.81 (m, 8H, $ArOCH_2CH_2$), 3.58-3.51 (m, 8H, OCH_2CH_3), 3.33, 3.26 and 3.18 (d, *J* = 13.7 Hz, 4H, $ArCH_{ax}H_{eq}Ar$), 1.24-1.17 (m, 12H, OCH_2CH_3).

The spectroscopic data found are in agreement with those reported in literature.[33]

5,17-bis(hydroxymethyl)-25,26,27,28-tetrakis(2-ethoxyethoxy)calix[4]arene (15)

In a round-bottom flask, the mixture containing compound **13** (1.31 g, 1.70 mmol) and its regioisomer was solubilized in absolute EtOH (55 mL). $NaBH_4$ (0.19 g, 5.11 mmol) was then added, and the reaction was allowed to proceed under magnetic stirring for 16 hours. The reaction was monitored by TLC (hexane/AcOEt eluent 6:4). The solvent was removed under reduced pressure. The solid thus obtained was dissolved in DCM (150 mL), the organic phase washed with distilled H_2O (2x100 mL), separated from the aqueous one and dried with anhydrous Na_2SO_4. The solvent was evaporated under reduced pressure. The product 5,17-dihydroxymethyl-25,26,27,28-tetrakis(2-ethoxyethoxy)-calix[4]arene was separated from its isomer 5,11-dihydroxymethyl-25,26,27,28-tetrakis(2-ethoxyethoxy)-calix[4]arene by flash column chromatography (stationary phase: silica, eluent: DCM/AcOEt/hexane 5:5:2) obtaining a white solid.
Yield of 1,3 isomer: 57% (0.76 g)
^{1}H NMR (400 MHz, $CDCl_3$) δ (ppm): 6.93 (d, *J* = 7.5 Hz, 4H, ArH), 6.80 (t, *J* = 7.2 Hz, 2H, ArH), 6.43 (s, 4H, ArH), 4.54 (d, *J* = 13.3 Hz, 4H, $ArCH_{ax}H_{eq}Ar$), 4.28 (t, *J* = 6.2 Hz, 4H, $ArOCH_2CH_2$), 4.18 (s, 4H, $ArCH_2OH$), 4.04 (t, *J* = 5.3 Hz, 4H, $ArOCH_2CH_2$), 3.93 (t, *J* = 6.2 Hz, 4H, $ArOCH_2CH_2$), 3.84 (t, *J* = 5.3 Hz, 4H, $ArOCH_2CH_2$), 3.63 – 3.53 (m, 8H, OCH_2CH_3), 3.18 (d, *J* = 13.3 Hz, 4H, $ArCH_{ax}H_{eq}Ar$), 1.26 (t, *J* = 7.0 Hz, 6H, OCH_2CH_3), 1.22 (t, *J* = 7.0 Hz, 6H, OCH_2CH_3).

The spectroscopic data found are in agreement with those reported in literature.[48]

5,17-bis(hydroxycarbonyl)-25,26,27,28-tetrakis(2-ethoxyethoxy)calix[4]arene (16)
Compound **15** (0.34 g, 0.44 mmol) was solubilized in benzene (8 mL), then $KMnO_4$ (0.70 g, 4.44 mmol), 6% aqueous NaOH (20 mL) and a catalytic amount of $Bu_4N^+HSO_4^-$ were added. The reaction was allowed to proceed under magnetic stirring at room temperature for 16 hours. AcOEt (200 mL) and 1 M HCl aqueous solution (200 mL) were added, the organic phase washed with distilled H_2O (3x100 mL), separated and finally anhydrified with anhydrous Na_2SO_4. The solvent was evaporated under reduced pressure. A white solid was collected.

Yield: 84% (0,33 g)

^{1}H NMR (400 MHz, $CDCl_3$) δ (ppm): 7.18 (d, *J* = 7.4 Hz, 4H, ArH), 7.06 (t, *J* = 7.1 Hz, 2H, ArH), 6.80 (s, 4H, ArH), 4.50 (d, *J* = 13.6 Hz, 4H, $ArCH_{ax}H_{eq}Ar$), 4.29 (t, *J* = 6.4 Hz, 4H, $ArOCH_2CH_2$), 3.99 – 3.92 (m, 4H, $ArOCH_2CH_2$), 3.87 (t, *J* = 6.4 Hz, 4H, $ArOCH_2CH_2$), 3.80 – 3.73 (m, 4H, $ArOCH_2CH_2$), 3.58 (q, *J* = 7.0 Hz, 4H, OCH_2CH_3), 3.51 (q, *J* = 7.0 Hz, 4H, OCH_2CH_3), 3.17 (d, *J* = 13.7 Hz, 4H, $ArCH_{ax}H_{eq}Ar$), 1.25 (t, *J* = 7.0 Hz, 6H, OCH_2CH_3), 1.18 (t, *J* = 6.9 Hz, 6H, OCH_2CH_3).

The spectroscopic data found are in agreement with those reported in literature.[49]

5,17-bis(chlorocarbonyl)-25,26,27,28-tetrakis(2-ethoxyethoxy)calix[4]arene (17)
In a two-necked round-bottom flask under nitrogen atmosphere, compound **16** (0.27, 0.34 mmol) was dissolved in dry DCM (20 mL), then $C_2Cl_2O_2$ (0.83 mL, 9.47 mmol) and DMF (catalytic amount) were added. The reaction was left stirring for 3 hours. Upon completion (TLC Hex/AcOEt, 1:1 eluent). The solvent was removed under reduced pressure and the yellow resin obtained was used without further purifications.

Quantitative Yield (0.28 g)

^{1}H NMR (400 MHz, $CDCl_3$) δ 7.72 (s, 4H, ArH), 6.58 – 6.52 (m, 2H, ArH), 6.48 (d, *J* = 7.6 Hz, 4H, ArH), 4.63 (d, *J* = 13.6 Hz, 4H, $ArCH_{ax}H_{eq}Ar$), 4.41 (t, *J* = 5.2 Hz, 4H, $ArOCH_2CH_2$), 4.10 (t, *J* = 5.0 Hz, 4H, $ArOCH_2CH_2$), 3.91 (t, *J* = 5.2 Hz, 4H, $ArOCH_2CH_2$), 3.85 (t, *J* = 5.1 Hz, 4H, $ArOCH_2CH_2$), 3.61 (q, *J* = 8.3, 7.6 Hz, 4H, OCH_2CH_3), 3.56 (q, *J* = 7.1 Hz, 4H, OCH_2CH_3), 3.31 (d, *J* = 13.7 Hz, 4H, $ArCH_{ax}H_{eq}Ar$), 1.29 (t, *J* = 7.0 Hz, 6H, OCH_2CH_3), 1.22 (t, *J* = 7.0 Hz, 6H, OCH_2CH_3).

5,17-((N^1,N^7-bis((L)-alaninamide)-N^4-tert-butoxycarbonyl-1,4,7-triazaheptane)-dicarboxyamide)-25,26,27,28-tetrakis(2-ethoxyethoxy)calix[4]arene (18)
A solution of compound **4** (0.14 g, 0.42 mmol) in dry DCM (20 mL) and Et_3N (50 µL) was loaded into a 20 mL syringe. Compound **17** (0.28 g, 0.34 mmol) was solubilized in dry DCM (20 mL) and loaded in another syringe. The two solutions are dripped simultaneously and at the same rate through automated drippers into a three-necked round-bottom flask under inert atmosphere containing dry DCM (160 mL) and Et_3N (0.28 mL, 2.03 mmol). The reaction was allowed to proceed under magnetic stirring for 1 hour from the end of the additions (33 minutes drip time). The reaction completion was determined by TLC (Hex/THF, eluent 4:6). The solvent was evaporated under reduced pressure and the crude was subjected to flash column chromatography (Hex/THF, 4:6) to obtain a white solid.

Yield: 13% (0,051 g)

^{1}H NMR (400 MHz, $CDCl_3$) δ (ppm): 8.10 – 8.02 (m, 2H, N*H*CH_2), 7.15 (d, *J* = 7.5, 4H, ArH), 6.99-6.90 (m, 2H, ArH), 6.74 + 6.54 (bs, 2H, NHCOAr), 6.51 + 6.32 (s, 4H, ArH), 4.64 – 4.48 (m, 6H, ArC*H*$_{ax}$H$_{eq}$Ar, CH), 4.42-4.30, 4.03 – 3.88 and 3.78 (m, m, t, *J* = 4.9 Hz, 16H, $ArOCH_2CH_2$), 3.71-3.64 + 3.44-3.27 + 3.06-2.99 (m, 6H, CH_2N), 3.59 (q, *J* = 7.0 Hz, 4H, OC*H*$_2$$CH_3$), 3.51 (q, *J* = 7.0 Hz, 4H, OC*H*$_2$$CH_3$), 3.21 – 3.12 (m, 6H, $ArCH_{ax}H_{eq}Ar$ and CH_2N), 1.54 (s, 9H, $C(CH_3)_3$), 1.35 (d, *J* = 10.8 Hz, 6H, CH_3), 1.26 (t, *J* = 7.0 Hz, 6H, OCH_2C*H*$_3$), 1.18 (t, *J* = 7.0 Hz, 6H, OCH_2C*H*$_3$).

^{13}C NMR (101 MHz, $CDCl_3$) δ (ppm): 173.6, 170.7, 169.9 and 157.5 (C=O), 157.1 and 155.3 (Ar_{ipso}), 136.4, 135.9, 134.2 and 133.0 (Ar_{ortho}), 129.0, 127.6, 124.8 (Ar_{meta}), 122.6, 122.5 (Ar_{para}), 80.3 (*C*$(CH_3)_3$), 74.2, 72.4, 69.6, 69.4 ($ArOCH_2CH_2$), 66.5, 66.1 (OCH_2CH_3), 48.8 (CH), 48.2, 47.8, 40.3, 39.8 (CH_2N), 30.7 ($ArCH_2Ar$), 28.5 ((CH_3)$_3$C), 17.2, 16.1 (CH_3), 15.5, 15.2 (OCH_2CH_3).

ESI-MS (m/z) calc (1109.36) oss: 1110.32 $[M+H]^+$ (100%)

5,17-((N^1,N^7-bis((L)-alaninammide)-1,4,7-triazaeptano)dicarboxyammide)-25,26,27,28-tetrakis(2-ethoxyethoxy)calix[4]arene (20)

37% HCl (0.2 mL) was added to a solution of compound **19** (0.051 g, 0.046 mmol) in 1,4-dioxane (1 mL). The reaction proceeded under magnetic stirring for 16 hours. Upon completion (TLC Hexane/THF eluent 4:6) the solvent was evaporated under reduced pressure. The product was purified by trituration in EtO_2 followed by centrifugation, obtaining a white solid.

Quantitative yield (0,045 g, 0.046 mmol)

^{1}H NMR (400 MHz, MeOD) δ (ppm): 7.69–7.56 and 6.46-6.36 (m, 4H, ArH), 7.30-7.32 (m, 2H, ArH), 6.98 (d, *J* = 8.4 Hz, 4H, ArH), 4.71 – 4.57 (m, 4H, ArC*H*$_{ax}$H$_{eq}$Ar), 4.46 and 4.03 (t, *J* = 6.1 Hz, 6H, $ArOCH_2CH_2$), 4.41-4.37, 3.99-3.95 and 3.92-3.85 (m, 8H, $ArOCH_2CH_2$), 4.22 (q, *J* = 7.0 Hz, 2H, CH), 3.83 (t, *J* = 4.3 Hz, 2H, $ArOCH_2CH_2$) 3.68 – 3.51 (m, 8H, OC*H*$_2$$CH_3$), 3.51 – 3.38 and 3.21 – 3.11 (m, 4H, CH_2N), 3.29-3.23 (m, 8H, $ArCH_{ax}H_{eq}Ar$ and CH_2N), 1.37 (d, *J* = 7.0 Hz, 6H, CH_3), 1.28 (t, *J* = 6.9 Hz, 6H, OCH_2C*H*$_3$), 1.19 (t, *J* = 7.0 Hz, 6H, OCH_2C*H*$_3$).

^{13}C NMR (101 MHz, MeOD) δ (ppm): 174.92, 168.31 (C=O), 158.19, 157.40 (Ar_{ipso}), 136.08, 136.03, 133.98, 133.70 (Ar_{orto}), 129.04 (Ar_{para}), 127.89, 126.54, 122.71, 122.19 (Ar_{meta}), 74.47, 73.81, 73.21, 72.21, 70.01, 69.80, 69.61, 69.39 ($ArOCH_2CH_2$), 66.13, 65.94 ($ROCH_2CH_3$), 49.68 (CH), 47.88 44.40, 35.71, 35.54 (CH_2N), 30.70, 30.55 ($ArCH_2Ar$), 15.79 (CH_3), 14.44 ($ROCH_2CH_3$).

ESI-MS (m/z) calc (1009.31) oss: 1010.34 $[M+H]^+$ (100%)

5,11,17,23-tetra-tert-butyl-[25,26,27,28-tetrakis(ethoxycarbonylmethoxy)]calix[4]arene (21)

In a two-necked round-bottom flask, tetratertbutyl-tetrahydroxycalix[4]arene (3.0 g, 4.62 mmol) was dissolved in acetone (100 mL), then Bromo-ethylAcetate (6.17 g, 36.96 mmol) was slowly added to the solution. The reaction was left stirring at room temperature, and after 15 hours it was completed (TLC, hexane/Ethyl Acetate 8/2). It was then quenched with H_2O (200 mL) and extracted with DCM (2x100 mL). The organic phases were combined and dried over anhydrous Na_2SO_4, the solvent was then evaporated under reduced pressure. The solid was purified by recrystallization in DCM/MeOH obtaining white needle crystals of pure product in a 63% yield (2.84 g, 2.91 mmol).

^{1}H NMR (400 MHz, $CDCl_3$) δ (ppm): 6.80 (s, 8H, ArH), 4.88 (d, *J* = 13.0 Hz, 4H, ArCH_{ax}H$_{eq}$Ar), 4.83 (s, 8H, ArOCH_2), 4.23 (q, *J* = 7.2 Hz, 8H, OCH_2CH$_3$), 3.21 (d, *J* = 12.8 Hz, 4H, ArCH$_{ax}$$H_{eq}$Ar), 1.31 (t, *J* = 8.1, 6.3 Hz, 12H, OCH$_2$CH_3), 1.10 (s, 36H, ArC(CH$_3$)$_3$).

The spectroscopic data found are in agreement with those reported in literature.[50]

5,11,17,23-tetranitro-25,26,27,28-tetrakis(ethoxycarbonylmethoxy)]calix[4]arene (22)

Calixarene **21** (1.92 g; 2.94 mmol) was dissolved, under inert atmosphere, with DCM in a two-necked round-bottom flask previously flame dried. The temperature was then lowered to 0°C then glacial acetic acid (30 mL, 525 mmol) and sequently fuming HNO_3 (9.75 mL, 235 mmol) were added to the solution. The mixture was stirred at room temperature and upon completion (TLC, hexane/Ethyl Acetate 6/4) it was quenched by addition of ice. The aqueous phase was extracted with DCM (2x 100 mL), the organic phases were combined, dried over anhydrous Na_2SO_4 and the solvent was evaporated under reduced pressure. The crude was purified by column chromatography (eluent: hexane/acetate 8/2), obtaining a pale orange solid in a 34% yield (948 mg, 1 mmol).

^{1}H NMR (400 MHz, $CDCl_3$) δ (ppm): 7.64 (s, 8H, ArH), 5.08 (d, *J* = 14.4 Hz, 4H, ArCH_{ax}H$_{eq}$Ar), 4.78 (s, 8H, ArOCH_2), 4.26 (q, *J* = 7.4 Hz, 8H, OCH_2CH$_3$), 3.51 (d, *J* = 14.4 Hz, 4H, ArCH$_{ax}$$H_{eq}$Ar), 1.33 (t, *J* = 7.1, 1.0 Hz, 12H, OCH$_2$CH_3).

The spectroscopic data found are in agreement with those reported in literature.[37]

5,11,17,23-tetraamino-tetrakis[25,26,27,28-(ethoxycarbonylmethoxy)]-calix[4]arene (23)

In a round-bottom flask, compound **22** (436 mg, 0.46 mmol) was solubilized in MeOH, then $CoCl_2x6H_2O$ (766 mg, 3.22 mmol) was added to the solution which turned pink. After that, $NaBH_4$ (574 mg, 15 mmol) was added batchwise to the mixture. The rection was stirred for 16 hours at room temperature and monitored by TLC (DCM/MeOH 95/5). Upon completion, it was quenched by the addition of 3N HCl (20 mL). A pink suspension formed and then NH_3 (30% in water, 50 mL) was added to it. The aqueous layer was extracted with DCM (2x30 mL), the organic phases combined, dried over anhydrous Na_2SO_4 and the solvent was removed under reduced pressure. A withe solid was obtained after trituration in Et_2O with a 65% yield (247 mg, 0.3 mmol).

^{1}H NMR (400 MHz, CD_3OD) δ (ppm): 6.62 (s, 8H, ArH), 4.45 (s, 8H, $ArOCH_2$), 4.38 (q, *J* = 7.1 Hz, 8H, OCH_2), 4.20 (d, *J* = 11.9 Hz, 4H, $ArCH_{ax}H_{eq}Ar$), 3.20 (d, *J* = 12.2 Hz, 4H, $ArCH_{ax}H_{eq}Ar$), 1.41 (t, *J* = 7.1 Hz, 12H, OCH_2CH_3).

The spectroscopic data found are in agreement with those reported in literature.[51]

5,11,17,23-tetrakis(bisBocguanidino)-tetrakis[25,26,27,28-(ethoxycarbonylmethoxy)]calix[4]arene (24)

Compound **23** (436 mg, 0.526 mmol) was dissolved in 10 mL of DMF, then Bis-Boc-Thiourea (872mg, 3.16 mmol), $HgCl_2$ (1.14 g, 4.21 mmol) and TEA (0.6 mL) were added in sequence. The mixture was stirred for 16 hours and monitored by TLC (hexane/ethyl acetate 7/3) and upon completion it was quenched by addition of water (20 mL). It was then extracted with DCM (2x20 mL), the organic phases were combined and dried over anhydrous Na_2SO_4, then the solvent was removed under reduced pressure. The crude was purified by column chromatography (eluent, hexane/ethyl acetate 8/2) and the product was obtained as a yellowish solid in 41% yield (385 mg, 0.21 mmol).

^{1}H NMR (400 MHz, $CDCl_3$) δ (ppm): 11.59 (s, 4H, NHBoc), 9.85 (s, 4H, N*H*C(=NBoc)NHBoc), 6.98 (s, 8H, ArH), 4.89 (d, *J*=13.3, 4H, $ArCH_{ax}H_{eq}Ar$), 4.73 (s, 8H, $ArOCH_2$), 4.20 (q, J = 7.0 Hz, 8H, OCH_2), 3.23 (d, *J*=13.3, 4H, $ArCH_{ax}H_{eq}Ar$), 1.47 (s, 72H, $OC(CH_3)_3$), 1.29 (t, *J*=7.2, 12H, OCH_2CH_3).

^{13}C NMR (101 MHz, $CDCl_3$) δ (ppm): 170.1 (COOEt), 163.5, 153.4, 152.9, 134.2, 131.4, 123.3 (Ar), 83.1, 79.1, 71.4 (OCH_2), 60.4, 31.8 ($ArCH_2Ar$), 28.1, 14.2.

ESI-MS: m/z calc 1796.86 obs: 1797.86 [8%, M + 2H]$^+$, 1697.92 [5%, (M-Boc) + H]$^+$, 1597.95 [5%, (M-2Boc) + H]$^+$.

5,11,17,23-tetra-guanidino-tetrakis[25,26,27,28-(hydroxycarbonylmethoxy)]calix[4]arene, tetrahydrochloride (25)

In a round-bottom flask compound **24** (100 mg, 0.056 mmol) was dissolved in 1,4-Dioxane (1 mL) then HCl (37% in water, 1 mL) was added to the solution. The mixture was stirred for 1 hour, then the solvent was evaporated. Trituration in Et_2O of the yellowish solid afforded the product as a white powder in 70% yield (35 mg, 0.039 mmol).

^{1}H NMR (400 MHz, D_2O) δ (ppm): 6.80 (s, 8H, ArH), 4.75 (s, 8H, $ArOCH_2$), 4.67 (d, *J*=13.6, 4H, $ArCH_{ax}H_{eq}Ar$), 3.36 (d, *J*=13.6, 4H, $ArCH_{ax}H_{eq}Ar$).

^{13}C NMR (101 MHz, D_2O) δ = 173.6 (COOH), 156.2, 154.0, 136.2, 129.7 (Ar), 126.1 (Ar_{meta}), 71.5 (OCH_2), 30.5 ($ArCH_2Ar$).

ESI-MS: m/z calc 888.35 obs: 889.32 [100%, M+H]$^+$

5,11,17,23-tetrakis[(p-carboxyphenyl)azo]-25,26,27,28-tetrahydroxycalix[4]arene (26)

In a round-bottom flask, 4-aminobenzoic acid (686 mg, 5mmol) and 1 mL (10 mmol) of concentrated hydrochloric acid were dissolved in 15 mL of water. After cooling the solution to 2 °C, a solution of sodium nitrite (350 mg, 5 mmol) in 10 mL of water was slowly added to the mixture. The obtained solution was then slowly added into a solution of 25,26,27,28-tetrahydroxycalix[4]arene (500 mg, 1.18 mmol) and sodium acetate (1.23 g, 15 mmol) in 26 mL MeOH-DMF (5:8, v:v) obtaining a red suspension. After stirring at room temperature for 2 h, 150 mL of 0.25% solution of hydrochloric acid was added. The temperature was then increased to 60 °C and the reaction continued under stirring for 30 minutes. The mixture was then filtered and washed with water and MeOH to obtain a red solid in a quantitative yield (1.2 g, 1.18 mmol).
^{1}H NMR (400 MHz, DMSO-d_6) δ (ppm): 8.04 (d, *J*=8.6, 8H, $ArHCO_2H$), 7.84 (s, 8H, ArH), 7.82 (d, *J*=8.6, 8H, NArH), 4.08 (bs, 8H, $ArCH_2Ar$).

The spectroscopic data found are in agreement with those reported in literature.[38]

5,11,17,23-tetraamino-25,26,27,28-tetrahydroxycalix[4]arene (27)

Compound **26** (100 mg, 0.098 mmol) was dissolved in 12 mL of an NaOH solution (1% in water) and reacted with sodium hydrosulfite (600 mg, 3.45 mmol) for 1 h at 90 °C to give a white suspension. It was then cooled rapidly to 20 °C, filtered, and washed with

water to give unstable scale-like white crystals of the desired product (47 mg, 0.097 mmol) in 99% yield. To avoid oxidation the product was immediately used in the following reaction.

5,11,17,23-tetrakis(bisBoc-guanidino)-25,26,27,28-tetrahydroxycalix[4]arene (28)

Compound **27** (47 mg, 0.097 mmol) was dissolved in 2 mL of DMF, then Bis-Boc-Thiourea (162 mg, 0.59 mmol), $HgCl_2$ (212 mg, 4.21 mmol) and TEA (0.27 mL) were added in sequence. The mixture was stirred for 16 hours and monitored by TLC (hexane/ethyl acetate 7/3) and upon completion it was quenched by addition of water (10 mL). It was then extracted with DCM (2x 10 mL), the organic phases were combined and dried over anhydrous Na_2SO_4, then the solvent was removed under reduced pressure. The crude was purified by column chromatography (eluent, hexane/ethyl acetate 8/2) and the product was obtained as a yellowish solid in 87% yield (124 mg, 0.085 mmol).

^{1}H NMR (400 MHz, $CDCl_3$) δ (ppm): 11.49 (s, 4H, NHBoc), 10.03 (s, 4H, N*H*C(=NBoc)NHBoc), 7.01 (s, 8H, ArH), 4.43 – 4.24 (m, 4H, ArC$H_{ax}$$H_{eq}$Ar), 3.91 – 3.75 (m, 4H, ArC$H_{ax}$$H_{eq}$Ar), 1.46 (s, 72H, OC($CH_3$)$_3$).

ESI-MS: m/z calc 1453.66 obs: 1454.64 [10%, M+H]$^+$, 1354.64 [30%, (M - Boc)+H]$^+$, 1254.64 [50%, (M - 2Boc)+H]$^+$

5,11,17,23-tetraguanidinium-25,26,27,28-tetrahydroxycalix[4]arene (29)

Compound **28** (34 mg, 0.0205 mmol) was dissolved in DCM (1 mL) then TFA (1 mL) was added to the solution. After 1 hour the solvent was removed under reduced pressure and a yellowish solid was obtained. The product was purified by trituration in Et_2O which afforded a white solid (13 mg, 0.0198 mmol) in 88% yield.

^{1}H NMR (400 MHz, D_2O, 353K) δ = 7.49 (s, 4H, ArH), 4.38 (s, 8H, ArCH_2Ar).

ESI-MS: m/z calc 656.75 obs: 657.73 [100%, M+H]$^+$

5,11,17,23-Tetrakis(bromomethyl)-25,26,27,28-tetrahydroxycalix[4]arene (30)

To a suspension of 25,26,27,28-tetrahydroxycalix[4]arene (1.67g, 3.94 mmol) and paraformaldehyde (2.36 g, 79 mmol) in glacial acetic acid (30 mL) was dripped hydrogen bromide (30% in acetic acid, 9.5 mL) at room temperature. The mixture was stirred for 2 h. The product was filtered and washed 3 times with water (30 mL), then dried to give a pale yellow powder (2.25 g, 2.84 mmol) in 72% yield.

^{1}H NMR (400 MHz, $CDCl_3$) δ (ppm): 10.12 (s, 4H, ArOH), 7.12 (s, 8H, ArH), 4.36 (s, 8H, $ArCH_2Br$), 4.23 (bs, 4H, $ArCH_{ax}H_{eq}Ar$), 3.56 (bs, 4H, $ArCH_{ax}H_{eq}Ar$).

The spectroscopic data found are in agreement with those reported in literature.[39]

5,11,17,23-Tetrakismethylen(bisBoc-guanidino)-25,26,27,28-tetrahydroxycalix[4]arene (31)

Compound **30** (500mg, 0.63 mmol) was dissolved in 15 mL of DMF, then potassium carbonate (504 mg, 3.65 mmol) and bis-Boc-guanidine (947 mg, 3.65 mmol) were added in sequence. The mixture was heated at 70°C and stirred for 48 hours. Upon completion it was quenched by addition of water (40 mL). It was then extracted with DCM (2x30 mL), the organic phases were combined and dried over anhydrous Na_2SO_4, then the solvent was removed under reduced pressure. The crude was purified by column chromatography (eluent, hexane/ethyl acetate 7/3) and the product was obtained as a yellowish solid in 34% yield (124 mg, 0.085 mmol).

^{1}H NMR (400 MHz, $CDCl_3$) δ (ppm): 9.29 (bs, 4H, OH), 6.88 (bs, 8H, ArH), 4.38 – 4.26 (m, 8H, $ArCH_2$), 3.60 – 3.08 (m, 8H, $ArCH_2Ar$), 1.49 (bs, 72H, $C(CH_3)_3$).

ESI-MS: m/z calc 1508.78 obs: 1509.74 [100%, M+H]$^+$

5,11,17,23-tetramethylenguanidinium-25,26,27,28-tetrahydroxycalix[4]arene (32)

Compound **31** (100 mg, 0.133 mmol) was dissolved in DCM (3 mL) then TFA (3 mL) was added to the solution. After 1 hour the solvent was removed under reduced pressure and a brown solid was obtained. The product was purified by trituration in Et_2O which afforded a yellow solid (21 mg, 0.029 mmol) in 22% yield.

^{1}H NMR (400 MHz, D_2O) δ (ppm): 7.02 (s, 8H, ArH), 4.09 (s, 8H, $ArCH_2N$), 3.86 (bs, 8H, $ArCH_2Ar$).

^{13}C NMR (101 MHz, D_2O) δ (ppm): 162.8($C_{guanidinium}$), 128.9, 127.6 (Ar_{meta}), 114.8, 43.9 ($ArCH_2$), 30.4 ($ArCH_2Ar$).

ESI-MS: m/z calc 712.86 obs: 713.83[100%, M+H]$^+$

5,17-bis(propargylamido)-25,26,27,28-tetrapropoxycalix[4]arene (33)

Compound **7** (0.1g, 0.14 mmol) was dissolved in dry DCM, then a catalytic amount of DMAP and TEA (0.04 mL, 0.28 mmol) were added. The temperature was lowered to 0°C

then propargylamine (0.018 mL, 0.28mmol) was slowly added to the solution. The reaction was stirred for 3 hours. Upon completion the solvent was evaporated, and the crude purified by flash column chromatography (eluent, hexane/AcOEt 6/4) obtaining a white solid (42 mg, 0.056 mmol) in 40% yield.

^{1}H NMR (400 MHz, $CDCl_3$) δ (ppm): 7.00 (s, 4H, ArHCO), 6.74 (d, *J* = 6.5 Hz, 4H, ArH_{meta}), 6.68 (dd, *J* = 8.5, 6.1 Hz, 2H, ArH_{para}), 6.29 (s, 2H, CONH), 4.47 (d, *J* = 13.4 Hz, 4H, Ar$CH_{ax}H_{eq}$Ar), 4.13 (d, *J* = 2.6 Hz, 4H, CONHCH_2CCH), 3.91 and 3.85 (2t, *J* = 7.6 and 7.4 Hz, 4H each, OC$H_2CH_2CH_3$), 3.21 (d, *J* = 13.4 Hz, 4H, Ar$CH_{ax}H_{eq}$Ar), 2.25 (t, *J* = 2.5 Hz, 2H, CONHCH_2CC*H*), 1.94 (m, *J* = 7.4 Hz, 8H, $OCH_2CH_2CH_3$), 1.03 and 0.99 (2t, *J* = 7.4 and 7.5 Hz, 6H each, $OCH_2CH_2CH_3$).

^{13}C NMR (101 MHz, $CDCl_3$) δ (ppm): 167.5 (Ar*C*O), 159.5 (Ar), 156.5 (Ar), 135.2 (Ar), 134.8 (Ar), 128.7 (C_{meta} Ar), 127.6 (Ar), 127.1 (C *Ar*CO), 122.6 (C_{para} Ar), 80.0 (CONHCH_2*C*CH), 77.4 (OC$H_2CH_2CH_3$), 77.1 (O*C*$H_2CH_2CH_3$), 71.3 (CONHCH_2*C*CH), 31.0 (ArCH_2Ar), 29.6 (CONHCH_2CCH), 23.3 (OCH_2*C*H_2CH_3), 23.2 (OCH_2*C*H_2CH_3), 10.4 ($OCH_2CH_2CH_3$), 10.2 ($OCH_2CH_2CH_3$).

ESI-MS: calc. (754.974), obs. 755.972 (100%) $[M + H]^+$

5,17-bis(propargylamido)-25,26,27,28-tetrakis(ethoxyethoxy)calix[4]arene (34)

Compound **17** was dissolved in dry DCM and the temperature was lowered to 0 °C. 0.07 mL (1.1 mmol) of propargylamine and 0.24 mL (1.7 mmol) of NEt_3 were added. The reaction was allowed to proceed for 3 hours at room temperature under magnetic stirring while it was monitored via TLC (eluent hexane/ethyl acetate 7:3). The reaction was then quenched with 10 mL of 1 M HCl and the organic phase extracted with DCM (3x10 mL). The combined organic phases were dried under reduced pressure. The crude reaction mixture (yellow-orange solid) was then purified by column chromatography with hexane/AcOEt as the eluent (6:4). A white solid (0.24 g, 0.27 mmol) was obtained in 49% yield.

^{1}H NMR (400 MHz, $CDCl_3$) δ (ppm): 7.11 (s, 4H, Ar*H*-CONHR), 6.63 (m, 6H ArH), 6.19 (t, *J* = 5.3 Hz, 2H, Ar-CON*H*R), 4.56 (d, *J* = 13.4 Hz, 4H, H_{ax} di Ar$CH_{ax}H_{eq}$Ar), 4.25 - 4.08 (m, 8H + 4H, ArOC$H_2CH_2OCH_2CH_3$-CONHR + Ar-CONHCH_2CCH), 3.84 (t+t, *J* = 5.5, Hz, 8H, $ArOCH_2CH_2OCH_2CH_3$), 3.55 (q+q, *J* = 7.0, 8H, $ArOCH_2CH_2OCH_2CH_3$), 3.21 (d, *J* = 13.4 Hz, 4H, H_{eq} di Ar$CH_{ax}H_{eq}$Ar), 2.27 (t, *J* = 2.5 Hz, 2H, Ar-CONHCH_2CC*H*), 1.22 (t, *J* = 6.9 Hz, 12H, $ArOCH_2CH_2OCH_2CH_3$).

^{13}C NMR (101 MHz, $CDCl_3$) δ (ppm): 167.5 (Ar-*C*ONHR), 159.7 (Ar*C*-$OCH_2CH_2OCH_2CH_3$-CONHR), 155.6 (Ar*C*-$OCH_2CH_2OCH_2CH_3$), 135.6 (Ar*C*-CH_2Ar), 134.3 (Ar*C*-CONHR),

128.53 (ArCH), 127.9 (ArC-CH_2Ar-CONHR), 127.2 (ArCH-CONHR), 122.8 (ArCH), 79.94 (Ar-CONHCH$_2$CCH) 73.5 + 73.3 (ArOCH$_2$CH$_2$OCH$_2$CH$_3$), 71.4 (Ar-CONHCH$_2$CCH), 69.7 + 69.6 (ArOCH$_2$CH$_2$OCH$_2$CH$_3$), 66.4 (ArOCH$_2$CH$_2$OCH$_2$CH$_3$), 30.9 (ArCH_2Ar), 29.6 (Ar-CONHCH$_2$CCH), 15.29 (ArOCH$_2$CH$_2$OCH$_2$CH$_3$).

ESI-MS: m/z calc (874.44) obs: 897.58 (100%) $[M + Na]^+$

5,11,17,23-tetraformyl-25,26,27,28-tetrakis(ethoxyethoxy)calix[4]arene (35)

In a round-bottom flask, dissolve 1.3 g (1.8 mmol) of compound 25,26,27,28-tetrakisethoxyethoxycalix[4]arene in 50 mL of TFA and add 8.0 g (57 mmol) of HMTA. The temperature is brought to 125°C and the reaction is left to proceed at reflux for 3 days under magnetic stirring, monitored by TLC (Ethyl Acetate/Hexane 6:4). After 3 days, the reaction is quenched with 100 mL of distilled water and left under magnetic stirring for 1 hour. The mixture changes color from amber to milky white and is extracted with 100 mL of DCM. The combined organic phases are dried over anhydrous Na_2SO_4 and dried under reduced pressure. A light-yellow oil (5 g) is obtained which is purified by column chromatography using Ethyl Acetate/Hexane (6.4) as the eluent to give compound **35** (0.8 g, 0.97 mmol) with a yield of 54%.

^{1}H NMR (400 MHz, $CDCl_3$) δ (ppm): 9.62 (s, 4H, CHO), 7.19 (s, 8H, Ar*H*-CHO), 4.65 (d, *J* = 13.9 Hz, 4H, ArC$H_{ax}H_{eq}$Ar), 4.23 (t, *J* = 5.0 Hz, 8H, ArOCH_2CH$_2$OCH$_2$CH$_3$), 3.81 (t, *J* = 5.0 Hz, 8H, ArOCH$_2$CH_2OCH$_2$CH$_3$-), 3.53 (q, *J* = 7.0 Hz, 8H, ArOCH$_2$CH$_2$OCH_2CH$_3$), 3.36 (d, *J* = 13.9 Hz, 4H, ArCH$_{ax}H_{eq}$Ar), 1.20 (t, *J* = 7.0 Hz, 12H, ArOCH$_2$CH$_2$OCH$_2$CH_3).

The spectroscopic data found are in agreement with those reported in literature.[52]

5,11,17,23-tetracarboxy-25,26,27,28-tetrakis(ethoxyethoxy)calix[4]arene (36)

In a round-bottom flask, dissolve compound **35** (0.80 g, 0.97 mmol) in 60 mL of $CHCl_3$ and 60 mL of acetone. Add 0.97 g (10.7 mmol) of $NaClO_2$ and 1.2 g (12.6 mmol) of $^+H_3NSO_4^-$, previously dissolved in the minimum amount of water. The reaction is allowed to proceed at room temperature for 3 days and is monitored by TLC (Hexane/Ethyl Acetate 3:7). The mixture is concentrated with a rotary evaporator and 100 mL of 1 M HCl is added. A precipitate forms which is filtered, washed with distilled water, and dried under reduced pressure. White solid compound **36** is obtained (0.85 g, 0.96 mmol) with a yield of 99%.

^{1}H NMR (400 MHz, CD_3OD) δ (ppm): 7.42 (s, 8H, Ar*H*), 4.67 (d, *J* = 13.5 Hz, 4H, ArC$H_{ax}H_{eq}$Ar), 4.25 (t, *J* = 5.0 Hz, 8H, ArOCH_2CH$_2$OCH$_2$CH$_3$), 3.90 (t, *J* = 5.0 Hz, 8H,

$ArOCH_2CH_2OCH_2CH_3$), 3.58 (t, *J* = 7.0 Hz, 8H, $ArOCH_2CH_2OCH_2CH_3$) 3.33 (d, J = 13.5 Hz, 4H, $ArCH_{ax}H_{eq}Ar$), 1.21 (t, *J* = 7.0 Hz, 12H, $ArOCH_2CH_2OCH_2CH_3$).

ESI-MS: m/z calc (888.36) oss: 911.35 (100%) $[M + Na]^+$

The spectroscopic data found are in agreement with those reported in literature.[53]

5,11,17,23-tetrakis(chlorocarbonyl)-25,26,27,28-tetrakis(ethoxyethoxy)calix[4]arene (37)

In a round-bottom flask, dissolve compound **36** (0.85 g, 0.96 mmol) in 4 mL of dry DCM and add 0.80 mL (10.1 mmol) of $Cl_2C_2O_2$ and a catalytic amount of DMF.. The reaction is allowed to proceed under magnetic stirring at room temperature for 1 hour and is monitored by TLC (Hexane/Ethyl Acetate 3:7). The reaction mixture is dried under reduced pressure and re-dissolved in dry DCM for the next reaction.

5,11,17,23-tetrakis(propargilamido)-25,26,27,28-tetrakis(ethoxyethoxy)calix[4]arene (38)

Compound **37** is dissolved in dry DCM and the temperature is brought to 0°C. 0.4 mL (6.2 mmol) of propargylamine and 0.8 mL (5.8 mmol) of NEt_3 are added. The reaction is allowed to proceed for 3 hours at room temperature under magnetic stirring and monitored by TLC (Hexane/Ethyl Acetate 4:6). The reaction is quenched with 10 mL of 1 M HCl and the organic phase is extracted with DCM (3x10 mL). The combined organic phases are dried under reduced pressure. The reaction crude (0.7 g) (yellow-orange solid) is purified by column chromatography with Hexane/Ethyl Acetate as eluent (2:8). A white solid (0.32 g, 0.31 mmol) is obtained with a total yield of 32%.

^{1}H NMR (400 MHz, CD_3OD) δ (ppm): 7.29 (s, 8H, ArH), 4.73–4.63 (d, *J* = 13.7 Hz, 4H, $ArCH_{ax}H_{eq}Ar$), 4.26 (t, *J* = 5.0 Hz, 8H, $ArOCH_2CH_2OCH_2CH_3$-CONHR), 4.07 (d, *J* = 2.4 Hz, 8H, Ar-$CONHCH_2CCH$), 3.91 (t, *J* = 5.0 Hz, 8H, $ArOCH_2CH_2OCH_2CH_3$-CONHR), 3.58 (q, *J* = 7.0 Hz, 8H, $ArOCH_2CH_2OCH_2CH_3$-CONHR), 3.36 (d, *J* = 13.7 Hz , 4H, $ArCH_{ax}H_{eq}Ar$), 2.56 (t, *J* = 2.5 Hz, 4H, Ar-$CONHCH_2CCH$), 1.21 (t, *J* = 7.0 Hz, 12H, $ArOCH_2CH_2OCH_2CH_3$-CONHR).

^{13}C NMR (101 MHz, CD_3OD) δ (ppm): 168.1 (Ar-*C*ONHR), 159.4 (ArC-$OCH_2CH_3OCH_2CH_3$), 134.9 (ArC-CONHR), 127.9 (ArC-CH_2Ar), 127.6 (Ar*C*H), 79.5 (Ar-$CONHCH_2CCH$), 73.6 ($ArOCH_2CH_2OCH_2CH_3$-CONHR), 70.4 (Ar-$CONHCH_2CCH$), 69.7 ($ArOCH_2CH_2OCH_2CH_3$-CONHR), 66.0 ($ArOCH_2CH_2OCH_2CH_3$-CONHR), 30.6 ($ArCH_2Ar$), 28.5 (Ar-$CONHCH_2CCH$), 14.3 ($ArOCH_2CH_2OCH_2CH_3$-CONHR).

ESI-MS: m/z calc (1036.48) oss: 1037.52 (100%) $[M + H]^+$

6-O-(diphenoxyphosphoryl)-D-trehalose (39)

Trehalose (2.5 g, 7.3 mmol) was suspended in anhydrous pyridine (33 mL) then diphenylphosphorylchloride (1.5 mL, 7.3 mmol) was slowly added. The mixture was stirred at room temperature for 16 hours then it was quenched by addition of methanol (10 mL). The solvents were removed under reduced pressure and the crude was purified by column chromatography (eluent, water/2-propanol/ethyl acetate 1/3/13) obtaining a white solid (800 mg, xx mmol) in 20% yield.

^{1}H NMR (400 MHz, CD_3OD) δ (ppm): 7.44 – 7.21 (m, 10H, ArH), 5.09 (t, *J* = 4.0 Hz, 2H, H_1), 4.59 – 4.42 (m, 2H, H_{6a} H_{6b}), 4.09 (ddt, *J* = 10.2, 4.4, 2.1 Hz, 1H, H_5), 3.90 – 3.77 (m, 4H, H_3, H_3', H_5',H_{6b}'), 3.70 (dd, *J* = 12.0, 5.5 Hz, 1H, H_{6a}'), 3.48 (dd, *J* = 9.8, 3.7 Hz, 1H, H_2'), 3.46 – 3.36 (m, 3H, H_4', H_4, H_2).

The spectroscopic data found are in agreement with those reported in literature.[54]

6-O-diphenoxyphosphoryl-2,2',3,3',4,4',6'-hepta-O-benzoyl-α,α-D-trehalose (40)

Compound **38** (0.7 g, 1.22 mmol) was dissolved in anhydrous pyridine (15 mL) at 0°C, then benzoyl chloride (1.56 mL, 13.41 mmol) was slowly added. The reaction was stirred at room temperature for 16 hours. It was then quenched by addition of 1M HCl (20 mL) and extracted with DCM (2x20 mL). The organic phases were combined, dried over anhydrous Na_2SO_4 and the solvent evaporated under reduced pressure. The crude was then purified by column chromatography (eluent, hexane/ethyl acetate 6/4) obtaining a colorless oil (470 mg, 0.36 mmol) in 30% yield.

^{1}H NMR (400 MHz, $CDCl_3$) δ (ppm): 8.11 (d, *J* = 7.3 Hz, 2H, Bz ArH_{orto}), 8.08 (d, *J* = 7.3 Hz, 2H, Bz ArH_{orto}), 8.00 – 7.95 (m, 2H, Bz ArH_{orto}), 7.94 – 7.90 (m, 4H, Bz ArH_{orto}), 7.83 – 7.76 (m, 4H, Bz ArH_{orto}), 7.61 -7.09 (m, 31H, ArH), 6.27 (t, *J* = 9.9 Hz, 1H, H_3'), 6.23 (t, *J* = 9.9 Hz, 1H, H_3), 5.73 – 5.60 (m, 3H, H_1, H_1', H_4), 5.55 (t, *J* = 9.9 Hz, 1H, H_4), 5.48 (dd, *J* = 10.2, 3.8 Hz, 1H, H_2'), 5.32 (dd, *J* = 10.1, 3.7 Hz, 1H, H_2), 4.28 (ddd, *J* = 10.3, 4.9, 2.9 Hz, 1H, H_5'), 4.16 (m, 1H, H_5), 4.08 (dd, *J* = 12.4, 2.9 Hz, 1H, H_{6b}'), 4.02 – 3.80 (m, 3H, H_{6a}, H_{6b}, H_{6a}').

The spectroscopic data found are in agreement with those reported in literature.[54]

6-azido-diphenoxyphosphoryl-2,2',3,3',4,4',6'-hepta-O-benzoyl-α,α-D-trehalose (41)

Compound **40** (470 mg, 0.37 mmol) and sodium azide (48 mg, 0.74 mmol) were dissolved in dry DMF (15 mL). The solution was heated at 80°C for 24 hours. Upon rection completion water (50 mL) and Ethyl Acetate (50 mL) were added to the mixture. The organic phase was separated, dried over anhydrous Na_2SO_4 and evaporated under reduced pressure. The oily crude obtained was purified by column chromatography (eluent, hexane/ethyl acetate 6/4) which gave the pure product as a colorless oil (353 mg, 0.32 mmol) in 87% yield.

^{1}H NMR (400 MHz, $CDCl_3$) δ (ppm): 8.21 – 8.13 (m, 2H, ArH_{ortho}), 8.12 – 8.06 (m, 2H, ArH_{ortho}), 8.01 – 7.91 (m, 6H, ArH_{ortho}), 7.85 (dd, *J* = 8.1, 1.4 Hz, 4H, ArH_{ortho}), 7.63 – 7.53 (m, 3H, ArH), 7.52 – 7.31 (m, 19H, ArH), 6.42 – 6.22 (m, 2H, H_4, H_3'), 5.78 (t, *J* = 3.8 Hz, 2H, H_1, H_1'), 5.71 (t, *J* = 9.9 Hz, 1H, H_4'), 5.58 (t, *J* = 9.8 Hz, 1H, H_4), 5.51 (dd, *J* = 10.2, 3.8 Hz, 2H, H_2, H_2'), 4.33 (ddd, *J* = 10.4, 4.5, 2.8 Hz, 1H, H_5'), 4.19 – 4.10 (m, 1H, H_5), 4.05 (dd, *J* = 12.4, 2.7 Hz, 1H, H_{6b}'), 3.92 (dd, *J* = 12.4, 4.7 Hz, 1H, H_{6a}'), 2.97 – 2.87 (m, 2H, H_{6a}, H_{6b}).

The spectroscopic data found are in agreement with those reported in literature.[54]

4'-hydroxy-2,2',3,3',4,6,6'-hepta-O-benzoyl-α,α-D-trehalose (42)

Trehalose (500 mg, 1.32 mmol) was dissolved in dry pyridine (20 mL) then the temperature was lowered to -40 °C. Benzoyl chloride (1.1 mL, 9.24 mmol) was then slowly added to the solution. The mixture was stirred for 60 minutes and kept for 16 hours at room temperature. The reaction was quenched by addition of 1M HCl (30 mL), then extracted with DCM (30 mL). The organic phase was dried over anhydrous Na_2SO_4 and the solvent was removed under reduced pressure. The crude was purified by column chromatography (eluent, DCM/ethyl acetate 95/5) obtaining a colorless oil (220 mg, 0.21 mmol) in 16% yield.

^{1}H NMR (400 MHz, $CDCl_3$) δ (ppm): 8.14 – 7.83 (m, 14H, ArH), 7.62 – 7.27 (m, 22H, ArH), 6.31 (t, *J* = 9.9 Hz, 1H, H_3), 6.04 (dd, *J* = 10.2, 9.2 Hz, 1H, H_3'), 5.75 – 5.67 (m, 3H, H_4, H_1, H_1'), 5.55 (dd, *J* = 10.3, 3.8 Hz, 1H, H_2), 5.49 (dd, *J* = 10.2, 3.9 Hz, 1H, H_2'), 4.40 (ddd, *J* = 10.2, 4.7, 2.8 Hz, 1H, H_5), 4.24 (dd, *J* = 12.3, 4.3 Hz, 1H, H_{6a}), 4.15 (m, 1H, H_5'), 4.01 (dd, *J* = 12.5, 2.8 Hz, 1H, H_{6b}'), 3.96 – 3.84 (m, 3H, $H_{6'a}$, H_4', H_{6b}), 3.76 (s, 1H, OH).

The spectroscopic data found are in agreement with those reported in literature.[40]

2,3,6-Tri-O-benzoyl-α-D-galactopyranosyl-2,3,4,6-tetra-O-benzoyl-α-D-glucopyranoside (43)

Compound **42** (420 mg, 0.39 mmol) was dissolved in dry DCM (3 mL) and dry pyridine (0.06 mL), the solution was then cooled to 0 °C. Triflic anhydride (0.1 mL, 0.59 mmol) was then slowly added to the mixture which was stirred for 30 minutes. Upon completion, the reaction was quenched by the addition of water (5 mL) and extracted with DCM (2x5 mL). The organic phases were combined and washed with 1% HCl (10 mL), $NaHCO_3$ (10 mL), and water (2x10 mL), then dried over anhydrous Na_2SO_4 and evaporated under reduced pressure. The oily crude obtained was used immediately without further purification.

The crude (471 mg, 0.39 mmol) was solubilized in dry DMF (5 mL) then $NaNO_2$ (108 mg, 1.57 mmol) was added to the solution. The mixture was stirred at room temperature for 48 hours. Upon completion the reaction was quenched by addition of water (10 mL) and extracted with DCM (2x10 mL). The organic phases were combined, dried over anhydrous Na_2SO_4 and evaporated under reduced pressure. The crude was purified by column chromatography (eluent, DCM/ethyl acetate 95/5) obtaining a colorless oil (160 mg, 0.14 mmol) in 36% yield.

^{1}H NMR (400 MHz, $CDCl_3$) δ (ppm): 8.20 – 7.76 (m, 15H, ArH), 7.65 – 7.29 (m, 21H, ArH), 6.30 (t, *J* = 10.0 Hz, 1H, H_3), 6.03 – 5.90 (m, 2H, H_2', H_3'), 5.78 (2x d, 3.7 Hz, 2H, H_1, H_1'), 5.68 (t, *J* = 9.9 Hz, 1H, H_4), 5.53 (dd, *J* = 10.3, 3.8 Hz, 1H, H_2), 4.43 – 4.34 (m, 2H, H_5, H_4'), 4.31 – 4.23 (m, 2H, H_{6b}', H_{6a}'), 4.15-4.05 (m, 2H, H_{6b}, H_5'), 3.99 (dd, *J* = 12.4, 5.0 Hz, 1H, H_{6a}), 3.36 (bs, 1H, OH).

The spectroscopic data found are in agreement with those reported in literature.[40]

4'-azido-2,2',3,3',4,6,6'-hepta-O-benzoyl-α,α-D-trehalose (44)

Compound **43** (160 mg, 0.14 mmol) was dissolved in dry DCM (1 mL) and dry pyridine (0.024 mL), the temperature was then lowered to 0 °C and triflic anhydride (0.038 mL, 0.022 mmol) was slowly added. The mixture was stirred at room temperature for 30 minutes then it was quenched by addition of water (2 mL). The organic phase was separated and the aqueous one was washed two times with DCM (3 mL). The combine organic phases were washed with 1% HCl (3 mL), $NaHCO_3$ (5 mL), water (5 mL) and brine (5 mL), the solvent was then evaporated under reduced pressure. The oily product was used without further purification.

The crude (179 mg, 0.14 mmol) was solubilized in dry DMF (1 mL) then sodium azide (39 mg, 0.60 mmol) and 15-crown-5 (0.012 mL, 0.60 mmol) were added to the solution, which was then stirred at room temperature for 120 minutes. Upon completion the mixture was diluted with DCM (5 mL), washed with water (5x5 mL), and brine (5 mL), the solvent was evaporated, and the crude purified by column chromatography (eluent, DCM/ethyl acetate 95/5). A colorless glassy solid was obtained (60 mg, 0.05 mmol) in 36% yield.

^{1}H NMR (400 MHz, $CDCl_3$) δ (ppm): 8.14 – 7.84 (m, 14H, ArH), 7.66 – 7.30 (m, 21H, ArH), 6.29 (t, *J* = 10.0 Hz, 1H, H_3), 6.19 (t, *J* = 10.0 Hz, 1H, H'_3), 5.77 – 5.62 (m, 3H, H_1, H_1', H_4), 5.52 (dd, *J* = 10.3, 3.8 Hz, 1H, H_2), 5.43 (dd, *J* = 10.2, 3.8 Hz, 1H, H_2'), 4.35 (ddd, *J* = 10.2, 4.6, 2.7 Hz, 1H, H_5), 4.10 – 3.93 (m, 4H, H_{6b}, H_5', H_{6a}', H_{6b}'), 3.93 – 3.78 (m, 2H, H_{6a}, H_4').

The spectroscopic data found are in agreement with those reported in literature.[40]

2',3'-di-O-benzyl-α-D-glucopyranosyl-2,3-di-O-benzyl-4,6-O-benzylidene-α-D-glucopyranoside (47)

Dimethoxymethylbenzne (1.98 mL, 12.16 mmol) was dissolved in DMF (10 mL) then a catalytic amount of TsOH was added to the solution. Trehalose (2.00 g, 5.84 mmol) was suspended in dry DMF (10 mL), and heated to 100 °C, then the previously prepared solution of dimethoxymethylbenzne was added in three steps (40%, 40%, 20% of the total volume respectively for the first, second and last addition) waiting 20 minutes between each addition. The mixture was further stirred at 100 °C for 60 minutes, then the solvent was distilled away. The brown oily crude was solubilized with DMF (30 mL) and cooled to 0 °C, then NaH (1.40 g, 58.4 mmol) was slowly added to the solution. After 5 minutes benzyl bromide (4.50 g, 26.28 mmol) was dripped into the mixture, which was left stirring for 3 hours.

Upon reaction completion water (30 mL) was added to quench excess NaH. the mixture was then diluted with EtOAc (30 mL) and washed with H_2O (3x20 mL) and brine (20 mL). The organic layer was dried over anhydrous Na_2SO_4 and concentrated to yield a pale-yellow residue. The oily crude obtained was redissolved in 20 mL of 9:1 MeOH–DCM, and trifluoroacetic acid (2 mL) was added. After 3 h, TLC anaylsis indicated the formation of two new products along with unreacted starting material. A saturated solution of $NaHCO_3$ was added (30 mL), and the resulting mixture was extracted with EtOAc (30 mL) which was then washed with water (20 mL) and brine (20 mL). The organic layer was adsorbed onto silica gel and purified by flash chromatography (eluent hexane/ethyl acetate 6/4) obtaining a colorless oil (1.50 g, 1.89 mmol) in 33% yield (over three steps).

^{1}H NMR (400 MHz, $CDCl_3$) δ (ppm): 7.57 – 7.29 (m, 25H, ArH), 5.59 (s, 1H, O_2CHPh), 5.17 (2x d, *J* = 3.7 Hz, 2H, H_1, H_1'), 5.10 – 4.68 (m, 8H, OCH_2Ph), 4.28 (td, *J* = 10.0, 4.9 Hz, 1H, H_5'), 4.20 – 4.10 (m, 2H, H_3', H_{6a}'), 4.04 (dt, *J* = 10.0, 3.8 Hz, 1H, H_5), 3.90 (t, *J* = 9.2 Hz, 1H, H_3), 3.75 – 3.54 (m, 7H, H_2, H_2', H_4, H_4', H_{6a}, H_{6b}, H_{6b}').

The spectroscopic data found are in agreement with those reported in literature.[42]

2,3,2',3'-tetra-O-benzyl-4,6-O-benzylidene-6'-O-tert-butyldimethylsilyl-α,α-D-trehalose (48)

Compound **47** (1.00 g, 1.26 mmol) was dissolved in dry DCM (10 mL), and DMAP (14 mg, 0.120 mmol) and Et_3N (0.7 mL, 5 mmol) were added to the solution, followed by TBDMSCl (574 mg, 3.80 mmol). The resulting solution was stirred at room temperature for 48 h. Upon completion, the mixture was washed with water and the organic phase was adsorbed onto silica gel and purified by flash chromatography (eluent, hexane/ethyl acetate 8/2) obtaining the desired product as a colorless oil (1104 mg, 1.22 mmol) in 97% yield.

^{1}H NMR (400 MHz, $CDCl_3$) δ (ppm): 7.57 – 7.29 (m, 25H, ArH), 5.57 (s, 1H, O_2CHPh), 5.19 (d, *J* = 3.6 Hz, 2H, H_1, H_1'), 5.00 (2x d, *J* = 11.2 Hz, 2H, OBn), 4.86 (m, 2H, OBn), 4.81 – 4.72 (m, 4H, OBn), 4.28 (td, *J* = 10.0, 4.9 Hz, 1H, H_5'), 4.20 – 4.08 (m, 2H, H_3', H_{6a}'), 4.02 (dt, *J* = 9.7, 3.8 Hz, 1H, H_5'), 3.92 (t, *J* = 9.3 Hz, 1H, H_3), 3.79 – 3.51 (m, 7H, H_2, H_2', H_4, H_4', H_{6a}, H_{6b}, H_{6b}'), 0.89 (s, 9H, $C(CH_3)_3$), 0.05 (s, 6H, $Si(CH3)_2$).

The spectroscopic data found are in agreement with those reported in literature.[42]

2,3,2',3'-tetra-O-benzyl-4'-carbonyl-4,6-O-benzylidene-6'-O-tert-butyldimethylsilyl-α,α-D-trehalose (49)

Oxalyl chloride (0.27 mL, 3.11 mmol) was dissolved in dry DCM (15 mL) and then cooled to -78 °C and dry DMSO (0.45 mL, 6.21 mL) was dripped in. The mixture was stirred for 30 minutes then a solution of compound **48** (1404 mg, 1.55 mmol) in dry DCM (10 mL) was added. After 60 minutes of stirring dry NEt_3 (1.73 mL, 12.41 mmol) was added to the mixture which was stirred for 10 additional minutes while it was allowed to reach room temperature. The reaction was then quenched by addition of water (30 mL). The organic phase was separated and the aqueous one was washed with DCM (10 mL). The combined organic phases were dried over anhydrous Na_2SO_4 and evaporated under reduced pressure. The yellowish oil obtained (1230 mg, 1.37 mmol) in 89% yield was

used without further purification.

^{1}H NMR (400 MHz, $CDCl_3$) δ (ppm): 7.58 – 7.29 (m, 25H, ArH), 5.59 (s, 1H, O_2CHPh), 5.34 (d, *J* = 3.4 Hz, 1H, H_1'), 5.28 (d, *J* = 3.7 Hz, 1H, H_1), 5.01 (d, *J* = 11.0 Hz, 1H, OCH_2Ph), 4.96 (d, *J* = 11.2 Hz, 1H, OCH_2Ph), 4.86 (d, *J* = 12.0 Hz, 1H, OCH_2Ph), 4.82 (d, *J* = 11.2 Hz, 1H, OCH_2Ph), 4.78 – 4.73 (m, 2H, OCH_2Ph), 4.72 – 4.65 (m, 2H, OCH_2Ph), 4.56 (dd, *J* = 6.1, 3.3 Hz, 1H, H_5'), 4.50 (d, *J* = 10.0 Hz, 1H, H_3'), 4.30 (td, *J* = 10.0, 4.9 Hz, 1H, H_5), 4.20 (dd, *J* = 10.2, 4.9 Hz, 1H, H_4), 4.10 (t, *J* = 9.3 Hz, 1H, H_3), 3.92 (dd, *J* = 11.3, 3.3 Hz, 1H, H_{6b}'), 3.86 (dd, *J* = 10.0, 3.4 Hz, 1H, H_2'), 3.80 (dd, *J* = 11.4, 6.1 Hz, 1H, H_{6a}'), 3.76 – 3.64 (m, 3H, H_2, H_{6a}, H_{6b}), 0.89 (s, 9H, $C(CH_3)_3$), 0.07 (d, *J* = 2.9 Hz, 6H, $Si(CH_3)_2$).

^{13}C NMR (101 MHz, $CDCl_3$) δ = 202.9, 138.7, 137.9, 137.9, 137.8, 137.5, 128.9, 128.5, 128.5, 128.4, 128.3, 128.2, 128.1, 128.0, 127.9, 127.8, 127.8, 127.7, 127.6, 101.3, 94.2, 93.6, 82.7, 82.3, 79.6, 78.9, 78.5, 75.3, 74.9, 74.4, 73.9, 69.0, 63.0, 61.3, 45.8, 41.0, 26.0, 18.4, 8.6, -5.2, -5.4.

2',3'-di-O-benzyl-6'-O-tert-butyldimethylsilyl-α-D-galactopyranosyl-2,3,-di-O-benzyl-4,6-O-benzylidene-α-D-glucopyranoside (50)

Compound **49** (500 mg, 0.55 mmol) was dissolved in dry THF (5 mL) and cooled to -78 °C. A solution of L-selectride 1M in THF (1.11 mL, 1.11 mmol) was slowly dripped in, then the mixture was left stirring for 120 minutes. The temperature was then slowly increased to room temperature and the reaction was quenched by addition of water (10 mL) followed by DCM (10 mL). The organic layer was separated and adsorbed onto silica gel. The crude was purified by flash column chromatography (eluent, hexane/ethyl acetate 8/2) obtaining a colorless oil (400 mg, 0.44 mmol) in 81% yield.

^{1}H NMR (400 MHz, $CDCl_3$) δ (ppm): 7.58 – 7.29 (m, 25H, ArH), 5.57 (s, 1H, OCHPh), 5.31 – 5.18 (m, 2H, H_1, H_1'), 4.96 (d, *J* = 11.2 Hz, 1H, OCH_2Ph), 4.88 – 4.68 (m, 7H, OCH_2Ph), 4.29 (td, *J* = 9.9, 4.9 Hz, 1H, H_5), 4.20 – 3.99 (m, 6H, H_2', H_3, H_3', H_{6a}', H_5'), 3.86 – 3.59 (m, 6H, H_2, H_4, H_4', H_{6a}, H_{6b}, H_{6b}'), 0.91 (s, 9H, $C(CH_3)_3$), 0.08 (m, 6H, $Si(CH_3)_2$).

^{13}C NMR (101 MHz, $CDCl_3$) δ = 138.9, 138.5, 138.4, 138.2, 137.7, 128.9, 128.5, 128.5, 128.5, 128.3, 128.2, 127.9, 127.8, 127.8, 127.8, 127.7, 127.6, 126.2, 101.3, 94.8, 94.2, 93.9, 82.5, 81.2, 79.3, 79.1, 78.6, 77.9, 77.4, 77.1, 76.8, 75.5, 75.3, 73.7, 73.5, 72.4, 71.0, 69.9, 69.1, 68.0, 63.2, 63.0, 62.8, 31.7, 26.0, 22.7, 18.5, 18.4, 14.2, -5.3, -5.4.

2,3,2',3'-tetra-O-benzyl-4'-azido-4,6-O-benzylidene-6'-O-tert-butyldimethylsilyl-α,α-D-trehalose (51)

Compound **50** (400 mg, 0.44 mmol) was dissolved in dry THF (5 mL), then the solution was cooled at 0 °C and triphenyphosphine (127 mg, 0.48 mmol) was added, followed by diisopropyl azodicarboxylate (0.095 mL, 0.48 mmol). Diphenyphosphoryl azide (0.104 mL, 0.48 mmol) was then slowly dripped in over 15 minutes. The mixture was allowed to warm up to room temperature and left stirring for 16 hours. Upon completion the reaction was quenched by addition of water (5 mL), and it was extracted with DCM (10 mL). The organic phase was dried over anhydrous Na_2SO_4 and adsorbed onto silica gel. The crude was purified by flash column chromatography obtaining a colorless oil (135 mg, 0.14 mmol) in 32% yield.

^{1}H NMR (400 MHz, $CDCl_3$) δ (ppm): 7.63 – 7.29 (m, 25H, ArH), 5.64 (s, 1H, O_2CHPh), 5.23 (d, *J* = 3.5 Hz, 1H, H_1), 5.21 (d, *J* = 3.7 Hz, 1H, H_1'), 5.14 – 4.74 (m, 8H, OCH_2Ph), 4.72 (d, *J* = 11.8 Hz, 1H, OCH_2Ph), 4.32 (td, *J* = 10.0, 4.9 Hz, 1H, H_5), 4.24 – 4.16 (m, 2H, H_{6a}, H_3'), 4.00 (t, *J* = 9.6 Hz, 1H, H_3), 3.91 (ddd, *J* = 10.4, 2.9, 1.7 Hz, 1H, H_5'), 3.80 – 3.56 (m, 6H, H_2, H_2', H_4, H_4', $H_{6'a}$, H_{6b}), 3.52 (dd, *J* = 11.7, 1.7 Hz, 1H, H_{6b}'), 0.96 (s, 9H, $C(CH_3)_3$), 0.11 (d, *J* = 4.8 Hz, 6H, $Si(CH_3)_2$).

^{13}C NMR (101 MHz, $CDCl_3$) δ (ppm): 138.8, 138.2, 138.1, 137.9, 137.6, 130.1, 129.9, 129.8, 129.1, 129.0, 128.6, 128.6, 128.5, 128.5, 128.4, 128.3, 128.0, 127.9, 127.9, 127.8, 127.7, 127.6, 127.4, 126.2, 125.7, 120.3, 120.3, 120.2, 120.2, 101.3, 95.0, 94.3, 82.5, 81.9, 79.9, 79.6, 79.2, 78.7, 77.4, 77.1, 76.8, 75.8, 75.7, 75.3, 73.9, 73.6, 73.2, 72.7, 70.9, 69.1, 68.2, 63.1, 62.8, 62.4, 62.0, 61.9, 61.1, 29.5, 26.1, 22.0, 18.5, -5.3, -5.4, -5.6.

Methyl-2,3,4-tri-O-benzoyl-6-azido-6-deoxy-α-D-mannopyranose (54)

In a round-bottom flask, 1.0 g (5.5 mmol) of Methyl α-D-mannopyranoside is dissolved in 5 mL of dry pyridine (30 mL) and 1.0 g (5.5 mmol) of TsCl is added. The reaction is allowed to proceed for 1 night at room temperature under magnetic stirring. The reaction is monitored through TLC (Hexane / Ethyl Acetate 5:5). To the reaction mixture, 2.0 mL (17 mmol) of BzCl is added after lowering the temperature to 0°C. The reaction is allowed to proceed for 3 days at room temperature under magnetic stirring. The reaction mixture is dried under reduced pressure, redissolved in DCM (50 mL) and extracted with a saturated solution of NaCl (3x50 mL). The crude product is not further purified but is redissolved in 10 mL of DMF and 0.65 g (10 mmol) of NaN_3 and LiBr (100 mg) are added. The temperature is brought to 120°C and the reaction is allowed to reflux for 2 days under magnetic stirring, monitored through TLC (Hexane/Ethyl Acetate 7:3). The reaction mixture is cautiously quenched with distilled water (10 mL) and with a saturated solution of $NaHCO_3$ (2mL), extracted with DCM (3x10 mLl). The combined organic phases are dried over anhydrous Na_2SO_4 and dried under reduced pressure. The crude product obtained (brown oil, 3 g) is purified through column

chromatography, using Hexane/Ethyl Acetate (8:2, 7:3) as the eluent to give compound 21 (0.94 g, 1.87 mmol) with a total yield of 34%.

^{1}H NMR (400 MHz, $CDCl_3$) δ (ppm): 8.17-8.10 (m, 2H, ArH of OBz), 8.02-7.95 (m, 2H, ArH of OBz), 7.87-7.79 (m, 2H, ArH of OBz), 7.71-7.61 (m, 1H, ArH of OBz), 7.59-7.49 (m, 3H, ArH of OBz), 7.48-7.37 (m, 3H, ArH of OBz), 7.33-7.25 (m, 2H, ArH of OBz), 5.95-5.81 (m, 2H, H_4 + H_3), 5.70 (dd, *J* = 2.9, 1.8 Hz, 1H, H_2), 5.03 (d, *J* = 1.8 Hz, 1H, H_1), 4.28 (ddd, *J* = 9.1, 6.6, 2.6 Hz, 1H, H_5), 3.59 (s, 3H, OCH_3), 3.58-3.52 (m, 1H, H_{6A}), 3.48 (dd, *J* = 13.3, 2.6 Hz, 1H, H_{6B}).

The spectroscopic data found are in agreement with those reported in literature.[55]

5,17-bis-[N-((1-(2,2',3,3',4,4',6,-hepta-O-benzoyl-6-deoxy-trehalos-6-yl)-1H-1,2,3-triazol-4-yl)methyl)aminocarbonyl]-25,26,27,28-tetrapropoxycalix[4]arene (55a)

Calixarene **34** (27 mg, 0.037 mmol) and compound **41** (120 mg, 0.11 mmol) were dissolved in DMF/water (3 mL and 0.5 mL respectively). $CuSO_4$ pentahydrate (2.8 mg, 0.011 mmol) and sodium ascorbate (4.4 mg, 0.022 mmol) were added to the solution. The reaction was microwaved at 80°C (150 W) for 90 minutes, then it was extracted with DCM (2x 10 mL). The organic phase was dried over anhydrous Na_2SO_4 and the solvent was removed under reduced pressure. The crude was purified by column chromatography (eluent, hexane/ethyl acetate 6/4) obtaining a white solid (50 mg, 0.017 mmol) in 46% yield.

^{1}H NMR (400 MHz, CDCl3) δ 8.21 – 7.71 (m, 30H, ArH), 7.67 – 7.21 (m, 44H, ArH), 7.07 (s, 2H, $CH_{triazole}$), 6.35 – 6.22 (m, 10H, H_3', H_3, ArH), 5.80 (d, *J* = 3.7 Hz, 2H, H_1'), 5.64 – 5.53 (m, 4H, H_4, H_1), 5.47 (dd, *J* = 10.2, 3.7 Hz, 2H, H_2'), 5.43 (dd, *J* = 10.3, 3.8 Hz, 2H, H_2), 5.31 (t, *J* = 9.8 Hz, 2H, H_4'), 4.73 (d, *J* = 4.6 Hz, 2H, CCH_2NH), 4.44 (2x d, *J* = 13.3 Hz, 4H, $ArCH_{ax}H_{eq}Ar$), 4.35 (ddd, *J* = 9.8, 6.1, 2.9 Hz, 2H, H_5'), 4.29 – 4.22 (m, 2H, H_5), 4.22 – 4.09 (m, 4H, $H_{6'a}$, $H_{6'b}$), 4.08 – 3.90 (m, 8H, H_{6a}, H_{6b}, $NHCOArOCH_2$), 3.70 (t, *J* = 7.1 Hz, 4H, $ArOCH_2$), 3.19 (2x d, *J* = 13.4 Hz, 4H, $ArCH_{ax}H_{eq}Ar$), 2.00 – 1.81 (m, 8H, $ArOCH_2CH_2$, $NHCOArOCH_2CH_2$), 1.03 (t, *J* = 7.4 Hz, 6H, $NHCOArOCH_2CH_2CH_3$), 0.90 (t, *J* = 7.5 Hz, 6H, $ArOCH_2CH_2CH_3$).

^{13}C NMR (101 MHz, $CDCl_3$) δ = 165.8, 165.6, 165.5, 165.2, 165.0, 164.8, 144.5, 136.4, 134.0, 133.8, 133.5, 133.3, 133.2, 130.1, 130.0, 129.9, 129.8, 129.7, 129.3, 128.9, 128.7, 128.6, 128.5, 128.4, 128.3, 127.4, 122.4, 92.2, 92.0, 77.3, 77.0, 76.7, 71.2, 70.8, 70.1, 69.9, 69.2, 69.0, 68.7, 62.1, 35.0, 31.0, 29.7, 23.3, 23.2, 14.1, 10.5, 10.0, 9.8, 1.0.

ESI-MS: m/z calc (2947.10) oss: 1474.60 (100%) $[M + 2H]^{2+}$

5,17-bis-[N-((1-(6-deoxy-trehalos-6-yl)-1H-1,2,3-triazol-4-yl)methyl)aminocarbonyl]-25,26,27,28-tetrapropoxycalix[4]arene (55)

Compound **55a** (50 mg, 0.017 mmol) has been dissolved in MeOH (2 mL) then sodium methoxide (26 mg, 0.48 mmol) has been added. The mixture was stirred at room temperature for 60 minutes then Amberlyst IR-120 was added. The suspension was stirred for an additional 30 minutes then the resin was filtered off. After lyophilization a white solid (24 mg, 0.017 mmol) was obtained in quantitative yield.

^{1}H NMR (400 MHz, DMSO-d_6) δ(ppm): 8.89 (bs, 2H, CONH), 7.92 (s, 2H, $CH_{triazole}$), 7.68 (s, 4H, ArH), 6.23 (t, *J* = 7.3 Hz, 2H, ArH_{para}), 6.17 (d, *J* = 7.7 Hz, 4H, ArH_{meta}), 5.31 (d, *J* = 5.5 Hz, 2H, H1), 4.99 – 4.31 (m, 22H, Ar$CH_{ax}H_{eq}$Ar, H_1', H_3, H_3', H_4, H_4', H_5, H_5' ,H_{6a}', H_{6b}'), 4.21 – 3.99 (m, 4H, O$CH_2CH_2CH_3$), 3.70 – 3.39 (m, 12H, O$CH_2CH_2CH_3$, CCH_2NH, H_{6a}, H_{6b}), 3.23 (d, *J* = 12.5 Hz, 4H, Ar$CH_{ax}H_{eq}$Ar), 3.16 - 2.95 (m, 4H, H_2, H_2'), 2.02 – 1.80 (m, 8H, $OCH_2CH_2CH_3$), 1.09 (t, *J* = 7.4 Hz, 6H, $OCH_2CH_2CH_3$), 0.89 (t, *J* = 7.4 Hz, 6H, $OCH_2CH_2CH_3$).

ESI-MS: m/z calc (1489.59) oss: 1490.60 (100%) $[M + H]^+$

5,17-bis-N-[((1-(2,2',3,3',4,4',6,-hepta-O-benzoyl-6-deoxy-trehalos-6-yl)-1H-1,2,3-triazol-4-yl)methyl)aminocarbonyl]-25,26,27,28-tetrakis(ethoxyethoxy)calix[4]arene (56a)

Compound **38** (10 mg, 0.011 mmol) and compound **41** (38 mg, 0.034 mmol) were loaded in a microwave vial and dissolved in a mixture of DMF and water (800 uL and 200 uL respectively), then $CuSO_4$ pentahydrate (0.86 mg, 0.0034 mmol) and sodium ascorbate (1.4 mg, 0.007 mmol) were added to the solution which was then heated at 90 °C for 40 minutes. Upon water (5 mL) and ethyl acetate (10 mL) were added. The organic phase was separated, and the aqueous one was washed two time with ethyl acetate (10 mL each). The combined organic phases were anhydrified over $NaSO_4$ and the solvent was evaporated under reduced pressure. The crude was purified by column chromatography (eluent, heane/ethyl acetate 6/4) obtaining a white solid (26 mg, 0.0085 mmol) in 41% yield.

^{1}H NMR (400 MHz, $CDCl_3$) δ(ppm): 8.19 – 8.03 (m, 8H, ArH of Bz), 7.99 – 7.74 (m, 23H, ArH of Bz), 7.65 – 7.51 (m, 11H, ArH of Bz), 7.50 – 7.30 (m, 39H ArH of Bz, ArH), 6.44 – 6.03 (m, 6H, ArH), 5.81 (d, J = 3.7 Hz, 2H, H_1), 5.69 – 5.56 (m, 4H), 5.48 (dd, J = 10.2, 3.6 Hz, 2H), 5.40 (dd, J = 8.4, 4.9 Hz, 2H), 5.38 – 5.26 (m, 2H), 4.88 – 4.76 (m, 3H), 4.57 – 4.19 (m, 15H), 4.10 – 3.08 (m, 28H), 1.25 – 1.08 (m, 12H, OCH_2CH_3).

^{13}C NMR (101 MHz, $CDCl_3$) δ(ppm): 167.6, 165.8, 165.5, 165.5, 165.3, 165.2, 164.9, 164.8, 161.1, 160.7, 155.0, 144.8, 136.6, 136.6, 134.0, 133.7, 133.5, 133.3, 133.2, 133.2, 133.0, 130.1, 130.0, 129.9, 129.8, 129.7, 129.4, 129.0, 128.9, 128.9, 128.7, 128.7, 128.5, 128.4, 128.3, 128.3, 128.1, 127.8, 127.6, 123.4, 122.7, 92.1, 92.0, 73.8, 72.9, 71.2, 70.8, 70.1, 70.0, 69.8, 69.6, 69.3, 69.1, 68.8, 68.7, 66.4, 66.2, 62.1, 49.9, 35.4, 30.9, 29.7, 15.3, 15.3.

ESI-MS: m/z calc (3067.21) oss: 1534.12 (100%) $[M + 2H]^{2+}$

5,17-bis-N-[((1-(6-deoxy-trehalos-6-yl)-1H-1,2,3-triazol-4-yl)methyl)aminocarbonyl]-25,26,27,28-tetrakis(ethoxyethoxy)calix[4]arene (56)

In a round-bottom flask, compound **56a** (26 mg, 0.0085 mmol) was dissolved in methanol (5 mL), then sodium methoxide (13 mg, 0.24 mmol) was added to the solution. The mixture was stirred for 60 minutes at room temperature then it was quenched by addition of Dowex 50W-X8(H) and stirred for 30 additional minutes. The resin was then filtered off and the solvent evaporated under reduced pressure obtaining a white solid (13 mg, 0.008 mmol) in 94% yield.

^{1}H NMR (600 MHz, D_2O) δ (ppm): 8.06 (s, 2H, $CH_{triazole}$), 7.39 (s, 4H, COArH), 6.90 (m, 4H, Ar$H_{meta}$$OCH_2$), 6.82 (t, *J* = 7.5 Hz, 2H, Ar$H_{para}$$OCH_2$), 5.19 (d, *J* = 3.8 Hz, 2H, H_1), 4.92 (d, *J* = 12.5 Hz, 1H, H_{6b}), 4.69(under solvent signal, H_{6a}, H_1', Ar$CH_{ax}H_{eq}$Ar), 4.34 (t, *J* = 5.0 Hz, 4H, $COArOCH_2$), 4.27 (t, *J* = 5.0 Hz, 4H, $ArOCH_2$), 4.25 – 4.18 (m, 2H, H_5), 4.07 (m, 8H, $COArOCH_2CH_2$, $ArOCH_2CH_2$), 3.93 (t, *J* = 9.4 Hz, 2H, H_3), 3.90 – 3.79 (m, 6H, H_3', H_4', H_5'), 3.79 – 3.63 (m, 10H, H_2, $H_{6'a}$, $H_{6'b}$, CCH_2NH), 3.48 (d, *J* = 10.0 Hz, 2H, Ar$CH_{ax}H_{eq}$Ar), 3.44 – 3.36 (m, 4H, H_4, H_2'), 3.29 (t, *J* = 9.5 Hz, 2H, H_4'), 1.33 (q, *J* = 6.9 Hz, 12H, $ArOCH_2CH_2CH_3$).

^{13}C NMR (101 MHz, CD_3OD) δ(ppm): 136.2, 133.6, 128.1, 127.7, 124.3, 93.8, 93.6, 73.4, 73.1, 73.0, 72.9, 72.4, 71.5, 70.4, 70.2, 69.8, 69.6, 66.2, 66.1, 61.2, 51.0, 48.3, 48.1, 47.9, 47.7, 47.5, 47.3, 47.0, 34.8, 30.5, 14.3.

ESI-MS: m/z calc (1713.80) oss: 1714.76 (100%) $[M + H]^+$

5,17-bis-N-[((1-(2,2',3,3',4',6,6'-hepta-O-benzoyl-4-deoxy-trehalos-4-yl)-1H-1,2,3-triazol-4-yl)methyl)aminocarbonyl]-25,26,27,28-tetrakis(etthoxyethoxy)calix[4]arene (57a)

In a microwave vial, 15 mg (0.017 mmol) of compound **38** and 70 mg (0.064 mmol) of compound **44** were dissolved in 2 mL of DMF. Then 2.5 mg (0.010 mmol) of $CuSO_4$ pentahydrate and 11.5 mg (0.058 mmol) of NaAsc, previously dissolved in the minimum amount of water, were added. The reaction heated for 20 minutes at 100°C under magnetic stirring. DCM was added to the mixture which was then extracted with a

saturated NaCl solution. The crude product was purified by column chromatography (eluent hexane/ethyl acetate 6:4) to give compound **57a** (40 mg, 0.013 mmol) with a yield of 76%.

^{1}H NMR (400 MHz, $CDCl_3$) δ (ppm): 8.11 (d, *J* = 8.4 Hz, 4H, ArH_{orto} of OBz), 8.06 (d, *J* = 8.4 Hz, 4H, ArH_{orto} of OBz), 7.95 (d+d+d, *J* = 8.4 Hz, 12H, ArH_{orto} of OBz), 7.84 (d+d, *J* = 8.4, Hz, 8H, ArH_{orto} of OBz), 7.65 – 7.31 (m, 44H, ArH_{para} of OBz + ArH_{meta} of OBz + ArH_{meta}, $CH_{triazole}$), 6.73 (bs, 2H, Ar-CON*H*R), 6.52 (t, *J* = 10.3 Hz, 2H, H_3'), 6.35 (t, *J* = 9.9 Hz, 2H, H_3), 6.31-6.20 (m,, 6H, ArH_{meta}-CONHR + ArH_{para}), 5.83 (d, *J* = 3.8 Hz, 2H, H_1'), 5.80 (d, *J* = 3.8 Hz, 2H, H_1), 5.72 (t, *J* = 9.9 Hz, 2H, H_4), 5.61 (dd, *J* = 10.0, 3.8 Hz, 2H, H_2'), 5.52 (dd, *J* = 10.2, 3.8 Hz, 2H, H_2), 5.07 (dd, *J* = 10.6 Hz, 2H, H_4'), 4.77 (ddd, *J* = 10.8, 3.5 Hz, 2H, H_5'), 4.64 (ddd, *J* = 4.8 Hz, 4H, Ar-CONHC*H*$_2$R), 4.54 (d, *J* = 13.4 Hz, 4H, ArC*H*$_{ax}$H$_{eq}$Ar), 4.40-4.26 (m, 4H + 2H, Ar-OC*H*$_2$CH$_2$OCH$_2$CH$_3$ + H_5), 4.05 (dd, *J* = 12.5, 2.7 Hz, 2H, H_{6A}), 3.99 (t, *J* = 6.0, 4H, Ar-OC*H*$_2$CH$_2$OCH$_2$CH$_3$), 3.94 (dd+dd, 4H, H_{6B}' , H_{6B}), 3.88 (t, *J* = 5.8 Hz, 4H, Ar-OCH$_2$C*H*$_2$OCH$_2$CH$_3$), 3.79 (t, *J* = 5.4 Hz, 4H, Ar-OCH$_2$C*H*$_2$OCH$_2$CH$_3$), 3.60 (bs, 2H, H_{6A}'), 3.54 (q+q, *J* = 7.0 Hz, 4H + 4H, ArOCH$_2$CH$_2$OC*H*$_2$CH$_3$), 3.22 (d, *J* = 13.7, 4H, ArCH$_{ax}$*H*$_{eq}$Ar), 1.20 (t+t, *J* = 7.0 Hz, 6H + 6H, ArOCH$_2$CH$_2$OCH$_2$C*H*$_3$).

^{13}C NMR (101 MHz, $CDCl_3$) δ (ppm): 167.3 (Ar-CONHR), 165.8 + 165.6 +165.3 (*C*-OBz), 160.9 (Ar*C*-OCH$_2$CH$_2$OCH$_2$CH$_3$), 136.7 (Ar*C*-CONHR), 134.3, 133.9, 133.6 + 133.5 + 133.43+ 133.3 + 133.2 + 133.0 (Ar*C*-H_{meta} of OBz + Ar*C*H_{para} di OBz) 129.8 (Ar*C*-H_{orto} of OBz), 128.4 (Ar*C*-H_{meta} of OBz + Ar*C*H_{para} of OBz), 128.1 (Ar*C*H), 127.6 (Ar*C*H), 122.7 (C=*C*HN), 92.7 (*C*-H_1), 73.8 (Ar-O*C*H$_2$CH$_2$OCH$_2$CH$_3$), 73.0 (Ar-OCH$_2$*C*H$_2$OCH$_2$CH$_3$), 71.3 (C-H_2), 70.1 (*C*-H_3), 69.7 (*C*-H_3'), 69.6 (ArOCH$_2$CH$_2$O*C*H$_2$CH$_3$), 68.7 (*C*-H_5), 68.6 (*C*-H_5'), 68.6 (*C*-H_4), 66.4 (ArOCH$_2$CH$_2$O*C*H$_2$CH$_3$), 61.7 (C-H_6), 60.6 (*C*-H_4'), 35.3 (Ar-CONH*C*H$_2$R), 30.9 (C di Ar*C*H$_2$Ar), 15.3 (ArOCH$_2$CH$_2$OCH$_2$*C*H$_3$).

ESI-MS: m/z calc (3094.09) oss: 1547.73 $[M+2H]^{2+}$

5,17-bis-N-[((1-(4-deoxy-trehalos-4-yl)-1H-1,2,3-triazol-4-yl)methyl)aminocarbonyl]-25,26,27,28-tetrakis(ethoxyethoxy)calix[4]arene (57)

Compound **57a** (40 mg, 0.013 mmol) was dissolved in MeOH, then a solution of NaOMe (25% in MeOH) was slowly added until pH 9. The mixture was stirred at room temperature for 30 minutes, then it was quenched by the addition of Amberlyst IR-120 (200 mg). After 10 minutes of stirring the suspension was filtered and the solvent evaporated under reduced pressure. A white solid (18 mg ,0.013 mmol) was obtained with quantitative yield.

^{1}H NMR (400 MHz, CD_3OD) δ (ppm): 8.09 (s, 2H, C_2N_3H), 7.53 (s, 4H, Ar*H*CONH), 6.52 – 6.35 (m, 6H, ArH), 5.31 (d, J = 3.7 Hz, 2H, H_1'), 5.17 (d, J = 3.7 Hz, 2H, H_1), 4.72 – 4.56 (m,

8H, ArC*H*$_{ax}$H$_{eq}$Ar, ArCONHC*H*$_2$R), 4.53 – 4.42 (m, 4H, H_4, H_3'), 4.35 (t, J = 5.5 Hz, 4H, OC*H*$_2$CH$_2$OCH$_2$CH$_3$), 4.04 (t, J = 5.6 Hz, 4H, OCH$_2$CH$_2$OC*H*$_2$CH$_3$), 3.99 – 3.81 (m, 15H, 2 x OCH$_2$C*H*$_2$OCH$_2$CH, H_3, H_{6b}, H_5, H_5'), 3.75 – 3.67 (m, 4H, H_{6a}, H_2'), 3.65 – 3.36 (m, 14H, H_4', H_2, H_{6b}', 2x Ar-OCH$_2$C*H*$_2$OCH$_2$CH$_3$), 3.25 (d, J = 13.4 Hz, 4H, ArCH$_{ax}$*H*$_{eq}$Ar), 3.19 (dd, J = 12.4, 4.0 Hz, 2H, $H_{6'a}$), 1.25 (t, J = 7.0 Hz, 6H, ArOCH$_2$CH$_2$OCH$_2$C*H*$_3$), 1.18 (t, J = 7.0 Hz, 6H, ArOCH$_2$CH$_2$OCH$_2$C*H*$_3$).

^{13}C NMR (101 MHz, CD$_3$OD) δ (ppm): 168.8 (Ar-*C*ONHR), 160.7 (Ar), 155.2 (*C*=CHN), 145.2 (Ar), 136.3 (Ar), 133.2 (Ar), 127.9 (Ar), 127.7 (Ar), 127.4 (Ar), 123.5 (C=*C*HN), 122.3 (Ar), 94.1 (C1'), 93.9 (C1), 73.7 (OCH$_2$*C*H$_2$OCH$_2$CH$_3$), 73.1 (O*C*H$_2$CH$_2$OCH$_2$CH$_3$), 72.5 (C3, C3'), 72.3 (C2'), 71.8 (C2), 70.7 (C4, C5, C5'), 70.5 (O*C*H$_2$CH$_2$OCH$_2$CH$_3$), 70.4 (OCH$_2$*C*H$_2$OCH$_2$CH$_3$), 69.9 (OCH$_2$*C*H$_2$OCH$_2$CH$_3$), 69.6 (OCH$_2$CH$_2$O*C*H$_2$CH$_3$), 66.1 (OCH$_2$C*H*$_2$OCH$_2$CH$_3$), 65.9 (OCH$_2$C*H*$_2$OCH$_2$CH$_3$), 62.6 (C4'), 61.2 (C6), 60.0 (C6'), 34.9 (Ar-CONH*C*H$_2$R), 30.5 (Ar*C*H$_2$Ar), 14.3 (ArOCH$_2$CH$_2$OCH$_2$*C*H$_3$).

ESI-MS: m/z calc (1608.69) oss: 1609.72 [M+H]$^+$

5,17-bis[-N-((1-(2,3,4-tri-O-benzoyl-6-deoxy-α-D-mannopyranos-6-yl)-1H-1,2,3-triazol-4-yl)methyl)aminocarbonyl]-25,26,27,28-tetrakis(ethoxyethoxy)calix[4]arene (58a)

In a microwave vial, 18 mg (0.023 mmol) of compound **38** and 27 mg (0.057 mmol) of compound **54** were dissolved in 2 mL of DMF. Then, 3 mg (0.011 mmol) of $CuSO_4$ pentahydrate and 23 mg (0.11 mmol) of NaAsc, previously dissolved in the minimum amount of water, were added. The reaction was heated at for 15 minutes at 100°C (150W). The reaction mixture was then diluted with DCM (5 mL) and extracted with a saturated NaCl solution. The crude product was purified by column chromatography (eluent DCM/MeOH 95:5) to give compound **58a** (15 mg, 0.008 mmol) with a yield of 34%.

^{1}H NMR (400 MHz, $CDCl_3$) δ (ppm): 8.07 (d, J = 7.0 Hz, 4H, ArH$_{orto}$ of OBz), 8.00 (d, J = 7.0 Hz, 4H, ArH$_{orto}$ of OBz), 7.88 (s, 2H, C_2N_3H), 7.83 (d, J = 7.0 Hz, 4H, ArH$_{orto}$ of OBz), 7.70-7.60 (m, 2H, ArH$_{para}$ of OBz), 7.59–7.37 (m, 12H, ArH$_{para}$ of OBz + ArH$_{meta}$ of OBz), 7.32 – 7.24 (m, 4H + 2H, ArH$_{meta}$ of OBz + ArH$_{para}$), 7.20 (bs, 4H, ArH$_{meta}$), 6.78 (bs, 2H, Ar-CON*H*R), 6.49 (s, 4H, ArH$_{meta}$-CONHR), 5.89 (dd, *J* = 10.0, 3.4 Hz, 2H, H_3), 5.75 (t, *J* = 10.0 Hz, 2H, H_4), 5.66 (dd, *J* = 3.4, 1.7 Hz, 2H, H_2), 4.95 (d, *J* = 1.8 Hz, 2H, H_1), 4.75 (dd, *J* = 14.2, 2.3 Hz, 2H, H_{6A}), 4.61 (d, *J* = 6.4 Hz, 4H, Ar-CONHC*H*$_2$R), 4.58-4.51 (m, 4H + 2H, ArC*H*$_{ax}$H$_{eq}$Ar + H_{6B}), 4.50 (dd, *J* = 10.4 Hz, 2H, H_5), 4.22 (t, *J* = 5.5 Hz, 4H, ArOC*H*$_2$CH$_2$OCH$_2$CH$_3$-CONHR), 4.09 (t, *J* = 5.4 Hz, 4H, ArOC*H*$_2$CH$_2$OCH$_2$CH$_3$), 3.83 (t, *J* = 5.4 Hz, 8H, ArOCH$_2$C*H*$_2$OCH$_2$CH$_3$), 3.62-3.45 (m, 8H, ArOCH$_2$CH$_2$OC*H*$_2$CH$_3$), 3.26-3.13 (m, 4H + 6H, ArCH$_{ax}$*H*$_{eq}$Ar + OCH$_3$), 1.21 (t+t, *J* = 7.0 Hz, 12H, ArOCH$_2$CH$_2$OCH$_2$C*H*$_3$).

^{13}C NMR (101 MHz, $CDCl_3$) δ (ppm): 167.7 (Ar-*C*ONHR), 165.8 - 165.4 (C-OBz), 160.1 (Ar*C*-$OCH_2CH_2OCH_2CH_3$), 155.6 ($NHCH_2C$(=CH)N), 136.0 (ArC-CONHR), 133.8 + 133.8 + 133.7 + 133.3 (Ar*C*-H_{meta} of OBz + Ar*C*H_{para} of OBz), 129.9 + 129.7 (Ar*C*-H_{orto} of OBz) 129.2 + 128.9 + 128.7 + 128.6 (Ar*C*-H_{para} + Ar*C*-CH_2Ar) , 128.3 (Ar*C*-H_{meta}-CONHR), 127.2 (Ar*C*-H_{meta}), 124.2 (C-C_2N_3H), 122.1 (ArC_{meta}-CONHR), 98.6 (C-H_1), 73.4 (ArO*C*$H_2CH_2OCH_2CH_3$), 70.3 (*C*-H_2), 69.6 (*C*-H_3), 68.2 (*C*-H_4), 66.4 ($ArOCH_2CH_2OCH_2CH_3$), 55.5 (OCH_3), 51.2 (C-H_6), 35.3 (Ar-CONH*C*H_2R), 30.9 (C di Ar*C*H_2Ar), 15.29 ($ArOCH_2CH_2OCH_2CH_3$).

ESI-MS: m/z calc (1938.11) oss: 1939.15 $[M+H]^+$

5,17-bis[-N-((1-(6-deoxy-α-D-mannopyranos-6-yl)-1H-1,2,3-triazol-4-yl)methyl)aminocarbonyl]-25,26,27,28-tetrakis(ethoxyethoxy)calix[4]arene (58)

Compound **58a** (15 mg, 0.008 mmol) was dissolved in MeOH, then a solution of NaOMe (25% in MeOH) was slowly added until pH 9. The mixture was stirred at room temperature for 30 minutes, then it was quenched by the addition of Amberlyst IR-120 (200 mg). After 10 minutes of stirring the suspension was filtered and the solvent evaporated under reduced pressure. A white solid (9 mg ,0.008 mmol) was obtained with quantitative yield.

1H NMR (400 MHz, DMSO-d_6) (ppm):8.74 (t, J = 5.8 Hz, 2H, ArCONH), 7.93 (s, 2H, C_2N_3H), 7.64 (s, 4H, ArH_{meta}), 6.23 (m, 6H, ArH), 4.76 (dd, J = 14.1, 2.2 Hz, 2H, H_{6a}), 4.60 – 4.44 (m, 10H, Ar-CONHC*H*$_2$R, ArC*H*$_{ax}$H$_{eq}$Ar, OHs), 4.39 (dd, J = 14.1, 9.0 Hz, 2H, H_{6b}), 4.31 (t, J = 6.0 Hz, 4H, ArOC*H*$_2$$CH_2OCH_2CH_3$-CONHR), 3.92 – 3.86 (m, 8H, ArOC*H*$_2$$CH_2OCH_2CH_3$, OHs), 3.76 (t, J = 5.8 Hz, 4H, $ArOCH_2CH_2$O*H*$_2$$CH_2CH_3$), 3.68 – 3.38 (m, 18H, H1, H2, H3, H4, H5, $ArOCH_2CH_2OCH_2$C*H*$_3$), 3.19 (under solvent peak, ArCH$_{ax}$*H*$_{eq}$Ar), 2.93 (s, 6H, OCH_3), 1.18 (t, J = 7.0 Hz, 6H, $ArOCH_2CH_2OCH_2$C*H*$_3$), 1.10 (t, J = 7.0 Hz, 7H, $ArOCH_2CH_2OCH_2$C*H*$_3$).

13C NMR (101 MHz, DMSO-d_6) (ppm): 166.8 (Ar-*C*ONHR), 160.6 (Ar), 155.1 ($NHCH_2C$(=CH)N), 145.7 (Ar), 136.4 (Ar), 133.1 (Ar), 128.5 (ArC_{para}), 128.3 (ArC_{meta}-CONHR), 128.0 (Ar), 124.2 (C-C_2N_3H), 122.4 (ArC_{meta}), 101.7 (C_1), 74.5 ($ArOCH_2CH_2OCH_2CH_3$), 73.0 ($ArOCH_2CH_2OCH_2CH_3$), 72.3(C_2), 71.3 (C_3), 70.6 (C_5), 69.8 ($ArOCH_2CH_2OCH_2CH_3$), 69.6 ($ArOCH_2CH_2OCH_2CH_3$), 68.7 (C_4), 66.1 ($ArOCH_2CH_2OCH_2CH_3$), 65.9 ($ArOCH_2CH_2OCH_2CH_3$), 54.5 (OCH_3), 51.5 (C_6), 35.3 (Ar-CONH*C*H_2R), 30.8 (Ar*C*H_2Ar), 15.6 ($ArOCH_2CH_2OCH_2CH_3$), 15.5 ($ArOCH_2CH_2OCH_2CH_3$).

ESI-MS: m/z calc (1313.47) oss: 1314.52 $[M+H]^+$

5,11,17,23-tetrakis[-N-((1-(2,2',3,3',4,4',6'-hepta-O-benzoyl-6-deoxy-trehalos-6-yl)-1H-1,2,3-triazol-4-yl)methyl)aminocarbonyl]-25,26,27,28-tetrakis(ethoxyethoxy)calix[4]arene (59a)

In a microwave vial, 15 mg (0.014 mmol) of compound **38** and 70 mg (0.064 mmol) of compound **41**, were dissolved in 2 mL of DMF. Then, 2.5 mg (0.010 mmol) of $CuSO_4$ pentahydrate and 11.5 mg (0.058 mmol) of NaAsc, dissolved in the minimum amount of water, were added. The reaction was heated for 20 min at 100°C (150W). DCM (5 mL) was added to the reaction mixture and extracted with a saturated NaCl solution. The crude product was purified by column chromatography (hexane/Acetate 6:4) to give compound **59a** (40 mg, 0.007 mmol) with a yield of 50%.

^{1}H NMR (400 MHz, $CDCl_3$) δ (ppm): 8.13 (d, *J* = 7.7 Hz, 8H, ArH_{orto} of OBz), 8.04 (d, *J* = 7.7 Hz, 8H, ArH_{orto} of OBz), 7.90 (m, 16H + 8H, ArH_{orto} of OBz + ArH_{para} of OBz), 7.79 (m, 16H, ArH_{orto} of OBz), 7.53 (m, 16H, ArH_{para} of OBz), 7.43 – 7.35 (m, 48H, ArH_{meta} of OBz), 7.33– 7.04 (m, 8H, ArH), 6.26 (dd, *J* = 9.8, 5.8 Hz, 8H, H_3), 5.78 (d, *J* = 3.8 Hz, 4H, H_1'), 5.70-5.60 (m, 4H, H_4), 5.60-5.53 (m, 4H, H_1), 5.47 (dd, *J* = 10.1, 3.8 Hz, 8H, H_2), 5.32 (t, *J* = 9.1 Hz, 4H, H_4'), 4.76-4.45 (m, 4H + 8H, Ar$CH_{ax}H_{eq}$Ar + Ar-CONHCH_2R), 4.45-4.24 (m, 8H, H_5) 4.18 (dd, *J* = 14.4 Hz, 5.9 Hz, 8H, H_6'), 4.15-4.07 (m, 8H, Ar-OCH_2CH$_2$OCH$_2$CH$_3$), 3.97 (dd, *J* = 12.4, 5.0 Hz, 8H, H_6), 3.76 (t, *J* = 5.4 Hz, 8H, Ar-OCH$_2$CH_2OCH$_2$CH$_3$), 3.47 (q+q, *J* = 7.0 Hz, 8H, Ar-OCH$_2$CH$_2$OCH_2CH$_3$), 3.23 (d, *J* = 13.6 Hz, 4H, Ar$CH_{ax}H_{eq}$Ar), 1.16 (t+t, 12H, Ar-OCH$_2$CH$_2$OCH$_2$CH_3).

^{13}C NMR (101 MHz, $CDCl_3$) δ (ppm): 165.8 + 165.5 + 165.2 + 164.9 (Ar-*C*ONHR + *C*-OBz), 133.4 (Ar*C*H$_{meta}$ di OBz + Ar*C*H$_{para}$ of OBz), 129.8 (ArH_{orto} of OBz), 128.7 (Ar*C*-CH$_2$Ar), 128.3 (ArH), 91.9 (*C*-H$_1$), 123.4 (*C*-H of C_2N_3H), 73.4 (Ar-OCH$_2$CH$_2$OCH2CH$_3$), 70.9 (C-H$_2$), 70.2 (*C*-H$_3$), 69.5 (Ar-OCH$_2$*C*H$_2$OCH$_2$CH$_3$), 68.9 (C-H$_4$), 68.5 (C-H$_5$), 66.3 (Ar-OCH$_2$CH$_2$O*C*H$_2$CH$_3$), 62.2 (C-H$_6$), 30.9 (C di Ar*C*H$_2$Ar), 15.3 (Ar-OCH$_2$CH$_2$OCH$_2$*C*H$_3$).

ESI-MS: m/z calc (5420.72) oss: 1362.20 (21%) [M + 3H, Na]$^{4+}$, 1367.52 (64%) [M + 2H, 2Na]$^{4+}$

5,11,17,23-tetrakis[-N-((1-(6-deoxy-trehalos-6-yl)-1H-1,2,3-triazol-4-yl)methyl)aminocarbonyl]-25,26,27,28-tetrakis(ethoxyethoxy)calix[4]arene (59)

Compound **59a** (40 mg, 0.007 mmol) was dissolved in MeOH, then a solution of NaOMe (25% in MeOH) was slowly added until pH 9. The mixture was stirred at room temperature for 30 minutes, then it was quenched by the addition of Amberlyst IR-120 (200 mg). After 10 minutes of stirring the suspension was filtered and the solvent evaporated under reduced pressure. A white solid (18 mg, 0.007mmol) was obtained with quantitative yield.

^{1}H NMR (400 MHz, CD_3OD) (ppm): 8.59 (s, 1H), 7.97 (s, 5H), 7.33 (s, 7H), 5.09 (d, J = 3.9 Hz, 5H), 4.86 – 4.73 (m, 13H), 4.61 – 4.50 (m, 16H), 4.35 – 4.16 (m, 14H), 3.90 (t, J = 5.2 Hz, 9H), 3.88 – 3.39 (m, 53H), 1.40 – 1.26 (m, 57H), 1.25 – 1.16 (m, 22H).

ESI-MS: m/z calc (2506.46) oss: 1254.23 $[M + 2H]^{2+}$

5,11,17,23-tetrakis[-N-((1-(2,3,4-tri-O-benzoyl-6-deoxy-α-D-mannopyranos-6-yl)-1H-1,2,3-triazol-4-yl)methyl)aminocarbonyl]-25,26,27,28-tetrakis(ethoxyethoxy)calix[4]arene (60a)

In a microwave vial, 17 mg (0.016 mmol) of compound **38** and 39 mg (0.074 mmol) of compound **54** were dissolved in 2 mL of DMF. Then, 2 mg (0.008 mmol) of $CuSO_4$ pentahydrate and 16 mg (0.08 mmol) of NaAsc, previously dissolved in the minimum amount of water, were added. The reaction was heated for 15 minutes at 100°C (150W). The reaction mixture was then diluted with DCM (5 mL)) and extracted with a saturated NaCl solution. The crude product is purified by column chromatography (eluent DCM/MeOH 96:4) to give compound **60a** (20 mg, 0.006 mmol) with a yield of 39%.

^{1}H NMR (400 MHz, $CDCl_3$) δ (ppm): 8.05 (d, *J* = 8.4 Hz, 8H, ArH_{orto} of OBz), 7.98 (d, *J* = 7.6, 8H, ArH_{orto} of OBz), 7.90 – 7.80 (m, 12H, ArH_{orto} of OBz + C-*H* of C_2N_3H), 7.62 (t, *J* = 7.3 Hz, 4H, ArH_{para} of OBz), 7.56 – 7.34 (m, 24H, Ar*H*$_{meta}$ of OBz + Ar*H*$_{para}$ of OBz), 7.26 (t, *J* = 7.9 Hz, 8H, ArH_{meta} of OBz), 7.08 (s, 8H ArH-CONHR), 5.87 (dd, *J* = 9.6, 3.3 Hz, 4H, H_3), 5.75 (t, *J* = 9.9 Hz, 4H, H_4), 5.65 (bs, 4H, H_2), 4.93 (bs, 4H, H_1), 4.73 (d, *J* = 13.8 Hz, 4H, H_{6A}), 4.64 – 4.51 (m, 8 H + 4H + 4H, Ar-CONHC*H*$_2$R + H_{6B} + ArC*H*$_{ax}$H$_{eq}$Ar), 4.49 (d, *J* = 10.5 Hz, 4H, H_5), 4.16 (t, J = 5.3 Hz, 8H, OC*H*$_2$CH$_2$OCH$_2$CH$_3$), 3.79 (t, *J* = 5.2 Hz, 8H, OCH$_2$C*H*$_2$OCH$_2$CH$_3$), 3.51 (q, *J* = 6.9 Hz, 8H, OCH$_2$CH$_2$OC*H*$_2$CH$_3$), 3.20 (d, *J* = 14.2 Hz, 4H, ArCH$_{ax}$*H*$_{eq}$Ar), 3.14 (s, 12H, OCH_3), 1.25-1.09 (m, 12H, OCH$_2$CH$_2$OCH$_2$C*H*$_3$).

^{13}C NMR (101 MHz, $CDCl_3$) δ (ppm): 167.6-165.4 (Ar-*C*ONHR + *C*-OBz)), 162.6 (C-OBz) 159.0 (Ar*C*-OCH$_2$CH$_2$OCH$_2$CH$_3$), 134.8 (Ar*C*-CONHR), 133.7 (Ar*C*H$_{para}$ of OBz), 133.2 (Ar*C*H$_{meta}$ of OBz + Ar*C*H$_{para}$ of OBz, 129.9 (Ar*C*H$_{orto}$ of OBz), 129.7 (Ar*C*H$_{orto}$ of OBz), 129.2 (Ar*C*H$_{orto}$ of OBz), 129.0 + 128.7 + 128.5 (Ar*C*H$_{meta}$ of OBz + Ar*C*H$_{para}$ of OBz), 128.31 (Ar*C*H$_{meta}$ of OBz), 127.4 (Ar*C*H + Ar*C*-CH$_2$Ar), 124.2 (*C*-C_2N_3H), 98.5 (*C*-H_1), 73.6 (OCH$_2$CH$_2$OCH$_2$CH$_3$) , 70.3 (*C*-H_2), 69.7 (*C*-H_3), 69.5 (OCH$_2$*C*H$_2$OCH$_2$CH$_3$), 69.4 (*C*-H_5), 68.2 (*C*-H_4), 66.4 (OCH$_2$CH$_2$O*C*H$_2$CH$_3$), 55.5 (O-*C*H$_3$), 51.2 (*C*-H_6), 35.1 (Ar-CONH*C*H$_2$R), 30.9 (C di Ar*C*H$_2$Ar), 15.3 (OCH$_2$CH$_2$OCH$_2$*C*H$_3$).

ESI-MS: m/z calc (3163.30) oss: 1582.65 $[M + 2H]^{2+}$

5,11,17,23-tetrakis[-N-((1-(6-deoxy-α-D-mannopyranos-6-yl)-1H-1,2,3-triazol-4-yl)methyl)aminocarbonyl]-25,26,27,28-tetrakis(ethoxyethoxy)calix[4]arene (60)

Compound **60a** (20 mg, 0.006 mmol) was dissolved in MeOH, then a solution of NaOMe (25% in MeOH) was slowly added until pH 9. The mixture was stirred at room temperature for 30 minutes, then it was quenched by the addition of Amberlyst IR-120 (200 mg). After 10 minutes of stirring the suspension was filtered and the solvent evaporated under reduced pressure. A white solid (9 mg, 0.006 mmol) was obtained with quantitative yield.

^{1}H NMR (400 MHz, DMSO-d_6) δ(ppm): 8.46 – 8.31 (m, 4H, ArCONH), 7.84 (s, 4H, C_2N_3H), 7.33 (s, 8H, ArH), 4.72 (dd, J = 14.1, 2.2 Hz, 4H, H_{6a}), 4.52 (d, J = 13.0 Hz, 4H, ArC$H_{ax}H_{eq}$Ar), 4.49 – 4.32 (m, 16H, H_1, H_{6b}, Ar-CONHCH_2), 4.14 (t, J = 5.3 Hz, 8H, OCH_2CH$_2$OCH$_2$CH$_3$), 3.81 (t, J = 5.2 Hz, 8H, OCH$_2$CH_2OCH$_2$CH$_3$), 3.66 - 3.36 (m, 38H, OCH$_2$CH$_2$OCH_2CH$_3$, H_2, H_3, H_4, H_5), 3.22 (under solvent peak, ArCH$_{ax}H_{eq}$Ar) 2.91 (s, 12H, OCH$_3$), 1.13 (t, J = 7.0 Hz, 12H, CH$_2$CH$_2$OCH$_2$CH_3).

^{13}C NMR (101 MHz, DMSO) δ (ppm): 166.3 (Ar-*C*ONHR), 128.1 (Ar), 124.2 (C-C_2N_3H), 101.2 (C_1), 74.0 (OCH$_2$CH$_2$OCH$_2$CH$_3$), 72.2 (C_2), 71.3 (C_3), 70.4 (C_4), 69.5 (OCH$_2$*C*H$_2$OCH$_2$CH$_3$), 68.6 (C_5), 66.0 (OCH$_2$CH$_2$O*C*H$_2$CH$_3$), 54.5 (O*C*H$_3$), 51.3 (C_6), 30.8 (Ar*C*H$_2$Ar), 15.5 (OCH$_2$CH$_2$OCH$_2$*C*H$_3$).

ESI-MS: m/z calc (1914.01) oss: 1915.02 $[M + H]^+$

NMR experiments material and methods

Bacterial strains and media

Pseudomonas putida (ATCC® 47054™), *Staphylococcus epidermidis* (ATCC® 700926™) and *Mycobacterium smegmatis* (ATCC® 700084™) were grown in LB broth at 37 °C aerobically under agitation in orbital shaker at 150 rpm, for 24 hours; Staphylococcus epidermidis (ATCC® 12228™) was grown in Nutrient Broth at 37 °C aerobically under agitation in orbital shaker at 150 rpm, for 24 hours. Bacterial cells were harvested and washed 2 times with PBS 10 mM at 1500 ×g for 15 minutes at 4°C. Pellets were resuspended in PBS 10 mM (OD600nm = 1.5) and freeze-dried in 750 µL aliquots.

On-cell STD NMR experiments

- Sample preparation

8 µL of 10 mM stock solution in d6-DMSO of test molecule were added to Disposable Kel-F inserts for 4 mm ZrO_2 MAS rotor (final concentration 2 mM).

For experiments with ligand alone, 32 µL of deuterated PBS 10 mM were added to the disposable insert (total volume 40 µL).

For experiments with cells, 2 aliquots of freeze-dried cells (OD600nm = 1.5 in 750 µL) were resuspended in distilled water and then washed in d-PBS 10 mM, by centrifuging for 7.5 min at 3000 ×g. Pellets were reunited and suspended in 32 µL of d-PBS and added to the disposable insert (total volume 40 µL).

- NMR spectra acquisition

NMR spectra were acquired by using a Bruker Avance III 600 MHz NMR spectrometer, equipped with a HR-MAS probe. 1H-NMR spectra were acquired with 16 scans. STD NMR spectra were acquired with 256 scans, selective irradiation frequency 5.15, 0.5 or -1.0 ppm, saturation time 3.0 s, off-resonance irradiation frequency 30 ppm, at 310 K and at a spinning rate of 3 kHz.

5. BIBLIOGRAPHY

(1) Belkaid, Y.; Hand, T. W. Role of the Microbiota in Immunity and Inflammation. *Cell* **2014**, *157* (1), 121.

(2) Cani, P. D.; Knauf, C. How Gut Microbes Talk to Organs: The Role of Endocrine and Nervous Routes. *Mol. Metab.* **2016**, *5* (9), 743.

(3) Murray, C. J.; Ikuta, K. S.; Sharara, F.; Swetschinski, L.; Robles Aguilar, G.; Gray, A.; Han, C.; Bisignano, C.; Rao, P.; Wool, E.; et al. Global Burden of Bacterial Antimicrobial Resistance in 2019: A Systematic Analysis. *Lancet* **2022**, *399* (10325), 629–655.

(4) Bousbia, S.; Raoult, D.; La Scola, B. Pneumonia Pathogen Detection and Microbial Interactions in Polymicrobial Episodes. *Future Microbiol.* **2013**, *8* (5), 633–660.

(5) Braga, P. A. C.; Tata, A.; Gonçalves Dos Santos, V.; Barreiro, J. R.; Schwab, N. V.; Veiga Dos Santos, M.; Eberlin, M. N.; Ferreira, C. R. Bacterial Identification: From the Agar Plate to the Mass Spectrometer. *RSC Adv.* **2012**, *3* (4), 994–1008.

(6) EL, van D.; H, A.; Y, J.; C, T. Ten Years of Next-Generation Sequencing Technology. *Trends Genet.* **2014**, *30* (9), 418–426.

(7) Tsuchido, Y.; Horiuchi, R.; Hashimoto, T.; Ishihara, K.; Kanzawa, N.; Hayashita, T. Rapid and Selective Discrimination of Gram-Positive and Gram-Negative Bacteria by Boronic Acid-Modified Poly(Amidoamine) Dendrimer. *Anal. Chem.* **2019**, *91* (6), 3929–3935.

(8) Mikagi, A.; Manita, K.; Tsuchido, Y.; Kanzawa, N.; Hashimoto, T.; Hayashita, T. Boronic Acid-Based Dendrimers with Various Surface Properties for Bacterial Recognition with Adjustable Selectivity. *ACS Appl. Bio Mater.* **2022**, 5(11):5255-5263.

(9) Casnati, A.; Sansone, F.; Ungaro, R. Peptido- and Glycocalixarenes: Playing with Hydrogen Bonds around Hydrophobic Cavities. *Acc. Chem. Res.* **2003**, *36* (4), 246–254.

(10) Casnati, A.; Fabbi, M.; Pelizzi, N.; Pochini, A.; Sansone, F.; Ungaro, R.; Di Modugno, E.; Tarzia, G. Synthesis, Antimicrobial Activity and Binding Properties of Calix[4]Arene Based Vancomycin Mimics. *Bioorg. Med. Chem. Lett.* **1996**, *6* (22), 2699–2704.

(11) Baldini, L.; Casnati, A.; Sansone, F. Multivalent and Multifunctional Calixarenes in Bionanotechnology. *Eur. J. Org. Chem.* **2020**, *2020* (32), 5056–5069.

(12) Baldini, L.; Casnati, A.; Sansone, F. Multivalent and Multifunctional Calixarenes in Bionanotechnology. *Eur. J. Org. Chem.* **2020**, *2020* (32), 5056–5069.

(13) Grare, M.; Mourer, M.; Fontanay, S.; Regnouf-de-Vains, J. B.; Finance, C.; Duval, R. E. In Vitro Activity of Para-Guanidinoethylcalix[4]Arene against Susceptible and Antibiotic-Resistant Gram-Negative and Gram-Positive Bacteria. *J. Antimicrob. Chemother.* **2007**, *60* (3), 575–581.

(14) Dibama, H. M.; Clarot, I.; Fontanay, S.; Salem, A. Ben; Mourer, M.; Finance, C.; Duval, R. E.; Regnouf-de-Vains, J. B. Towards Calixarene-Based Prodrugs: Drug Release and Antibacterial Behaviour of a Water-Soluble Nalidixic Acid/Calix[4]Arene Ester Adduct. *Bioorg. Med. Chem. Lett.* **2009**, *19* (10), 2679–2682.

(15) Baldini, L.; Cacciapaglia, R.; Casnati, A.; Mandolini, L.; Salvio, R.; Sansone, F.; Ungaro, R. Upper Rim Guanidinocalix[4]Arenes as Artificial Phosphodiesterases. *J. Org. Chem.* **2012**, *77* (7), 3381–3389.

(16) Arena, G.; Bonomo, R. P.; Calì, R.; Lombardo, G. G.; Sciotto, D.; Gulino, F. G.; Ungaro, R.; Casnati, A. Water-Soluble Calixarenes as Synthetic Receptors. Remarkable Influence of Stereochemistry on the Coordination Properties of Two New Conformational Isomers of a Calix[4]arene Tetracarboxylate1. **2006**, *4* (4), 287–295.

(17) Abrahams, K. A.; Besra, G. S. Mycobacterial Cell Wall Biosynthesis: A Multifaceted Antibiotic Target. *Parasitology* **2018**, *145* (2), 116–133.

(18) O'Neill, M. K.; Piligian, B. F.; Olson, C. D.; Woodruff, P. J.; Swarts, B. M. Tailoring Trehalose for Biomedical and Biotechnological Applications. *Pure Appl. Chem.* **2017**, *89* (9), 1223–1249.

(19) Swarts, B. M.; Holsclaw, C. M.; Jewett, J. C.; Alber, M.; Fox, D. M.; Siegrist, M. S.; Leary, J. A.; Kalscheuer, R.; Bertozzi, C. R. Probing the Mycobacterial Trehalome with Bioorthogonal Chemistry. **2012**, 16123–16126.

(20) Ishikawa, E.; Ishikawa, T.; Morita, Y. S.; Toyonaga, K.; Yamada, H.; Takeuchi, O.; Kinoshita, T.; Akira, S.; Yoshikai, Y.; Yamasaki, S. Direct Recognition of the Mycobacterial Glycolipid, Trehalose Dimycolate, by C-Type Lectin Mincle. *J. Exp. Med.* **2009**, *206* (13), 2879–2888.

(21) Kamariza, M.; Shieh, P.; Ealand, C. S.; Peters, J. S.; Chu, B.; Rodriguez-Rivera, F. P.; Babu Sait, M. R.; Treuren, W. V.; Martinson, N.; Kalscheuer, R.; et al. Rapid Detection of Mycobacterium Tuberculosis in Sputum with a Solvatochromic Trehalose Probe. *Sci. Transl. Med.* **2018**, *10* (430), 6310.

(22) McBride, M. J.; Ensign, J. C. Effects of Intracellular Trehalose Content on Streptomyces Griseus Spores. *J. Bacteriol.* **1987**, *169* (11), 4995–5001.

(23) Foley, H. N.; Stewart, J. A.; Kavunja, H. W.; Rundell, S. R.; Swarts, B. M.

Bioorthogonal Chemical Reporters for Selective In Situ Probing of Mycomembrane Components in Mycobacteria. *Angew. Chemie Int. Ed.* **2016**, *55* (6), 2053–2057.

(24) Hodges, H. L.; Brown, R. A.; Crooks, J. A.; Weibel, D. B.; Kiessling, L. L. Imaging Mycobacterial Growth and Division with a Fluorogenic Probe. *Proc. Natl. Acad. Sci. U. S. A.* **2018**, *115* (20), 5271–5276.

(25) De Smet, K. A. L.; Weston, A.; Brown, I. N.; Young, D. B.; Robertson, B. D. Three Pathways for Trehalose Biosynthesis in Mycobacteria. *Microbiology* **2000**, *146* (1), 199–208.

(26) Grzegorzewicz, A. E.; Pham, H.; Gundi, V. A. K. B.; Scherman, M. S.; North, E. J.; Hess, T.; Jones, V.; Gruppo, V.; Born, S. E. M.; Korduláková, J.; et al. Inhibition of Mycolic Acid Transport across the Mycobacterium Tuberculosis Plasma Membrane. *Nat. Chem. Biol. 2012 84* **2012**, *8* (4), 334–341.

(27) Tahlan, K.; Wilson, R.; Kastrinsky, D. B.; Arora, K.; Nair, V.; Fischer, E.; Whitney Barnes, S.; Walker, J. R.; Alland, D.; Barry, C. E.; et al. SQ109 Targets MmpL3, a Membrane Transporter of Trehalose Monomycolate Involved in Mycolic Acid Donation to the Cell Wall Core of Mycobacterium Tuberculosis. *Antimicrob. Agents Chemother.* **2012**, *56* (4), 1797–1809.

(28) Kalscheuer, R.; Weinrick, B.; Veeraraghavan, U.; Besra, G. S.; Jacobs, W. R. Trehalose-Recycling ABC Transporter LpqY-SugA-SugB-SugC Is Essential for Virulence of Mycobacterium Tuberculosis. *Proc. Natl. Acad. Sci. U. S. A.* **2010**, *107* (50), 21761–21766.

(29) Furze, C. M.; Delso, I.; Casal, E.; Guy, C. S.; Seddon, C.; Brown, C. M.; Parker, H. L.; Radhakrishnan, A.; Pacheco-gomez, R.; Stansfeld, P. J.; et al. Structural Basis of Trehalose Recognition by the Mycobacterial LpqY-SugABC Transporter. *J. Biol. Chem.* **2021**, *296*, 100307.

(30) Arosio, D.; Fontanella, M.; Baldini, L.; Mauri, L.; Bernardi, A.; Casnati, A.; Sansone, F.; Ungaro, R. A Synthetic Divalent Cholera Toxin Glycocalix[4]Arene Ligand Having Higher Affinity than Natural GM1 Oligosaccharide. *J. Am. Chem. Soc.* **2005**, *127* (11), 3660–3661.

(31) Bernardi, S.; Fezzardi, P.; Rispoli, G.; Sestito, S. E.; Peri, F.; Sansone, F.; Casnati, A. Clicked and Long Spaced Galactosyl- and Lactosylcalix[4]Arenes: New Multivalent Galectin-3 Ligands. *Beilstein J. Org. Chem. 10175* **2014**, *10* (1), 1672–1680.

(32) Dalcanale, E. Selective Oxidation of Aldehydes to Carboxylic Acids with Sodium Chlorite-Hydrogen Peroxide. *J. Org. Chem.* **1985**, *51* (1), 567–569.

(33) Molenveld, P.; Engbersen, J. F. J.; Kooijman, H.; Spek, A. L.; Reinhoudt, D. N.

Efficient Catalytic Phosphate Diester Cleavage by the Synergetic Action of Two Cu(II) Centers in a Dinuclear Cis-Diaqua Cu(II) Calix[4larene Enzyme Model. *J. Am. Chem. Soc.* **1998**, *120* (27), 6726–6737.

(34) Sartori, A.; Casnati, A.; Mandolini, L.; Sansone, F.; Reinhoudt, D. N.; Ungaro, R. The First Synthesis and Characterisation of Elusive Cone 1,2-Diformyl Tetralkoxycalix[4]Arenes and Their Derivatives. *Tetrahedron* **2003**, *59* (29), 5539–5544.

(35) Thordarson, P. Determining Association Constants from Titration Experiments in Supramolecular Chemistry. *Chem. Soc. Rev.* **2011**, *40* (3), 1305–1323.

(36) Frish, L.; Sansone, F.; Casnati, A.; Ungaro, R.; Cohen, Y. Complexation of a Peptidocalix[4]Arene, a Vancomycin Mimic, with Alanine-Containing Guests by NMR Diffusion Measurements. *J. Org. Chem.* **2000**, *65* (16), 5026–5030.

(37) Verboom, W.; Durie, A.; Egberink, R. J. M.; Asfari, Z.; Reinhoudt, D. N. Ipso Nitration of P-Tert-Butylcalix[4]Arenes. *J. Org. Chem.* **1992**, *57* (4), 1313–1316.

(38) Geng, W. C.; Jia, S.; Zheng, Z.; Li, Z.; Ding, D.; Guo, D. S. A Noncovalent Fluorescence Turn-on Strategy for Hypoxia Imaging. *Angew. Chemie Int. Ed.* **2019**, *58* (8), 2377–2381.

(39) Filby, M. H.; Humphries, T. D.; Turner, D. R.; Kataky, R.; Kruusma, J.; Steed, J. W. Modular Assembly of a Preorganised, Ditopic Receptor for Dicarboxylates. *Chem. Commun.* **2006**, No. 2, 156–158.

(40) Bassily, R. W.; El-Sokkary, R. I.; Silwanis, B. A.; Nematalla, A. S.; Nashed, M. A. An Improved Synthesis of 4-Azido-4-Deoxy- and 4-Amino-4-Deoxy-α,α-Trehalose and Their Epimers. *Carbohydr. Res.* **1993**, *239* (C), 197–207.

(41) Dong, H.; Pei, Z.; Ramström, O. Stereospecific Ester Activation in Nitrite-Mediated Carbohydrate Epimerization. *J. Org. Chem.* **2006**, *71* (8), 3306–3309..

(42) Lin, F. L.; van Halbeek, H.; Bertozzi, C. R. Synthesis of Mono- and Dideoxygenated α,α-Trehalose Analogs. *Carbohydr. Res.* **2007**, *342* (14), 2014–2030.

(43) Meyer, C.; Scherer, M.; Schönberg, H.; Rüegger, H.; Loss, S.; Gramlich, V.; Grützmacher, H. Coordination Chemistry of Phosphanyl Amino Acids: Solid State and Solution Structures of Neutral and Cationic Rhodium Complexes. *Dalt. Trans.* **2006**, No. 1, 137–148.

(44) Chawla, H. M.; Pant, N.; Kumar, S.; Mrig, S.; Srivastava, B.; Kumar, N.; Black, D. S. Synthesis and Evaluation of Novel Tetrapropoxycalix[4]Arene Enones and Cinnamates for Protection from Ultraviolet Radiation. *J. Photochem. Photobiol. B Biol.* **2011**, *105* (1), 25–33.

(45) Kim, H. J.; Kim, J. S. BODIPY Appended Cone-Calix[4]Arene: Selective Fluorescence Changes upon Ca2+ Binding. *Tetrahedron Lett.* **2006**, *47* (39), 7051–7055.

(46) Jørgensen, M.; Larsen, M.; Sommer-Larsen, P.; Petersen, W.; Synthesis of functionalised fluorescent dyes and their coupling to amines and amino acids. *J. Chem. Soc.* **1997**, *19*, 2851–2855.

(47) Verboom, W.; Datta, S.; Asfari, Z.; Harkema, S.; Reinhoudt, D. N., Tetra-O-Alkylated Calix[4]arenes in the 1,3-Alternate Conformation. *J. Org. Chem.* **1992**, *57* (20), 5394–5398.

(48) Arduini, A.; Manfredi, G.; Pochini, A.; Sicuri, A. R.; Ungaro, R. Selective Formylation of Calix[4]Arenes at the 'Upper Rim' and Synthesis of New Cavitands. *J. Chem. Soc. Chem. Commun.* **1991**, No. 14, 936–937.

(49) Vreekamp, R. H.; Verboom, W.; Reinhoudt, D. N. Lower Rim-Upper Rim Hydrogen-Bonded Adducts of Calix[4]arenes. *J. Org. Chem.* **1996**, *61* (13), 4282–4288.

(50) Iwamoto, K.; Fujimoto, K.; Matsuda, T.; Shinkai, S. Remarkable Metal Template Effects on Selective Syntheses of P-t-Butylcalix[4]Arene Conformers. *Tetrahedron Lett.* **1990**, *31* (49), 7169–7172.

(51) Scheerder, J.; Duynhoven, J. P. M. van; Engbersen, Johan F. J.; Reinhoudt, D. N. Solubilization of NaX Salts in Chloroform by Bifunctional Receptors. *Angew. Chem.* **1996**, *108* (10), 1172.

(52) Arduini, A.; Fanni, S.; Manfredi, G.; Pochini, A.; Ungaro, R.; Sicun, A. R.; Ugozzoli, F. Direct Regioselective Formylation of Tetraalkoxycalix[4]Arenes Fixed in the Cone Conformation and Synthesis of New Cavitands. *J. Org. Chem.* **1995**, *60* (5), 1448–1453.

(53) Corbellini, F.; Van Leeuwen, F. W. B.; Beijleveld, H.; Kooijman, H.; Spek, A. L.; Verboom, W.; Crego-Calama, M.; Reinhoudt, D. N. Multiple Ionic Interactions for Noncovalent Synthesis of Molecular Capsules in Polar Solvents. *New J. Chem.* **2005**, *29* (1), 243–248.

(54) Barry, C. S.; Backus, K. M.; Barry, C. E.; Davis, B. G. ESI-MS Assay of M. Tuberculosis Cell Wall Antigen 85 Enzymes Permits Substrate Profiling and Design of a Mechanism-Based Inhibitor. *J. Am. Chem. Soc.* **2011**, *133* (34), 13232–13235.

(55) Bodnár, B.; Mernyák, E.; Szabó, J.; Wölfling, J.; Schneider, G.; Zupkó, I.; Kupihár, Z.; Kovács, L. Synthesis and in Vitro Investigation of Potential Antiproliferative Monosaccharide–d-Secoestrone Bioconjugates. *Bioorg. Med. Chem. Lett.* **2017**, *27* (9), 1938–1942.